

UNCLASSIFIED

AD NUMBER
AD452824
NEW LIMITATION CHANGE
TO Approved for public release, distribution unlimited
FROM Distribution authorized to U.S. Gov't. agencies only; Administrative/Operational Use; OCT 1964. Other requests shall be referred to Office of the Deputy Administrator for SST Development, Federal Aviation Agency, 800 Independence Avenue, SW, Washington, DC.
AUTHORITY
AFWAL ltr dtd 20 Jan 1976

THIS PAGE IS UNCLASSIFIED

ML-TDR-64-236

THICK SECTION FRACTURE TOUGHNESS

TECHNICAL DOCUMENTARY REPORT NO. ML-TDR-64-236

October 1964

Supersonic Transport Research Program
Sponsored by the
FEDERAL AVIATION AGENCY

Jointly Directed by: RTD, FAA and NASA

Air Force Materials Laboratory
Research and Technology Division
Air Force Systems Command
Wright-Patterson Air Force Base, Ohio

Project No. 648D

Prepared under Contract No. AF33(657)-11461 by the
BOEING-NORTH AMERICAN, A JOINT VENTURE,
International Airport
Los Angeles 9, California

THIS DOCUMENT CONTAINED
BLANK PAGES THAT HAVE
BEEN DELETED

NOTICES

The information contained herein is a part of a national undertaking sponsored by the Federal Aviation Agency with administrative and technical support provided by the Department of Defense, Research and Technology Division, Air Force Systems Command with contributing basic research and technical support provided by the National Aeronautics and Space Administration.

When Government drawings, specifications, or other data are used for any purpose other than in connection with a definitely related Government procurement operation, the United States Government thereby incurs no responsibility nor any obligation whatsoever; and the fact that the Government may have formulated, furnished, or in any way supplied the said drawings, specifications, or other data, is not to be regarded by implication or otherwise as in any manner licensing the holder or any other person or corporation, or conveying any rights or permission to manufacture, use, or sell any patented invention that may in any way be related thereto.

Copies have been placed in the DDC collection. U. S. Government agencies may obtain copies from DDC. Other qualified DDC users may request through:

Office of the Dep/Adm for SST Development
Federal Aviation Agency
800 Independence Ave. S. W.
Washington 25, D. C.

DDC release to OTS not authorized.

This report must not be cited, abstracted, reprinted, or given further distribution without written approval of the above-named controlling office.

Copies of this report should not be returned to the Research and Technology Division unless return is required by security considerations, contractual obligations, or notice on a specific document.

FOREWORD

This report describes work accomplished under Contract AF33(657)11461, Exhibit "B", entitled, "Thick Section Fracture Toughness." This program was performed as a joint venture of The Boeing Company and North American Aviation, Incorporated.

Mr. D. L. Posner of North American Aviation was program manager, and Mr. L. T. Goodmanson of Boeing was assistant program manager. The Boeing Company had prime responsibility for work accomplished under Exhibit "B". Technical direction of the program was carried out by Mr. D. R. Donaldson of The Boeing Company and Mr. J. W. Ellis of North American Aviation. Mr. D. F. Bulloch of Boeing was principal project leader and Mr. R. R. Ferguson of North American Aviation was assistant project leader.

Significant contributions to this project were made by the following personnel at Boeing: Mrs. S. Clarke, Structures Laboratory, Mr. W. Larson, Structures Laboratory, Mr. E. Schwenk, Structures Laboratory, Mr. J. C. McMillan, Metals Technology, Mr. W. Spurr, Structures Research, Mr. S. H. Smith, Fail-Safe Group. Significant contributions to this project were made by the following personnel at North American Aviation: Mr. T. Tanaka, Structures Laboratory, Mr. J. Warren, Structures Laboratory.

This program, Project No. 648D, was administered under the direction of the Air Force Materials Laboratory, Research and Technology, by Mr. C. L. Harmsworth, Project Engineer. The contract time period covered by this final summary report is July 1, 1963 to June 30, 1964.

ABSTRACT

The purpose of this program was to evaluate plane stress and plane strain fracture toughness for eight alloys suitable for thick section application on the supersonic transport.

A preliminary heat treat study was conducted using precracked Charpy specimens to determine a relative optimum toughness condition for each alloy. Data is presented for several exploratory heat treatments for each alloy.

Plane stress and plane strain critical stress intensity values are presented for three thicknesses of center notched specimens at four temperatures from -110°F to 650°F. Plane strain values were obtained from discontinuous cracking, "pop-in," indications. Plane strain values were also obtained from round notched tensile specimens and surface cracked specimens. Data were obtained from specimens, of three different grain directions, which were cut from large forged blocks.

The effect of service conditions was investigated on four of the most promising alloys (9 Ni-4Co, Maraging 250, Inco 718 and Ti 6Al-4V). Data is presented for round notched specimens subjected to 1000 hour exposure at high temperature, sustained loading in distilled water and high load rate fracture testing.

This technical documentary report has been reviewed and is approved.



D. A. Shinn
Chief, Materials Information Branch
Materials Application Division
AF Materials Laboratory

TABLE OF CONTENTS

Section	Page
1. INTRODUCTION	1
2. SUMMARY	3
3. PROGRAM OUTLINE	7
Material Selection	7
Heat Treat Study	7
Central Notched Panel Testing	8
Notched Round Specimens	8
Critical Surface Crack Determination	10
Stress and Temperature Exposure Testing	10
High Load Rate Testing	10
Environmental Testing	11
4. BASIC CONCEPTS OF FRACTURE MECHANICS	13
Griffith-Irwin Theory of Crack Instability	13
Stress Intensity Factors of Fracture	18
5. MATERIAL	27
Block Dimensions	27
Forging Procedures	27
6. HEAT TREAT STUDY	37
Test Procedure	37
Experimental Results	39
Discussion	39
7. CENTER-NOTCHED SPECIMENS	79
Test Procedure	79
Experimental Results	89
Discussion	110
Electron Fractography	135
8. ROUND-NOTCHED SPECIMENS	143
Test Procedure	143
Experimental Results	161
Discussion	175

TABLE OF CONTENTS (continued)

Section	Page
9. CRITICAL SURFACE CRACK DETERMINATION	179
Test Procedure	179
Results and Discussion	188
10. PRECRACKED CHARPY EXPOSURE TESTING	195
Test Procedure	195
Results and Discussion	195
11. SELECTION OF FOUR MOST PROMISING ALLOYS	211
12. ROUND-NOTCHED SPECIMENS EXPOSURE TESTING	225
Results and Discussion	225
13. ENVIRONMENTAL TESTING	233
Test Procedure	233
Experimental Results	234
Discussion	234
Electron Fractography	242
14. HIGH LOAD RATE TESTING	247
Test Procedure	247
Test Results	247
15. CONCLUSIONS	255
16. RECOMMENDATIONS	261
17. REFERENCES	263

LIST OF ILLUSTRATIONS

Figure		Page
1	Program Flow Chart	9
2	Griffith Plate Configuration	14
3	Plane Stress and Plane Strain Failure Modes	16
4	Stresses Acting on an Element of Material Near Crack Front	17
5	Centrally-Cracked Panel Configuration with Infinite and Finite Widths	22
6	Circumferentially Cracked Cylindrical Specimen	25
7	Surface Flawed Specimen Configuration	25
8	Typical Sub-Block Layout of First 9 x 9 Billet for Steel and Nickel Alloys	30
9	Typical Sub-Block Layout of Second 9 x 9 Billet for Steel and Nickel Alloys	31
10	Typical Sub-Block Layout of Forged Down Billet for Steel Alloys	32
11	Typical Sub-Block Layout of First Billet for Titanium Alloys	33
12	Typical Sub-Block Layout of Second Billet for Titanium Alloys	34
13	Typical Sub-Block Layout of Third Billet for Titanium Alloys	35
14	Typical Sub-Block Layout of Fourth Billet for Titanium Alloys	36
15	Precracked Charpy Specimen	38
16	Smooth Tensile Specimen	38
17	Variation of Precracked Charpy Toughness and Ultimate Strength with Temperature for Heat Treatments of 4340	57
18	Variation of Precracked Charpy Toughness and Ultimate Strength with temperature for Heat Treatments of 9Ni-4Co	58
19	Variation of Precracked Charpy Toughness and Ultimate Strength with Temperature for Heat Treatments of AM355	59

LIST OF ILLUSTRATIONS (continued)

Figure		Page
20	Variation of Precracked Charpy Toughness and Ultimate Strength with Temperature for Heat Treatments of MARAGING 250	60
21	Variation of Precracked Charpy Toughness and Ultimate Strength with Temperature for Heat Treatments of INCO 718	61
22	Variation of Precracked Charpy Toughness and Ultimate Strength with Temperature for Heat Treatments of Ti 6Al-4V	62
23	Variation of Precracked Charpy Toughness and Ultimate Strength with Temperature for Heat Treatments of Ti 6Al-6V-2Sn ANN	63
24	Variation of Precracked Charpy Toughness and Ultimate Strength with Temperature for Heat Treatments of Ti 6Al-6V-2Sn STA	64
25	Variation of Precracked Charpy Toughness and Ultimate Strength with Temperature for Heat Treatments of PH 13-8 Mo	65
26	Micrographs of Selected Heat Treat Condition for 4340	66
27	Micrographs of Selected Heat Treat Condition for 9 Ni-4Co	67
28	Micrographs of Selected Heat Treat Condition for AM355	68
29	Micrographs of Selected Heat Treat Condition for MARAGING 250	69
30	Micrographs of Selected Heat Treat Condition for INCO 718	70
31	Micrographs of Selected Heat Treat Condition for Ti 6Al-4V	71
32	Micrographs of Selected Heat Treat Condition for Ti 6Al-6V-2Sn ANN	72
33	Micrographs of Selected Heat Treat Condition for Ti 6Al-6V-2Sn STA	73
34	Micrographs of Selected Heat Treat Condition for PH 13-8 Mo	74
35	3/16 Inch Center Notch Specimen	80
36	3/8 Inch Center Notch Specimen	81

LIST OF ILLUSTRATIONS (continued)

Figure		Page
37	1 Inch Center Notch Specimen	82
38	1 Inch Center Notch Speciment During Fatigue Cracking	84
39	3/8 Inch Center Notch - 110°F Test Setup	85
40	3/16 Inch Center Notch High Temperature Test Setup	87
41	1 Inch Center Notch High Temperature Test Setup	88
42	K _C Data for Center Notch Panels of 4340	100
43	K _C Data for Center Notch Panels of 9Ni-4Co	100
44	K _C Data for Center Notch Panels of AM355	101
45	K _C Data for Center Notch Panels of MARAGING 250	101
46	K _C Data for Center Notch Panels of INCO 718	102
47	K _C Data for Center Notch Panels of Ti 6Al-4V	102
48	K _C Data for Center Notch Panels of Ti 6Al-6V-2Sn ANN	103
49	K _C Data for Center Notch Panels of Ti 6Al-6V-2Sn STA	103
50	K _C Data for Center Notch Panels of PH 13-8 Mo	104
51	K _{C(p)} Data for Center Notch Panels of 4340	104
52	K _{C(p)} Data for Center Notch Panels of 9Ni-4Co	105
53	K _{C(p)} Data for Center Notch Panels of AM355	105
54	K _{C(p)} Data for Center Notch Panels of MARAGING 250	106
55	K _{C(p)} Data for Center Notch Panels of INCO 718	106
56	K _{C(p)} Data for Center Notch Panels of Ti 6Al-4V	107
57	K _{C(p)} Data for Center Notch Panels of Ti 6Al-6V-2Sn ANN	107
58	K _{C(p)} Data for Center Notch Panels of Ti 6Al-6V-2Sn STA	108

LIST OF ILLUSTRATIONS (continued)

Figure		Page
59	$K_{C(p)}$ Data for Center Notch Panels of PH 13-8 Mo	108
60	Center Notch Specimen Load Displacement Curves at -110° F	109
61	Center Notch Specimen Load Displacement Curves at Room Temperature	109
62	Center Notch Specimen Load Displacement Curves at 400° F	110
63	Typical Load Accelerometer Center Notch Trace	111
64	3/16 Inch Thick Panel Residual Strength for 4340	112
65	3/16 Inch Thick Panel Residual Strength for 9Ni-4Co	112
66	3/16 Inch Thick Panel Residual Strength for AM355	113
67	3/16 Inch Thick Panel Residual Strength for MARAGING 250	113
68	3/16 Inch Thick Panel Residual Strength for INCO 718	114
69	3/16 Inch Thick Panel Residual Strength for Ti 6Al-4V	114
70	3/16 Inch Thick Panel Residual Strength for Ti 6Al-6V-2Sn ANN	115
71	3/16 Inch Thick Panel Residual Strength for Ti 6Al-6V-2Sn STA	115
72	3/16 Inch Thick Panel Residual Strength for PH 13-8 Mo	116
73	Center Notch Panel Fracture Faces of 4340	117
74	Center Notch Panel Fracture Faces of 9Ni-4Co	118
75	Center Notch Panel Fracture Faces of AM355	119
76	Center Notch Panel Fracture Faces of MARAGING 250	120
77	Center Notch Panel Fracture Faces of INCO 718	121
78	Center Notch Panel Fracture Faces of Ti 6Al-4V	122
79	Center Notch Panel Fracture Faces of Ti 6Al-6V-2Sn STA	123
80	Center Notch Panel Fracture Faces of Ti 6Al-6V-2Sn ANN	124
81	Center Notch Panel Fracture Faces of PH 13-8 Mo	125

LIST OF ILLUSTRATIONS (continued)

Figure		Page
82	Comparison of K_{1C} from Panel "Pop-In" and Round Notch Tensile for 4340	127
83	Comparison of K_{1C} from Panel "Pop-In" and Round Notch Tensile for 9Ni-4Co	127
84	Comparison of K_{1C} from Panel "Pop-In" and Round Notch Tensile for AM355	128
85	Comparison of K_{1C} from Panel "Pop-In" and Round Notch Tensile for MARAGING 250	128
86	Comparison of K_{1C} from Panel "Pop-In" and Round Notch Tensile for INCO 718	129
87	Comparison of K_{1C} from Panel "Pop-In" and Round Notch Tensile for Ti 6Al-4V	129
88	Comparison of K_{1C} from Panel "Pop-In" and Round Notch Tensile for Ti 6Al-6V-2Sn ANN	130
89	Comparison of K_{1C} from Panel "Pop-In" and Round Notch Tensile for Ti 6Al-6V-2Sn STA	130
90	Comparison of K_{1C} from Panel "Pop-In" and Round Notch Tensile for PH 13-8 Mo	131
91	Electron Fractograph of Center Notched 9Ni-4Co	137
92	Electron Fractograph of Center Notched MARAGING 250	138
93	Electron Fractograph of Center Notched INCO 718	139
94	Electron Fractograph of Center Notched Ti 6Al-4V	140
95	Load-Displacement Curve of 4340 Center Notch CA88 Specimen	141
96	Macrograph of CA 88 Specimen with Surface Markings Indicative of Discontinuous Cracking	141
97	Fractograph Zones of Specimen CA88 from Fig. 96	142
98	1-1/8 Inch Fatigue Cracked Notch Tensile Specimen	144
99	Fatigue Cracking of 1-1/8 Inch Round Notch Tensile Specimen	145
100	Fracture Testing of 1-1/8 Inch Round Notch Tensile Specimen	147

LIST OF ILLUSTRATIONS (continued)

Figure		Page
101	Wire Loop Attachments for 1-1/8 Inch Round Notch Specimen	148
102	1-1/8 Inch Round Notch Specimen Heating or Cooling Setup	149
103	2-3/4 Inch Diameter Round Notch Specimen	159
104	2-3/4 Inch Round Notch Specimen Test Setup	160
105	2-3/4 Inch Round Notch Specimen Extensometer	162
106	K_{1C} Data for Round Notch Specimens of 4340	165
107	K_{1C} Data for Round Notch Specimens of 9Ni-4Co	165
108	K_{1C} Data for Round Notch Specimens of AM355	166
109	K_{1C} Data for Round Notch Specimens of MARAGING 250	166
110	K_{1C} Data for Round Notch Specimens of INCO 718	167
111	K_{1C} Data for Round Notch Specimens of Ti 6Al-4V	167
112	K_{1C} Data for Round Notch Specimens of Ti 6Al-6V-2Sn ANN	168
113	K_{1C} Data for Round Notch Specimens of Ti 6Al-6V-2Sn STA	168
114	K_{1C} Data for Round Notch Specimens of PH 13-8 Mo	169
115	$K_{1C(p)}$ Data for Round Notch Specimens of 4340	170
116	$K_{1C(p)}$ Data for Round Notch Specimens of 9Ni-4Co	170
117	$K_{1C(p)}$ Data for Round Notch Specimens of AM355	171
118	$K_{1C(p)}$ Data for Round Notch Specimens of MARAGING 250	171
119	$K_{1C(p)}$ Data for Round Notch Specimens of INCO 718	172
120	$K_{1C(p)}$ Data for Round Notch Specimens of Ti 6Al-4V	172
121	$K_{1C(p)}$ Data for Round Notch Specimens of Ti 6Al-6V-2Sn ANN	173
122	$K_{1C(p)}$ Data for Round Notch Specimens of Ti 6Al-6V-2Sn STA	173
123	$K_{1C(p)}$ Data for Round Notch Specimens of PH 13-8 Mo	174

LIST OF ILLUSTRATIONS (continued)

Figure		Page
124	2-3/4 Inch Round Notch Specimen Load Displacement Curves	174
125	Surface Crack Specimen	180
126	Fatigue Cracking Setup for Surface Cracked Specimens	184
127	Fracture Faces of Surface Crack Specimens	185
128	Fracture Testing Setup for Surface Cracked Specimens	187
129	Effect of Failure Stress Level on Surface Cracked Specimen Toughness Values	190
130	Effect of Failure Stress Level on Relationship Between Actual and Predicted Fracture Stresses	190
131	Relationship Between Round Notch and Surface Cracked Specimen Toughness Values for Various Alloys	191
132	Effect of Alloy Toughness Level on Relationship Between Actual and Predicted Fracture Stresses	191
133	Typical Load-Displacement Data for Surface Cracked Specimens	193
134	Exposure Setup for Long Charpy Specimens	196
135	Long Exposure Charpy Specimens	197
136	Effect of 1000 Hour Exposure on the Precracked Charpy Toughness for 4340	200
137	Effect of 1000 Hour Exposure on the Precracked Charpy Toughness for 9 Ni-4Co	200
138	Effect of 1000 Hour Exposure on the Precracked Charpy Toughness for AM 355	201
139	Effect of 1000 Hour Exposure on the Precracked Charpy Toughness for MARAGING 250	201
140	Effect of 1000 Hour Exposure on the Precracked Charpy Toughness for INCO 718	202
141	Effect of 1000 Hour Exposure on the Precracked Charpy Toughness for Ti 6Al-4V	202

LIST OF ILLUSTRATIONS (continued)

Figure		Page
142	Effect of 1000 Hour Exposure on the Precracked Charpy Toughness for Ti 6Al-6V-2Sn ANN	203
143	Effect of 1000 Hour Exposure on the Precracked Charpy Toughness for Ti 6Al-6V-2Sn STA	203
144	Effect of 1000 Hour Exposure on the Precracked Charpy Toughness for PH 13-8 Mo	204
145	Exposure Effects of 1000 Hours on Modified 9 Ni-4Co for Heat 580	207
146	Exposure Effects of 1000 Hours on Modified 9 Ni-4Co for Heat 655	208
147	Exposure Effects of 1000 Hours on Modified 9 Ni-4Co for Heat 656	209
148	9 Ni-4Co Exposure Effects Comparison of Initial Heat 881 and Best Modified Heat 665	210
149	3/16 Inch Thick Plate K_C Comparison	213
150	3/16 Inch Thick Plate K_C -Density Ratio Comparison	214
151	3/8 Inch Thick Plate K_C Comparison	215
152	3/8 Inch Thick Plate K_C -Density Ratio Comparison	216
153	1 Inch Thick Plate K_C Comparison	217
154	1 Inch Thick Plate K_C -Density Ratio Comparison	218
155	Round Notch Tensile K_{1C} Comparison	219
156	Round Notch Tensile K_{1C} -Density Ratio Comparison	220
157	Ultimate Strength Comparison	221
158	Strength-Density Ratio Comparison	222
159	Effects of 1000 Hour Stress and Temperature on Properties for 9 Ni-4Co	229

LIST OF ILLUSTRATIONS (continued)

Figure		Page
160	Effects of 1000 Hour Stress and Temperature on Properties for MARAGING 250	230
161	Effects of 1000 Hour Stress and Temperature on Properties for INCO 718	231
162	Effects of 1000 Hour Stress and Temperature on Properties for Ti 6Al-4V	232
163	200° F Test Setup for Environmental Specimens	235
164	Environmental Effects on 9 Ni-4Co	240
165	Environmental Effects on MARAGING 250	240
166	Environmental Effects on INCO 718	241
167	Environmental Effects on Ti 6Al-4V	241
168	Electron Fractographs of Environmental Specimens for 9 Ni-4Co	243
169	Electron Fractographs of Environmental Specimens for MARAGING 250	244
170	Electron Fractographs of Environmental Specimens for INCO 718	245
171	Electron Fractographs of Environmental Specimens for Ti 6Al-4V	246
172	Hydraulic System of High Load Rate Test Rig	248
173	Load Control System of High Load Rate Test Rig	249
174	Typical High Load Rate Curve	252
175	Effect of Stress Rate on K_{1C} Values for 9 Ni-4Co	253
176	Effect of Stress Rate on K_{1C} Values for MARAGING 250	253
177	Effect of Stress Rate on K_{1C} Values for INCO 718	254
178	Effect of Stress Rate on K_{1C} Values for Ti 6Al-4V	254
179	3/8 Inch Thick Plate K_C - Density Ratio Comparison	256

LIST OF ILLUSTRATIONS (continued)

Figure		Page
180	1 Inch Thick Plate K_C - Density Ratio Comparison	256
181	Round Notch Tensile K_{1C} - Density Ratio Comparison	257
182	Variation in K_{1C} Test Results with Specimen Type	258

LIST OF TABLES

Table	Page
T-1 Chemical Composition of Alloys	29
T-2 Heat Treatments and Resulting Mechanical Properties for 4340	40
T-3 Heat Treatments and Resulting Mechanical Properties for 9 Ni-4Co	42
T-4 Heat Treatments and Resulting Mechanical Properties for AM 355	43
T-5 Heat Treatments and Resulting Mechanical Properties for Maraging 250	46
T-6 Heat Treatments and Resulting Mechanical Properties for Inco 718	49
T-7 Heat Treatments and Resulting Mechanical Properties for Ti 6Al-4V	50
T-8 Heat Treatments and Resulting Mechanical Properties for Ti 6Al-6V-2Sn ANN	52
T-9 Heat Treatments and Resulting Mechanical Properties for Ti 6Al-6V-2Sn STA	54
T-10 Heat Treatments and Resulting Mechanical Properties for PH 13-8 Mo	56
T-11 Center Notch Specimen Details	79
T-12 Fatigue Crack Details	83
T-13 Center Notch Panel Data for 4340	90
T-14 Center Notch Panel Data for 9 Ni-4Co	91
T-15 Center Notch Panel Data for AM 355	92
T-16 Center Notch Panel Data for Maraging 250	93
T-17 Center Notch Panel Data for Inco 718	94
T-18 Center Notch Panel Data for Ti 6Al-4V	95
T-19 Center Notch Panel Data for Ti 6Al-6V-2Sn ANN	96

LIST OF TABLES (continued)

Table	Page
T-20 Center Notch Panel Data for Ti 6Al-6V-2Sn STA	97
T-21 Center Notch Panel Data for PH 13-8Mo	98
T-22 Round Notch Tensile Data for 4340	150
T-23 Round Notch Tensile Data for 9 Ni-4Co	151
T-24 Round Notch Tensile Data for AM 355	152
T-25 Round Notch Tensile Data for Maraging 250	153
T-26 Round Notch Tensile Data for Inco 718	154
T-27 Round Notch Tensile Data for Ti 6Al-4V	155
T-28 Round Notch Tensile Data for Ti 6Al-6V-2Sn ANN	156
T-29 Round Notch Tensile Data for Ti 6Al-6V-2Sn STA	157
T-30 Round Notch Tensile Data for PH 13-8Mo	158
T-31 Large Round Notch Tensile Data	163
T-32 Surface Cracked Specimen Data	181
T-33 Exposure Precracked Charpy Data	198
T-34 Chemical Composition for 9 Ni-4Co	205
T-35 Modified 9 Ni-4Co Mechanical Properties	205
T-36 Exposure Data of Modified 9 Ni-4Co Heats	206
T-37 Alloy Rating Chart by Toughness and Toughness Density Ratio	223
T-38 Exposure Round Notch Tensile Data	227
T-39 Exposure Tensile Data	228
T-40 Environmental Test Data for 9 Ni-4Co	236
T-41 Environmental Test Data for Maraging 250	237
T-42 Environmental Test Data for Inco 718	238

LIST OF TABLES (continued)

Table	Page
T-43 Environmental Test Data for Ti 6Al-4V	239
T-44 High Load Rate Data	250

LIST OF SYMBOLS

μ_T	Total Potential Energy Change
T	Surface Tension
σ_g, σ	Gross Area Stress
σ_o	Gross Area Stress at Pop-in
σ_p	Predicted Failure Stress
a	Half Crack Length
a_c	Half Critical Crack Length
a_o	Half Initial Crack Length (Fatigue Crack)
a_i	Half Initial Saw Slot Length
a_e	Equilibrium Half Crack Length
E	Young's Modulus of Elasticity
P	Energy Dissipation by Plastic Deformation
x, y, z	Rectangular Coordinates
r, θ	Polar Coordinates
$\sigma_x, \sigma_y, \sigma_z$	Normal Stress Components
$\tau_{xy}, \tau_{yz}, \tau_{xz}$	Shear Stress Components
ϵ_z	Normal Strain Component
γ_{xz}, γ_{yz}	Shear Strain Components
ν	Poisson's Ratio
K_1, K_2	Symmetric and Skew-Symmetric Stress Intensity Factor Components
G_C	Plane Stress Fracture Toughness or Strain Energy Release Rate
G_{1C}	Plane Strain Fracture Toughness or Strain Energy Release Rate
K_C	Plane Stress Critical Stress Intensity Factor

LIST OF SYMBOLS (continued)

$K_{C(p)}$	Plane Stress Critical Stress Intensity Factor with Plastic Zone Correction
K_{1C}	Plane Strain Critical Stress Intensity Factor
$K_{1C(p)}$	Plane Strain Critical Stress Intensity Factor with Plastic Zone Correction
ϕ	Airy Stress Function
∇	Del Operator
ζ	Complex Variable $\zeta = x + iy$
$Z(\zeta)$	Westergaard Stress Function
K	Opening Mode Stress Intensity Factor
W	Centrally-Cracked Panel Width
σ_{ys}	Yield Stress
w	Plastic Zone Width
σ_n	Net-Section Stress
σ_{max}	Maximum Stress at Notch Root
ρ	Notch Root Radius
K_t	Theoretical Stress Concentration Factor
D	Round Notch Bar Major Diameter
A_{net}	Net-Section Area
A_{gross}	Gross-Section Area
d	Round Notch Bar Net Section Diameter
Φ	Complete Elliptical Integral of the Second Kind
b	Surface Flaw Depth
t	Plate Thickness
l	Length Dimension

LIST OF SYMBOLS (continued)

R	Ratio of Minimum and Maximum Fatigue Stress Level
A	Charpy Specimen Net-Area at Fracture

SECTION 1 INTRODUCTION

In aircraft structural design and analysis, and the selection of a structural material for a specific structural application, one of the primary material mechanical properties considered is fracture toughness. The fracture toughness property of a structural material is a measure of material resistance to brittle fracture. In addition, the material property allows a means of predicting the unstable flaw or crack length of a structure at a maximum operating stress level.

According to the "fail-safe" design philosophy, cracks that are present or occur in an aircraft structure must be contained within the structure without danger of catastrophic failure. In the case of thick-section structure, the major problem is the presence or occurrence of embedded or surface type flaws or cracks. The growth of flaws of this type, either by sustained or fatigue loading, will occur in one of the following manners. First, the structural operating load level may be such that flaw growth and final instability will occur while the flaw remains in the embedded or surface flaw geometrical shape. This type of flaw produces a plane strain fracture mode. Secondly, the flaw growth may be such that the flaw becomes a through-the-thickness type of crack with final instability occurring in this state. This type of flaw or crack results in either the plane strain or plane stress fracture mode or a combination depending on structural geometry, operating load level, and material ductility.

The concept of the supersonic commercial transport will impose new requirements on the fail-safe capability of airframe materials. Higher speeds, altitudes, and load carrying capabilities of a successful transport will make it increasingly difficult to contain cracks within the structure without sufficient material fracture toughness. New structural alloys have been developed in recent years with greatly increased resistance to the growth of embedded flaws. The present problem then is the selection of those alloys most suited for this application and the determination of their fracture toughness in both the plane stress and plane strain states.

With these considerations in mind, the FAA funded a program to determine the fracture toughness of eight alloys suitable for thick section application on the supersonic transport. The fracture properties were to be investigated over the service temperature range and under the various service conditions.

The eight alloys selected for investigation were:

- 4340
- 9 Ni-4Co
- AM 355
- Maraging 250
- Inco 718
- Ti 6Al-4V
- Ti 6Al-6V-2Sn
- PH 13-8Mo

Manuscript was released by author October, 1964 for publication as a RTD Technical Documentary Report.

To ensure testing each of the alloys in the optimum toughness condition, a heat treat study using precracked Charpy specimens preceded the main program.

Plane stress and plane strain fracture toughness was determined on the eight alloys by means of fatigue-cracked center notched, round notched, and surface cracked specimens fabricated from large forged blocks.

Service conditions were simulated on notched rounds by sustained load in distilled water, exposure to stress and temperature, and high load rate testing.

This one-year program under the administrative direction of the Air Force and with the technical assistance of NASA has extended from July 1, 1963 to June 30, 1964.

SECTION 2 SUMMARY

The purpose of this program was to evaluate the plane stress and plane strain fracture toughness characteristics of eight forging alloys suitable for thick section application on the supersonic transport.

Fracture test specimens were fabricated from 9 x 9 x 24-inch forged blocks for the steel alloys and 3 x 9 x 24-inch forged blocks for titanium. Three steel alloys in forged down 3 x 9-inch cross sections were also tested.

A heat treat study using precracked Charpy specimens and tensile specimens was conducted to ensure that the main fracture toughness program was performed on each alloy in an optimum strength-toughness condition. The optimum heat treatment determined from this study for each alloy, is listed below with the room temperature strength and precracked Charpy toughness.

<u>Alloy</u>	<u>Ultimate Strength, ksi</u>	<u>Yield Strength, ksi</u>	<u>Toughness, $\frac{W}{A}$ in-lbs/in²</u>	<u>Heat Treatment</u>
4340	217.1	202.2	811	Austenitized at 1525°F, salt quenched at 375°F, and double tempered at 800°F.
9Ni-4Co	212.8	204.7	2273	Austenitized at 1450°F, salt quenched at 450°F, and double tempered at 700°F.
AM355	210.8	161.1	589	Solution annealed at 1925°F, oil quenched and sub-cooled to -100°F. Condition tempered at 850°F, oil quenched and sub-cooled to -100°F. Tempered at 850°F.
Maraging 250	239.0	216.5	738	Solution annealed at 1700°F, air cooled and aged at 1050°F.
Inco 718	185.3	154.5	1835	Solution annealed at 1975°F, and air cooled. Aged at 1400°F for 10 hours and furnace cooled 20°F/hr to 1200°F.
Ti 6Al-4V	165.4	152.2	535	Solution annealed at 1650°F, water quenched and aged at 1100°F.

<u>Alloy</u>	<u>Ultimate Strength, ksi</u>	<u>Yield Strength, ksi</u>	<u>Toughness, $\frac{W}{in-lbs/in^2}$</u>	<u>Heat Treatment</u>
Ti 6Al-6V -2Sn - Annealed	151.8	142.5	314	Annealed at 1300°F for 2 hrs, and air cooled.
Ti 6Al-6V -2Sn - STA	176	168.5	216	Solution annealed at 1575°F, water quenched and aged at 1200°F.
PH 13-8Mo	207.1	195.4	827	Solution annealed at 1700°F, air cooled to below 60°F and aged at 1025°F.

Plane stress, K_{IC} , values were determined on three thicknesses of material (3/16", 3/8" and 1") utilizing center notched panels. Testing was accomplished over the service range for the supersonic transport, -110°F to 650°F. K_{IC} values as derived from the center notched specimens increased with test temperature and decreased as panel thickness increased for every alloy. In many cases, particularly at elevated temperature, these characteristics were obscured by the depressing of the K_{IC} values caused by net stresses above 0.8 of the yield strength. A summary of K_{IC} values is shown in Figs. 179 and 180 for the 3/8-inch and 1-inch thick center notched panels. Data for only the most critical testing temperature of -110°F is plotted.

Plane strain, K_{IIC} , values were also determined on the center notched specimens from discontinuous cracking (pop-in) indications on load-displacement curves and accelerometer recordings. Plane strain fracture toughness was also determined from fatigue-cracked notched specimens tested in two sizes and three forging directions. These specimens were tested over the same temperature range. A comparison of the notched round specimen K_{IIC} values, normalized by density is shown in Fig. 181 for the most critical testing conditions; transverse and -110°F. Plane strain critical stress intensity values from these specimens were compared with those determined from the center notched specimen pop-in indications. The correlation was only fair in some and poor in others. It was considered that in general the alloys had too high a fracture toughness to yield satisfactory pop-in data.

The relationship between theoretical and experimentally determined fracture stresses for surface cracked specimens was determined using the K_{IIC} values from the notched round specimens. Theoretically predicted fracture stresses were based on ratios of fracture stress to yield stress of 0.8 to 1.0. Theoretically determined fracture stresses ranged from 28 percent above to 39 percent below the experimental results. The relationship between the predicted and actual stresses was a function of alloy toughness level. The results indicated the critical stress intensity equation for surface cracks was only valid for gross area stresses up to about 90 percent of the yield strength.

The rating order of K_C and K_{1C} values for the alloys varied considerably over the temperature range from -110°F to 650°F for various thicknesses of center notched panels and for the notched round specimens. However, four of the alloys; 9Ni-4Co, Maraging 250, Inco 718 and Ti 6Al-4V (not in order of preference) were concluded to be the most promising for further study. Although Ti 6Al-6V-2Sn was not selected for further study, the fracture toughness of this alloy in the annealed condition was rated very closely to the first four alloys.

The following tests were conducted on the four most promising alloys to determine the effect of simulated service conditions on the K_{1C} values.

- 1) 1000 hour exposure to stress and temperature.
- 2) Sustained loading in distilled water at room temperature and 200°F .
- 3) High load rate testing at 10^5 and 10^6 psi/sec.

Exposure testing of notched round specimens for 1000 hours at 650°F under stress revealed significant instability in only the Maraging 250. K_{1C} values were decreased an average of 16 percent for the Maraging 250 and increased 6 percent for the Inco 718 when stressed to 40 ksi. The Ti 6Al-4V specimens stressed to 25 ksi were increased only an average of 5 percent of K_{1C} .

The 9Ni-4Co was exposed at the lower temperature of 400°F and at a stress level of 40 ksi which caused an average increase of less than one percent in K_{1C} values.

Environmental testing of transverse notched round specimens in distilled water at room temperature and 200°F caused delayed fracture to occur in each of the four most promising alloys within 100 hours. Sustained loading in room temperature distilled water caused delayed fracture stress intensity values as low as 78 percent of K_{1C} for 9Ni-4Co, 65 percent for Maraging 250, 78 percent for Inco 718 and 82 percent for Ti 6Al-4V.

Raising the distilled water temperature to 200°F lowered the delayed fracture stress intensity values to 48 percent of K_{1C} for 9Ni-4Co, 48 percent for Maraging 250, 77 percent for Inco 718 and 62 percent for Ti 6Al-4V.

Increasing the rate of loading from 2.5×10^3 psi/sec to 10^6 psi/sec for notched round specimens tested at room temperature, increased the room temperature K_{1C} values for 9Ni-4Co 19 percent, decreased the Maraging 250 values 2 percent, increased the Inco 718 values 11 percent, and increased the Ti 6Al-4V values 20 percent.

SECTION 3 PROGRAM OUTLINE

MATERIAL SELECTION

Eight forging alloys which appeared promising for supersonic transport application were selected for this program. They represent several alloy systems which possess characteristics desirable for severe design requirements. These alloys are:

- 1) 4340
- 2) 9 Ni-4Co-.45C
- 3) AM 355
- 4) Maraging 250
- 5) Inco 718
- 6) Ti 6Al-4V
- 7) Ti 6Al-6V-2Sn
- 8) PH 13-8Mo

The steel alloys were forged to 9 x 9 x 24-inch blocks in order to obtain specimens in both the longitudinal and transverse direction. It was felt that this size would result in excessively low properties for the titanium alloys so these alloys were forged to 3 x 9 x 24-inch.

To investigate the effect of forging reduction, 4340, AM 355, and Maraging 250 blocks were forged down to 3 x 9-inch cross sections. These blocks were tested only in the short transverse direction.

HEAT TREAT STUDY

At the time the program was planned, there was comparatively little plane strain fracture toughness data available for most of the selected alloys. It was, therefore, not known if the vendor recommended heat treatment would result in a suitably tough condition. Heat treat sequences have generally been developed on the basis of tensile strength and ductility. Since ductility is not necessarily a good indication of fracture toughness, a systematic investigation of comparative toughness values for several likely heat treatments for each alloy was considered necessary. In addition, chemistry variations within heats of the same alloy can result in toughness variations. Therefore, the correct heat treatment for the particular heat obtained for the program had to be determined.

Because of the large amount of testing required, precracked Charpy specimens were selected for this phase of the program. Several investigators (Refs. 1 and 2) have reported a satisfactory correlation between fracture energy per unit area, $\frac{W}{A}$, and the strain energy release rate G , as determined from center notched panels. It was, therefore, considered that these specimens would provide a preliminary toughness review of each alloy.

It was considered that at least three trial heat treatments for each of the eight alloys would be necessary. It was also necessary to investigate the results of each heat treatment at each of the proposed testing temperatures (-110°F, room temperature, 400°F and 650°F).

The heat treatments selected as resulting in the best compromise of strength and toughness for the particular alloy and heat were then used in the remainder of the program, as shown in Fig. 1.

CENTER NOTCHED PANEL TESTING

Center notched panels were fabricated from the forged blocks to provide both plane stress and plane strain fracture toughness data. Three panel thicknesses, 3/16, 3/8 and 1 inch thick, were tested to determine the variation of plane stress fracture toughness with thickness. It was anticipated that the transition from plane stress to plane strain would occur in each alloy before the specimen thickness increased to one inch.

During testing the panels were instrumented to detect discontinuous cracking. The load occurring during pop-in was then used to determine plane strain fracture toughness. Plane strain fracture toughness, K_{IC} , obtained in this way was to be compared to the K_{IC} values obtained from the notched round and surface cracked specimens.

Specimens were tested at -110°F, room temperature, 400°F and 650°F to determine the variation of both plane strain and plane stress fracture toughness with temperature. Because of the size of the specimens testing was replicated at room temperature only.

It was desired to investigate the change in toughness with grain direction. However, because of the limitation of forged block size, only the 3/16-inch thick specimens could be tested in both the longitudinal and transverse direction.

NOTCHED ROUND SPECIMENS

Plane strain fracture toughness was also determined by the use of fatigue-cracked notched tensile specimens in two sizes. The first set of specimens tested were made 3 inches long by 1-1/8 inches in diameter to allow testing of each of the grain directions of the forged blocks.

Specimens were fracture tested at -110°F, room temperature, 400°F and 650°F. Because of the number of variables it was originally planned to have duplicate testing only at -110°F and 650°F. After original testing indicated excessively high net section stresses at 650°F duplicate testing was changed to -110°F and room temperature.

After testing was completed on the 1-1/8 inch diameter specimens, 2-3/4 inch diameter specimens were fabricated and retesting of conditions which resulted in net section stress to yield stress ratios above 1.1 was accomplished. Fracture tests at 650°F were not retested because of the excessively high net section stresses and the relatively lower importance of this temperature to SST application.

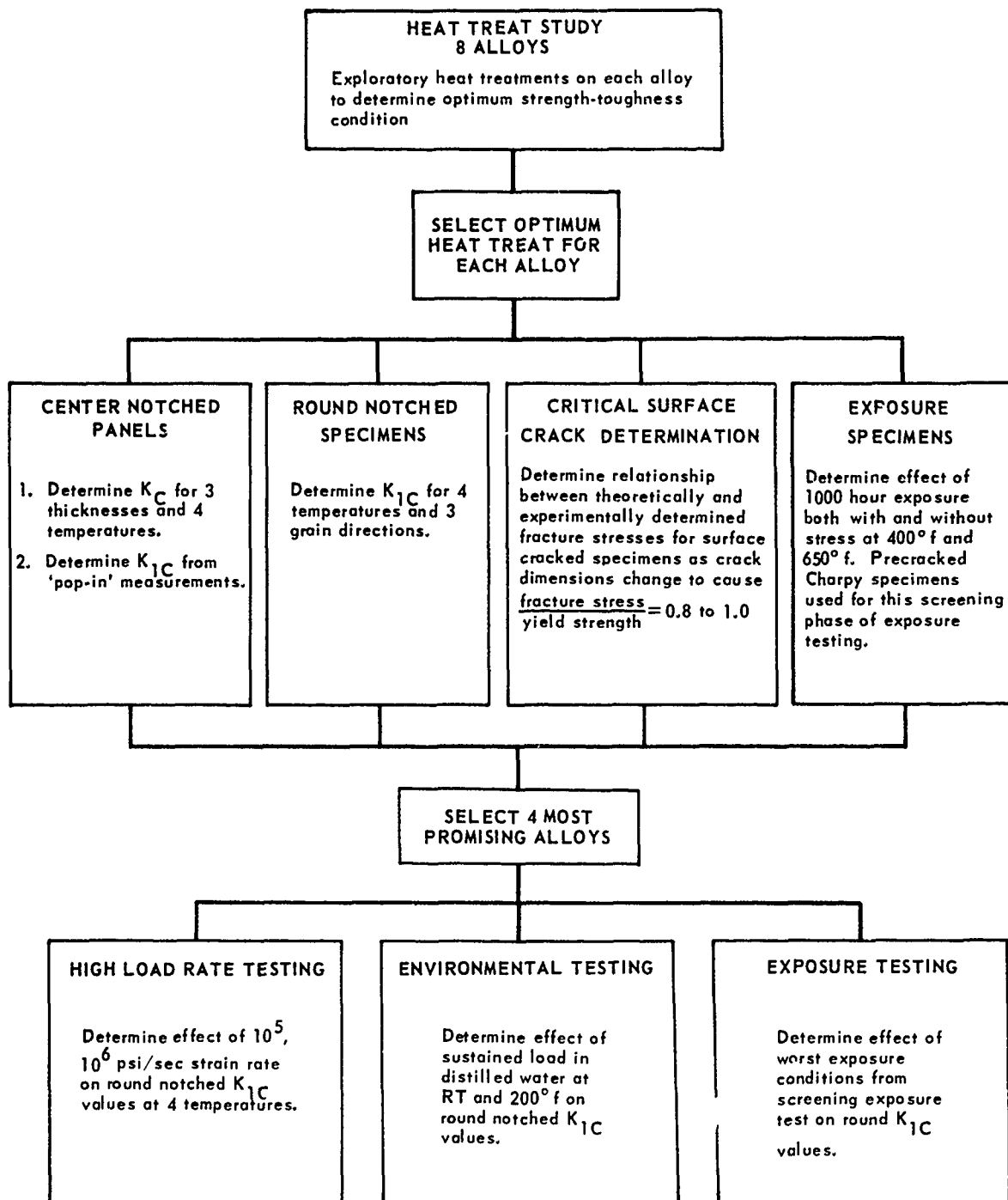


FIG. 1 PROGRAM FLOW CHART

CRITICAL SURFACE CRACK DETERMINATION

It was also the objective of the program to determine the relationship of plane strain fracture toughness obtained from both notched round and surface cracked specimens. Assuming that K_{IC} was a material constant, the K_{IC} values from the notched round specimens were used to calculate critical crack sizes on surface cracked specimens which result in fracture stress to yield stress ratios of .8, .9 and 1.0. The predicted values for the surface crack specimen fracture stress were then compared with experimental results.

Specimens were all fabricated from the longitudinal grain direction. Fracture testing was accomplished at room temperature except for AM 355 and PH 13-8Mo which were tested at -110°F. The Inco 718 was not included in this test because of its very high toughness.

STRESS AND TEMPERATURE EXPOSURE TESTING

To simulate aircraft service experience, material from all eight alloys was exposed for 1000 hours at 400°F and 650°F, in creep ovens. The titanium alloys were subjected to a stress of 25,000 psi and the remaining alloys to 40,000 psi as recommended by the NASA Supersonic Transport Materials Committee. Material was also exposed to the same temperatures without stress to assess the effect of stress on stability.

Precracked Charpy specimens were fabricated from the exposed material and impact tested at -110°F, room temperature, 400°F and 650°F. This preliminary phase was intended to indicate any serious instability and to aid in selection of the four most promising alloys.

A more quantitative phase, using 1-1/8 inch notched round exposure specimens, was then performed on the four most promising alloys. The specimens were exposed to the more severe temperature and stress conditions as determined from the preliminary tests.

Specimens were tested only in the transverse grain direction and at -110°F, room temperature, 400°F, and 650°F. Test procedure was identical to that in section 6 and therefore, exposed and unexposed results could be compared.

HIGH LOAD RATE TESTING

Notched round specimens in this program were all loaded to failure at a rate of 2.5×10^3 psi/sec. Since some alloys are known to be sensitive to changes in rate of loading, specimens of the four most promising alloys were subjected to a series of tests at high load rates. Notched round specimens identical to the specimens in section 6 were fracture tested at rates of 10^5 and 10^6 psi/sec. Test procedure was also the same, except for the load rate, so that the data could be directly compared.

Specimens were tested only in the transverse grain direction and at -110°F, room temperature, 400°F, and 650°F.

ENVIRONMENTAL TESTING

Fatigue cracked 1-1/8 inch notched round specimens from the four most promising alloys were also exposed to the effects of distilled water under sustained loading. Specimens were exposed at various percentages of their K_{1C} values (determined in section 8) to both room temperature and 200°F for 100 hours or until failure. If fracture did not occur by 100 hours the specimen was loaded to failure still in the test environment.

The object of this test was to develop a relationship between time to failure and load level in terms of percent of K_{1C} . Specimens were tested in the transverse grain direction only.

SECTION 4 BASIC CONCEPTS OF FRACTURE MECHANICS APPLIED TO THICK SECTIONS

The Griffith-Irwin fracture mechanics theory has become the classical approach in treating the mechanics of material crack growth and crack instability. This approach is used in treating material fracture toughness evaluation of the thick-section alloys. The following subsections discuss the basic concepts of the theory, crack tip stress analysis, and associated elastic stress analysis of fracture test specimen configurations used in this investigation.

"GRIFFITH-IRWIN THEORY" OF CRACK INSTABILITY

Griffith (Ref. 3) developed his original theory for the treatment of stability and instability of cracks or imperfections in ideally brittle solids. The theory is based on an energy balance or equilibrium concept of the fracture process.

In a linear elastic media (i. e., brittle solid) subjected to boundary stresses, the formation of a crack results in a change in potential energy. The total change in potential energy is equivalent to the sum of changes in strain energy due to boundary stress displacements and surface energy or surface tension dissipation of the material. According to the theorem of minimum potential energy, equilibrium or crack stability occurs when the change in potential energy is a minimum upon introducing the crack.

As an example of the application of the stability theory, Griffith considered the wide plate configuration of Fig. 2. Incorporating the crack tip stress analysis by Inglis (Ref. 4), Griffith showed that the total change in potential energy per unit plate thickness, μ_T , is given by:

$$\mu_T = 4Ta - \frac{\pi \sigma^2 a^2}{E} \quad (1)$$

where T is the material surface tension dissipation, a is the half crack length, σ is the uniformly applied boundary stress and E is Young's modulus of elasticity. Now, for equilibrium $\frac{\partial \mu_T}{\partial a} = 0$ or:

$$\frac{\pi \sigma^2 a}{E} = 2T \quad (2)$$

Therefore, the equilibrium half crack length, a_e , is:

$$a_e = \frac{2TE}{\pi \sigma^2} \quad (3)$$

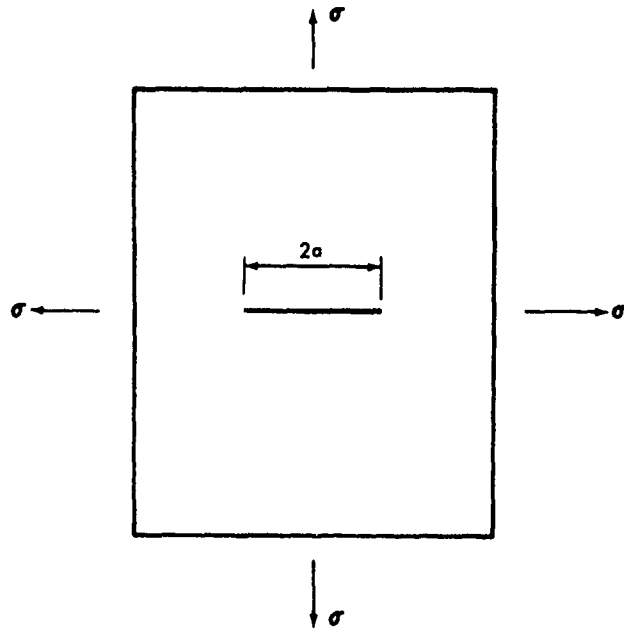


FIG. 2 GRIFFITH PLATE CONFIGURATION

Thus, referring to Equation (2), it can be seen that at the onset of rapid fracture or crack instability the strain energy release rate per unit of crack extension will be a maximum and proportional to the surface tension dissipation of the brittle material. Griffith's experiments on glass spherical bulbs and cylinders substantiated the above statement. Moreover, the experiments demonstrated that the strain energy release rate at onset of rapid fracturing was a constant for glass. In addition, applied stresses parallel to the direction of crack extension had no significant effect on the material constant.

The above Griffith energy concept of the fracture process did not consider the surface energy dissipation associated with local plasticity at the crack tip. An extension of the Griffith theory to consider plastic energy dissipation was pursued by Irwin (Refs. 5, 6) and Orowan (Ref. 7). However, the results of Irwin's analysis, which was based on a work rate analysis of the fracture process, allows a practical means of evaluating brittle fracture characteristics of ductile materials. In essence, the results are expressed in a modified form of Equations (2) and (3).

$$\frac{\pi \sigma^2 a}{E} = 2T + p \quad (4)$$

where p is the energy dissipation, during crack extension, associated with plastic deformation.

A more rigorous approach to the crack stability problem is given by Irwin (Refs. 8, 9) which involves elastic stress analysis of the crack tip stress field and its relationship to strain energy release rate. The approach is based on the state of stress and strain that exists along the leading edge of the crack. The predominant state governs the mode of fracture that will occur in a cracked structure.

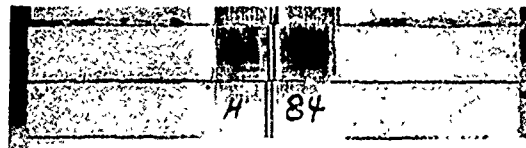
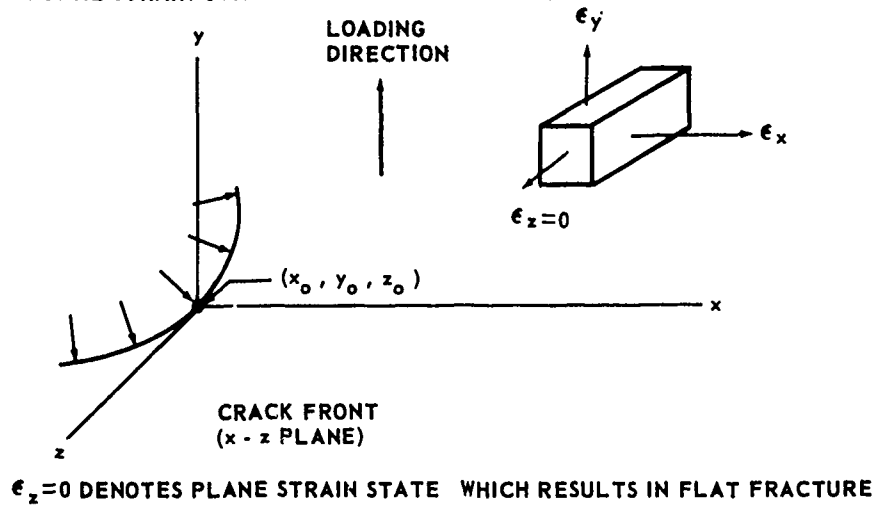
Fig. 3 shows the extreme conditions, namely, the state of plane strain and state of plane stress. In the schematic diagram of Fig. 3, the strain in the Z-direction, ϵ_z , of an element of material near the crack front is zero, except at the free surface, resulting in a state of plane strain. This state at the crack front causes a flat fracture appearance or plane-strain failure mode, as seen in the photograph. Moreover, this type of failure mode indicates a brittle behavior of the structural material. In the diagram of Fig. 3, the stress in the Z-direction, σ_z , is zero resulting in material deformation in the same direction (Ref.10). Such a state is plane-stress producing a complete shear fracture appearance or plane-stress failure mode and indicates ductile behavior of the structural material. A combined state of plane stress and plane strain results in a mixed failure mode producing shear and flat fracture across the fracture face.

A linear elastic analysis for the stresses acting on an element of material near the crack tip in an infinite solid, Fig. 4, is given by Irwin (Ref. 8). On the basis of Westergaard's (Ref.11) semi-inverse stress function method, Irwin demonstrated that the crack tip stress field can be expressed in terms of a stress intensity factor K. The general equations for normal and shear stresses near the crack front for the states of plane stress and plane strain are as follows:

For plane stress state,

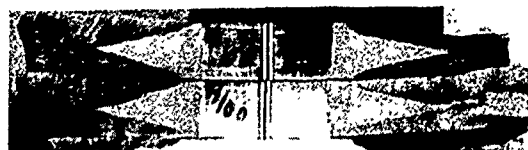
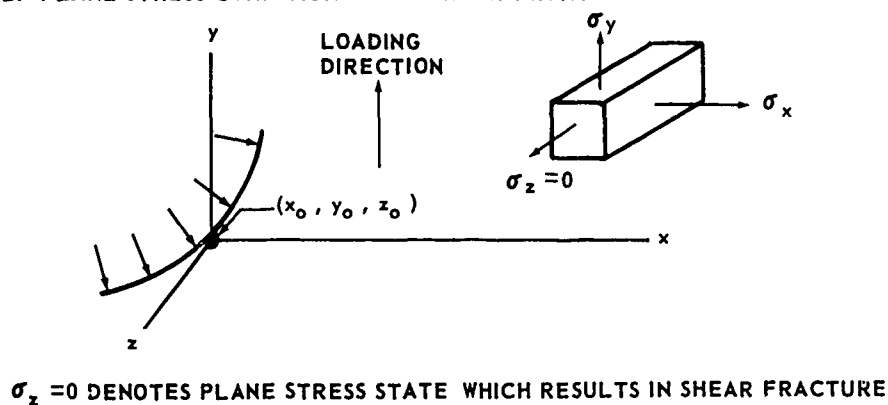
$$\begin{aligned}\sigma_x &= \frac{K_1}{\sqrt{2\pi r}} \cos \frac{\theta}{2} \left(1 - \sin \frac{\theta}{2} \sin \frac{3\theta}{2} \right) \\ &\quad - \frac{K_2}{\sqrt{2\pi r}} \sin \frac{\theta}{2} \left(2 + \cos \frac{\theta}{2} \cos \frac{3\theta}{2} \right) \\ \sigma_y &= \frac{K_1}{\sqrt{2\pi r}} \cos \frac{\theta}{2} \left(1 + \sin \frac{\theta}{2} \sin \frac{3\theta}{2} \right) \\ &\quad + \frac{K_2}{\sqrt{2\pi r}} \sin \frac{\theta}{2} \cos \frac{3\theta}{2} \cos \frac{\theta}{2}\end{aligned}$$

A. PLANE STRAIN CONDITION NEAR CRACK FRONT



BRITTLE BEHAVIOR

B. PLANE STRESS CONDITION NEAR CRACK FRONT



DUCTILE BEHAVIOR

FIG. 3 PLANE STRESS AND PLANE STRAIN FAILURE MODES

$$\tau_{xy} = \frac{K_1}{\sqrt{2\pi r}} \sin \frac{\theta}{2} \cos \frac{\theta}{2} \cos \frac{3\theta}{2} + \frac{K_2}{\sqrt{2\pi r}} \cos \frac{\theta}{2} \left(1 - \sin \frac{\theta}{2} \sin \frac{3\theta}{2} \right)$$

$$\sigma_z = \tau_{xz} = \tau_{yz} = 0 \quad (5)$$

For plane strain state,

$$\sigma_z = \nu (\sigma_x + \sigma_y)$$

$$\epsilon_z = \gamma_{xz} = \gamma_{yz} = 0$$

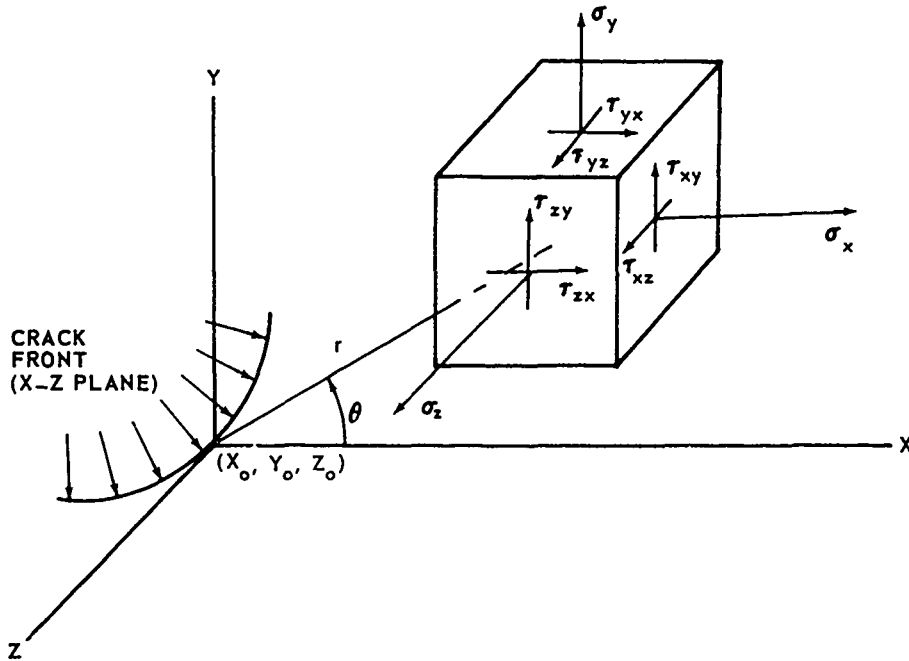


FIG. 4 STRESS ACTING ON AN ELEMENT OF MATERIAL NEAR CRACK FRONT

where K_1 and K_2 are, respectively, the symmetric and skew-symmetric stress intensity factors relative to applied crack extension loadings, ν is Poisson's ratio, and r and θ are polar coordinates (x, y plane) of the material element under consideration. In examining Equation (5), it can be seen that a stress singularity exists at the crack tip (i.e., $r = 0$). In addition, the crack tip stress

analysis of Williams (Ref. 12) and Sneddon (Ref. 13) have shown similar general equations in comparison to Equations (5). Moreover, an elastic analysis of the crack tip stress field gives a satisfactory description of the stress field if the crack tip plastic zone is small compared to the crack size.

In considering symmetrically applied loading or $K_2 = 0$, the strain energy release rate, G , at onset of rapid fracture is expressed in terms of the crack tip stress field or stress intensity factor (Ref. 9). For the state of plane stress, the strain energy release rate, G_C , is

$$G_C = \frac{K_C^2}{E} \quad (6)$$

where K_C (i.e., K_1) is the plane stress critical stress intensity factor. In addition, for the state of plane strain, the strain energy release rate, G_{1C} , is

$$G_{1C} = \frac{(1 - \nu^2) K_{1C}^2}{E} \quad (7)$$

where K_{1C} (i.e., K_1) is the plane strain critical stress intensity factor. The parameters G_C and G_{1C} are commonly referred to as plane stress and plane strain fracture toughness respectively.

Now, the approach is to evaluate the material constants K_C and K_{1C} through experimental methods. The following discusses the analytical solutions for the stress intensity factor of fracture test specimen configurations of interest in the investigation.

STRESS INTENSITY FACTORS OF FRACTURE TEST SPECIMEN CONFIGURATIONS

The primary fracture test specimen configurations used in material fracture toughness evaluation are the centrally cracked panel, circumferentially cracked cylindrical specimen (or round-notched bar), and surface-flawed plate. The analytical results and discussion of the crack tip stress intensity factors for these specimen configurations are based on the analytical works of Irwin (Refs. 8, 14, 15, 16, 17) and are subsequently presented.

Centrally Cracked Panel Configuration

An analysis technique for the general solution of problems of cracks in elastic sheets is given by Westergaard (Ref. 11). Westergaard's approach to elastic stress problems is based on a semi-inverse stress function method, which involves the following mathematical model and general theory of elasticity.

The problem under consideration is a centrally cracked infinite panel loaded in the x-y plane (Fig. 5a). An Airy stress function, ϕ , must satisfy the equilibrium and compatibility equations in solving for the normal and shear stresses acting on a differential element (dx by dy) of material in the elastic stress field near the crack tip.

For equilibrium and a state of plane stress, $\sigma_z = 0$,:

$$\begin{aligned}\frac{\partial \sigma_x}{\partial x} + \frac{\partial \tau_{xy}}{\partial y} &= 0 \\ \frac{\partial \sigma_y}{\partial y} + \frac{\partial \tau_{xy}}{\partial x} &= 0 \\ \tau_{xy} &= \tau_{yx}\end{aligned}\quad (8)$$

and the compatibility equation is:

$$\nabla^2 (\sigma_x + \sigma_y) = 0$$

$$\text{where } \nabla^2 = \frac{\partial^2}{\partial x^2} + \frac{\partial^2}{\partial y^2} \quad (9)$$

In addition, the normal and shear stresses are given in terms of ϕ as:

$$\sigma_x = \frac{\partial^2 \phi}{\partial y^2}; \quad \sigma_y = \frac{\partial^2 \phi}{\partial x^2}; \quad \tau_{xy} = - \frac{\partial^2 \phi}{\partial x \partial y} \quad (10)$$

Combining Equations (8), (9), and (10) results in the well known biharmonic equation:

$$\nabla^4 \phi = 0; \quad \text{where } \nabla^4 = \frac{\partial^4}{\partial x^4} + 2 \frac{\partial^4}{\partial x^2 \partial y^2} + \frac{\partial^4}{\partial y^4} \quad (11)$$

By defining ϕ as:

$$\phi = \text{Re } \bar{\bar{Z}} + y \text{Im } \bar{Z} \quad (12)$$

where $\bar{\bar{Z}}$ is an analytic function of the complex variable ζ ,

$\zeta = x + iy$, and

$$\bar{Z} = \frac{d\bar{Z}}{d\zeta} ; \quad Z = \frac{d\bar{Z}}{d\zeta} ; \quad Z' = \frac{dZ}{d\zeta} \quad (13)$$

results in $\nabla^4 \phi = 0$. Equations (10) then reduce to:

$$\begin{aligned} \sigma_x &= \text{Re}Z - y \text{Im} Z' \\ \sigma_y &= \text{Re}Z + y \text{Im} Z' \\ \tau_{xy} &= -y \text{Re}Z' \end{aligned} \quad (14)$$

The stress function, $Z(\zeta)$, which solves the infinite panel problem of Fig. 5(a) is:

$$Z(\zeta) = \sigma \left[1 - \left(\frac{a}{\zeta} \right)^2 \right]^{-\frac{1}{2}} \quad (15)$$

where σ is a uniformly applied tension stress. Now, along the line of expected crack extension (i.e., x axis where $\theta = 0$, $y = 0$), the normal stress in the y-direction is:

$$\sigma_y = \text{Re}Z = \sigma \left[1 - \left(\frac{a}{x} \right)^2 \right]^{-\frac{1}{2}} \quad (16)$$

In addition, referring to Equations (5), σ_y can be expressed as

$$\sigma_y = \frac{K}{\sqrt{2\pi r}} \quad (17)$$

Therefore, combining Equations (16) and (17) results in

$$K = \sigma \left[\frac{2\pi r x^2}{x^2 - a^2} \right]^{\frac{1}{2}} \quad (18)$$

where $x = a + r$. Since the stress intensity factor describes the stress field near the crack tip, the following limiting process is taken.

$$K = \lim_{r \rightarrow 0} \sigma \left[\frac{2\pi (a+r)^2}{2a+r} \right]^{\frac{1}{2}} = \sigma \sqrt{\pi a} \quad (19)$$

Equation (19) is an infinite panel solution for the crack tip stress intensity factor K . However, it is of practical interest to determine the stress intensity factor for a centrally cracked panel of finite width.

The approach is to consider a collinear array of cracks of length $2a$ subjected to uniform tension, σ , and spaced at equidistant W as shown in Fig. 5b. The appropriate Westergaard stress function that solves the given problem is,

$$Z(\zeta) = \frac{\sigma \sin \frac{\pi \zeta}{W}}{\left[\left(\sin \frac{\pi \zeta}{W} \right)^2 - \left(\sin \frac{\pi a}{W} \right)^2 \right]^{1/2}} \quad (20)$$

Therefore, along the x-axis:

$$\sigma_y = \text{Re}Z = \frac{\sigma \sin \frac{\pi x}{W}}{\left[\left(\sin \frac{\pi x}{W} \right)^2 - \left(\sin \frac{\pi a}{W} \right)^2 \right]^{1/2}} \quad (21)$$

where $x = a + r$. The resulting stress intensity factor is:

$$K = \lim_{r \rightarrow 0} \sigma \sin \frac{\pi(a+r)}{W} \left[\frac{2 \pi r}{\left(\sin \frac{\pi(a+r)}{W} \right)^2 - \left(\sin \frac{\pi a}{W} \right)^2} \right]^{1/2} \quad (22)$$

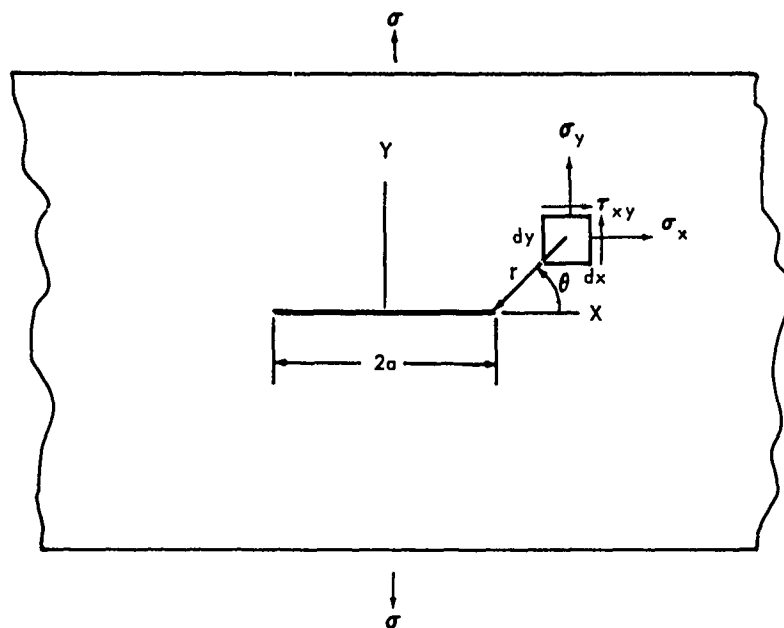
or

$$K = \sigma \sqrt{\pi a} \left[\frac{W}{\pi a} \text{TAN} \frac{\pi a}{W} \right]^{1/2} \quad (23)$$

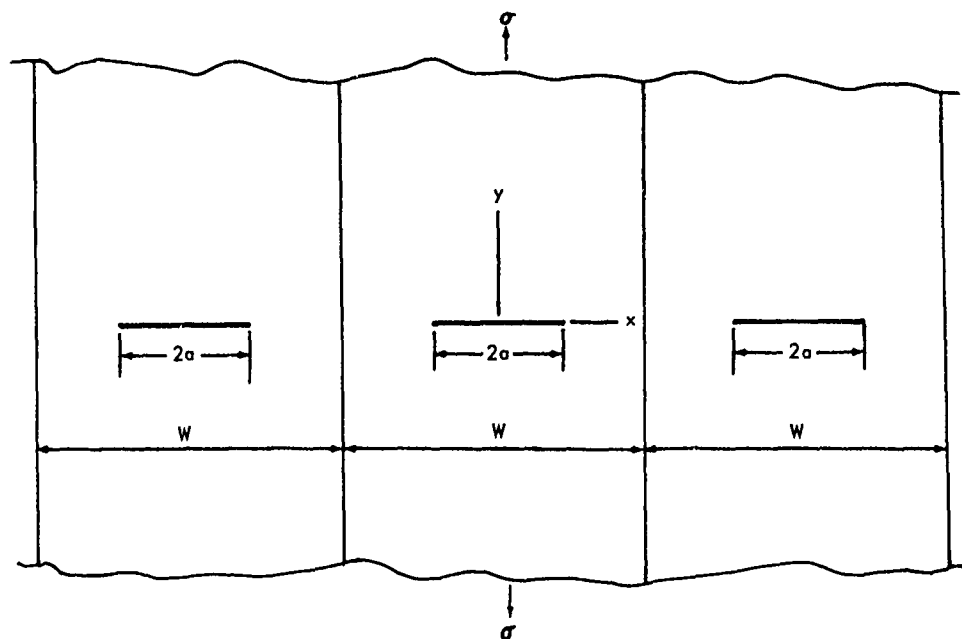
Therefore, Equation (23) is the stress intensity factor for a finite centrally cracked panel loaded in uniform tension. In comparing Equations (19) and (23), the term $\left[\frac{W}{\pi a} \text{TAN} \frac{\pi a}{W} \right]^{1/2}$ is a stress field correction factor for the finite geometry.

The previous stress analysis of the crack tip stress field and stress intensity factor for the centrally cracked panel fracture specimen configuration is based on mathematical elastic theory techniques. Therefore, certain corrections and limitations will be placed on the solution for the stress intensity factor due to localized plastic deformation at the crack tip.

Of primary interest is the size of the plastic enclave or zone at the tip of the crack. This is readily determined by applying a yield criterion and incorporating the stress field equations given previously, Equation (5). The yield criterion which gives results in good agreement with test results is the Henky-



(A) INFINITE PANEL SUBJECTED TO UNIFORM TENSION



(B) COLLINEAR ARRAY OF CRACKS SUBJECTED TO UNIFORM TENSION

FIG. 5 CENTRALLY-CRACKED PANEL CONFIGURATION WITH INFINITE AND FINITE WIDTHS

von Mises distortional energy criterion (see Ref. 10). For the state of plane stress or biaxial stress condition, the yielding theory can be expressed as:

$$\sigma_x^2 - \sigma_x \sigma_y + \sigma_y^2 + 3 \tau_{xy}^2 = \sigma_{ys}^2 \quad (24)$$

where σ_{ys} is the yield stress as determined from an axial test. Substitution of Equations (5) into the above Equation (24) results in the following expression, which defines the extent of the plastic zone in terms of polar coordinates r and θ .

$$r = \frac{K^2}{2\pi\sigma_{ys}^2} \cos^2 \frac{\theta}{2} \left[1 + 3 \sin^2 \frac{\theta}{2} \right] \quad (25)$$

Along the line of crack extension, i.e., $\theta = 0^\circ$, the width of the plastic zone, w , is

$$w = r = \frac{K^2}{2\pi\sigma_{ys}^2} \quad (26)$$

The width of the plastic zone is considered as an added effective crack length. Therefore, Equation (23) when corrected for this additional crack length becomes:

$$K = \sigma \left[W \tan\left(\frac{\pi a}{W} + \frac{K^2}{2W\sigma_{ys}^2}\right) \right]^{1/2} \quad (27)$$

Based on observations of experimental data, the ASTM Committee on Fracture Testing of High-Strength Materials (Ref. 18) recommends that center-cracked panels be so designed that $\sigma_n = 0.8 \sigma_{ys}$, where σ_n is the net section failure stress.

Circumferentially Cracked Cylindrical Specimen (Round-Notched Bar)

The basic stress intensity factor equation for this fracture test specimen configuration (Fig. 6) is given by Irwin (Ref. 19) as:

$$K = \lim_{\rho \rightarrow 0} \sigma_{MAX} \sqrt{\pi\rho} \quad (28)$$

where ρ is the notch root radius and σ_{MAX} is the maximum stress at the notch root. Equation (28) can be rewritten by considering $\sigma_{MAX} = K_t \sigma_n$. Therefore,

$$K = \sigma_n \sqrt{\pi D} \lim_{\frac{\rho}{D} \rightarrow 0} \frac{K_t}{2} \sqrt{\frac{\rho}{D}} \quad (29)$$

where σ_n is the net section stress, D is the major bar diameter, K_t is a theoretical stress concentration factor, and it is assumed $A_{net} = 1/2 A_{gross}$. An analysis by Irwin (Ref. 19) shows that for $\frac{d}{D} = 0.707$, where d is the net section diameter, Equation (29) reduces to:

$$K = 0.233 \sigma_n \sqrt{\pi D} \quad (30)$$

The plane strain plastic zone width at the crack tip was derived by Irwin (Ref. 14, 15) and is given as:

$$w = \frac{K^2}{4 \pi \sqrt{2} \sigma_{ys}^2} \quad (31)$$

By considering the plastic zone width as an effective radial increase in crack depth, Equation (30) becomes:

$$K = 0.233 \left(\frac{\frac{D}{2\sqrt{2}}}{\frac{D}{2\sqrt{2}} - \frac{K^2}{4 \pi \sqrt{2} \sigma_{ys}^2}} \right)^2 \sigma_n \sqrt{\pi D} \quad (32)$$

The Equation for K then reduces to:

$$K \left[1 - \frac{K^2}{2 \pi D \sigma_{ys}^2} \right]^2 = 0.233 \sigma_n \sqrt{\pi D} \quad (33)$$

The ASTM Committee on Fracture Testing of High-Strength Materials (Ref. 18) recommends that notched bars be of sufficient size to assure $\sigma_n \leq 1.1 \sigma_{ys}$ at failure. This recommendation is substantiated by experimental results reported by the committee.

Surface-Flawed Plate Configuration

The stress intensity factor for a semielliptical surface flaw in a plate subjected to a uniform tension stress, Fig. 7, as derived by Irwin (Ref. 16, 17) is:

$$K = \frac{1.1 \sigma \sqrt{\pi b}}{\Phi} \quad (34)$$

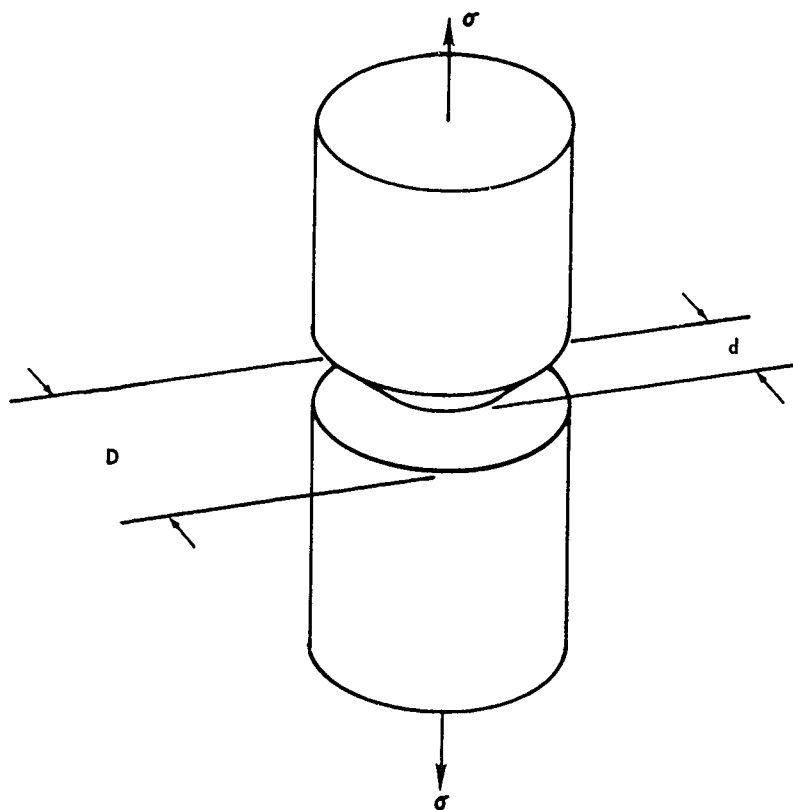


FIG. 6 CIRCUMFERENTIALLY CRACKED CYLINDRICAL SPECIMEN

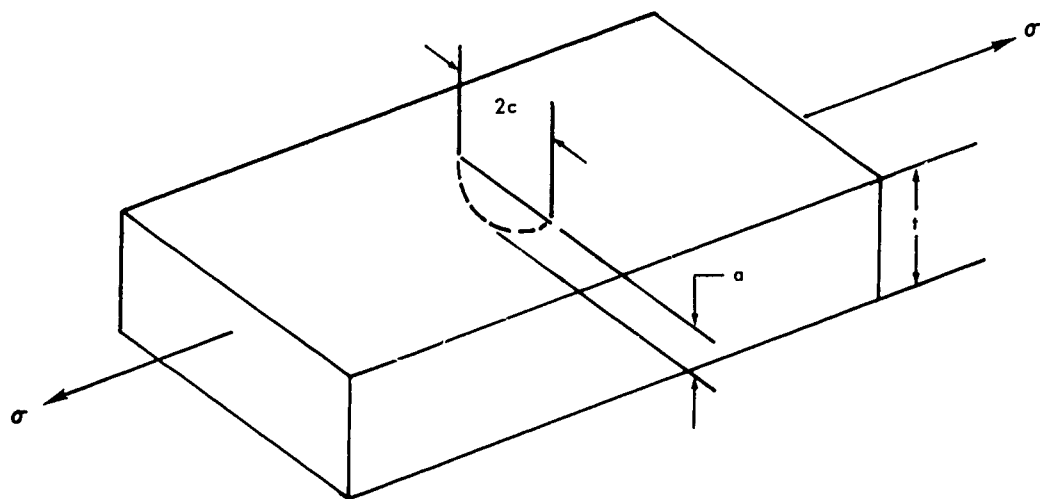


FIG. 7 SURFACE FLAWED SPECIMEN CONFIGURATION

where b is the flaw depth and Φ is the following complete elliptical integral of the second kind.

$$\Phi = \int_0^{\pi/2} \left(1 - \left(\frac{a^2 - b^2}{a^2}\right) \sin^2 \theta\right)^{1/2} d\theta \quad (35)$$

Equation (34) is valid for $\frac{b}{a} < 1$ where a is the half flaw length and $\frac{b}{t} < 0.5$ where t is the plate thickness. Correcting Equation (34) for the plane strain plastic zone width, Equation (3), results in:

$$K = \frac{1.1 \sigma \sqrt{\pi b}}{\left[\Phi^2 - 0.212 \left(\frac{\sigma}{\sigma_{ys}}\right)^2\right]^{1/2}} \quad (36)$$

The ASTM Committee on Fracture Testing of High Strength Materials (Ref. 18) recommends that surface flawed plates be of sufficient size that $\sigma \leq \sigma_{ys}$ and $\sigma \geq 0.9\sigma_n$ at fracture.

SECTION 5 MATERIAL

BLOCK DIMENSIONS

Forged blocks 9 x 9 x 24 inches were obtained for the fabrication of steel specimens. Blocks this large were necessary in order to test panels up to one inch thick. The width-to-thickness ratio of 9 to 1 was as low as considered advisable; the ASTM Fracture Committee recommends 16 to 1. A 16-inch square billet was considered too large to obtain sufficient working in forging reduction from the cast ingot. A 9 x 9-inch cross section was the compromise size selected as a good trade between fracture properties and satisfactory test specimens. In addition, specimen sizes were considered representative of SST part sizes.

It was realized that some variation in fracture properties might occur across the block which would obscure results obtained from testing variables. In an effort to minimize this undesirable variable, consutrode melted material with its inherently better homogeniety was used and in addition the transverse specimens were all taken from a 3-inch slab from the top of one block. The longitudinal specimens tend to be less affected by position in the block as is generally found with the reduction in area values from tensile specimens. The locations of the specimens in the forged blocks are shown in Figs. 8 through 14.

To ensure that there was not a large variation in properties across the blocks, three transverse tensile specimens from each block were tested. One specimen was taken from the center, edge, and midpoint areas of each block. Reduction in area values revealed only minor variations.

Because titanium requires greater forging reduction to obtain satisfactory properties, 3 x 9 x 24-inch blocks were obtained. In addition, to determine the effects of forging reduction, 3 x 9-inch cross section blocks of 4340, AM 355 and Maraging 250 were also obtained.

Forged blocks for each alloy were from a single heat to eliminate chemistry variations. A wet chemical analysis and vacuum gas analysis were run on each alloy and the results are listed in Table 1. The supplier, melting procedure, and heat number for each alloy was included for additional information.

Ultrasonic inspection was conducted on each alloy using a 3/32-inch indication as basis for rejection. A slab from the cross section of each block was macro-etched to inspect for evidence of gross segregation.

The above inspection procedures indicated that each material was within specification requirements and free from harmful defects.

FORGING PROCEDURE

Because it was impossible to obtain material from each alloy with the same degree of forging, a short description of the melting and forging process is given. The amount of forging reduction from the cast ingot to the final forged block will have an effect on the fracture properties and should be considered in the analysis.

4340

This material was air melted in an electric furnace and then, vacuum consumable electrode, remelted to a 16-inch diameter ingot. Forging from 2200° F was used to reduce the ingot to a 12-inch round cornered square. The billet was conditioned and final forged to a 9 x 9-inch cross section. The heat treatment as supplied was 1600°F with a 70°F/hour furnace cool to room temperature.

9 Ni-4Co

First melting was in air in an electric furnace with a subsequent vacuum arc remelt using a 27-inch electrode. The final ingot size was 30-inches and forged in the temperature range of 2050° F down to 1800° F. The final 9 x 9 inch forging was slow cooled in vermiculite.

AM 355

This alloy was air melted in an electric furnace and then consumable electrode vacuum remelted with a 22-inch electrode to a final 20-inch ingot. The ingot was forged to the final 9 x 9-inch size then equalized and aged by heating at 1375°F for 3 hours, air cooled then heated to 1050°F for 3 hours and air cooled.

Maraging 250

This material was air melted in an electric furnace and vacuum consumable remelted using a 16-inch electrode. The final 20-inch ingot was homogenized for 3 hours at 2300°F, then forged to a 12-inch square and air cooled. The 12-inch square was then reheated to 2000°F, held for 3 hours and forged to the final 9 x 9 inch size. The forged blocks were solution annealed at 1500°F for 6 hours and air cooled to room temperature.

Inco 718

This material was vacuum arc remelted using a 13-inch consumable electrode. The final ingot 16 inches in diameter was forged between 2000° F and 1800° F to the final 9 x 9 inch size. The forged blocks were then annealed at 1800° F for 1 hour.

Ti 6Al-4V

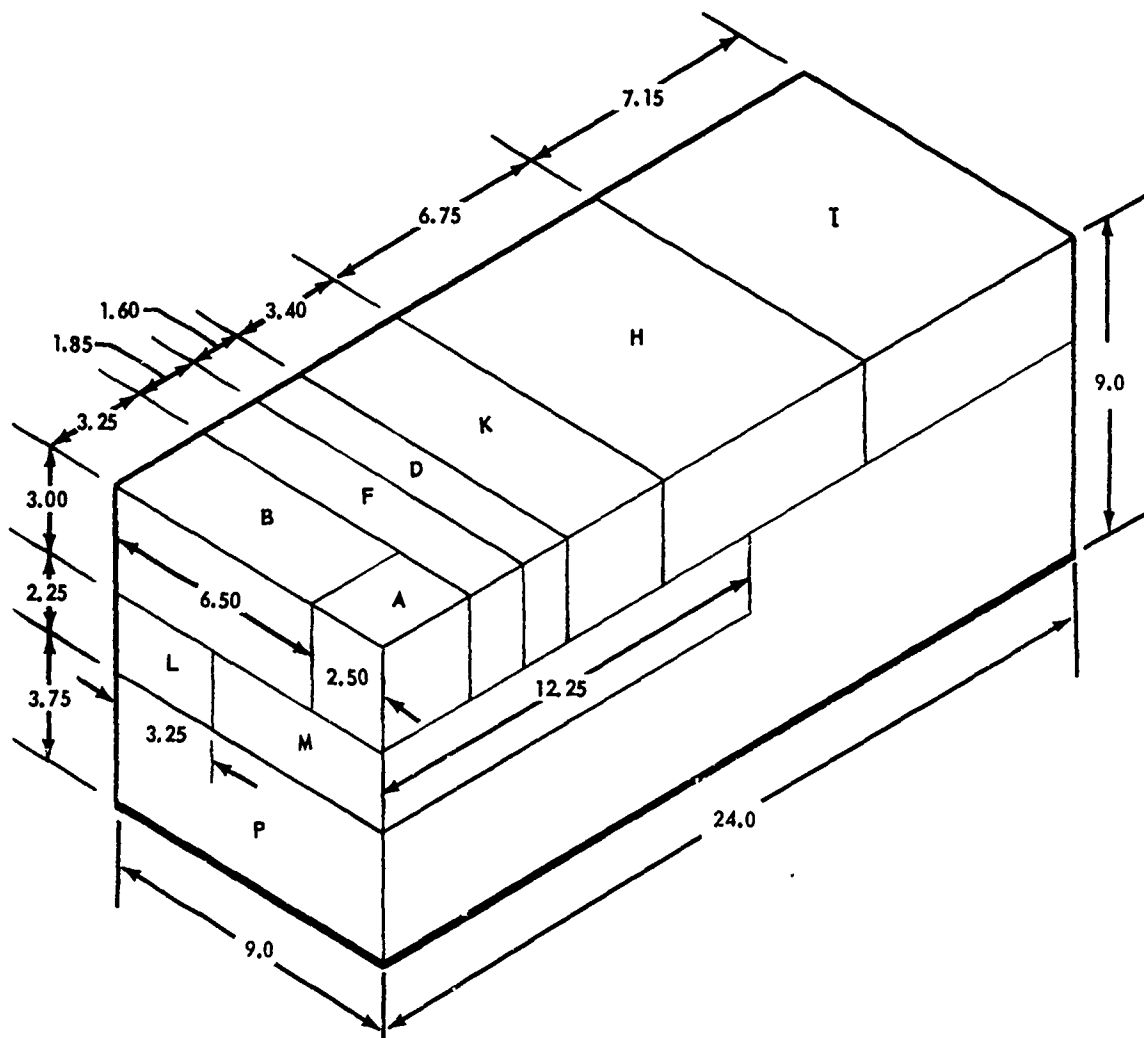
This material was consumable electrode vacuum melted using a 16-inch electrode. The first melt resulted in a 24-inch diameter ingot and the second resulted in a 30-inch ingot. The ingot was forged to a 12-inch round cornered square (R.C.S.) and reformed to a 9-inch R.C.S. reconditioned again and finally reformed to the 3 x 9-inch size. Heat treatment at time of delivery was an anneal at 1300°F for 1 hour and air cooled.

Ti 6Al-6V-2Sn

This material was consumable electrode vacuum melted using a 12-inch electrode. The first melt resulted in an 18-inch diameter ingot and the second resulted in a 24-inch diameter ingot. This was forged to a 12-inch R.C.S., conditioned and reformed to a 9-inch R.C.S., conditioned and final forged to the 3 x 9-inch size. Heat treatment at time of delivery was an anneal at 1300°F for one hour and air cooled.

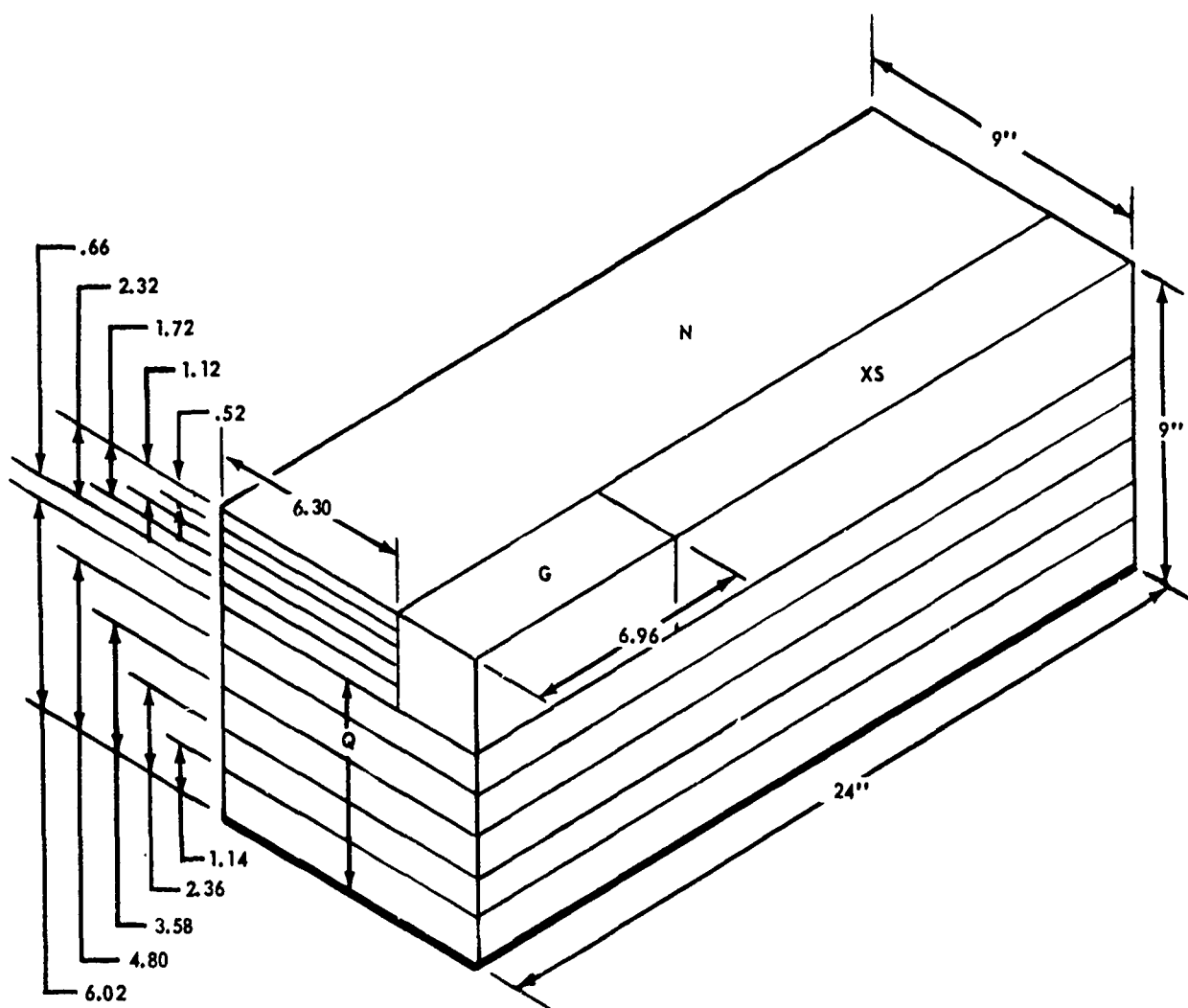
PH 13-8Mo

This steel was vacuum induction melted and cast into a 12-inch diameter electrode which was consumable electrode vacuum melted to a 16-inch diameter ingot. The ingot was then forged to the final 9 x 9-inch size.



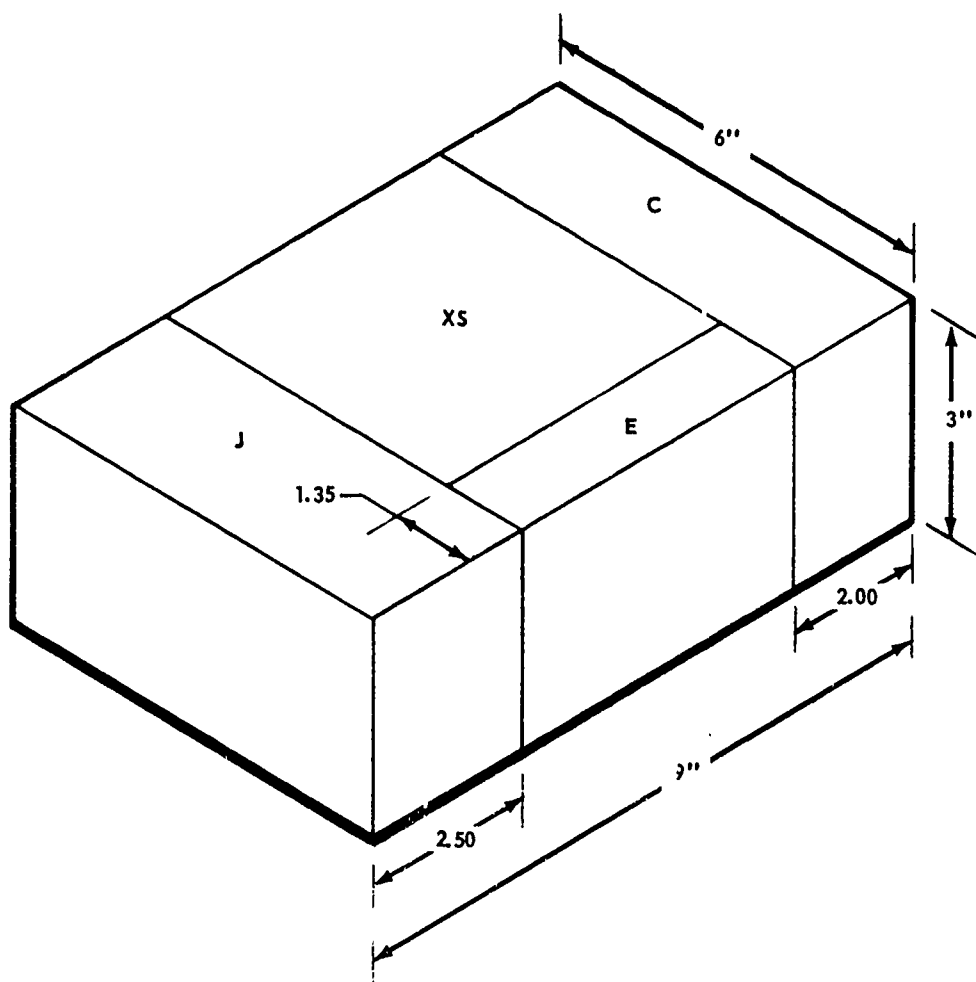
SUB BLOCK	NUMBER AND TYPE OF SPECIMENS
A	10 LONGITUDINAL GRAIN ROUND SMOOTH TENSILES
B	30 TRANSVERSE GRAIN ROUND SMOOTH TENSILES
D	38 TRANSVERSE GRAIN CHARPY SPECIMENS
F	8 TRANSVERSE GRAIN LONG CHARPY SPECIMENS
H	22 TRANSVERSE GRAIN 1-1/8 INCH DIAMETER ROUND NOTCH TENSILES
I	20 TRANSVERSE GRAIN 1-1/8 INCH DIAMETER ROUND NOTCH TENSILES
K	5 TRANSVERSE GRAIN PANEL 3/16 X 3 X 9
L	5 LONGITUDINAL GRAIN PANEL 3/16 X 3 X 9
M	5 LONGITUDINAL GRAIN PANEL 3/16 X 5 X 12
P	3 LONGITUDINAL GRAIN 2-3/4 INCH DIAMETER ROUND NOTCH TENSILES
P	3 TRANSVERSE GRAIN 2-3/4 INCH DIAMETER ROUND NOTCH TENSILES

FIG. 8 TYPICAL SUB-BLOCK LAYOUT OF FIRST 9 X 9 BILLET FOR STEEL AND NICKEL ALLOYS



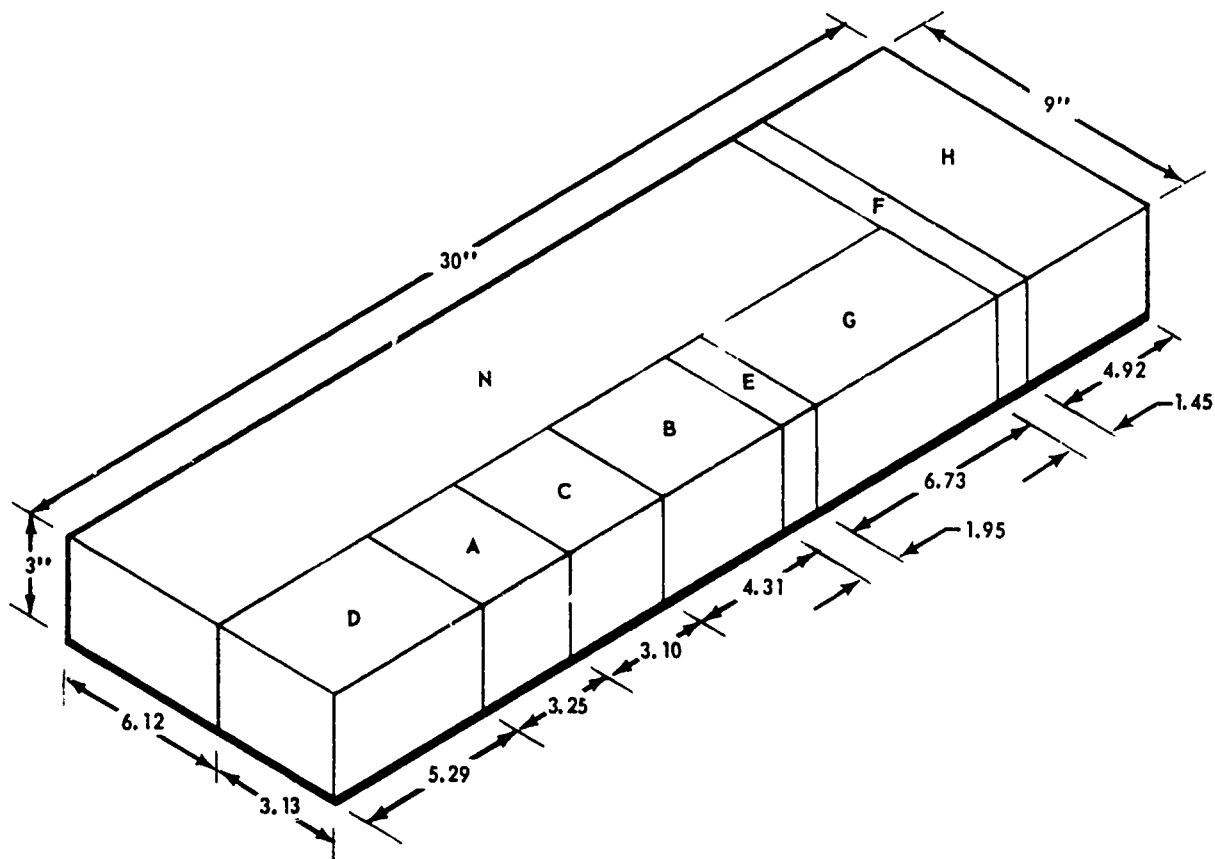
SUB BLOCK	NUMBER AND TYPE OF SPECIMENS
G	8 LONGITUDINAL GRAIN 1-1/8 INCH DIAMETER ROUND NOTCH TENSILES
N	5 LONGITUDINAL GRAIN PANEL 3/8 X 6 X 24
Q	5 LONGITUDINAL GRAIN PANEL 1 X 9 X 24

FIG. 9 TYPICAL SUB-BLOCK LAYOUT OF SECOND 9 X 9 BILLET FOR STEEL AND NICKEL ALLOYS



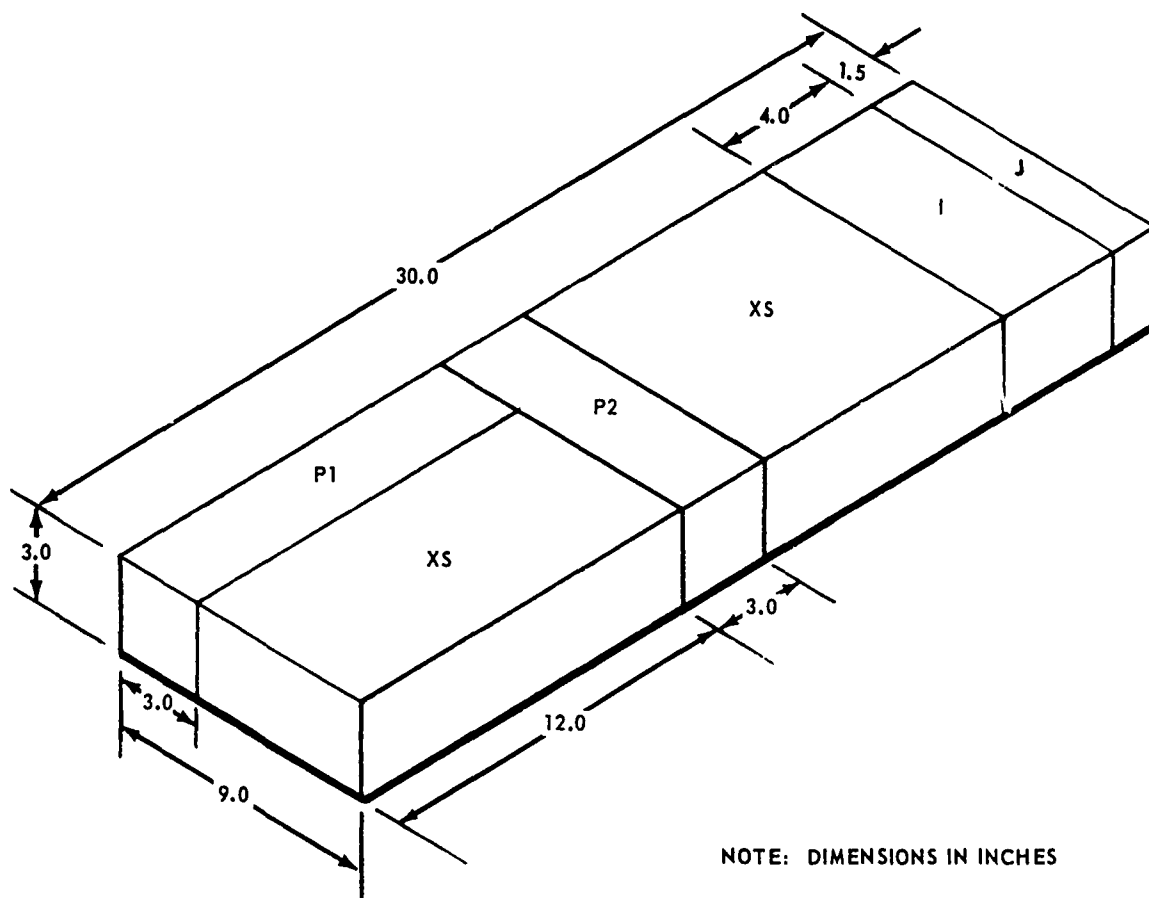
SUB BLOCK	NUMBER AND TYPE OF SPECIMENS
C	24 SHORT TRANSVERSE GRAIN ROUND SMOOTH TENSILES
E	16 SHORT TRANSVERSE GRAIN CHARPY SPECIMENS
J	8 SHORT TRANSVERSE GRAIN 1-1/8 INCH DIAMETER ROUND NOTCH TENSILES

FIG. 10 TYPICAL SUB-BLOCK LAYOUT OF FORGED DOWN BILLET FOR STEEL ALLOYS



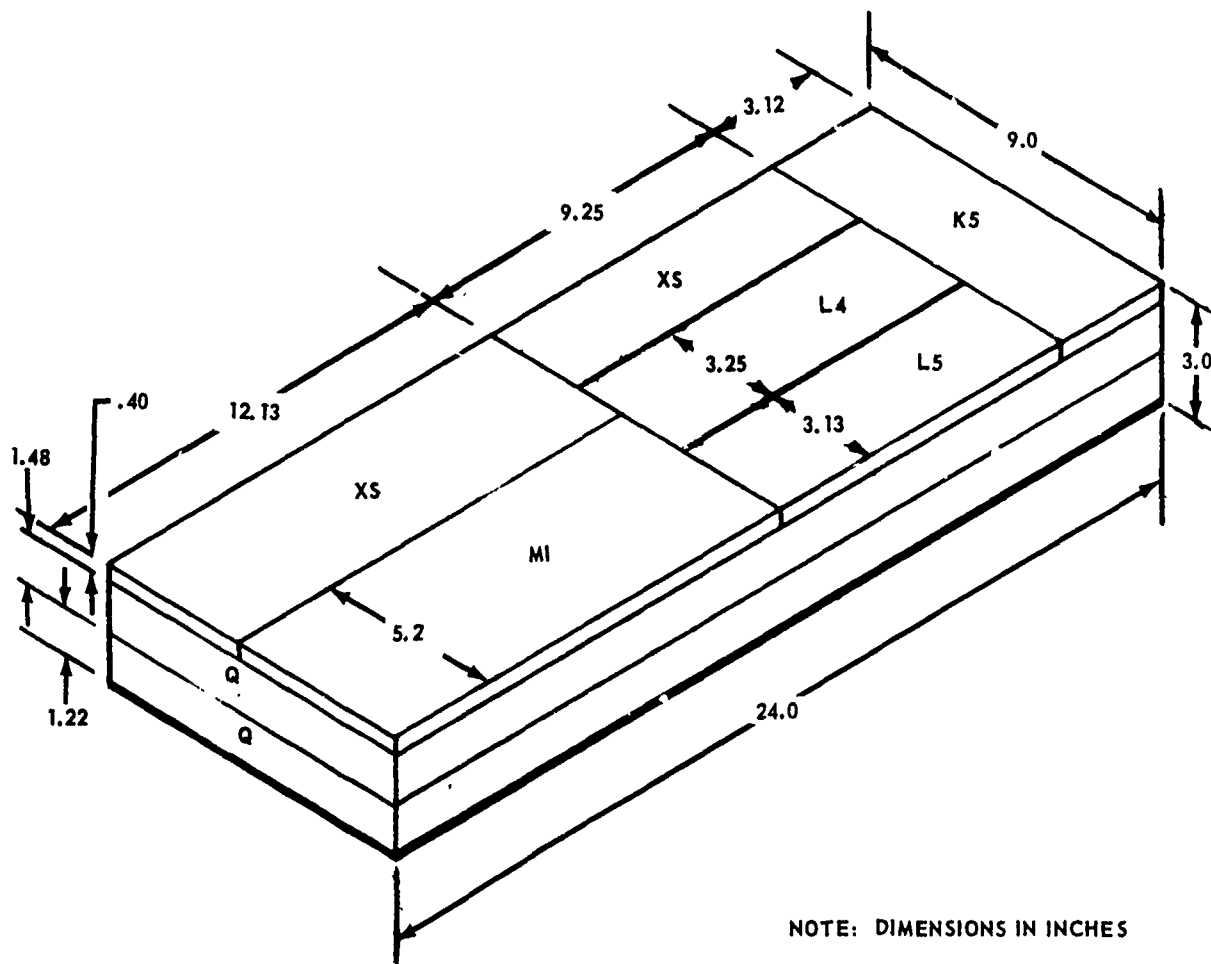
SUB BLOCK	NUMBER AND TYPE OF SPECIMENS
A	10 LONGITUDINAL GRAIN ROUND SMOOTH TENSILES
B	30 TRANSVERSE GRAIN ROUND SMOOTH TENSILES
C	24 SHORT TRANSVERSE GRAIN ROUND SMOOTH TENSILES
D	38 TRANSVERSE CHARPY SPECIMENS
E	16 SHORT TRANSVERSE GRAIN CHARPY SPECIMENS
F	8 TRANSVERSE GRAIN LONG CHARPY SPECIMENS
G	8 LONGITUDINAL GRAIN 1-1/8 INCH DIAMETER ROUND NOTCH TENSILE
H	22 TRANSVERSE GRAIN 1-1/8 INCH DIAMETER ROUND NOTCH TENSILE
N	5 LONGITUDINAL GRAIN PANEL 3/8 X 6 X 24

FIG. 11 TYPICAL SUB-BLOCK LAYOUT OF FIRST BILLET FOR TITANIUM ALLOYS



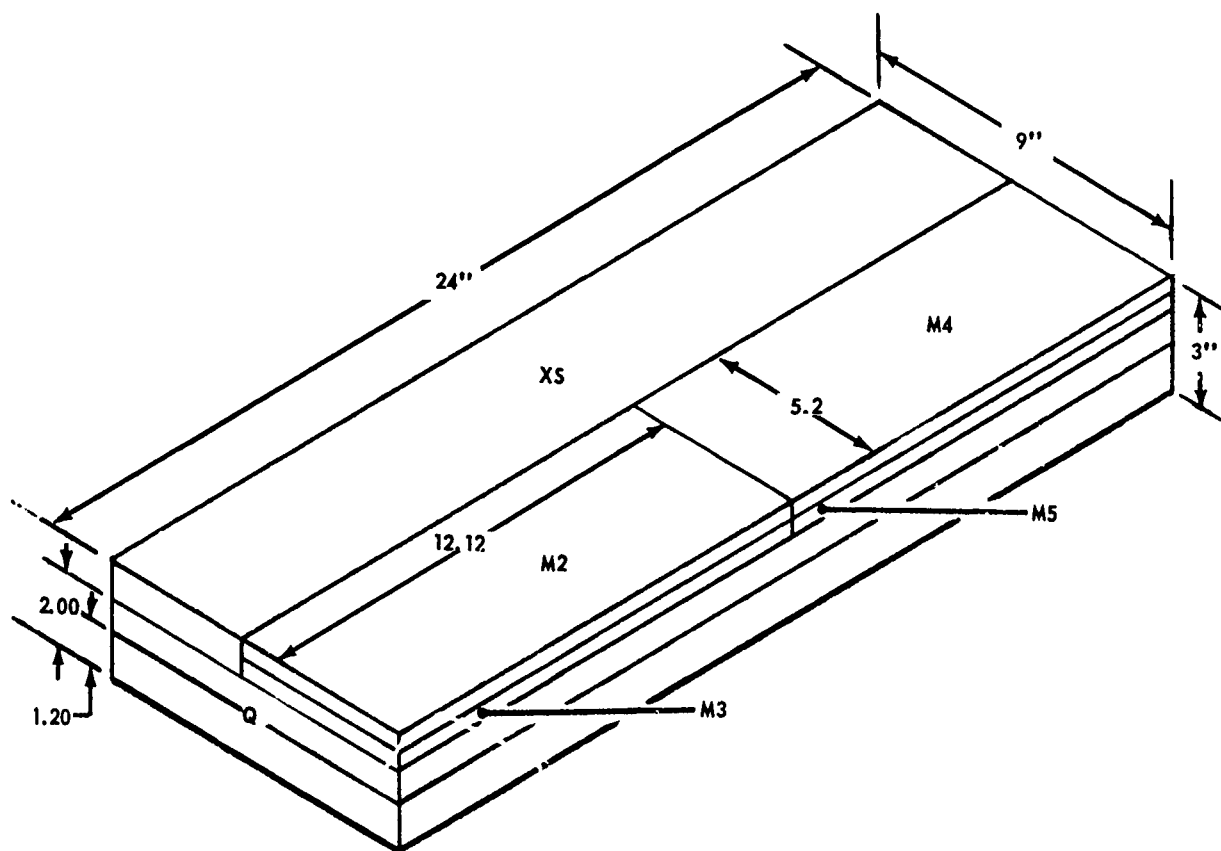
SUB BLOCK	NUMBER AND TYPE OF SPECIMENS
I	20 TRANSVERSE GRAIN 1-1/8 INCH DIAMETER ROUND NOTCH TENSILES
J	8 SHORT TRANSVERSE GRAIN 1-1/8 INCH DIAMETER ROUND NOTCH TENSILES
P1	1 LONGITUDINAL GRAIN 2-3/4 DIAMETER ROUND NOTCH TENSILES
P2	1 TRANSVERSE GRAIN 2-3/4 DIAMETER ROUND NOTCH TENSILES

FIG. 12 TYPICAL SUB-BLOCK LAYOUT OF SECOND BILLET FOR TITANIUM ALLOYS



SUB BLOCK	NUMBER AND TYPE OF SPECIMENS
K	5 TRANSVERSE GRAIN PANELS 3/16 X 3 X 9
L	2 LONGITUDINAL GRAIN PANELS 3/16 X 3 X 9
Q	2 LONGITUDINAL GRAIN PANELS 1 X 9 X 24
M	1 LONGITUDINAL GRAIN PANEL 3/16 X 5 X 12

FIG. 13 TYPICAL SUB-BLOCK LAYOUT OF THIRD BILLET FOR TITANIUM ALLOYS



SUB BLOCK	NUMBER AND TYPE OF SPECIMENS
M	4 LONGITUDINAL PANEL 3/16 x 5 x 13
Q	2 LONGITUDINAL GRAIN PANEL 1 x 9 x 24

FIG. 14 TYPICAL SUB-BLOCK LAYOUT OF FOURTH BILLET FOR TITANIUM ALLOYS

SECTION 6 HEAT TREAT STUDY

TEST PROCEDURE

- 1) Charpy specimens were tested only in the transverse direction, which was considered more sensitive to fracture property changes and the most discriminating in choosing the optimum heat treatment. Specimens were also fabricated from the short transverse directions of the forged-down 3 x 9 inch blocks since this was the grain direction of greatest interest from these blocks. These specimens were then compared with the transverse direction in the 9 x 9-inch blocks to determine the effect of added forging reduction. Specimens were rough machined leaving approximately 0.030 inch on each dimension, then heat treated and final machined.

Finished Charpy impact specimens of standard dimensions as shown in Fig. 15 were fatigued in a Manlabs Fatigue Precracking Machine to form a crack at the root of the machined notch. This machine applies simple beam bending loads to the specimen at 1800 cpm and shuts off automatically as deflection increases with initiation of the crack. Uniform cracks approximately 0.020 inch deep were grown by this method. Impact testing was then accomplished in a Wiedeman-Baldwin Impact Tester on the 240 ft-lb scale at 17 fps. One scale was used for all alloys in an attempt to obtain more reproducible data. Specimens not tested at room temperature were held for at least 15 minutes at temperature in a furnace before testing to ensure reaching the desired temperature.

After reaching temperature the specimens were rapidly transferred to the impact tester and fractured. The area remaining after fatigue cracking was readily visible and measured under a low power microscope. Toughness values were then calculated as energy to fracture in inch-pounds divided by the area fractured during impact.

- 2) Tensile specimens used in the heat treat study are shown in Fig. 16. The size was dictated by the dimensions of the short transverse direction of the forged down blocks. Specimens were tested in a Wiedeman-Baldwin 20-kip universal testing machine at a strain rate of 0.005 in/in/sec up to the yield strength and at 0.020 in/in/sec to failure.

A clamshell furnace with quartz radiant heating lamps was used for the high-temperature testing. A cold box using nitrogen gas released from a liquid nitrogen tank was used for the -110° F testing. Three thermocouples were attached to each specimen during testing to ensure uniform temperature control. Temperatures recorded by each thermocouple, were within $\pm 5^\circ\text{F}$ of the desired test temperature before testing proceeded. Specimens were held at temperature for at least 15 minutes before testing. Load-strain curves to failure were obtained for each specimen.

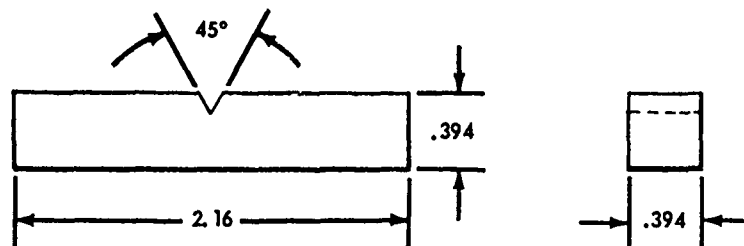


FIG. 15 PRECRACKED CHARPY SPECIMEN

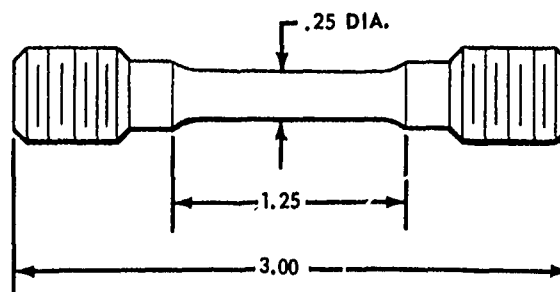


FIG. 16 SMOOTH TENSILE SPECIMEN

EXPERIMENTAL RESULTS

Heat treat steps for the nine heat treat investigations are listed with the resulting Charpy and tensile data in Tables 2 through 10. Heat treatments were based on data obtained from the vendors and from a review of the literature. Where valid fracture toughness data was available it was usually given for a single standard condition. Therefore, the heat treatments selected for study were generally based on impact studies because they were more plentiful in the literature.

Optimum heat treatments are indicated for each alloy where the best combination of strength and fracture toughness resulted. Selection of the optimum heat treatment was made by referring to the plots of variation of precracked Charpy toughness and ultimate strength with temperature shown in Figs. 17 through 25. In most instances selection was determined by toughness for one heat treatment being considerably better than the others. Where the toughness did not vary appreciably the resulting heat treatment in the highest strength was chosen.

Metallographic studies were made with optical and electron microscopes of all heat treat conditions. Photomicrographs of the optimum heat treatment for each alloy are shown in Figs. 26 through 34.

DISCUSSION

Heat treat results of each individual alloy in the program are as follows:

4340

The requirement for metallurgical stability after 1000 hours exposure to 650° F dictated a tempering temperature of at least 800° F. Strengths below 200 ksi were considered to be too low to be of interest and not comparable in strength to the other steel alloys. These considerations led to the selection of the 800° F tempering temperature.

The standard oil quench and double temper was picked as the first trial heat treatment. Previous work (Ref. 20) has shown that an increase in impact toughness was attained by including a sub-cool to -110° F between the tempering cycles. Other data (Ref. 21) has shown increases in toughness by martempering at 375° F. It was thought probable that the increased toughness was due to the reduction in residual microstresses. Therefore, these variations were included in the trial heat treatments. Tensile and fracture data for the martempering treatment A, the sub-cooling treatment B, and the normal quench and temper C are shown in Fig. 17. Of the three, the martempering process resulted in the highest strength and precracked Charpy toughness.

Optical and electron photomicrographs of the 4340 with the optimum heat treatment are shown in Fig. 26. The extremely fine martensitic platelets are readily observable at 5000X in the electron micrographs. The microstructure also contains spheroidal and plate-like carbides of the M_3C type typical of 4340 tempered at 800° F (Ref. 22).

TABLE 2 HEAT TREATMENTS AND RESULTING MECHANICAL PROPERTIES FOR 4340


HEAT * TREAT	GRAIN	TEST TEMP °F	ULTIMATE STRENGTH psi	.2% YIELD STRENGTH psi	ELONG 1 inch percent	RA percent	PRECRACKED CHARPY W/A (in/lbs in ²)
(OPTIMUM)							
A	T	-100	228,200	212,800	10	29	210
A	T	-100	231,600	215,000	9	29	152
A	T	RT	217,600	202,200	9	36	734
A	T	RT	216,600	202,200	9	36	888
A 	T	400	215,200	183,700	12	39	997
A	T	400	217,100	187,400	11	37	1147
A	T	650	188,400	154,900	15	50	1180
A	T	650	189,700	155,500	15	54	1252
A	ST	-100	234,400	217,600	9	25	158
A	ST	-100	228,100	212,400	9	25	157
A	ST	RT	210,800	196,600	6	14	-
A	ST	RT	212,000	197,200	7	25	-
A	ST	400	215,500	184,400	6	16	
A	ST	400	215,100	184,300	6	15	
A	ST	650	189,200	157,900	13	39	918
A	ST	650	188,400	155,600	14	44	895
A	L	-110	248,000	231,600	12	47	
A	L	-110	240,800	227,100	14	50	
A	L	RT	226,400	214,100	13	52	
A	L	RT	224,800	212,100	12	52	
A	L	400	215,300	183,100	15	53	
A	L	400	217,400	186,200	15	56	
A	L	650	190,900	159,500	5	12	
A	L	650	193,400	165,200	18	68	
B	T	-100	224,100	209,400	9	28	204
B	T	-100	225,700		10	32	154
B	T	RT	209,700	194,200	8	36	824
B	T	RT	212,200	196,300	9	35	833
B	T	650	184,700	152,200	16	53	1430
B	T	650	183,100	150,700	17	57	1556
B	ST	-100	227,100	211,700	6	19	155
B	ST	-100	222,800	209,700	7	21	158
B	ST	RT	219,000	201,800	8	20	-
B	ST	RT	214,100	199,100	7	25	-
B	ST	650	177,800	152,400	12	38	1041
B	ST	650	177,900	161,100	10	25	1093

TABLE 2 HEAT TREATMENTS AND RESULTING MECHANICAL PROPERTIES FOR 4340
(continued)

HEAT * TREAT	GRAIN	TEST TEMP °F	ULTIMATE STRENGTH psi	.2% YIELD STRENGTH psi	ELONG 1 inch percent	RA percent	PRECRACKED CHARPY W A (in lbs in ²)
C	T	-100	223,300	208,500	10	31	185
C	T	-100	224,200	207,800	9	27	210
C	T	RT	211,400	195,400	9	36	839
C	T	RT	210,700	195,000	9	36	928
C	T	650	182,800	149,600	16	60	1149
C	T	650	182,400	151,700	16	56	1150
C	ST	-100	225,500	212,100	7	18	197
C	ST	-100	226,200	212,500	4	10	208
C	ST	RT	212,300	197,900	8	19	-
C	ST	RT	211,800	197,900	6	19	-
C	ST	650	186,800	153,200	14	44	-
C	ST	650	186,500	154,000	13	40	1048

*HEAT TREATMENTS

- A. (1) Cycle annealed at 1625°F for 45 minutes and air cool, then heat to 1250°F for 90 minutes and air cool.
- (2) Austenitize at 1525°F for 45 minutes and quench in salt to 375°F. Hold until part reaches bath temperature then air cool to below 160°F.
- (3) Temper at 800°F for 1-1/2 hours.
- (4) Temper at 800°F for 1-1/2 hours.
- B. (1) Cycle anneal at 1625°F for 45 minutes and air cool. Reheat to 1250°F for 90 minutes and air cool.
- (2) Austenitize at 1525°F for 45 minutes and oil quench.
- (3) Temper at 800°F for 90 minutes.
- (4) Subcool to -110°F for 2 hours.
- (5) Temper at 800°F for 90 minutes.
- C. (1) Cycle anneal at 1625°F for 45 minutes and air cool, then reheat-treat to 1250°F for 90 minutes and air cool.
- (2) Austenitize at 1525°F for 45 minutes and oil quench.
- (3) Temper at 800°F for 90 minutes and air cool.
- (4) Temper at 800°F for 90 minutes and air cool.

TABLE 3 HEAT TREATMENTS AND RESULTING MECHANICAL PROPERTIES FOR 9Ni-4Co

HEAT * TREAT	GRAIN	TEST TEMP °F	ULTIMATE STRENGTH psi	.2% YIELD STRENGTH psi	ELONG 1 inch percent	RA percent	PRECRACKED CHARPY W. A (in/lbs in ²)
(OPTIMUM)							
A	T	-100	227,800	220,800	14	57	863
A	T	-100	226,900	220,400	14	53	835
A	T	RT	213,000	205,100	14	55	2336
A	T	RT	212,600	204,300	14	57	2210
A	T	400	192,900	163,900	24	75	3059
A	T	400	196,900	166,300	22	70	3032
A	T	650	171,100	150,500	22	80	2869
A	T	650	173,100	148,400	21	79	2855
A	L	-110	218,800	209,400	16	58	
A	L	-110	224,300	213,100	15	60	
A	L	RT	208,200	200,600	15	63	
A	L	RT	203,700	196,200	15	61	
A	L	400	202,000	173,400	18	64	
A	L	400	195,800	164,900	22	71	
A	L	650	151,900	133,400	21	79	
A	L	650	149,800	129,300	21	80	
B	T	-100	203,200	190,300	16	57	1655
B	T	-100	203,700	190,400	16	59	1684
B	T	RT	190,300	178,400	15	58	3630
B	T	RT	189,000	177,300	17	59	3780
B	T	650	157,900	135,200	23	80	4695
B	T	650	156,500	133,900	22	81	4789
C	T	-100	222,100	206,300	14	48	916
C	T	-100	222,200	205,700	14	52	983
C	T	RT	206,600	190,000	14	57	1769
C	T	RT	206,600	191,100	14	58	1780
C	T	650	165,100	139,300	23	78	2948
C	T	650	167,300	139,800	23	79	3055

*HEAT TREATMENTS

- A. (1) Normalize at 1600°F for 1 hour and air cool.
 (2) Austenitize at 1450°F for 30 minutes and quench in salt at 450°F and hold for 6 hours, then air cool.
 (3) Temper at 700°F for 1 hour.
 (4) Temper at 700°F for 1 hour.
- B. (1) Normalize at 1600°F for 1 hour and air cool.
 (2) Austenitize at 1450°F for 30 minutes, and quench into salt at 550°F and hold for 6 hours, then air cool.
 (3) Temper at 700°F for 1 hour.
 (4) Temper at 700°F for 1 hour.
- C. (1) Normalize at 1650°F for 1 hour and air cool.
 (2) Austenitize at 1450°F for 30 minutes, and oil quench to below 120°F.
 (3) Subcool to -110°F for 2 hours.
 (4) Temper at 750°F for 1 hour and air cool.
 (5) Temper at 750°F for 1 hour and air cool.

TABLE 4 HEAT TREATMENTS AND RESULTING MECHANICAL PROPERTIES
FOR AM 355

HEAT * TREAT	GRAIN	TEST TEMP °F	ULTIMATE STRENGTH psi	.2% YIELD STRENGTH psi	ELONG 1 inch percent	RA percent	PRECRACKED CHARPY W/A (in 'lbs in ²)
A	T	-100	217,600	199,500	2	.2	105
A	T	-100	218,400		2	2	107
A	T	RT	218,000	175,300	8	18	222
A	T	RT	217,400	174,200	10	20	203
A	T	650	198,700		8	19	811
A	T	650	198,300	134,700	8	19	649
A	ST	-100	211,500	205,700			155
A	ST	-100	208,800	204,300			105
A	ST	RT	220,900	179,900	5	6	
A	ST	RT	222,000	179,300	3	3	
A	ST	650	201,000	140,600	4	11	956
A	ST	650	202,100	143,200	7	22	1128
B	T	-100	238,100	209,800	3	2	159
B	T	-100	236,200	205,900	2	2	159
B	T	RT	226,800	192,900	11	22	318
B	T	RT	229,400	183,900	15	30	316
B	T	650	207,100	145,800	8	23	842
B	T	650	207,600	142,300	8	23	873
B	ST	-100	207,300		1	.2	158
B	ST	-100	215,500		1	.2	162
B	ST	RT	226,800	185,200	5	1.5	
B	ST	RT	224,600	186,000	5	3	
B	ST	650	205,100	142,000	7	17	947
B	ST	650	206,700	143,600	7	18	1231
C	T	-100	273,300	127,300	18	29	218
C	T	-100	270,000	199,100	18	31	261
C	T	RT	225,400	159,300	20	43	750
C	T	RT	228,600	170,700	20	42	655
C	T	650	206,100	134,500	10	26	1211
C	T	650	206,400	143,100	8	14	1327
C	ST	-100	230,200	201,600	1	2	207
C	ST	-100	228,500	200,800	1	1	256
C	ST	RT	225,000	179,500	3	1.5	
C	ST	RT	226,700	173,600	7	7	
C	ST	650	204,300	128,200	9	17	1409
C	ST	650	204,500	137,600	6	14	1421

TABLE 4 HEAT TREATMENTS AND RESULTING MECHANICAL PROPERTIES
FOR AM 355 (continued)

HEAT * TREAT	GRAIN	TEST TEMP °F	ULTIMATE STRENGTH psi	.2% YIELD STRENGTH psi	ELONG 1 inch percent	RA percent	PRECRACKED CHARPY W/A (in lbs in ²)
D	T	-110	240,500	208,800	7	9	159
D	T	-110	249,900	214,100			161
D	T	RT	221,400	176,700	13	34	436
D	T	RT	219,900	173,800	12	29	389
D	T	650	200,400	134,700	11	28	1009
D	T	650	200,000	134,500	10	24	1111
D	ST	-110	228,600	202,700	1	0	159
D	ST	-110	222,200		1	1	161
D	ST	RT	217,800	173,300	8	16	
D	ST	RT	217,600	174,400	4	9	
D	ST	650	206,400	154,300	8	14	673
D	ST	650	201,600	140,200	8	4	811
(OPTIMUM)							
E	T	-110	253,700	186,000	16	19	204
E	T	-110	250,300	173,100			198
E	T	RT	210,500	162,100	18	39	637
E	T	RT	211,200	160,000	17	38	541
E	T	400	193,000	133,700	11	37	1221
E	T	400	194,200	152,600	12	37	972
E	T	650	185,800	110,400	9	19	1565
E	T	650	185,800	142,400	9	12	1745
E	ST	-110	249,200	186,100	12		207
E	ST	-110	234,500	181,600	7		209
E	ST	RT	211,400	153,700	18	28	
E	ST	RT	210,800	153,600	16	22	
E	ST	400	193,800	146,300	11	33	
E	ST	400	193,400	138,800	12	29	
E	ST	650	185,200	135,700	11	21	2015
E	ST	650	183,000	134,300	10	28	1746
E	L	-110	250,200	202,800	24	56	
E	L	-110	250,200	203,600	23	55	
E	L	RT	217,100	164,000	20	58	

TABLE 4 HEAT TREATMENTS AND RESULTING MECHANICAL PROPERTIES
FOR AM 355 (continued)

HEAT * TREAT	GRAIN	TEST TEMP °F	ULTIMATE STRENGTH psi	.2% YIELD STRENGTH psi	ELONG 1 inch percent	RA percent	PRECRACKED CHARPY W/A (in/lbs in ²)
E	L	RT	217,300	169,400	22	58	
E	L	400	196,500	148,600	17	58	
E	L	400	194,600	139,500	16	57	
E	L	650	195,000	148,200	9	27	
E	L	650	195,300	148,100	10	28	

*HEAT TREATMENTS

- A. (1) Solution anneal at 1925° F for 30 min. and oil quench.
(2) Condition anneal at 1710° F for 30 min. and oil quench.
(3) Subcool (within 1 hour after quenching) to -110° F for 3 hours.
(4) Temper at 850° F for 3 hours and air cool.
- B. (1) Solution anneal to 1925° F for 30 min. and oil quench.
(2) Subcool (within 1 hour after quenching) to -110° F for 3 hours.
(3) Condition anneal at 1800° F for 30 min. and oil quench.
(4) Subcool (within 1 hour after quenching) to -110° F for 3 hours.
(5) Temper at 850° F for 3 hours and air cool.
- C. (1) Solution anneal at 1500° F for 3 hours, transfer to 1925° F for 20 min. without cooling below 800° F, oil quench.
(2) Subcool (within 20 min. after quench) to -110° F for 3 hours.
(3) Temper at 850° F for 2 hours and oil quench.
(4) Subcool (within 20 min. after quench) to -110° F for 3 hours.
(5) Temper at 850° F for 1 hour and air cool.
- D. MODIFIED EQUALIZED AND OVERAGED TREATMENT
 - (1) Anneal at 1550° F for 30 min., oil quench to room temperature.
 - (2) Subcool to -100° F for 1 hour.
 - (3) Reanneal at 1550° F for 10 hours air cool.

HARDENING TREATMENT

- (1) Carbide solution anneal at 1890° F for 45 min., oil quench.
- (2) Subcool to -100° F for 3 hours within 20 min. of quenching.
- (3) Condition temper at 850° F for 2 hours oil quench.
- (4) Subcool to -100° F for 3 hours within 20 min. of quenching.
- (5) Temper at 850° F for 1 hour, air cool.

E. MODIFIED EQUALIZED AND OVERAGED TREATMENT

- (1) Solution anneal at 1850° F for 45 min., oil quench.
- (2) Subcool to -100° F for 1 hour.
- (3) Over-temper at 1075° F for 3 hours, air cool.

HARDENING TREATMENT

- (1) Carbide solution anneal at 1925° F for 30 min., oil quench.
- (2) Subcool to -100° F for 3 hours within 20 min.
- (3) Condition temper at 850° F for 2 hours, oil quench.
- (4) Subcool to -100° F for 3 hours within 20 min.
- (5) Temper at 850° F for 1 hour, air cool.

TABLE 5 HEAT TREATMENTS AND RESULTING MECHANICAL PROPERTIES
FOR MARAGING 250

HEAT * TREAT	GRAIN	TEST TEMP °F	ULTIMATE STRENGTH psi	.2% YIELD STRENGTH psi	ELONG 1 inch percent	RA percent	PRECRACKED CHARPY W/A (in/lbs in ²)
A	T	-100	269,700	252,000	8	29	211
A	T	-100	271,900	237,800	10	39	212
A	T	RT	240,700	220,600	10	39	427
A	T	RT	236,900	213,800	10	38	319
A	T	650	209,700	189,400	3	9	720
A	T	650	207,700	195,700	3	9	664
A	ST	-100	298,100	257,400	6	28	270
A	ST	-100	285,000	262,300	8	34	233
A	ST	RT	258,200	238,000	9	38	-
A	ST	RT	253,200	231,100	8	41	-
A	ST	650	218,400	202,500	8	34	857
A	ST	650	219,700	207,100	7	34	818
B	T	-100	270,800	258,100	9	37	270
B	T	-100	279,300	271,100	10		234
B	T	RT	254,600	242,200	9	44	329
B	T	RT	253,600	240,400	10	46	362
B	T	650	206,900	194,000	3	13	895
B	T	650	206,500	194,600	3	15	842
B	ST	-100	305,600	285,800	7		421
B	ST	-100	298,900	286,200	8	37	429
B	ST	RT	260,600		8		-
B	ST	RT	258,700		10		-
B	ST	650	222,800	207,900	8	40	947
B	ST	650	203,200	202,400	1	12	956
C	T	-100	285,700	273,000	8	40	308
C	T	-100	306,900	284,100	8		305
C	T	RT	256,700	242,600	8	42	440
C	T	RT	257,200	241,700	9	38	474
C	T	650	220,700	205,300	1	8	804
C	T	650	221,200	211,600	4	16	658
C	ST	-100	303,000	283,600	8	42	456
C	ST	-100	315,100	294,800	8	36	449
C	ST	RT	265,200		7	34	-
C	ST	RT	272,000		10	41	-

TABLE 5 HEAT TREATMENTS AND RESULTING MECHANICAL PROPERTIES
FOR MARAGING 250 (continued)

HEAT * TREAT	GRAIN	TEST TEMP °F	ULTIMATE STRENGTH psi	.2% YIELD STRENGTH psi	ELONG 1 inch percent	RA percent	PRECRACKED CHARPY W. A (in lbs in ²)
C	ST	650	221,600	220,200	6	22	903
C	ST	650	226,300	221,000	10	41	850
D	T	-100	292,100	274,700	7	33	307
D	T	-100	288,300	279,100	7	33	287
D	T	RT	258,400	246,200	8	37	473
D	T	RT	258,000	244,600	10	45	417
D	T	650	220,000	207,200	3	5	638
D	T	650	222,600	209,900	3	7	647
D	ST	-100	307,800	297,000	8	36	359
D	ST	-100	295,800		8	40	314
D	ST	RT	264,600	253,000	8	40	
D	ST	RT	266,500	258,700	8	38	
D	ST	650	211,600		3	10	936
D	ST	650	220,100	206,500	3	11	956
(OPTIMUM)							
E	T	-110	254,000	233,400	13	39	316
E	T	-110	253,600	232,300	12	41	324
E	T	RT	230,500	216,000	14	49	750
E	T	RT	231,500	217,300	13	47	726
E	T	400	204,400	192,300	11	47	1042
E	T	400	204,900	187,200	13	49	1043
E	T	650	197,500		8	28	1582
E	T	650	197,900	187,000	7	15	1458
E	ST	-110	250,400	231,100	10	31	340
E	ST	-110	251,000	233,900	11	35	358
E	ST	RT	231,500	217,600	11	36	
E	ST	RT	231,800	218,900	12	40	
E	ST	400	211,400	199,100	12	45	
E	ST	400	209,400	197,200	13	45	
E	ST	650	199,600	187,200	11	42	1256
E	ST	650	199,500	188,500	7	18	1274
E	L	-110	246,400	230,100	13	51	
E	L	-110	247,400	230,900	13	50	
E	L	RT	226,000	211,800	14	55	
E	L	RT	226,200	212,900	14	56	

TABLE 5 HEAT TREATMENTS AND RESULTING MECHANICAL PROPERTIES
FOR MARAGING 250 (continued)

HEAT * TREAT	GRAIN	TEST TEMP °F	ULTIMATE STRENGTH psi	.2% YIELD STRENGTH psi	ELONG 1 inch percent	RA percent	PRECRACKED CHARPY W/A (in·lbs in ²)
E	L	400	198,700	185,200	13	57	
E	L	400	196,300	182,600	15	58	
E	L	650	168,700	150,200	18	68	
E	L	650	172,400	156,100	11	38	

*HEAT TREATMENTS

- A. (1) Solution anneal at 1500°F for 1 hour and air cool.
(2) Age at 850°F for 6 hours and air cool.
- B. (1) Solution anneal at 1500°F for 1 hour and air cool.
(2) Age at 900°F for 3 hours and air cool.
- C. (1) Solution anneal at 1500°F for 1 hour and air cool.
(2) Age at 950°F for 3 hours and air cool.
- D. (1) Solution anneal at 1700°F for 30 minutes and air cool.
(2) Age at 950°F for 3 hours and air cool.
- E. (1) Solution anneal at 1700°F for 1 hour and air cool.
(2) Age at 1050°F for 3 hours and air cool.

TABLE 6 HEAT TREATMENTS AND RESULTING MECHANICAL PROPERTIES FOR INCO 718

HEAT * TREAT	GRAIN	TEST TEMP °F	ULTIMATE STRENGTH psi	.2% YIELD STRENGTH psi	ELONG 1 inch percent	RA percent	PRECRACKED CHARPY W/A (in/lbs in ²)
A	T	-110	201,600	157,700	17	22	1947
A	T	-110	205,700	160,400	18	22	1730
A	T	RT	182,200	144,300	15	19	1719
A	T	RT	178,300	143,400	14	15	1768
A	T	650	163,300	133,300	11	19	2230
A	T	650	168,300	133,600	16	21	1979
(OPTIMUM)							
B	T	-110	199,300	166,900	18	24	1831
B	T	-110	190,100	161,500	12	15	1470
B	T	RT	185,700	153,800	19	24	1927
B	T	RT	184,800	155,100	20	31	1742
B	T	400	174,400	143,700	13	22	2131
B	T	400	175,900	146,400	17	26	1709
B	T	650	155,700	136,100	16	23	2534
B	T	650	162,700	138,500	10	15	2756
B	L	-110	209,900	174,500	19	26	
B	L	-110	207,400	169,000	18	23	
B	L	RT	190,500	156,400	20	27	
B	L	RT	193,000	155,500	20	25	
B	L	400	174,800	145,100	19	31	
B	L	400	177,700	147,000	17	25	
B	L	650	177,400	145,000	17	22	
B	L	650	170,600	142,800	19	31	
C	T	-110	184,800	151,800	18	22	1183
C	T	-110	181,800	143,800	22	22	1731
C	T	RT	165,500	138,300	19	23	1617
C	T	RT	162,000	141,400	13	23	1954
C	T	650	147,000	126,600	16	23	2046
C	T	650	149,200	126,300	18	19	1874

*HEAT TREATMENTS

- A. (1) Solution anneal at 1975°F for 1 hour and air cool.
 (2) Age 1450°F for 8 hours and furnace cool 20°F hr. to 1200°F.
- B. (1) Solution anneal at 1975°F for 1 hour and air cool.
 (2) Age 1400°F for 10 hours and furnace cool 20°F hr. to 1200°F.
- C. (1) Solution anneal at 1800°F for 1 hour and air cool.
 (2) Age 1325°F for 8 hours and furnace cool 20°F hr. to 1150°F.

TABLE 7 HEAT TREATMENTS AND RESULTING MECHANICAL PROPERTIES FOR Ti 6Al-4V

HEAT * TREAT	GRAIN	TEST TEMP °F	ULTIMATE STRENGTH psi	.2% YIELD STRENGTH psi	ELONG 1 inch percent	RA percent	PRECRACKED CHARPY W/A (in/lbs in ²)
A	T	-110	199,500	186,600	9	33	144
A	T	-110	198,700	185,000	10	39	165
A	T	RT	172,700	161,700	13	50	
A	T	RT	173,500		13	49	408
A	T	650	122,500	97,500	8	29	1789
A	T	650	123,600	105,200	9	25	2479
A	ST	-110	195,800	184,000	7	31	
A	ST	-110	191,800	181,100	8	39	
A	ST	RT	171,600	158,000	12	48	
A	ST	RT	170,000	156,300	14	55	
A	ST	650	119,500	99,300	13	52	
A	ST	650	122,900	106,100	13	60	
(OPTIMUM)							
B	T	-110	189,300	174,500	10	31	294
B	T	-110	189,400	131,300	12	34	327
B	T	RT	165,100	152,100	14	38	471
B	T	RT	165,600	152,300	14	38	600
B	T	400	129,400	110,400	12	57	1421
B	T	400	130,600	113,000	15	59	1598
B	T	650	116,400	96,700	7	25	2989
B	T	650	120,600	99,100	15	67	2970
B	ST	-110	181,600	170,700	7	36	
B	ST	-110	188,200	181,000	9	36	
B	ST	RT	165,500	152,800	11	36	
B	ST	RT	162,100	150,900	12	36	
B	ST	400	129,300	108,000	13	51	
B	ST	400	130,600	109,100	14	55	
B	ST	650	120,900	97,100	13	57	
B	ST	650	120,900	96,400	13	52	
B	L	-110	188,100	178,000	-	-	
B	L	-110	186,300	174,800	11	39	
B	L	RT	160,200	146,900	13	43	
B	L	RT	160,000	147,300	13	45	
B	L	400	129,100	109,000	16	63	
B	L	400	125,900	107,300	17	62	
B	L	650	116,600	94,200	16	65	
B	L	650	115,200	95,900	16	63	

TABLE 7 HEAT TREATMENTS AND RESULTING MECHANICAL PROPERTIES
FOR Ti 6Al-4V (continued)

HEAT * TREAT	GRAIN	TEST TEMP °F	ULTIMATE STRENGTH psi	.2% YIELD STRENGTH psi	ELONG 1 inch percent	RA percent	PRECRACKED CHARPY W/A (in/lbs/in ²)
C	T	-110	178,500	168,200	10	32	333
C	T	-110	178,100	169,400	10	33	328
C	T	RT	153,400	142,700	14	37	538
C	T	RT	154,500	143,900	14	38	577
C	T	650	106,300	86,900	15	67	3156
C	T	650	110,400	91,300	11	29	3133
C	ST	-110	176,600	164,100	10	35	
C	ST	-110	178,700	166,500	11	39	
C	ST	RT	152,600	143,300	10	32	
C	ST	RT	156,600	143,100	11	33	
C	ST	650	107,700	87,000	16	63	
C	ST	650	98,900	76,300	16	60	

*HEAT TREATMENTS

- A. (1) Solution treat at 1725°F for 1 hour water quench.
(2) Age at 1150°F for 4 hours and air cool.
- B. (1) Solution treat at 1650°F for 1 hour and water quench.
(2) Age 1100°F for 4 hours and air cool.
- C. (1) Solution treat at 1550°F for 1 hour and water quench.
(2) Age at 1100°F for 4 hours and air cool.

TABLE 8 HEAT TREATMENTS AND RESULTING MECHANICAL PROPERTIES FOR
Ti 6Al-6V-2Sn ANN

HEAT * TREAT	GRAIN	TEST TEMP °F	ULTIMATE STRENGTH psi	.2% YIELD STRENGTH psi	ELONG 1 inch percent	RA percent	PRECRACKED CHARPY W/A (in·lbs in ²)
A	T	-110	178,500	168,600	10	29	103
A	T	-110	182,500	172,500	11	36	98
A	T	RT	151,900	145,100	13	42	253
A	T	RT	151,800	145,200	13	43	216
A	T	650	121,100	100,200	18	53	1648
A	T	650	122,200	101,000	12	58	1996
A	ST	-110	177,000	166,600	8	26	
A	ST	-110	174,300	164,900	9	30	
A	ST	RT	148,600	138,600	12	33	
A	ST	RT	149,700	136,500	12	24	
A	ST	650	120,300	95,600	19	45	
A	ST	650	118,600	95,800	9	22	
B	T	-110	189,900	183,500	10	29	108
B	T	-110	184,700	175,800	10	27	112
B	T	RT	158,300		14	36	229
B	T	RT	157,100	148,500	15	35	270
B	T	650	116,400	101,200	11	29	1527
B	T	650	115,200	100,600	14	55	1484
B	ST	-110	177,500	172,300	11	35	
B	ST	-110	181,800	179,400	10	37	
B	ST	RT	157,700	148,900	13	34	
B	ST	RT	157,700	148,200	14	36	
B	ST	650	113,500	101,400	4	13	
B	ST	650	121,800	101,600	12	41	
(OPTIMUM)							
C	T	-110	179,800	175,900	8	28	136
C	T	-110	174,200	163,000	8	32	112
C	T	RT	151,500	142,500	14	39	320
C	T	RT	152,100	142,500	14	32	308
C	T	400	123,200	105,900	16	48	962
C	T	400	119,100	103,200	15	43	1293
C	T	650	116,900	100,800	15	54	2192
C	T	650	112,700	99,700	8	25	1865
C	ST	-110	175,200	169,000	12	36	
C	ST	-110	175,100	169,900	12	35	
C	ST	RT	148,000	139,600	15	44	
C	ST	RT	149,200	137,500	13	48	

TABLE 8 HEAT TREATMENTS AND RESULTING MECHANICAL PROPERTIES FOR
Ti 6Al-6V-2Sn ANN (continued)

HEAT * TREAT	GRAIN	TEST TEMP °F	ULTIMATE STRENGTH psi	.2% YIELD STRENGTH psi	ELONG 1 inch percent	RA percent	PRECRACKED CHARPY W. A (in lbs in ²)
C	ST	400	124,500	107,600	15	47	
C	ST	400	125,200	109,600	14	56	
C	ST	650	114,200	96,700	17	62	
C	ST	650	112,500	97,700	12	29	
C	L	-110	178,300	176,500	13	46	
C	L	-110	178,200	172,000	13	45	
C	L	RT	151,600	145,400	15	52	
C	L	RT	147,400	138,800	16	41	
C	L	400	119,900	103,200	18	56	
C	L	400	122,600	108,200	18	57	
C	L	400	122,300	106,900	18	57	
C	L	650	111,100	91,700	16	57	

*HEAT TREATMENTS

- A. Anneal at 1400°F for 2 hours air cool.
- B. Anneal at 1300°F for 2 hours furnace cool 50°F hour to 1000°F.
- C. Anneal at 1300°F for 2 hours air cool.

TABLE 9 HEAT TREATMENTS AND RESULTING MECHANICAL PROPERTIES
FOR Ti 6Al-6V-2Sn STA

HEAT * TREAT	GRAIN	TEST TEMP °F	ULTIMATE STRENGTH psi	.2% YIELD STRENGTH psi	ELONG 1 inch percent	RA percent	PRECRACKED CHARPY W A (in lbs in ²)
A	T	-110	210,300	200,000	9	31	109
A	T	-110	208,200	203,900	8	14	113
A	T	RT	175,200	167,400	12	43	224
A	T	RT	176,900	170,100	13	42	103
A	T	650					955
A	T	650	122,100	102,400	12	32	1087
A	ST	-110	210,800	202,200		26	
A	ST	-110	200,800	195,300	8	31	
A	ST	RT	176,700	168,900	10	40	
A	ST	RT	176,200	168,000	11	39	
A	ST	650	126,500	111,900	8	18	
A	ST	650	116,300	112,600	2	5	
(OPTIMUM)							
B	T	-110	195,000	186,800	8	30	110
B	T	-110	200,400	193,800	5	19	116
B	T	RT	173,400	164,200	13	39	218
B	T	RT	177,800	172,700	8	21	214
B	T	400	143,200	126,000	14	42	561
B	T	400	143,700	127,700	13	59	631
B	T	650	81,900	63,700	7	27	1122
B	T	650	102,200	84,800	7	24	1244
B	ST	-110	194,400	188,800	7	31	
B	ST	-110	194,600	189,800	8	35	
B	ST	RT	169,400	161,200	12	36	
B	ST	RT	166,300	159,900	9	25	
B	ST	400	134,600	116,300	11	52	
B	ST	400	134,900	116,900	15	55	
B	ST	650	96,200		4	8	
B	ST	650	129,900	115,300	14	51	
B	L	-110	192,000	188,500	11	29	
B	L	-110	194,700	191,600	11	30	
B	L	RT	166,300	160,600	14	53	
B	L	RT	168,500	160,000	14	40	
B	L	400	142,400	127,800	16	51	
B	L	400	140,700	124,900	16	51	
B	L	650	114,100	98,900	30	76	
B	L	650	129,700	113,600	9	28	

TABLE 9 HEAT TREATMENTS AND RESULTING MECHANICAL PROPERTIES
FOR Ti 6Al-6V-2Sn STA (continued)

HEAT * TREAT	GRAIN	TEST TEMP °F	ULTIMATE STRENGTH psi	.2% YIELD STRENGTH psi	ELONG 1 inch percent	RA percent	PRECRACKED CHARPY W/A (in ² lbs in ²)
C	T	-110	203,200	191,400	6	21	103
C	T	-110	207,800	193,800	6	20	113
C	T	RT	180,700	164,300	9	27	114
C	T	RT	175,300	163,800	10	19	113
C	T	650	121,400	101,400	8	31	960
C	T	650	123,900	101,600	8	21	894
C	ST	-110	202,600	193,600	7	26	
C	ST	-110	200,000	191,300	8	25	
C	ST	RT	172,100	163,900	12	35	
C	ST	RT	179,800	169,800	8	27	
C	ST	650	129,500	111,600	5	13	
C	ST	650	125,000	108,600	7	24	

*HEAT TREATMENTS

- A. (1) Solution anneal at 1625°F for 1 hour water quench.
(2) Age at 1200°F for 4 hours air cool.
- B. (1) Solution anneal at 1575°F for 1 hour water quench.
(2) Age at 1200°F for 4 hours air cool.
- C. (1) Solution anneal at 1525°F for 1 hour water quench.
(2) Age at 1150°F for 4 hours air cool.

TABLE 10 HEAT TREATMENTS AND RESULTING MECHANICAL PROPERTIES
FOR PH 13-8 Mo

HEAT * TREAT	GRAIN	TEST TEMP °F	ULTIMATE STRENGTH psi	.2% YIELD STRENGTH psi	ELONG 1 inch percent	RA percent	PRECRACKED CHARPY W/A (in/lbs/in ²)
A	T	-110	248,900	225,500	2	1.4	314
A	T	RT	227,500	205,700	7	15	545
A	T	RT	226,200	207,500	10	37	491
A	T	650	187,700	162,100	8	19	1833
B	T	-110	245,500	224,400	2	5	119
B	T	RT	223,800	201,600	13	55	343
B	T	650	186,900	160,800	13	54	1943
C	T	-110	238,900	229,000	12	50	130
C	T	RT	223,000	211,000	13	54	416
C	T	650	184,000	164,400	13	53	2062
(OPTIMUM)							
D	T	-110	222,800	215,400	12	41	275
D	T	-110	223,900	220,500	11	42	251
D	T	RT	207,100	196,900	12	57	900
D	T	RT	207,100	193,800	12	49	755
D	T	400	186,800	179,300	12	58	2607
D	T	400	186,500	178,800	14	60	2614
D	T	650	172,300	162,700	13	58	3126
D	T	650	170,600	160,800	13	59	3192
D	L	-110	228,600	219,000	14	54	
D	L	-110	228,200	219,200	14	58	
D	L	RT	209,700	204,800	14	60	
D	L	RT	211,000	205,300	14	59	
D	L	400	188,500	179,000	14	63	
D	L	400	186,500	181,300	14	63	
D	L	650	174,700	165,200	7	27	
D	L	650	176,600	165,600	9	36	

*HEAT TREATMENTS

- A. (1) Solution anneal at 1700°F for 30 min. air cool to below 60°F for 30 min.
(2) Age at 950°F for 4 hours, air cool.
- B. (1) Solution anneal at 1700°F for 30 min. air cool to below 60°F for 30 min.
(2) Age at 1000°F for 1 hour, air cool.
- C. (1) Solution anneal at 1700°F for 30 min. air cool to below 60°F for 30 min.
(2) Age at 1000°F for 4 hours, air cool.
- D. (1) Solution anneal at 1700°F for 30 min. air cool to below 60°F for 30 min.
(2) Age at 1025°F for 4 hours, air cool.

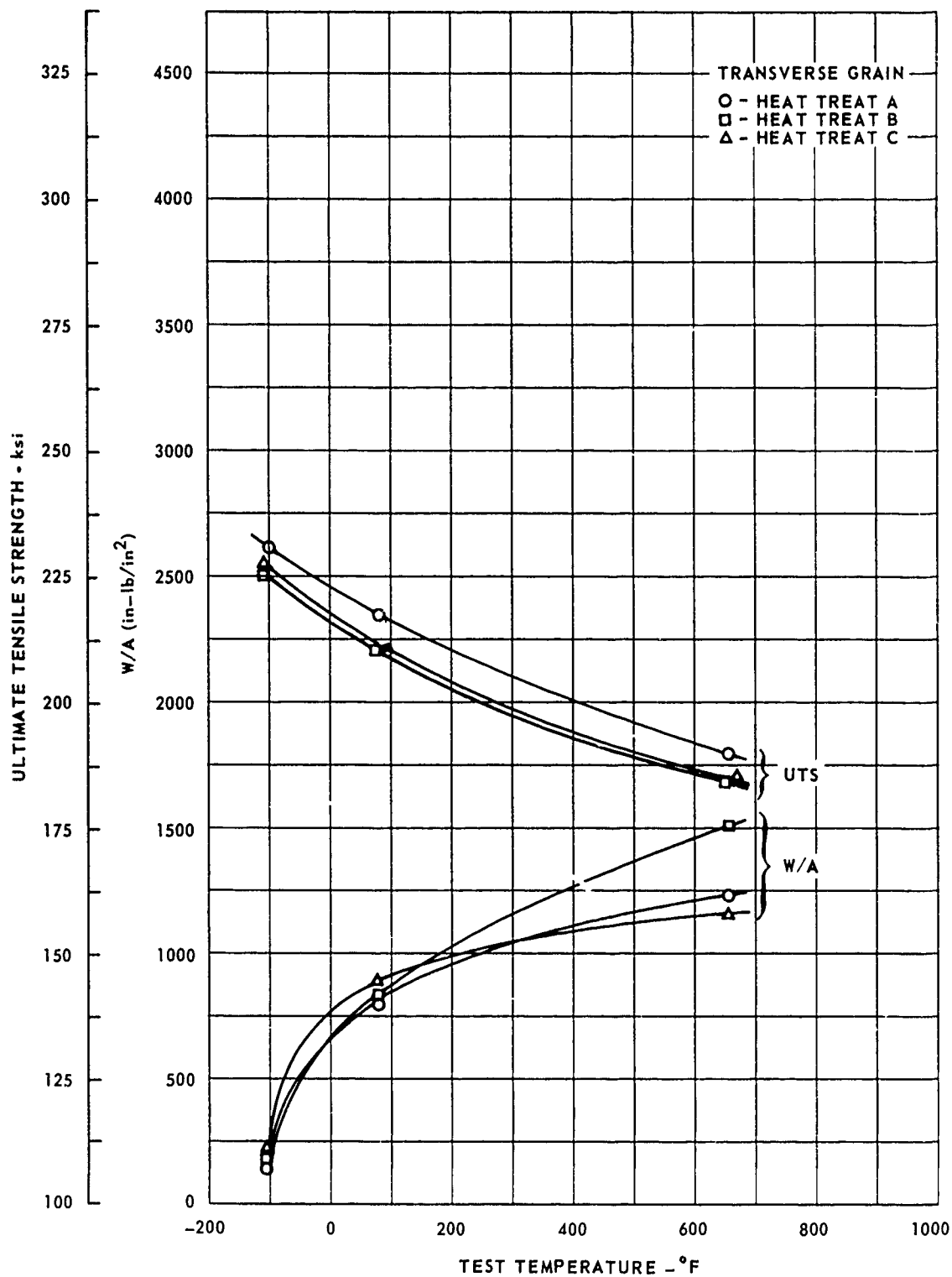


FIG. 17 VARIATION OF PRECRACKED CHARPY TOUGHNESS AND ULTIMATE STRENGTH WITH TEMPERATURE FOR HEAT TREATMENTS (OF 4340

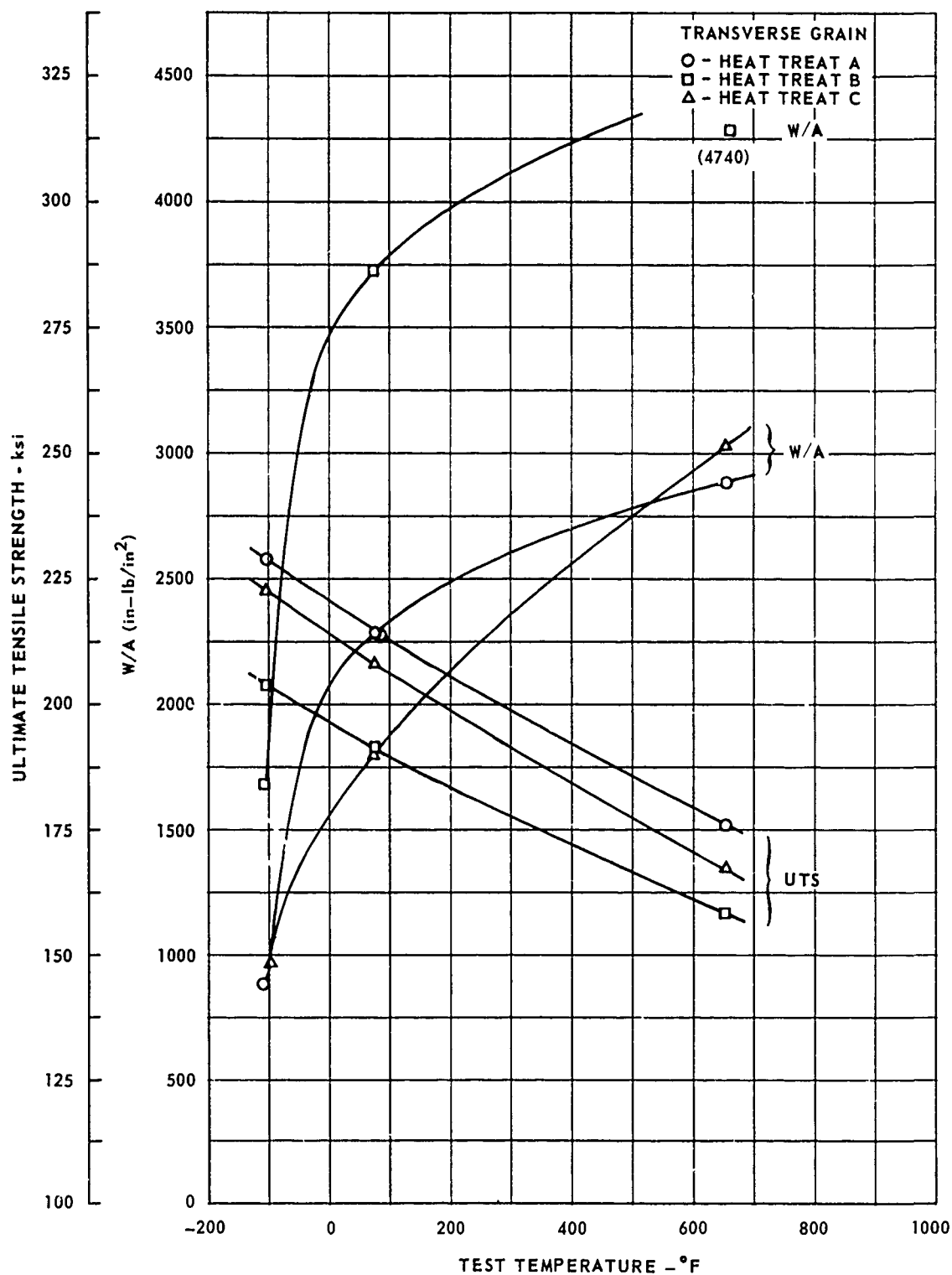


FIG. 18 VARIATION OF PRECRACKED CHARPY TOUGHNESS AND ULTIMATE STRENGTH WITH TEMPERATURE FOR HEAT TREATMENTS OF 9Ni-4Co

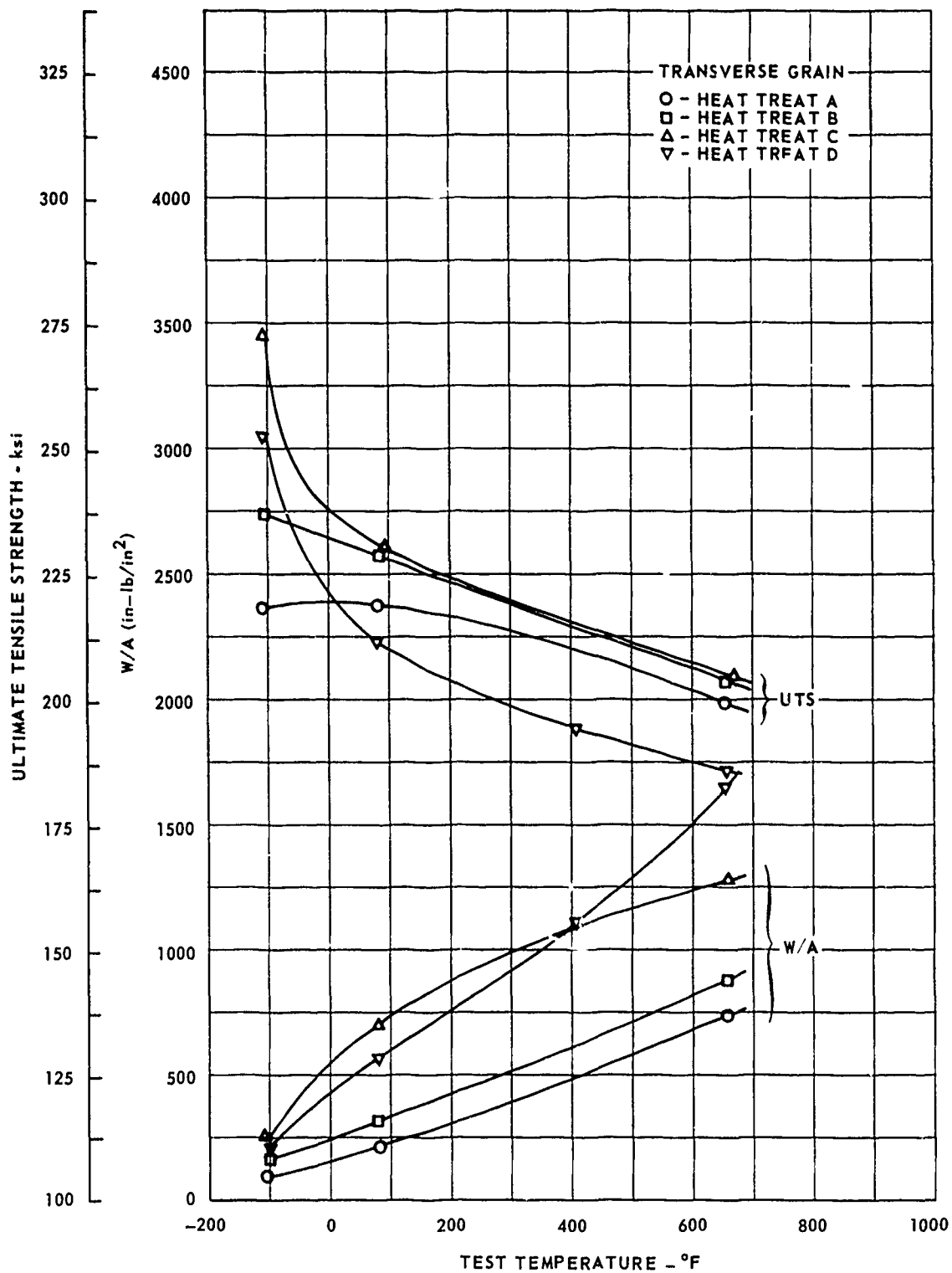


FIG. 19 VARIATION OF PRECRACKED CHARPY TOUGHNESS AND ULTIMATE STRENGTH WITH TEMPERATURE FOR HEAT TREATMENTS OF AM 355

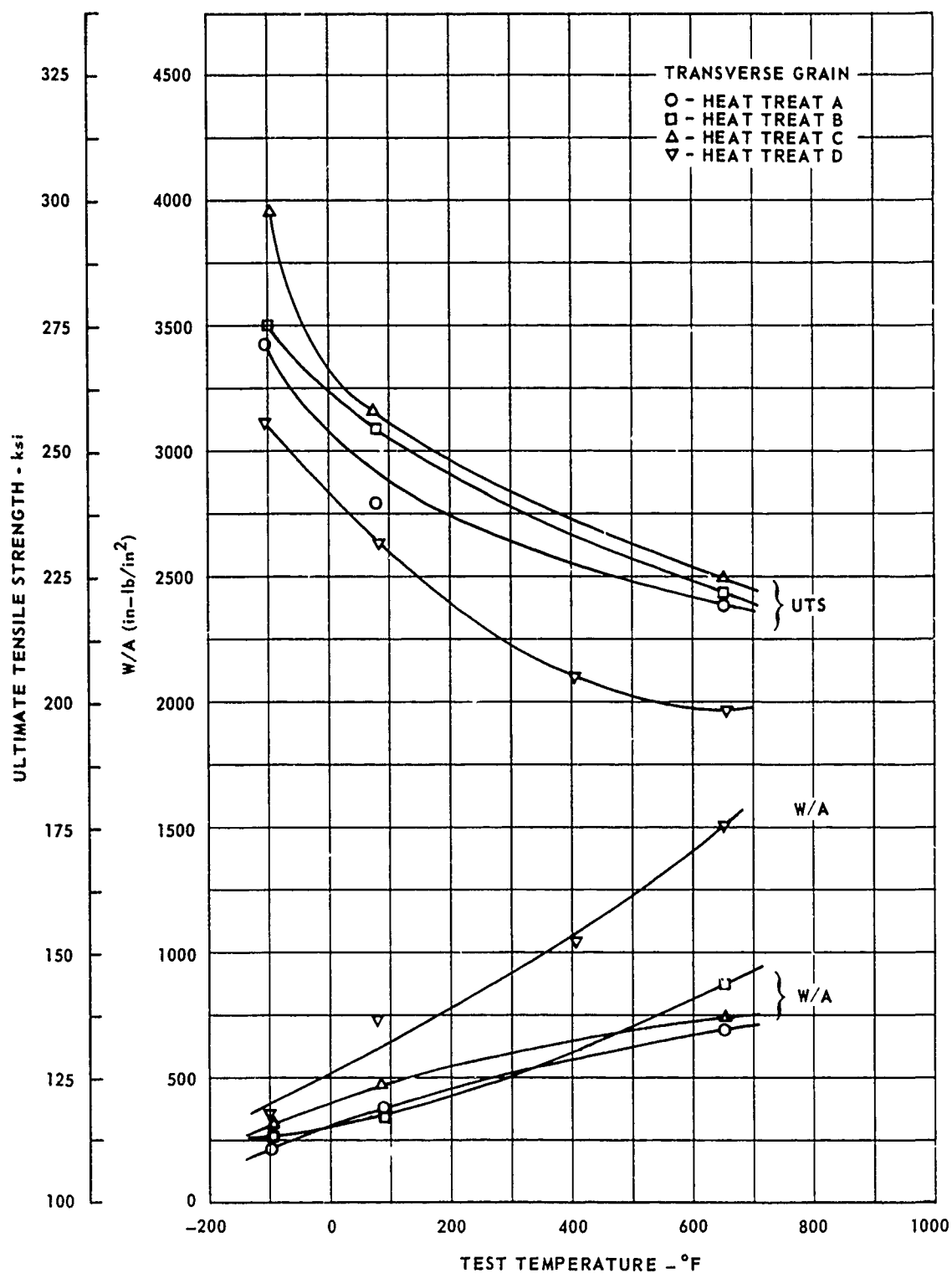


FIG. 20 VARIATION OF PRECRACKED CHARPY TOUGHNESS AND ULTIMATE STRENGTH WITH TEMPERATURE FOR HEAT TREATMENTS OF MARAGING 250

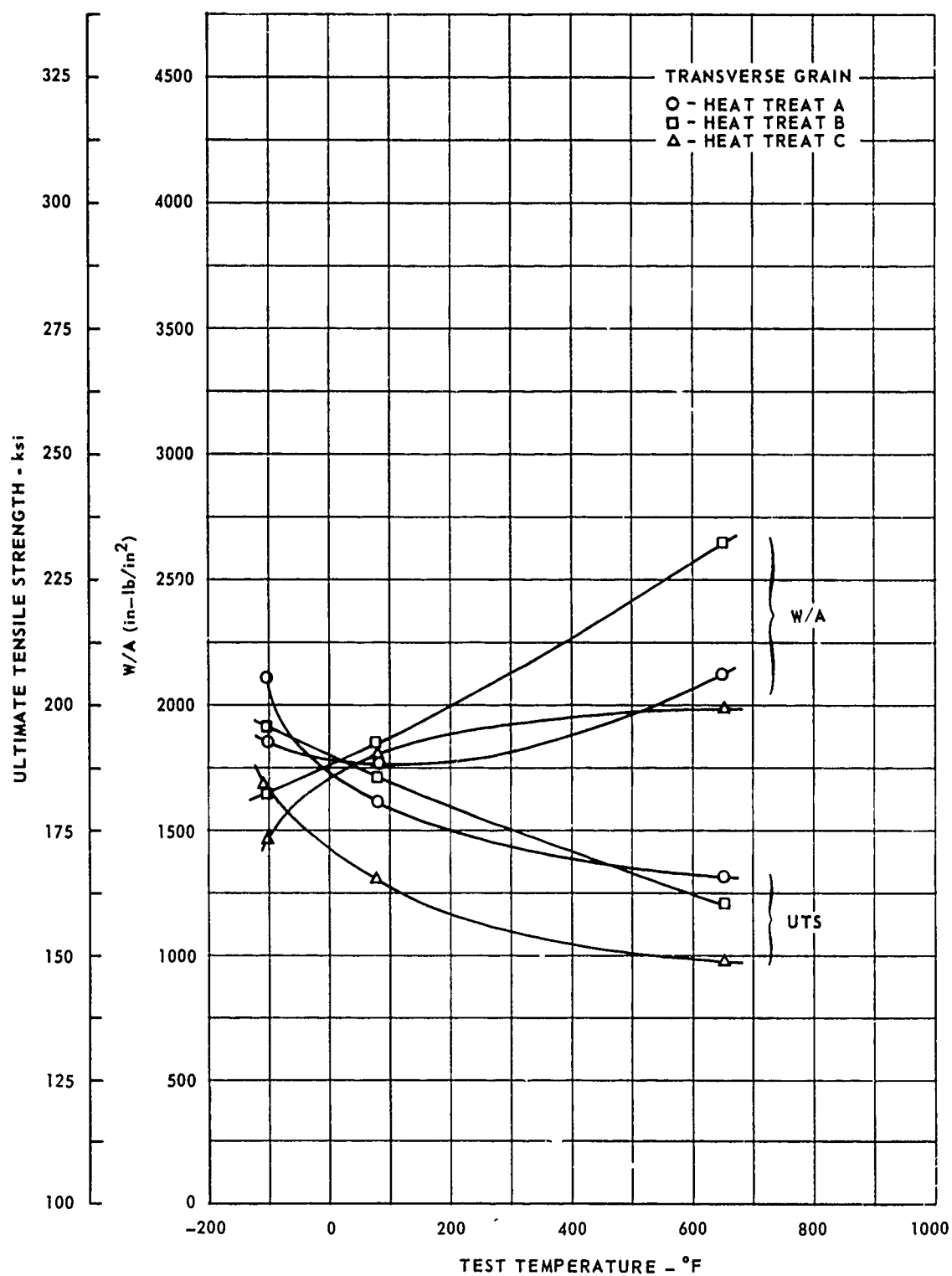


FIG. 21 VARIATION OF PRECRACKED CHARPY TOUGHNESS AND ULTIMATE STRENGTH WITH TEMPERATURE FOR HEAT TREATMENTS OF INCO 718

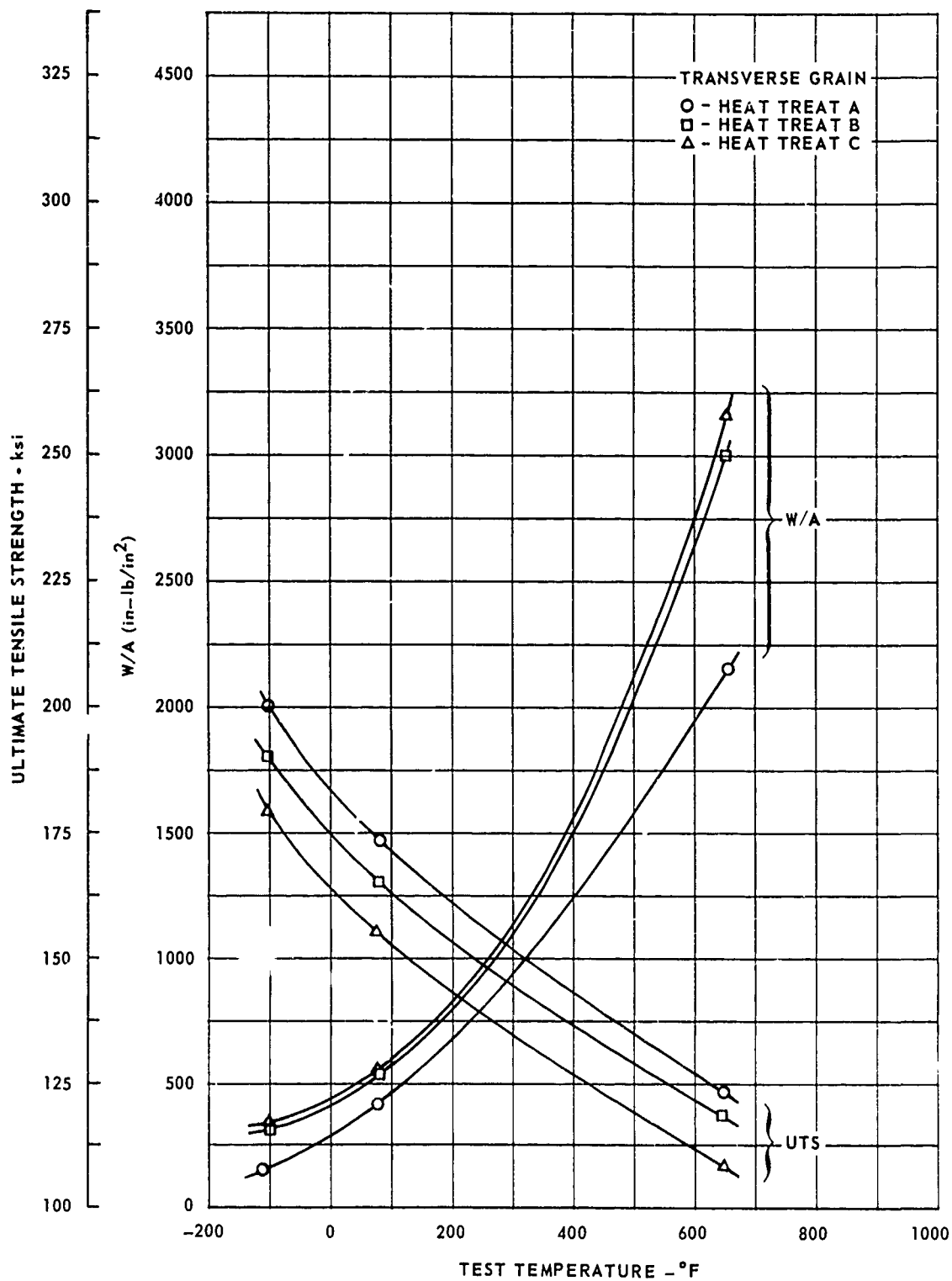


FIG. 22 VARIATION OF PRECRACKED CHARPY TOUGHNESS AND ULTIMATE STRENGTH WITH TEMPERATURE FOR HEAT TREATMENTS OF Ti-6Al-4V

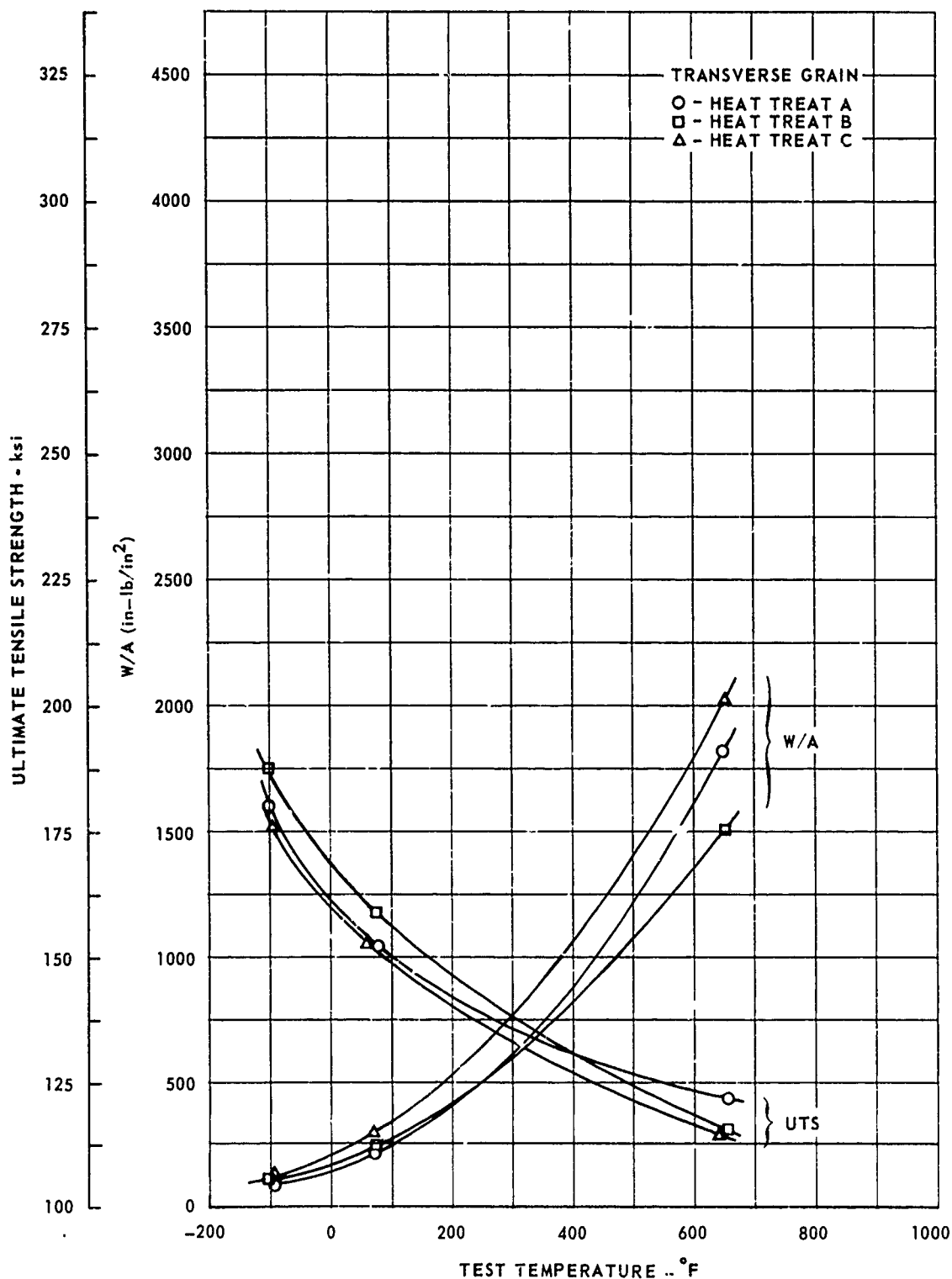


FIG. 23 VARIATION OF PRECRACKED CHARPY TOUGHNESS AND ULTIMATE STRENGTH WITH TEMPERATURE FOR HEAT TREATMENTS OF Ti 6Al-6V-2Sn ANN

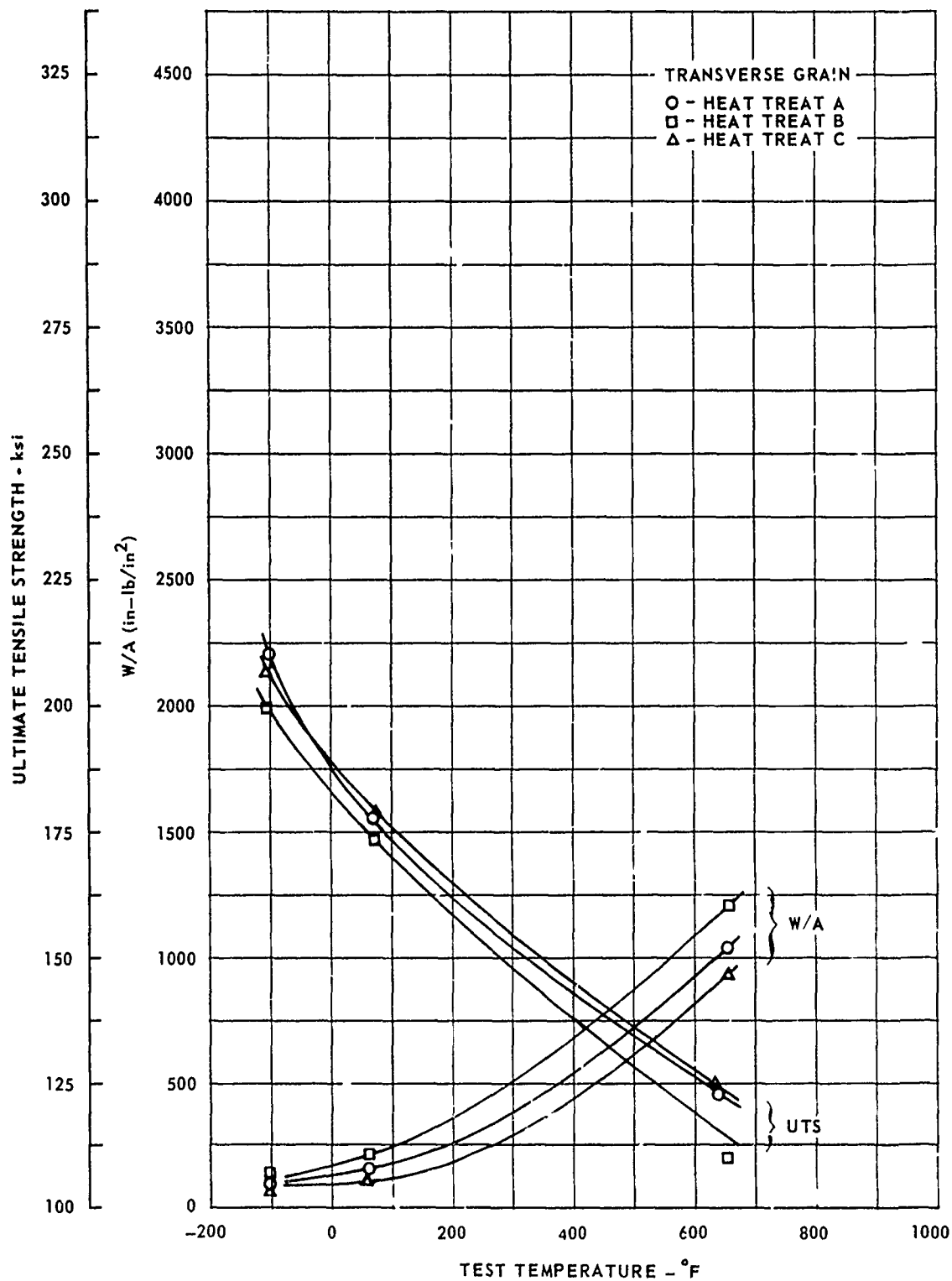


FIG. 24 VARIATION OF PRECRACKED CHARPY TOUGHNESS AND ULTIMATE STRENGTH WITH TEMPERATURE FOR HEAT TREATMENTS OF Ti-6Al-6V-2Sn STA

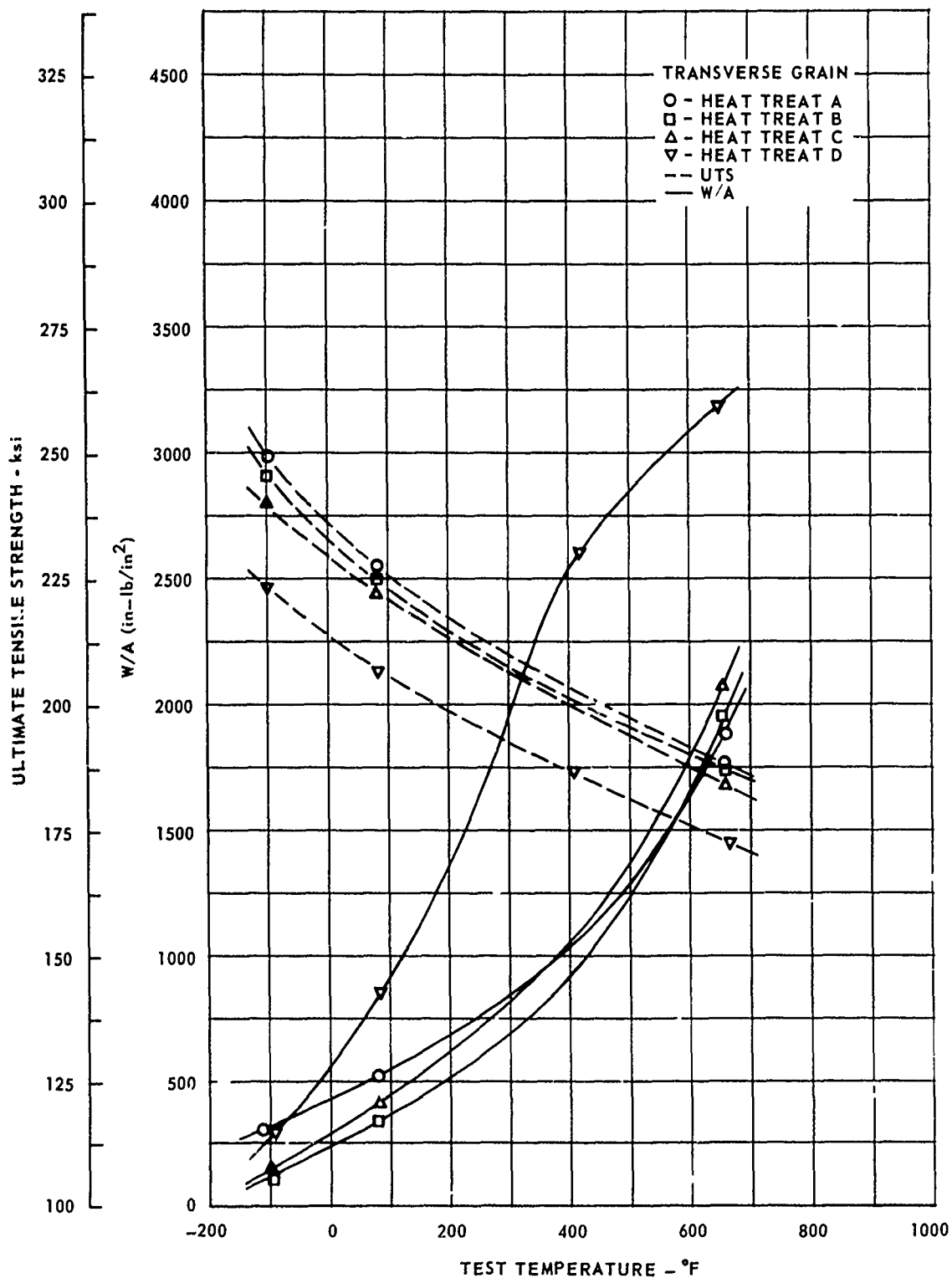
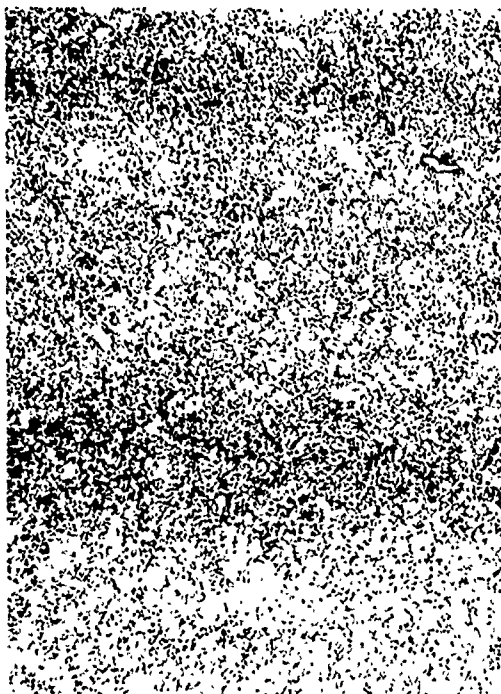


FIG. 25 VARIATION OF PRECRACKED CHARPY TOUGHNESS AND ULTIMATE STRENGTH WITH TEMPERATURE FOR HEAT TREATMENTS OF PH 13-8Mo



100x



1000x



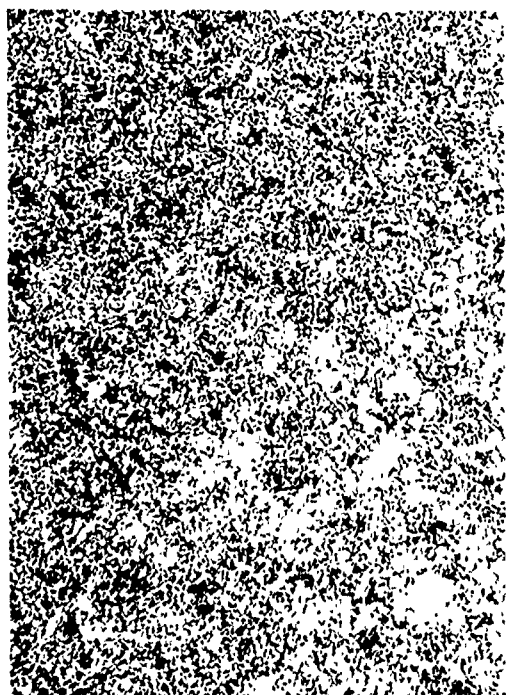
5000x



5000x

ETCHANT: Vilella's REAGENT

FIG. 26 MICROGRAPHS OF SELECTED HEAT TREAT CONDITION FOR 4340



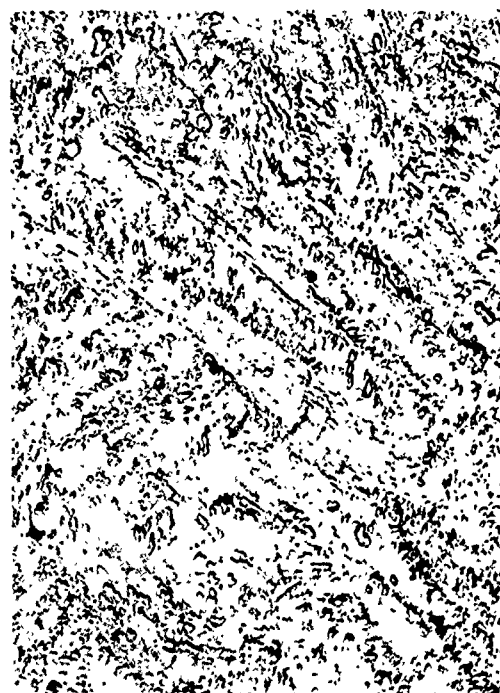
100x



1000x



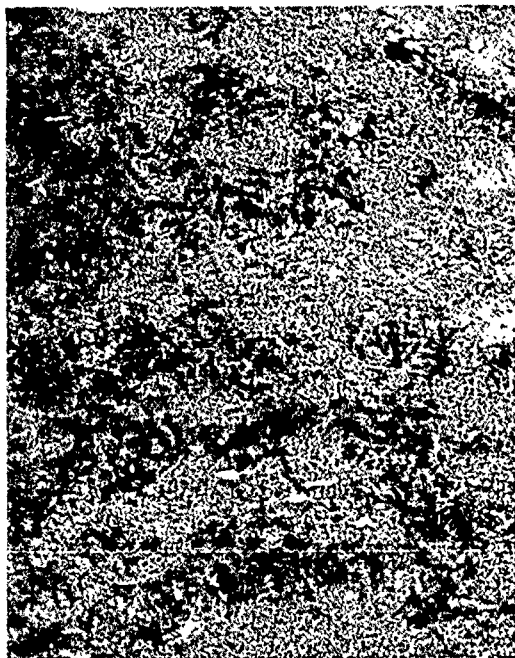
5000x



5000x

ETCHANT: 60% HCl, 12% HNO₃, 12% Acetic Acid

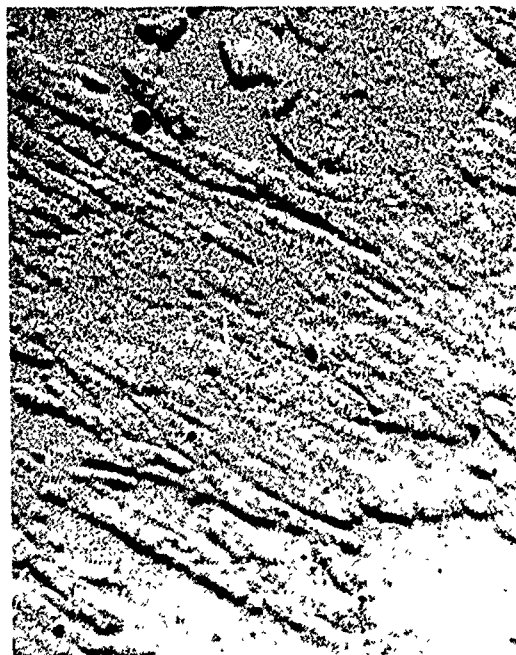
FIG. 27 MICROGRAPHS OF SELECTED HEAT TREAT CONDITION FOR 9Ni-4Co



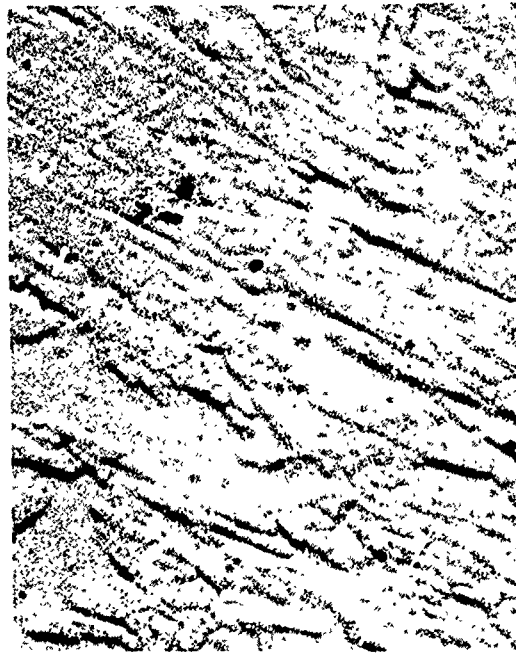
(100x)



(1000x)



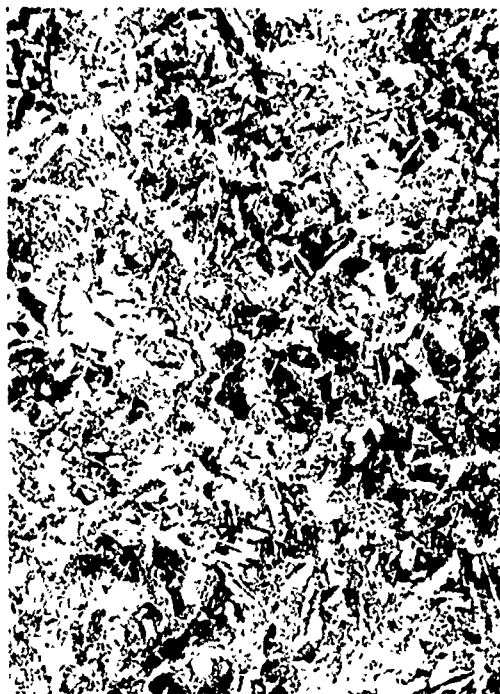
(5000x)



(5000x)

NOTE: Villela's Etch for 100x and 1000x 10% $(\text{NH}_4)_2\text{S}_2\text{O}_8$ Electrolytic Etch for 5000x

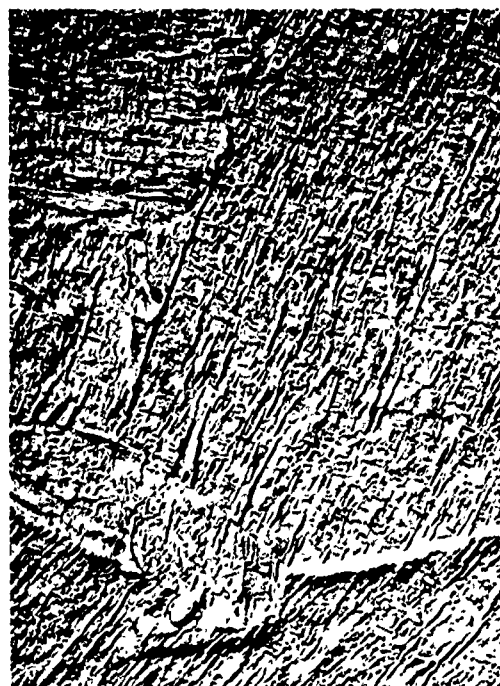
FIG. 28 MICROGRAPHS OF SELECTED HEAT TREAT CONDITION FOR AM 355



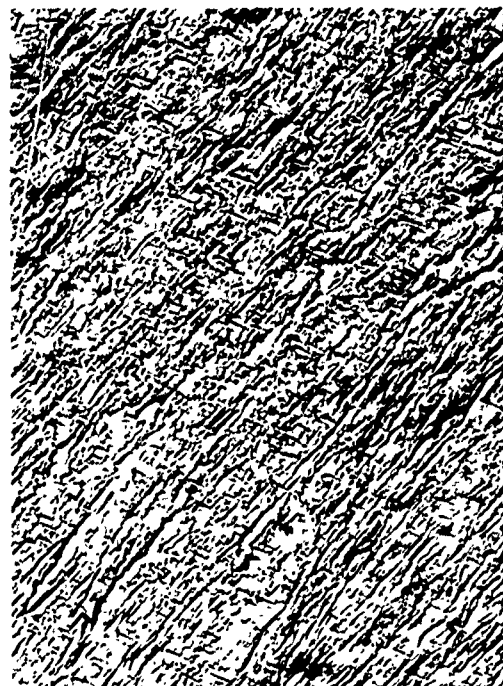
100x



1000x



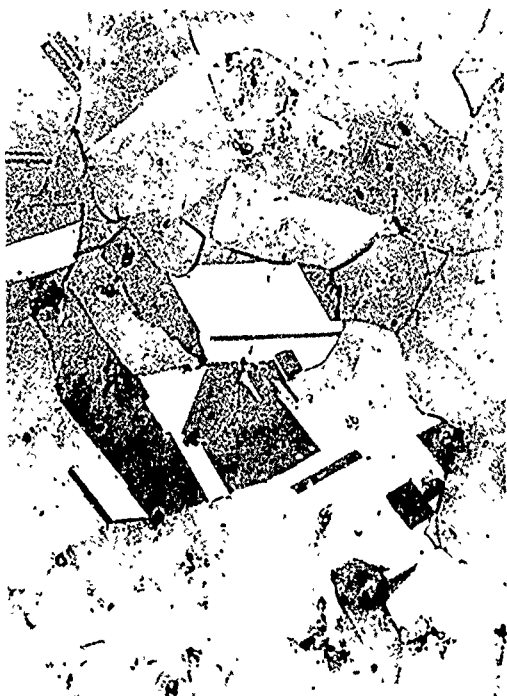
5000x



5000x

ETCHANT: 60% HCl, 12% HNO_3 , 12% Acetic Acid

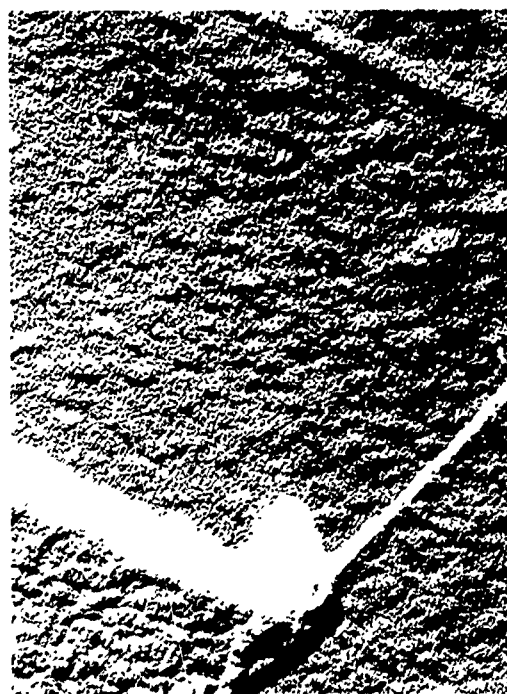
FIG. 29 MICROGRAPHS OF SELECTED HEAT TREAT CONDITION FOR MARAGING 250



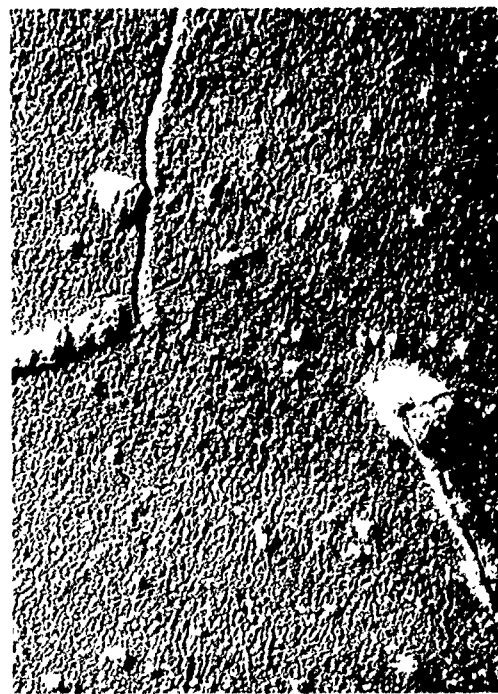
100x



2500x



5000x



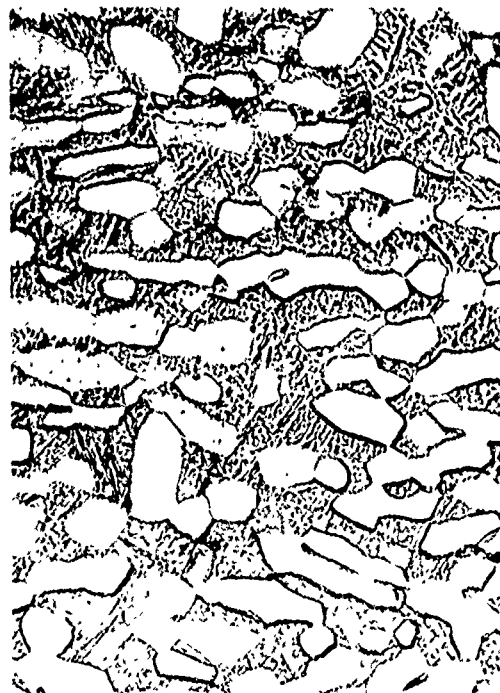
5000x

ETCHANT: 12% HCl, 12% HNO₃, 12% Acetic Acid

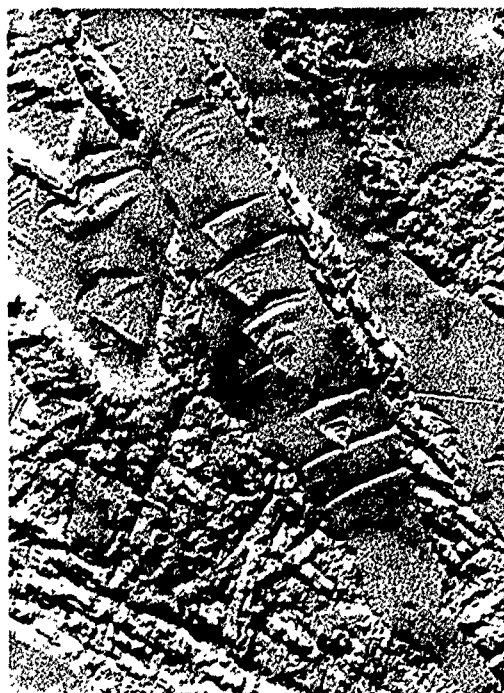
FIG. 3C MICROGRAPHS OF SELECTED HEAT TREAT CONDITION FOR INCO 718



100x



1000x



5000x



5000x

ETCHANT: 20% H_2SO_4 followed by 1% HF (emitted for electron micrographs)

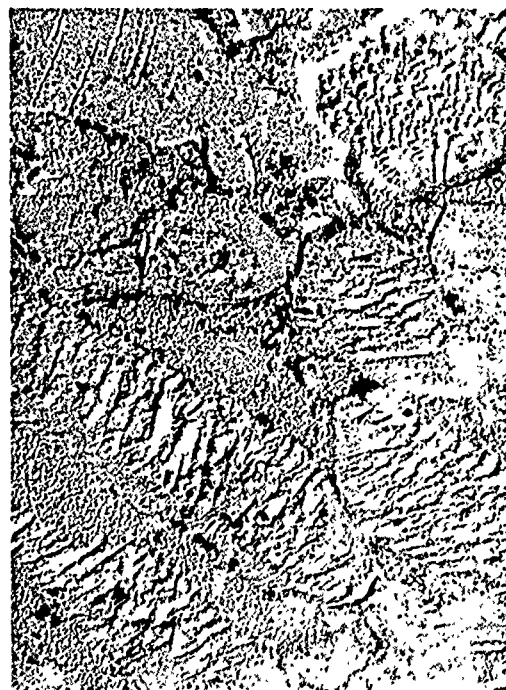
FIG. 31 MICROGRAPHS OF SELECTED HEAT TREAT CONDITION FOR Ti 6Al-4V



100x



1000x



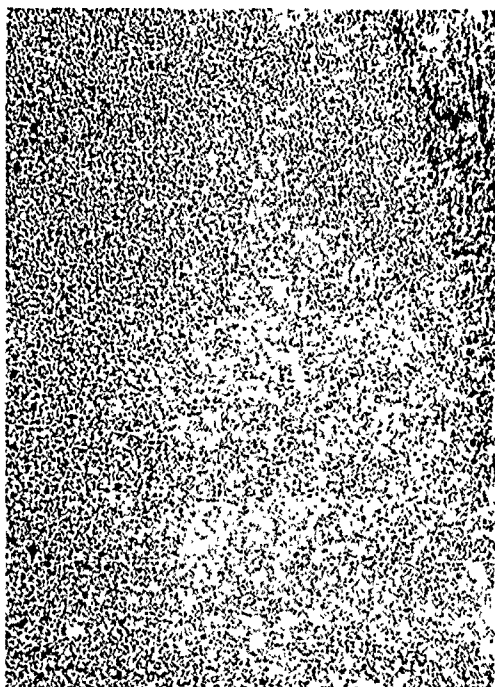
5000x



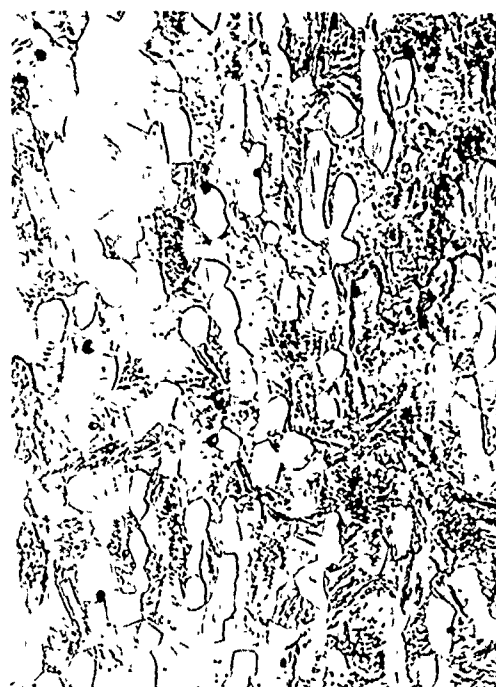
5000x

ETCHANT: 20% H_2SO_4 followed by 1% HF (emitted for electron micrographs)

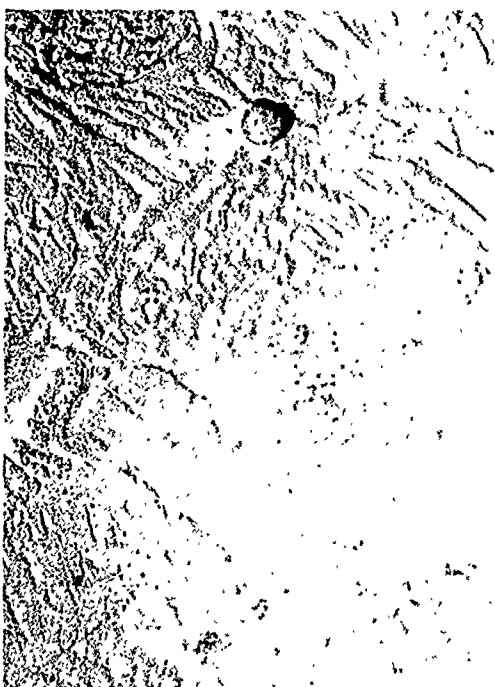
FIG. 32 MICROGRAPHS OF SELECTED HEAT TREAT CONDITION FOR Ti 6Al-6V-2Sn ANN



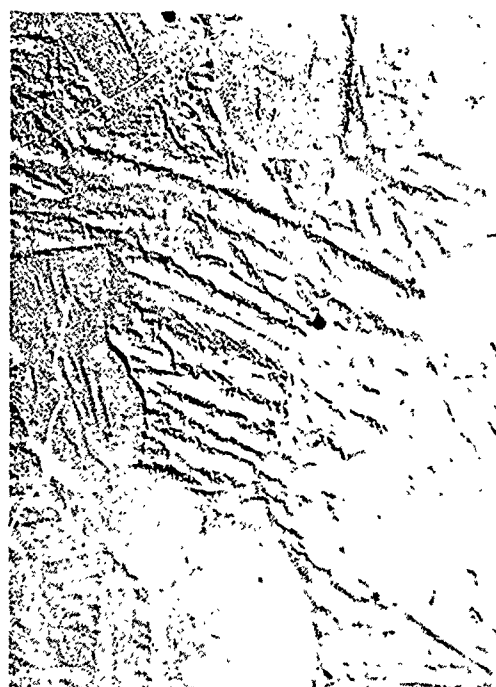
100x



1000x



5000x



5000x

ETCHANT: 20% H_2SO_4 FOLLOWED BY 1% HF (EMITTED FOR ELECTRON MICROGRAPH)

FIG. 33 MICROGRAPHS OF SELECTED HEAT TREAT CONDITION FOR Ti 6Al-6V-2Sn STA



100x



1000x



5000x



5000x

ETCHANT: 60% HCl, 12% HNO₃, 12% Acetic Acid

FIG. 34 MICROGRAPHS OF SELECTED HEAT TREAT CONDITION FOR PH 13-8 Mo

9 Ni-4Co-.45C

Preliminary data was obtained from the producer on the use of an isothermal quench to develop a bainitic structure. This procedure indicated an improvement in fracture toughness over the quenched and tempered martensitic condition. Excellent toughness had been obtained with isothermal quenching in the range from 450°F to 650°F. The requirement for metallurgical stability after exposure to 650°F and 40 ksi required a final tempering temperature above 650°F. 700°F was considered the minimum tempering temperature which would provide stability.

The three trial heat treatments listed in Table 3 consisted of a martensitic quench followed by tempering at 750°F, a 450°F isothermal quench followed by tempering at 700°F and a 550°F isothermal quench followed by tempering at 700°F. The tensile and fracture data plotted in Fig. 18 indicate the 450°F bainitic treatment developed exceptional toughness with strength in the same range as the 4340. Therefore, this heat treatment was selected for heat treatment of the subsequent specimens.

The bainitic structure of this alloy is revealed in Fig. 27.

AM 355

Experimental heat treatments of the AM 355 consisted of variations of the sub cooled and tempered condition listed in Table 4 as the SCT condition. It involved the solution of carbides at 1925°F, conditioning of the austenite at 1710°F, transformation to martensite at -100°F, and tempering at temperatures of 850°F. The second was similar to the first except it included an additional subcool at -100°F after the carbide solution treatment in an attempt to form some martensite before precipitation of carbides. The third was similar to the second, however, the austenite conditioning treatment was done at a temperature of 850°F rather than 1710°F to obtain a finer carbide precipitate. Properties resulting from the third heat treatment were somewhat lower than anticipated. The existence of delta-ferrite in the microstructure was considered to be the cause of the poorer toughness properties. Several attempts were made to reduce the delta-ferrite content by the equalized and overaged treatment initially given to forged AM 355 before the hardening treatment. These attempts were unsuccessful in either reducing the delta-ferrite content or improving the toughness. All of these heat treatments involved final tempering at 850°F rather than 1000°F because the higher tempering temperature results in strength levels which were considered too low for supersonic transport application. The tensile and fracture data plotted in Fig. 19 show the austenite conditioning treatment at 850°F resulted in superior properties.

The microstructures for this heat treatment are shown in Fig. 28. The microstructure differs from the standard SCT condition in that more austenite is apparent due to the low conditioning treatment. Delta ferrite islands with $M_{23}C_6$ carbides precipitated at the interface with the austenite are also shown in Fig. 28. These carbides result in a brittle interface and cause the lower, than expected, fracture toughness.

Maraging 250

The three heat treatments chosen consisted of the standard 900°F age, an 850°F under-age and a 950°F over-age. It was thought that the 950°F over-age would provide a slightly lower strength with increased toughness over the standard heat treat. However, the 950°F over-age increased the strength and toughness slightly. The toughness for the three heat treatments as shown by precracked Charpy specimens was lower than the other alloys previously tested. Preliminary work indicated that a higher annealing temperature would provide lower strength and increased elongation. Two additional heat treatments were tried involving higher annealing temperatures at 1700°F and aging at 950°F and 1050°F. The 950°F age resulted in strengths above the previous data with the same relative precrack Charpy toughness. The 1050°F age resulted in a decrease in strength and a marked increase in toughness (Fig. 20). This microstructure showed some reversion to austenite as shown in Fig. 20. This 1050°F age was the heat treatment selected as the optimum. Mechanical properties are included in Table 5.

Inco 718

Preliminary work showed that the standard heat treatment did not provide the expected properties shown by other typical heats. Conversations with Huntington Alloys, the alloy producer, together with the supplier data suggested higher solution annealing temperatures and higher aging temperatures than normally used would yield increased strength and toughness over that of standard heat treat. This was verified by the testing done for this project. Solution annealing at 1975°F and aging at 1400°F proved to provide optimum properties as shown in Table I and Fig. 3.

Ti 6Al-4V

The strength level of Ti 6Al-4V depends on the temperature of solution treating which determines the amount of beta phase formed. The higher recommended solution treating at 1750°F enables greater response during subsequent aging. For a solution treatment at 1750°F, lower aging temperatures in the range of 900°F yield higher strengths. Discussions with alloy producers indicated that a slightly over-aged condition would provide the maximum toughness for a given strength level. Most of the data found in the literature involved heat treatments yielding high strengths and poor toughness. Three heat treatments listed in Table 7 were chosen with solution temperature at 1725°F, 1650°F and 1550°F which provided three levels of strength after aging at 1100°F with corresponding differences in precracked Charpy toughness. The heat treatment at 1650°F with the intermediate strength level was considered the optimum for strength and toughness as shown in Table 7 and Fig. 22. The microstructure for this heat treatment is shown in Fig. 31.

Ti 6Al-6V-2Sn STA

Solution treated and aged heat treatments for the Ti 6Al-6V-2Sn alloy involved similar considerations to that of the Ti 6Al-4V. Previous experience showed the high strength level to have poor toughness. Heat treatments were chosen

that resulted in lower strength levels. The structures obtained were considered to be slightly over-aged. The variation in strength was not great, therefore, the heat treatment providing the highest precracked Charpy toughness was selected as optimum. The optimum heat treatment involved solution treating at 1575°F and aging at 1200°F. The three trial heat treatments and resulting properties are shown in Table 9 and Fig. 24.

Ti 6Al-6V-2Sn ANN

Data from the literature was extremely limited on various annealing treatments of Ti 6Al-6V-2Sn. The standard mill anneal consisted of heating to 1300°F for two hours and air cooling. A 1400°F anneal has also been reported in the literature by some alloy producers. The effect of furnace cooling has been found to be significant in changing the toughness of other titanium alloys and was chosen as another variable. The three heat treatments were 1300°F air cool, 1300°F furnace cool and 1400°F air cool. The tensile and precracked Charpy test data proved the standard mill anneal to be the optimum process as shown in Table 8 and Fig. 23.

PH 13-8Mo

Tensile and precracked Charpy specimen data provided by Armco for PH 13-8Mo was used in the selection of the four heat treatments listed in Table 10. The solution anneal at 1700°F resulted in the best toughness-strength relationship regardless of the aging conditions. Aging temperatures in the neighborhood of 1000°F seemed to be the most likely; therefore, 950°F, 1000°F, and 1025°F were selected. The relative toughness as measured by the precracked Charpy specimens was rather low for the 950°F and 1000°F. At 1025°F the toughness increased considerably with little drop in tensile yield strength although the drop in ultimate strength was somewhat greater. Fig. 25 indicates the very little change in properties for heat treatments A, E, and C tempered at 950°F and 1000°F. Heat treatment D shows the sudden increase in toughness with only a 25°F increase in tempering temperature.

SECTION 7 CENTER-NOTCHED SPECIMENS

TEST PROCEDURE

Center-notch fracture toughness tests were conducted for each alloy in its optimum heat treat condition. Three thicknesses, with the other dimensions compatible with recommended ASTM proportions and block dimensions, were tested at four temperatures. Table 11 shows a general outline of specimen dimensions and test details.

TABLE 11 CENTER NOTCH SPECIMEN DETAILS

THICKNESS (inches)	WIDTH (inches)	LENGTH (inches)	GRAIN DIRECTION	FATIGUE CRACK LENGTH (inches)	TEST TEMPERATURE °F
3/16	3.0	9.0	T AND L	1.0	-110, RT, 400, 650
3/8	6.0	24.0	L	2.0	-110, RT, 400, 650
1.00	9.0	24.0	L	3.0	-110, RT, 400, 650

Specimen drawings are shown in Figs. 35, 36 and 37.

Fatigue Crack Growth

All center-notch specimens were fatigue-cycled so that $K = 26,400$ when $2a_i$ grew to $2a_0$ (some exceptions were made and are discussed below). It was felt that this would assure a consistent crack tip sharpness in all specimens.

For each specimen thickness, the fatigue crack extension was approximately equal to three-fourths of the panel thickness. Fatigue crack details for the center-notch specimens are shown in Table 12.

The 3/16 x 3 x 9-inch specimens were cycled in a Sonntag Universal Test Machine, Model SF10U. All 3/16-inch thick specimens except Ti 6Al-6V-2Sn STA were cycled at $\sigma_{FAT} = 19840$. Since Charpy tests indicated Ti 6Al-6V-2Sn STA was relatively brittle, the stress was reduced to 13250 psi to avoid possible specimen failure while fatigue cracking. Surface fatigue cracks were observed and measured with a 50X Gaertner Microscope.

All 3/8 x 6 x 24-inch specimens were cycled in a Riehle-Los hydraulically actuated, nonresonant, fatigue test machine. Due to certain operating characteristics, cycling for all specimens was initially at 120 cpm then continuously increased to 600 cpm. Ti 6Al-6V-2Sn STA and annealed specimens were load-cycled at a lower stress to avoid possible specimen failure. Surface fatigue cracks were observed with a 3X magnifying glass and measured with a steel scale.

All 1.0 x 9 x 24-inch specimens were fatigue cracked in a 350-kip resonant-beam fatigue machine. All titanium specimens were cycled at a lower stress

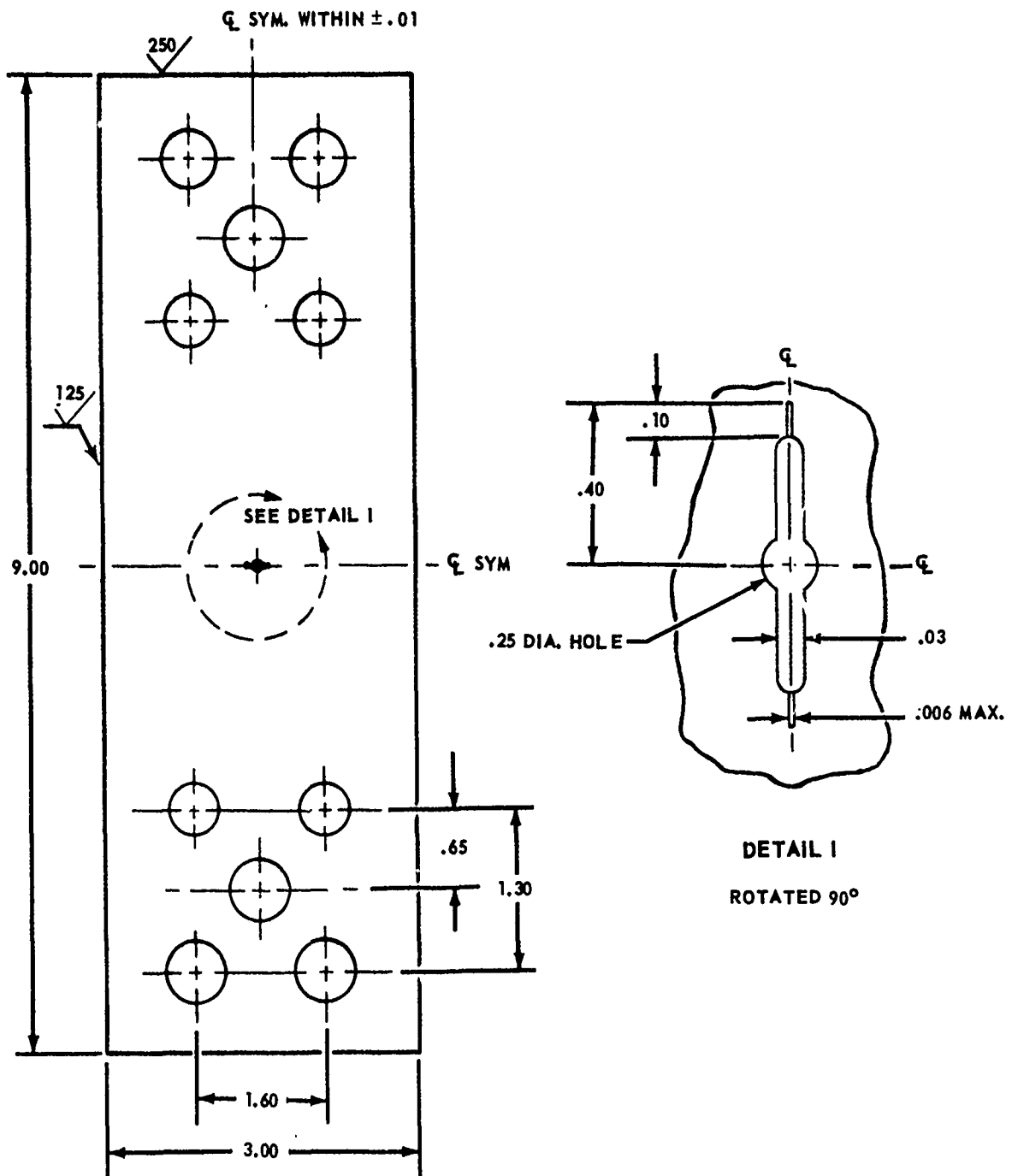


FIG. 35 3/16 INCH CENTER NOTCH SPECIMEN

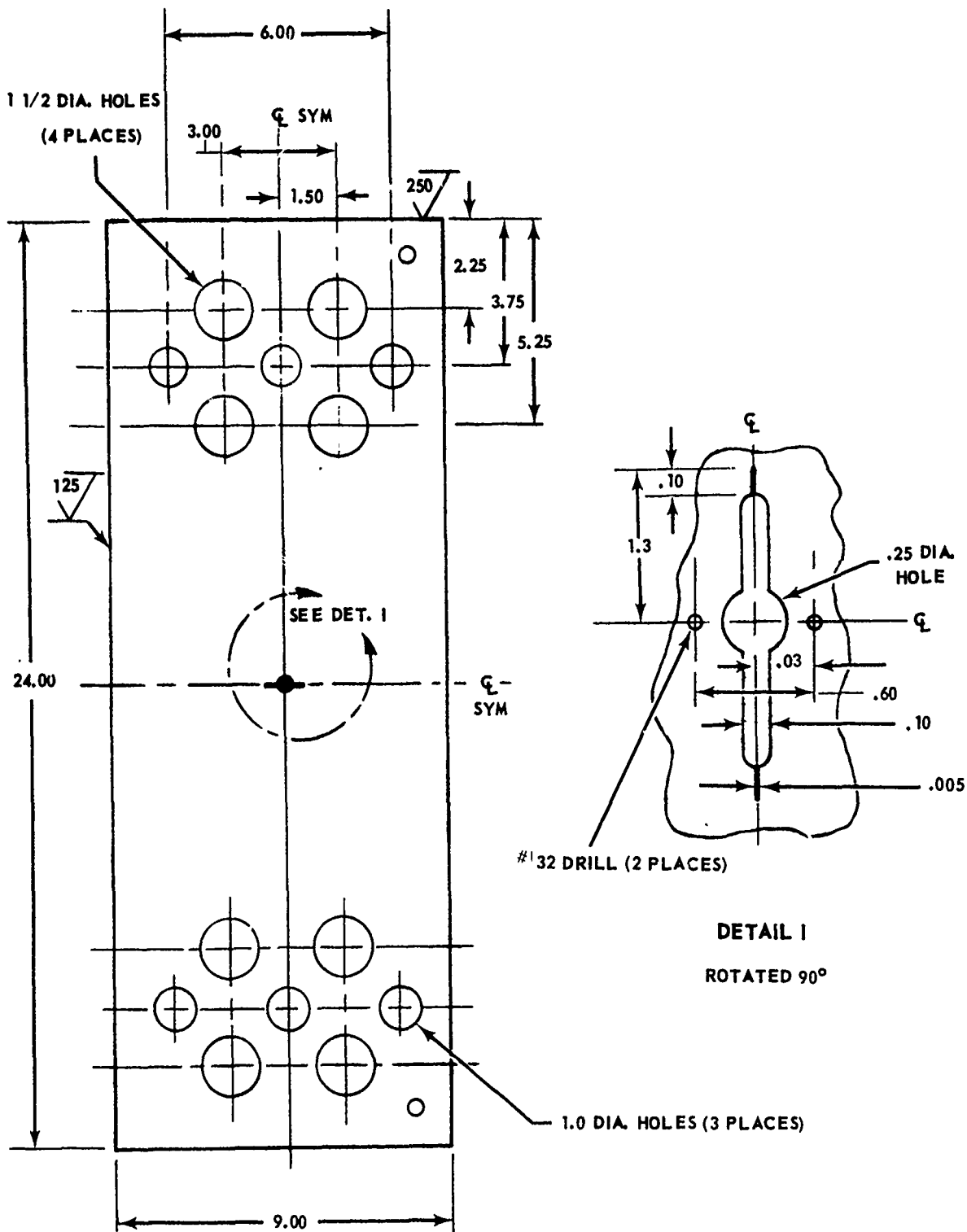


FIG. 37 1 INCH CENTER NOTCH SPECIMEN

TABLE 12 FATIGUE CRACK DETAILS

NOM'NAL THICKNESS (inches)	WIDTH (inches)	$2a_i$ (inches)	$2a_o$ (inches)	$\sigma_{FAT.}$ psi	R	$K \sqrt{\text{inches}}$	MACHINE	CYCLE RATE cpm
3/16	3.0	.85	1.0	19840 ^(b) (13250)	.05	26,400 (17,600)	SF10U	1800
3/8	6.0	1.70 ^(a) (2.0)	2.0 (2.30)	14000 ^(b) (9350)	.05	26,400 (17,600)	RIEHLE- LOS	120 TO 600
1.00	9.0	2.3	3.0	11500 ^(b) (7700)	.05	26,400 (17,600)	350 KIP MACHINE	1375 \pm 25 (1100 \pm 25)

(a) MACHINE NOTCHES WERE ACCIDENTALLY CUT OVERSIZE IN 3/8 x 6 x 24-INCH INCONEL SPECIMENS: $2a_i$ 2.0 INCHES, $2a_o$ 2.30 INCHES.

(b) CERTAIN SPECIMENS WERE TESTED UNDER A LOWER STRESS AND ARE DISCUSSED BELOW.

for the same reason mentioned above. The cyclic rate for the titanium specimens was lower due to lower LOAD requirements. Surface crack lengths were observed and measured with a 3X magnifying glass and a steel scale. All fatigue cracks on the 1 x 9 x 24-inch specimens were averaged from readings made on both sides of a given specimen. A photograph of the test setup is shown in Fig. 38.

All force sensing equipment used for measuring cyclic loads were calibrated against load cells whose calibration was directly traceable to National Bureau of Standards load cells.

All center-notch specimens (3/16, 3/8, and 1.0 inch thick) were loaded to failure at a gross area stress rate of 150,000 psi/min applied through pin-ended grips. All specimen cracks were photographed to the time of failure except for four specimens. Initially it was anticipated that crack lip displacements would be used to determine critical crack lengths (initial fatigue crack length plus slow growth). However, since net section yielding occurred at room temperature in the four 4340, 3/16-inch specimens, and might well occur in future specimens, motion picture photography was used thereafter.

Black and white film, 16mm, ASA 125, at 24 fps was used initially on several specimens; it was then replaced with 35mm film (of the same type) in order to improve image resolution. A steel scale was taped to the specimen in the field of view of the camera so critical crack lengths could be measured directly.

All -110° F specimens were brought to temperature and held there by controlling the flow of liquid nitrogen to the specimen cold chambers. A photograph of the test setup and double window cold chamber for the 3/8-inch thick specimen is shown in Fig. 39.

Negative test temperatures were measured on calibrated stamping recorders

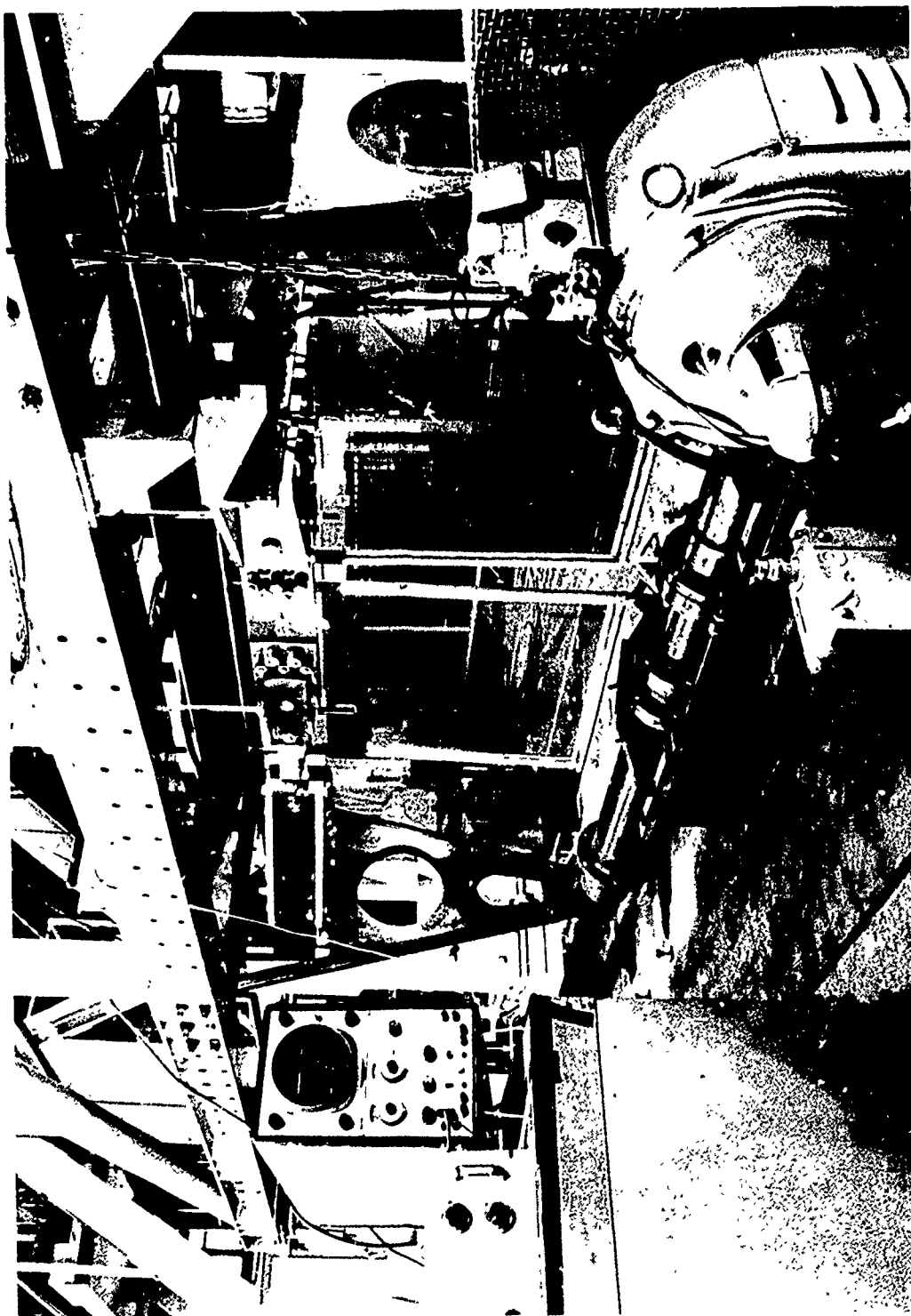


FIG. 38 1 INCH CENTER NOTCH SPECIMEN DURING FATIGUE CRACKING

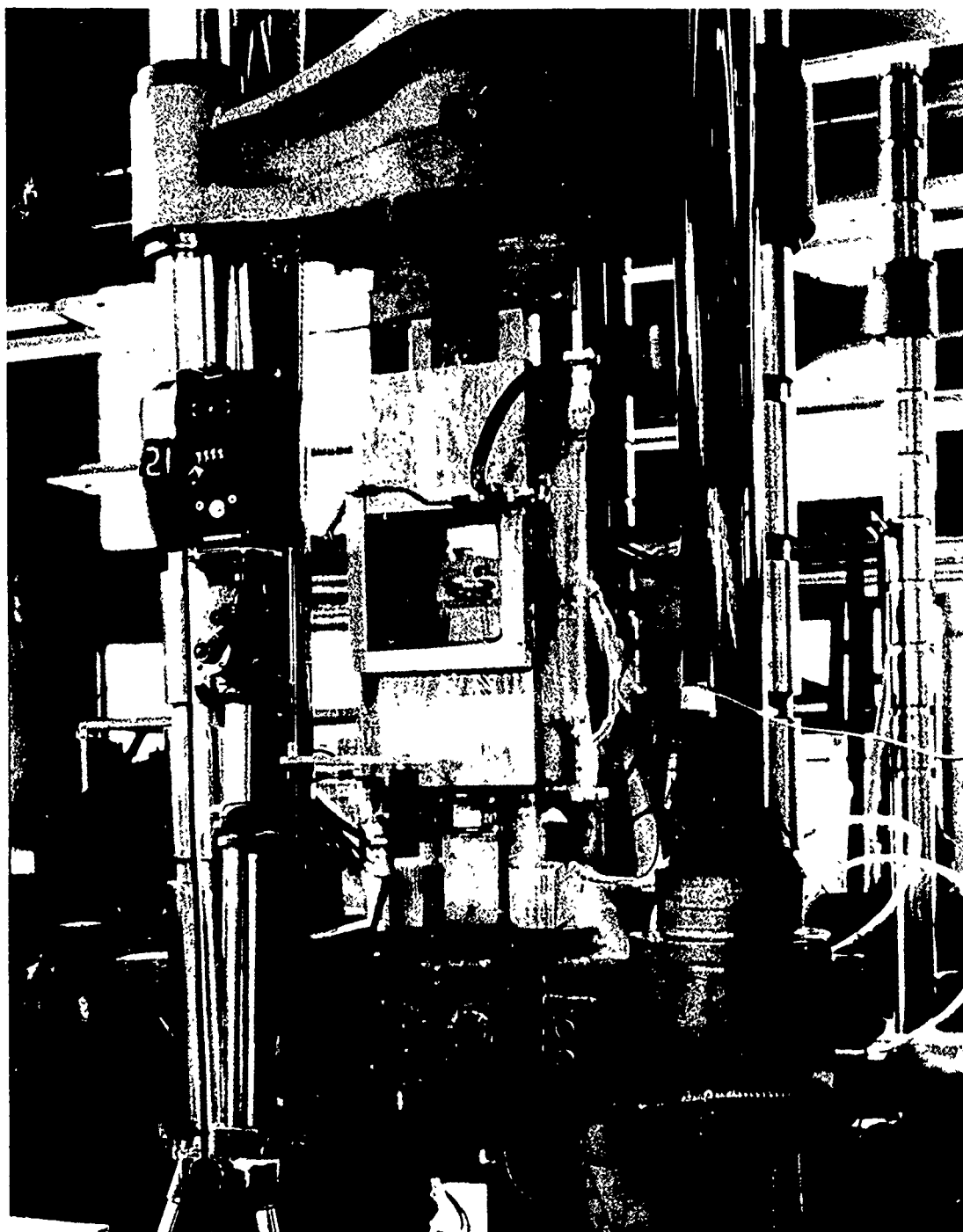


FIG. 39 3/8 INCH CENTER NOTCH -110°F TEST SETUP

using chromel-alumel thermocouples. A minimum of three thermocouples was used on all -110°F specimens. The specimens were soaked at temperature for a minimum time of 15, 30, and 45 to 60 minutes for the 3/16, 3/8, and 1.0-inch specimens, respectively, or until all thermocouples averaged out to -110°F . Temperatures were maintained to $\pm 5^{\circ}\text{F}$.

Specimens at 400°F and 650°F were brought to temperature and maintained with control thermocouples and an ignitron controlled radiant heat system. Photographs of the systems used on the 3/16 and 1.0-inch thick specimens are shown in Figs. 40 and 41.

Test temperatures were measured on calibrated stamping recorders using chromel-alumel thermocouples. A minimum of four, five, and six thermocouples were used on the 3/16, 3/8, and 1.0-inch thick specimens, respectively. Temperatures were maintained to $\pm 5^{\circ}\text{F}$.

Pop-in Detection

Pop-in is a term used to describe rapid, discontinuous crack extension. To detect this phenomenon, four different systems were investigated:

- 1) Load versus crack lip displacement or yawning;
- 2) An accelerometer;
- 3) Strain gages near a crack tip;
- 4) Load measurement with a high-response galvanometer using a time-based oscillograph.

From the investigation it was found that the most-to-least sensitive systems were 2, 3, 1, and 4 respectively. Systems 1 and 2 were used in this program because: Load versus crack displacement curves have been satisfactorily used by other investigators; yawning could be correlated to crack length for elastic specimens and; the accelerometer was by far more sensitive than any extensometer available. In fact, an investigation previously conducted on center notched specimens of 7178-T6 aluminum, indicated that rapid, discontinuous cracking was sensed at loads where the load-versus-yawning curves appeared and remained linear. Only the larger pop-ins were also detected by the load-displacement curve.

For each test specimen, an oscillograph plot of load versus time and accelerometer output versus time were recorded.

Calibrated load-signals were obtained from load cells in series with the specimen. Output from a Columbia Research Accelerometer, Model 606-1-HT, was conditioned, amplified, and recorded along with the load signal on a Consolidated Electrodynamic Oscillograph, Model 5-124. A high-frequency (2500 cps) galvanometer was used to graphically reproduce the accelerometer output. A photograph of the load and accelerometer signal conditioning equipment and oscillograph is shown in Fig. 40.

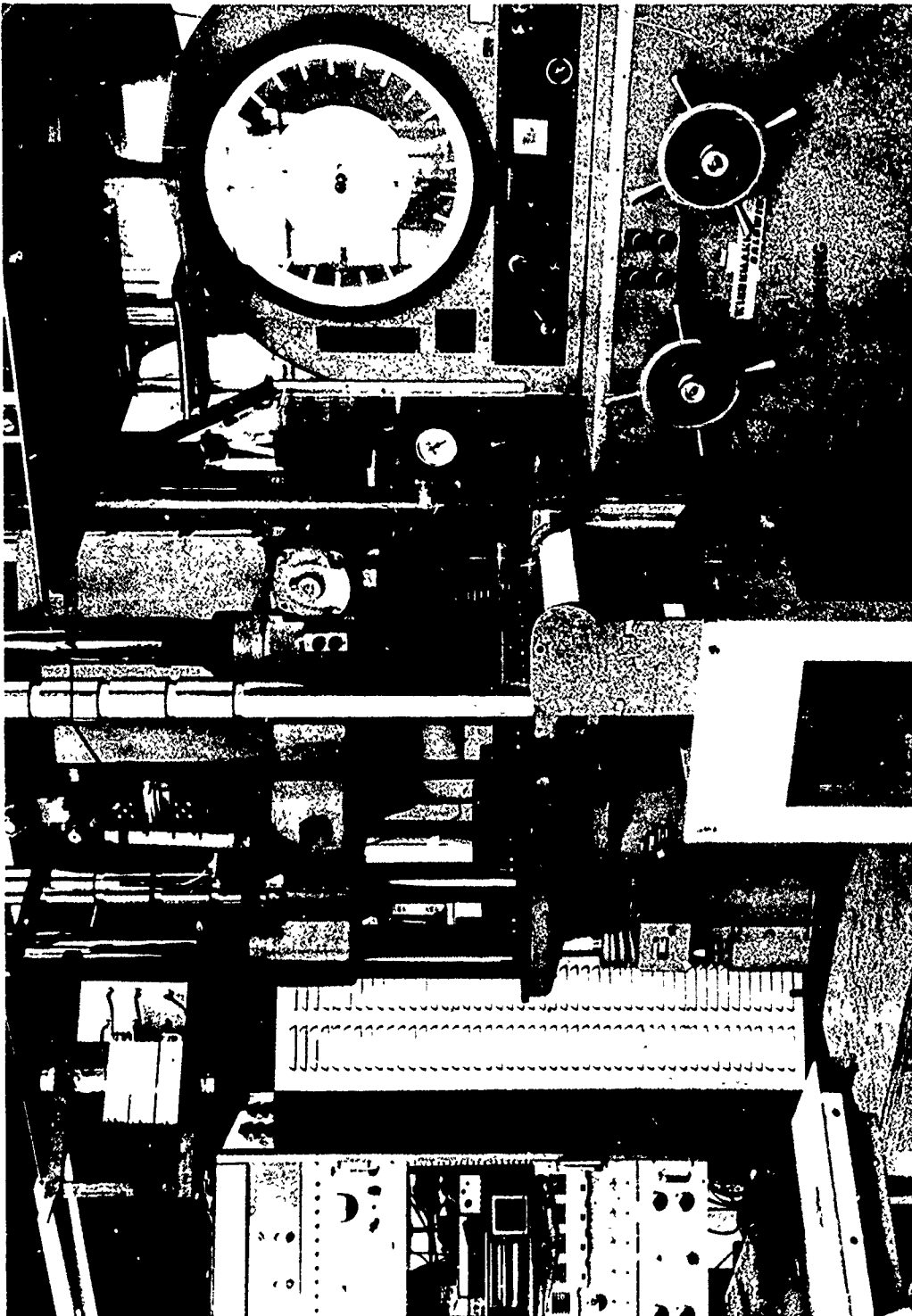


FIG. 40 3/16 INCH CENTER NOTCH HIGH TEMPERATURE TEST SETUP

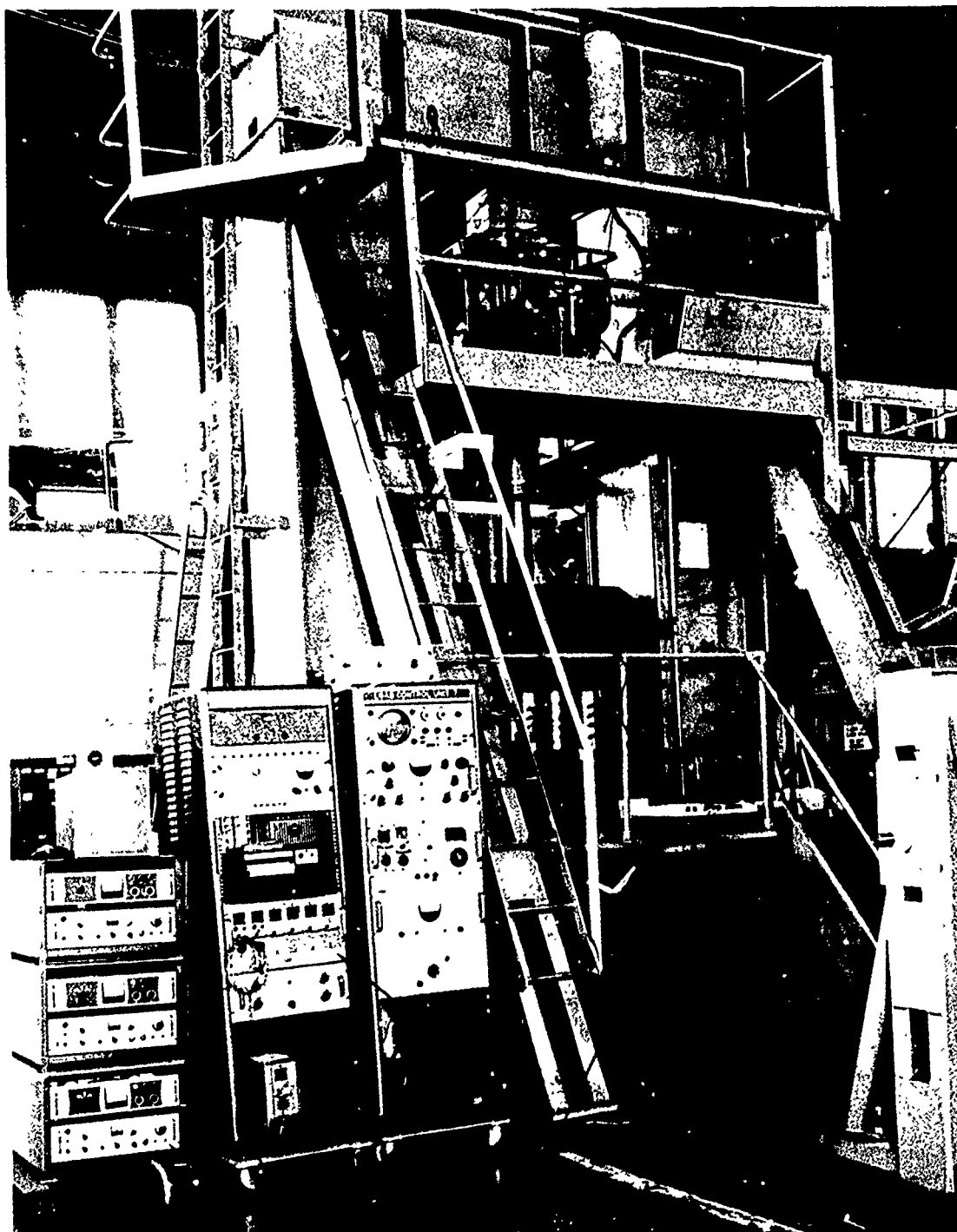


FIG. 41 1 INCH CENTER NOTCH HIGH TEMPERATURE TEST SETUP

It was found that the accelerometer could be placed anywhere on the specimen load path without significant signal attenuation. For room-temperature specimens the accelerometer was placed close to the crack; for -110°F , 400°F , and 650°F tests it was attached outside the temperature zone on the line of action. Double-back tape beneath the accelerometer foot and pressure tape against the foot adequately held it in position.

All 3/16-inch specimens were tested in a 120-kip Baldwin test machine as shown in Fig. 40. Clamps were secured 0.3 inch above and 0.3 inch below the notch centerline and on the specimen longitudinal centerline. Attached to the clamps were chains, which connected to a Baldwin TSMD Dual Range Extensometer below the test section. Shown also in Fig. 40 is the load-displacement plotter, load-accelerometer equipment, and oscillograph. The accelerometer can be seen in Fig. 40 on the top grip just below the load cell; for high-temperature tests the accelerometer was placed on the load cell. For low-temperature testing the accelerometer was placed on the lower load straps.

In general the test setup for the 3/8-inch thick specimens was the same as for the 3/16-inch thick. All specimens were tested in a 300-kip Baldwin Test Machine. Fig. 31 shows the low-temperature setup with the Extensometer and accelerometer below the cold chamber.

All 1.0-inch center-notch plates were tested in a Boeing-made 1000-kip hydraulic test machine shown in Fig. 41. The testing procedure was the same as for the 3/16-inch and 3/8-inch thick specimens. Crack lip displacement was measured with a calibrated Daytronic 104 BSS-160 linear variable differential transformer (LVDT). For high temperatures, a forced-air-cooled stainless steel jacket was placed around the LVDT core. The accelerometer was placed on a grip plate outside the temperature zone. It was considered that buckling restraint was unnecessary because of the low width-to-thickness ratios.

EXPERIMENTAL RESULTS

Fracture toughness data for the eight alloys are listed in Tables 13 through 21. Plane-stress critical-stress intensity values, K_{IC} , were calculated both with and without the plastic zone correction factor. Both values were included to show the effect of the plastic zone correction. Many specimens had net section stresses at or above the yield strength and at this point the worth of the plastic zone correction is questionable.

Because of their relevance to fracture measurements, the average yield strength, net section stress, and net-stress to yield-strength ratios were included in the tables. Because the stress intensity values tend to become conservative when the ratio increases above 0.8, these values are identified in the tables with an asterisk.

The critical stress intensity, K_{IC} , values were calculated from Equation (23) of Section 4:

$$K_{IC} = \sigma_g \left[w \tan \left(\frac{\pi a}{W} \right) \right]^{1/2}$$

TABLE 13 CENTER NOTCH PANEL DATA FOR 4340

SPECIMEN NO.	TEST TEMP. °F	GRAIN DIRECTION	GAGE inches	WIDTH inches	MAX. LOAD kips	LOAD AT "POP-IN" kips	SHEAR** percent	INITIAL 1/2 CRACK LENGTH inches	CRITICAL 1/2 CRACK LENGTH inches	σ_G ksi	σ_{ys} ksi	K_{1Cp} ksi√in	K_{1C} ksi√in	K_{IC} ksi√in	σ_N ksi	σ_N / σ_{ys}
CA 81	-110	L	.197	3.00	31.6	27.7	11	.50	.50	53.6	229.4	63.4	72.2	61.7	70.5	.350
CA 82	-110	L	.375	6.00	52.5	52.5	0	1.00	1.00	23.3	229.4	43.7	43.7	43.4	43.4	.153
CA 84	-110	L	1.06	9.02	168.0	168.0	0	1.50	1.50	18.6	229.4	42.6	42.6	42.3	42.3	.359
CA 85	RT	L	.197	3.00	65.9		98	.50	.70	111.5	213.1	85.8	222.0		184.2	.523
CA 86	RT	L	.197	3.00	66.2		98	.51	.70	112.0	213.1	113.0	223.0		185.2	.526
CA 98	RT	L	.376	6.00	125.5	120.0	32	1.00	1.30	55.7	213.1	88.2	126.3		122.5	.413
CA 88	RT	L	.375	6.00	108.3	98.3	17	.99	1.23	48.2	213.1	82.2	104.3	81.1	102.3	.383
CA 91	RT	L	1.01	9.02	383.8	383.8	8	1.50	1.55	42.2	213.1	97.6	99.6	96.2	97.6	.301
CA 92	RT	L	1.01	9.02	388.9	388.9	7	1.50	1.50	42.9	213.1	99.1	99.1	97.8	97.8	.300
CA 93	400	L	.197	3.00	57.1	50.7	98	.50	.79	96.7	184.7	122.7	227.5	112.5	174.8	1.10*
CA 87	400	L	.376	6.01	115.8	108.8	68	1.00	1.67	52.2	184.7	92.1	149.0	89.6	139.5	.625
CA 96	400	L	1.00	9.02	384.0	350.0	24	1.50	2.27	42.4	184.7	83.9	131.5	79.0	127.0	.463
CA 97	650	L	.197	3.00	63.0	60.1	100	.50	.71	106.8	162.4	160.0	275.0	134.0	172.0	1.24*
CA 94	650	L	.375	6.00	108.8	90.3	79	1.00	1.94	48.4	162.4	76.7	168.0	74.6	151.0	.807
CA 100	650	L	1.06	9.02	494.0		35	1.50	2.10	51.9	162.4		156.6		147.0	.598
CA 101	-110	T	.197	3.00	30.9	26.5	9	.50	.50	52.3	213.9	60.3	70.5	59.2	68.9	.367
CA 102	RT	T	.198	3.01	62.1		98	.50	.70	104.5	202.2		204.2		172.3	.969*
CA 103	RT	T	.198	3.00	61.7		98	.51	.70	104.0	202.2		209.0		171.9	.958*
CA 104	400	T	.197	3.00	52.7	48.1	98	.51	.83	89.4	185.5	117.9	211.0	106.7	168.5	.994*
CA 105	650	T	.198	3.00	60.7	53.2	99	.50	.63	102.1	155.2	118.2		117.7	155.8	1.14*

NO BUCKLING RESTRAINT USED DURING FRACTURE TEST

FRACTURE TEST LOADING RATE WAS 150 ksi/min, GROSS AREA STRESS

* THESE RATIOS ARE ABOVE THE .8 LIMIT RECOMMENDED BY THE ASTM

COMMITTEE FOR FRACTURE TOUGHNESS

** PERCENT SHEAR MEASURED AT A DISTANCE EQUAL TO TWO THICKNESSES OF PANEL FROM OUTSIDE EDGE

MAX.

FATIGUE DATA
SPEC. SIZE
InchesCYCLING
STRESS
ksiCYCLING
RATE
cpm

R

.188 x 3 x 9
.375 x 6 x 24
1.00 x 9 x 2419.8
14.0
11.41800
120 to 600
1375.05
.05
.05

TABLE 14 CENTER NOTCH PANEL DATA FOR 9Ni-4Co

SPECIMEN NO.	TEST TEMP. °F	GRAIN DIRECTION	GAGE inches	WIDTH inches	MAX. LOAD kips	LOAD AT "POP-IN" kips	SHEAR** percent	INITIAL 1/2 CRACK LENGTH inches	CRITICAL 1/2 CRACK LENGTH inches	σ_G ksi	σ_{ys} ksi	K_{ICP} ksi√in	K_{ICP} ksi√in	K_{IC} ksi√in	K_{IC} ksi√in	σ_N ksi	σ_N ksi
CB81	-110	L	.185	3.0	64.5		98	.50	.67	115.8	211.3					184.0	210.0
CB82	-110	L	.375	6.01	114.5	111.0	31	1.00	1.29	50.9	211.3	92.9		91.2		112.0	89.1
CB84	-110	L	.991	8.99	214.0	214.0	6	1.50	1.61	24.0	211.3	55.0		54.0		57.1	38.5
CB85	RT	L	.185	3.0	68.1		98	.50	.67	123.5	198.4					196.0	222.0
CB86	RT	L	.185	3.0	68.3		100	.51	0.70	121.0	198.4					198.0	231.0
CB87	RT	L	.375	6.0	207.8		98	1.02	1.60	92.1	198.4					238.0	197.5
CB88	RT	L	.375	6.0	223.5	188.3	98	1.00	1.55	98.8	198.4	166.0		156.0		249.0	205.5
CB91	RT	L	.984	8.99	343.8	325.0	18	1.50	2.04	38.9	198.4					106.5	69.8
CB92	RT	L	.994	8.99	346.7		10	1.50	2.0	38.9	198.4					106.5	70.0
CB93	400	L	.185	3.0	58.5	49.4	100	.50	0.78	101.8	169.1	132.0		117.0		178.0	219.0
CB94	400	L	.374	6.0	186.5	162.0	98	1.00	1.83	82.9	169.1	144.0		134.0		242.0	213.0
CB96	400	L	.992	8.98	318.8	250.	36	1.50	2.20	35.8	169.1	37.3		36.8		105.2	70.3
CB97	650	L	.185	3.0	62.6		100	.50	1.05	111.5	131.4					270.0	•
CB98	650	L	.375	6.00	245.8	105.7	100	1.00	1.85	109.1	131.4	92.0		87.2		322.0	286.0
CB100	650	L	.993	8.95	1,015.0		100	1.50	1.66	113.4	131.4					275.0	180.0
CB101	-110	T	.185	3.0	65.1	26.4	98	.50	0.69	116.4	220.6	64.2		62.8		189.0	217.0
CB102	RT	T	.185	3.0	UNK		100	.50	0.70		204.7					207.0	237.0
CB103	RT	T	.185	3.0	68.6	54.5	100	.50	0.72	123.8	204.7					187.0	214.0
CB104	400	T	.185	3.0	60.2	57.4	100	.50	.74	108.5	165.1					•	•
CB105	650	T	.185	3.0	62.2		100	.50	1.15	112.6	149.5					315.0	•

NO BUCKLING RESTRAINT USED DURING FRACTURE TEST

FRACTURE TEST LOADING RATE WAS 150 ksi/min, GROSS AREA STRESS

* THESE RATIOS ARE ABOVE THE .8 LIMIT RECOMMENDED BY THE ASTM

COMMITTEE FOR FRACTURE TOUGHNESS

** PERCENT SHEAR MEASURED AT A DISTANCE EQUAL TO TWO THICKNESSES OF PANEL FROM OUTSIDE EDGE

▲ ASSUMED • EXTREME DUCTILE FAILURE

FATIGUE DATA

SPEC. SIZE
Inches

MAX.

CYCLING
STRESS
ksiCYCLING
RATE
cpm

R

19.8

14.0

11.4

1800

120 to 600

1375

.05

.05

.05

TABLE 15 CENTER NOTCH PANEL DATA FOR AM 355

SPECIMEN NO.	TEST TEMP. °F	GRAIN DIRECTION	GAGE inches	WIDTH inches	MAX. LOAD kips	LOAD AT "POP-IN" kips	SHEAR** percent	INITIAL 1/2 CRACK LENGTH inches	CRITICAL 1/2 CRACK LENGTH inches	σ_G ksi	σ_{ys} ksi	K_{ICP} ksi√in	K_{IC} ksi√in	K_C ksi√in	σ_N ksi	$\frac{\sigma_N}{\sigma_{ys}}$
CC81	-110	L	.181	3.02	15.5	10.48	0	.50	.54	28.4	203.2	25.4	25.2	39.4	44.6	.220
CC82	-110	L	.375	6.00	33.0	33.0	0	1.00	1.00	14.7	203.2	27.4	27.3	27.3	22.0	.108
CC84	-110	L	.994	8.99	121.0	79.0	0	1.50	1.53	13.6	203.2	20.4	20.4	31.4	20.6	.101
CC85	RT	L	.182	3.01	54.5	33.2	42	.50	.70	100.0	166.7	84.3	80.1	164.0	187.0	1.12*
CC86	RT	L	.181	3.01	62.4	38.4	100	.50	.71	114.0	166.7	99.3	95.0	189.5	218.0	1.31*
CC87	RT	L	.384	6.01	116.8	81.7	17	1.00	1.16	50.6	166.7	67.2	65.9	103.2	82.4	.494
CC88	RT	L	.381	6.01	228.0	158.2	75	1.00	1.67	99.5	166.7	139.0	128.7	265.0	225.0	1.35*
CC91	RT	L	1.00	8.99	374.0	275.0	13	1.50	2.25	41.6	166.7	70.9	69.7	124.5	83.1	.499
CC92	RT	L	1.00	9.00	285.0	215.0	7	1.50	1.69	31.7	166.7	55.1	52.1	77.6	50.8	.305
CC93	400	L	.180	3.01	65.2	40.8	100	.50	.63	120.0	144.0	107.5	99.3	183.0	20.7	1.44*
CC94	400	L	.385	6.00	252.8		100	1.00	1.25	110.0	144.0	400.0		238.0	192.0	1.33*
CC96	400	L	1.01	9.00	816.0		66	1.50	1.98	90.0	144.0	332.3		246.0	200.0	1.390*
CC97	650	L	.185	3.00	52.2		100	.50	.75	94.1	148.2	282.0		162.7	188.0	1.27*
CC98	650	L	.377	6.01	198.3	179.0	100	1.00	1.59	87.3	148.2	164.0	146.7	224.0	186.8	1.26*
CC100	650	L	.992	9.00	619.0	595.0	70	1.50	2.06	69.4	148.2	165.0	151.7	194.5	127.8	.863*
CC101	-110	T	.181	3.00	30.5	24.9	17	.50	.55	56.2	179.0	62.2	60.4	78.0	88.7	.496
CC102	RT	T	.181	3.00	38.0	26.7	17	.50	.69	70.0	161.1	67.2	63.4	113.7	129.5	.803
CC103	RT	T	.181	3.00	45.9	28.3	25	.50	.58	84.4	161.1	76.7	67.4	122.0	138.0	.857*
CC104	400	T	.182	3.01	52.3		83	.51	.55	95.7	143.1	170.3		133.2	151.0	1.05*
CC105	650	T	.181	3.00	44.7	43.0	100	.50	.79	82.3	142.0	118.7	104.0	148.7	174.0	1.22*

NO BUCKLING RESTRAINT USED DURING FRACTURE TEST

FRACTURE TEST LOADING RATE WAS 150 ksi/min, GROSS AREA STRESS

MAX.

CYCLING STRESS ksi

CYCLING RATE cpm

R

* THESE RATIOS ARE ABOVE THE .8 LIMIT RECOMMENDED BY THE ASTM

COMMITTEE FOR FRACTURE TOUGHNESS

** PERCENT SHEAR MEASURED AT A DISTANCE EQUAL TO TWO THICKNESSES OF PANEL FROM OUTSIDE EDGE

• EXTREME DUCTILE FAILURE

FATIGUE DATA SPEC. SIZE inches

.188 x 3 x 9

.375 x 6 x 24

1.00 x 9 x 24

CYCLING STRESS ksi

19.8

14.0

11.4

CYCLING RATE cpm

1800

120 to 600

1375

R

.05

.05

.05

TABLE 17 CENTER NOTCH PANEL DATA FOR INCO 718

SPECIMEN NO.	TEST TEMP. °F	GRAIN DIRECTION	GAGE inches	WIDTH inches	MAX. LOAD kips	LOAD AT "POP-IN" kips	SHEAR** percent	INITIAL 1/2 CRACK LENGTH inches	CRITICAL 1/2 CRACK LENGTH inches	σ_G ksi	K_{IcP} ksi√in	K_{Ic} ksi√in	K_{Cp} ksi√in	K_C ksi√in	σ_4 ksi	σ_N $\frac{\sigma_4}{\sigma_{ys}}$
CE81	-110	L	.185	3.00	65.9		100	.50	.59	118.6			229.0	173.0	195.5	1.14*
CE82	-110	L	.383	6.00	236.8		89	1.12	1.37*	106.2			338.0	243.0	171.0	.995*
CE84	-110	L	1.009	9.01	917.5		8	1.50	1.90	100.9			330.0	267.0	176.0	1.02*
CE85	RT	L	.194	3.00	65.0		100	.50	.64	111.8			306.	172.0	194.0	1.24*
CE86	RT	L	.196	3.00	65.2		100	.50	.63*	111.1			285.0	169.5	191.8	1.23*
CE87	RT	L	.380	6.01	225.0		100	1.15	1.45	98.5			349.0	234.2	191.0	1.22*
CE88	RT	L	.373	6.01	217.2		98	1.15	1.46	96.6			354.0	231.0	190.5	1.22*
CE91	RT	L	.985	9.00	870.0		25	1.50	1.89	98.3			341.0	258.0	169.5	1.09*
CE92	RT	L	.992	9.00	900.0		27	1.50	1.99	100.4			404.0	275.0	174.0	1.12*
CE93	400	L	.196	3.00	59.8		100	.50	.71	101.8			249.0	168.5	193.0	1.32*
CE94	400	L	.380	6.00	203.0		100	1.16	1.39	89.1			289.0	206.1	165.3	1.13*
CE96	400	L	1.000	9.00	864.0		68	1.50	1.62	96.1			288.0	229.0	150.0	1.02*
CE97	650	L	.195	3.00	58.0	52.6	100	.50	.84	99.1		123.6	330.0	188.0	255.0	1.77*
CE98	650	L	.383	6.00	197.5		100	1.15	1.42	85.9			274.0	201.0	163.0	1.13*
CE100	650	L	1.000	9.01	750.0	332.0	65	1.64	2.25*	83.3		189.0	345.0	249.0	166.5	1.16*
CE101	-110	T	.194	3.00	65.6	29.0	100	.50	.61	112.4		136.4	246.0	167.0	188.3	1.15*
CE102	RT	T	.194	3.00	63.6		100	.50	.62	109.3			281.0	164.7	186.0	1.20*
CE103	RT	T	.195	3.00	64.9		100	.50	.64	110.9			297.0	177.2	193.5	1.25*
CE104	400	T	.191	3.00	57.4		98	.50	.69	100.0			271.0	161.6	182.2	1.25*
CE105	650	T	.189	3.00	54.7		98	.50	.77	96.4			298.0	170.5	197.5	1.44*

NO BUCKLING RESTRAINT USED DURING FRACTURE TEST

FRACTURE TEST LOADING RATE WAS 150 ksi/min, GROSS AREA STRESS

MAX.

CYCLING STRESS

CYCLING RATE

R

FATIGUE DATA SPEC. SIZE

* THESE RATIOS ARE ABOVE THE .8 LIMIT RECOMMENDED BY THE ASTM

COMMITTEE FOR FRACTURE TOUGHNESS

** PERCENT SHEAR MEASURED AT A DISTANCE EQUAL TO TWO THICKNESSES

OF PANEL FROM OUTSIDE EDGE

• EXTREME DUCTILE FAILURE

Inches

ksi

cpm

.05

.188 x 3 x 9

19.8

1800

.05

.375 x 6 x 24

14.0

120 to 600

.05

1.00 x 9 x 24

11.4

1375

.05

TABLE 18 CENTER NOTCH PANEL DATA FOR Ti 6Al-4V

SPECIMEN NO.	TEST TEMP. °F	GRAIN DIRECTION	GAGE inches	WIDTH inches	MAX. LOAD kips	LOAD AT "POP-IN" kips	SHEAR ^{***} percent	INITIAL CRACK LENGTH inches	CRITICAL CRACK LENGTH inches	σ_G ksi	σ_{ys} ksi	K_{ICp} ksi√in	K_{IC} ksi√in	K_C ksi√in	σ_N ksi	$\frac{\sigma_N}{\sigma_{ys}}$
CF81	-110	L	.190	2.99	34.9		84	.50	.72	61.4	176.4			103.	118.0	.669
CF82	-110	L	.383	5.97	92.8	74.5	46	1.01	1.73	40.6	176.4	61.4	60.4	113.	96.5	.547
CF84	-110	L	.995	8.98	228.0	184.0	72	1.50	2.14	25.5	176.4	47.3	47.0	73.6	48.8	.277
CF85	RT	L	.190	2.99	38.8		100	.50	.81	68.4	147.1			126.3	149	1.01*
CF86	RT	L	.189	2.99	33.0		66	.50	.94	58.2	147.1			124.	157.4	1.07*
CF87	RT	L	.382	5.97	122.0		90	1.01	1.60	53.5	147.1			138.	113.2	.761
CF88	RT	L	.332	5.97	118.3		74	1.01	1.59	51.9	147.1			133.2	111.0	.756
CF91	RT	L	.998	8.97	253.0		18	1.50	2.60	28.3	147.1			95.6	67.3	.458
CF92	RT	L	.732	8.98	358.0		59	1.50	2.50 ^Δ	54.4	147.1			183.	123.0	.837
CF93	400	L	.190	2.99	46.3		100	.50	.86	81.6	108.1			159.	192	1.77*
CF94	400	L	.383	5.97	162.5		100	1.01	1.82	71.3	108.1			207.	187.0	1.73*
CF96	400	L	.999	8.98	595.0		69	1.50	2.28	67.0	108.1			203.	135	1.25*
CF97	650	L	.192	2.98	37.4		100	.50	.92	65.6	95.0			137.	171.4	1.80*
CF98	650	L	.383	5.97	140.5		100	1.00	1.85	61.6	95.0			182.	161.8	1.70*
CF100	650	L	1.005	8.98	569.0		100	1.50	2.35	63.0	95.0			196.	90.	.948*
CF101	-110	T	.189	2.99	25.2		45	.50	.68	44.6	174.0			71.8	81.8	.470
CF102	RT	T	.191	2.98	27.4		50	.50	.92	48.4	152.2			101.5	126.0	.828*
CF103	RT	T	.192	2.98	27.4		79	.50	.80	48.0	152.2			87.8	103.3	.679
CF104	400	T	.192	2.98	44.1		100	.50	.90 ^Δ	77.3	111.0			157.0	195.0	1.75*
CF105	650	T	.191	2.98	39.2		98	.50	.95	69.2	97.8			149.0	190.0	1.94*

NO BUCKLING RESTRAINT USED DURING FRACTURE TEST

FRACTURE TEST LOADING RATE WAS 150 ksi/min, GROSS AREA STRESS

* THESE RATIOS ARE ABOVE THE .8 LIMIT RECOMMENDED BY THE ASTM

COMMITTEE FOR FRACTURE TOUGHNESS

** PERCENT SHEAR MEASURED AT A DISTANCE EQUAL TO TWO THICKNESSES OF PANEL FROM OUTSIDE EDGE

Δ ESTIMATED • EXTREME DUCTILE FAILURE

MAX.

FATIGUE DATA
SPEC. SIZE
inchesCYCLING
STRESS
ksiCYCLING
RATE
cpm

R

.188 x 3 x 9
.375 x 6 x 24
1.00 x 9 x 2419.8
14.0
11.41800
120 to 600
1375.05
.05
.05

TABLE 19 CENTER NOTCH PANEL DATA FOR Ti 6Al-4V-2Sn ANN

SPECIMEN NO.	TEST TEMP. °F	GRAIN DIRECTION	GAGE inches	WIDTH inches	MAX. LOAD kips	LOAD AT "POP-IN" kips	SHEAR** percent	INITIAL CRACK LENGTH inches	CRITICAL 1/2 CRACK LENGTH inches	σ_G ksi	σ_{ys} ksi	K_{IC} ksi√in	K_{ICP} ksi√in	K_{ICP} ksi√in	K_C ksi√in	σ_N ksi	$\frac{\sigma_N}{\sigma_{ys}}$
CH81	-110	L	.183	2.99	39.1	21.4	67	.50	.64	71.3	171.8	51.4	119.7	52.4	110.0	124.9	.727
CH82	-110	L	.382	6.00	73.8	42.4	23	1.00	1.48	32.3	171.8	27.7	79.6	27.8	78.6	63.6	.370
CH84	-110	L	1.00	9.00	109.0	109.0	4	1.50	1.78	12.1	171.8	27.6	31.4	27.4	30.6	20.0	.116
CH85	RT	L	.194	2.99	46.1		100	.51	.77	79.2	142.1		194.0		139.5	162.9	1.15
CH86	RT	L	.182	2.99	43.9		100	.50	.74	80.6	142.1		182.0		138.5	159.5	1.12*
CH87	RT	L	.383	6.00	149.8		66	1.00	1.56	65.2	142.1		191.0		165.0	136.0	.957*
CH88	RT	L	.381	6.00	146.0	86.8	64	.98	1.58	63.8	142.1	71.6	191.7	70.2	166.5	135.0	.950*
CH91	RT	L	.994	9.00	315.7	209.0	20	1.50	1.75	35.3	142.1	53.3	90.4	54.0	88.5	57.8	.408
CH92	RT	L	.990	9.00	311.1	233.3	17	1.50	1.79	34.9	142.1	59.4	91.2	60.4	88.3	58.0	.408
CH93	400	L	.179	2.99	40.8		100	.51	.88	76.4	105.7				152.0	185.0	1.76*
CH94	400	L	.384	6.00	165.4		100	1.00	1.60	71.9	105.7				185.0	153.5	1.45*
CH96	400	L	1.01	9.00	585.0		57	1.50	1.91	64.7	105.7		221.0		172.0	112.0	1.06*
CH97	650	L	.188	2.99	35.7		100	.50	.92	63.5	91.7				137.5	154.5	1.68*
CH98	650	L	.382	6.00	150.8		100	.98	1.71	65.9	91.7				180.5	160.1	1.74*
CH100	650	L	1.00	9.01	563.0		68	1.50	1.99	62.4	91.7		296.0		171.0	116.0	1.26*
CH101	-110	T	.185	2.99	17.4	13.5	19	.51	.70	31.5	169.5	32.6	52.8	32.8	51.3	59.2	.349
CH102	RT	T	.190	2.99	40.6		76	.51	.75	71.5	142.5		151.5		124.0	145.0	1.02*
CH103	RT	T	.190	2.99	32.7		47	.51	.80	57.8	142.5		119.7		105.9	123.9	.869*
CH104	400	T	.195	2.99	43.1		98	.50	.85	73.9	104.6				142.5	171.5	1.64*
CH105	650	T	.194	2.99	38.8		100	.51	.91	66.8	100.3				136.8	171.0	1.71*

NO BUCKLING RESTRAINT USED DURING FRACTURE TEST

FRACTURE TEST LOADING RATE WAS 150 ksi/min, GROSS AREA STRESS

- * THESE RATIOS ARE ABOVE THE .8 LIMIT RECOMMENDED BY THE ASTM COMMITTEE FOR FRACTURE TOUGHNESS
- ** PERCENT SHEAR MEASURED AT A DISTANCE EQUAL TO TWO THICKNESSES OF PANEL FROM OUTSIDE EDGE
- EXTREME DUCTILE FAILURE

FATIGUE DATA			MAX.		
SPEC. SIZE			CYCLING		
Inches			STRESS		
			RATE		
			R		
.188 x 3 x 9			19.8		
.375 x 6 x 24			14.0		
1.00 x 9 x 24			11.4		
			1800		
			120 to 600		
			1375		
			.05		
			.05		
			.05		

TABLE 20 CENTER NOTCH PANEL DATA FOR Ti 6Al-6V-2Sn STA

SPECIMEN NO.	TEST TEMP. °F	GRAIN DIRECTION	GAGE inches	WIDTH inches	MAX. LOAD kips	LOAD AT "POP-IN" kips	SHEAR** percent	INITIAL 1/2 CRACK LENGTH inches	CRITICAL 1/2 CRACK LENGTH inches	σ_G ksi	K_{ICP} ksi√in	K_{IC} ksi√in	K_C ksi√in	σ_N ksi	$\frac{\sigma_N}{\sigma_{ys}}$
CG81	-110	L	.195	2.99	19.7	19.2	13	.50	.70	33.8	43.8	43.1	55.4	63.5	.33
CG82	-110	L	.383	6.00	46.5	39.8	0	1.00	1.05	20.2	37.8	37.2	38.7	31.2	.16
CG84	-110	L	1.00	9.00	105.0	87.0	0	1.50	1.56	11.6	26.6	26.3	27.0	17.8	.09
CG85	RT	L	.193	2.99	28.6		52	.50	.79	49.8	36.0		90.0	105.0	.65
CG86	RT	L	.197	2.99	27.9		45	.50	.84	47.4	92.5		90.5	108.0	.67
CG97	650	L	.197	2.98	44.6		95	.50	.78	75.7	261.0●		135.5	159.5	1.50*
CG98	650	L	.380	5.99	158.8		95	1.00	1.64	69.7	341.0●		182.0	154.0	1.45*
CG100	650	L	.987	8.96	490.0		45	1.50	2.25	55.4	203.0		166.6	111.5	1.05*
CG101	-110	T	.192	2.99	16.4	15.12	0	.50	.63	55.6	38.0	37.4	43.7	49.3	.26
CG102	RT	T	.195	2.99	29.8	22.2	40	.50	.69	50.9	70.5	66.7	82.9	92.0	.55
CG103	RT	T	.181	2.99	20.6	20.6	31	.50	.69	39.8	52.8	51.6	64.8	70.6	.42
CG105	650	T	.190	2.99	39.8	23.5	100	.50	.82	70.0	82.0	74.1	137.5	155.0	1.34*

NO BUCKLING RESTRAINT USED DURING FRACTURE TEST

FRACTURE TEST LOADING RATE WAS 150 ksi/min, GROSS AREA STRESS

* THESE RATIOS ARE ABOVE THE .8 LIMIT RECOMMENDED BY THE ASTM

COMMITTEE FOR FRACTURE TOUGHNESS

** PERCENT SHEAR MEASURED AT A DISTANCE EQUAL TO TWO THICKNESSES

OF PANEL FROM OUTSIDE EDGE

● EXTREME DUCTILE FAILURE

MAX.

FATIGUE DATA SPEC. SIZE	CYCLING STRESS	CYCLING RATE	R
inches	ksi	cpm	
.188 x 3 x 9	19.8	1800	.05
.375 x 6 x 24	14.0	120 to 600	.05
1.00 x 9 x 24	11.4	1375	.05

TABLE 21 CENTER NOTCH PANEL DATA FOR PH 13-8 Mo

SPECIMEN NO.	TEST TEMP. °F	GRAIN DIRECTION	GAGE inches	WIDTH inches	MAX. LOAD kips	LOAD AT "POP-IN" kips	SHEAR** percent	INITIAL 1/2 CRACK LENGTH inches	CRITICAL 1/2 CRACK LENGTH inches	σ_G ksi	σ_{ys} ksi	K_{ICP} ksi√in	K_{ICP} ksi√in	K_{IC} ksi√in	K_C ksi√in	σ_N ksi	$\frac{\sigma_N}{\sigma_{ys}}$
CJ81	-110	L	.183	2.99	20.3	19.6	0	.50	.50	37.1	219.1	47.6	49.5	47.1	48.7	55.6	.25
CJ82	-110	L	.378	6.00	51.8	47.8	0	1.00	1.06	22.8	219.1	39.3	44.3	39.1	47.4	35.3	.16
CJ84	-110	L	1.005	8.62	154.0	154.0	0	1.50	1.50	17.2	219.1	39.4	39.4	39.2	39.2	27.3	.12
CJ85	RT	L	.190	2.99	72.5	48.2	100	.50	.68	128.0	205.0	119	293	112	206	234	1.14*
CJ86	RT	L	.191	2.99	71.7	43.5	100	.50	.68	125.5	205.0	106	278	100	202	230	1.12*
CJ87	RT	L	.377	6.00	152.0	109.1	31	1.00	1.19	67.0	205.0	92.0	146	89.8	139	112	.55
CJ88	RT	L	.377	6.01	137.0	108.9	33	1.00	1.34	60.4	205.0	91.5	141	89.0	136	101	.49
CJ91	RT	L	1.004	8.62	381.0	381.0	5	1.50	1.60	44.0	205.0	97.5	106.6	95.4	104.8	69.8	.34
CJ92	RT	L	1.004	8.62	308.0	294.0	3	1.50	1.65	35.5	205.0	78.9	87.3	77.5	86.3	57.7	.28
CJ93	400	L	.190	2.99	67.6		100	.50	.68	119.6	180.2	292			192	218	1.21*
CJ94	400	L	.377	6.00	261.3		100	.99	1.17	115.0	180.2	298			236	189	1.05*
CJ96	400	L	1.004	8.61	884.0			1.50	1.63	102.0	180.2	289			246	164	.91*
CJ97	650	L	.189	2.99	61.7	31.6	98	.50	.57	109.0	165.4	76.6	202	73.5	155	176	1.06*
CJ98	650	L	.377	6.01	235.0		160	1.00	1.22	103.5	165.4		281		219	175	1.06*
CJ100	650	L	1.005	8.61	756.0		95	1.50	1.80	87.8	165.4		262		226	150	.91*
CJ101	-110	T	.192	2.99	24.9	24.9	0	.50	.50	43.4	218.0	58.2	58.2	57.1	57.1	62.8	.29
CJ102	RT	T	.197	2.99	50.3	42.5	37	.50	.77	85.7	195.4	101	171.0	95.3	151	176.0	.90*
CJ103	RT	T	.197	2.99	64.1	43.0	39	.50	.74	109.0	195.4	85.8	256	82.4	186	214	1.10*
CJ104	400	T	.196	2.99	65.1	57.7	100	.50	.75	111.0	179.1	148	278	130	171	223.0	1.25*
CJ105	650	T	.195	2.99	62.6		100	.50	.91	107.0	161.7		346 ●		220	275	1.70*

NO BUCKLING RESTRAINT USED DURING FRACTURE TEST

FRACTURE TEST LOADING RATE WAS 150 ksi/min, GROSS AREA STRESS

* THESE RATIOS ARE ABOVE THE .8 LIMIT RECOMMENDED BY THE ASTM

COMMITTEE FOR FRACTURE TOUGHNESS

** PERCENT SHEAR MEASURED AT A DISTANCE EQUAL TO TWO THICKNESSES OF PANEL FROM OUTSIDE EDGE

● EXTREME DUCTILE FAILURE

MAX.

FATIGUE DATA
SPEC. SIZE
InchesCYCLING
STRESS
ksiCYCLING
RATE
cpm

R

.188 x 3 x 9

.375 x 6 x 24

1.00 x 9 x 24

19.8

14.0

11.4

.05

.05

.05

Stress intensity values corrected for the plastic zone at the tip of the crack are shown in the tables as $K_{C(p)}$. Calculations were made using Equation (27) of Section 4:

$$K_{C(p)} = \sigma_g \left[w \tan \left(\frac{\pi a}{W} \right) + \frac{K_c^2}{2W\sigma_{ys}^2} \right]^{1/2}$$

The equation was solved graphically by the method presented by the ASTM Committee on Fracture Testing of High-Strength Materials.

In Fig. 42 through 50 the stress intensity values, K_C , are plotted against testing temperature. Variation of stress intensity with thickness is also shown by including the 3/16, 3/8, and 1-inch thick panels in the same plot. As a further reminder that some of the data are conservative, the data points with net-stress to yield-stress ratios greater than 0.8 are accompanied by a vertical arrow. Stress intensity values corrected for the plastic zone have been plotted against test temperature in Figs. 51 through 59. In several instances the corrected values were extremely high because of high net section stresses. These data were too high to plot conveniently and since it was of doubtful value the points were not plotted. The information, however, was included in the tables.

Pop-in loads, determined from load-displacement curves and load-accelerometer-oscillograph plots, are included in the tables. Typical load-displacement curves for center-notch specimens tested at -110° F, room temperature, and 400° F are shown in Figs. 60, 61 and 62. It should be noted that all center-notch displacement curves are essentially crack lip displacement curves. Due to the finite size of displacement sensing equipment, all measurements were referenced from points 0.3 inch above and below the notch centerline on the specimen longitudinal centerline.

A load-time trace and accelerometer-time trace is shown in Fig. 63; only the portion of the oscillograph plot where pop-in bursts were noted, is shown.

Gross area stresses, σ_g , were also included in the tables. Since the net-stress to yield-stress ratios were so high for most of the 3/16-inch panels, the gross area stress or residual strength was plotted against test temperature in Figs. 64 through 72. It was felt that residual strengths for these panels were of more significance than stress intensity values. Both longitudinal and transverse data were included in the same plot to compare the effect of grain direction on toughness.

Another measure of relative toughness made on the center notched specimens was the percent-of-shear zone on the fracture face. The procedure recommended by the ASTM Fracture Committee was to make the measurement at a point between one and two thicknesses from the specimen edge. In this study, the line of measurement was taken at twice the thickness from the panel edge. These measurements are also listed in the tables.

For a visual comparison of fracture characteristics, photographs of the 3/8 and 1-inch thick specimen fracture faces are included in Fig. 73 through 81.

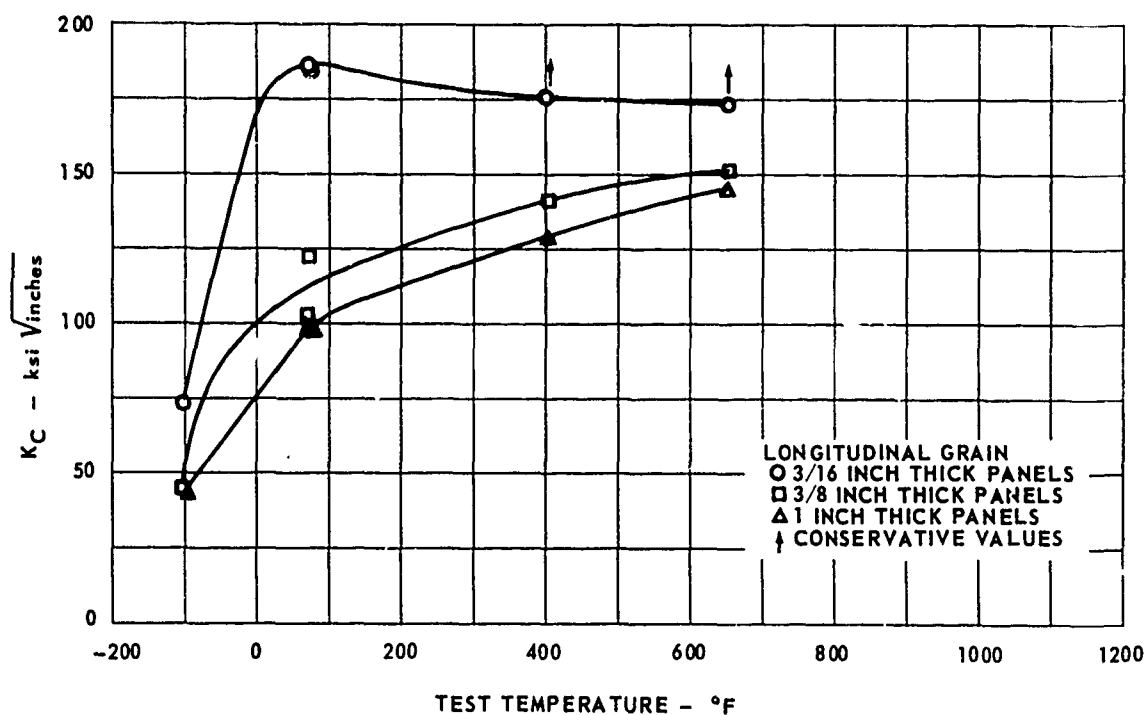


FIG. 42 K_C DATA FOR CENTER NOTCH PANELS OF 4340

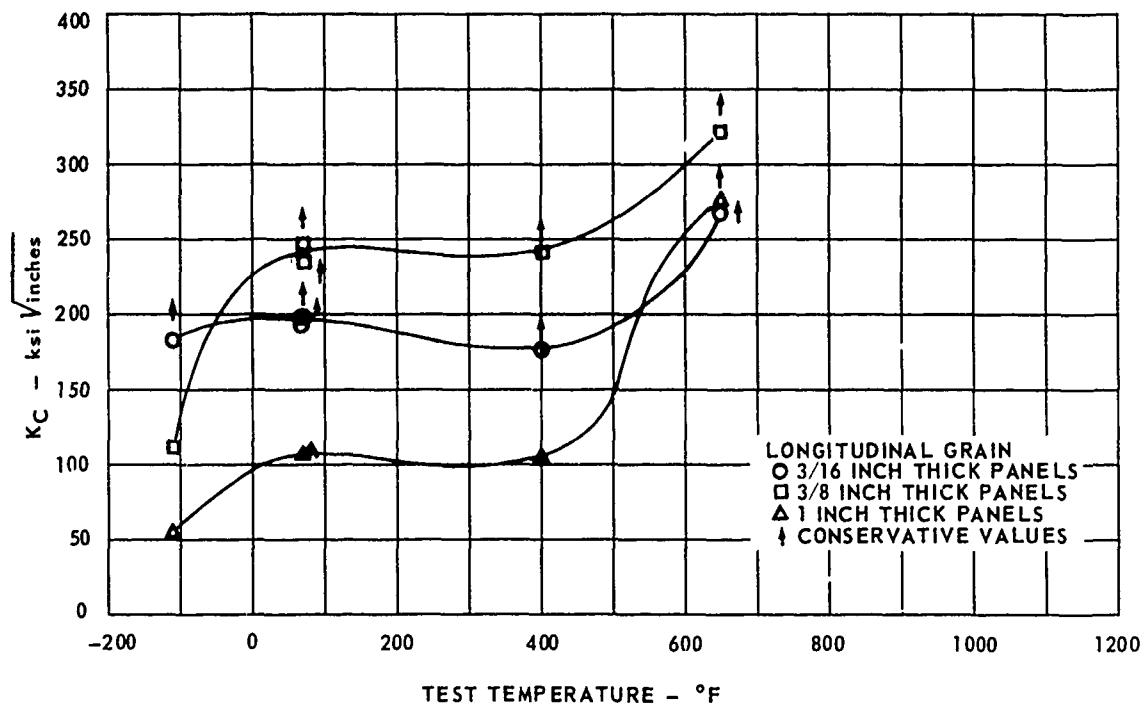


FIG. 43 K_C DATA FOR CENTER NOTCH PANELS OF 9 Ni-4Co

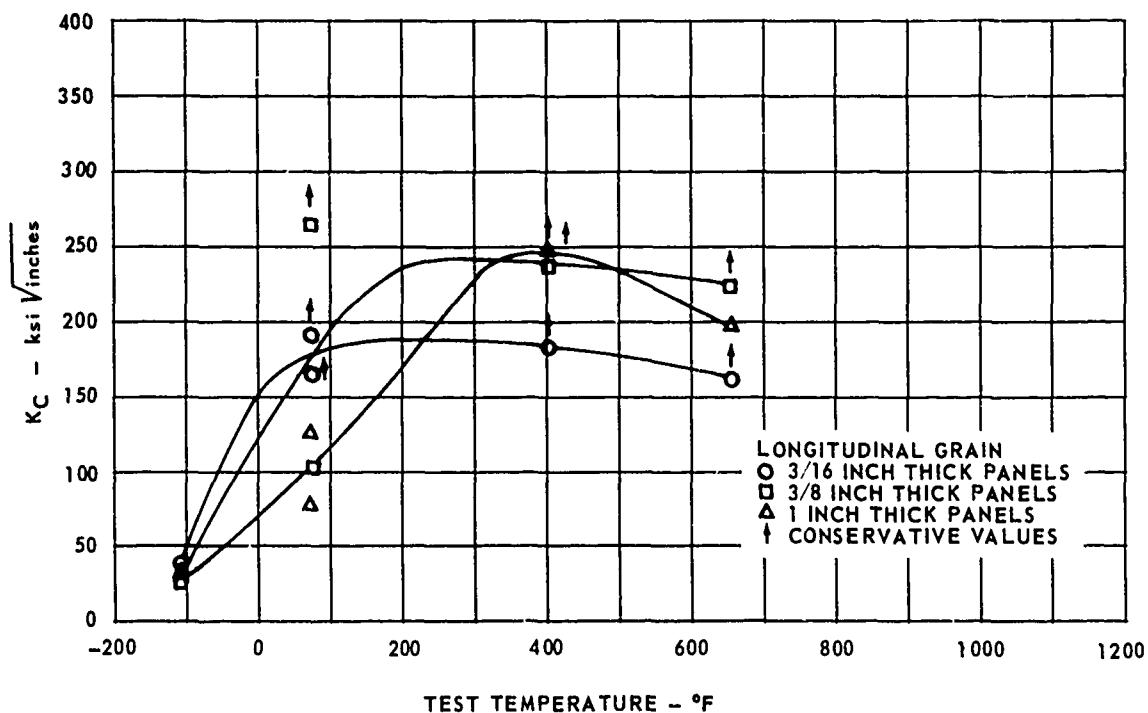


FIG. 44 K_{IC} DATA FOR CENTER NOTCH PANELS OF AM 355

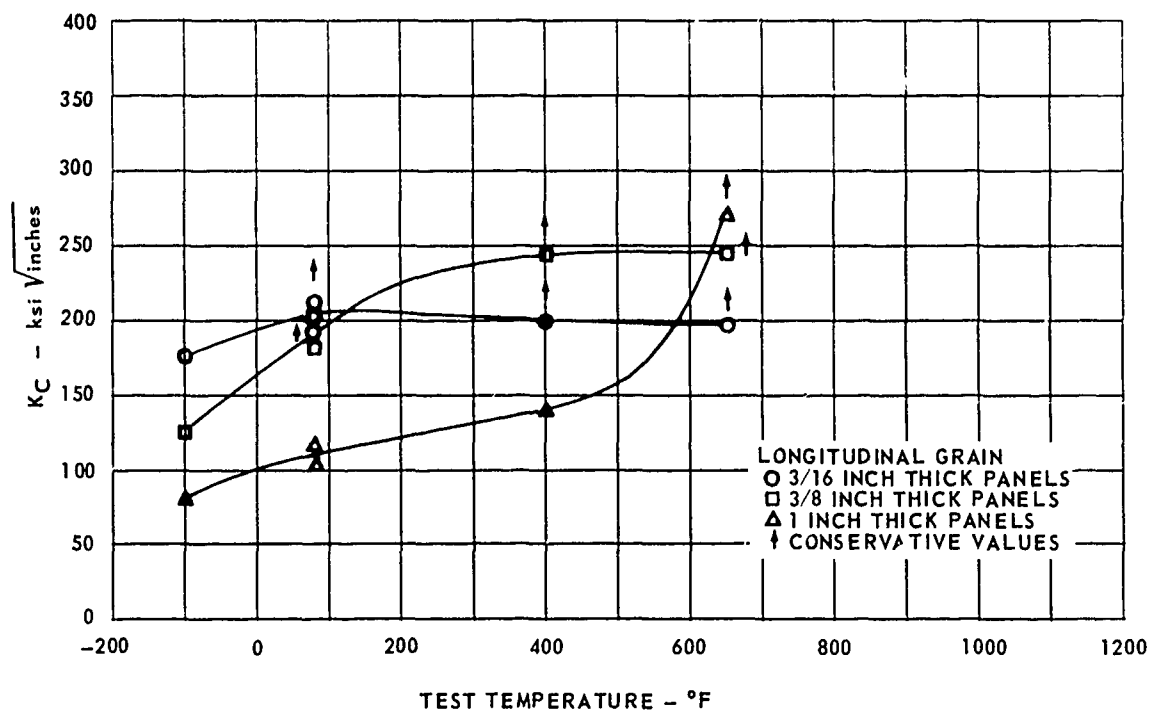


FIG. 45 K_{IC} DATA FOR CENTER NOTCH PANELS OF MARAGING 250

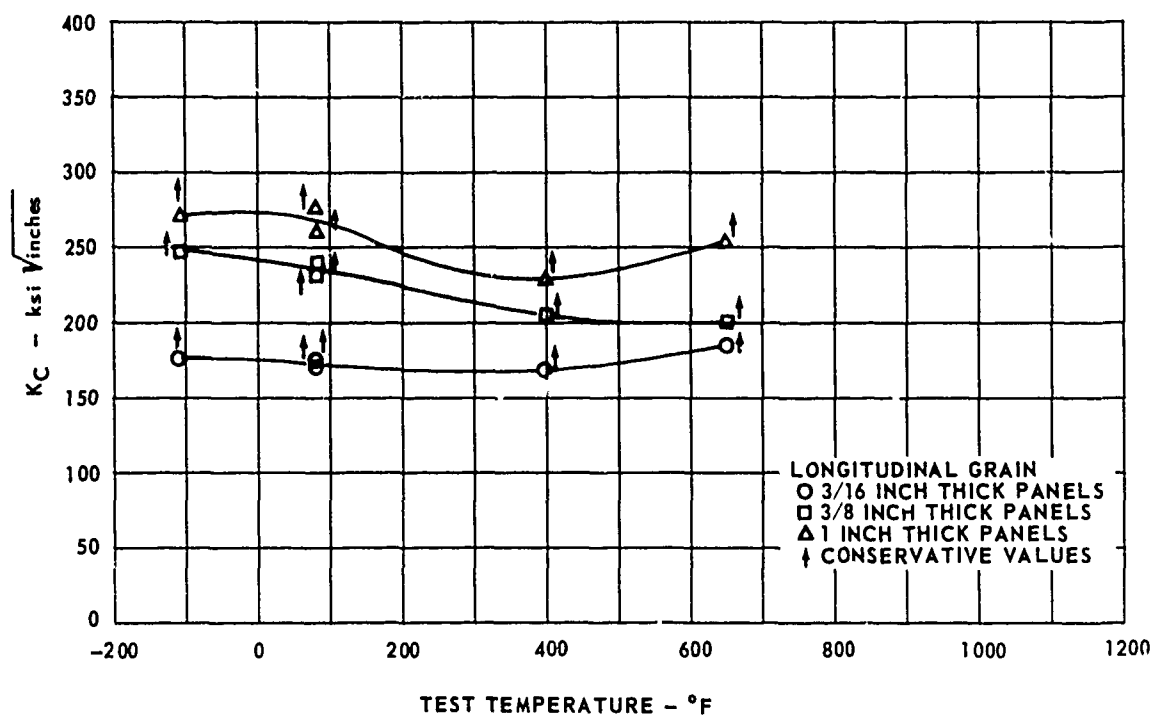


FIG. 46 K_{IC} DATA FOR CENTER NOTCH PANELS OF INCO 718

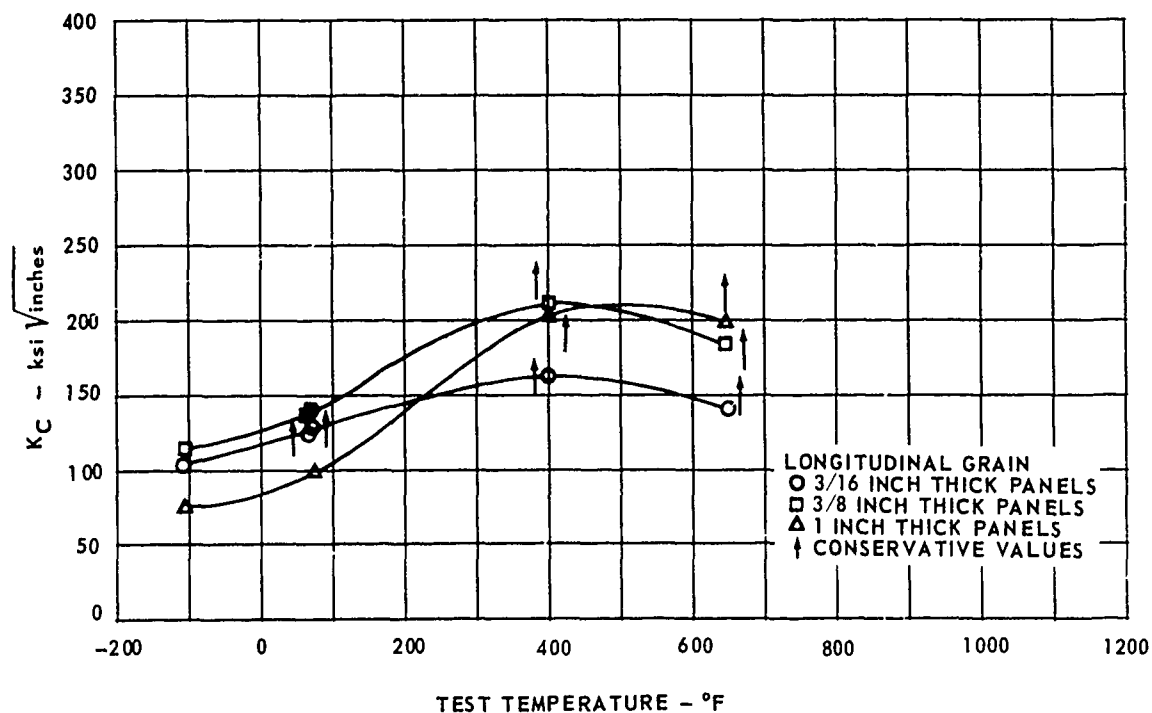


FIG. 47 K_{IC} DATA FOR CENTER NOTCH PANELS OF Ti 6Al-4V

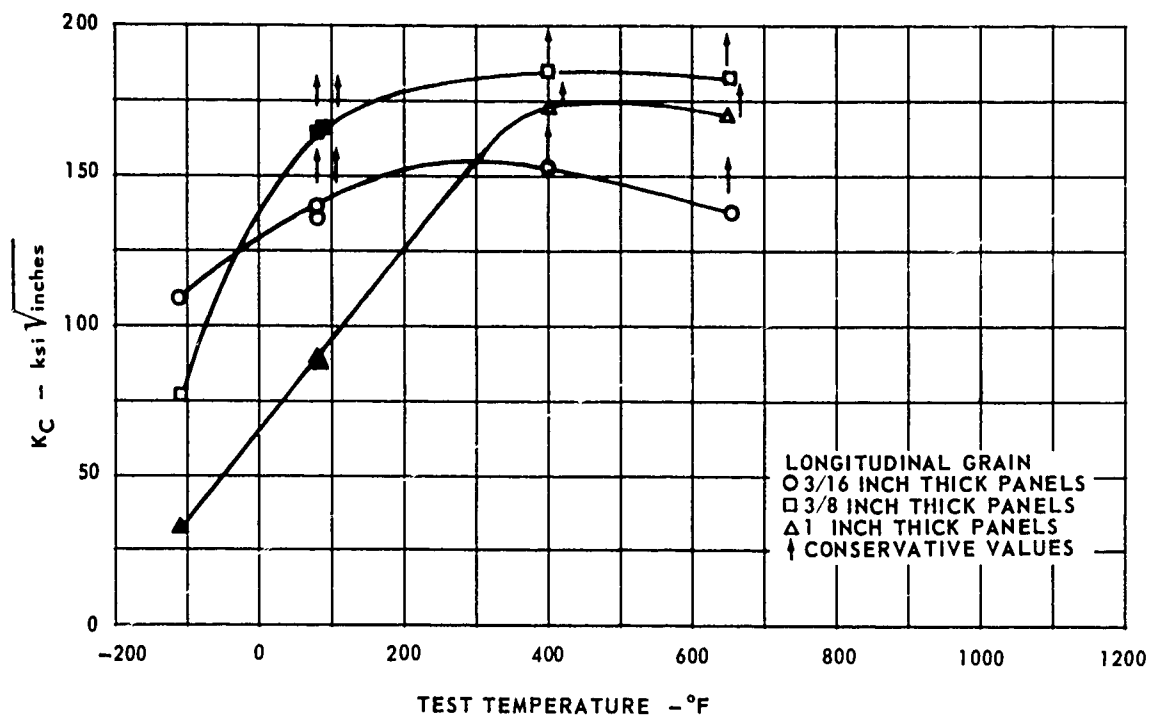


FIG. 48 K_C DATA FOR CENTER NOTCH PANELS OF Ti 6Al-6V-2Sn ANN

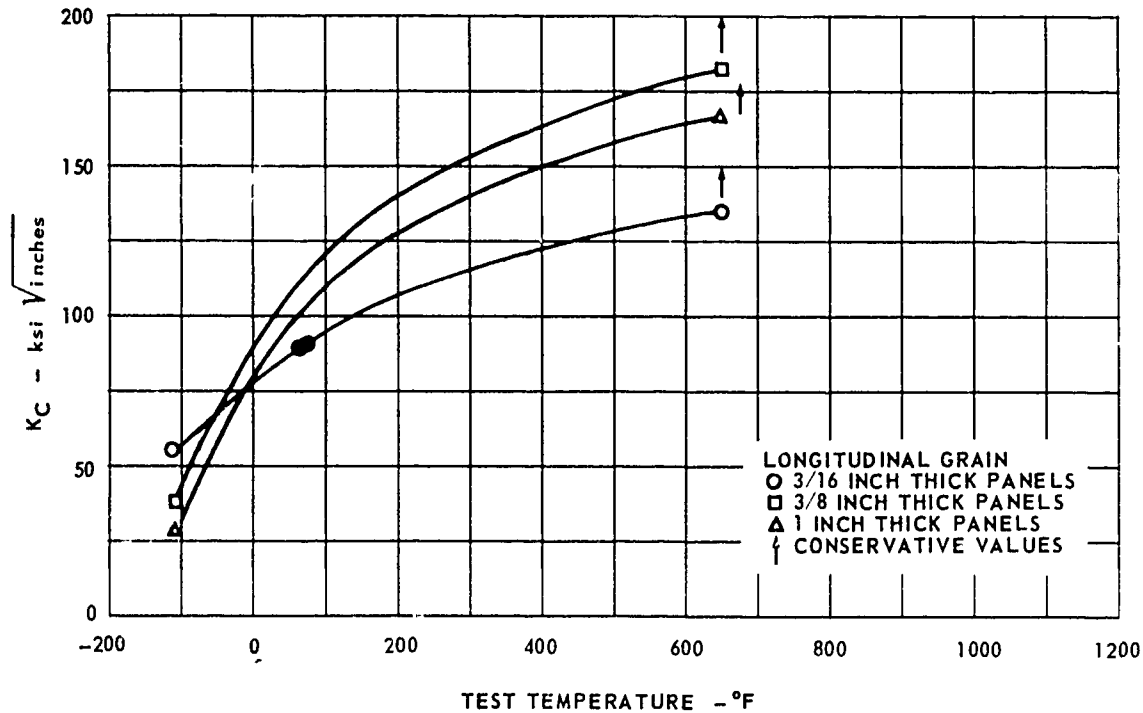


FIG. 49 K_C DATA FOR CENTER NOTCH PANELS OF Ti 6Al-6V-2Sn STA

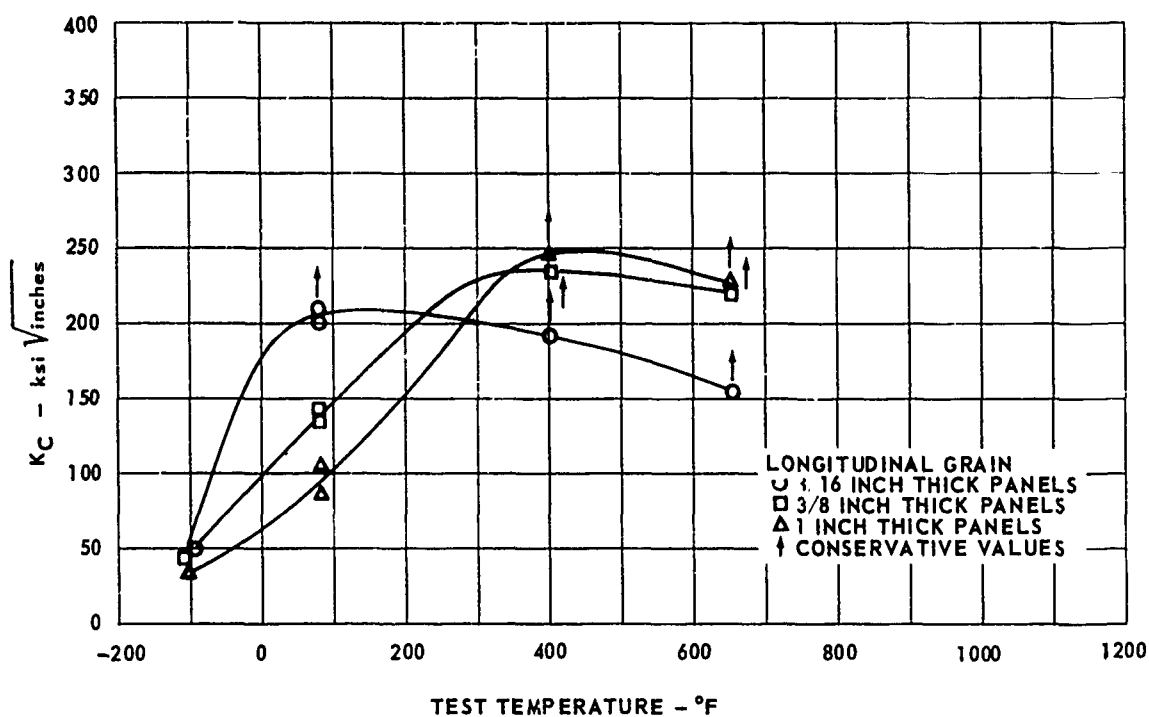


FIG. 50 K_C DATA FOR CENTER NOTCH PANELS OF PH 13-8 Mo

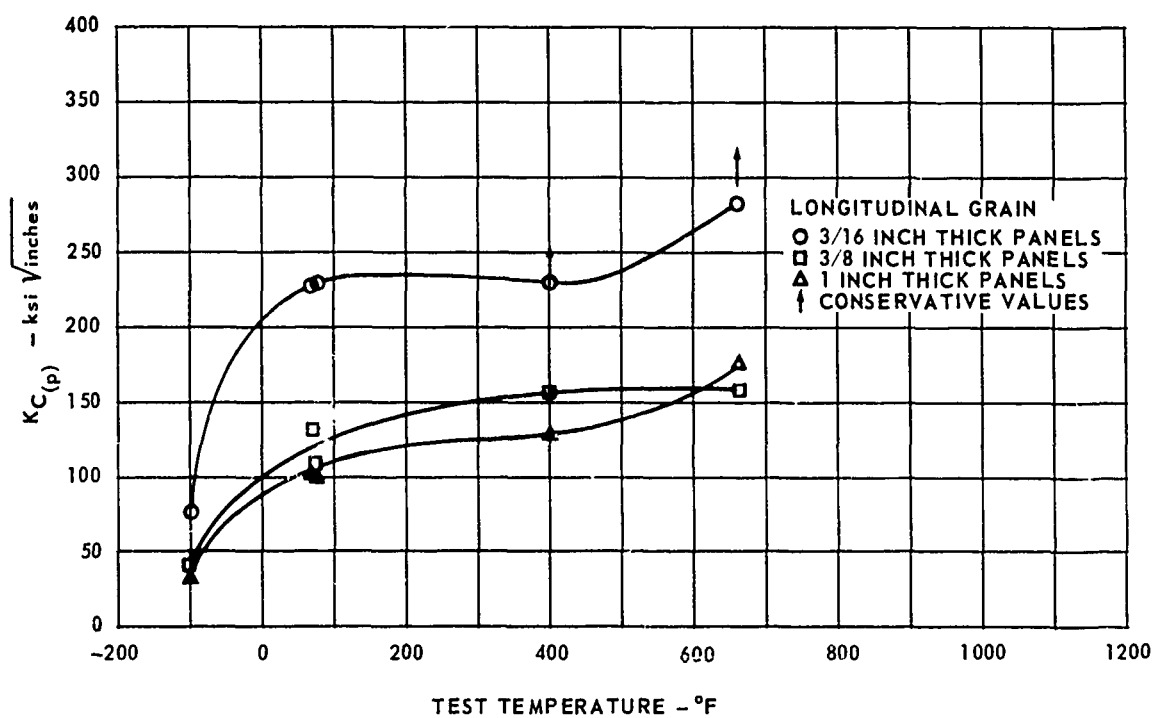


FIG. 51 $K_{C(p)}$ DATA FOR CENTER NOTCH PANELS OF 4340

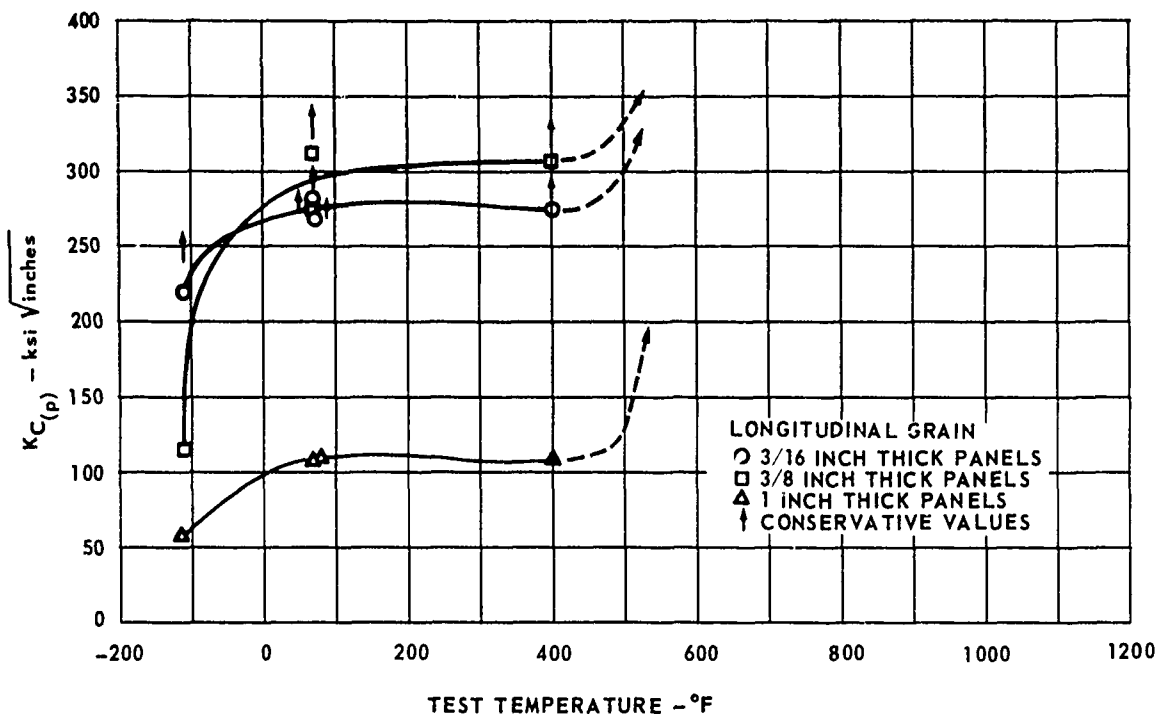


FIG. 52 $K_{C(p)}$ DATA FOR CENTER NOTCH PANELS OF 9 Ni-4Co

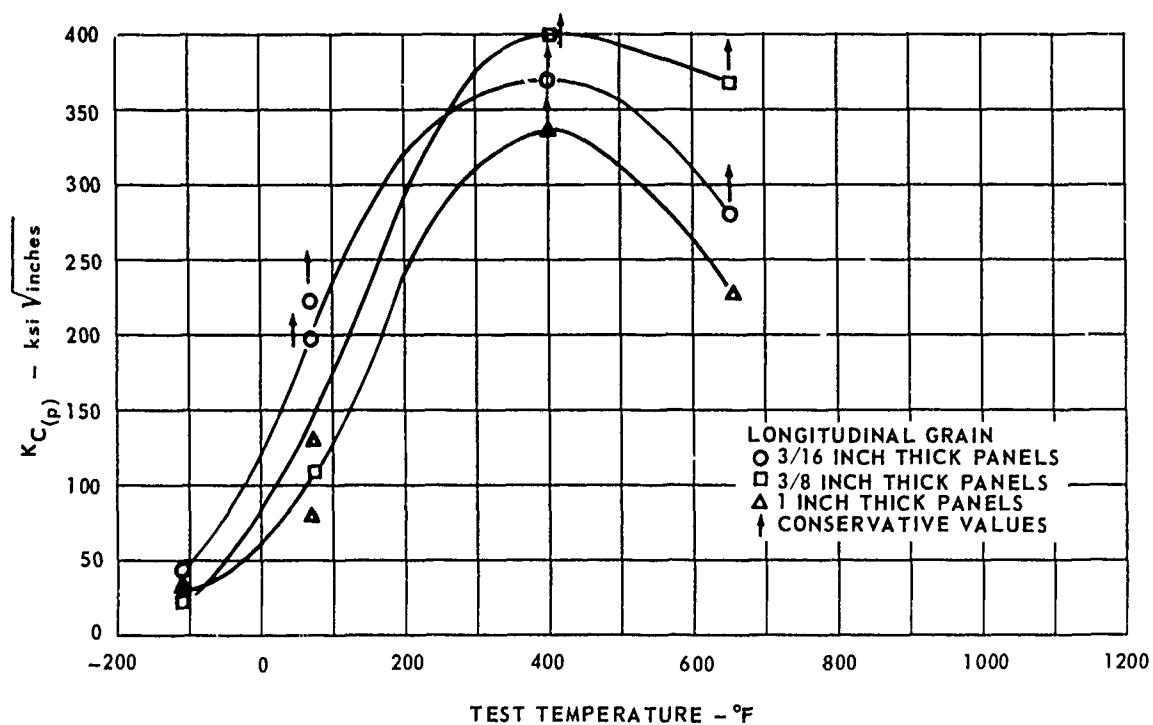


FIG. 53 $K_{C(p)}$ DATA FOR CENTER NOTCH PANELS OF AM 355

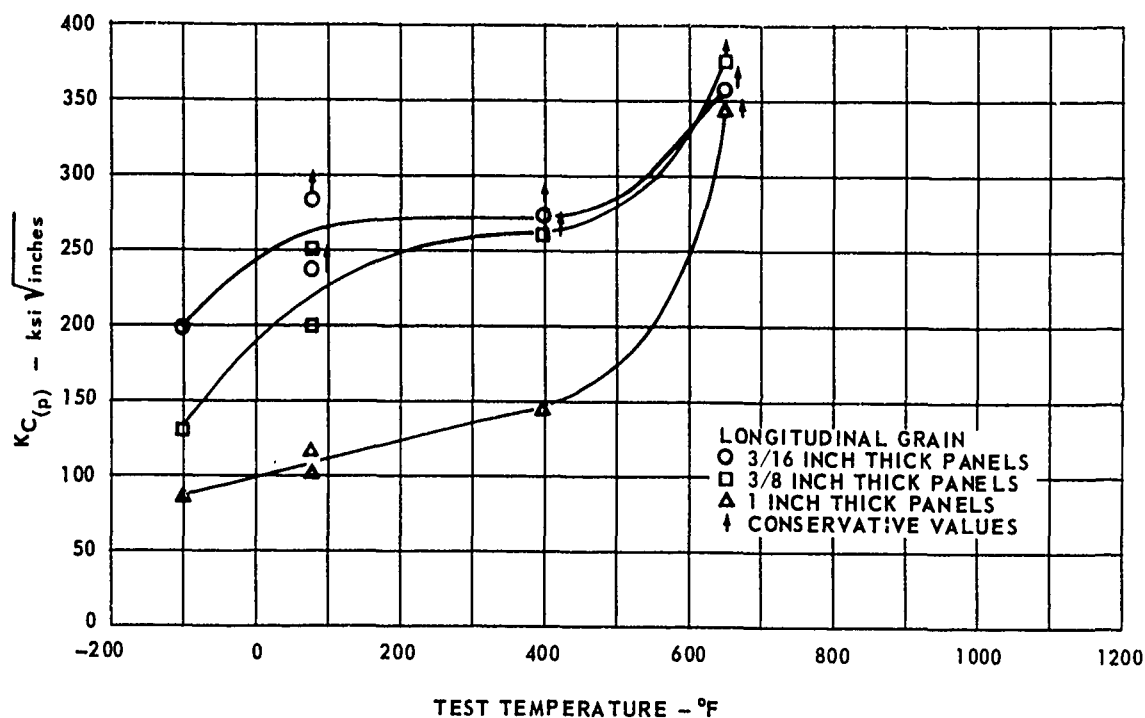


FIG. 54 $K_{C(p)}$ DATA FOR CENTER NOTCH PANELS OF MARAGING 250

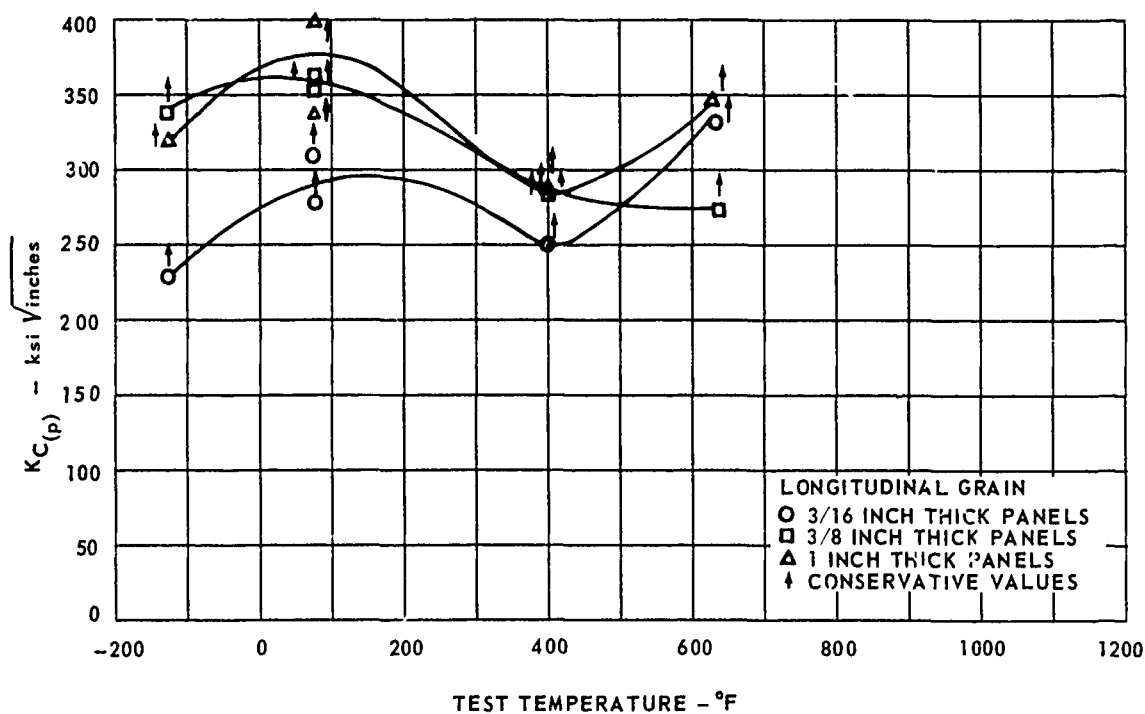


FIG. 55 $K_{C(p)}$ DATA FOR CENTER NOTCH PANELS OF INCO 718

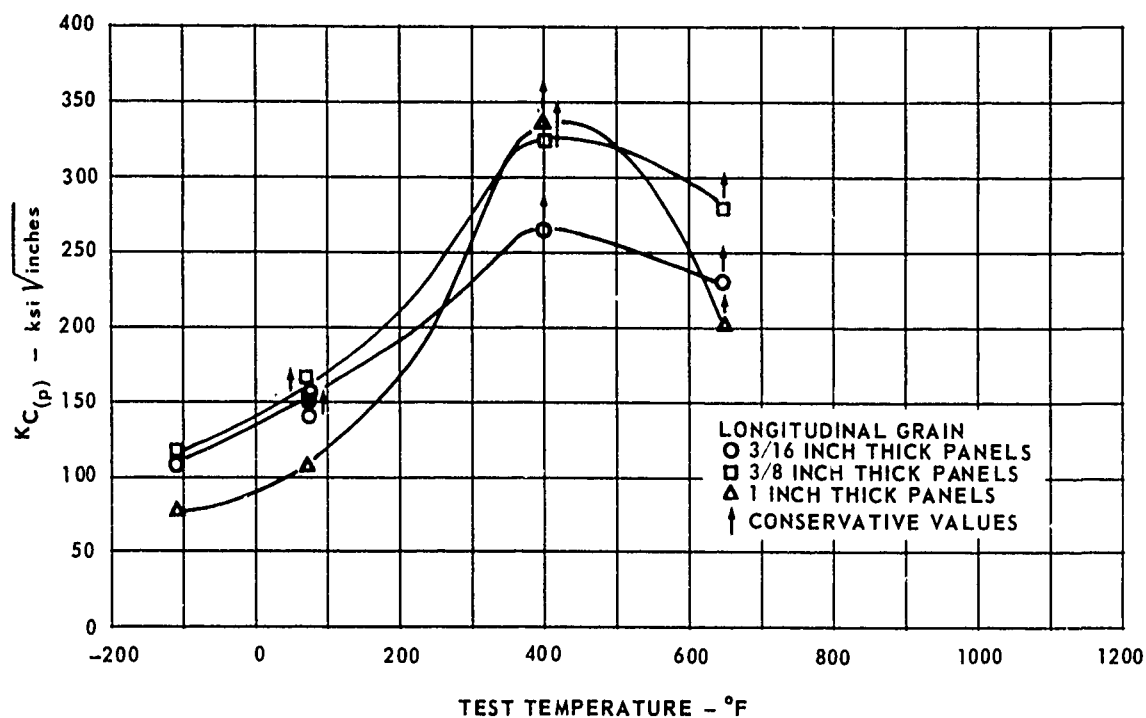


FIG. 56 $K_{C(p)}$ DATA FOR CENTER NOTCH PANELS OF Ti 6Al-4V

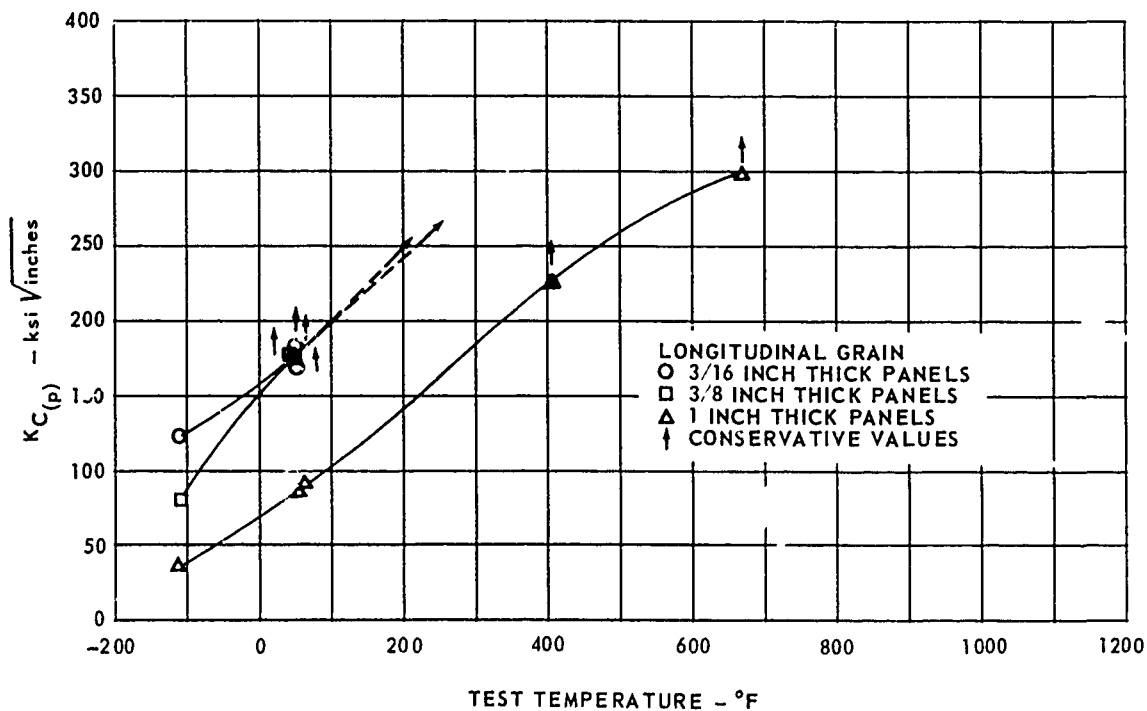


FIG. 57 $K_{C(p)}$ DATA FOR CENTER NOTCH PANELS OF Ti 6Al-6V-2Sn ANN

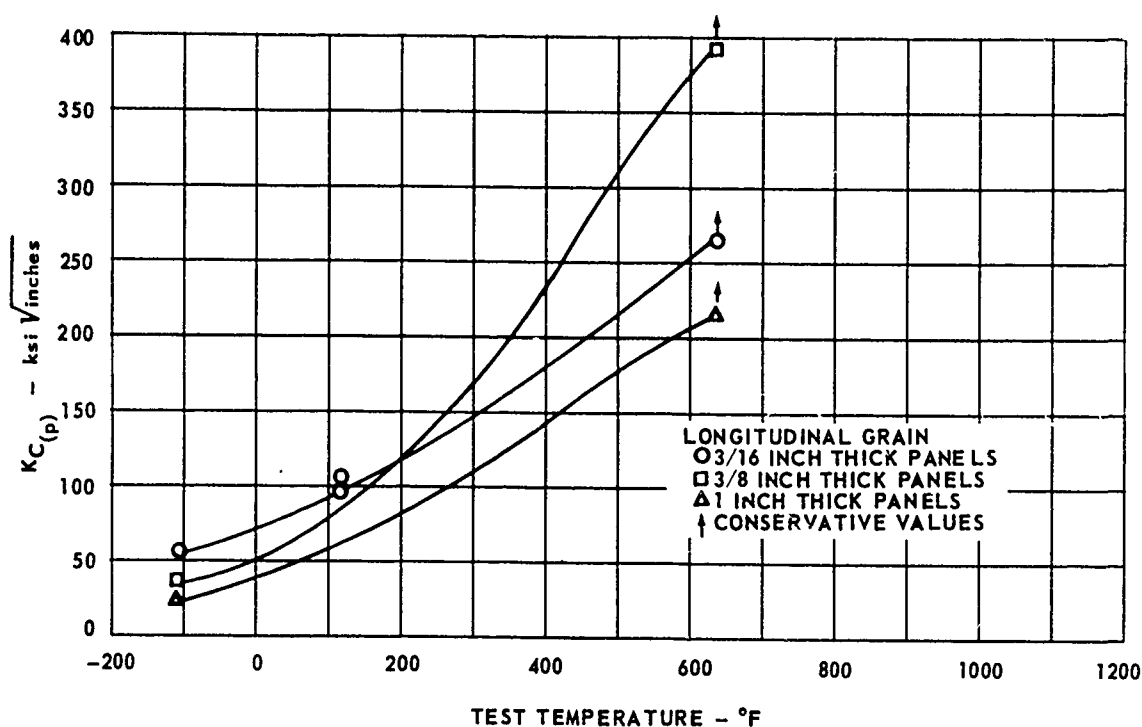


FIG. 58 $K_{IC(p)}$ DATA FOR CENTER NOTCH PANELS OF Ti 6Al-6V-2Sn STA

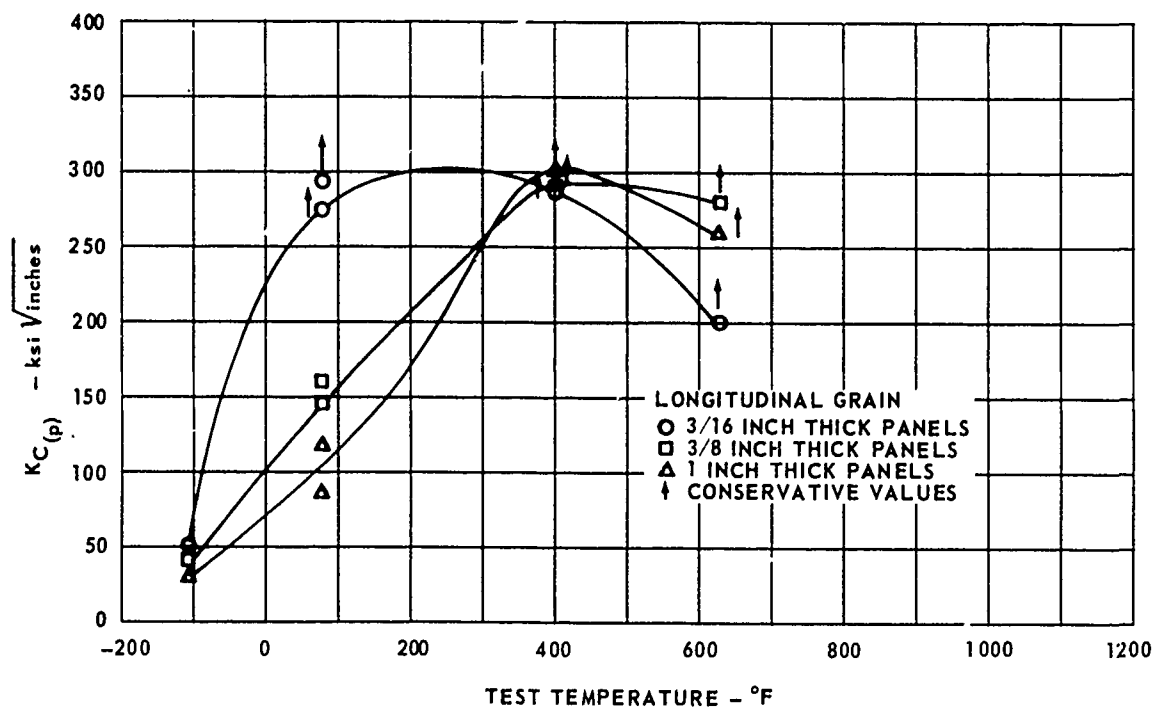


FIG. 59 $K_{IC(p)}$ DATA FOR CENTER NOTCH PANELS OF PH 13-8 Mo

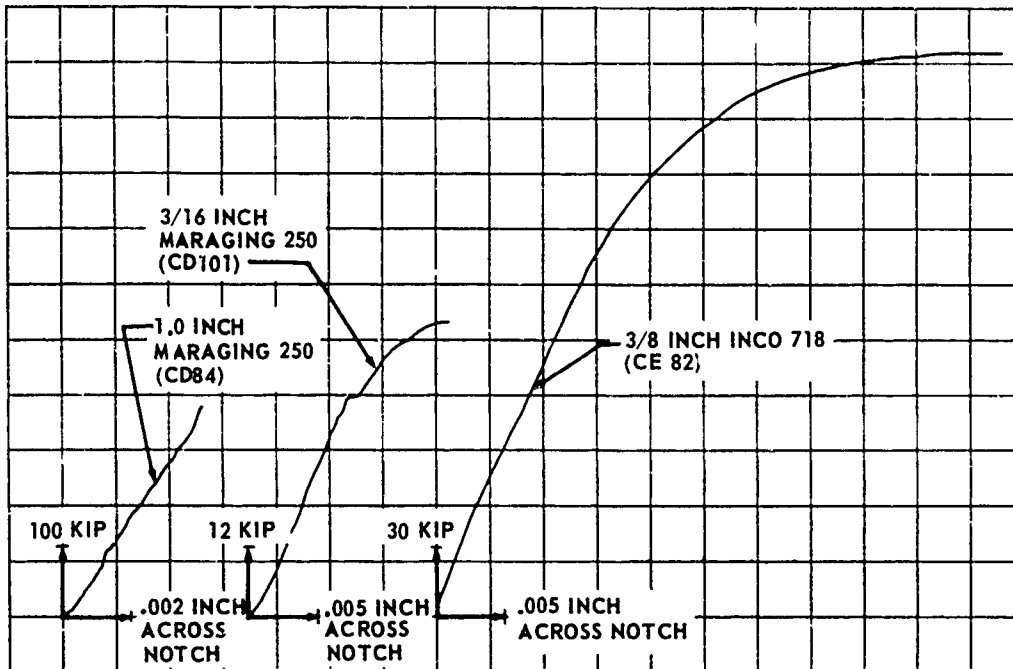


FIG. 60 CENTER NOTCH SPECIMEN LOAD DISPLACEMENT CURVES AT -110°F

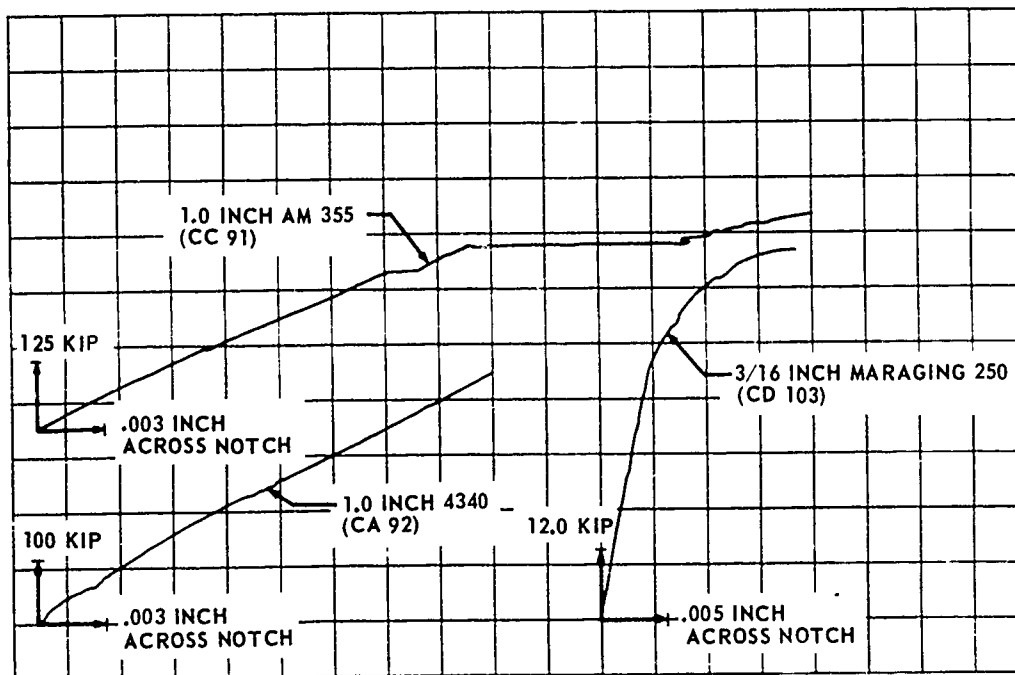


FIG. 61 CENTER NOTCH SPECIMEN LOAD DISPLACEMENT CURVES AT ROOM TEMPERATURE

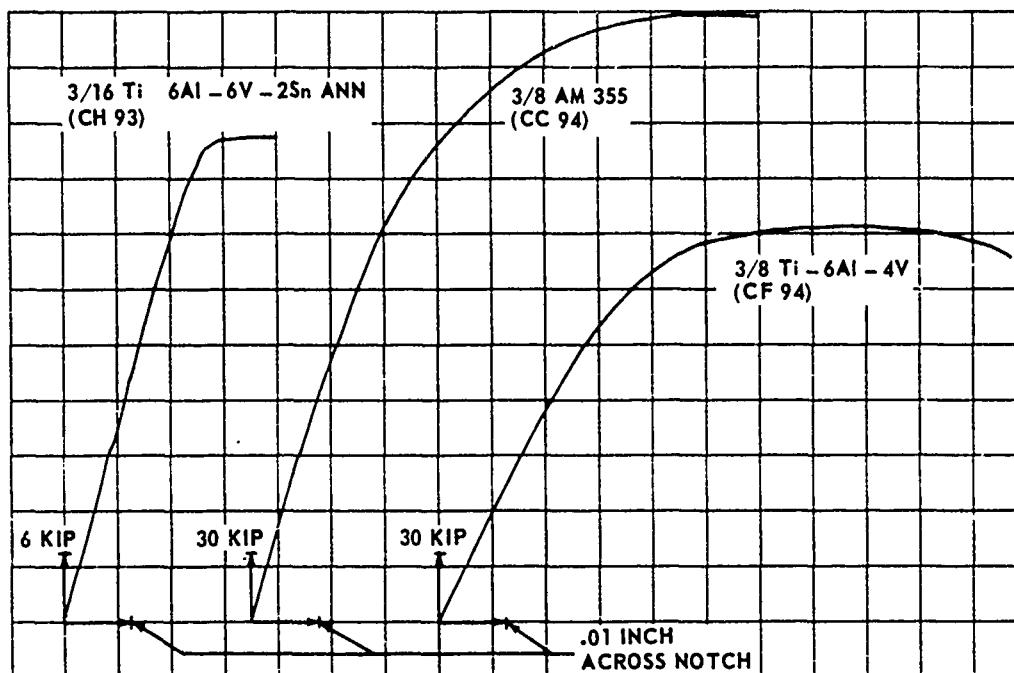


FIG. 62 CENTER NOTCH SPECIMEN LOAD DISPLACEMENT CURVES AT 400°F

Specimen numbers were lettered on the saw slot portion of the fracture face so that test temperature could be determined by referring to the tables. The specimens are stacked in increasing order of test temperature with the -110°F specimen being on the bottom. It is readily seen the percent-of-shear zone increases with test temperature for each alloy.

DISCUSSION

Plane Stress Determination

The variation of critical stress intensity with test temperature for three panel thicknesses of center-notched specimens is shown in Figs. 42 through 50. For most alloys, the stress intensity values varied from plane strain characterized by almost complete flat fracture at -110°F to a plane stress fracture at 650°F. The transition, shown by the increase in shear zone was illustrated by the photographs of center-notch specimen fracture faces in Figs. 73 through 81. This transition caused the critical stress intensity curves to generally increase with temperature. In most instances where this did not occur, it was probably because the net stress to yield stress ratio had increased to the point where the stress intensity values were depressed. This phenomenon is illustrated in the Fifth Report of the Special ASTM Committee on Fracture Testing (Ref. 18) where experimental data are plotted showing the decrease from actual K_{IC} as the net stress to yield stress ratio increases above approximately 0.8.

The ratio generally increased as panel thickness decreased, and presumably the

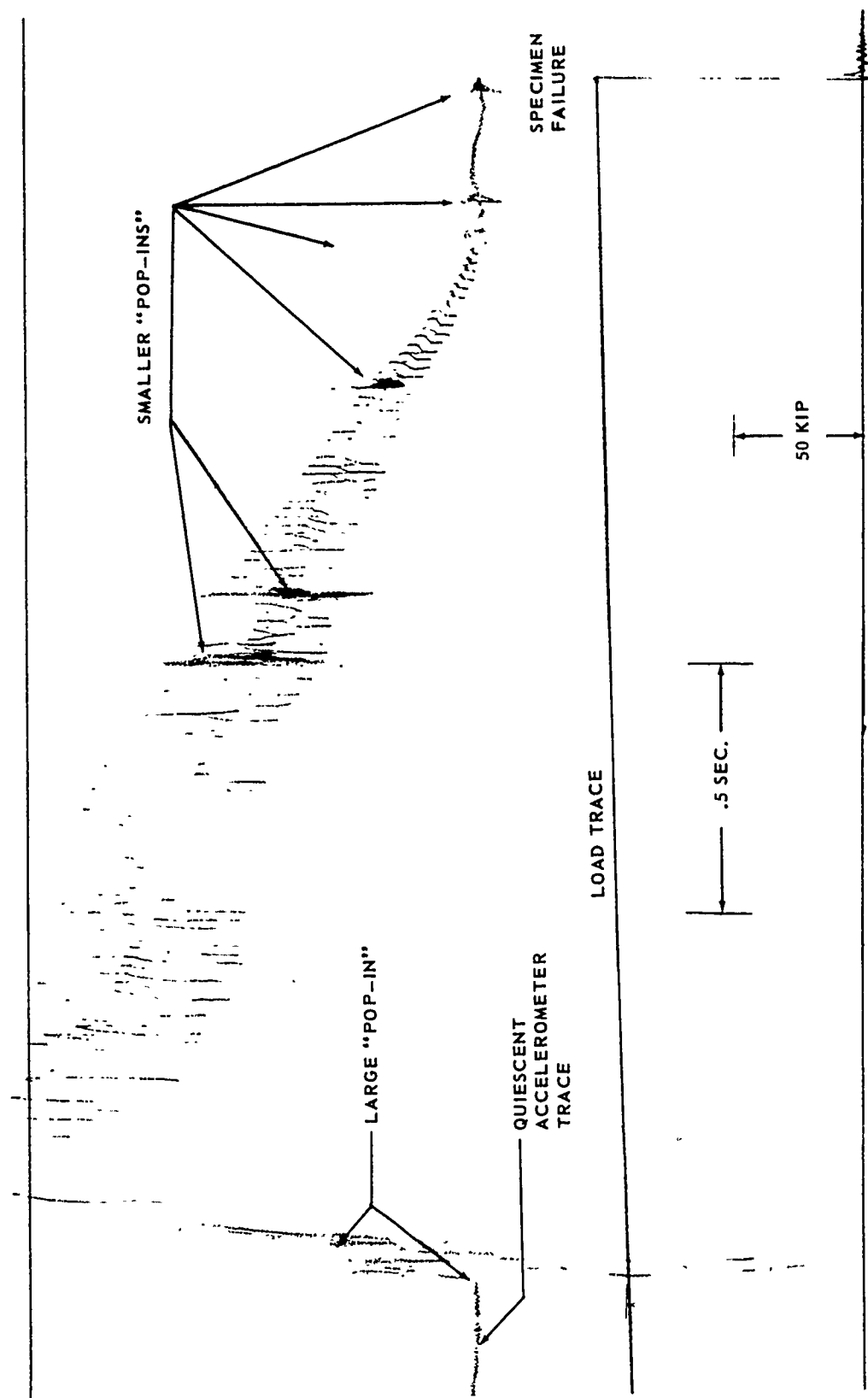


FIG. 63 TYPICAL LOAD-ACCELEROMETER CENTER NOTCH TRACE

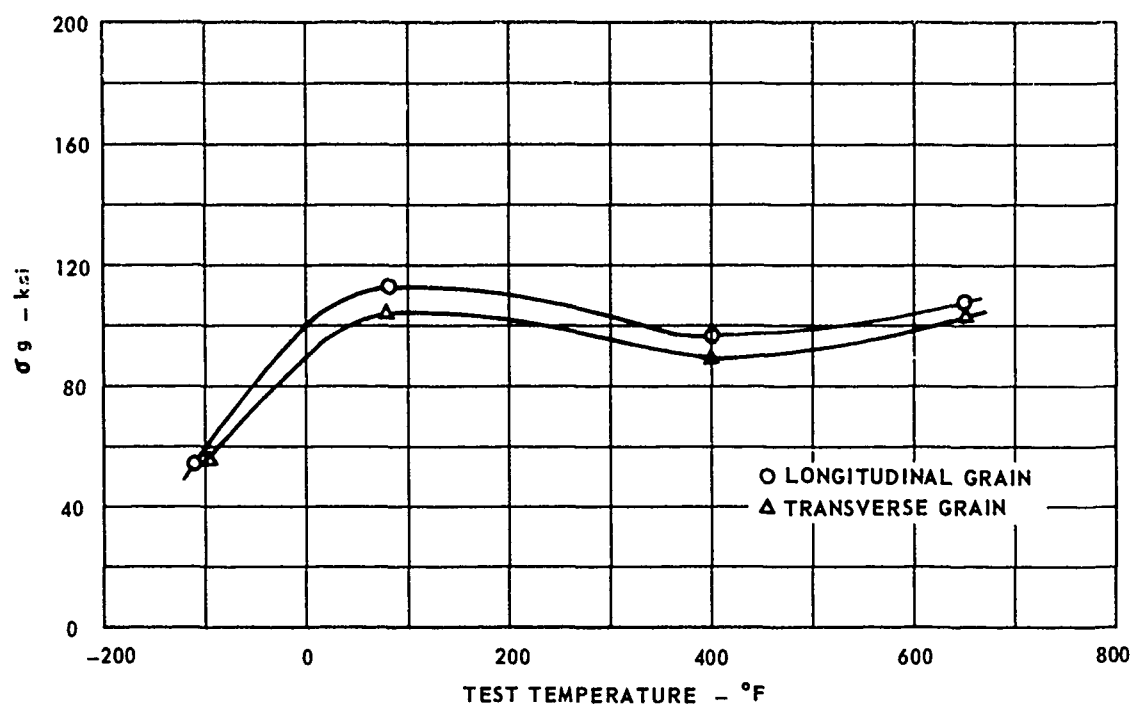


FIG. 64 3/16 INCH THICK PANEL RESIDUAL STRENGTH FOR 4340

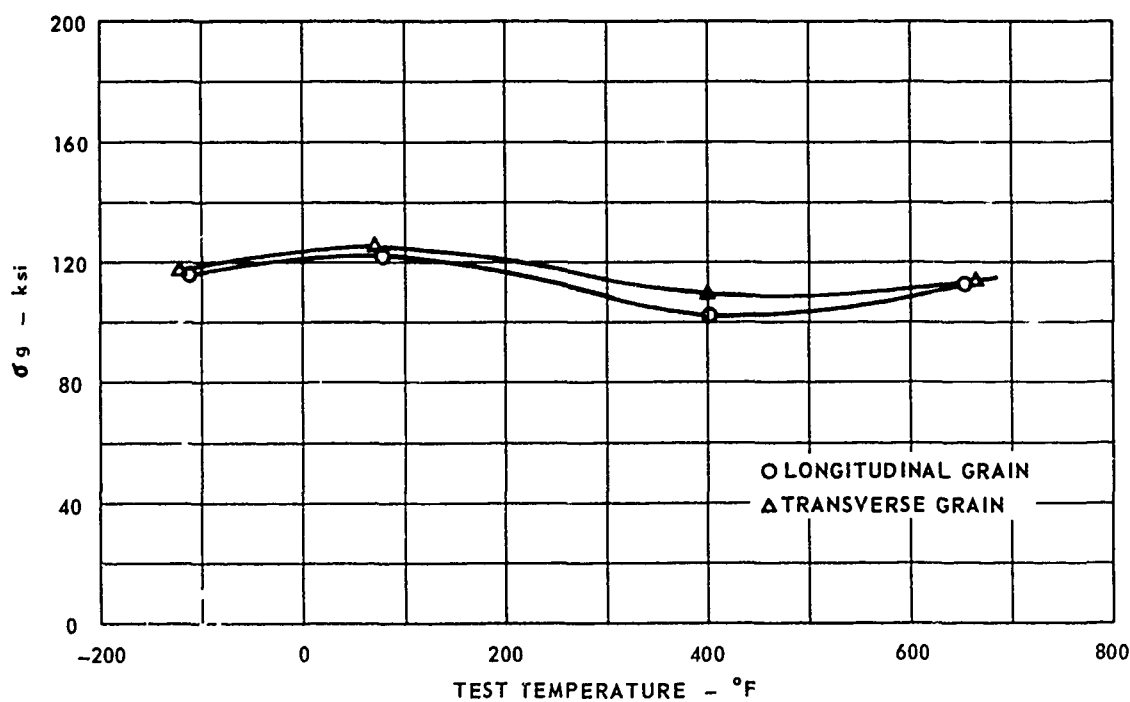


FIG. 65 3/16 INCH THICK PANEL RESIDUAL STRENGTH FOR 9Ni-4Co

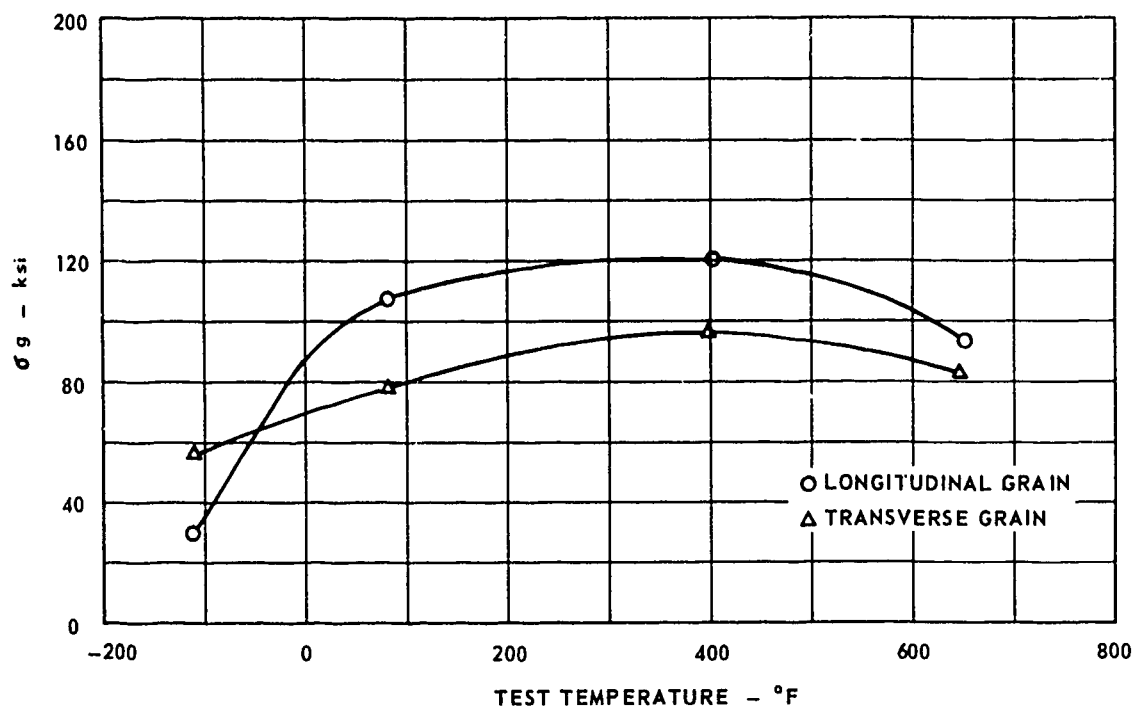


FIG. 66 3/16 INCH THICK PANEL RESIDUAL STRENGTH FOR AM 355

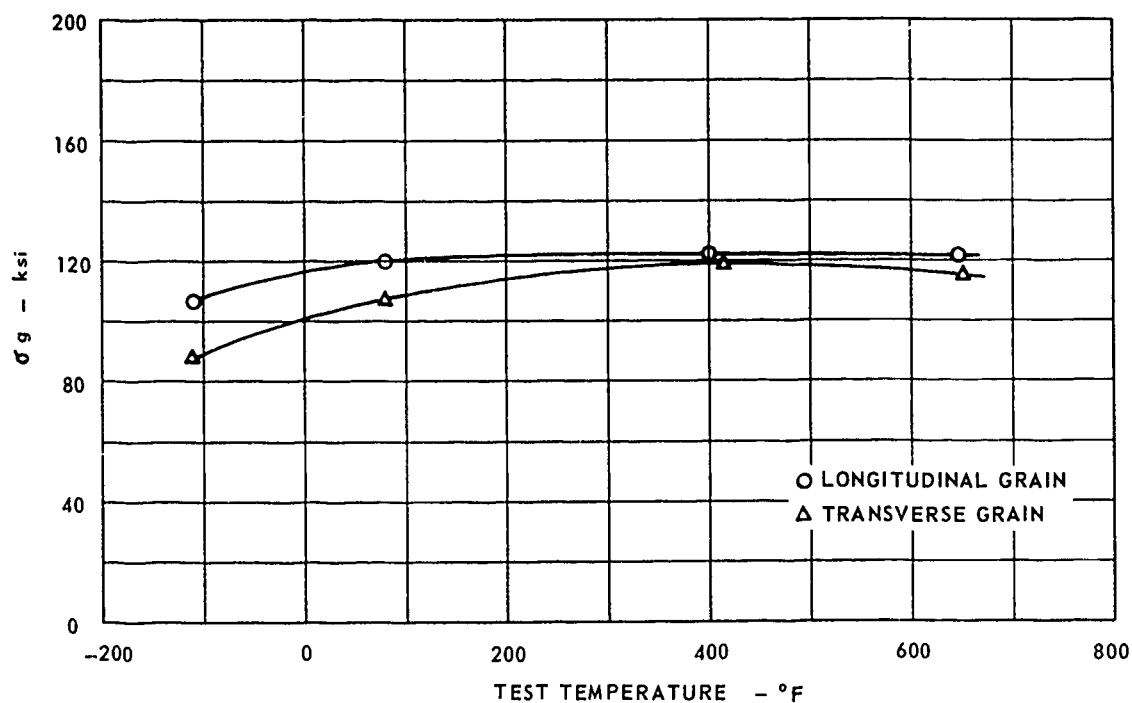


FIG. 67 3/16 INCH THICK PANEL RESIDUAL STRENGTH FOR MARAGING 250

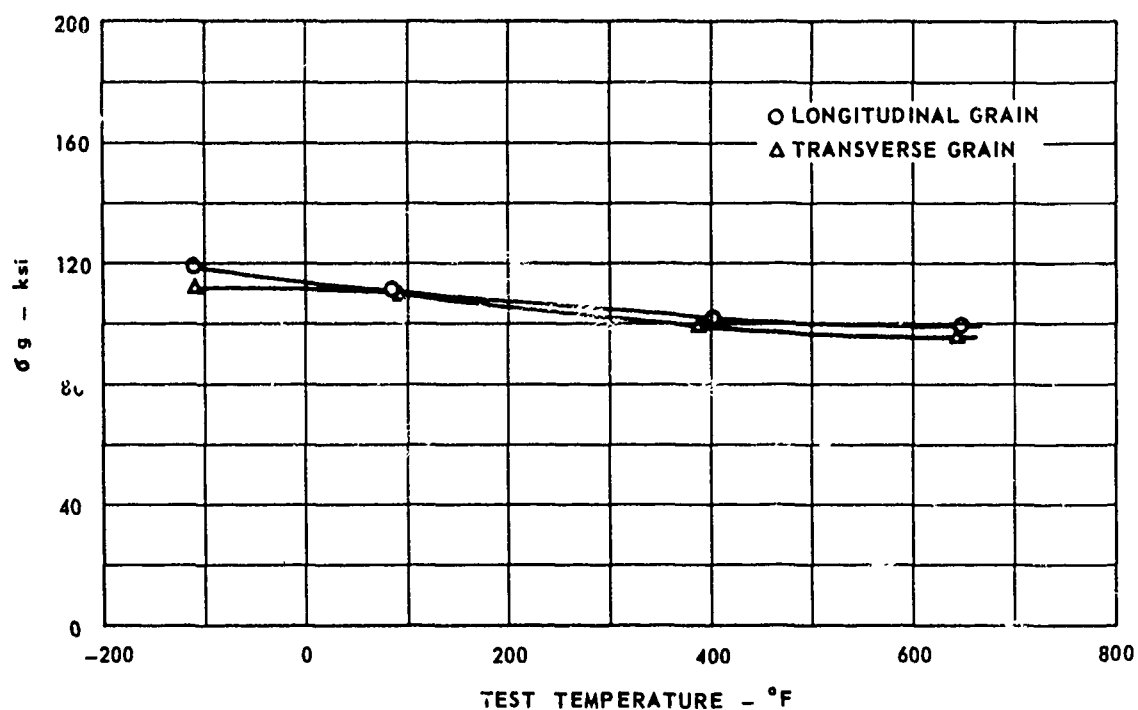


FIG. 68 3/16 INCH THICK PANEL RESIDUAL STRENGTH FOR INCO 718

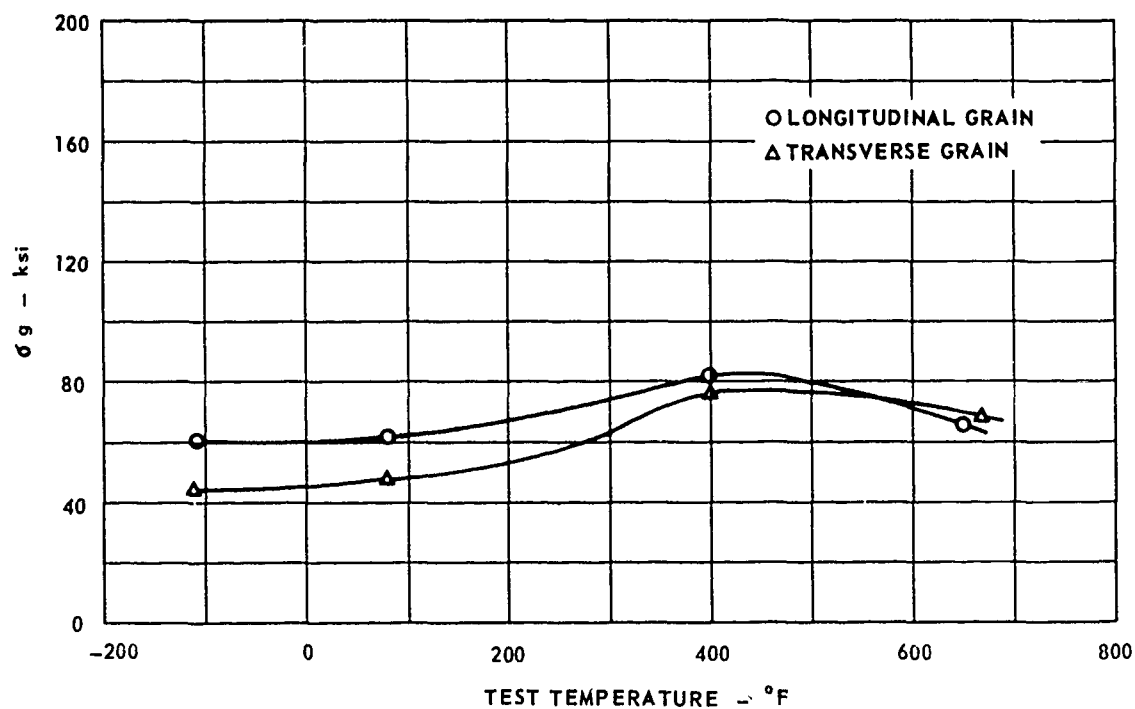


FIG. 69 3/16 INCH THICK PANEL RESIDUAL STRENGTH FOR Ti 6Al-4V

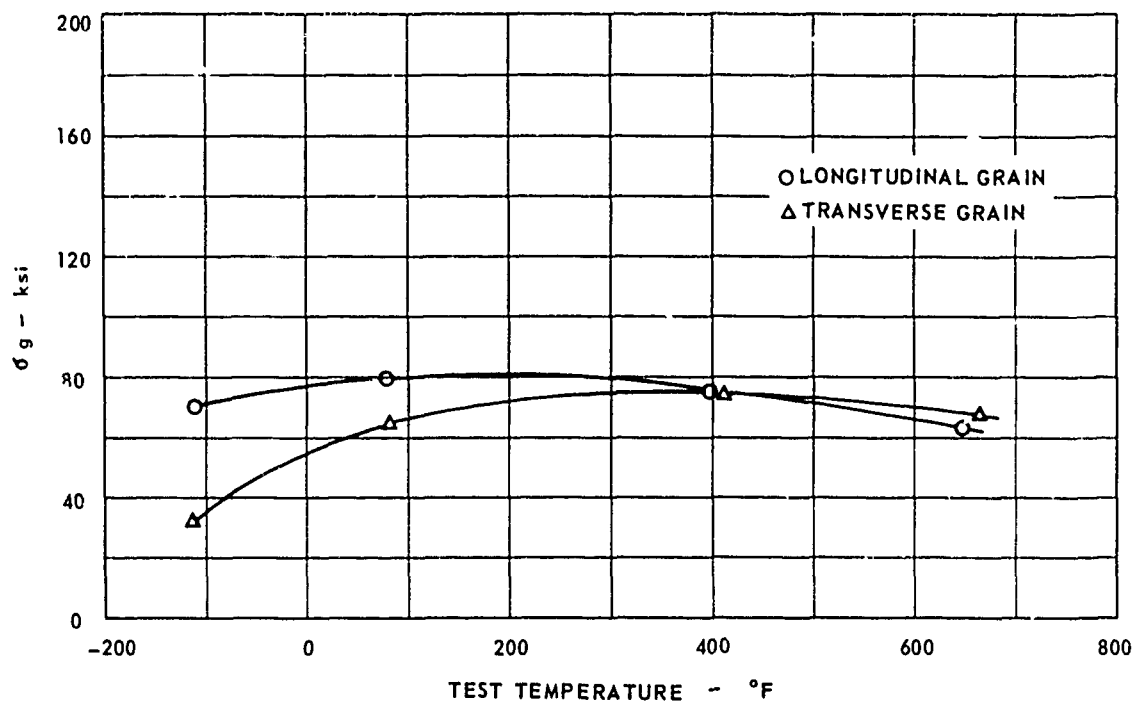


FIG. 70 3/16 INCH THICK PANEL RESIDUAL STRENGTH FOR Ti 6Al-6V-2Sn ANN

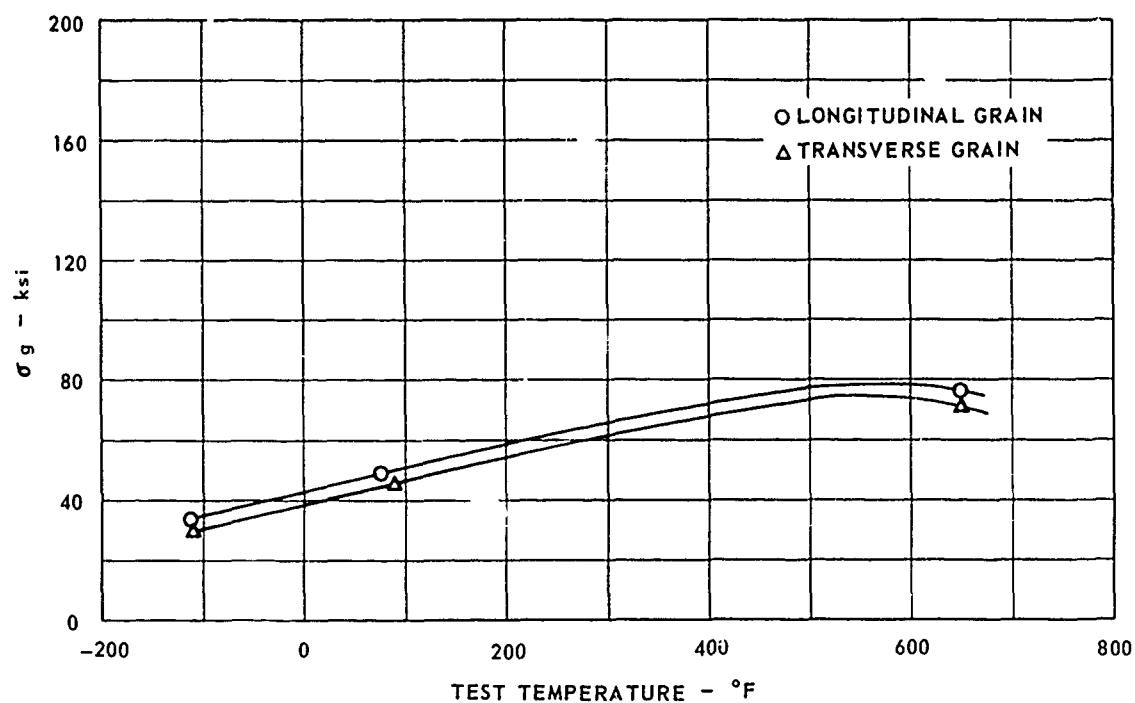


FIG. 71 3/16 INCH THICK PANEL RESIDUAL STRENGTH FOR Ti 6Al-6V-2Sn STA

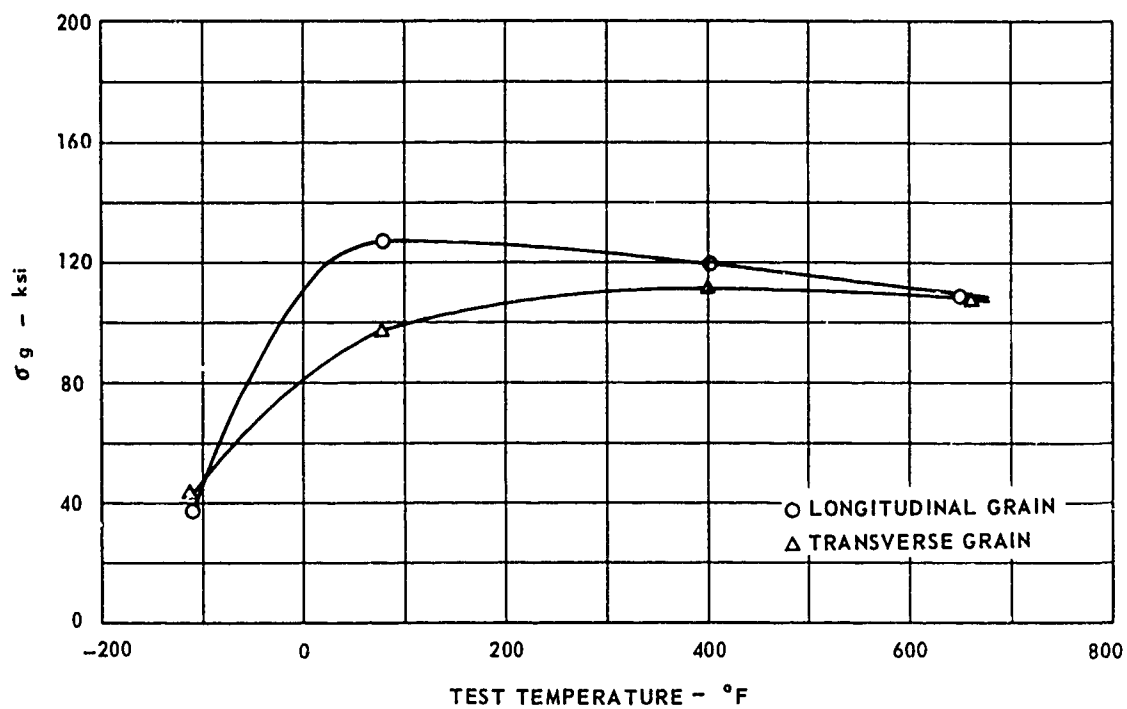


FIG. 72 3/16 INCH THICK PANEL RESIDUAL STRENGTH FOR PH 13-8 Mo

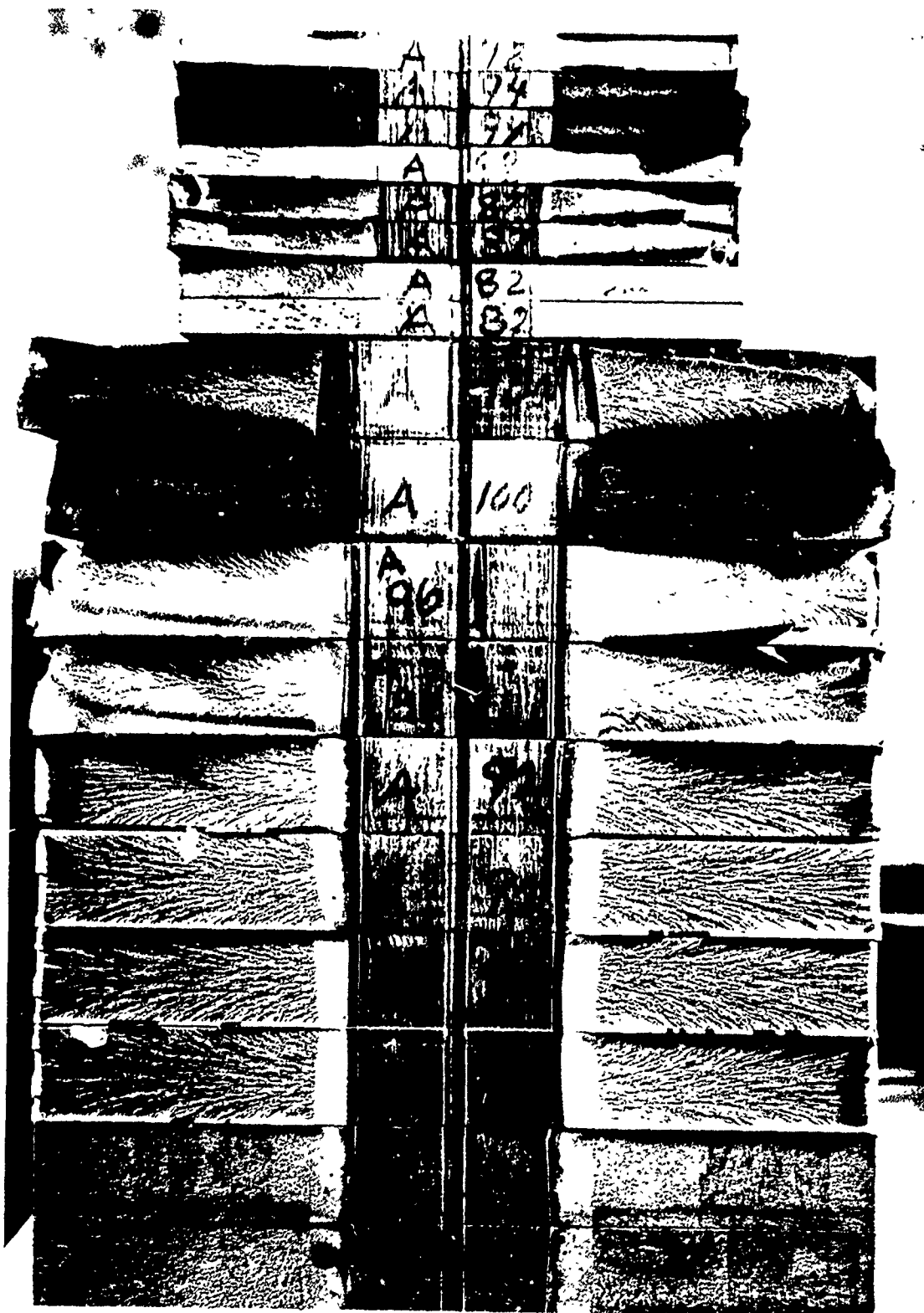


FIG. 73 CENTER NOTCH PANEL FRACTURE FACES OF 4340

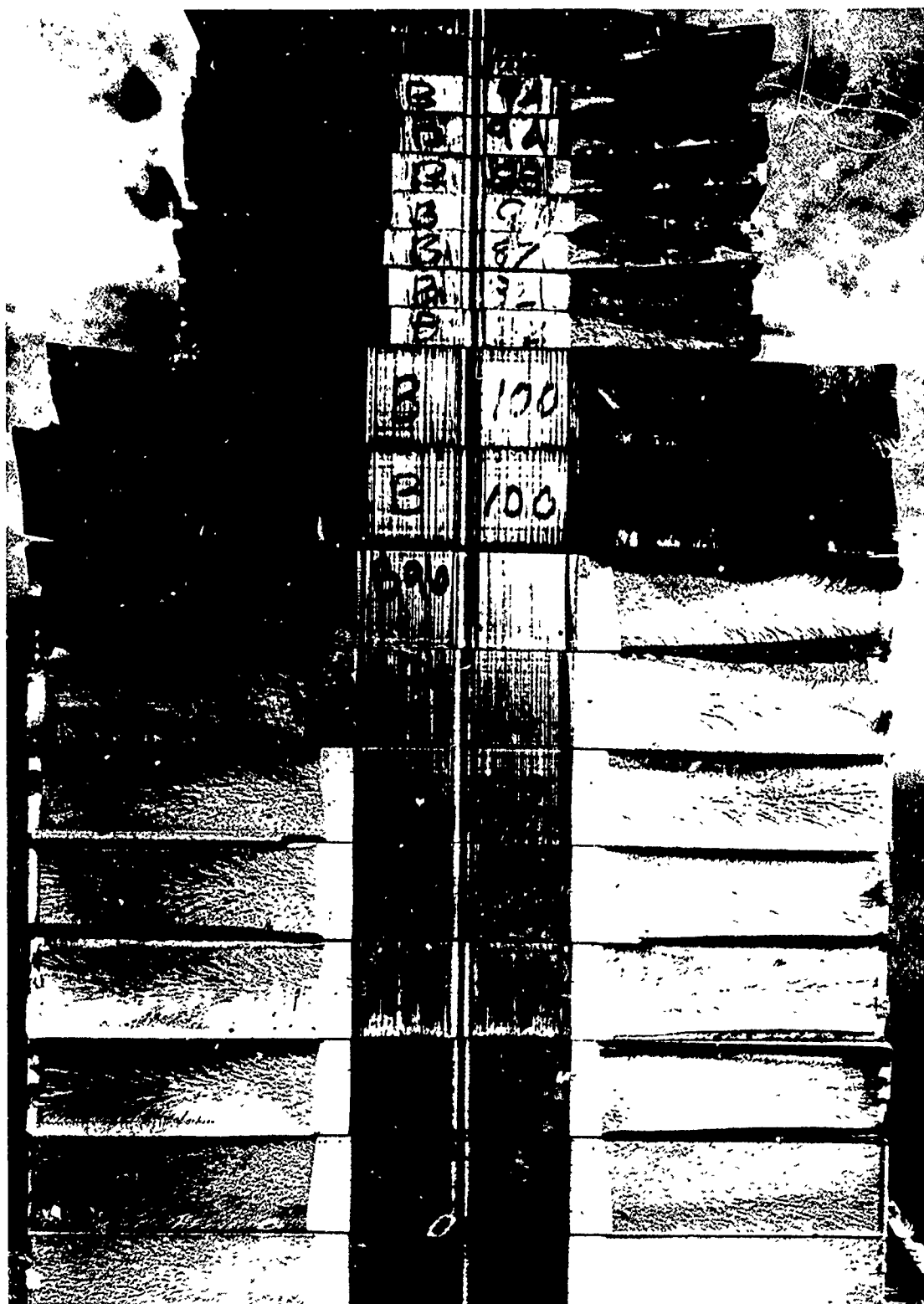


FIG. 74 CENTER NOTCH PANEL FRACTURE FACES OF 9Ni-4Co

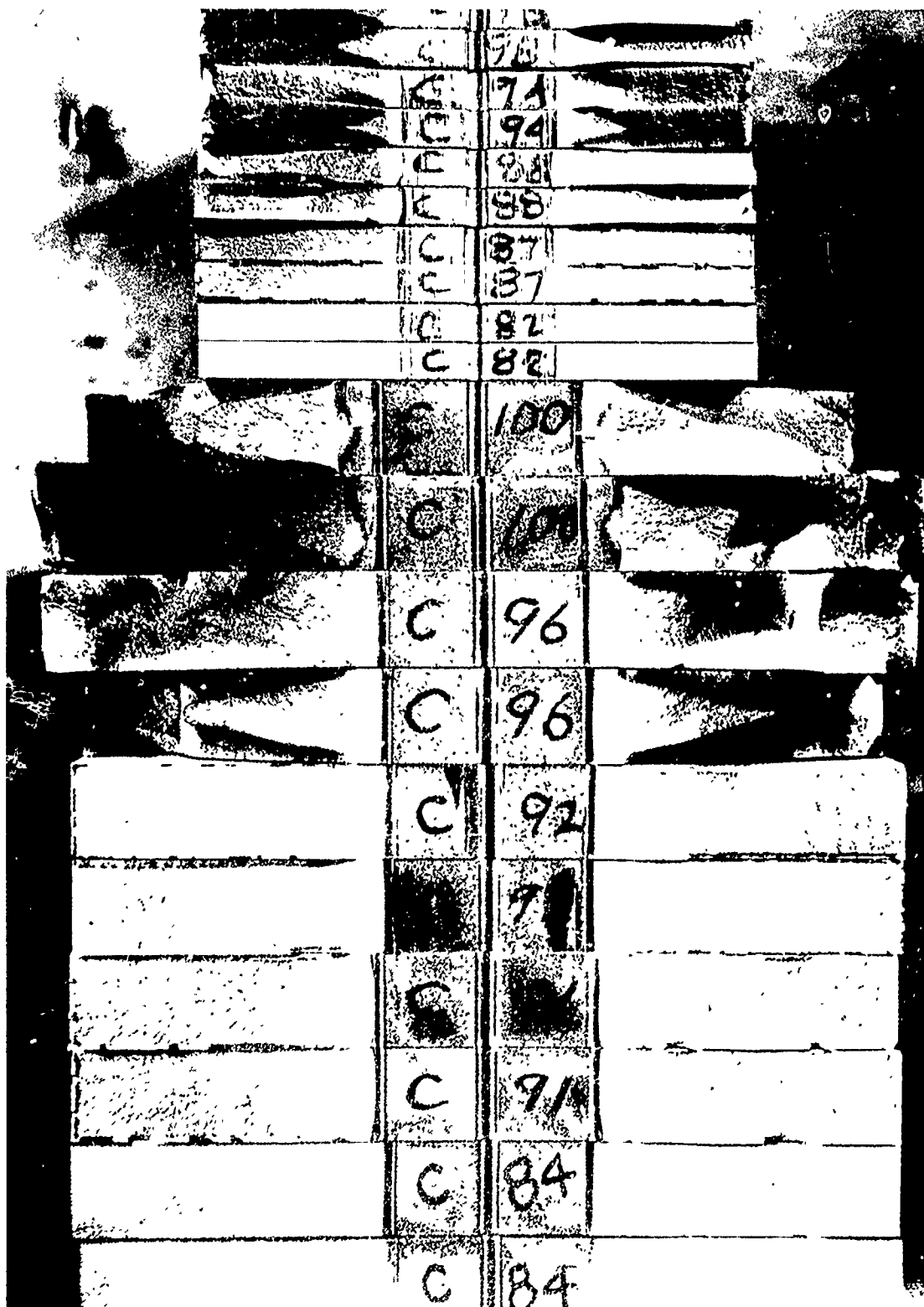


FIG. 75 CENTER NOTCH PANEL FRACTURE FACES OF AM 355

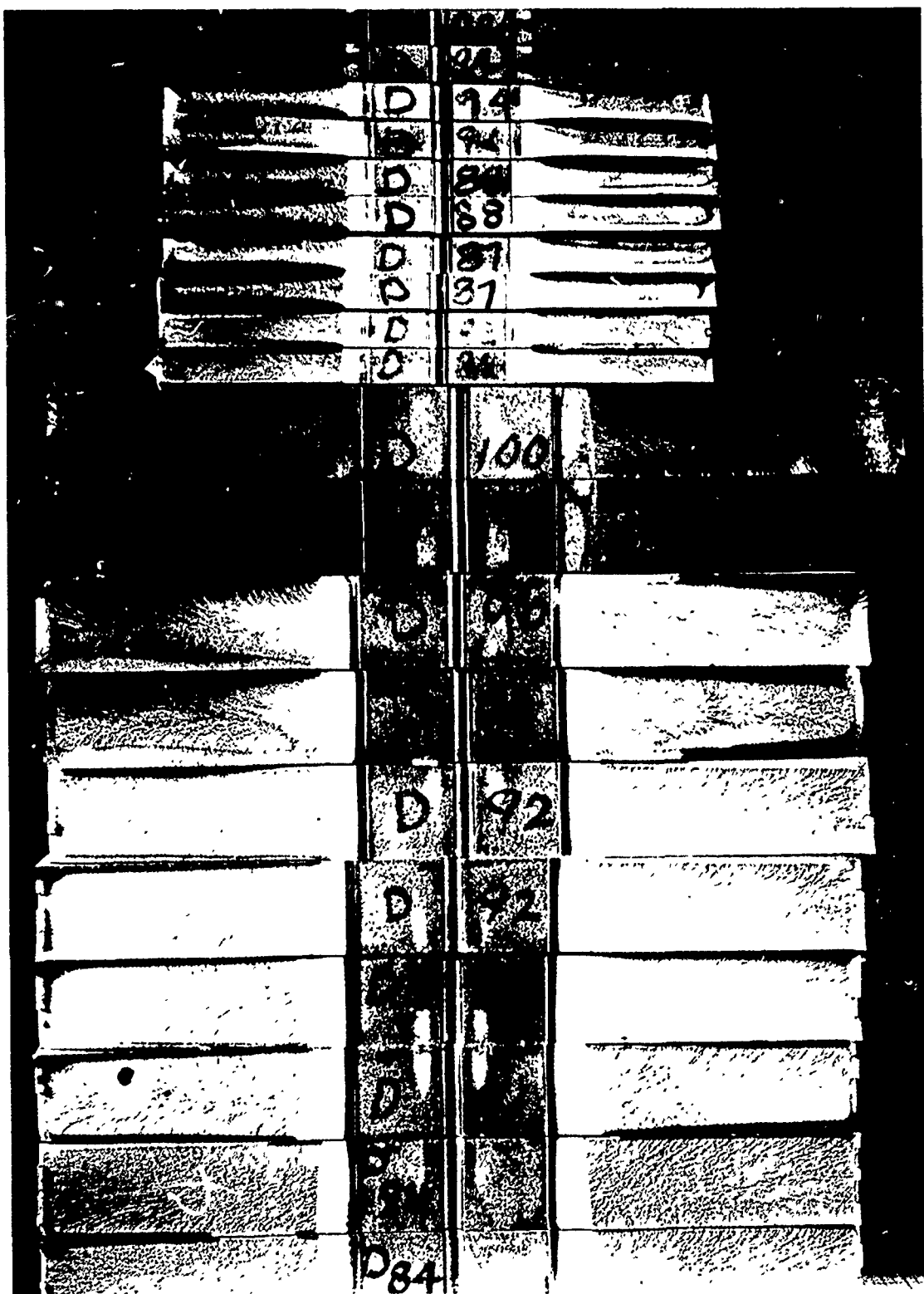


FIG. 76 CENTER NOTCH PANEL FRACTURE FACES OF MARAGING 250

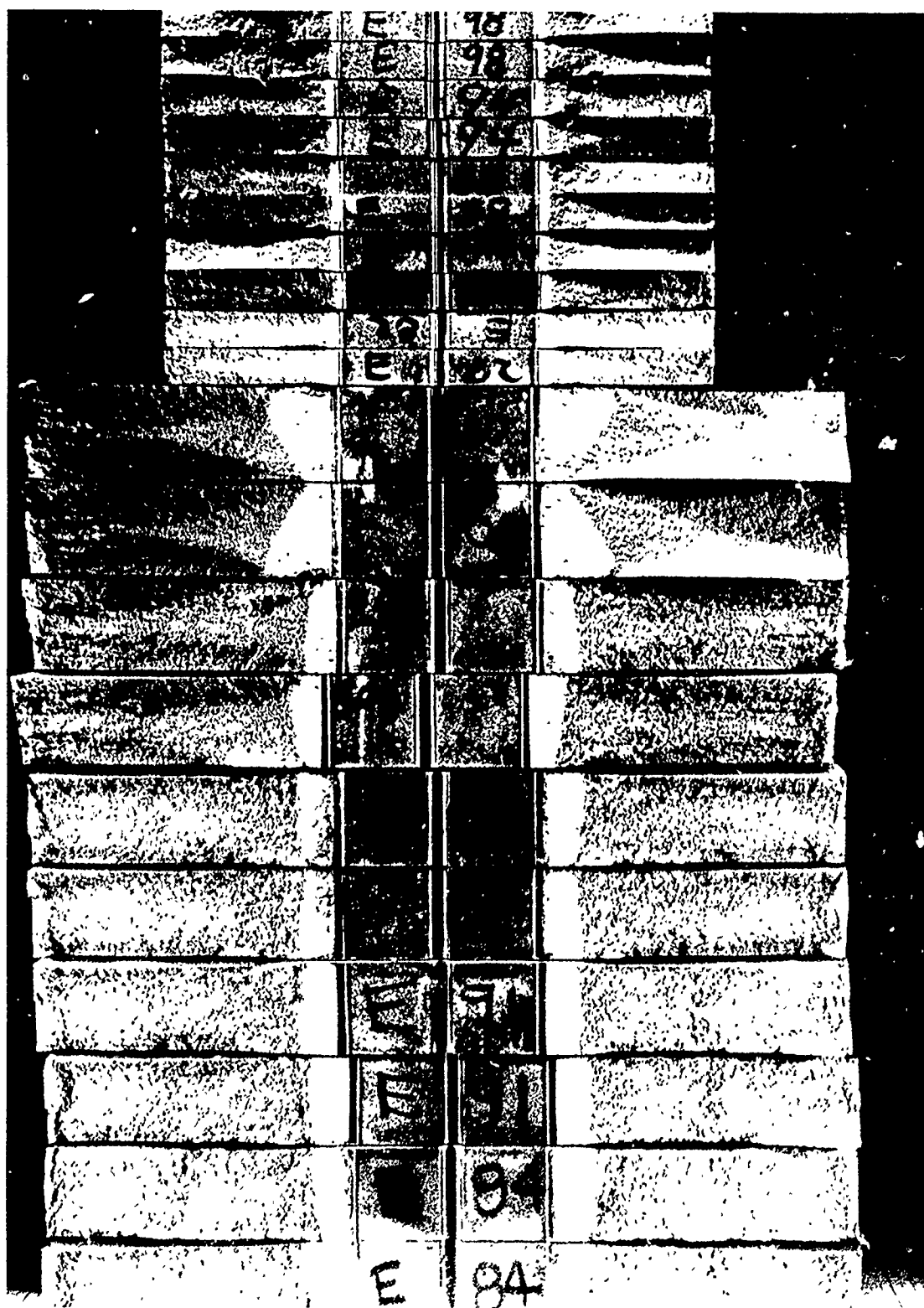


FIG. 77 CENTER NOTCH PANEL FRACTURE FACES OF INCO 718

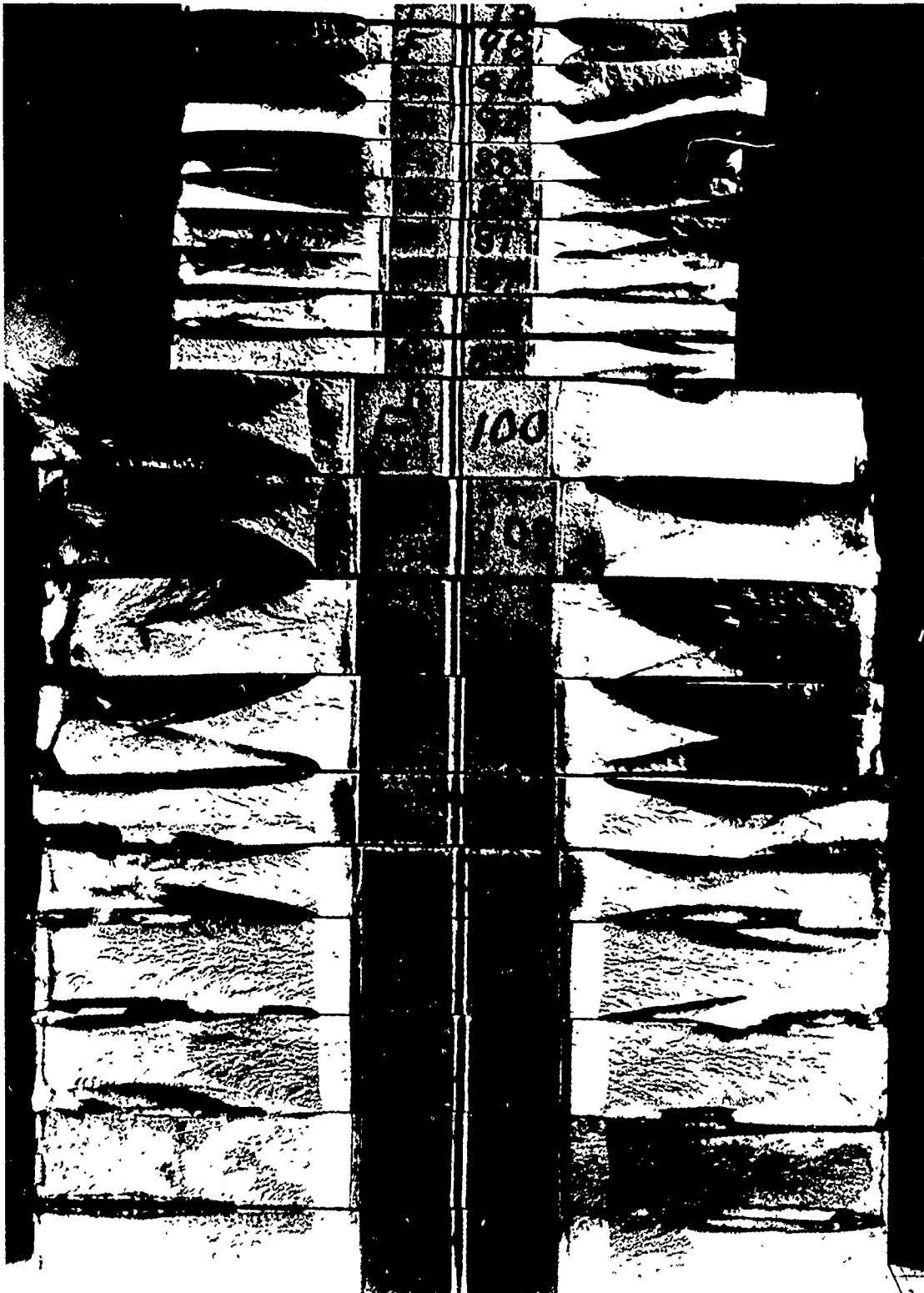


FIG. 78 CENTER NOTCH PANEL FRACTURE FACES OF T₁ 6Al-4V

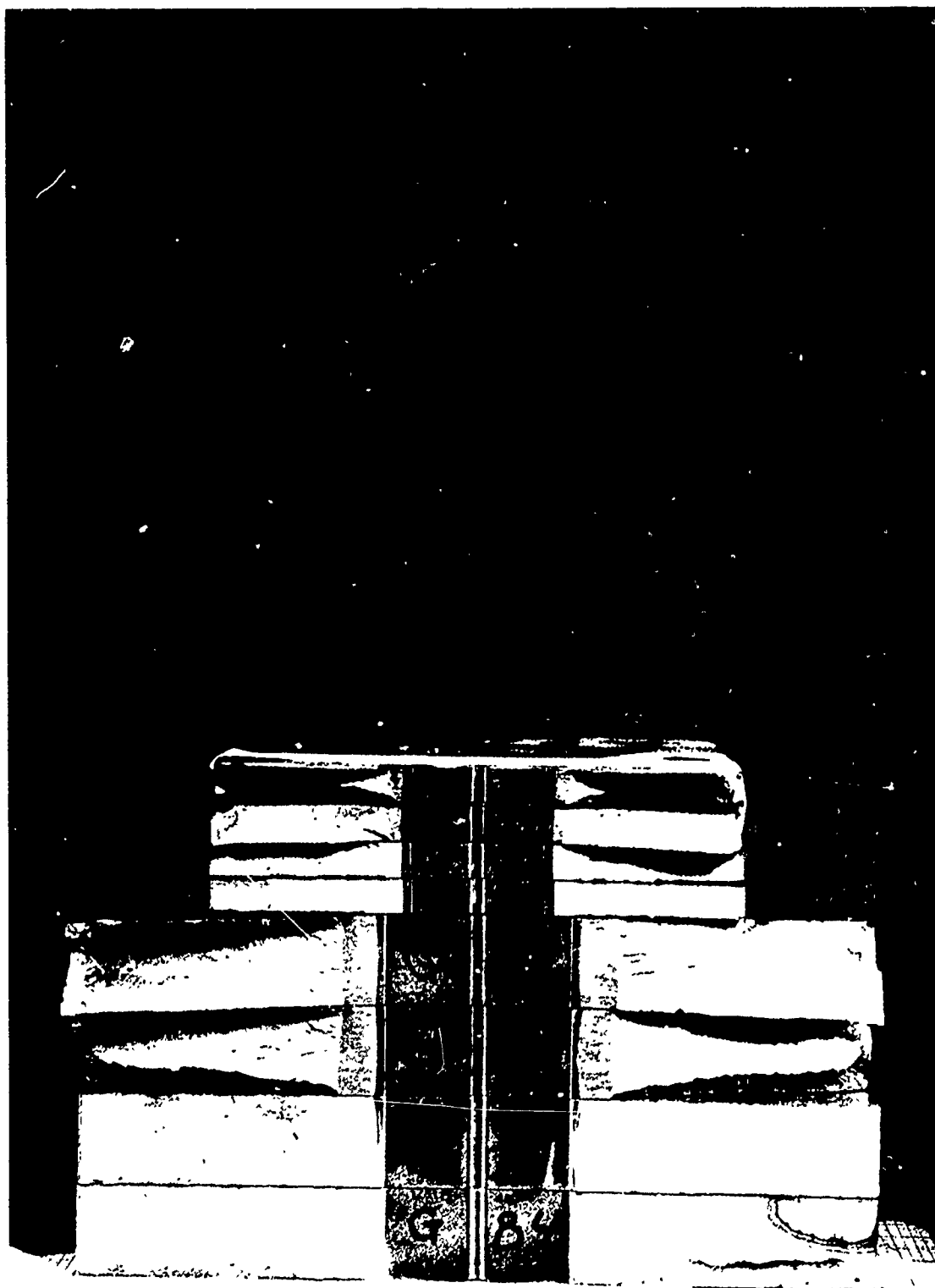


FIG. 79 CENTER NOTCH PANEL FRACTURE FACES OF T_1 6Al-6V-2Sn STA

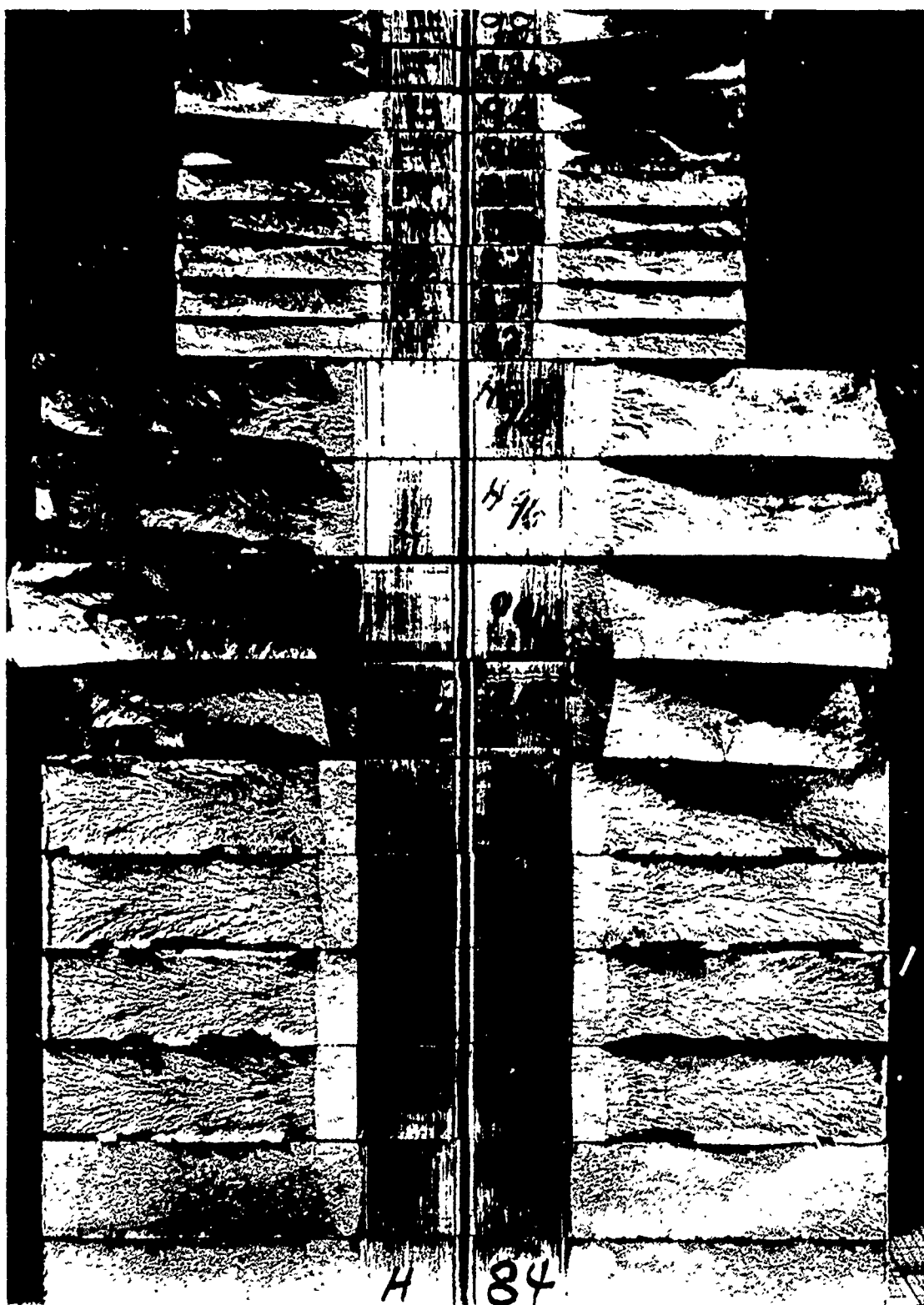


FIG. 80 CENTER NOTCH PANEL FRACTURE FACES OF T_1 6Al-6V-2Sn ANN

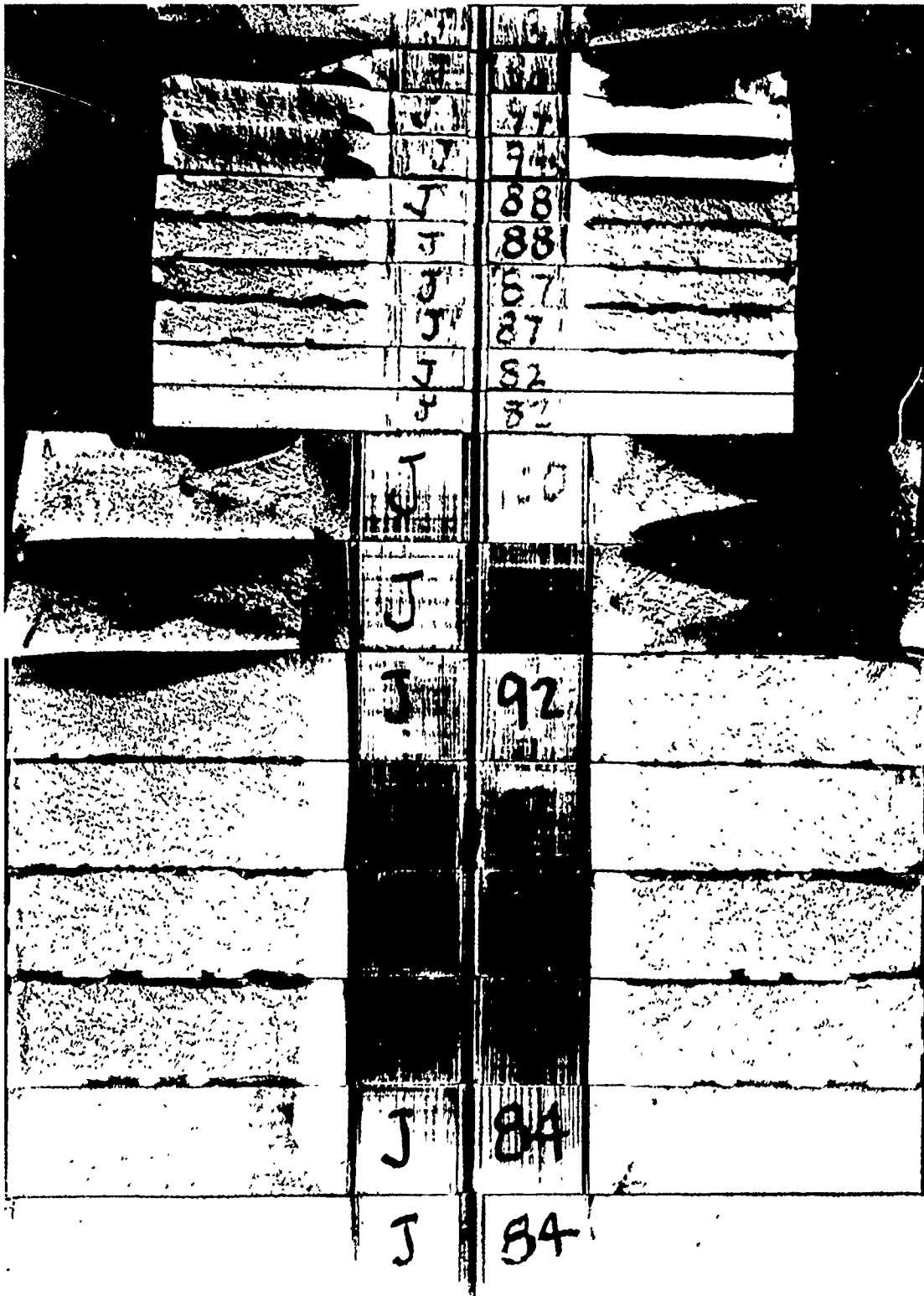


FIG. 81 CENTER NOTCH PANEL FRACTURE FACES OF PH 13-8 Mo

higher the ratio, the more conservative the K_C value. This would account for the fact that the curves of Figs. 42 through 50 for the 3/16-inch thick panels were generally highest at -110°F and dropped below the other K_C curves as the temperature increased. It had been expected that stress intensity values would decrease as panel thickness increased for AM 355 as was shown by Steigerwald and Hanna (Ref. 23). The alloy most closely showing this relationship was 4340, which had only 2 ratios above 0.8. The Inco 718 with all ratios above 0.8 showed a complete reversal of the curves.

The stress intensity values when corrected for the plastic zone as shown in Figs. 51 to 59 tend to be higher than the uncorrected values at the higher temperatures. It is evident, when comparing the K_C , $K_{C(p)}$ and $\frac{\sigma_N}{\sigma_{ys}}$ column in

Table 2, that the plastic zone correction is only significantly large when the net stress to yield stress ratio is large. Therefore, the plastic zone correction probably has less meaning as the net area stress increases above 80 percent of the tensile yield strength.

Plane Strain Stress Intensity Determination from Pop-In

Plane strain stress intensity values from pop-in measurements on the center-notched panels were disappointing. The pop-in indications obtained are listed as K_{IC} in the tables and are plotted with the round-notched data in Figs. 82 through 90 to show the correlation of K_{IC} values from the two methods of testing. The correlation for the two methods is only fair, even at low temperatures where almost complete flat fracture occurred.

It is possible that the difference in location of specimens within the large forged block contributed to the variation in K_{IC} values. Areas of the blocks from which the specimens were removed are shown in the first quarterly report. It is probable, however, that the pop-in technique for measuring plane strain stress intensity on very tough alloys will be of limited value. Published data (Ref. 24) showing good correlation between the pop-in method and notched round specimens has been obtained on more brittle alloys such as 7075-T6. It is probable that the lack of indications is a result of the high toughness of the alloys tested. In all center notch tests an extensometer and an accelerometer were used to detect pop-in. Both these techniques, especially the accelerometer are very sensitive. Therefore it is unlikely that any discontinuous cracking was not recorded.

In general when a specimen did crack discontinuously, it did so more than once. Pop-in was detected as many as nineteen times on one specimen. Sometimes the first pop-in was small and other times large as shown by discontinuities in load-displacement curves (Figs. 60 and 61). Moreover, these rapid bursts of cracking were also noted by the accelerometer as shown in Fig. 63. Even more complicating was the fact that the accelerometer practically always sensed small pop-ins at lower loads where the load-displacement curves were linear and showed no discontinuities.

A relationship between pop-in and K_{IC} may exist. However, the data obtained from the center-notch tests were not conclusive. For comparison, all pop-in

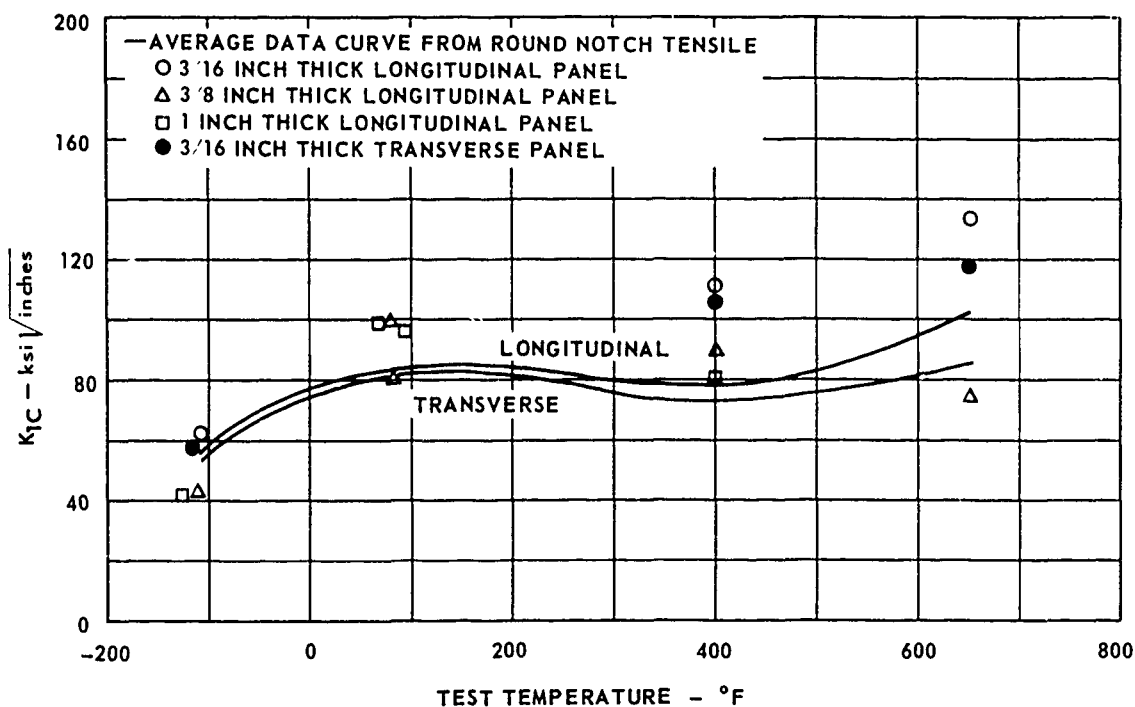


FIG. 82 COMPARISON OF K_{1C} FROM PANEL "POP-IN" AND ROUND NOTCH TENSILE FOR 4340

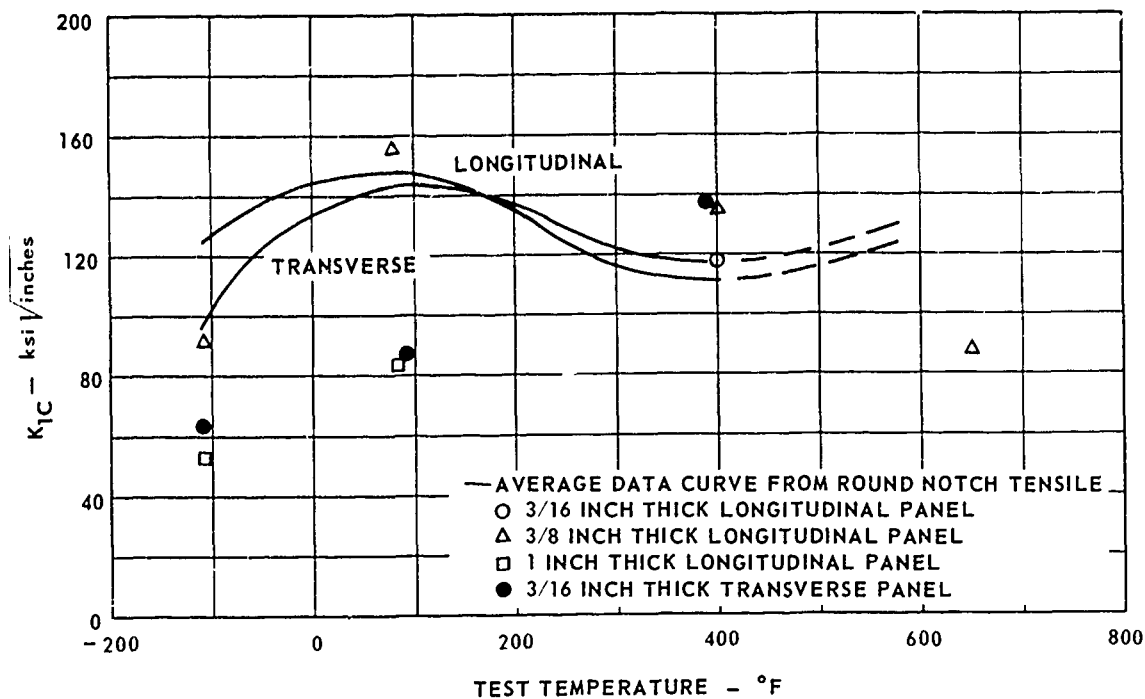


FIG. 83 COMPARISON OF K_{1C} FROM PANEL "POP-IN" AND ROUND NOTCH TENSILE FOR 9 Ni-4 Co

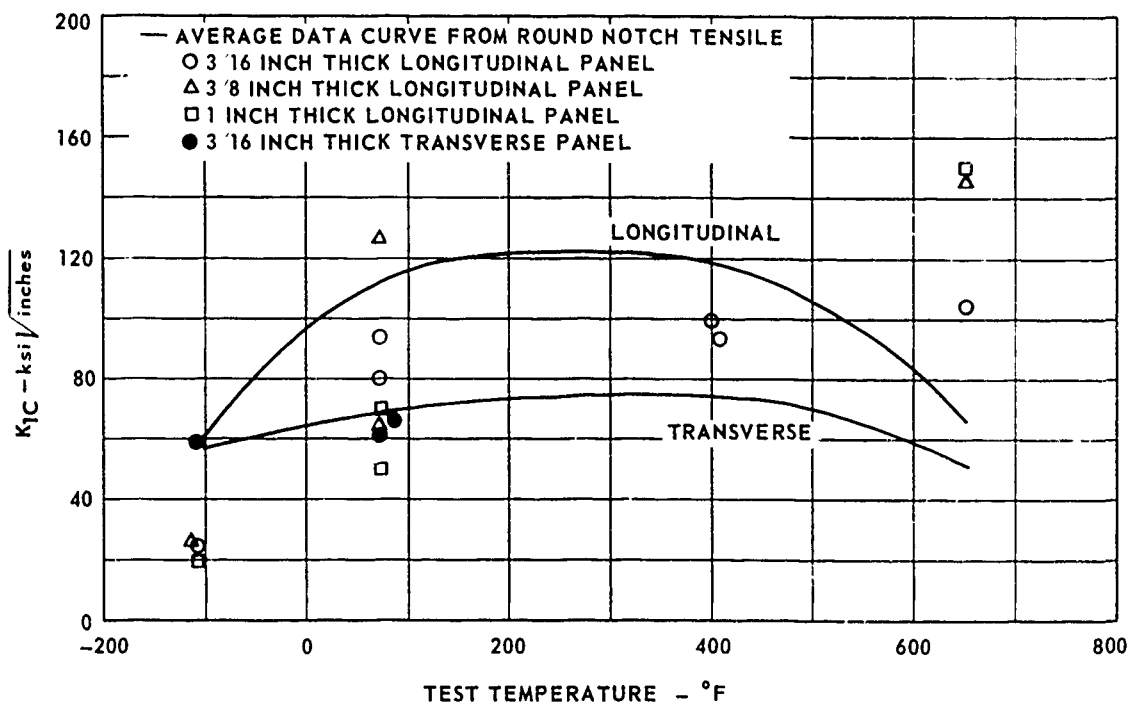


FIG. 84 COMPARISON OF K_{1C} FROM PANEL "POP-IN" AND ROUND NOTCH TENSILE FOR AM 355

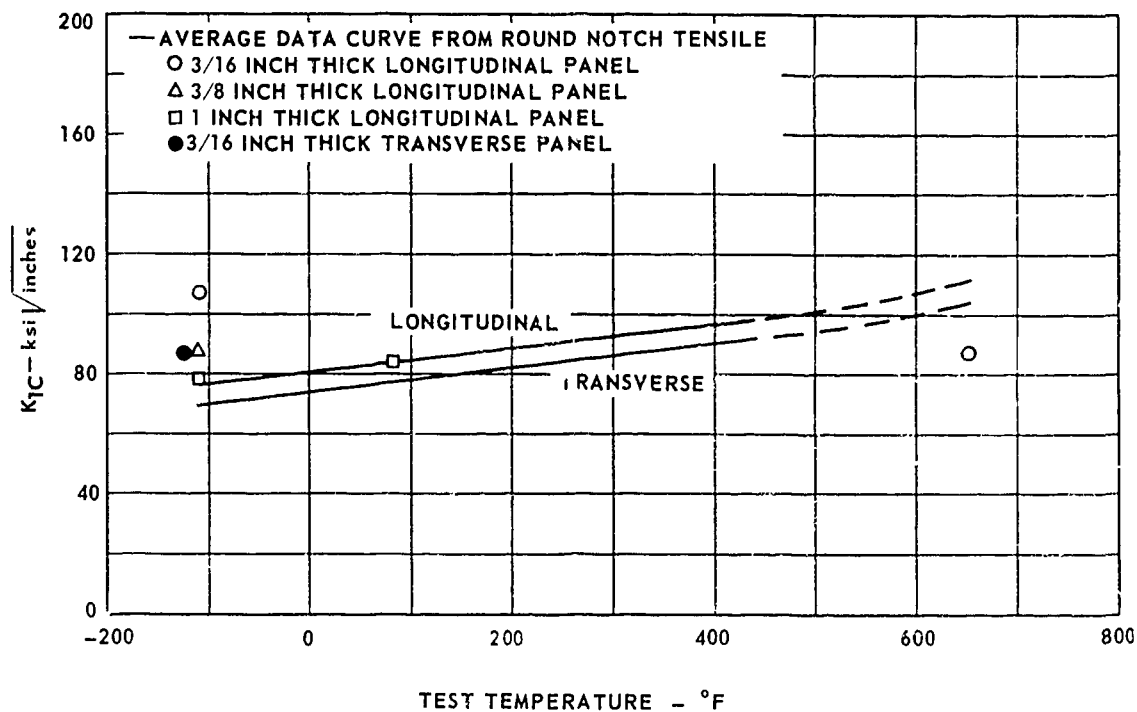


FIG. 85 COMPARISON OF K_{1C} FROM PANEL "POP-IN" AND ROUND NOTCH TENSILE MARGING 250

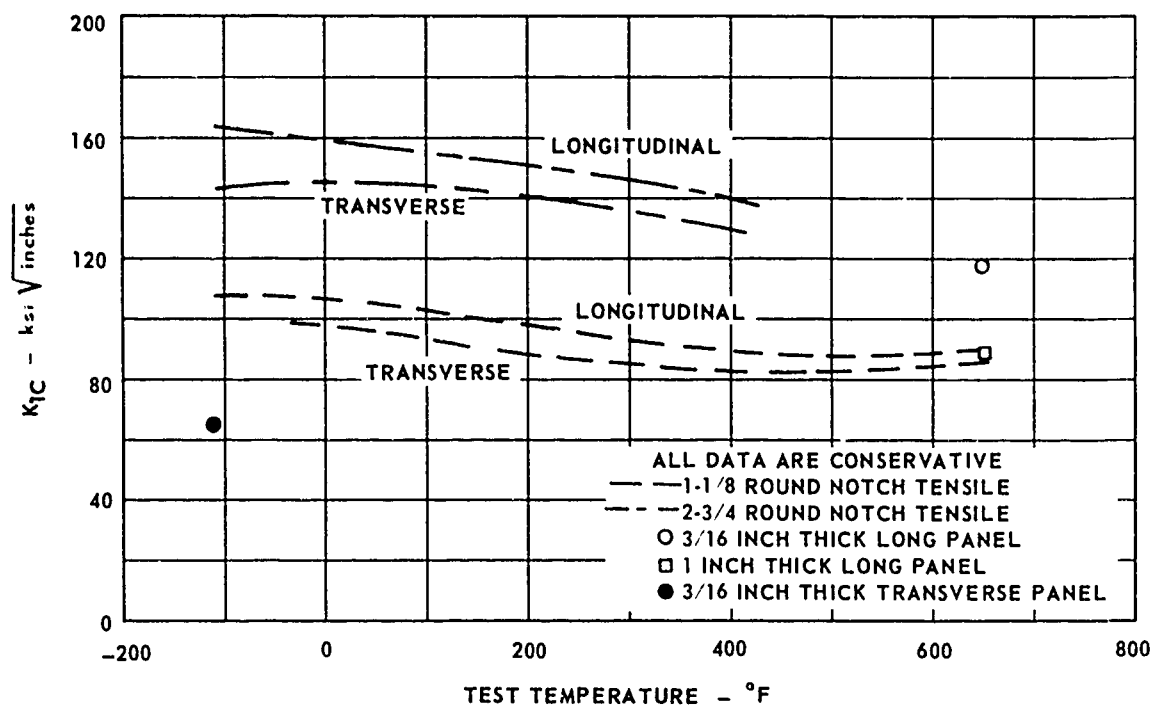


FIG. 86 COMPARISON OF K_{1C} FROM PANEL "POP-IN" AND ROUND NOTCH TENSILE FOR INCO 718

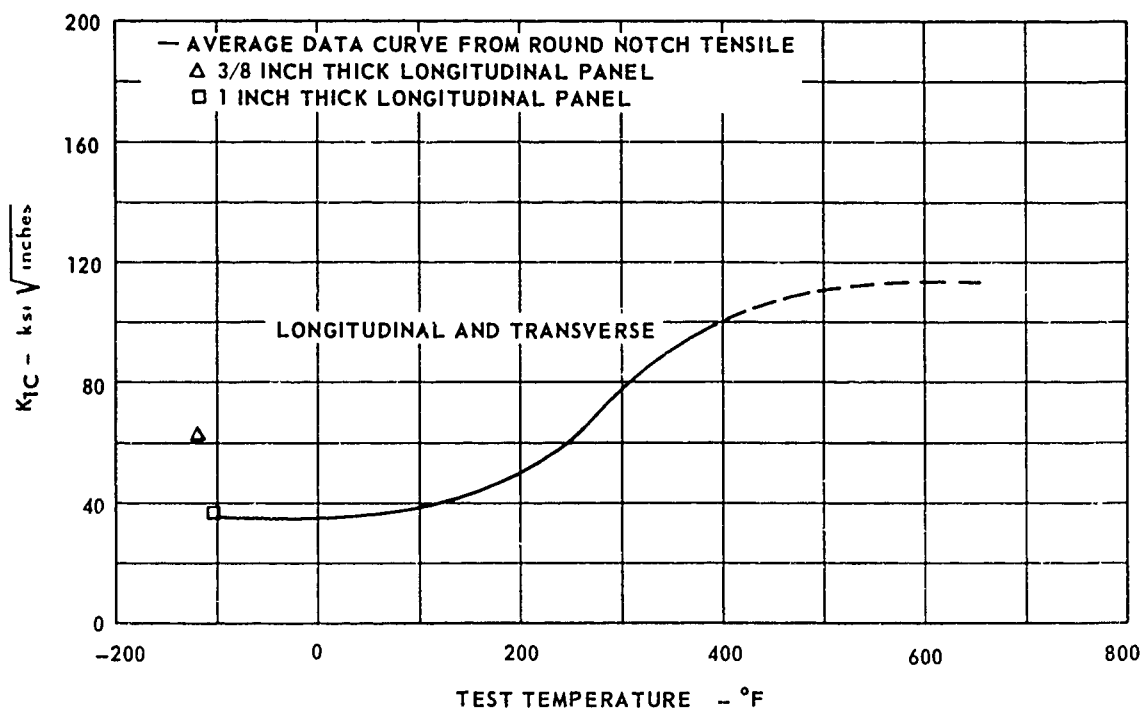


FIG. 87 COMPARISON OF K_{1C} FROM PANEL "POP-IN" AND ROUND NOTCH TENSILE FOR Ti 6Al-4V

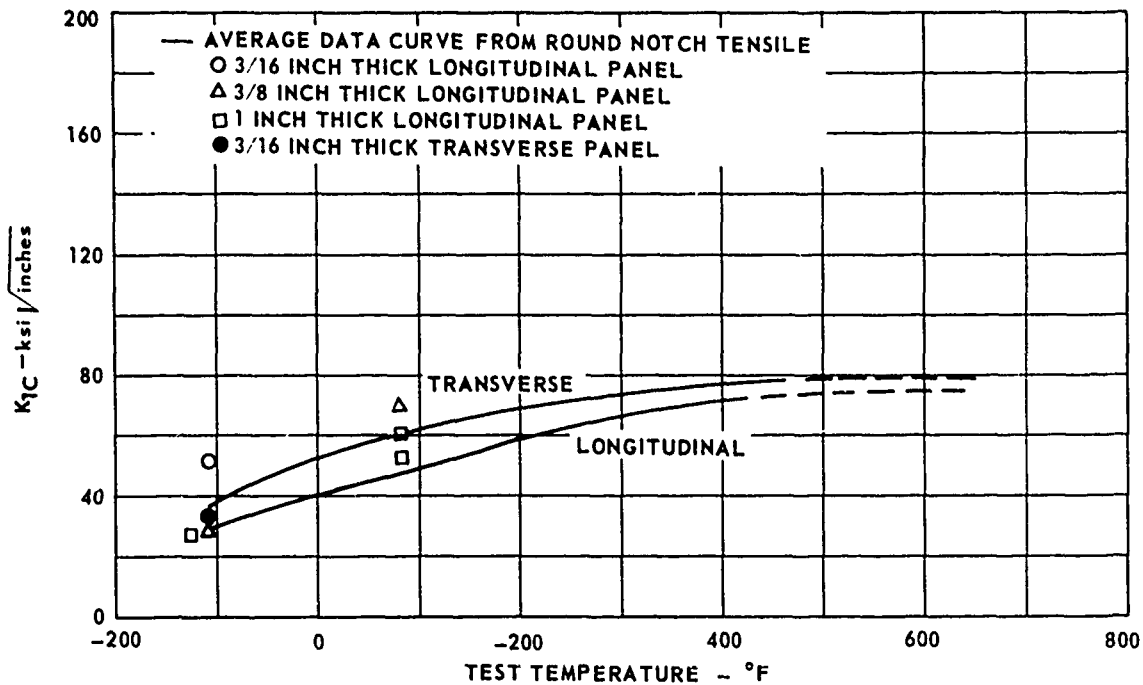


FIG. 88 COMPARISON OF K_{1C} FROM PANEL "POP-IN" AND ROUND NOTCH TENSILE FOR Ti 6Al-6V-2Sn ANN

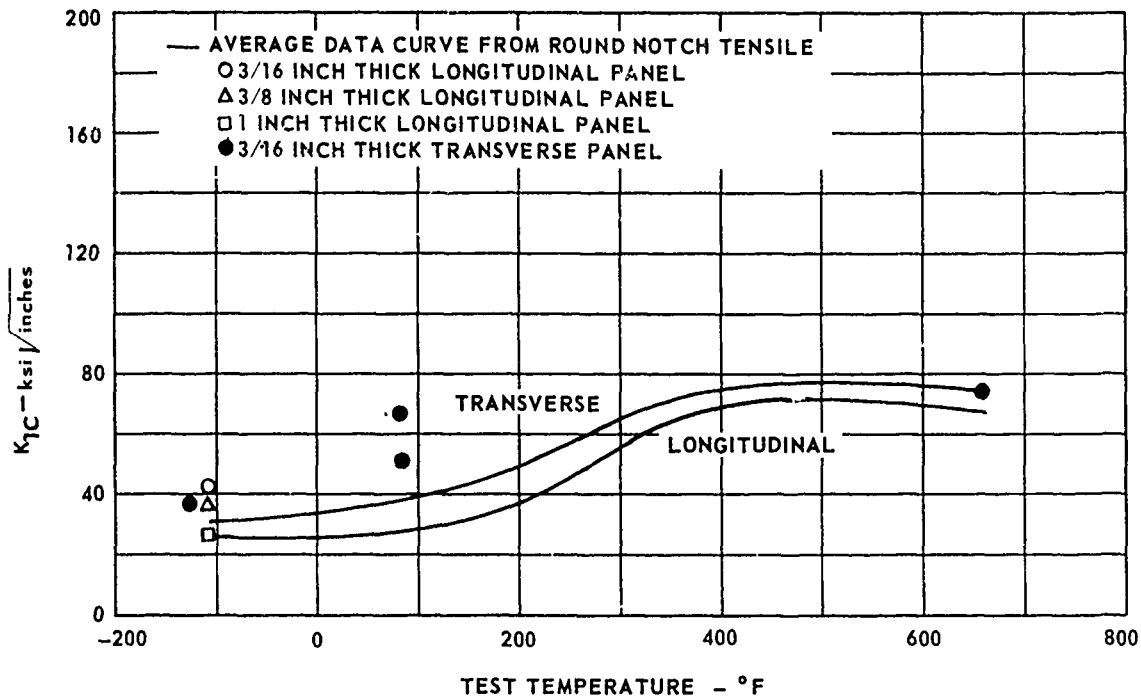


FIG. 89 COMPARISON OF K_{1C} FROM PANEL "POP-IN" AND ROUND NOTCH TENSILE FOR Ti 6Al-6V-2Sn STA

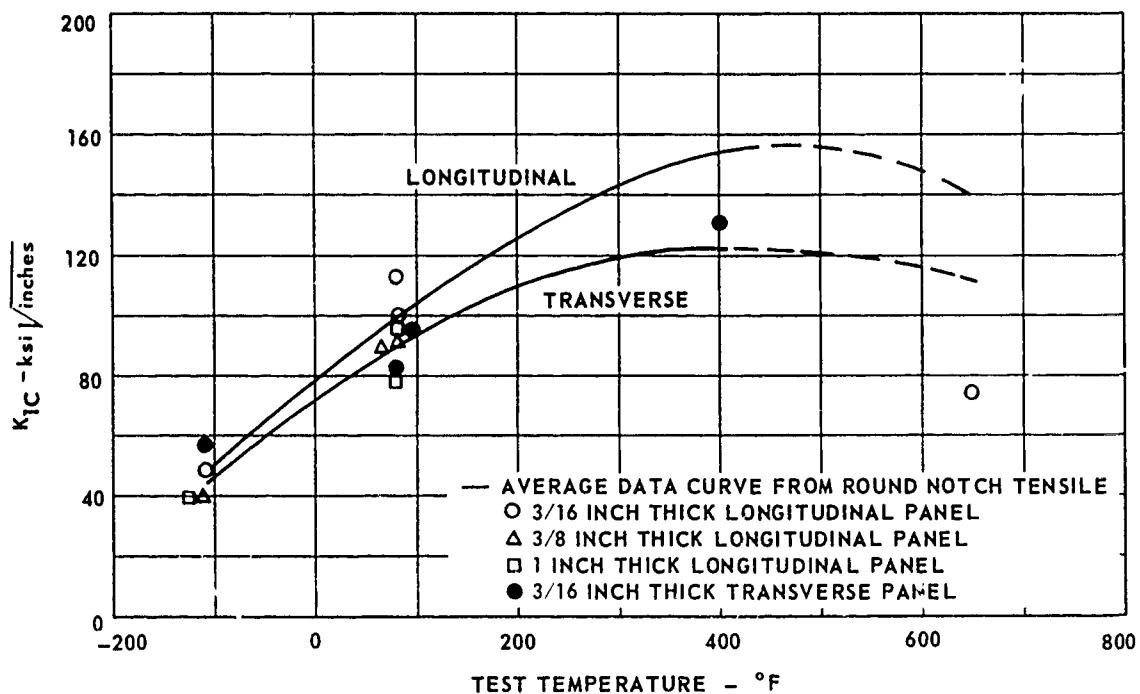


FIG. 90 COMPARISON OF K_{1C} FROM PANEL "POP-IN" AND ROUND NOTCH TENSILE FOR PH 13-8 Mo

loads shown in the tables correlate to the first pop-in detected by the extensometer.

There is considerable variation in the effect of temperature and thickness on the individual alloys. Results for each alloy will, therefore, be reviewed individually.

4340

In this alloy only the 3/16-inch thick specimens at higher temperatures had net stress to yield stress ratios above 0.8 (Fig. 42). Therefore, the thickness effect on K_{IC} was expected with increasing thickness lowering the values toward the plane strain condition. The 3/8 and 1-inch specimens at -110° F had no measurable shear lip and are approximately the same value and may be regarded as K_{IC} . The martensitic microstructure in this alloy has resulted in poor toughness at -110° F after which there is a constant rise with temperature.

Pop-in indications and flat fracture data plotted with the round notch K_{IC} curves (Fig. 82) indicate better correlation with 4340 than with most of the other alloys. However, even here some of the data showed wide variations.

Plastic zone correction of the data indicates a small increase in K_{IC} values except for the 3/16-inch thick specimens which increased rather sharply. This was due to the fact that the net stresses were high. Residual strength curves of the 3/16-inch thick specimens show the same general characteristics as the K_{IC} data with little variation between the longitudinal and transverse grain directions.

9 Ni-4Co

The greater toughness of this alloy has resulted in high net stresses, especially for the 3/16 and 3/8-inch thick specimens, as indicated by the number of arrows in Fig. 43. The effect of increasing K_{IC} values with decreasing panel thickness is seen at -110° F. As the temperature increased the net stress to yield stress ratio increased and the 3/16-inch values appear to be depressed.

A low point in the curve appears in the curve at the 400° F testing temperature which is also apparent in the round-notched data and as an increase in strength in the tensile data.

Plastic zone corrected data (Fig. 52) indicates an extreme increase due to the very high net stresses. At 650° F the values become so high they were not recorded.

AM 355

The martensitic microstructure appears to have resulted in low toughness at -110° F. The values for the three thicknesses are approximately the same and are somewhat below the round notch K_{IC} data (Fig. 44). All three specimens also had zero percent shear and therefore the values are undoubtedly K_{IC} values.

This alloy shows a very rapid rise in toughness to 400° F and a subsequent drop at 650° F which is very similar to the other stainless steel PH 13-8Mo. The reason for the drop is not known, although, as described in the test procedure, the specimens spend some time at 650° F under a negligible load and a microstructural change is doubtful.

Plastic zone correction results in exceptionally high values at higher temperatures (Fig. 53) where high net stress occurred. A comparison of residual strength of the 3/16-inch panels reveals a wide variation between the longitudinal and transverse grain direction.

AM 355 recorded numerous discontinuous cracking indications both on the load-displacement curve and on the accelerometer trace. The indications determined as valid pop-in are shown in Fig. 84 with the average curve for the round notch specimens included for comparison. Unfortunately the scatter prevents a satisfactory correlation. It is probable that the variation in fracture properties across a 9 x 9-inch cross-section from a forged block would result in some scatter. However, it is doubtful that this would account for the degree of scatter occurring in this test and it may indicate a limitation of pop-in data on tough alloys.

Maraging 250

An increase in toughness with decreasing thickness is seen at both -110° F and room temperature (Fig. 45). However, as net-stress to yield-strength ratios became large at higher temperatures the thickness effect reversed. Although the ratios above 0.8 cause a flattening of both the 3/16 and 3/8-inch thick specimen curves, the 1-inch thick specimen curve indicates a constant increase of toughness with temperature. The plastic zone correction (Fig. 54) has resulted in the toughness curves for all three thicknesses having the same slope and thickness effect, except at 650° F.

There were relatively fewer pop-in indications with this alloy and the ones that occurred were at lower temperatures. They tended in general to be above the plane strain data from the round notch specimens.

Inco 718

This alloy had exceptionally high toughness especially at low temperatures. The K_{IC} curves for the three thicknesses of specimens showed little effect from testing temperature (Fig. 46). The curves actually tended to be slightly higher at low temperatures. Table 17 indicates that the net stress ratio of every test was above 0.8 and therefore conservative. However, the ratios increased very little with increasing temperature and it is probable that the true K_{IC} values would not be affected significantly by temperature. This was the only alloy in which the data indicates the toughness increased with thickness. This may, however, be due to the fact that all the data were conservative. There were only three pop-in indications (Fig. 86) in this very tough alloy. The two values at 650° F may indicate the actual trend of the data.

Ti 6Al-4V

All values above room temperature were conservative and are, therefore, indicated with an arrow (Fig. 47). This is because of the rapid decrease of yield strength between room temperature and 400° F. The 3/16-inch thick panels appear to have depressed values over the whole temperature range. However, the 3/8-inch thick specimens show a higher toughness than the 1-inch thick specimens to above 400° F.

There were only two pop-in indications and these occurred at -110° F. One value agreed very well with the round K_{1C} values and the other was somewhat high.

Ti 6Al-6V-2Sn

This alloy was tested in both the heat treated and annealed conditions. The fewer number of STA specimens were tested at only the extreme temperature conditions so that annealed and STA curves could be compared. As expected, the annealed toughness was greater at -110° F; however, the values were very similar at 650° F (Figs. 48 and 49). The annealed data indicated a decrease in toughness from 400° F to 650° F as did the Ti 6Al-4V.

Both conditions showed an increase of toughness with thickness at -110° F and a complete reversal at 650° F. Again this was probably due to the high net stresses at high temperatures.

There were a number of pop-in indications for the alloy in both heat treated and annealed conditions showing fair correlation with K_{1C} from the round notch data. A number of the indications were readily observable on the fracture faces (Fig. 79).

Residual strength properties of the STA condition (Fig. 71) indicate very little directionality of fracture properties.

PH 13-8Mo

This alloy behaved similarly to the AM 355 stainless steel. The three thicknesses of specimens exhibited low fracture toughness at -110° F with the 3/8 and 1-inch specimens rising rapidly to 400° F. Above 400° F there appears to be a slight drop-off with testing temperature (Fig. 50).

Below 400° F the K_C values increase as the thickness decreases. As in most of the other alloys the trend reverses at high temperatures as the net-stress to yield-stress ratio increases above 0.8.

Numerous indications of discontinuous cracking were recorded for this alloy; as occurred in the AM 355. Those indications which were determined to be valid pop-ins were plotted with the average round notch K_{1C} curves in Fig. 90. In this case there is a fair correlation with most of the indications.

Residual strength properties of the 3/16-inch thick specimens (Fig. 72) reveal longitudinal grain direction to have higher fracture toughness than the transverse grain.

ELECTRON FRACTOGRAPHY

Fractographic studies have proven useful in relating test results to the fracture surface of specimens (Ref. 25). The fracture surface exhibits a topography characteristic of the mode of failure during propagation of the crack. The electron microscope with its high resolution and depth of field can be used to great advantage in this type of analysis. Therefore, an electron fractographic survey was conducted on each of the four most promising alloys of this program.

Replication Technique

Replicas in this survey were prepared utilizing the two-step cellulose acetate film method outlined below.

- 1) The fracture faces of each specimen had been protected by acrylic lacquer spray soon after testing. Therefore, the surface was cleaned by softening pieces of cellulose acetate in acetone and pressing them against the fracture surface and allowing them to dry. When the film was stripped off, the foreign material on the surface was removed.
- 2) A piece of acetate film wetted with a replicating solution of acetone with some dissolved cellulose acetate was applied to the fracture face. The acetone softens and partially dissolves the film which when pressed against the surface forms a plastic negative. The film was allowed to dry under pressure and stripped carefully from the surface.
- 3) A positive replica was prepared from the plastic negative by first shadowing with germanium at approximately 45°. Then carbon was deposited normal to the surface in a vacuum evaporator. The replicas were so oriented that the germanium shadowing direction was parallel to the general direction of crack propagation to aid in orientation of the picture.
- 4) Small 1/8-inch squares were cut from the replica in the regions of interest and the cellulose acetate was dissolved slowly in a mixture of acetone and distilled water. After the carbon replica had floated free, it was transferred to pure acetone and allowed to wash for a few hours. Specimen preparation was completed when the carbon replica was placed on a copper grid for viewing.

Effect of Temperature

In order to determine the effect of test temperature on the mode of fracture, the 3/8-inch thick center notched panels were selected. Specimens of 9 Ni-4Co, Maraging 250, Inco 718, and Ti 6Al-4V at each of the four test temperatures were replicated as described above.

The mechanism of the formation of dimples on the fracture surface of ductile alloys has been well documented (Refs. 26 and 27). The dimples are the result of plastic fracture in which microvoids form and coalesce into rounded, smooth concave depressions. Thus ductile rupture results in what has been termed dimples on the plastic replica.

The replicas in each case were taken from the slow growth area at the center of the panel thickness, adjacent to the fatigue crack. This was an area of apparent plane strain in even the toughest specimens. The fractographs of each of the alloys was characterized by dimples of varying sizes.

The size of the dimples tends to increase with testing temperature (Figs. 91, 92, 93 and 94); with a sudden large increase occurring between 400° F and 650° F. Even Inco 718, which showed very small dimples throughout the temperature range, showed considerable change between 400° F and 650° F. In this respect it was of interest to note that the toughness values for the Inco 718 decreased with temperature (Fig. 46). However, the yield strength also decreases, which may have more relevance to dimple size.

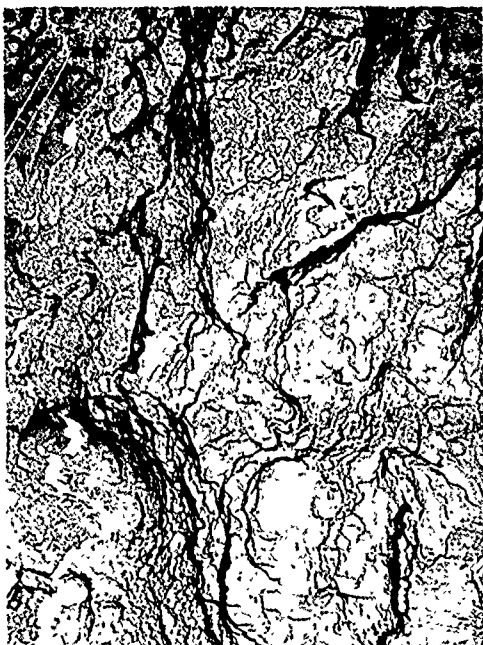
Ti 6Al-4V exhibits a much larger dimple size than the other alloys investigated. At 650° F, the size had become so large (Fig. 94) that individual dimples almost covered the field of vision of the photograph.

Effect of Crack Growth Rate

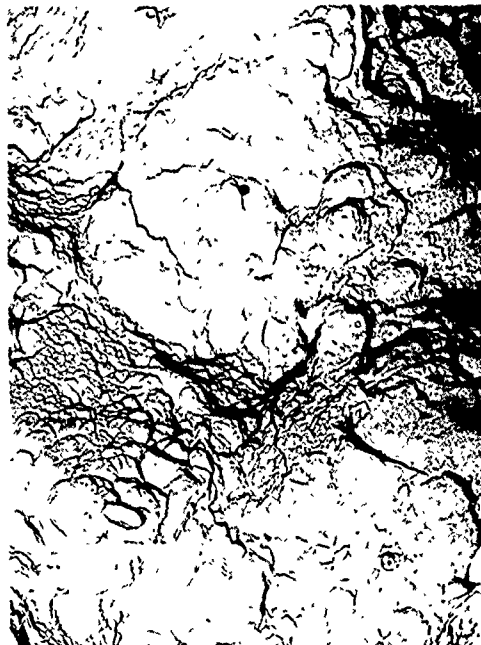
Several of the alloys displayed surface markings indicative of discontinuous cracking. Electron fractography was employed in an attempt to relate the fracture topography to the fracture test results. The 4340 room-temperature specimen (CA88) was selected because it displayed several readily discernible zones of fracture (Fig. 96) and its load-displacement curve gave a clear pop-in indication.

The load-displacement curve (Fig. 95) showed the linear elastic loading portion of the curve up to point A after which slow growth occurred to point B. Rapid unstable crack growth, referred to as pop-in, then occurred between B and C. The pop-in indication was recorded both by extensometer and by accelerometer. After pop-in, the crack again entered a zone of slow stable growth under load to point D. At this point the crack again became unstable and final rapid failure occurred.

An electron fractograph of the fatigue zone (1) in Fig. 96 revealed the typical transgranular appearance with faint fatigue striations (Fig. 97A). Several areas of intergranular crack propagation were also visible. The interface between the fatigue zone (1) and the slow, stable crack-growth zone (2) is shown in Fig. 97B. The slow-growth area at the lower side of the interface was characterized by a dimpled region. The slow crack-growth zones (2) and (4) were characterized by a dimpled structure shown in Fig. 97C. The rapid crack growth regions (3) and (5) revealed intergranular areas associated with the dimples (Fig. 97D).



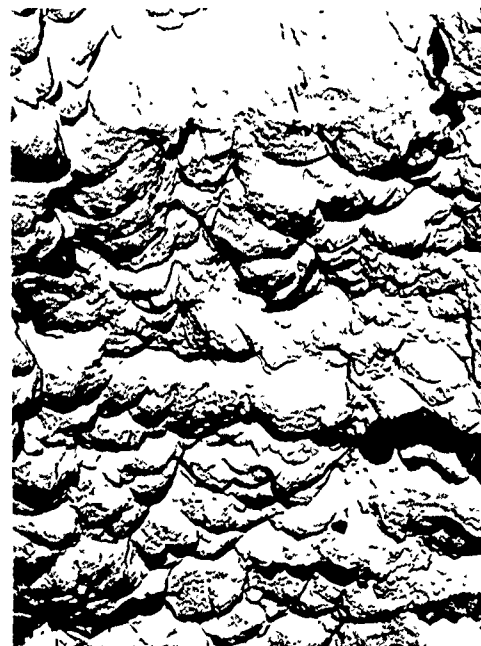
TESTED AT -110°F (Specimen CB 82)



TESTED AT R.T. (Specimen CB 87)



TESTED AT 400°F (Specimen CB 94)



TESTED AT 650°F (Specimen CB 98)

NOTE: Replicas taken from slow growth area adjacent to fatigue crack (1700x)

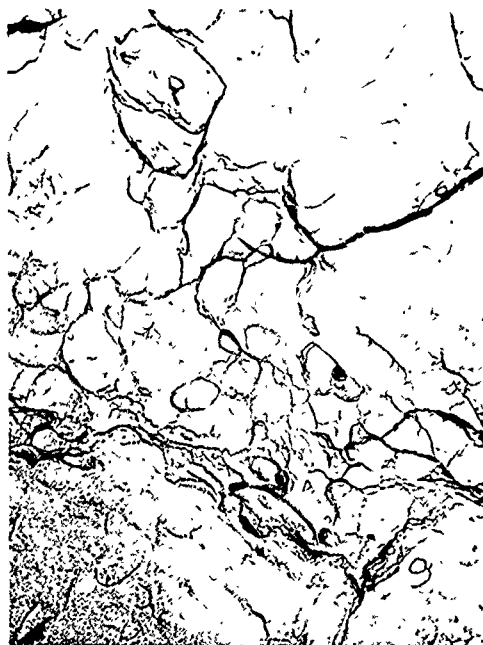
FIG. 91 ELECTRON FRACTOGRAPH OF CENTER NOTCHED 9 Ni-4Co



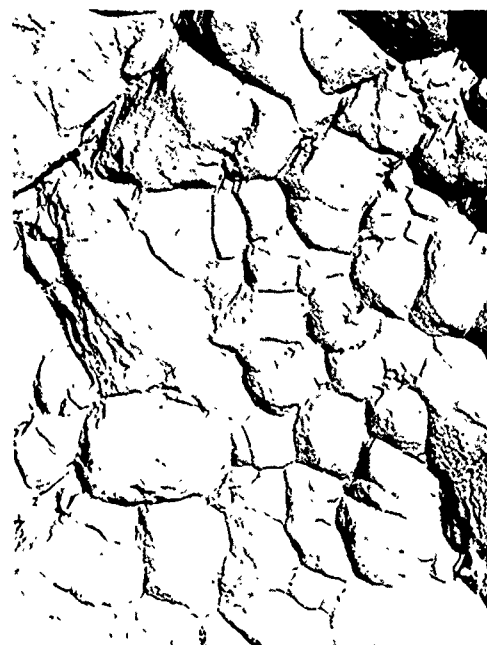
TESTED AT -110°F (Specimen CD 82)



TESTED AT R.T. (Specimen CD 87)



TESTED AT 400°F (Specimen CD 94)



TESTED AT 650°F (Specimen CD 98)

NOTE: Replicas taken from slow growth area adjacent to fatigue crack (1700x)

FIG. 92 ELECTRON FRACTOGRAPH OF CENTER NOTCHED MARAGING 250



TESTED AT -110°F (Specimen CE 82)



TESTED AT R.T. (Specimen CE 87)



TESTED AT 400°F (Specimen CE 94)



TESTED AT 650°F (Specimen CE 98)

NOTE: Replicas taken from slow growth area adjacent to fatigue crack (1700x)

FIG. 93 ELECTRON FRACTOGRAPH OF CENTER NOTCHED INCO 718



TESTED AT -110°F (Specimen CF 82)



TESTED AT R.T. (Specimen CF 87)



TESTED AT 400°F (Specimen CF 94)



TESTED AT 650°F (Specimen CF 98)

NOTE: Replicas taken from slow growth area adjacent to fatigue crack (1700x)

FIG. 94 ELECTRON FRACTOGRAPH OF CENTER NOTCHED Ti 6Al-4V

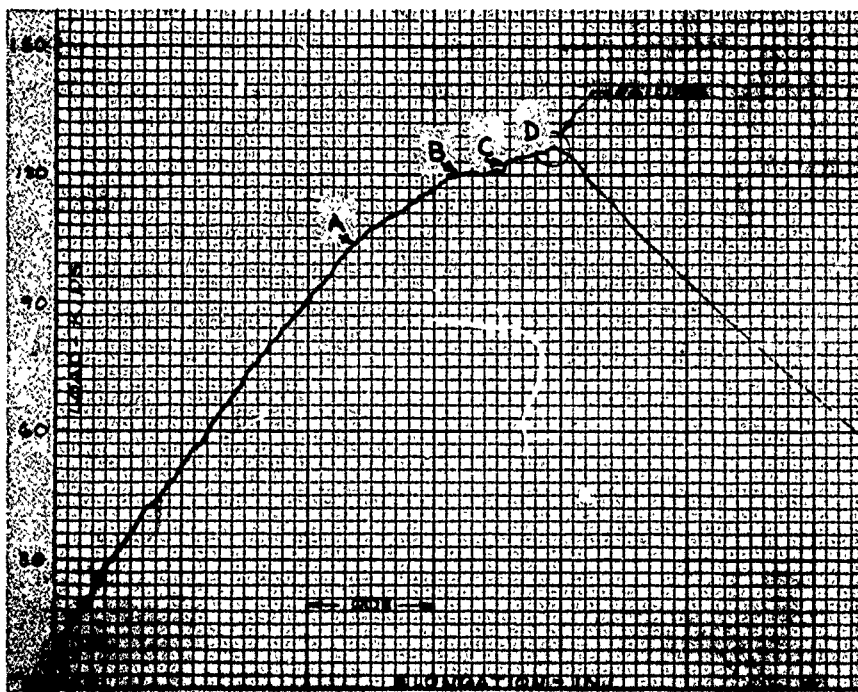


FIG. 95 LOAD-DISPLACEMENT CURVE OF 4340 CENTER NOTCH CA88 SPECIMEN

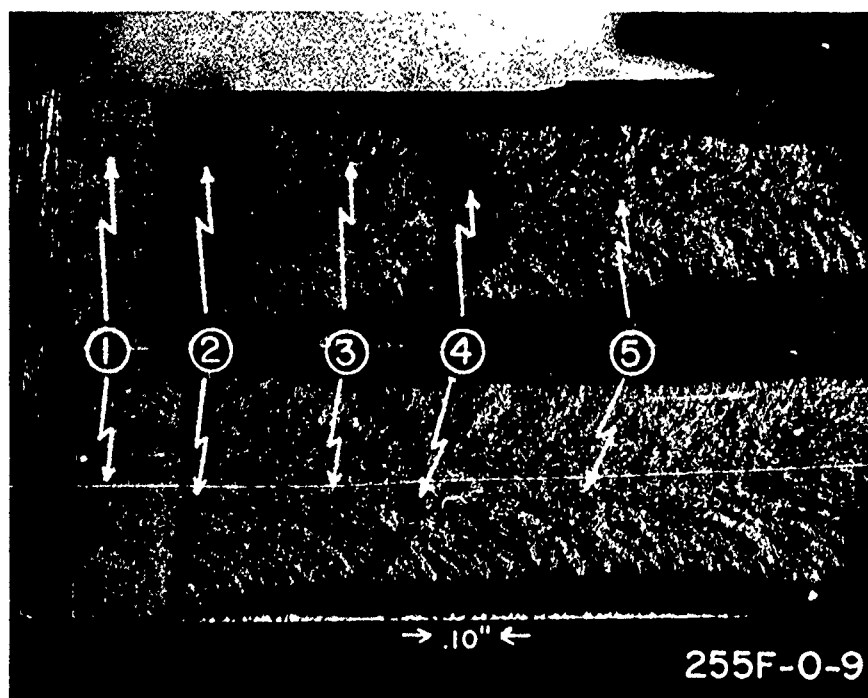
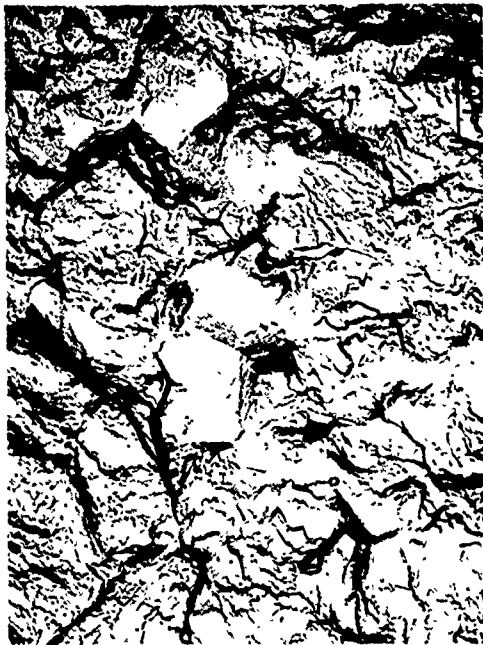


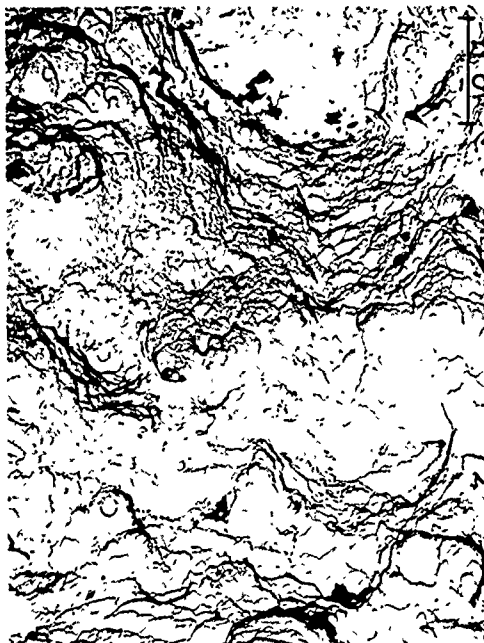
FIG. 96 MACROGRAPH OF CA88 SPECIMEN WITH SURFACE MARKINGS INDICATIVE OF DISCONTINUOUS CRACKING



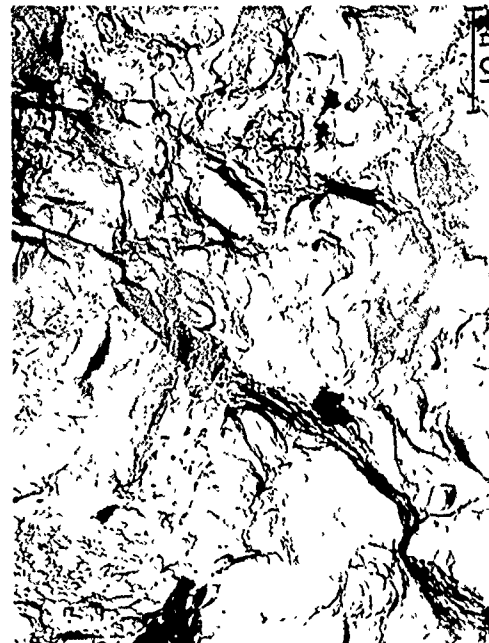
(A) TYPICAL FATIGUE AREA FROM ZONE 1



(B) FATIGUE INTERFACE BETWEEN ZONE 1 AND 2



(C) DIMPLED STRUCTURE TYPICAL OF ZONE 2 AND 4



(D) EVIDENCE OF INTERGRANULAR CRACKING IN FAST FRACTURE AREAS 3 AND 5

FIG. 97 FRACTOGRAPH ZONES OF SPECIMEN CA88 FROM FIG. 96

SECTION 8 ROUND-NOTCHED SPECIMENS

TEST PROCEDURE

Specimen Details

Fatigue-cracked notch tensile specimens shown in Fig. 98 were used to determine plane-strain fracture toughness. The specimens have a 1-1/8 inch major diameter with a ratio of net-to-major-diameter after fatigue cracking of approximately 0.7. This ratio results in minimum net section yielding and small variations in the ratio do not significantly affect the toughness equation parameters.

At the beginning of the program, it was realized that the 1-1/8 inch diameter specimen might not be large enough to avoid excessive net section yielding in all tests. Therefore, the program was planned so that additional specimens of a larger diameter could be run if excessive yielding occurred in some of the tests. As it turned out, excessive yielding occurred in many of the specimens and 2-3/4 inch diameter specimens were tested where needed.

Other plans considered at the beginning of the program were to increase the size of the specimens. However, a 1-1/8 inch diameter was as large as could be removed from the short transverse direction and still retain a reasonable length to diameter ratio. Also increasing the size of the specimens would have curtailed the quantity of data because of the high cost of testing larger specimens. Varying the specimen size to suit the alloy and test temperature was also considered. However, adequate data were not available to do this. Besides, consistent specimen size was desirable so that the data would be more comparable.

The billet location of the specimens is shown in the material section of the report. The specimen blanks were sawed from the billet, rough machined to a 1-3/16 inch diameter cylinder, heat treated, and then finish machined. The notches were machined by form grinding to a fine finish to facilitate viewing of the fatigue crack. The exact dimensions of each specimen are listed in the test data tables.

Fatigue Cracking

The specimens were fatigue cracked in a Sonntag SF-10-U fatigue machine equipped with a 5:1 load multiplier (Fig. 99) and a Riehle-Los hydraulic fatigue machine. Specimens were cycled axially at a load equivalent to one-third of the yield strength in the net section with an R of 0.05. This value of stress was used to minimize the plastic zone size at the crack tip and to reduce the danger of specimens failing during fatigue cracking. This loading produced adequate cracking in 6,000 to 10,000 cycles for all the alloys except AM 355 and Inco 718. A larger number of cycles were required for these two alloys because of the low loading resulting from low yield strengths. Specimens were rotated 120° at least three times during cycling to improve uniformity of crack depth around the notch circumference.

Crack propagation was observed with an alignment telescope and a stroboscopic light timed to flash at maximum crack opening. Care had to be taken to stop the

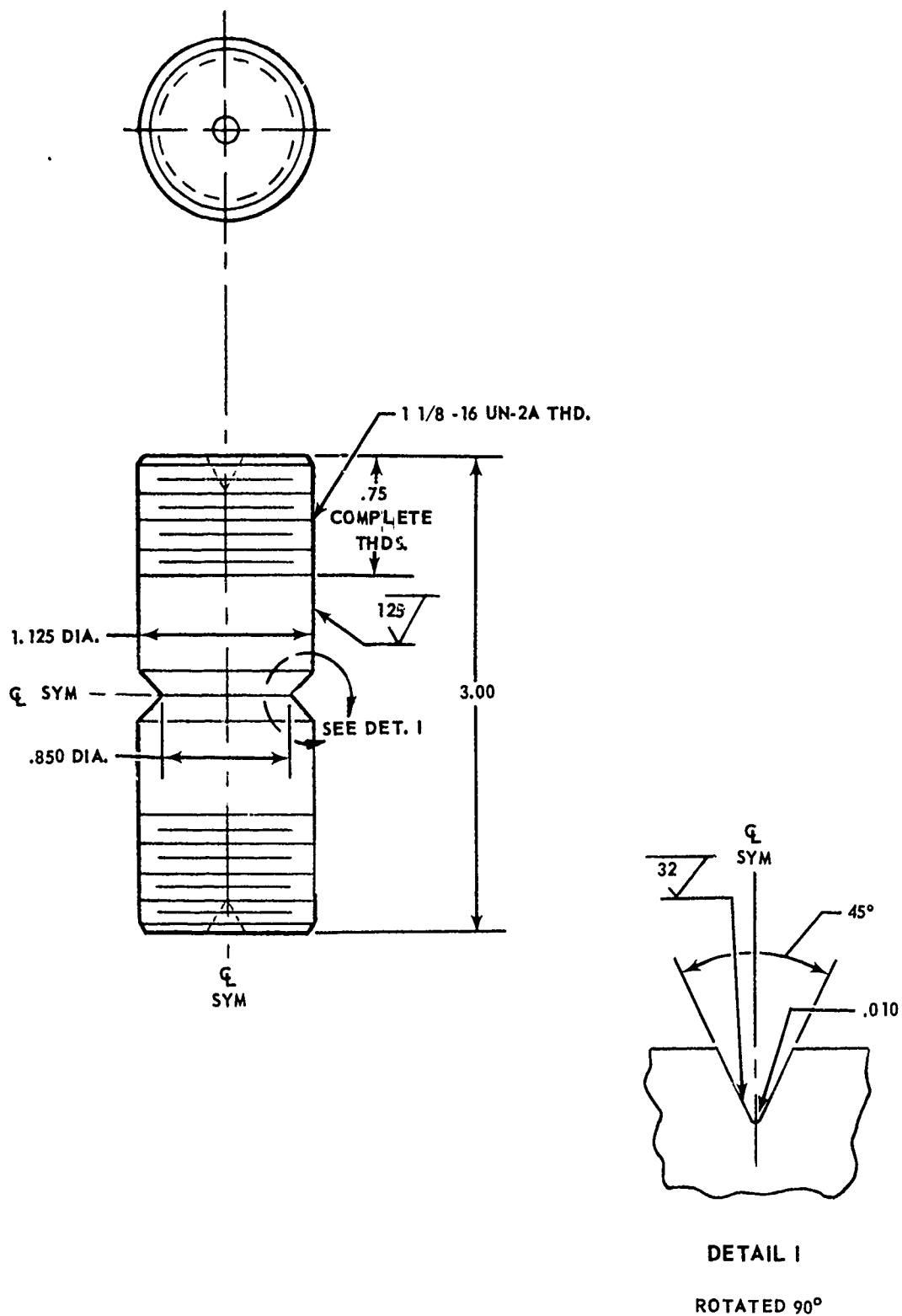


FIG. 98 1-1/8 INCH FATIGUE CRACKED NOTCH TENSILE SPECIMEN

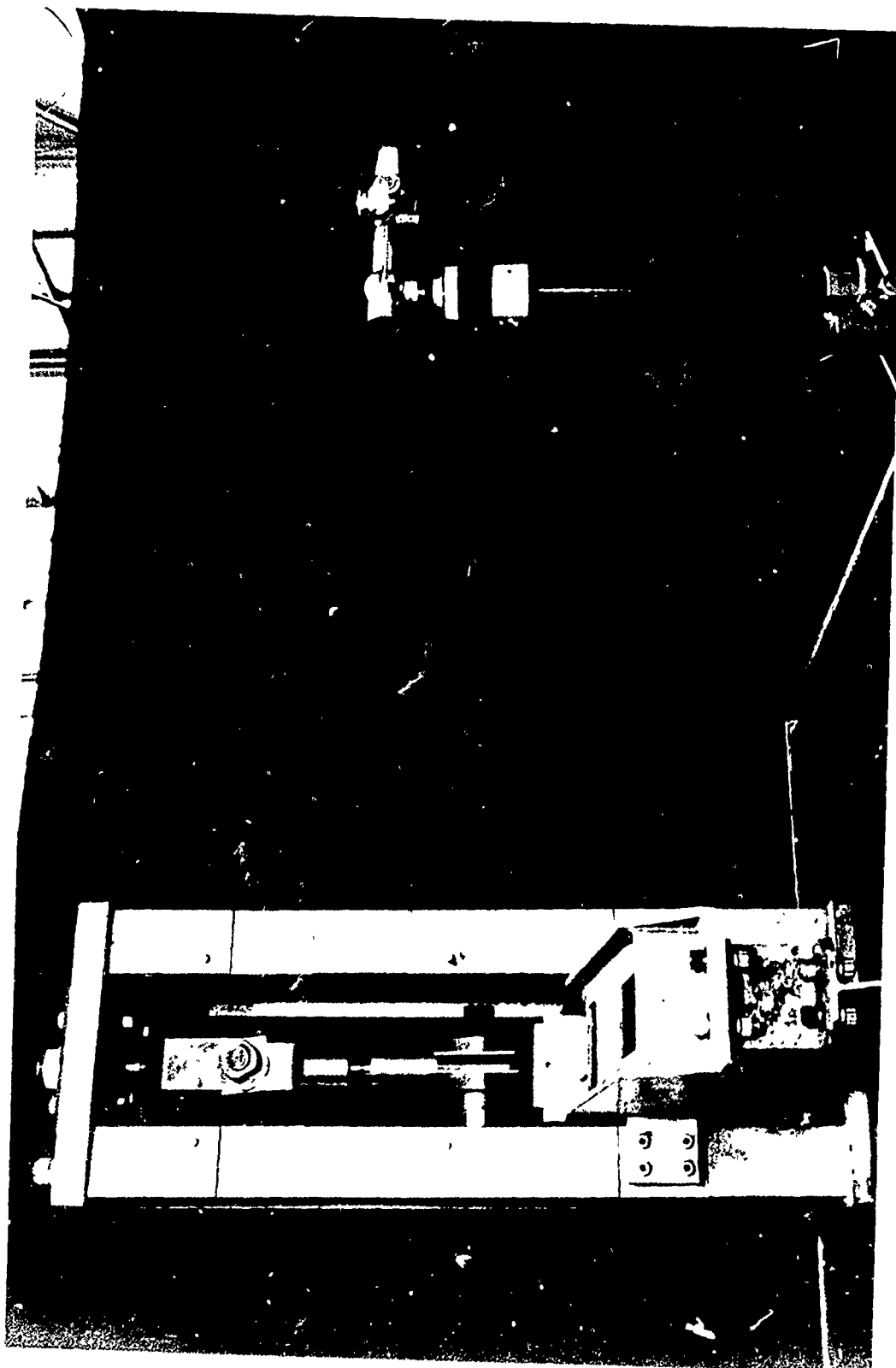


FIG. 99 FATIGUE CRACKING OF 1-1 8 INCH ROUND NOTCH TENSILE SPECIMEN

fatigue propagation at the proper time. When cracking was extended too long, the crack depth around the notch circumference tended to become less uniform. If cycling was stopped too soon, uncracked areas would be left in the notch root. In AM 355, many fine cracks formed in the notch root and gave the false appearance of adequate cracking, so a number of the AM 355 specimens contained uncracked areas. Most of the specimens had crack depths in the range of 0.030 to 0.060 inch.

Fracture Testing

The specimens were fracture tested in a Tinius-Olsen 440,000-pound capacity test machine (Fig. 100) and a 300,000-pound capacity Baldwin test machine. The load was applied through pin ended members, which screwed on to the specimen. The loading pins were maintained at right angles to each other to minimize loading eccentricities. Displacement across the notch was measured with an extensometer and recorded with load.

The extensometer arms were attached by means of wire loops spot welded to the notch edge (Fig. 101). This method of attachment permitted measurement directly at the notch. At specimen failure, the arms slipped out of the loops thus avoiding damage to the extensometer. High sensitivity was attained by using an arm pivot arrangement which produced a displacement magnification of two.

Cooling for the -110°F tests was accomplished by enclosing the specimen in an environmental box and injecting liquid nitrogen in the airstream of an enclosed circulation blower. A temperature within $\pm 5^{\circ}\text{F}$ of the test temperature was maintained by metering the nitrogen flow by a flow-control valve actuated by a control thermocouple. For the 400 and 650°F tests, an environmental box was again utilized to house the specimen. Pressurized air flowing through electrical resistance heated tubes and ducted to the box was used to heat the specimen. A control thermocouple and an ignitron maintained a temperature within $\pm 5^{\circ}\text{F}$ of the test temperature. Fig. 102 shows the heating and cooling system in detail. Four thermocouples were employed during each test to ensure a uniform specimen temperature.

The edge of the fatigue crack was clearly distinguishable on the fractured surface and the crack diameter was measured using a jeweler's magnifying glass and a 6 inch machinists' scale in 0.01 inch graduations. Four equally spaced diameter measurements were made on the fracture face in determining the average net diameter. The individual measurements were accurate to ± 0.002 inch. The average net diameter of each specimen is listed in Tables 22 through 30. The toughness calculations were based on the fatigue crack diameter.

Testing Procedures, 2-3/4 Inch Notched Rounds

The specimens (Fig. 103) were fatigue cracked and fractured in a 1,000-kip vertical hydraulic test machine, (Fig. 104). Loads were applied through pin-ended members screwed to the specimen. Load eccentricities were minimized through the universal joint design of the test machine. The specimens were cycled at loads equivalent to one-third to one-fifth the yield stress. The stress was reduced to one-fifth yield stress on some specimens to reduce the danger of failure during fatigue cracking. This loading produced adequate cracking in 3,000 to 25,000 cycles.

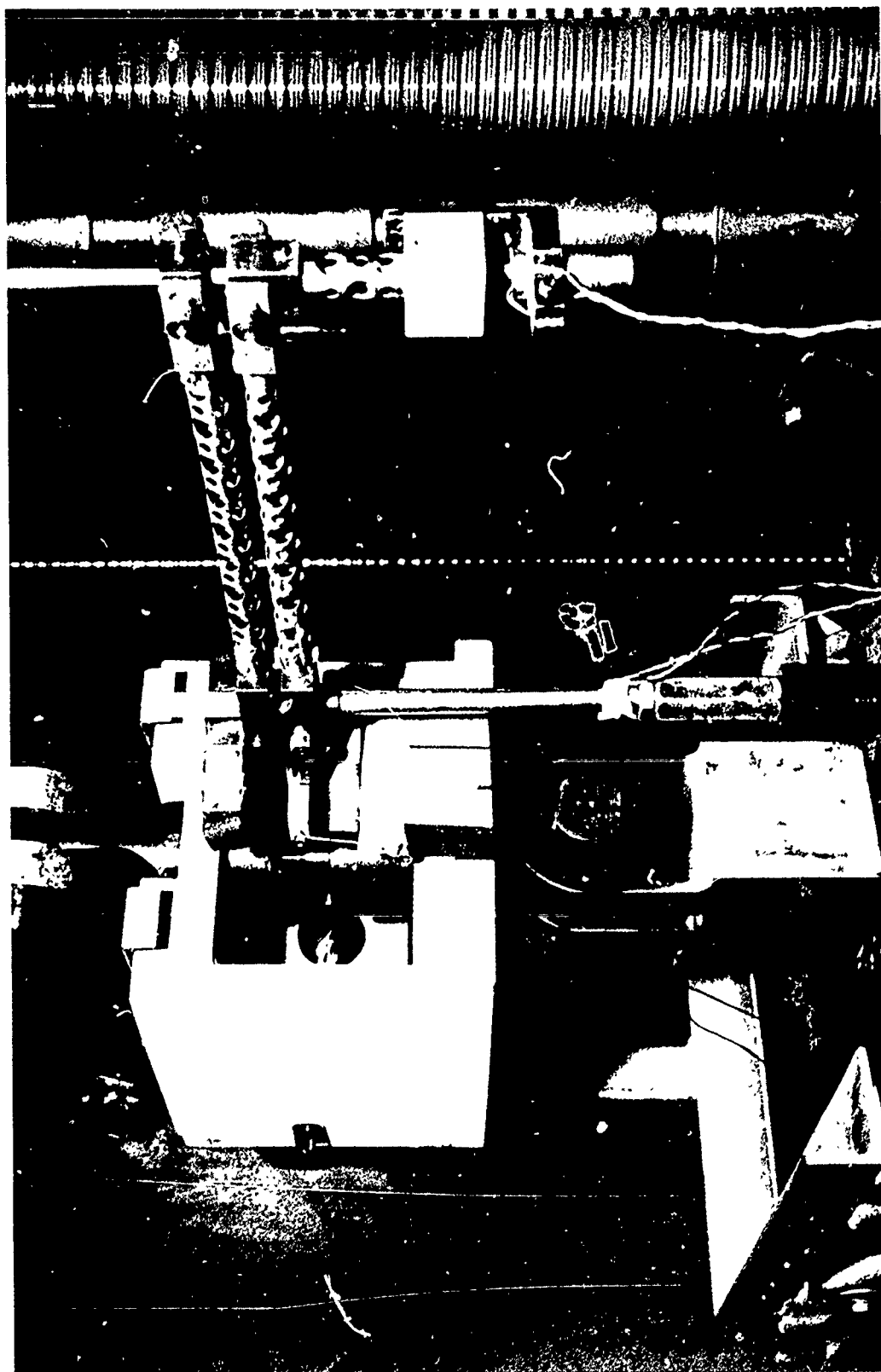


FIG. 100 FRACTURE TESTING OF 1-1 8 INCH ROUND NOTCH TENSILE SPECIMEN

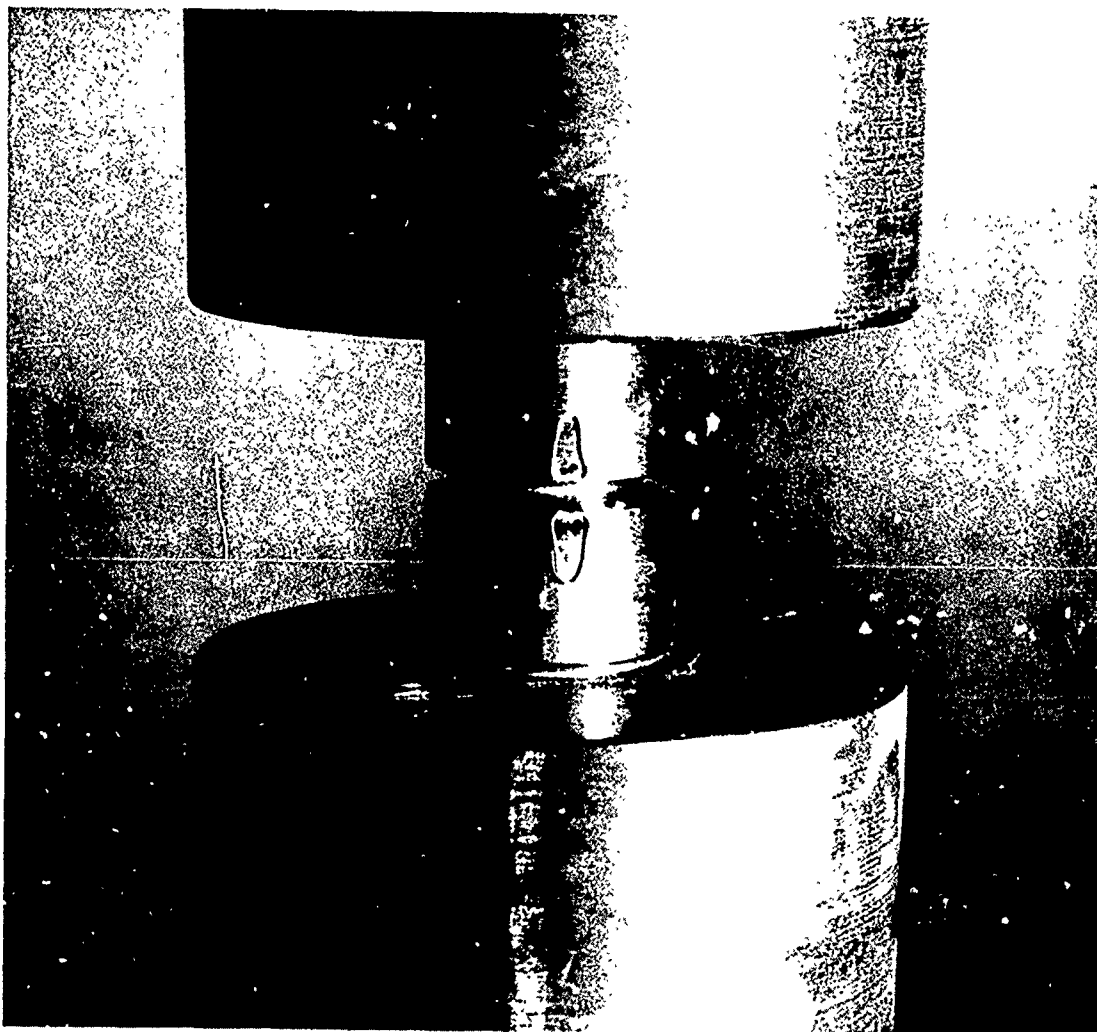


FIG. 101 WIRE LOOP ATTACHMENTS FOR 1-1 8 INCH ROUND NOTCH SPECIMEN

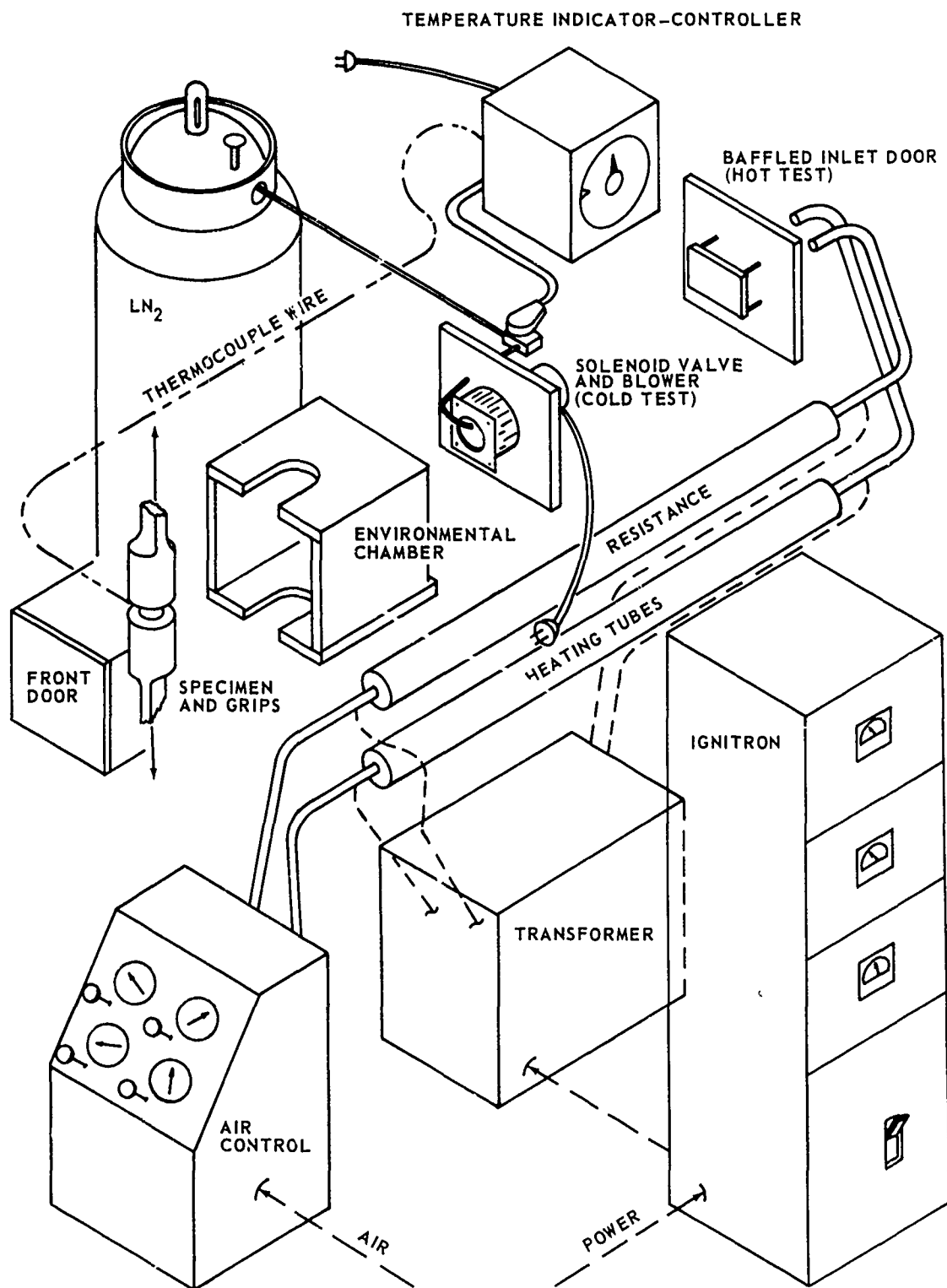


FIG. 102 1-1/8 INCH ROUND NOTCH SPECIMEN HEATING OR COOLING SETUP

TABLE 22 ROUND NOTCH TENSILE DATA FOR 4340

SPECIMEN NO.	TEST TEMP. °f	GRAIN DIRECTION	MAJOR DIAMETER (D) inches	NOTCH DIAMETER inches	NET DIAMETER inches	MAXIMUM LOAD kips	NET AREA in ²	σ_N ksi	K_{1C} ksi $\sqrt{\text{in}}$	YIELD STRENGTH .2% OFFSET ksi	$\frac{\sigma_N}{\sigma_{ys}}$	K_{1Cp} ksi $\sqrt{\text{in}}$
A3G1	-110	L	1.122	.846	.815	76.0	.521	145.8	63.5	229.4	.64	65.5
A3G4	-110	L	1.123	.845	.806	61.6	.510	120.7	52.9	229.4	.53	53.4
A211	-110	T	1.121	.844	.806	61.8	.510	121.0	52.9	213.9	.57	53.8
A212	-110	T	1.123	.845	.829	70.4	.540	130.3	56.8	213.9	.61	58.3
A1J6	-110	ST	1.123	.846	.768	45.8	.463	98.7	43.2	215.0	.46	43.6
A3G5	75	L	1.123	.846	.715	97.3	.402	189.1	82.8	213.0	.89	86.8
A214	75	T	1.122	.844	.788	89.0	.488	182.5	79.9	202.2	.90	83.9
A1J5	75	ST	1.123	.850	.788	76.8	.488	157.3	68.9	196.9	.80	71.7
A3G2	400	L	1.222	.847	.815	93.5	.522	179.0	78.2	184.7	.97	83.2
A1J1	400	ST	1.122	.846	.775	70.3	.472	149.0	65.4	184.4	.80	67.9
A3G3	650	L	1.123	.844	.787	119.0	.487	244.3	107.0	162.4	1.50*	128.7
A3G6	650	L	1.122	.845	.766	101.5	.461	220.1	96.3	162.4	1.36*	110.1
A215	650	T	1.122	.846	.744	84.4	.470	179.4	78.5	155.2	1.16*	85.7
A213	650	T	1.123	.845	.830	117.3	.541	216.7	94.5	155.2	1.40*	109.9
A1J2	650	ST	1.123	.845	.767	69.9	.463	151.0	66.1	156.7	.96	70.1
A1J3	650	ST	1.123	.845	.788	69.5	.488	142.3	62.3	156.7	.91	65.6
A1J4	650	ST	1.122	.846	.815	102.0	.522	195.3	85.3	156.7	1.25*	95.0

* THESE RATIOS ARE ABOVE THE 1.1 LIMIT RECOMMENDED BY THE ASTM COMMITTEE FOR FRACTURE TOUGHNESS

FATIGUE DATA:

MAX. CYCLING STRESS APPROXIMATELY 55 ksi, 6000 TO 12,000 CYCLES

R = .05

CYCLING RATE WAS 1800 cpm

FRACTURE TEST LOADING RATE WAS 150 ksi/min.

TABLE 23 ROUND NOTCH TENSILE DATA FOR 9N.-4Co

SPECIMEN NO.	TEST TEMP. of	GRAIN DIRECTION	MAJOR DIAMETER (D) inches	NOTCH DIAMETER inches	NET DIAMETER inches	MAXIMUM LOAD kips	NET AREA in ²	σ_N ksi	K_{IC} ksi $\sqrt{\text{in}}$	YIELD STRENGTH .2% OFFSET ksi	$\frac{\sigma_N}{\sigma_{ys}}$	K_{ICP} ksi $\sqrt{\text{in}}$
B3G4	-110	L	1.123	.846	.801	120.8	.504	239.8	105.0	211.3	1.14*	114.3
B211	-110	T	1.121	.851	.805	111.5	.509	219.0	95.9	220.6	.99	101.8
B217	-110	T	1.124	.846	.811	116.4	.517	225.3	98.7	220.6	1.02	105.8
B3G2	75	L	1.121	.845	.773	107.3	.470	228.2	99.9	198.4	1.15*	108.7
B316	75	T	1.120	.843	.765	105.4	.460	229.3	100.3	204.7	1.12*	108.7
B3G3	400	L	1.125	.846	.779	93.5	.477	195.9	85.8	169.1	1.16*	93.8
B213	400	T	1.124	.844	.786	90.3	.485	185.9	81.4	165.1	1.13*	89.3
B3G1	650	L	1.123	.846	.790	139.3	.490	284.0	124.4	131.4	2.16*	•
B3G5	650	L	1.123	.846	.771	136.5	.467	292.0	127.8	131.4	2.22*	•
B3G6	650	L	1.124	.846	.811	126.5	.517	244.6	106.7	131.4	1.86*	•
B214	650	T	1.124	.848	.808	137.5	.513	267.8	117.3	149.4	1.79*	•
B215	650	T	1.122	.846	.800	135.5	.503	269.6	118.0	149.4	1.81*	•

* THESE RATIOS ARE ABOVE THE 1.1 LIMIT RECOMMENDED BY THE ASTM COMMITTEE FOR FRACTURE TOUGHNESS

FATIGUE DATA:

MAX. CYCLING STRESS APPROXIMATELY 69 ksi, 6000 TO 8000 CYCLES

R = .05

CYCLING RATE WAS 1800 cpm

FRACTURE TEST LOADING RATE WAS 150 ksi/min.

• EXTREME DUCTILE FAILURE

TABLE 24 ROUND NOTCH TENSILE DATA FOR AM 355

SPECIMEN NO.	TEST TEMP. of	GRAIN DIRECTION	MAJOR DIAMETER (D) inches	NOTCH DIAMETER inches	NET DIAMETER inches	MAXIMUM LOAD kips	NET AREA in ²	σ_N ksi	K_{IC} ksi $\sqrt{\text{in}}$	YIELD STRENGTH .2% OFFSET ksi	$\frac{\sigma_N}{\sigma_{ys}}$	K_{ICP} ksi $\sqrt{\text{in}}$
C3G1	-110	L	1.123	.846	.846**	79.5	.562**	141.4**	61.5**	203.2	.70	63.7**
C3G4	-110	L	1.121	.847	.820	60.5	.528	114.6	50.0	203.2	.56	51.1
C2I1	-110	T	1.122	.844	.844**	85.8	.559**	153.3**	66.7**	179.5	.85	70.1**
C2I2	-110	T	1.121	.847	.847**	80.9	.563**	143.5**	62.4**	179.5	.80	65.4**
C1J1	-110	ST	1.121	.847	.805	47.3	.510	92.7	40.6	183.9	.48	41.1
C1J6	-110	ST	1.124	.847	.796	45.3	.498	90.9	39.8	183.9	.49	40.4
C3G5	75	L	1.123	.847	.805	121.8	.509	239.2	104.7	166.7	1.43*	122.7
C2I6	75	T	1.122	.849	.815	80.3	.522	153.8	67.3	161.1	.96	71.4
C1J2	75	ST	1.122	.847	.729	61.5	.417	147.5	64.6	153.6	.96	68.4
C1J5	75	ST	1.123	.840	.804	84.8	.507	167.0	73.1	153.6	1.09	78.8
C3G3	400	L	1.123	.839	.839**	146.3	.553**	264.6**	114.8**	144.1	1.84*	
C3G2	400	L	1.121	.847	.847**	145.3	.563**	257.8**	112.1**	144.1	1.79*	
C2I3	400	T	1.121	.845	.810	84.8	.515	164.6	71.9	143.2	1.15*	78.5
C1J4	400	ST	1.122	.847	.803	90.3	.507	178.1	78.0	142.5	1.25*	86.7
C3G6	650	L	1.123	.847	.795	78.8	.496	158.9	69.6	148.1	1.07	74.9
C2I5	650	T	1.123	.847	.720	46.3	.408	113.4	49.7	126.4	.79	51.6
C1J3	650	ST	1.122	.850	.719	46.8	.406	115.1	50.4	135.0	.85	52.7

* THESE RATIOS ARE ABOVE THE 1.1 LIMIT RECOMMENDED BY THE ASTM COMMITTEE FOR FRACTURE TOUGHNESS

** NOTCH ROOT CONTAINED AREAS WHICH WERE NOT FATIGUE CRACKED.

FATIGUE DATA:

MAX. CYCLING STRESS APPROXIMATELY 55 ksi, 6000 TO 17,000 CYCLES

R = .05

CYCLING RATE WAS 1800 cpm

FRACTURE TEST LOADING RATE WAS 150 ksi/min.

TABLE 25 ROUND NOTCH TENSILE DATA FOR MARAGING 250

SPECIMEN NO.	TEST TEMP. °f	GRAIN DIRECTION	MAJOR DIAMETER (D) inches	NOTCH DIAMETER inches	NET DIAMETER inches	MAXIMUM LOAD kips	NET AREA in ²	σ_N ksi	K_{1C} ksi $\sqrt{\text{in}}$	YIELD STRENGTH .2% OFFSET ksi	$\frac{\sigma_H}{\sigma_{ys}}$	K_{1Cp} ksi $\sqrt{\text{in}}$
D3G1	-110	L	1.122	.849	.764	76.5	.458	169.7	74.3	230.5	.74	76.6
D3G4	-110	L	1.120	.848	.765	80.3	.460	174.6	76.4	230.5	.76	78.7
D2I1	-110	T	1.121	.849	.750	72.0	.441	163.2	71.4	232.9	.70	73.4
D2I2	-110	T	1.120	.849	.750	69.3	.441	157.0	68.7	232.9	.67	70.3
D1J6	-110	ST	1.120	.848	.748	64.5	.439	146.8	64.2	232.5	.63	65.4
D1J8	-110	ST	1.119	.848	.759	68.3	.452	150.8	65.9	232.5	.65	67.6
D3G5	75	L	1.121	.849	.757	82.5	.450	183.3	80.2	212.5	.86	84.1
D3G3	75	L	1.120	.848	.754	86.3	.447	193.2	84.5	212.5	.91	88.9
D2I6	75	T	1.120	.849	.728	72.8	.416	175.0	76.6	216.7	.81	79.7
D2I4	75	T	1.120	.848	.698	64.0	.382	167.5	73.0	216.7	.77	76.0
D1J5	75	ST	1.119	.848	.781	71.5	.478	149.4	65.3	218.3	.68	67.1
D1J9	75	ST	1.118	.849	.734	61.8	.423	146.2	63.9	218.3	.67	65.5
D3G2	400	L	1.120	.850	.784	111.0	.483	230.0	100.6	183.9	1.25*	112.1
D2I3	400	T	1.118	.849	.767	94.0	.462	203.3	98.9	189.8	1.07	95.3
D1J4	400	ST	1.120	.848	.742	81.5	.433	188.4	82.4	198.2	.95	87.0
D3G6	650	L	1.120	.849	.742	105.6	.432	244.2	106.9	182.6	1.33*	121.6
D2I5	650	T	1.121	.848	.747	100.0	.438	228.4	100.0	187.0	1.22*	110.5
D1J10	650	ST	1.119	.849	.755	87.5	.447	195.7	85.5	187.9	1.04	91.6

* THESE RATIOS ARE ABOVE THE 1.1 LIMIT RECOMMENDED BY THE ASTM COMMITTEE FOR FRACTURE TOUGHNESS

FATIGUE DATA:

MAX. CYCLING STRESS APPROXIMATELY 72 ksi, 7000 TO 9000 CYCLES

R = .05

CYCLING RATE WAS 1800 cpm

FRACTURE TEST LOADING RATE \dot{W} A : 50 ksi min.

TABLE 26 ROUND NOTCH TENSILE DATA FOR INCO 718

SPECIMEN NO	TEST TEMP. of	GRAIN DIRECTION	MAJOR DIAMETER (D) inches	NOTCH DIAMETER inches	NET DIAMETER inches	MAXIMUM LOAD kips	NET AREA in ²	σ_N ksi	K_{IC} ksi $\sqrt{\text{in}}$	YIELD STRENGTH .2% OFFSET ksi	$\frac{\sigma_N}{\sigma_{ys}}$	K_{IC_p} ksi $\sqrt{\text{in}}$
E3G1	-110	L	1.122	.848	.757	113.3	.451	251.3	110.0	171.8	1.46*	130.3
E3G4	-110	L	1.123	.850	.745	109.3	.436	250.6	109.7	171.8	1.46*	129.7
E211	-110	T	1.124	.848	.700	84.8	.385	220.2	96.4	164.2	1.34*	109.8
E212	-110	T	1.121	.848	.779	114.5	.476	240.4	105.2	164.2	1.46*	124.5
E3G3	75	L	1.124	.848	.848**	130.5	.565**	231.1**	100.3**	156.0	1.48*	120.8
E3G5	75	L	1.122	.848	.777	117.0	.474	246.7	108.0	156.0	1.58*	135.3
E214	75	T	1.121	.849	.811	111.3	.517	215.2	94.2	154.5	1.39**	109.0
E216	75	T	1.123	.850	.753	98.8	.445	221.8	97.1	154.5	1.44*	114.0
E3G2	400	L	1.124	.849	.774	96.8	.471	205.6	90.0	146.1	1.41*	104.6
E213	400	T	1.122	.849	.765	89.0	.459	193.6	84.8	145.1	1.33*	96.2
E3G6	650	L	1.122	.850	.803	104.8	.506	207.1	90.7	143.9	1.44*	106.4
E215	650	T	1.120	.848	.746	86.8	.438	198.2	86.7	137.3	1.44*	102.0

* THESE RATIOS ARE ABOVE THE 1.1 LIMIT RECOMMENDED BY THE ASTM COMMITTEE FOR FRACTURE TOUGHNESS

** NOTCH ROOT CONTAINED AREAS WHICH WERE NOT FATIGUE CRACKED.

FATIGUE DATA:






MAX. CYCLING STRESS APPROXIMATELY 52 ksi, 40,000 TO 55,000 CYCLES

R = .05

CYCLING RATE WAS 1800 cpm

FRACTURE TEST LOADING RATE WAS 150 ksi/min.

TABLE 27 ROUND NOTCH TENSILE DATA FOR Ti 6Al-4V

SPECIMEN NO.	TEST TEMP. °f	GRAIN DIRECTION	MAJOR DIAMETER (D) inches	NOTCH DIAMETER inches	NET DIAMETER inches	MAXIMUM LOAD kips	NET AREA in ²	σ_N ksi	K_{1C} ksi $\sqrt{\text{in}}$	YIELD STRENGTH .2% OFFSET ksi	$\frac{\sigma_N}{\sigma_{ys}}$	K_{1Cp} ksi $\sqrt{\text{in}}$
F1G1	-110	L	1.122	.849	.746	34.3	.437	78.4	34.3	176.4	.44	34.8
F1G4	-110	L	1.121	.848	.770	39.6	.466	85.0	37.2	176.4	.48	37.7
F2I1	-110	T	1.121	.848	.740	34.3	.430	78.3	34.3	177.9	.44	34.7
F2I2	-110	T	1.120	.850	.765	38.0	.460	82.6	36.1	177.9	.46	36.4
F2J1	-110	ST	1.123	.848	.715	31.0	.402	77.2	33.8	171.3	.43	34.4
F2J6	-110	ST	1.121	.848	.799	45.7	.502	91.0	39.8	171.3	.52	40.3
F1G3	75	L	1.123	.849						147.1	.64	42.0
F1G5	75	L	1.120	.849	.774	39.9	.470	84.9	37.1	147.1	.58	37.8
F2I4	75	T	1.122	.849	.770	35.3	.465	75.8	33.2	152.2	.50	33.7
F2I6	75	T	1.121	.849	.753	39.5	.445	88.8	38.9	152.2	.58	39.7
F2J2	75	ST	1.122	.849	.758	38.5	.451	85.4	37.4	151.9	.56	38.2
F2J5	75	ST	1.120	.849	.739	38.0	.429	88.5	38.7	151.9	.58	39.6
F1G2	400	L	1.121	.849	.772	76.9	.468	164.3	71.9	108.2	1.52*	87.1
F2I3	400	T	1.122	.850	.729	68.7	.418	164.5	72.0	111.7	1.47*	85.6
F2J4	400	ST	1.121	.848	.775	82.3	.471	174.6	76.4	108.6	1.60*	97.4
F1G6	650	L	1.120	.850	.716	63.0	.403	156.4	68.4	95.1	1.64*	
F2I5	650	T	1.122	.848	.765	73.1	.457	160.1	70.1	97.9	1.64*	91.0
F2J3	650	ST	1.122	.849	.778	79.0	.475	166.2	72.8	96.8	1.72*	104.3

* THESE RATIOS ARE ABOVE THE 1.1 LIMIT RECOMMENDED BY THE ASTM COMMITTEE FOR FRACTURE TOUGHNESS

 THIS SPECIMEN FAILED IN FATIGUE MACHINE. THE K_{1C} VALUE FOR THIS SPECIMEN BASED ON THE MAXIMUM FATIGUELOAD IS 40,100 psi $\sqrt{\text{in}}$ ($\sigma_N = 93,800$ psi, NET AREA = .312 in²)

FATIGUE DATA:

MAX. CYCLING STRESS APPROXIMATELY 52 ksi, 6000 TO 7000 CYCLES

R = .05

CYCLING RATE WAS 1800 cpm

FRACTURE TEST LOADING RATE WAS 150 ksi/min.

TABLE 28 ROUND NOTCH TENSILE DATA FOR Ti 6Al-6V-2Sn ANN

SPECIMEN NO.	TEST TEMP. of	GRAIN DIRECTION	MAJOR DIAMETER (D) inches	NOTCH DIAMETER inches	NET DIAMETER inches	MAXIMUM LOAD kips	NET AREA in ²	σ_N ksi	K_{IC} ksi $\sqrt{\text{in}}$	YIELD STRENGTH .2% OFFSET ksi	$\frac{\sigma_N}{\sigma_{ys}}$	K_{ICp} ksi $\sqrt{\text{in}}$
H1G1	-110	L	1.124	.847	.742	39.0	.432	90.2	39.5	171.8	.52	40.0
H1G4	-110	L	1.125	.845	.726	28.0	.414	67.6	29.6	171.8	.39	30.0
H8I1	-110	T	1.124	.849	.712	32.8	.398	82.2	36.0	169.5	.48	36.6
H8I2	-110	T	1.125	.849	.747	42.3	.438	96.4	42.2	169.5	.56	43.0
H8J1	-110	ST	1.125	.850	.713	32.0	.399	80.1	35.1	169.5	.47	35.7
H8J6	-110	ST	1.125	.850	.770	42.9	.466	92.1	40.3	169.5	.54	41.1
H1G3	75	L	1.125	.850	.748	47.0	.439	107.1	46.9	143.1	.74	48.4
H1G5	75	L	1.125	.850	.677	34.9	.360	97.0	42.1	143.1	.67	43.6
H8I4	75	T	1.125	.850	.761	70.1	.455	154.3	67.6	142.5	1.08	72.9
H8I6	75	T	1.125	.851	.765	57.3	.460	124.6	54.6	142.5	.87	57.3
H8J2	75	ST	1.124	.851	.747	53.9	.439	122.8	53.8	138.6	.88	56.3
H8J5	75	ST	1.125	.850	.724	64.4	.412	156.3	68.5	138.6	1.12*	74.3
H1G2	400	L	1.125	.848	.758	69.9	.451	155.0	67.9	105.7	1.46*	80.5
H8I3	400	T	1.125	.849	.646	50.1	.328	153.0	66.1	104.6	1.46*	79.4
H8J4	400	ST	1.124	.851	.743	75.0	.433	173.2	75.9	108.6	1.59*	95.9
H1G6	650	L	1.125	.851	.760	70.7	.454	155.7	68.2	99.3	1.56*	84.9
H8I5	650	T	1.125	.848	.700	60.6	.385	157.5	68.7	100.3	1.57*	86.0
H8J3	650	ST	1.124	.850	.742	66.6	.433	154.0	67.4	97.2	1.58*	84.8

FATIGUE DATA:

MAX. CYCLING STRESS APPROXIMATELY 47 ksi, 7000 TO 8000 CYCLES

R = .05

CYCLING RATE WAS 1800 cpm

FRACTURE TEST LOADING RATE WAS 150 ksi/min.

*THESE RATIOS ARE ABOVE 1.1 LIMIT RECOMMENDED BY THE ASTM COMMITTEE FOR FRACTURE TOUGHNESS

TABLE 29 ROUND NOTCH TENSILE DATA FOR Ti 6Al-6V-2Sn STA

SPECIMEN NO.	TEST TEMP. °F	GRAIN DIRECTION	MAJOR DIAMETER (D) inches	NOTCH DIAMETER inches	NET DIAMETER inches	MAXIMUM LOAD kips/lbs	NET AREA in ²	σ_N ksi	K_{IC} ksi $\sqrt{\text{in}}$	YIELD STRENGTH 2% OFFSET ksi	$\sigma_N / \bar{\sigma}_Y$	$K_{IC} C_p$ ksi $\sqrt{\text{in}}$
G8G1	-110	L	1.125	.853	.783	30.3	.481	62.9	27.5	190.0	.33	27.7
G8I1	-110	T	1.124	.852	.797	33.0	.498	66.2	29.0	190.2	.35	29.3
G8I2	-110	T	1.126	.853	.828	37.5	.539	69.6	30.4	190.3	.37	30.8
G7J1	-110	ST	1.125	.854	.845	33.6	.561	60.0	26.1	189.3	.32	26.5
G7J6	-110	ST	1.122	.854	.765	21.8	.460	47.4	20.7	189.3	.25	21.2
G8G3	75	L	1.125	.852	.792	33.5	.493	68.0	29.8	160.3	.42	30.1
G8G4	75	L	1.126	.855	Δ	Δ	Δ	Δ	Δ	160.3	.41	28.9
G8G5	75	L	1.126	.854	.777	31.1	.474	65.5	28.7	168.5	.58	44.0**
**G8I4	75	T	1.124	.852	.836	53.9	.549	98.1	42.8	168.5	.47	35.4
G8I6	75	T	1.122	.854	.786	39.5	.485	79.4	34.8	160.6	.45	32.6**
G7J2	75	ST	1.122	.854	.836	40.1	.549	72.9	31.8	160.6	.45	32.6
G7J4	75	ST	1.124	.854	Δ	Δ	Δ	Δ	Δ	160.6	.47	32.6**
**G7J5	75	ST	1.088	.852	.834	40.8	.546	74.7	31.9	126.4	1.27*	78.7
G8G2	400	L	1.126	.854	.787	78.3	.486	161.0	70.5	126.9	1.29*	80.2
G8I3	400	T	1.124	.854	.812	84.8	.517	163.9	71.8	113.7	1.42*	77.1
G8G6	650	L	1.125	.853	.803	76.5	.506	151.2	66.2	113.0	1.41*	82.6
G8I5	650	T	1.123	.853	.777	77.0	.474	162.4	71.1	115.3	1.34*	77.2
G7J3	650	ST	1.123	.854	.816	80.8	.523	154.3	67.6			

NOTES:

* THESE RATIOS ARE ABOVE THE 1.1 LIMIT RECOMMENDED BY THE ASTM COMMITTEE FOR FRACTURE TOUGHNESS
 MAX FATIGUE CYCLING STRESS APPROXIMATELY 53 ksi,
 4000 TO 6000 CYCLES
 R = .05
 CYCLING RATE WAS 1800 CPM

Δ FAILED IN FATIGUE

** SOME AREAS DO NOT APPEAR FATIGUE CRACKED

*** ABOUT HALF OF NOTCH NOT CRACKED

FRACTURE TESTING LOAD RATE WAS 150 ksi/min

TABLE 30 ROUND NOTCH TENSILE DATA FOR PH 13-8 Mo

SPECIMEN NO.	TEST TEMP. °F	GRAIN DIRECTION	MAJOR DIAMETER (D) inches	NOTCH DIAMETER inches	NET DIAMETER inches	MAXIMUM LOAD kips	NET AREA in ²	σ_N ksi	K_{1C} ksi $\sqrt{\text{in}}$	YIELD STRENGTH .2% OFFSET ksi	σ_N / σ_{ys}	K_{1C_p} ksi $\sqrt{\text{in}}$
J2XSG1	-110	L	1.122	.850	.781	49.0	.478	102.4	44.8	219.1	.47	45.2
J2XSG4	-110	L	1.122	.850	.773	54.5	.470	116.1	50.8	219.1	.53	51.4
J211	-110	T	1.122	.851	.762	43.1	.455	94.7	41.5	218.0	.43	41.7
J212	-110	T	1.122	.850	.750	45.1	.441	102.3	44.8	218.0	.47	45.0
J2XSG3	75	L	1.122	.850	.799	113.3	.501	226.0	99.0	205.0	1.10	107.0
J2XSG5	75	L	1.122	.850	.785	101.8	.484	210.1	92.0	205.0	1.02	98.2
J214	75	T	1.122	.850	.754	92.3	.447	206.6	90.5	195.4	1.06	96.8
J216	75	T	1.123	.851	.778	104.5	.475	220.1	96.4	195.4	1.13*	105.0
J2XSG2	400	L	1.122	.851	.782	132.0	.480	275.0	120.4	180.2	1.53*	146.5
J213	400	T	1.122	.849	.785	132.3	.484	273.2	119.6	179.1	1.53*	145.3
J2XSG6	650	L	1.122	.850	.783	114.1	.481	237.3	103.9	165.4	1.44*	121.7
J215	650	T	1.122	.851	.782	111.7	.480	232.5	101.8	161.8	1.44*	119.4

FATIGUE DATA:

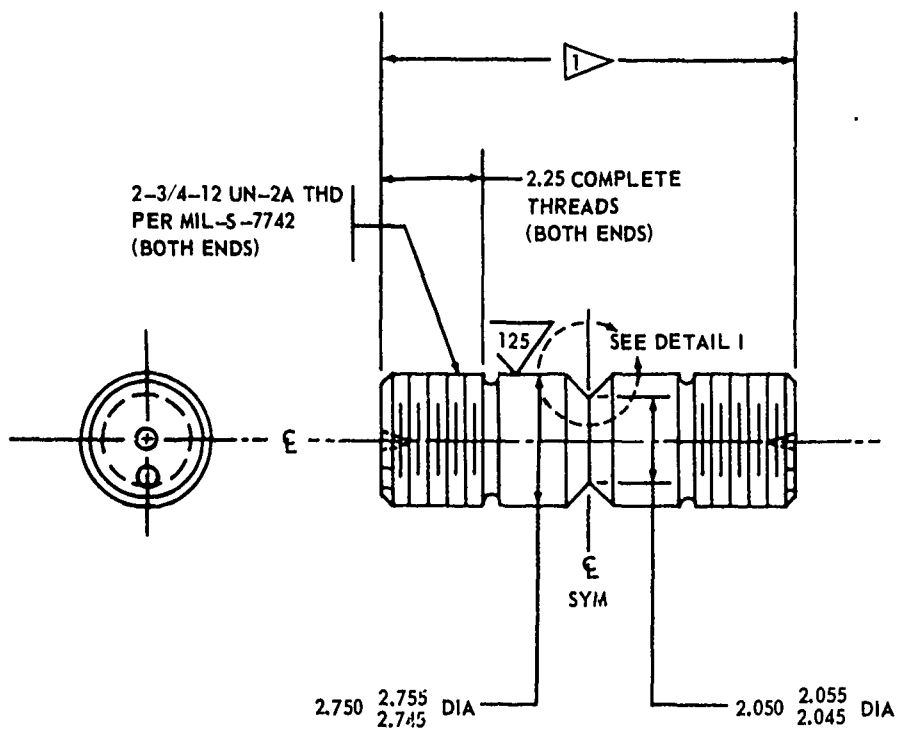
MAX. CYCLING STRESS APPROXIMATELY 67 ksi, 8000 TO 10,000 CYCLES

R = .05

CYCLING RATE WAS 1800 cpm

FRACTURE TEST LOADING RATE WAS 150 ksi/min.

*THESE RATIOS ARE ABOVE THE 1.1 LIMIT RECOMMENDED BY
ASTM COMMITTEE FOR FRACTURE TOUGHNESS



SPECIMEN DETAIL
1/4 SIZE

NOTE:

1 12 INCHES FOR
LONGITUDINAL GRAIN
DIRECTION

9 INCHES FOR
TRANSVERSE GRAIN
DIRECTION

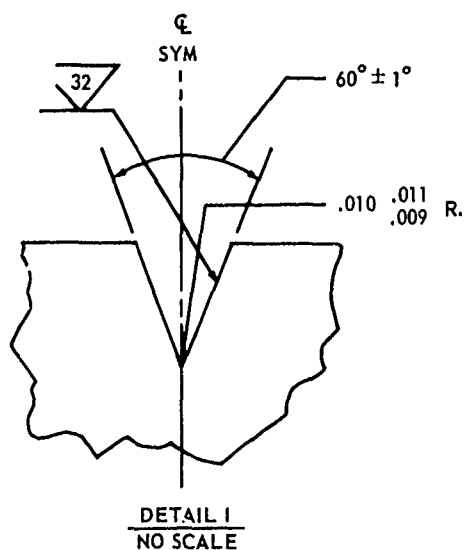


FIG. 103 2-3/4 INCH DIAMETER ROUND NOTCH SPECIMEN

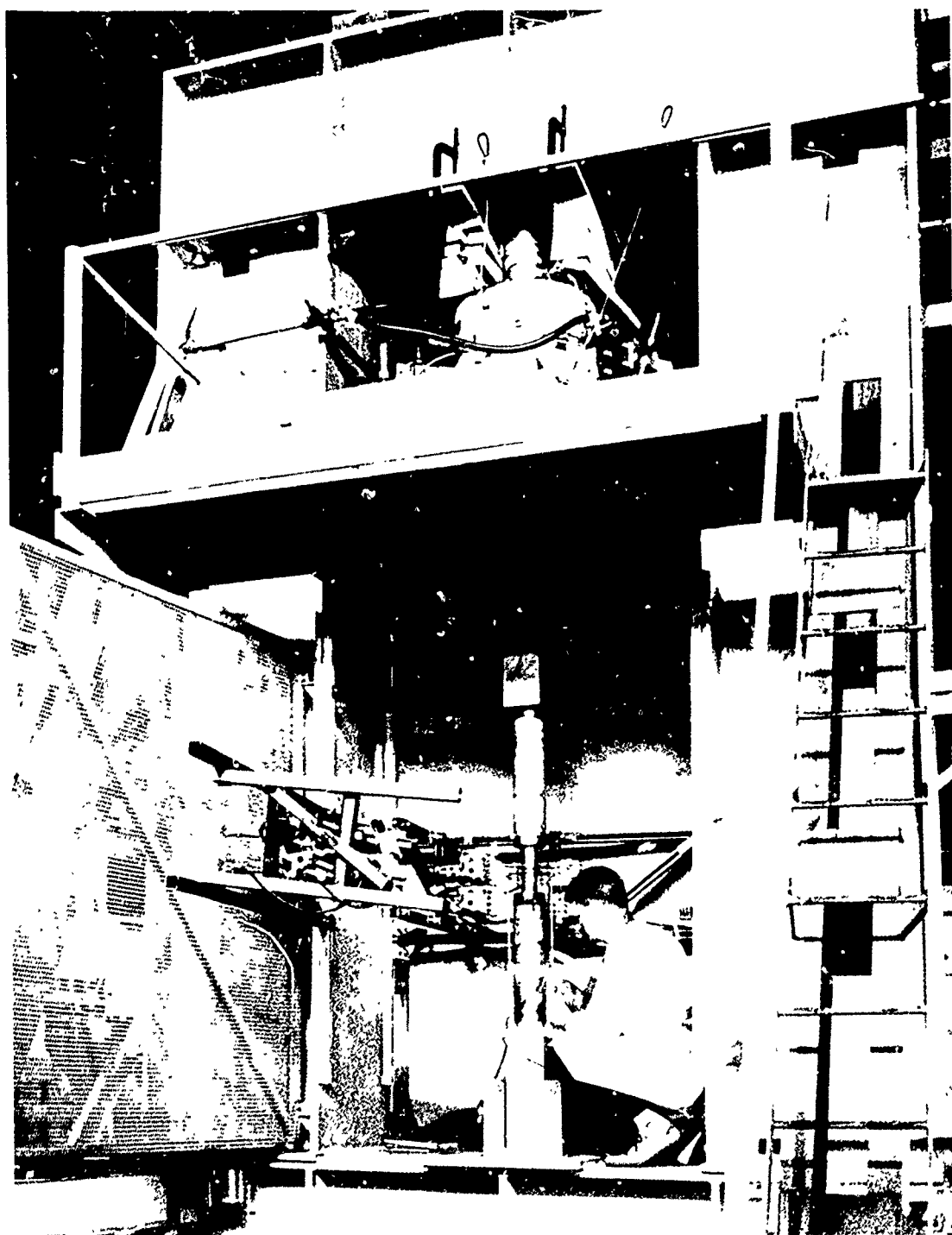


FIG. 104 2-3 4 INCH ROUND NOTCH!! SPECIMEN TEST S' TUP

Crack extension was viewed with a 50x Gaertner microscope. The specimens were rotated every 2000 to 4000 cycles to help produce uniform cracking.

Cooling and heating of the specimens was accomplished using liquid nitrogen and radiant heat as discussed in the test procedure for center-notched specimens.

Displacement across the notch was measured with an extensometer and recorded with load. A close-up view of the extensometer is shown in Fig. 105. Two algebraically adding, differential transformers were used to minimize specimen bending. The extensometer plate arms, shown in Fig. 105, were attached 0.05 inch above and below the notch using pointed set screws; the set screws were located along the longitudinal axis of the plate to further minimize the effect of any specimen bending.

EXPERIMENTAL RESULTS

Test results for the 1-1/8 inch diameter specimens are tabulated in Tables 22 through 30 and results for the 2-3/4 inch diameter specimens are tabulated in Table 31. Fatigue data for growing the crack in the root of the notch are also included. Net section stress, average tensile yield strength as well as the net-stress to yield-strength ratio are listed in the tables to aid in evaluating the plane-strain critical-stress intensity data. Ratios above the 1.1 limit recommended by ASTM Committee on Fracture Testing of High Strength Materials are indicated by an asterisk.

Plane-strain critical-stress intensity values calculated using Equations (37) and (33) of Section 4, are listed both with and without the plastic zone correction. To differentiate the two values, the plastic zone corrected values are identified as $K_{1C(p)}$, similar to the center notch specimen data. It was felt that both values should be included to provide evidence of how the correction varied as the net-stress to yield-strength ratio increased.

Both the 1-1/8 inch and 2-3/4 inch specimen K_{1C} values are plotted against testing temperature in Figs. 106 through 114. The effect of grain direction on fracture properties was also shown by including in the same plot the different grain directions tested.

Data points listed in the tables with an asterisk are also indicated in the figures with an arrow.

Plane strain stress intensity values corrected for the plastic zone $K_{1C(p)}$ are plotted against test temperature in Figs. 115 through 123.

Load-displacement curves were obtained for most of the 1-1/8 inch and 2-3/4 inch round notch specimens (curves were not obtained for 1-1/8 inch round notch specimens tested in Section 13 Environmental Testing). Typical curves for three 2-3/4 inch diameter round notch specimens are shown in Fig. 124.

Essentially, the curves measure notch displacement as a function of load. In all cases, no displacement discontinuities were noted like those which occurred in some center-notch specimens (Figs. 61 and 62). In some ways, however, the two sets of curves are similar. Brittle specimens (both round and center notch)

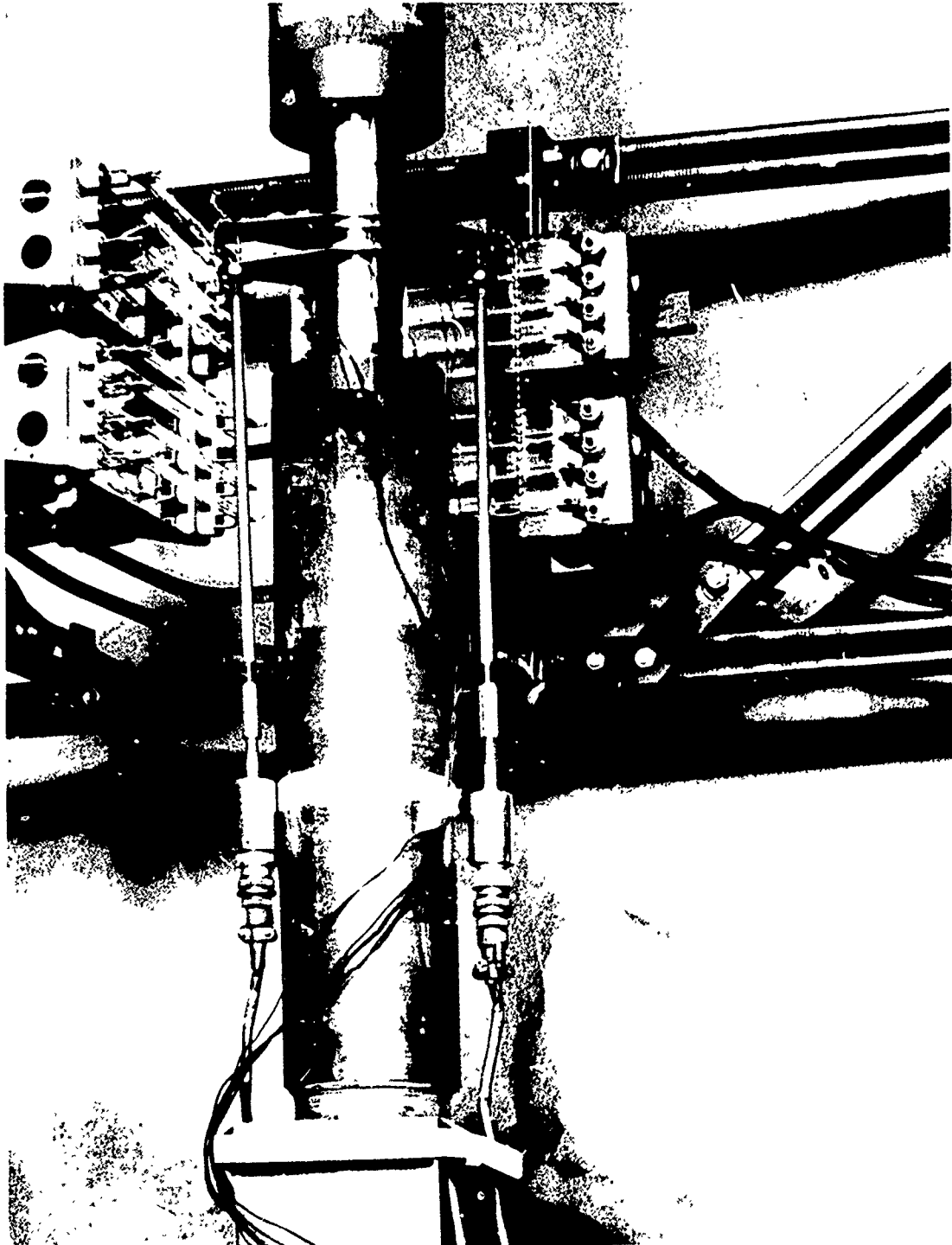


FIG. 105 2-3/4 INCH ROUND NOTCH SPECIMEN EXTENSOMETER

TABLE 31 LARGE ROUND NOTCH TENSILE DATA

SPECIMEN NO.	TEST TEMP. of	GRAIN DIRECTION	MAJOR DIAMETER (D) inches	NOTCH DIAMETER inches	NET DIAMETER inches	MAXIMUM LOAD kips	NET AREA in ²	σ_N ksi	K_{IC} ksi $\sqrt{\text{in}}$	YIELD STRENGTH .2% OFFSET ksi	$\frac{\sigma_N}{\sigma_{ys}}$	K_{IC_p} ksi $\sqrt{\text{in}}$
9 NI - 4 Co												
CB 202	-110	L	2.75	2.05	1.91	518	2.86	181	124.0	211.3	.86	130.5
CB 203	RT	T	2.75	2.04	1.90	601	2.83	213	145.8	204.7	1.04	155.5
CB 204	RT	L	2.75	2.04	1.91	621	2.86	217	148.6	198.4	1.09	160.0
CB 207	400	-	2.74	2.05	1.90	481	2.83	170	116.0	165.1	1.03	123.0
CB 208	400	L	2.75	2.04	1.92	466	2.89	161	110.3	169.1	.95	117.0
AM 355												
CC 204	RT	L	2.75	2.05	1.85	437	2.66	164	112.2	166.7	.98	120.0
CC 207	400	T	2.75	2.06	1.93	290	2.92	99.3	68.0	143.2	.69	69.5
CC 208	400	L	2.75	2.04	1.91	463	2.86	162	111.0	144.1	1.12*	121.0
MARAGING 250												
CD 208	RT	L	2.75	2.05	1.91	356	2.86	125	85.6	184.0	.64	89.3
INCO 718												
CE 201	-110	T	2.75	2.05	1.91	602	2.86	211	144.5	164.2	1.28*	161.5
CE 202	-110	L	2.74	2.04	1.90	683	2.83	241	164.5	171.8	1.40*	191.3
CE 203	RT	T	2.75	2.05	1.92	612	2.89	212	144.0	154.5	1.37*	168.0
CE 204	RT	L	2.74	2.05	1.94	681	2.95	231	158.3	156.0	1.48*	187.0
CE 207	400	T	2.75	2.05	1.92	560	2.92	192	131.5	145.1	1.32*	149.3
CE 208	400	L	2.75	2.04	1.92	596	2.89	206	141.0	146.1	1.41*	165.5
Ti 6Al-4V												
CF 207	400	T	2.74	2.05	1.86	383	2.71	141	96.2	111.0	1.27*	109.0
CF 208	400	L	2.73	2.04	1.90	406	2.83	143	97.5	108.1	1.32*	111.0

TABLE 31 LARGE ROUND NOTCH TENSILE DATA (continued)

SPECIMEN NO.	TEST TEMP. °F	GRAIN DIRECTION	MAJOR DIAMETER (D) inches	NOTCH DIAMETER inches	NET DIAMETER inches	MAXIMUM LOAD kips	NET AREA in ²	σ_N ksi	K_{IC} ksi $\sqrt{\text{in}}$	YIELD STRENGTH .2% OFFSET ksi	$\frac{\sigma_N}{\sigma_{ys}}$	K_{ICp} ksi $\sqrt{\text{in}}$
Ti 6Al-6V-2Sn ANN												
CH 207	400	T	2.75	2.05	1.80	276	2.54	109	74.6	104.6	1.04	80.0
CH 208	RT	L	2.75	2.05	1.76	135†	2.43	55.7	38.1	105.7	.53	38.8
Ti 6Al-6V-2Sn STA												
CG 207	400	T	2.75	2.05	1.97	331	3.05	109	74.6	126.9	.86	78.3
CG 208	400	L	2.75	2.05	1.95	288	2.98	96.7	66.2	126.4	.77	68.8
PH 13-8 Mo												
CJ 203	RT	T	2.75	2.03	1.97	248	3.04	81.6	55.9	195.4	.42	57.4
CJ 204	RT	L	2.75	2.04	1.96	264	3.02	87.4	59.9	205.0	.43	60.2
CJ 207	400	T	2.75	2.03	1.93	504	2.92	173	118.5	179.1	.97	126.3
CJ 208	400	L	2.74	2.03	1.94	668	2.95	227	155	180.2	1.26*	174.2

* THESE RATIOS ARE ABOVE THE 1.1 LIMIT RECOMMENDED BY THE ASTM COMMITTEE FOR FRACTURE TOUGHNESS

† FAILED DURING FATIGUE

FATIGUE DATA:

MAX. CYCLING STRESS .20 TO .33 YIELD STRENGTH

R = .05

CYCLING RATE WAS 60 TO 90 CPM

FRACTURE TEST LOADING RATE WAS 150 ksi/min.

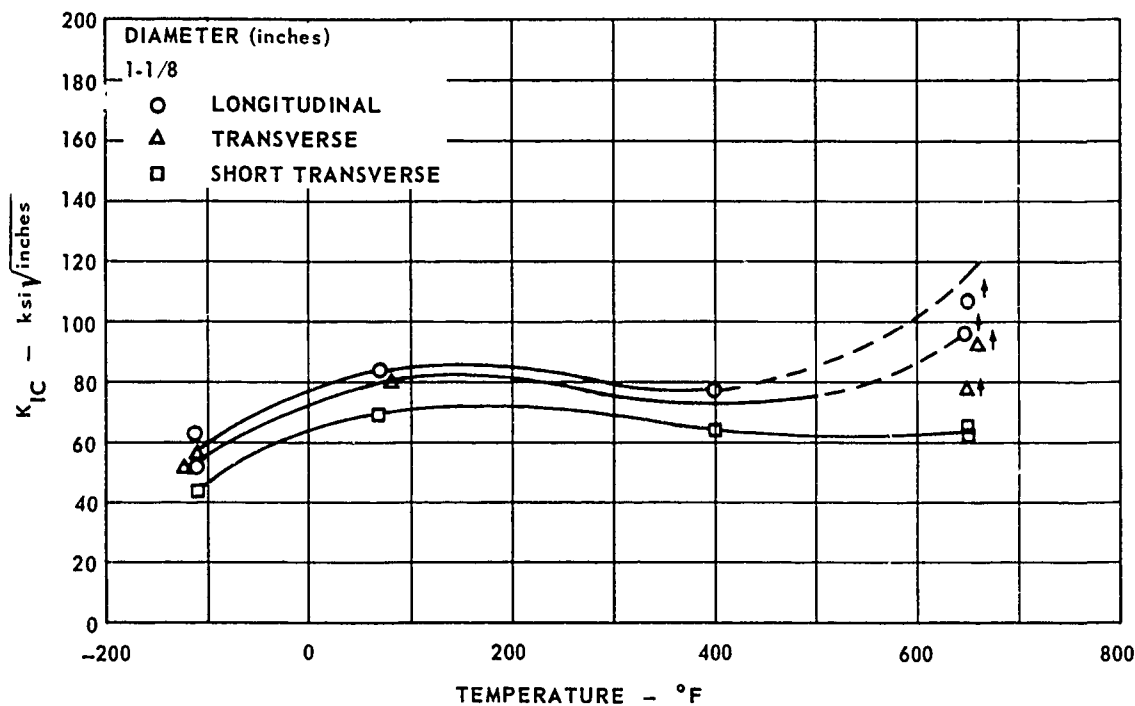


FIG. 106 K_{IC} DATA FOR ROUND NOTCH SPECIMENS OF 4340

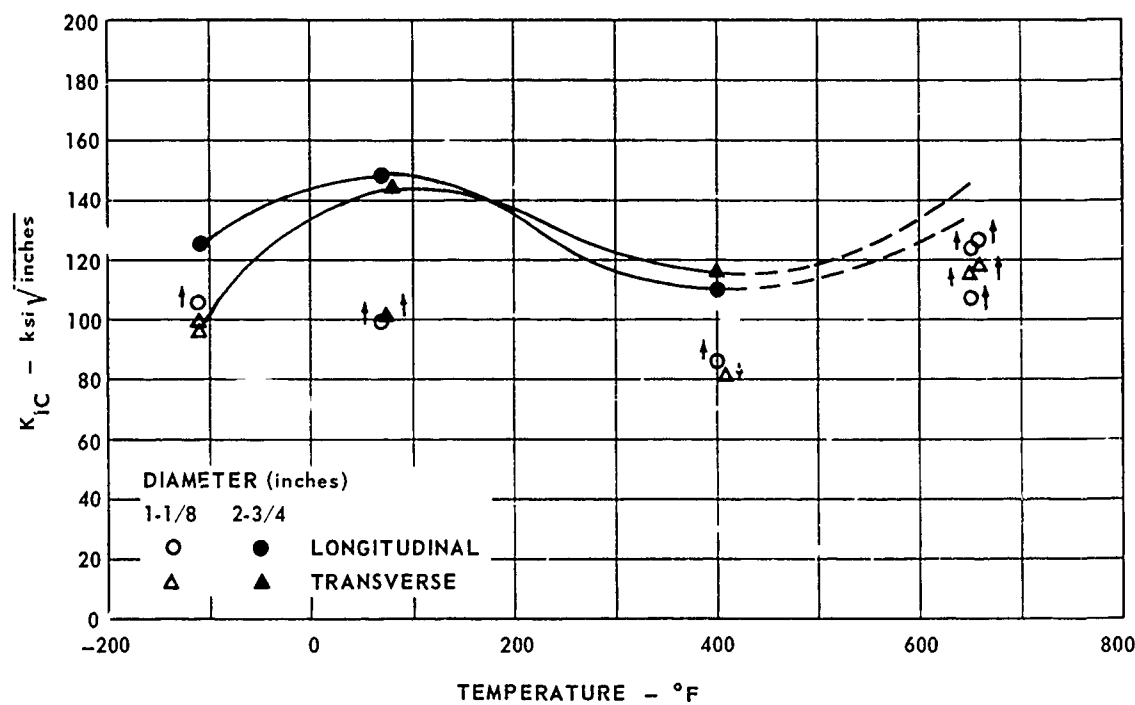


FIG. 107 K_{IC} DATA FOR ROUND NOTCH SPECIMENS OF 9Ni-4Co

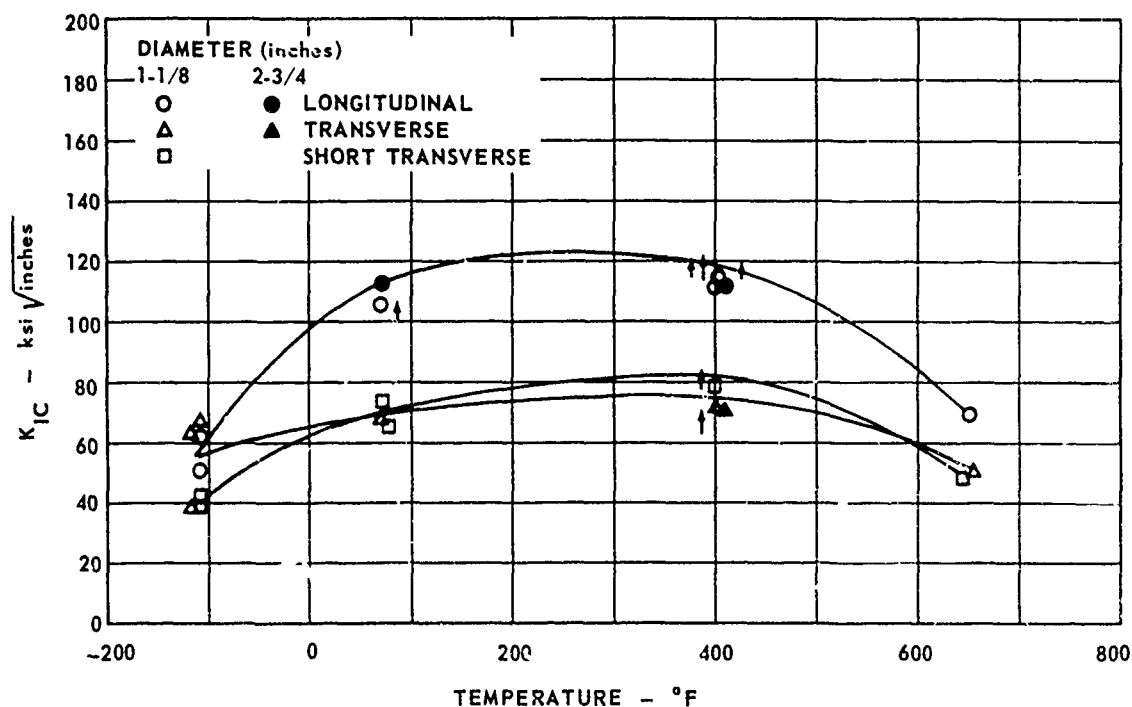


FIG. 108 K_{IC} DATA FOR ROUND NOTCH SPECIMENS OF AM 355

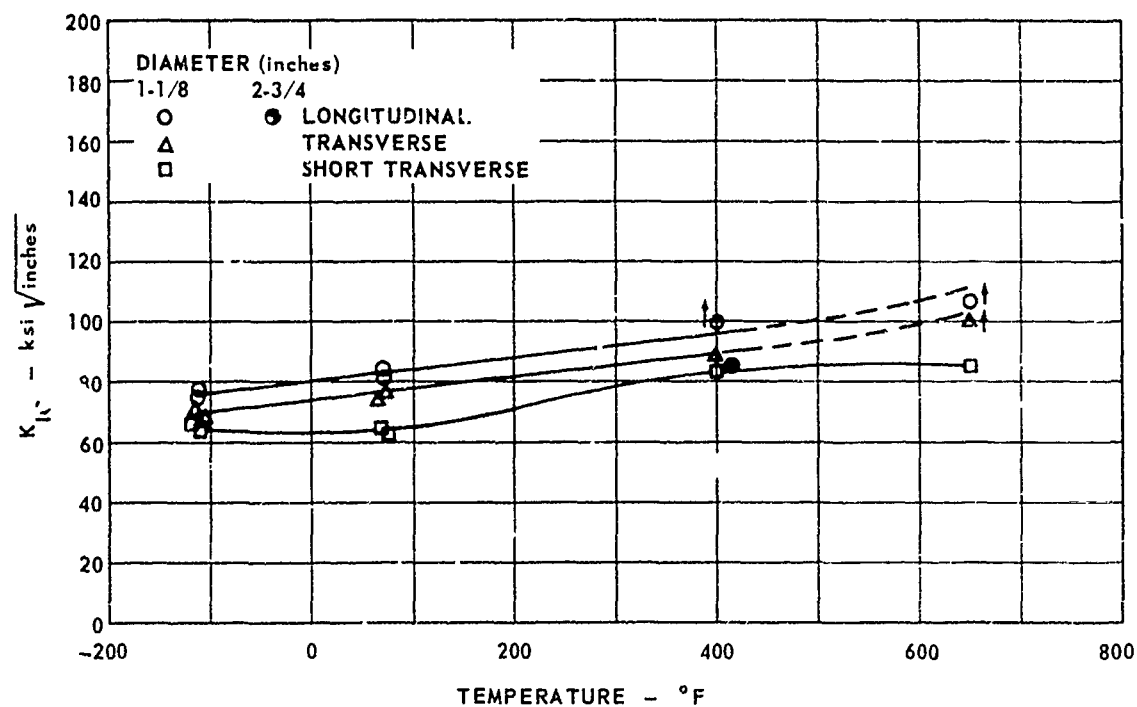


FIG. 109 K_{IC} DATA FOR ROUND NOTCH SPECIMENS OF MARAGING 250

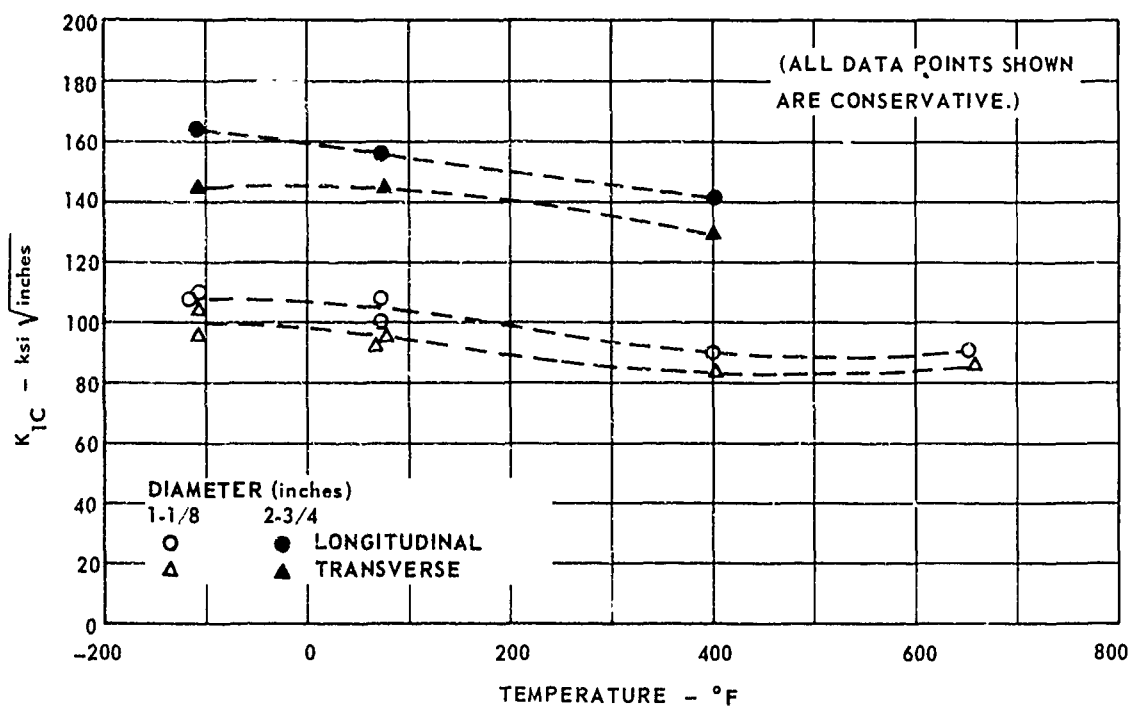


FIG. 110 K_{IC} DATA FOR ROUND NOTCH SPECIMENS OF INCO 718

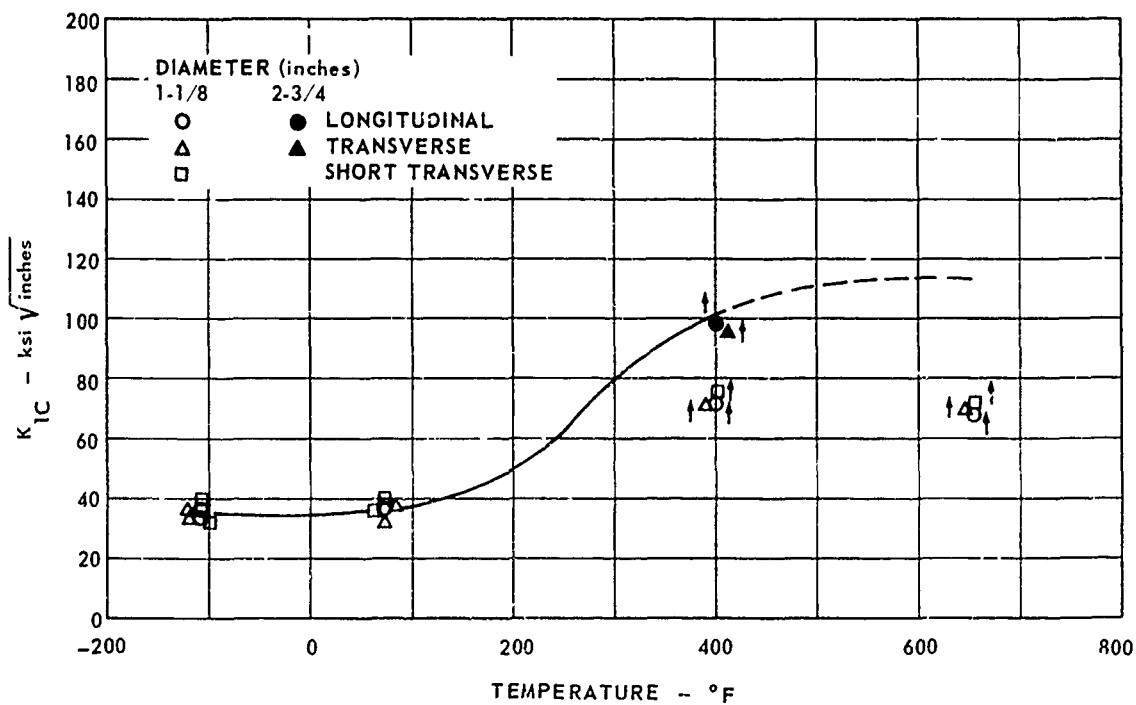


FIG. 111 K_{IC} DATA FOR ROUND NOTCH SPECIMENS OF Ti 6Al-4V

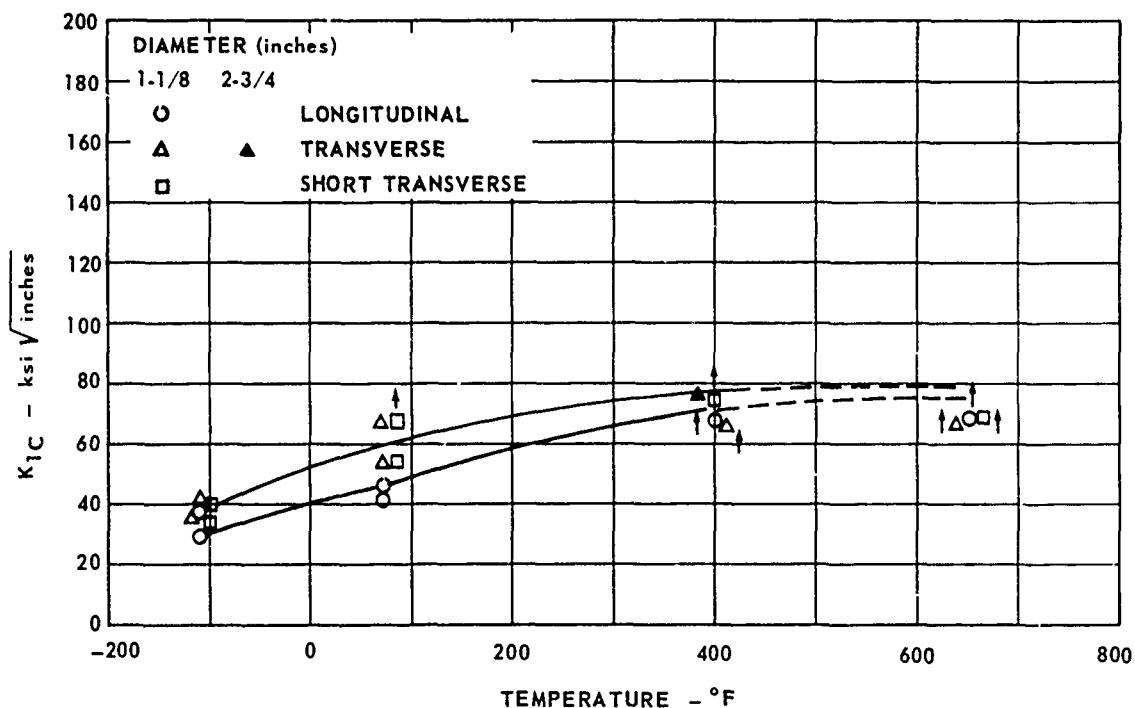


FIG. 112 K_{IC} DATA FOR ROUND NOTCH SPECIMENS OF Ti 6Al-6V-2Sn ANN

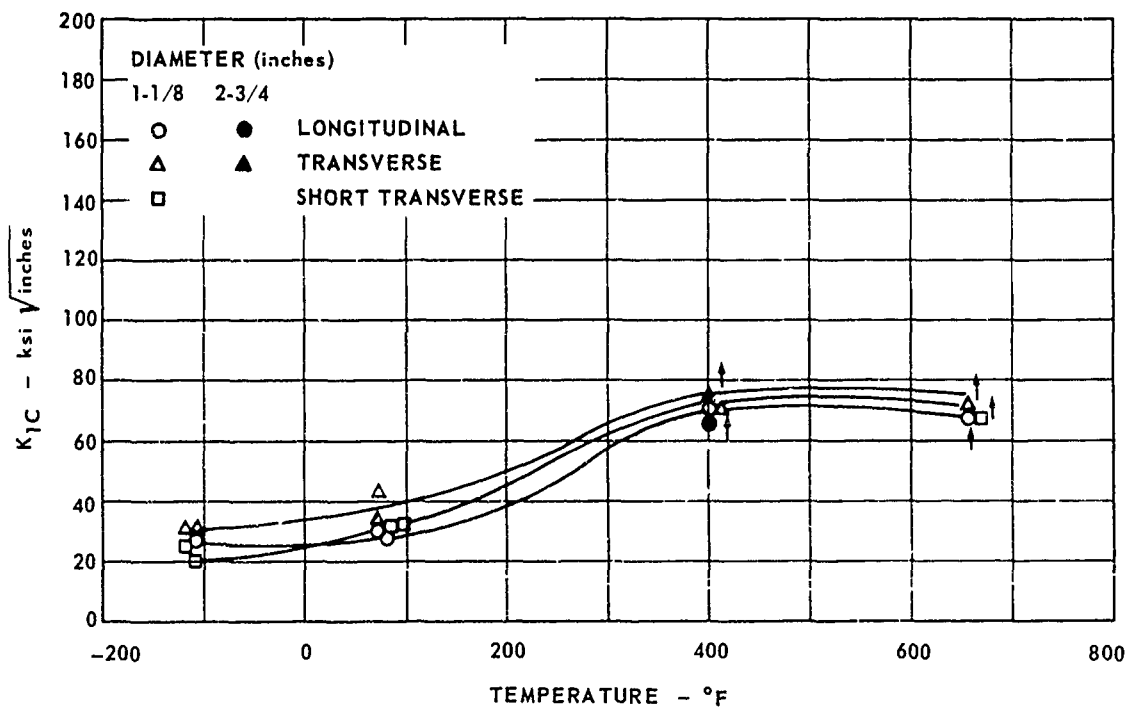


FIG. 113 K_{IC} DATA FOR ROUND NOTCH SPECIMENS OF Ti 6Al-6V-2Sn STA

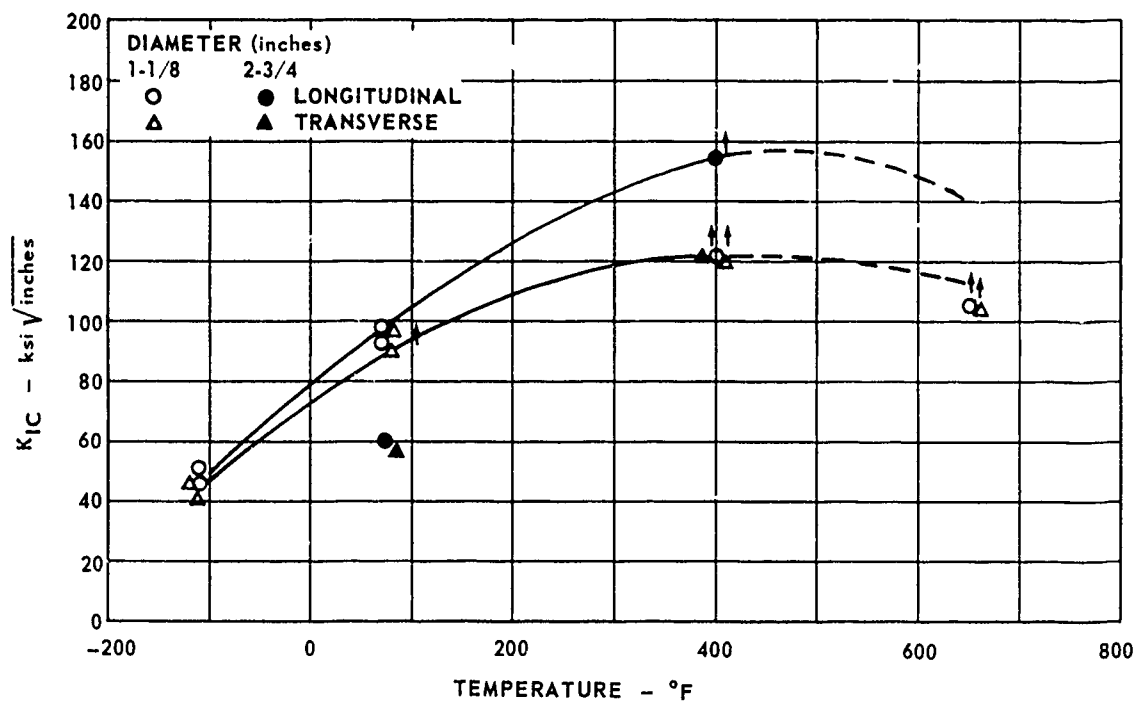


FIG. 114 K_{IC} DATA FOR ROUND NOTCH SPECIMENS OF PH 13-8 Mo

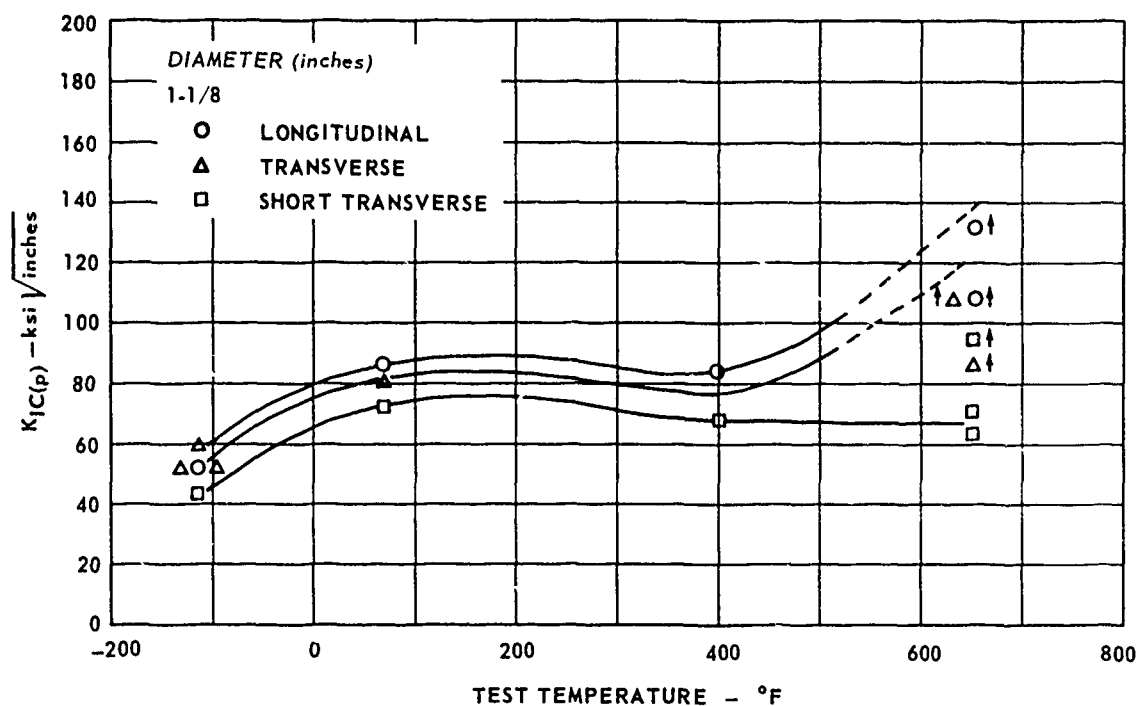


FIG. 115 $K_{IC(p)}$ DATA FOR ROUND NOTCH SPECIMENS OF 4340

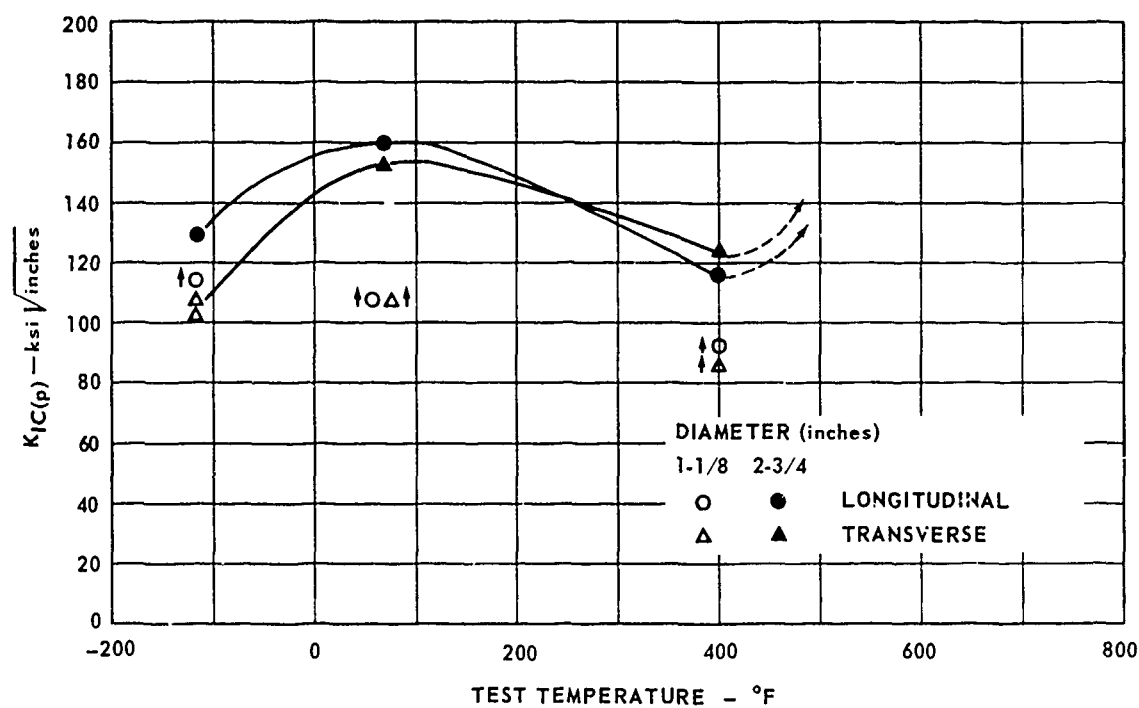


FIG. 116 $K_{IC(p)}$ DATA FOR ROUND NOTCH SPECIMENS OF 9Ni-4Co

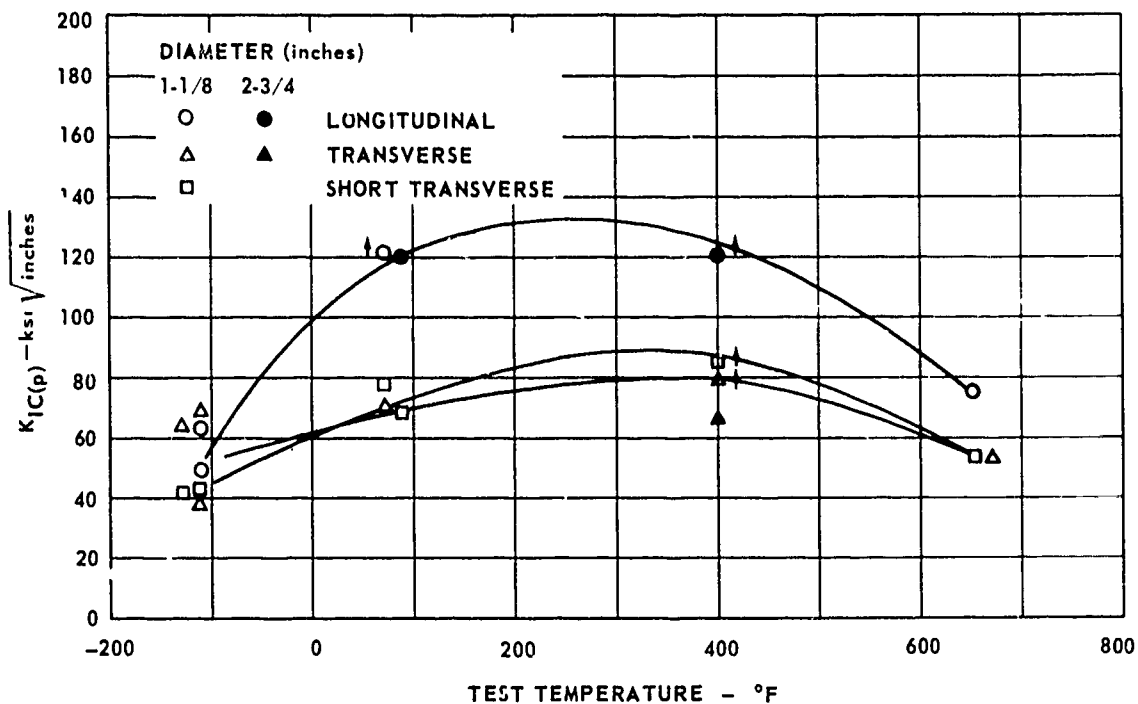


FIG. 117 $K_{IC(p)}$ DATA FOR ROUND NOTCH SPECIMENS OF AM 355

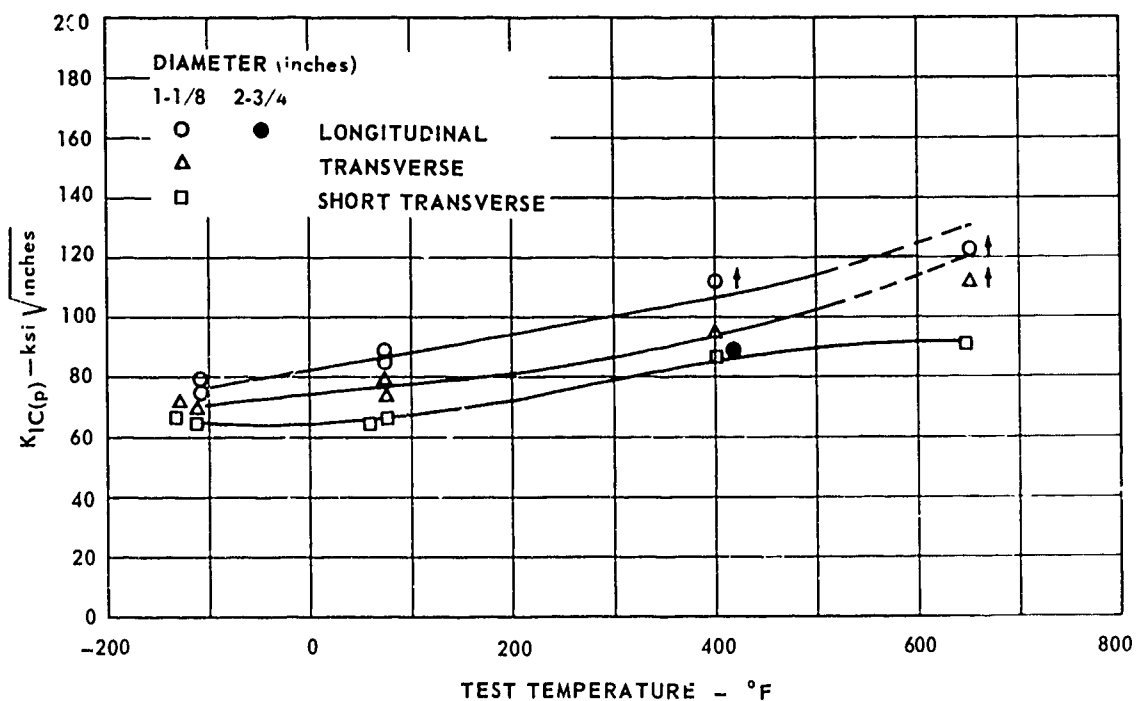


FIG. 118 $K_{IC(p)}$ DATA FOR ROUND NOTCH SPECIMENS OF MARAGING 250

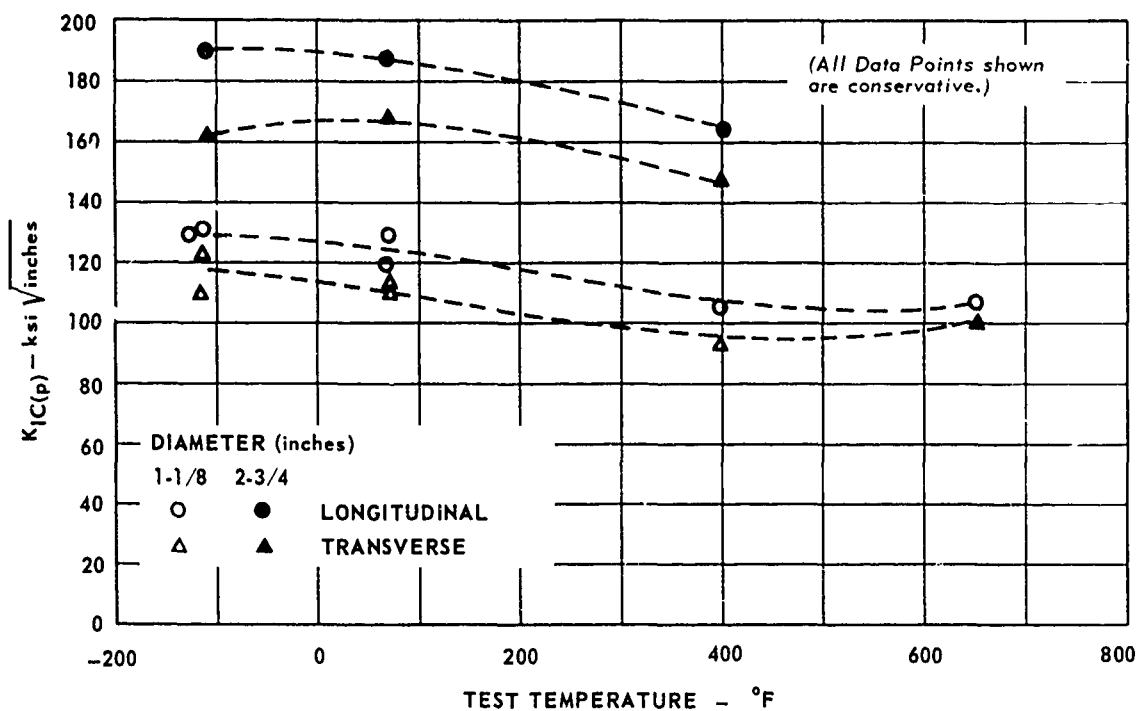


FIG. 119 $K_{IC(p)}$ DATA FOR ROUND NOTCH SPECIMENS OF INCO 718

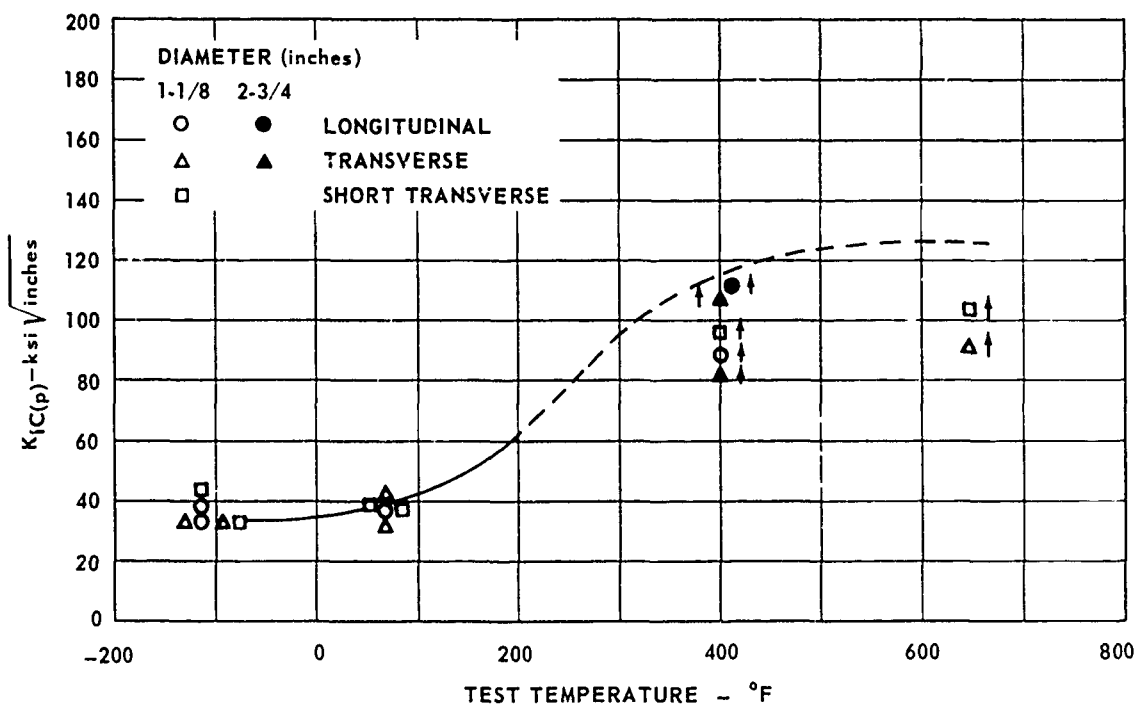


FIG. 120 $K_{IC(p)}$ DATA FOR ROUND NOTCH SPECIMENS OF Ti 6Al-4V

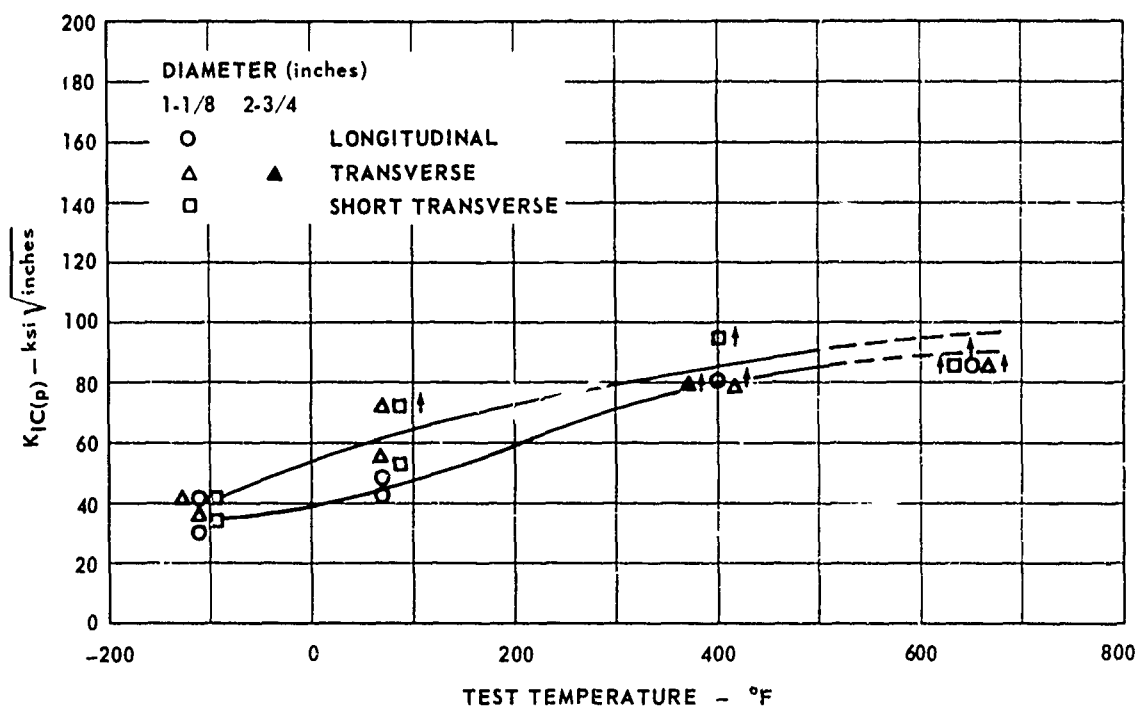


FIG. 121 $K_{IC(p)}$ DATA FOR ROUND NOTCH SPECIMENS OF Ti 6Al-6V-2Sn ANN

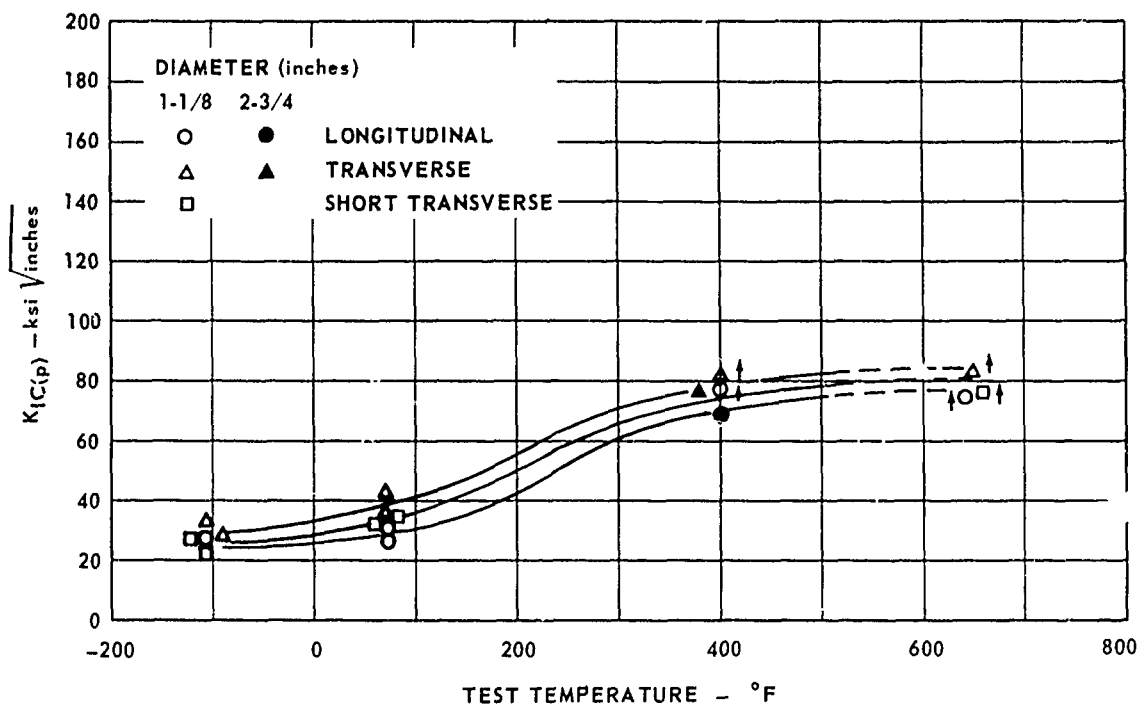


FIG. 122 $K_{IC(p)}$ DATA FOR ROUND NOTCH SPECIMENS OF Ti 6Al-6V-2Sn STA

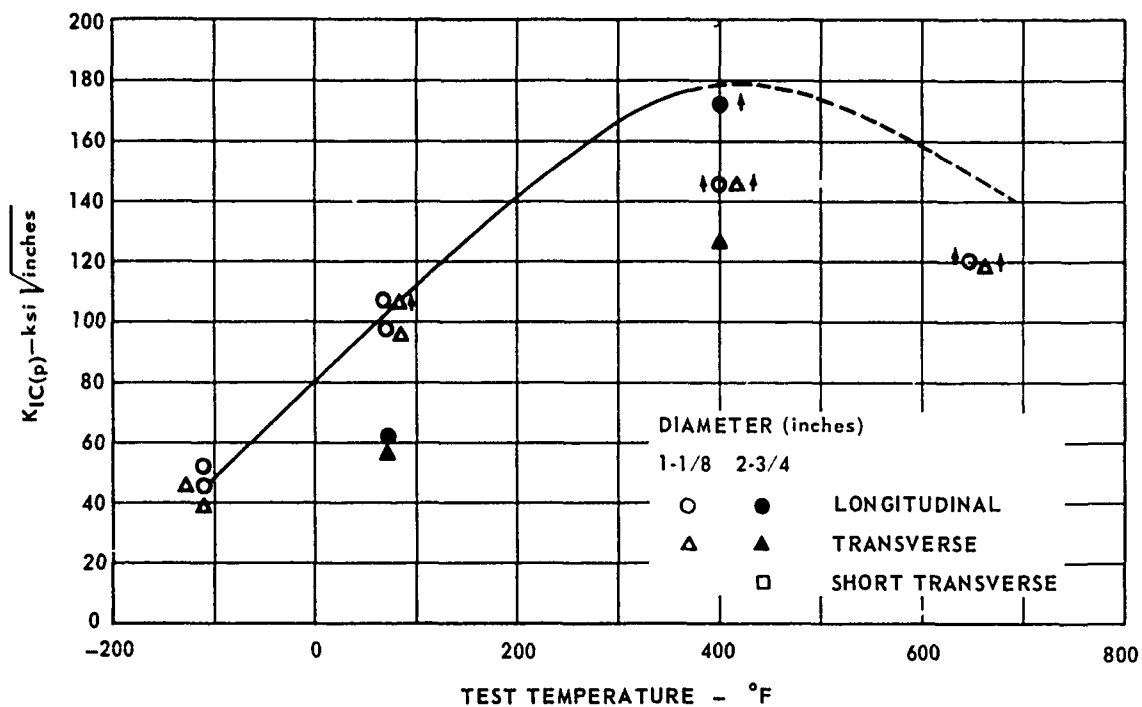


FIG. 123 $K_{IC(p)}$ DATA FOR ROUND NOTCH SPECIMENS OF PH 13-8Mo

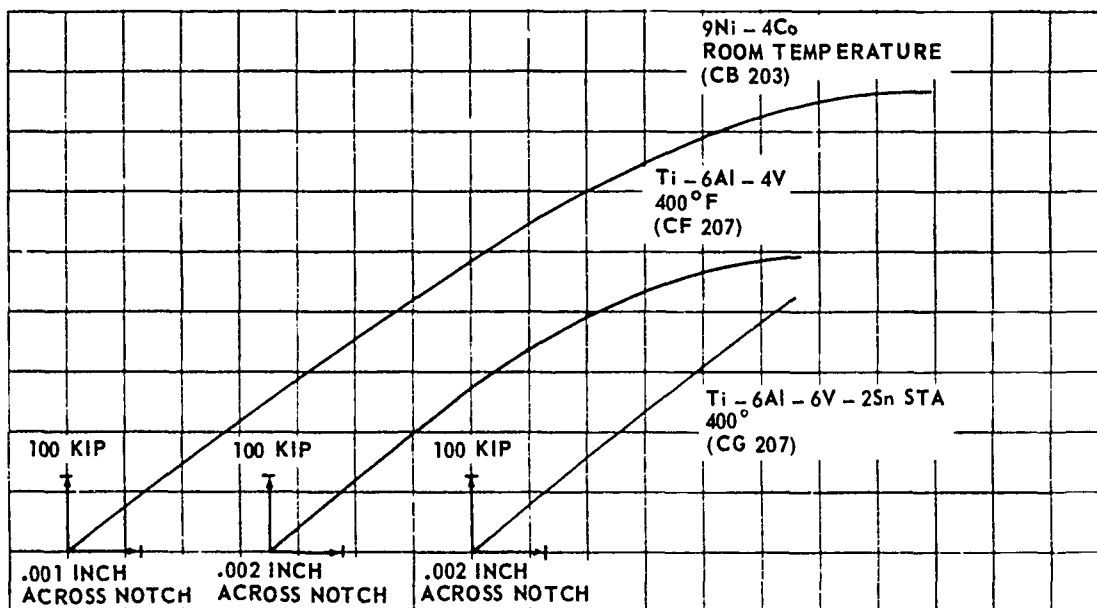


FIG. 124 2-3/4 INCH ROUND NOTCH SPECIMEN LOAD DISPLACEMENT CURVES

exhibit linear elastic curves to failure. As toughness increased, thereby increasing the net stress-yield strength ratio, the amount of nonlinearity shown in the curves also increased.

DISCUSSION

In general, the data obtained from the round notched specimens show an increase of K_{1C} with increasing temperature. This trend was somewhat obscured by the tendency for the net-stress to yield-stress ratio to increase with temperature. Data included in the Fifth Report of the Special ASTM Committee on Fracture (Ref. 18) revealed that ratios increasing above 1.1 result in decreasing K_{1C} values. It was also possible that some variations from the general trend were due to metallurgical changes in several alloys resulting from testing at elevated temperature.

The lower net-stress to yield-stress ratios of the large 2-3/4 inch diameter specimens did not always result in increased K_{1C} values as had been expected. It was not readily apparent what caused this reversal in expected behavior. To determine if heat treatment variations due to size changes had caused the anomalous results, hardness readings were taken. However, no hardness difference could be detected between the two sizes of notched round specimens.

Because of the different characteristics of each alloy, they are discussed individually.

4340

This martensitic low alloy steel showed the expected low toughness at -110°F with an increase at room temperature (Fig. 106). Above room temperature the toughness seemed fairly constant as indicated by the short transverse curve. At 650°F , the longitudinal and transverse data points were conservative and therefore should show a sharp rise. As would be expected, the longitudinal specimens had the highest toughness, followed by the transverse and short transverse. No large round specimens were tested in this alloy, since all the data points were valid below 650°F .

9 Ni-4Co

This bainitic steel showed high toughness at all temperatures although low points were seen for specimens tested at -110°F and 400°F (Fig. 107). Because of the high toughness, many of the 1-1/8 inch diameter specimens were conservative. Therefore, five 2-3/4 inch diameter specimens were also tested. As expected, the K_{1C} values for the large rounds were raised by the lower net-stress to yield-strength ratio. However, the increase in K_{1C} values was large for the small decrease in ratio. Hardness readings showed no difference in heat treat response between the large and small round specimens.

In this alloy, no forged down 3 x 9-inch bar was tested. Therefore, there is no short transverse data. However, the longitudinal and transverse curves show little difference in toughness.

AM 355

This semi-austenitic stainless steel showed a large variation in toughness depending on the grain direction tested (Fig. 108). The longitudinal toughness was much higher than the transverse and short transverse toughness. In this respect, the alloy differed from the other stainless steel, PH 13-8Mo which showed almost no directionality. It was possible that the variation in the AM 355 was due to the deleterious effects of the delta ferrite. The alloy also showed a very large variation in toughness with test temperature. As might be expected of a martensitic alloy with 5 percent nickel, the -110°F values were low. The toughness almost doubled at room temperature and 400°F . What was not expected was the large decrease upon testing at 650°F . This decrease had not been predicted by the precracked Charpy impact values shown in Fig. 19. This alloy was similar to the other stainless steel, PH 13-8Mo, which also showed a decrease in toughness at 650°F .

The only conservative K_{1C} values were at room temperature and 400°F , and the large specimens showed very little difference in toughness from the smaller specimens. At room temperature the small longitudinal specimen had a net-stress to yield-strength ratio of 1.43 and the large longitudinal specimen had a ratio of 0.98. This caused an increase in K_{1C} values. The longitudinal 400°F specimens showed a larger ratio difference; 1.83 for the small and 1.12 for the large specimen. However, the K_{1C} values were approximately the same for both sizes. This may be explained by the fact that both ratios were conservative and the actual K_{1C} differences were obscured.

The small transverse 400°F specimen had a ratio slightly above 1.1, and therefore the K_{1C} value was approximately the same as the value for the large specimen at the same point. The plastic zone correction (Fig. 117) caused a greater increase in $K_{1C(p)}$ for the large specimens than for the small. Therefore, the $K_{1C(p)}$ for the large specimen was actually below the small specimen value.

MARAGING 250

This alloy showed a small constant rise in toughness with temperature. The toughness was high over the whole temperature range from -110°F to 650°F (Fig. 109).

The toughness properties showed some variation with grain direction. The toughness decreased from longitudinal to transverse with the greatest decrease seen in short transverse properties. Only one specimen below 650°F was conservative, the 400°F longitudinal specimen, and its ratio was 1.21. When this condition was retested with a 2-3/4 inch diameter specimen, a lower K_{1C} value was obtained. Hardness values on both the large and small specimens indicated no difference in heat treatment. No unusual fracture face characteristics could be seen to account for the difference. It will be noticed by referring to the forged block drawings, Figs. 8 and 9, that the small and large longitudinal rounds were from different blocks. Although the blocks were from the same heat and forged to the same dimensions, it was possible that forging differences were influencing the results.

INCO 718

Toughness values for this alloy were so high that even at -110°F , they were conservative. Even after re-evaluating each condition below 650°F with the large notched rounds, the lowest net stress to yield stress ratio was 1.28. It is interesting to note that this was the only alloy which showed a constant decrease in toughness with increasing temperature (Fig. 110). This did not seem to be the result of increasingly conservative results as in other alloys because the net stress to yield stress ratio was exceptionally constant over the whole temperature range. Although the ratio was higher than the other alloys at -110°F , it was not as high as the other alloys at higher temperatures because of the constant yield strength.

The K_{1C} values from the large specimens showed a substantial increase over the values from the small specimens even though the net stress to yield stress ratio decreased only slightly. Both the large specimen and small specimen data exhibited the same shaped curve with a definite increase of longitudinal over transverse toughness.

Ti 6Al-4V

This heat-treated alpha-beta titanium alloy showed low K_{1C} values at both -110°F and room temperature (Fig. 111). However, it increased rapidly, between room temperature and 400°F . This was also the range in which the yield strength dropped off sharply from approximately 150 to 110 ksi. In this characteristic, the alloy was similar to the other heat-treated titanium, Ti 6Al-6V-2Sn STA. At 400°F and 650°F ratios were considerably above 1.1, and when re-tested at 400°F , with large specimens, the results were still conservative. Testing the large specimens resulted, however, in a large increase in toughness.

It was significant that the data showed no evidence of directionality so that only one line could be drawn through the data.

Although only one transverse small specimen at room temperature was slightly above the 1.1 recommended limit, both a longitudinal and transverse large specimen were tested. Both values were unexpectedly low. Hardness values showed the same heat-treat response as the smaller specimens. The fatigue crack depth and the fracture face did not reveal any apparent reason for the low readings. The large specimens were from a different block than the small specimens, however it was forged to the same dimensions. In addition, the 400°F large specimens are not lower than the 400°F small specimens.

Ti 6Al-6V-2Sn

This alloy, tested in both the annealed and STA condition, provided an opportunity to judge the effects of strength differences. The heat-treated specimens (Fig. 113) showed lower K_{1C} values at -110°F , and especially at room temperature, than the annealed (Fig. 112). However, the heat-treated specimens increased rapidly in toughness between room temperature and 400°F , similar to heat-treated Ti 6Al-4V. At 400°F , the toughness of the alloy in both conditions was approximately the same. It is interesting to note that the K_{1C} values for

the small specimens at 650° F was approximately the same for all three titanium alloys tested.

In both conditions, the K_{1C} values for the longitudinal grain were generally lower than for both the transverse and short transverse grain direction.

The specimens tested at 400° F and 650° F all resulted in ratios above 1.1 except for the annealed short transverse specimen. When retested with the larger specimens, the ratios were all below 1.1 and showed an increased toughness, except for the longitudinal STA specimen. The plastic zone correction which caused less increase in the large specimen $K_{1C(p)}$ values resulted in a reversal of the STA data (Fig. 122).

PH 13-8Mo

The general trend of the toughness versus temperature curve for this alloy (Fig. 114) was similar to the other stainless steel, AM 355. The low-nickel martensitic condition resulted in a low value at -110° F to a K_{1C} higher than any of the other alloys at 400° F. The apparent toughness decreased at 650° F even though the net-stress to yield-strength ratio was lower. Therefore, the mechanism which caused the decrease in toughness may have been the same as in the AM 355.

SECTION 9 CRITICAL SURFACE CRACK DETERMINATION

The primary purpose of this investigation was to determine the relationship between theoretical and experimentally determined fracture stresses for surface-cracked panel specimens. It was also desired to determine how the relationship changed as the crack dimensions varied to cause fracture-stress to yield-stress ratios over the range of 0.8 through 1.0.

Longitudinal panel specimens 3/16 to 1/4 inch thick were prepared containing various sizes of semielliptical shaped surface cracks. These specimens were fracture tested at 75° F or -110° F. The theoretical fracture stress, based on the round notched specimen K_{1C} value for the alloy, was calculated for each specimen and compared with the actual fracture stresses. The K_{1C} value for each specimen was also calculated and compared with the round notched specimen K_{1C} value for the particular alloy.

TEST PROCEDURE

Specimen

The specimens were fabricated as shown in Fig. 125 and were 1/4 inch thick for 9 Ni-4Co and PH 13-8Mo and were 3/16 inch thick for all the other alloys. It was attempted throughout the program to keep specimen thickness at least twice the crack depth because the standard toughness equation was derived for cracks having depths under half the thickness. The 9 Ni-4Co and PH 13-8Mo specimens were made thicker to allow for larger crack sizes caused by high toughness. The exact width and thickness of each specimen is listed in Table 32.

Location of the specimens within the forged blocks is shown in the material section of the report. The specimen blanks were sawed from the billet, rough machined, heat treated, and then finished machined. Correct grip-hole alignment was obtained by use of a drill jig. A starter notch for fatigue cracking was machined at the specimen center by the electric discharge process using a 0.010-inch thick brass electrode. The starter notch was made the length of the desired crack and was 0.010-inch deep.

Fatigue Cracking

The first three specimens (A2M1, 2 and 3) were fatigue cracked in axial loading. However, difficulty was encountered in controlling crack depth and the remaining specimens were all cracked in bending fatigue, as shown in Fig. 126, using a Sonntag SF-1-U fatigue machine. The specimens were held horizontally at the ends in pivoted jaws and the load was applied to the specimen center by a push rod connected to the machine drive. Cycling was interrupted periodically and the crack length determined by examining the notch with a 72x binocular microscope. Cycling was continued until the crack had progressed along the entire length of the notch.

The specimens were cycled 1,800 times per minute at a stress on the notched surface equal to about 39 percent of the yield stress with an R of 0.05. Most of the specimens required from 25,000 to 80,000 cycles for adequate cracking.

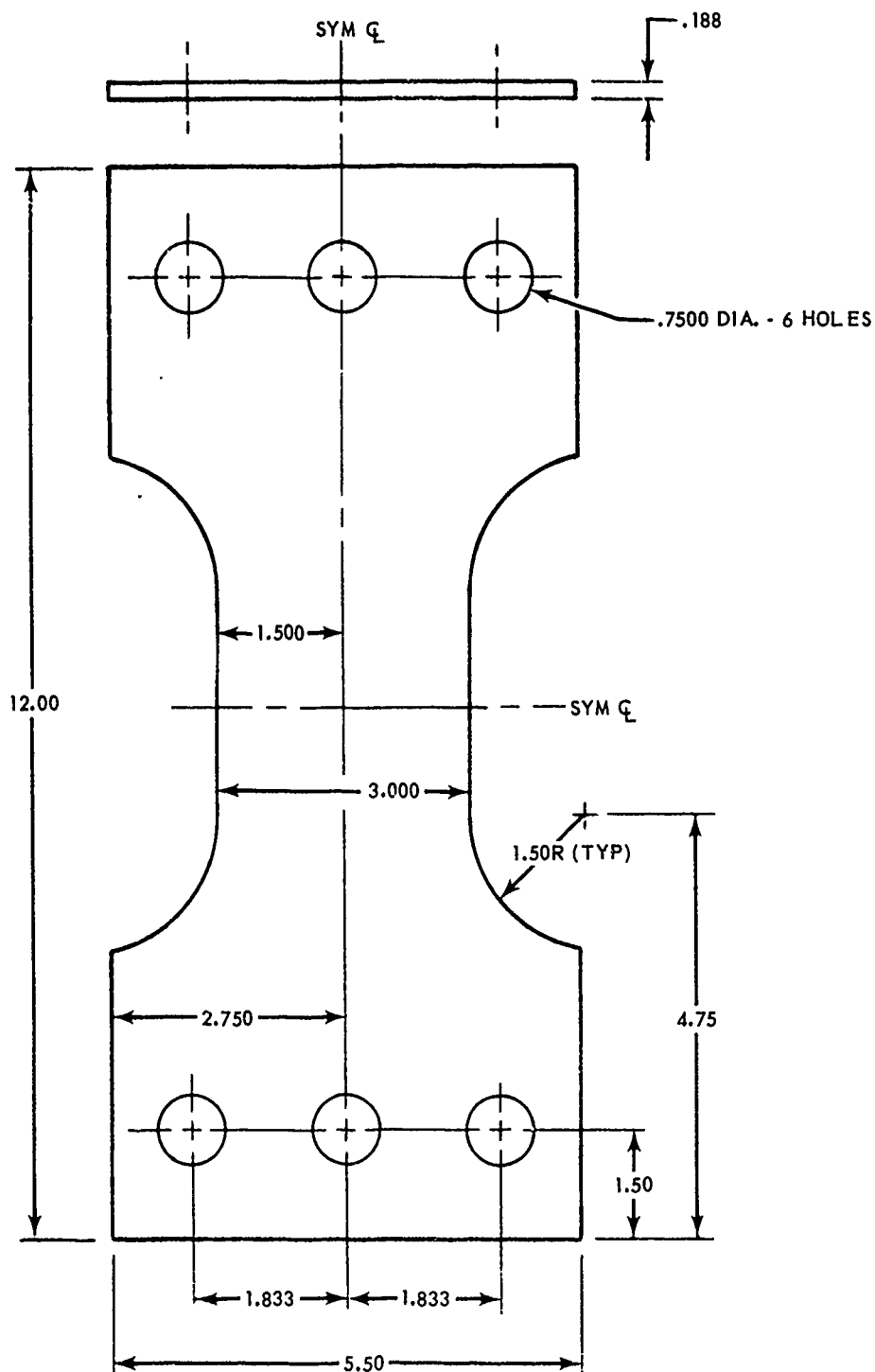


FIG. 125 SURFACE CRACK SPECIMEN

TABLE 32 SURFACE CRACKED SPECIMEN DATA

SPECIMEN DATA				FATIGUE DATA		FAILURE DATA		CRACK SIZE				FAILURE STRESS		$\frac{\sigma_p}{\sigma}$	K_{1C_p}				
NUMBER	THICKNESS inches	WIDTH inches	GROSS AREA in ²	MAXIMUM CYCLING STRESS ksi	CYCLES in 000's	TEST TEMP °F	MAXIMUM LOAD kips	1 inches (a)	2 inches (b)	CRACK DEPTH inches (b)	$\frac{b}{a}$	ϕ^2	$\frac{b}{Q}$	ACTUAL (σ) ksi	PREDICTED (σ_p) ksi	$\sigma - \sigma_p$	$\frac{\sigma}{\sigma_{ys}}$	K_{1C_p}	
4340																			
A2M1	.186	2.997	.558	60.5	26	75	102.3	.375	.048	.128	1.06	.053		183.2	192.1	-8.9	1.04	82.2	
A2M5	.192	2.988	.574	80.0	35	75	107.8	.375	.058	.155	1.06	.064		187.7	177.2	10.5	.94	92.4	
A2M4	.190	2.974	.565	62.0/80.0	75/24	75	105.5	.375	.060	.160	1.07	.066		186.7	175.4	11.3	.94	93.0	
A2M3	.184	2.992	.551	67.3	26	75	101.2	.376	.068	.181	1.09	.073		183.7	166.9	16.8	.91	96.6	
A2M2	.187	2.945	.551	67.3	29	75	78.5	.388	.160	.412	1.34	.129		142.5	132.6	9.9	.93	99.2	
9 Ni-4Co																			
BROKE THROUGH GRIP HOLES																			
B2M1																			
B2M5	.199	2.988	.595	78.0	76.0	75	117.8	.125	.070	.560	1.56	.052		197.9	314.9	-117.0	1.59	1.00	87.5
B2M4	.250	2.985	.746	78.0	90.0	75	138.5	.280	.128	.457	1.40	.105		185.6	240.2	-54.6	1.29	.93	117.0
B2M2	.220	2.989	.658	78.0	90.0	75	114.9	.350	.135	.386	1.30	.119		174.6	226.9	-52.3	1.30	.88	116.0
B2M3	.253	2.987	.756	78.0	55.0	75	132.9	.370	.148	.400	1.32	.128		175.8	220.4	-44.6	1.25	.89	121.0
AM 355																			
C2M1	.191	2.996	.572	65.0	135.0	75	97.5	.362	.118	.326	1.23	.117		170.5	181.1	10.5	1.06	1.02	113.2
C2M2	.192	2.984	.573	65.0	87.0	-110	111.5	.075	.049	.653	1.72	.032		194.6	150.6	44.0	.77	.96	67.6
C2M4	.190	2.988	.568	65.0	70.0	-110	109.5	.103	.057	.553	1.55	.042		192.8	133.2	59.6	.69	.95	76.6
C2M5	.190	2.993	.569	65.0	95.0	-110	82.5	.130	.060	.461	1.40	.047		145.0	123.5	21.5	.85	.71	60.6
	.193	2.985	.576	65.0	128.0	-110	56.8	.225	.093	.413	1.34	.072		98.5	98.0	.5	.99	.48	51.4

SPECIMENS A2M 1,2 AND 3 WERE FATIGUE CRACKED UNDER AXIAL LOADING. (R=.05 CRACK SURFACE).

ALL OTHER SPECIMENS WERE FATIGUE CRACKED UNDER FLECTURE LOADING (1800 CPM, R = .05)

ACTUAL FAILURE STRESS BASED ON GROSS AREA

FRACTURE TEST LOAD RATE WAS 150 ksi/min

 σ_{ys} = 213.0, 198.4 ksi FOR 4340 AND 9Ni - 4Co, RESPECTIVELY AND 166.7 AT 75°F and 203.2 at -110°F FOR AM 355 K_{1C_p} = ROUND NOTCHED SPECIMEN TOUGHNESS VALUE OF 86.7, 160.0 ksi√inches FOR 4340 AND 9Ni - 4Co, RESPECTIVELY AND 122.7 AT 75°F AND 51.1 AT -110°F FOR AM 355.

$$\sigma_p^2 = \frac{K_{1C_p}^2 \phi^2}{3.77 b - .212 K_{1C_p}^2 / \sigma_{ys}^2}$$

 σ_p = PREDICTED FAILURE STRESS

$$Q = \phi^2 - .212 (\sigma / \sigma_{ys})^2$$

TABLE 32 SURFACE CRACKED SPECIMEN DATA (continued)

SPECIMEN DATA				FATIGUE DATA			FAILURE DATA		CRACK SIZE				FAILURE STRESS		$\frac{\sigma_p}{\sigma}$	$K_{Ic} \rho_{ys}$
NUMBER	THICKNESS inches	WIDTH inches	GROSS AREA in ²	MAXIMUM CYCLING STRESS ksi	CYCLES in 000's	TEST TEMP °F	MAXIMUM LOAD kips	1/2 CRACK LENGTH (a) inches	CRACK DEPTH (b) inches	$\frac{b}{a}$	ϕ^2	$\frac{b}{Q}$	ACTUAL (σ) ksi	PRE- DICTED (σ_p) ksi		
MARAGING 250																
D2M1	.186	2.998	.557	85.0	54	75	126.0	.120	.012	.100	1.03		226.2	213.3	1.00	1.06
D2M5	.191	2.998	.573	85.0	40	75	120.5	.106	.057	.538	1.52	.044	210.3	195.2	1.01	.99
D2M4	.190	3.005	.571	85.0	46	75	116.8	.127	.073	.575	1.58	.053	204.5	184.4	.95	.96
D2M3	.192	2.995	.575	85.0	69	75	115.5	.147	.080	.544	1.53	.060	200.9	166.0	.92	.94
D2M2	.191	2.998	.573	85.0	104	75	105.5	.202	.090	.445	1.38	.074	184.1		.90	.87
TITANIUM 6Al-4V																
F4M2	.184	2.995	.551	60.0	32	75	90.8	.042	.029	.690	1.64	.021	164.7	137.9	.84	1.12
F3M1	.176	2.990	.526	60.0	15	75	80.1	.082	.039	.476	1.43	.033	152.3	112.6	.74	1.04
F4M3	.188	2.995	.563	60.0	34	75	79.8	.135	.070	.518	1.49	.054	141.7	87.5	.62	.96
F4M4	.182	2.994	.545	60.0	26	75	72.4	.165	.078	.473	1.42	.062	132.8	81.2	.61	.90
F4M5	.192	2.995	.575	60.0	34	75	74.0	.181	.080	.442	1.38	.066	128.7	79.0	.61	.87
Ti 6Al-6V-2Sn ANN																
H7M3	.189	2.996	.566	56.0	30.0	75	79.9	.110	.064	.582	1.59	.046	141.1	113.0	.80	.99
H7M2	.189	2.996	.566	56.0	38.0	75	77.1	.137	.065	.474	1.42	.053	136.3	106.1	.78	.95
H7M1	.189	2.995	.566	56.0	29.0	75	77.0	.171	.068	.398	1.32	.060	136.0	105.1	.77	.95
H7M4	.191	2.996	.572	56.0	22.0	75	74.8	.198	.078	.394	1.31	.069	130.8	93.7	.72	.91
H7M5	.188	3.000	.564	56.0	34.0	75	69.9	.256	.100	.391	1.31	.087	123.8	83.4	.67	.86

ACTUAL FAILURE STRESS BASED ON GROSS AREA

FRACTURE TEST LOAD RATE WAS 150 ksi/min

 σ_{ys} = 212.5, 147.1 AND 143.1 ksi, FOR MARAGING 250 Ti 6Al-4V AND Ti 6Al-6V-2Sn ANN, RESPECTIVELY K_{IC} = ROUND NOTCHED SPECIMEN TOUGHNESS VALUE OF 86.5, 37.8 AND 46.0 ksi $\sqrt{\text{inches}}$, FOR MARAGING 250, Ti 6Al-4V AND Ti 6Al-6V-2Sn ANN, RESPECTIVELY.

$$\sigma_p^2 = \frac{K_{IC}^2 \phi^2}{3.77 b + .212 K_{IC}^2 \sigma_{ys}^2}$$

 σ_p = PREDICTED FAILURE STRESS

$$Q = \phi^2 - .212 (\sigma_{ys})^2$$

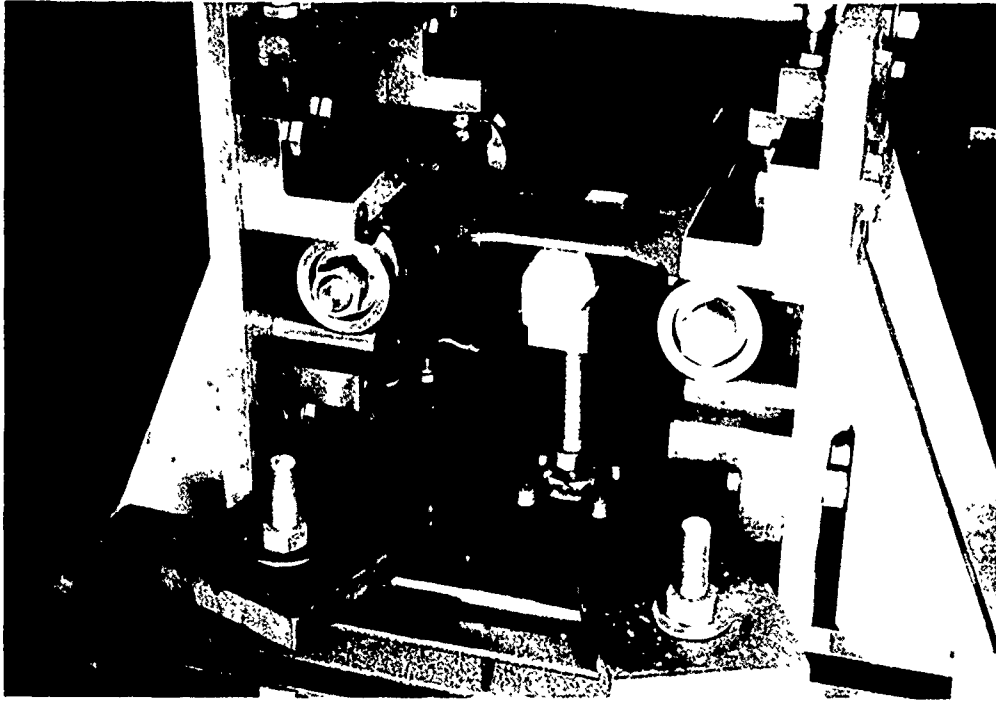


FIG. 126 FATIGUE CRACKING SETUP FOR SURFACE CRACKED SPECIMENS

Fatigue conditions for each specimen including cycling stress, crack depth, and crack length are listed in Table 32. The shape of the cracks are shown in the photograph of the fracture surfaces (Fig. 127).

Initially, it was planned to maintain crack lengths constant at 0.75 inch and the starter notch in all 4340 specimens was made 0.75 inch long. Crack depth was to be varied by changing the number of cycles. However, cracks as shallow and as elliptical in shape as desired could not be obtained with the 0.75 inch notch. This problem was solved by shortening the starter notches to a length of three to five times the desired crack depth. Crack depth was controlled essentially by the length of the starter notch.

The original test plan was to produce theoretical crack sizes for fracture-stress to yield-stress ratios of 1.0, 0.9, and 0.8. However, this approach was abandoned when it was discovered that the experimental fracture stresses were much higher than the theoretical and that this procedure would result in most of the specimens having fracture stresses above the yield stress. The approach then adopted was to determine, for each alloy, the approximate effect of crack size on fracture stress by first testing two of the five program specimens. Crack sizes were then selected for the remaining three specimens based on the results of the first two specimens.

SURFACE CRACK SPECIMENS

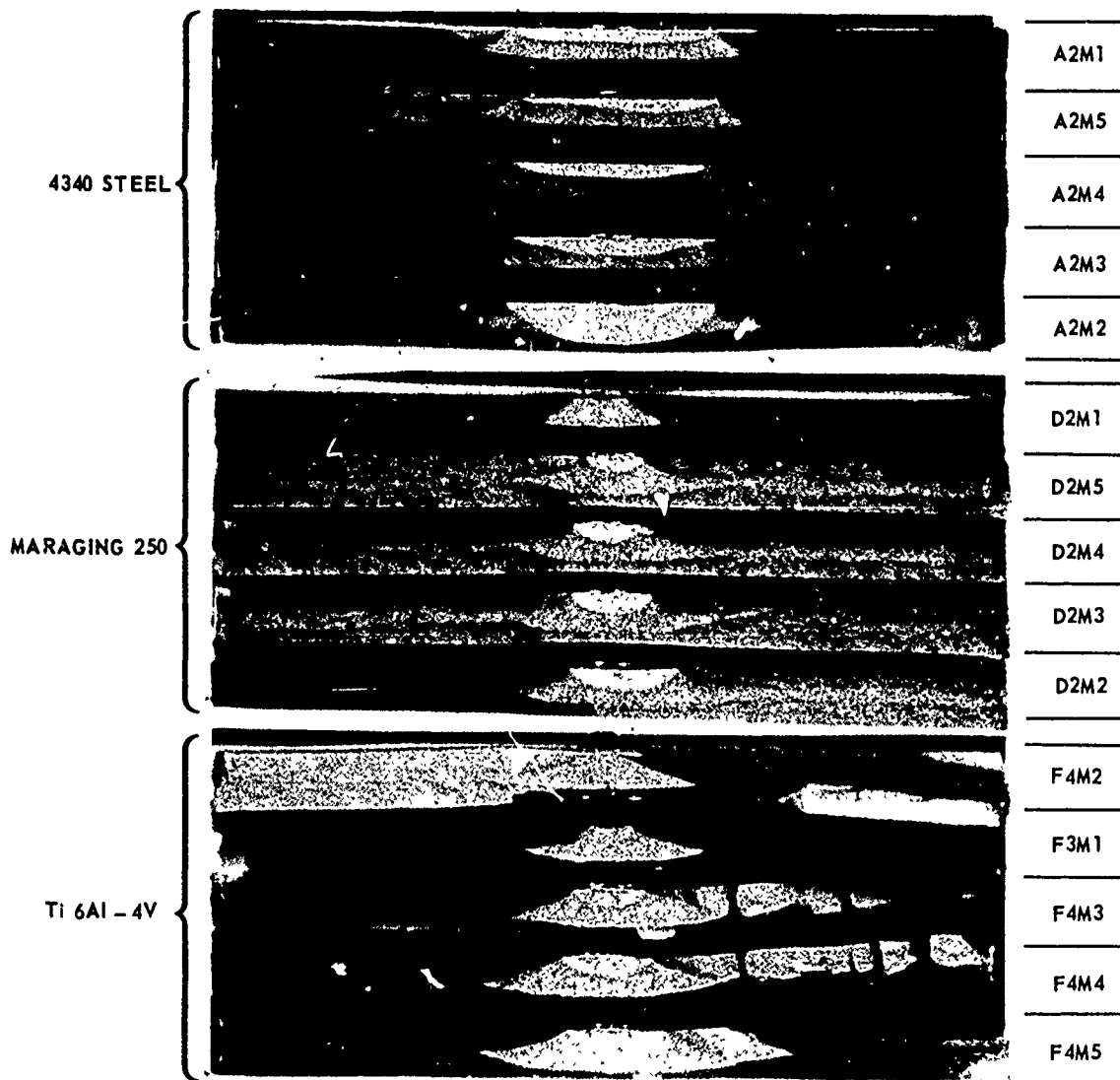


FIG. 127 FRACTURE FACES OF SURFACE CRACK SPECIMENS

SURFACE CRACK SPECIMENS

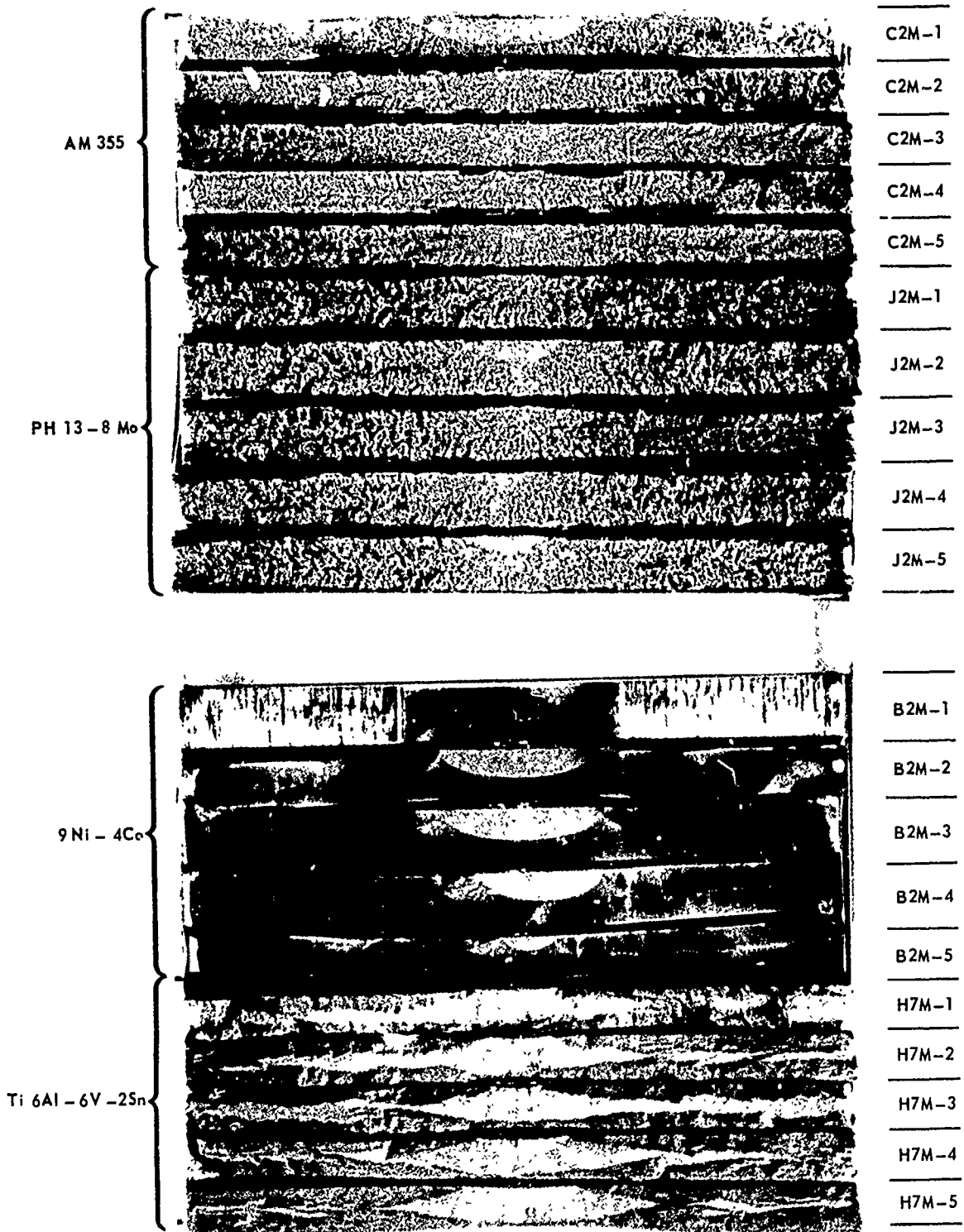


FIG. 127 FRACTURE FACES OF SURFACE CRACK SPECIMENS (continued)

Fracture Testing

The specimens were fracture tested, as shown in Fig. 128, in a Tinius-Olsen 440,000-pound capacity tensile machine at a stress rate of 150,000 psi per minute. Loading eccentricities were minimized by pin loading the specimen by means of load plates bolted to the specimen. Displacement across the crack was measured with an extensometer and recorded versus load. The extensometer arms were attached by means of wire loops spotwelded to the crack edge. This method of attachment permitted measurement directly at the crack and prevented damage to the extensometer at failure as the arms would slip through the loops. High sensitivity was obtained by using an arm pivot arrangement that produced a displacement magnification of two.

All specimens were tested at room temperature except those of AM 355 and PH 13-8Mo. These alloys were tested at -110°F to keep crack depth under half the specimen thickness. At room temperature, the toughness of these alloys was so high that crack depths considerably over half the specimen thickness would have been necessary to produce fracture below the yield strength.

An environmental chamber and liquid nitrogen were used for the -110°F tests. The cooling setup was the same as that described previously for the round notched specimens.

After failure, the fatigue crack length and depth were measured on the fracture face using a jewelers' magnifying glass and a 6-inch machinists' scale containing 0.01-inch graduations. In the toughness calculations, it was assumed that the crack size was the same as that of the fatigue crack at onset of rapid failure.

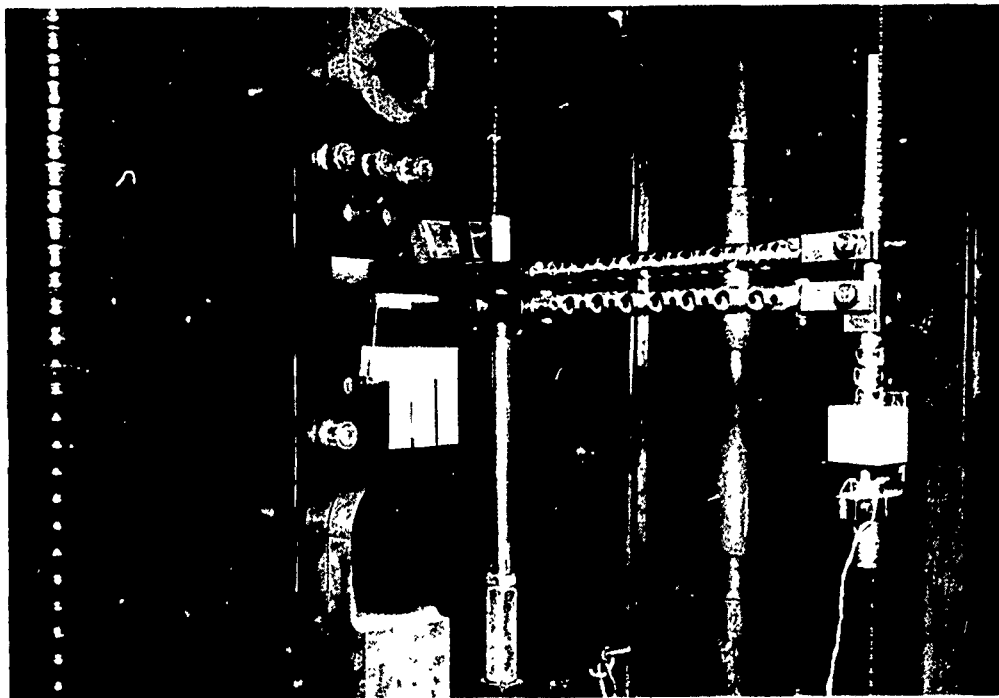


FIG. 128 FRACTURE TESTING SETUP FOR SURFACE CRACKED SPECIMENS

RESULTS AND DISCUSSION

The K_{1C} values were calculated for each specimen using the stress intensity expression, Equation (36), of Section 4. The predicted fracture stress σ_p , based on the round notched specimen $K_{1C(p)}$ value, was calculated for each specimen by rearranging Equation (36) to the form shown below and solving for the fracture stress using the $K_{1C(p)}$ value determined for the longitudinal direction of the alloy in the round notched specimen tests.

$$\sigma_p^2 = \frac{K_{1C(p)}^2 \Phi^2}{3.77b + 0.212 K_{1C(p)}^2 / \sigma_{ys}^2}$$

The test data are tabulated in Table 32. The table lists the predicted fracture stress as well as the experimentally determined fracture stress for each material. The table also lists the actual K_{1C} toughness value exhibited by each specimen, which was calculated from the actual fracture stress and crack dimensions. The ratio of the fracture stress to the yield strength is also listed to aid in the analysis.

The critical stress intensity values will be discussed first since the relationship between the predicted and actual fracture stresses depends on these values. These stress intensity values versus the fracture-stress to yield-strength ratio are plotted in Fig. 129. The curves show that the toughness values decrease rapidly with increasing fracture stress at stresses greater than about 90 percent of the yield strength. This behavior results from the onset of general plastic yielding. When plastic yielding occurs, the toughness equation is no longer valid and the apparent K_{1C} values fall below the true values. The large effect of the onset of yielding on the apparent toughness values is evident from the curves.

The curve for Ti 6Al-6V-2Sn annealed does not show a knee and indicates general yielding was occurring at fracture stresses as low as 86 percent of the yield stress. It is felt that this is possibly due to test scatter and that further test results would show that the curve has a knee at about the same ratio as the other alloys.

The fracture stresses reported are based on gross area. Net area is about 5 percent less for most of the specimens.

The test data indicate that the maximum fracture-stress to yield-strength ratio at which the toughness equation is valid is about 0.90 for gross fracture stresses and about 0.95 for net fracture stresses. These are also the maximum fracture stress to yield strength ratios at which it could be hoped to predict fracture stresses using the present equation. These ratios are lower than the maximum net fracture stress to yield strength ratio of 1.1 accepted for valid toughness measurements using round notched specimens.

At fracture stresses less than about 90 percent of the yield strength, Fig. 129 curves indicate that the stress intensity values remain fairly constant with decreasing fracture stress except for Ti 6Al-6V-2Sn annealed and AM 355. The Ti 6Al-6V-2Sn curve was discussed previously.

The curve for AM 355 shows a large decrease in toughness with decreasing fracture stress. This behavior was unexpected and no explanation is offered except that AM 355 showed considerable test data scatter throughout the entire program.

The specimen K_{1C} value determines the relationship between the predicted and actual fracture stresses. This may be seen from the expression shown below which relates the ratio of the predicted-to-actual fracture stress to the toughness values.

$$\sigma_p/\sigma = \left[\frac{K_{1C}^2(\text{round}) \Phi^2 / [3.77 b + 0.212 K_{1C}^2(\text{round}) / \sigma_{ys}^2]}{K_{1C}^2(\text{surface cracked}) \Phi^2 / [3.77 b + 0.212 K_{1C}^2(\text{surface cracked}) / \sigma_{ys}^2]} \right]^{1/2}$$

A plot of the predicted to actual fracture ratio for each specimen versus the fracture-stress to yield-stress ratio is shown in Fig. 130. The curves reflect the changes in apparent toughness with fracture stress level shown in Fig. 129. At a fracture stress of 90 percent or less of the yield strength, the predicted stresses for the alloys ranged from 29 percent above to 39 percent below the actual stresses. Only two alloys had predicted stresses within 10 percent of the actual stress. The predicted stresses were below the actual stresses for all alloys except one.

Since most of the predicted stresses were below the actual stress, the possibility that the start of rounding on the load-displacement curves might be the start of slow crack growth and that the predicted loads might coincide with this point was considered. However, they did not. For the titanium alloys, the predicted loads were far below the point at which rounding began (Fig. 133).

A plot of the round bar $K_{1C(p)}$ value versus the surface-cracked specimen $K_{1C(p)}$ value for each alloy is shown in Fig. 131. The surface-cracked specimen values were taken from Fig. 129 at a fracture stress level of 90 percent of the yield strength. The curve indicates that the difference between round bar and surface cracked specimen stress intensity values is related to the stress intensity level. At stress intensity levels below about 100 ksi $\sqrt{\text{in.}}$ (round bar), the surface cracked specimen values are higher and the difference between the two specimen values increases with decreasing stress intensity level. Above a stress intensity level of 100 ksi $\sqrt{\text{in.}}$ (round bar), it would seem that the round notched values would be higher. However, the upper part of the curve is only based on one point and therefore has questionable accuracy. Both types of specimens rank the alloys in approximately the same toughness order. However, the round notched specimen toughness values show a much greater stress intensity difference between the alloys than the surface-cracked specimen values. This would indicate that the round notched specimen is more toughness sensitive than the surface cracked specimen.

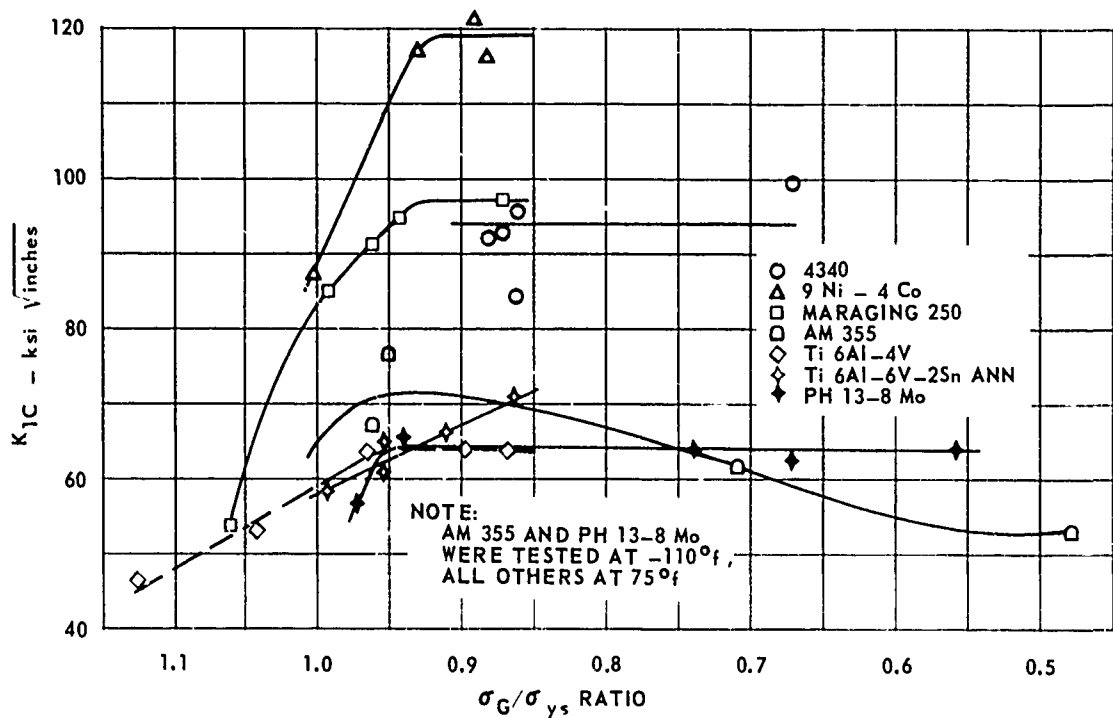


FIG. 129 EFFECT OF FAILURE STRESS LEVEL ON SURFACE CRACKED SPECIMEN TOUGHNESS VALUES

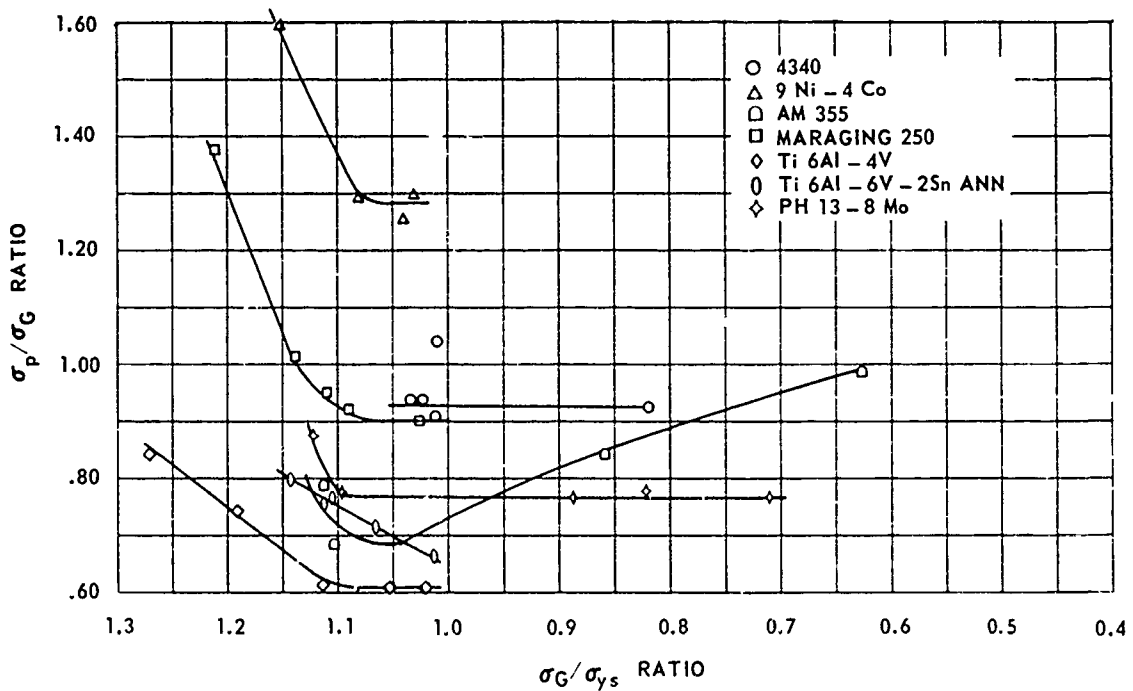


FIG. 130 EFFECT OF FAILURE STRESS LEVEL ON RELATIONSHIP BETWEEN ACTUAL AND PREDICTED FRACTURE STRESSES

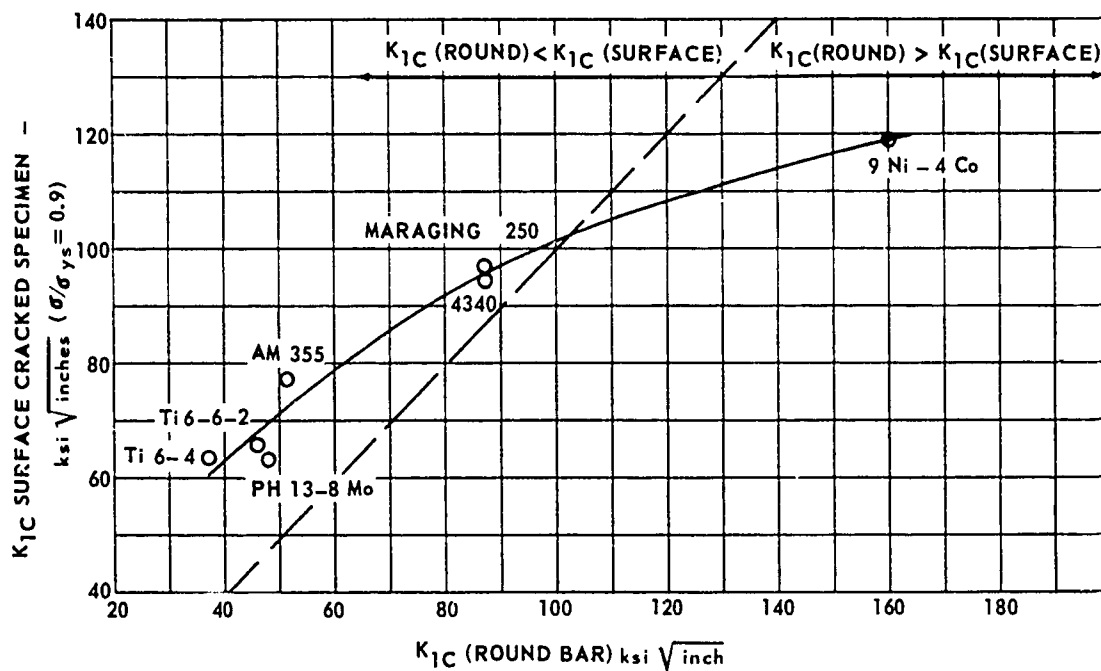


FIG. 131 RELATIONSHIP BETWEEN ROUND NOTCH AND SURFACE CRACKED SPECIMEN TOUGHNESS VALUES FOR VARIOUS ALLOYS

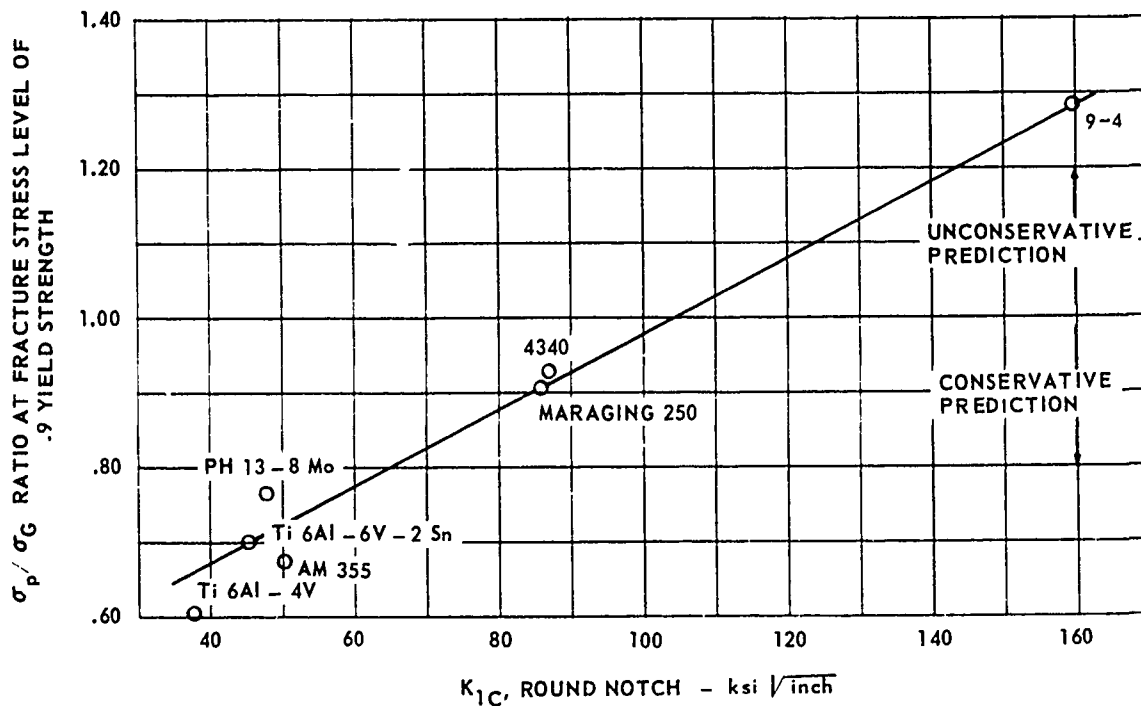
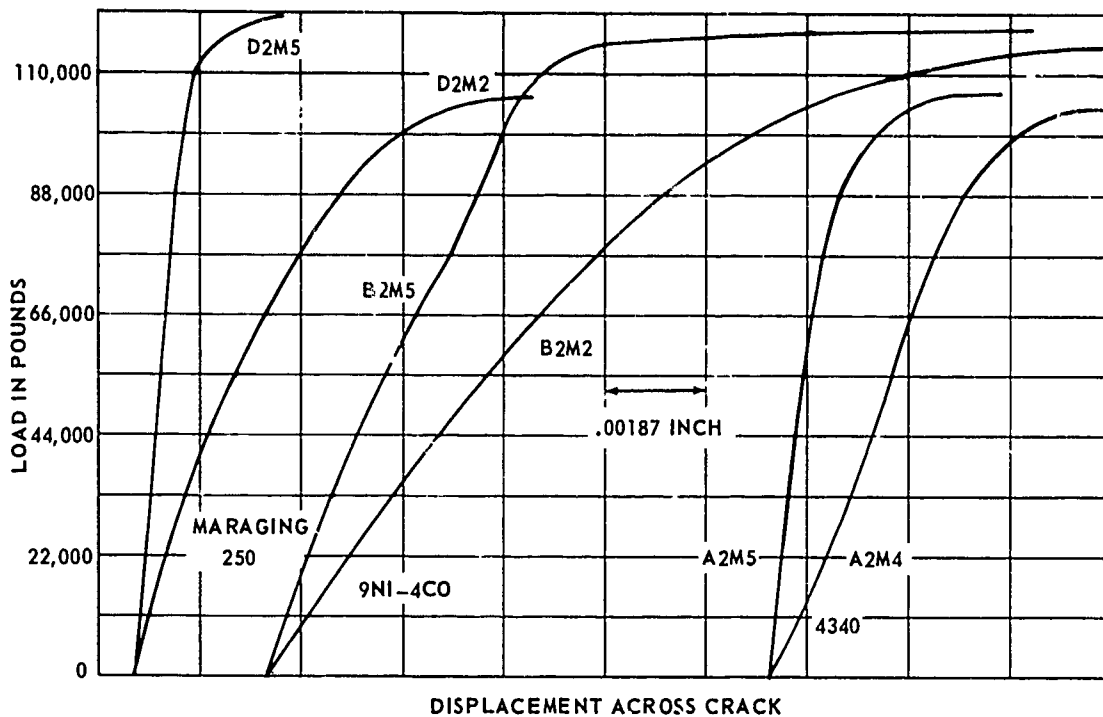


FIG. 132 EFFECT OF ALLOY TOUGHNESS LEVEL ON RELATIONSHIP BETWEEN ACTUAL AND PREDICTED FRACTURE STRESSES

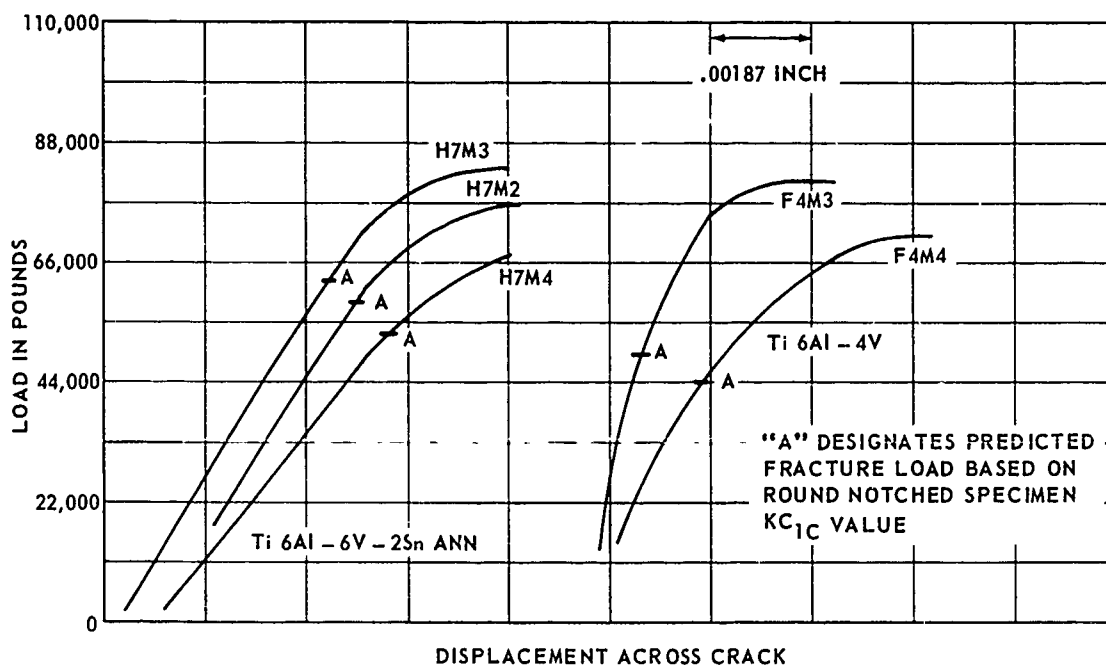
Since the difference between the round notched and surface-cracked specimen toughness values is related to the toughness level, the predicted-to-actual fracture stress ratio is also related to the stress intensity level. A plot of this ratio versus stress intensity level for the various alloys is shown in Fig. 132. According to the plot, an alloy would have to have a stress intensity value in the range of 85 to 125 ksi $\sqrt{\text{in.}}$ (round notched) for the predicted stresses to be within 10 percent of the actual stresses.

If the round notched specimen toughness values were converted to an equivalent surface cracked stress intensity value according to the Fig. 131 curve, then the predictions for all the alloys would be within 10 percent of the actual stresses.

The differences between the $K_{IC(p)}$ values for the two types of specimen indicates the stress condition in the round notched specimens as coming closer to a plane strain condition than that in the surface cracked specimens. This would result in the surface cracked specimens exhibiting lower material toughness sensitivity and higher toughness values for six out of the seven alloys. The lower fracture stress-to-yield strength ratio at which toughness values become invalid in the surface-cracked than in the round notched specimens also supports the above mentioned stress condition difference. A comparison of the load-displacement curves for these two specimen types also supports the above possibility. These curves for the surface-cracked specimens (Fig. 133) always showed rounding just prior to fracture, whereas, those for the round specimens were essentially linear for specimens having fracture stresses under 130 percent of the yield strength.



(A) 4340, 9 Ni-4 Co and MARAGING 250 Specimens



(B) Ti 6Al-4V and Ti 6Al-6V-2Sn ANN Specimens

FIG. 133 TYPICAL LOAD-DISPLACEMENT DATA FOR SURFACE CRACKED SPECIMENS

SECTION 10 PRECRACKED CHARPY EXPOSURE TESTING

To simulate aircraft service experience, 1000-hour exposure testing was accomplished at both 400°F and 650°F. Stress conditions were those recommended by the NASA Materials Committee for the Supersonic Transport; 40,000 psi for steel and 25,000 psi for titanium. To assess the effect of temperature only, specimens were also exposed to the same temperatures at zero stress.

A preliminary evaluation of all eight alloys was made with precracked Charpy specimens. It was considered that these preliminary specimens would indicate any serious problems with metallurgical stability and aid in selecting the four most promising alloys. A second evaluation was made on the four most promising alloys with exposure specimens of the same design as the 1-1/8-inch diameter notched rounds in previous testing. These specimens were tested at only the more extreme exposure conditions. The second evaluation will be discussed later in the sequence of testing (Section 12).

TEST PROCEDURE

Material for the exposure specimens was exposed in recirculating air, resistance heated creep ovens (Fig. 134). The material for the Charpy specimens was exposed under load in lengths referred to as long Charpy specimens (Fig. 135) suitable for subsequent fabrication into three precracked Charpy specimens identical to those used in the heat treat study. Lengths of material for zero stress precracked Charpy specimens were placed in the same creep ovens so they would be exposed to the identical temperature. Material for the round notched specimens was exposed in rods 3 inches long, with 6 coupled together in the same type of creep ovens. Exposed Charpy and round notched specimens were at least 0.030 inch oversized on each surface. The 0.030 inch excess was removed after exposure by the final machining operation.

Temperature in the creep ovens was controlled by Minneapolis-Honeywell time-proportioning temperature controllers using chromel-alumel (Type K) thermocouple sensing elements. Overheating protection was provided by similar equipment. Thermocouples were placed at the top and bottom of each specimen (6 inches apart) to ensure temperature uniformity.

After 1000 hours exposure, the material was removed and finish machined into specimens identical to the procedure used previously. Fatigue cracking and fracture testing were the same as procedure described in Section 6.

RESULTS AND DISCUSSION

Precracked Charpy exposure data is tabulated in Table 33. The data is plotted against test temperature in Figs. 136 through 144. Unexposed data for comparative purposes is included from Section 6, Heat Treat Study. Stability characteristics for the individual alloys are discussed separately.



FIG. 134 EXPOSURE SETUP FOR LONG CHARPY SPECIMENS

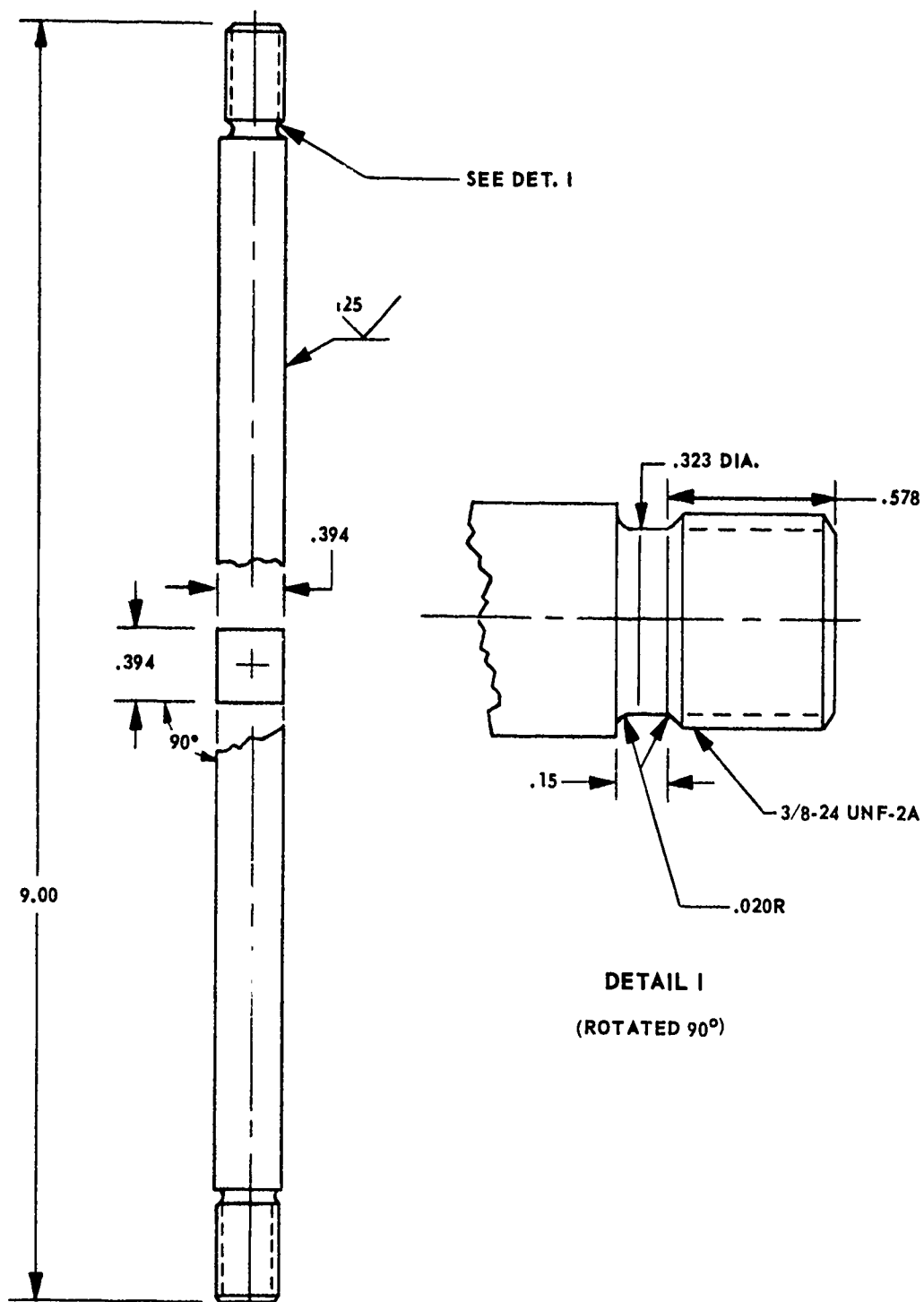


FIG. 135 LONG EXPOSURE CHARPY SPECIMEN

TABLE 33 EXPOSURE PRECRACKED CHARPY DATA

CONDITIONS				W/A (in-lbs/in ²)								
EXPOSURE TEMP °F	EXPOSURE STRESS psi	GRAIN DIRECTION	TEST TEMP °F	4340	9 Ni-4Co	AM 355	MARAGING 250	INCO 718	Ti 6Al-4V	Ti 6Al-6V-2Sn ANN	Ti 6Al-6V-2Sn STA	PH 13-8Mo
400	0	T	-110	272	945	195	425	1358	351	111	118	191
400	0	T	-110	241	935	226	407	1735	339	147	98	264
400	0	T	RT	537	2769	470	605	1662	582	330	202	763
400	0	T	400	1274	2317	947	1015	2542	1418	1096	540	2251
400	0	T	650	1378	3835	1200	1497	2191	2570	1881	1275	1810
400	0	T	650	1389	3761	1190	1367	2358	3003	720	1002	2333
650	0	T	-110	250	2062	207	276	1279	327	139	87	148
650	0	T	-110	229	1861	168	294	1753	360	114	107	313
650	0	T	RT	546	3068	424	527	1497	549	349	131	349
650	0	T	400	1101	4882	1091	793	1620	1596	356	545	1407
650	0	T	650	1168	5356	1211	1346	2286	3161		953	2145
650	0	T	650	1280	5218	1211	1409	2493	2994	610	992	2323
400	40,000*	T	-110	305	1200	212	410	2379	330	109		207
400	40,000*	T	-110	284	1168	221	410	2182	313	109		171
400	40,000*	T	RT	716	3860	568	678	2140	577	291		733
400	40,000*	T	400	1065	5049	1179	1098	2837	1513	905		2900
400	40,000*	T	650	1051	4736	1200	1313	2113	3415	2125		3175
400	40,000*	T	650	1236	4024	1019	1355	3036	3105	1687		3297
650	40,000*	T	-110	295	1743	196	275	1980	351	93		115
650	40,000*	T	-110	251	2210	190	292	1768	346	106		109
650	40,000*	T	RT	467	3929	517	466	2154	561	121		353
650	40,000*	T	400	1194	5319	956	762	2542	1653	339		1449
650	40,000*	T	650	1274	6389	1111	1138	2400	3033	410		2084
650	40,000*	T	650	1378	6685	1112	1252	2990	2712	708		2539

* 25,000 psi for Titanium Alloys

4340

Exposure conditions did not effect 4340 stability significantly. The plotted data (Fig. 136) indicated an embrittlement at room temperature and an increase in toughness at elevated temperatures. However, the room temperature data for 40 ksi exposed at 400°F, which would be expected to be next to the most extreme condition, is very close to the room temperature unexposed point. Therefore, this data probably indicates the amount of scatter possible with this type of specimen.

AM 355

The AM 355 data indicates a possible embrittling reaction at 650°F. Published sharp edge notched data at 650°F (Ref.28) showed the same decrease. Investigations have shown that, with long creep exposure carbides of the $M_{23}C_6$ type precipitate in the matrix of stainless steels of this type with long creep exposure. The data showed the toughness to be at least as great as the 4340 at 650°F.

MARAGING 250

The 650°F exposure both with and without stress appeared to cause a small decrease in the toughness of Maraging 250. The 400°F exposure, however, did not seem to affect the properties. The stability of the alloy based on this preliminary testing appeared to be only slightly affected by high temperature exposure.

INCO 718

The Inco 718 alloy exposure testing showed greater scatter than encountered with the other alloys. Stress and heat tended to increase the toughness, whereas, heat alone tended to decrease the toughness.

It is difficult to explain these contradictory results other than that it represents metallurgical differences in areas of the block from which specimens were removed. In any event, the most severe exposure conditions did not cause embrittlement.

Ti 6Al-4V And Ti 6Al-6V-2Sn

One thousand hours of exposure with stresses as high as 25,000 psi and temperatures as high as 650°F had no noticeable effect on Ti 6Al-4V and Ti 6Al-6V-2Sn STA, as indicated by precracked Charpy specimens. However, the 650°F exposure, both with and without stress, appears to have an embrittling effect on the annealed condition of Ti 6Al-6V-2Sn as shown in Fig. 142. The 400°F exposure seemed to have no effect. Both the exposed and unexposed specimens were heat treated together, exposed in the same creep oven, and tested at the same time. Therefore, the indication seems to be that the annealed condition is less stable under stress than the aged condition at 650°F. It might be expected that the exposure conditions would age the annealed material till it approached the STA toughness. However, it can be seen from a comparison of Figs. 142 and 143 that the toughness of the exposed annealed

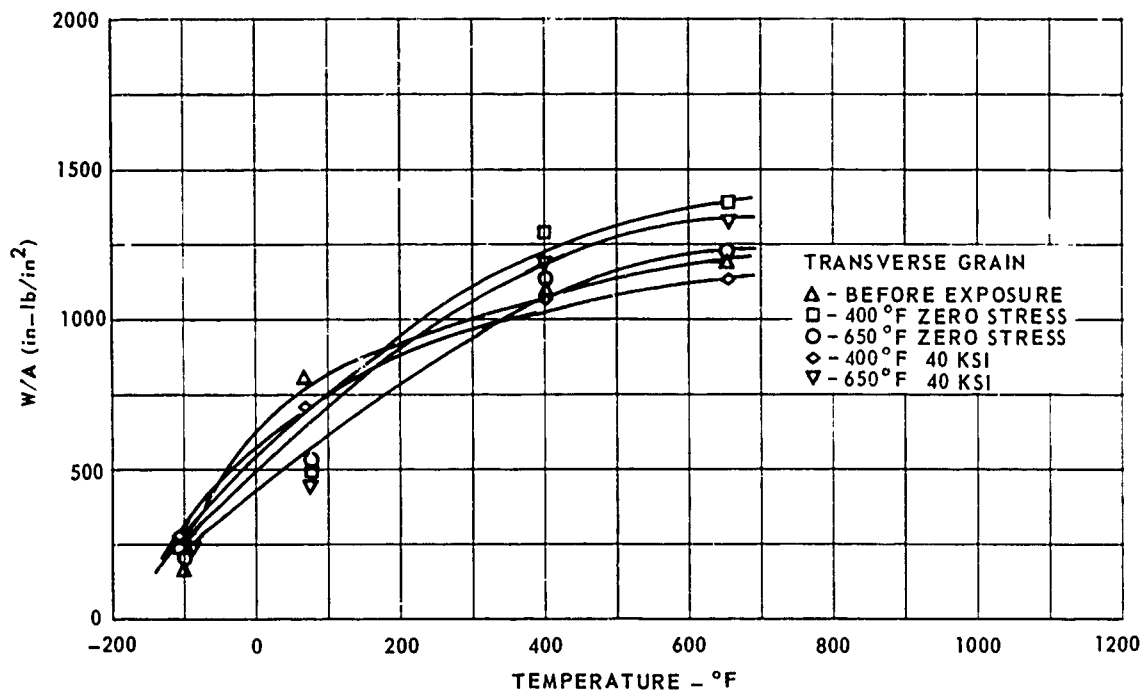


FIG. 136 EFFECT OF 1000 HOUR EXPOSURE ON THE PRECRACKED CHARPY TOUGHNESS FOR 4340

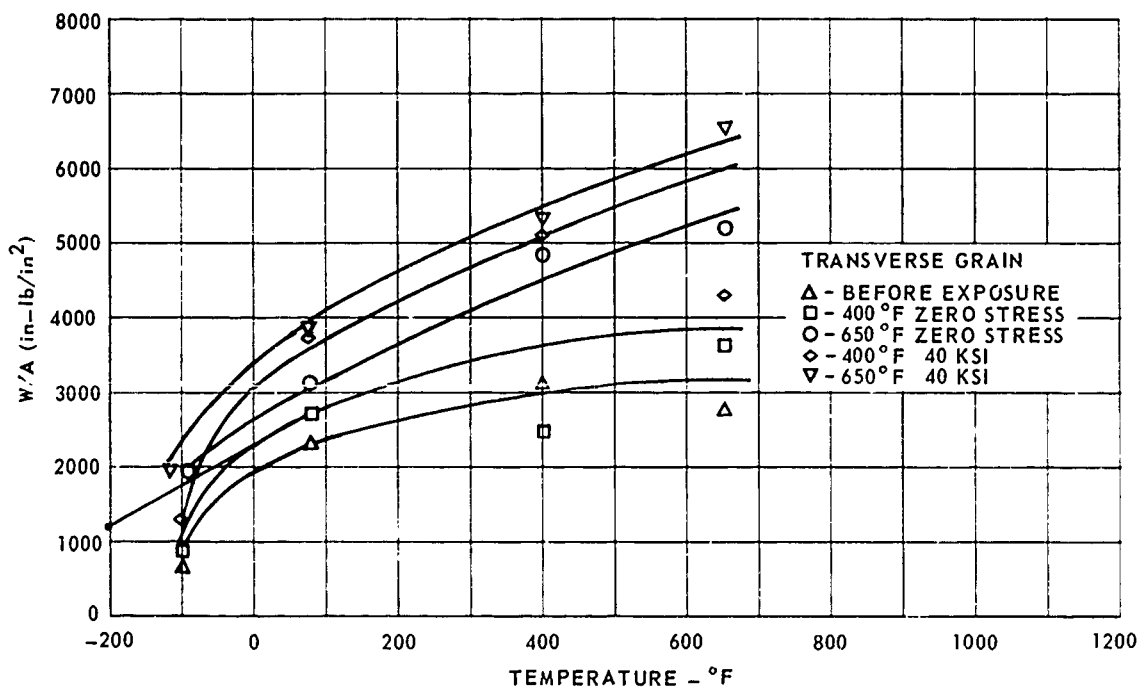


FIG. 137 EFFECT OF 1000 HOUR EXPOSURE ON THE PRECRACKED CHARPY TOUGHNESS FOR 9 Ni - 4 Co

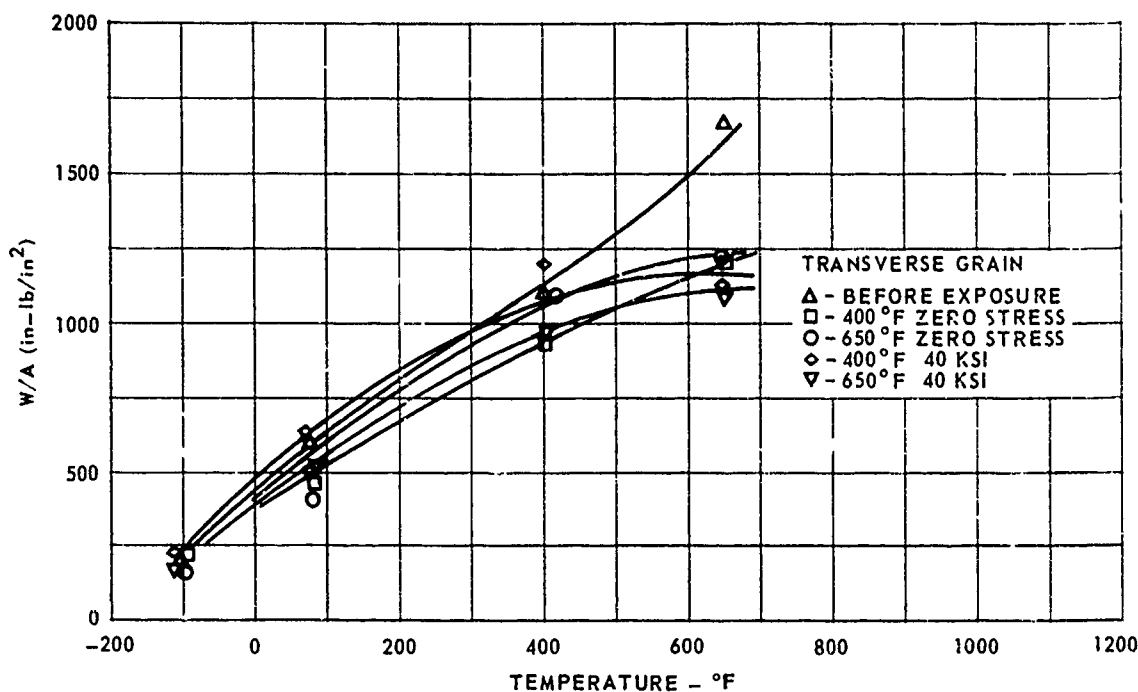


FIG. 138 EFFECT OF 1000 HOUR EXPOSURE ON THE PRECRACKED CHARPY TOUGHNESS FOR AM 355.

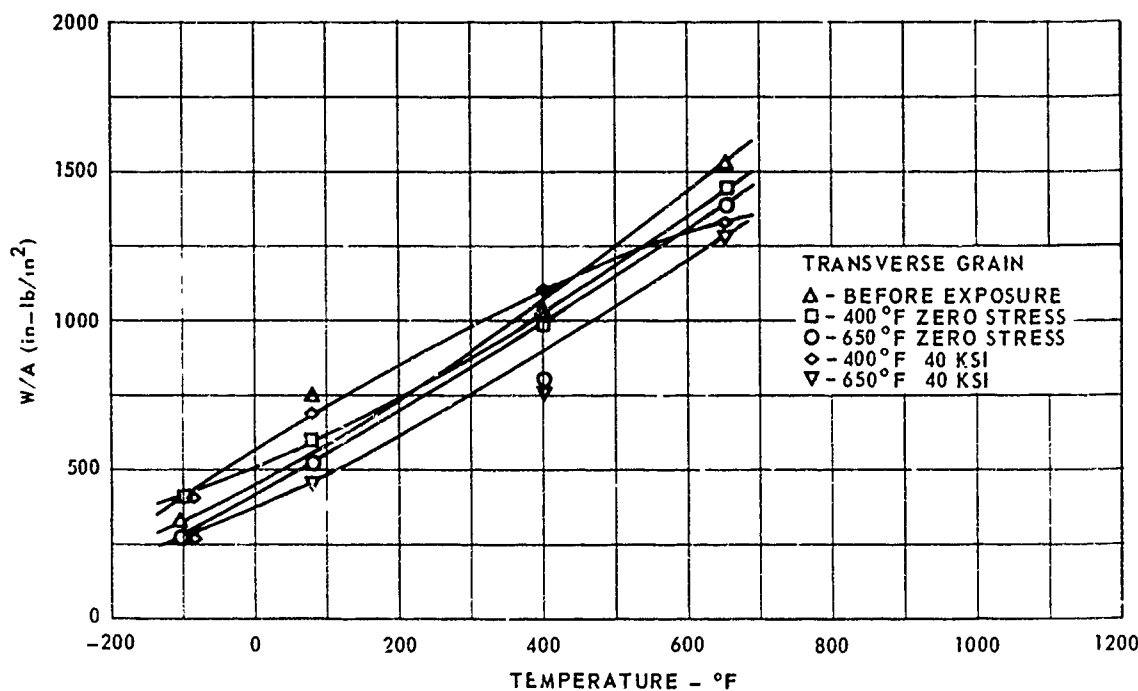


FIG. 139 EFFECT OF 1000 HOUR EXPOSURE ON THE PRECRACKED CHARPY TOUGHNESS FOR MARAGING 250

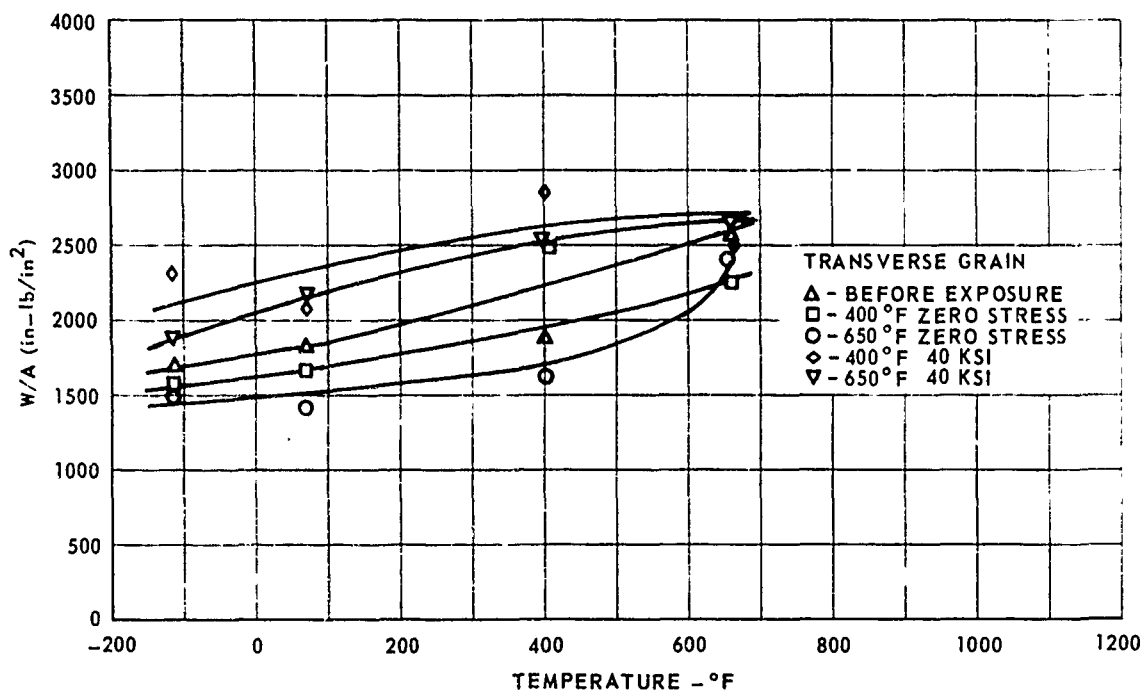


FIG. 140 EFFECT OF 1000 HOUR EXPOSURE ON THE PRECRACKED CHARPY TOUGHNESS FOR INCO 718

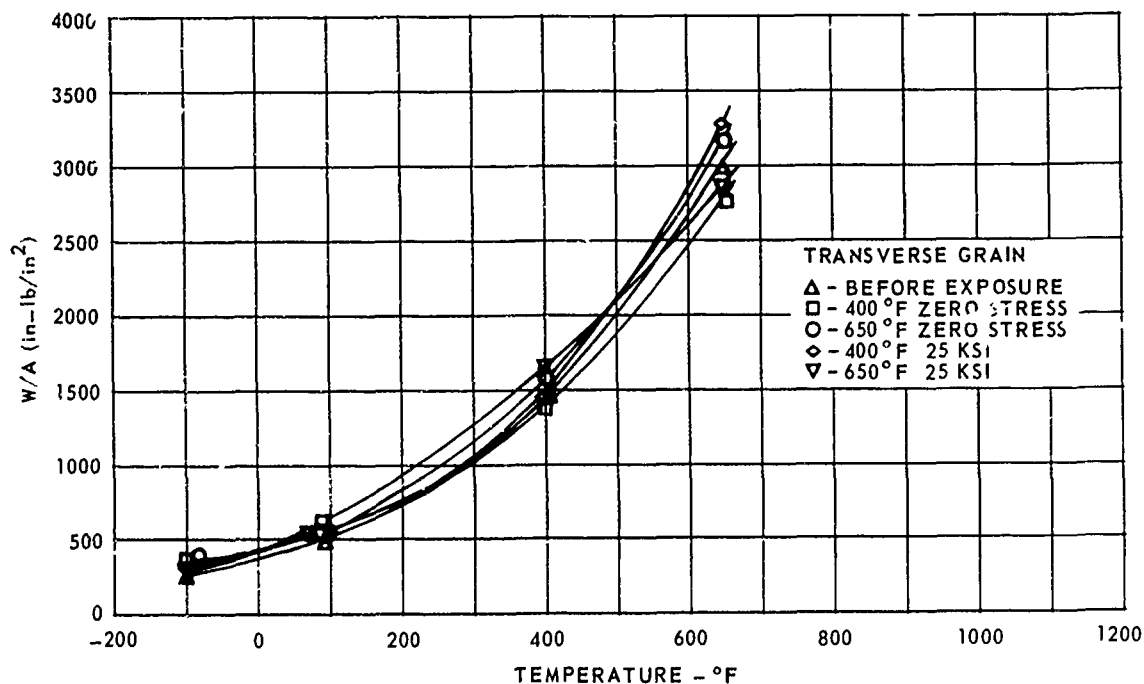


FIG. 141 EFFECT OF 1000 HOUR EXPOSURE ON THE PRECRACKED CHARPY TOUGHNESS FOR Ti 6Al-4V

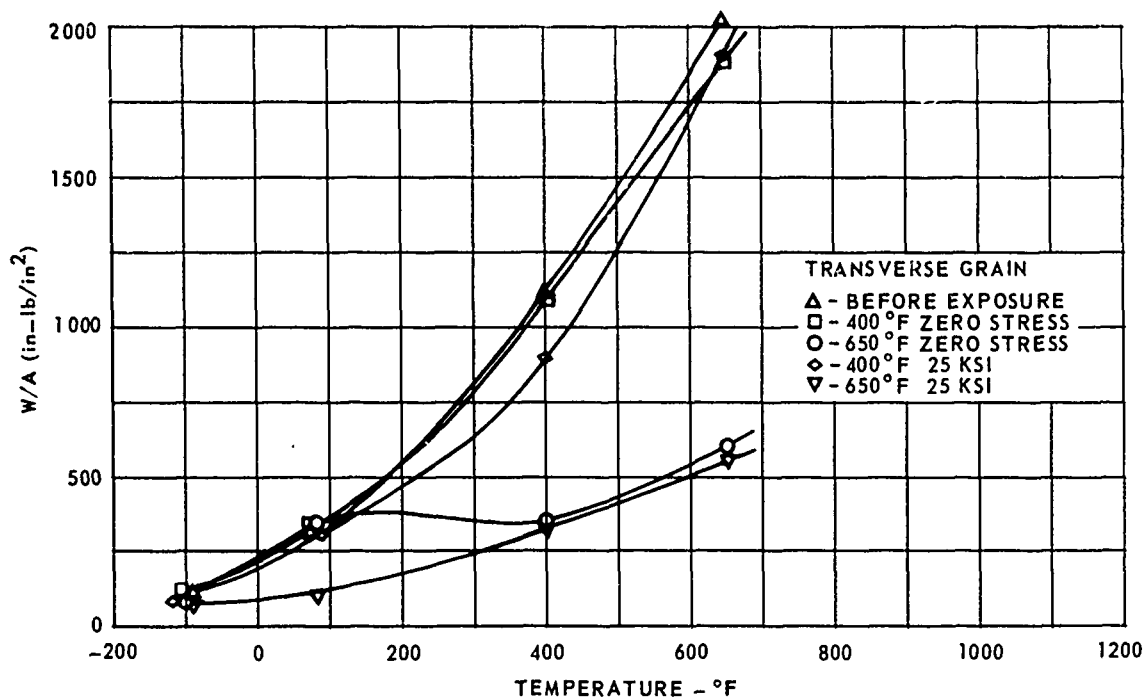


FIG. 142 EFFECT OF 1000 HOUR EXPOSURE ON THE PRECRACKED CHARPY TOUGHNESS FOR Ti 6Al-6V-2Sn ANN

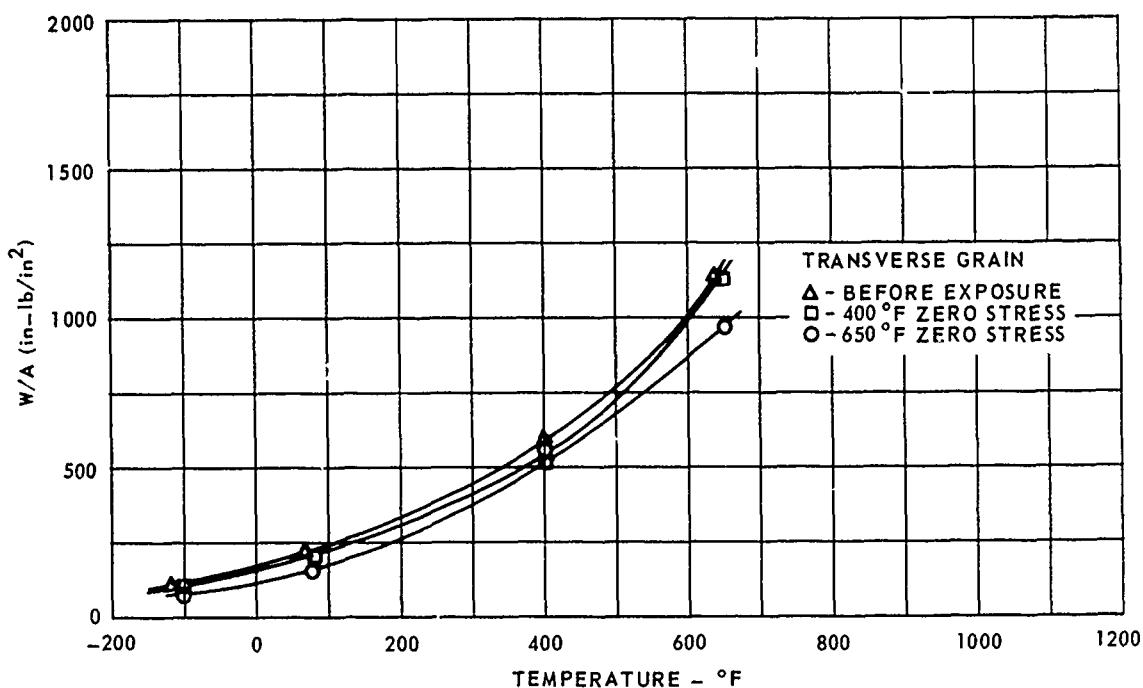


FIG. 143 EFFECT OF 1000 HOUR EXPOSURE ON THE PRECRACKED CHARPY TOUGHNESS FOR Ti 6Al-6V-2Sn STA

material falls below the exposed STA condition.

PH 13-8Mo

The PH 13-8Mo also indicated the same embrittling effect from the 650°F exposure as the AM 355, (Fig. 144), possibly for the same reason. It is questionable that the low values for 400°F exposure at zero stress indicates embrittlement since the stressed exposure at this temperature showed no effect.

9 Ni-4Co

An adverse effect of exposure conditions on 9 Ni-4Co was clearly indicated by the test data. The impact toughness nearly doubled in many instances and hardness measurements on the specimens correspondingly decreased. The increase in toughness, therefore, appeared to be caused by continued tempering. When contacted the material supplier advised that additions of chromium and molybdenum would improve the temper resistance of the alloy. Because of the excellent toughness of this alloy it was considered advisable to test material available from several modified heats.

Three 300-pound heats of modified chemistries had been poured and rolled into 1-inch thick plates. The modified chemistries are listed in Table 34.

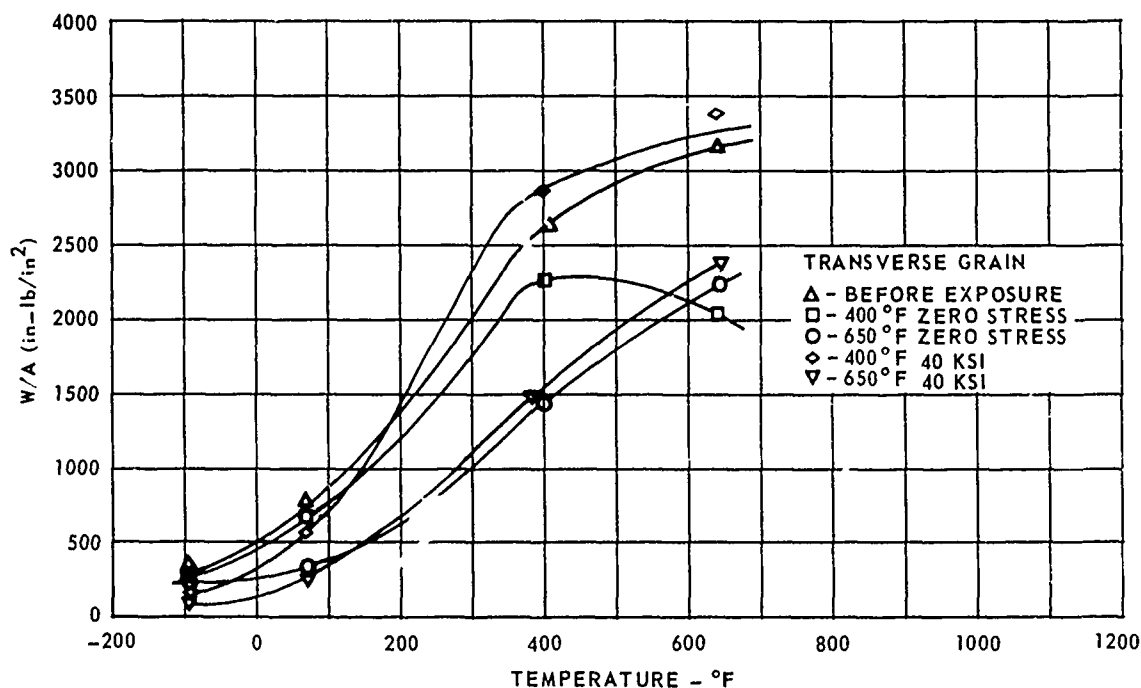


FIG. 144 EFFECT OF 1000 HOUR EXPOSURE ON THE PRECRACKED CHARPY TOUGHNESS FOR PH 13-8Mo

TABLE 34 CHEMICAL COMPOSITION FOR 9 Ni-4Co

HEAT NO.	C	Mn	Si	Ni	Cr	Mo	V	Co
3950881*	.43	.13	.01	8.09	.13	.11	.09	3.81
3920588	.41	.21	.03	8.00	.34	.28	.12	4.00
3888655	.31	.30	.01	7.76	1.10	.98	.12	3.10
3888656	.27	.32	.01	7.74	1.23	1.30	.08	3.14

*Initial Heat

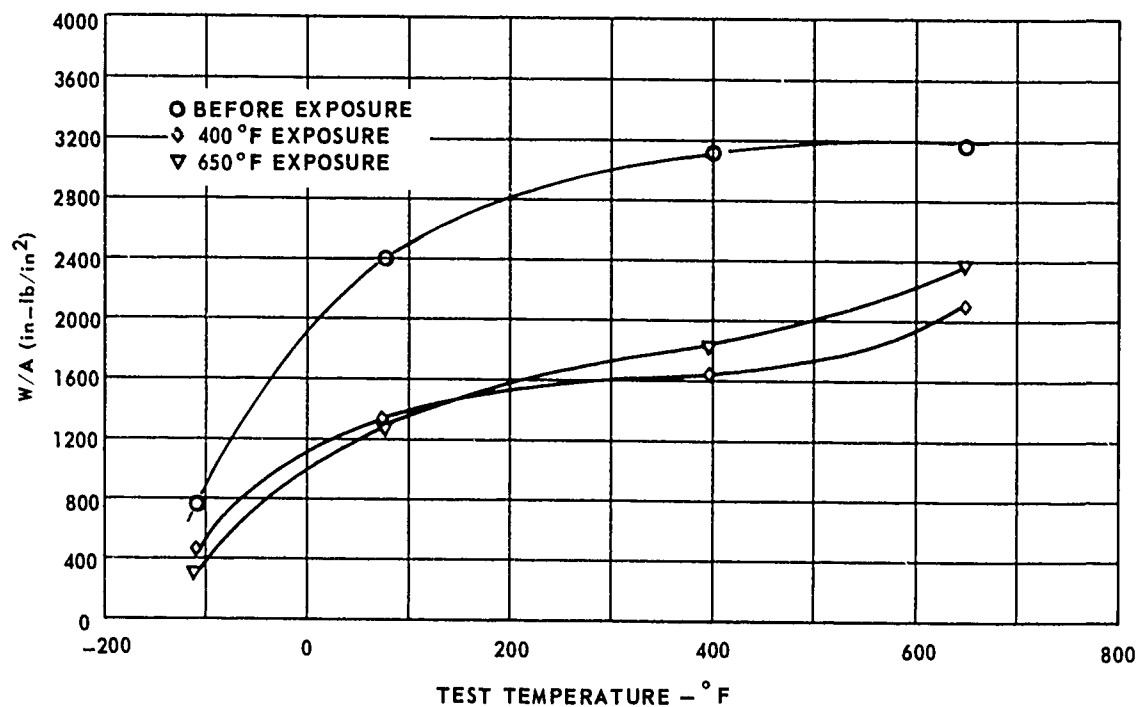
The manufacturer provided short-time tensile data on the three heats (Table 35). Tensile and exposure Charpy specimens were fabricated from the plate and heat treated. The 0.41 carbon heat (3920588) was given a 475°F bainitic heat treatment tempered at 750°F, similar to the initial heat, and the lower carbon heats were heat treated to the martensitic condition by oil quenching to room temperature and double tempering at 1000°F. The specimens were exposed to conditions similar to those used previously. The tensile and exposure data is presented in Table 36. The precracked Charpy impact values and ultimate tensile strengths for the three modified heats are shown in Figs. 145, 146, and 147. Heat 3888655 indicated the greatest precracked Charpy toughness and ultimate tensile strength of the three heats. In Fig. 148 the effect of exposure is compared for heat 3888655 and the original heat, 3950881. The 400°F, and 650°F exposure specimens had a lower toughness than the unexposed specimens, especially at high temperature. This indicates that even with increased chromium and molybdenum some instability still exists. It appears that with the martensitic microstructure, exposure does not decrease strength and increase toughness as it does with the bainitic structure. However, after exposure the -110°F and 650°F testing results in approximately the same toughness for both steels.

TABLE 35 MODIFIED 9Ni-4Co MECHANICAL PROPERTIES

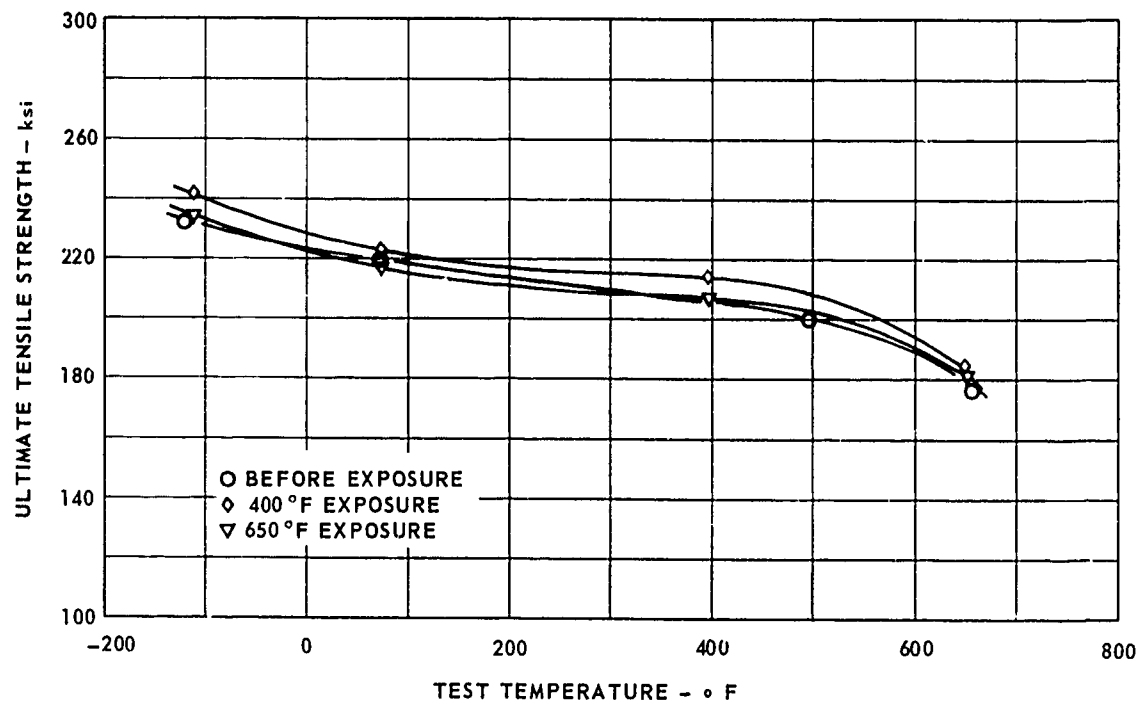
HEAT	GRAIN	TEST TEMP °F	ULTIMATE STRENGTH ksi	.2% YIELD STRENGTH ksi	ELONG. 1 inch percent	RA percent	PRECRACKED CHARPY W/A (in-lbs/in ²)
VENDOR DATA							
3920588	T	-110	235.2	234.5			791
	T	75	220.4	220.0	11	52	2403
	T	400		170.6			3135
	T	500	199.9	185.0	19	64	
	T	650	178.9	164.2	17	69	3166
3888655	T	-90	242.6	206.5			1264
	T	75	229.0	200.0	15	56	2136
	T	400	209.0	184.0			3314
	T	650	194.8	171.0			4110
3888655	T	75	226.0	201.0	15	56	
BOEING TEST DATA							
3888655	T	-110	238.7	213.6	15	59	1055
	T	-110	238.3	213.1	15	58	1090
	T	75	220.6	199.1	16	63	1585
	T	75	221.1	199.3	16	63	1633
	T	400	202.0	180.6	15	63	2182
	T	400	201.2	178.7	16	62	2140
	T	650	193.4	166.7	15	70	2486
	T	650	192.2	168.5	14	63	2454

TABLE 36 EXPOSURE DATA OF MODIFIED 9 Ni-4Co HEATS
(TRANSVERSE GRAIN DIRECTION)

EXPOSURE TEMP °f	EXPOSURE STRESS ksi	TEST TEMP °f	ULTIMATE STRENGTH ksi	.2% YIELD STRENGTH ksi	ELONG. 1 inch percent	RA percent	PRECRACKED CHARPY W A (in·lbs in ²)
HEAT 3920588							
400	40	-110	239.3	229.7	11	43	450
400	40	-110	242.7	231.0	13	43	441
400	40	RT	224.7	217.2	12	47	1430
400	40	RT	221.5	211.1	12	48	1250
400	40	400	213.9	187.3	14	50	1628
400	40	650	182.9	158.3	17	70	2096
650	40	-110	235.0	229.2	11	38	311
650	40	-110	233.4	229.7	11	44	312
650	40	RT	216.3	207.8	12	48	1419
650	40	RT	217.7	211.2	12	48	1186
650	40	400	205.7	189.1	14	42	1820
650	40	650	182.0	179.8	16	68	2360
HEAT 3888655							
400	40	-110	245.9	214.5	16	60	1202
400	40	-110	243.1	213.9	14	56	1071
400	40	RT	228.9	203.8	16	61	2021
400	40	RT	229.3	205.2	16	59	1929
400	40	400	208.1	185.4	16	63	2575
400	40	650	195.9	172.5	16	66	2974
650	40	-110	247.6	221.5	15	50	717
650	40	-110	246.7	220.5	14	55	802
650	40	RT	229.0	208.8	16	52	1713
650	40	RT	229.1	208.3	14	59	1752
650	40	400	209.8	191.8	15	60	25.71
650	40	650	197.1	179.8	16	65	2968
HEAT 3888656							
400	40	-110	242.3	210.2	14	49	1160
400	40	-110	241.3	210.4	15	51	1117
400	40	RT	225.0	199.1	14	57	1757
400	40	RT	223.4	199.7	15	57	1777
400	40	400	206.1	180.7	16	64	2205
400	40	650	193.8	171.7	16	66	2451
650	40	-110	245.3	220.8	15	56	844
650	40	-110	243.7	222.4	14	56	764
650	40	RT	225.4	204.9	14	59	1572
650	40	RT	224.8	205.1	15	53	1552
650	40	400	206.1	188.1	16	63	2211
650	40	650	196.7	175.5	15	65	2436

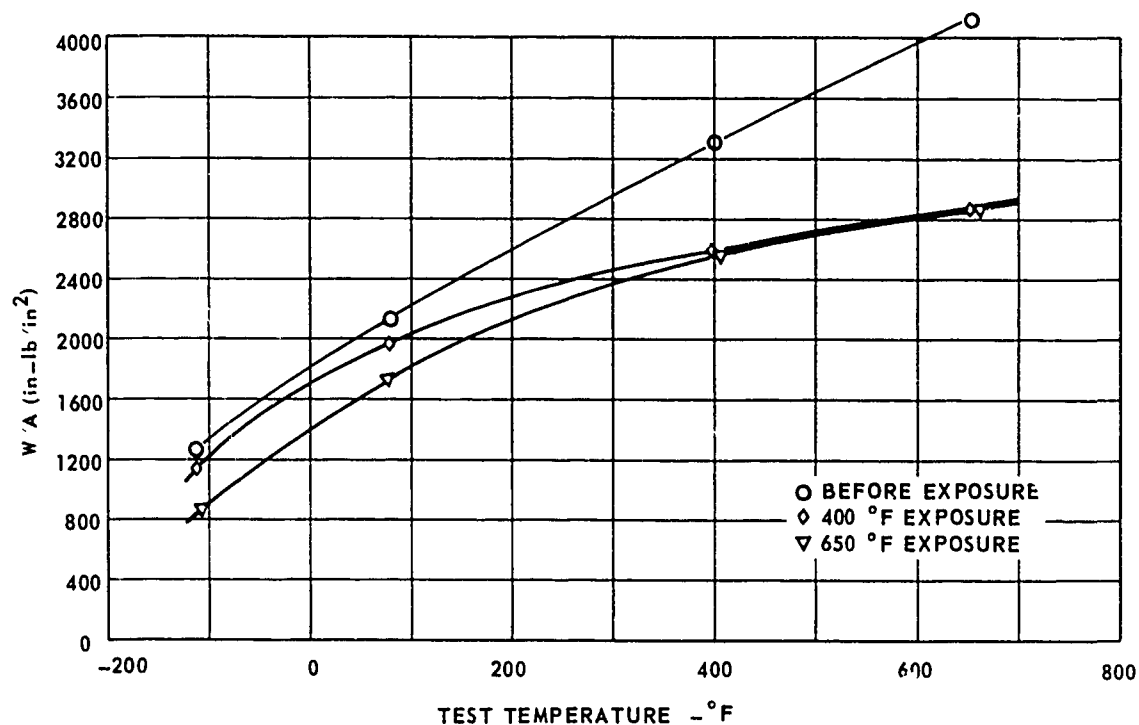


A. CHARPY TOUGHNESS PROPERTIES

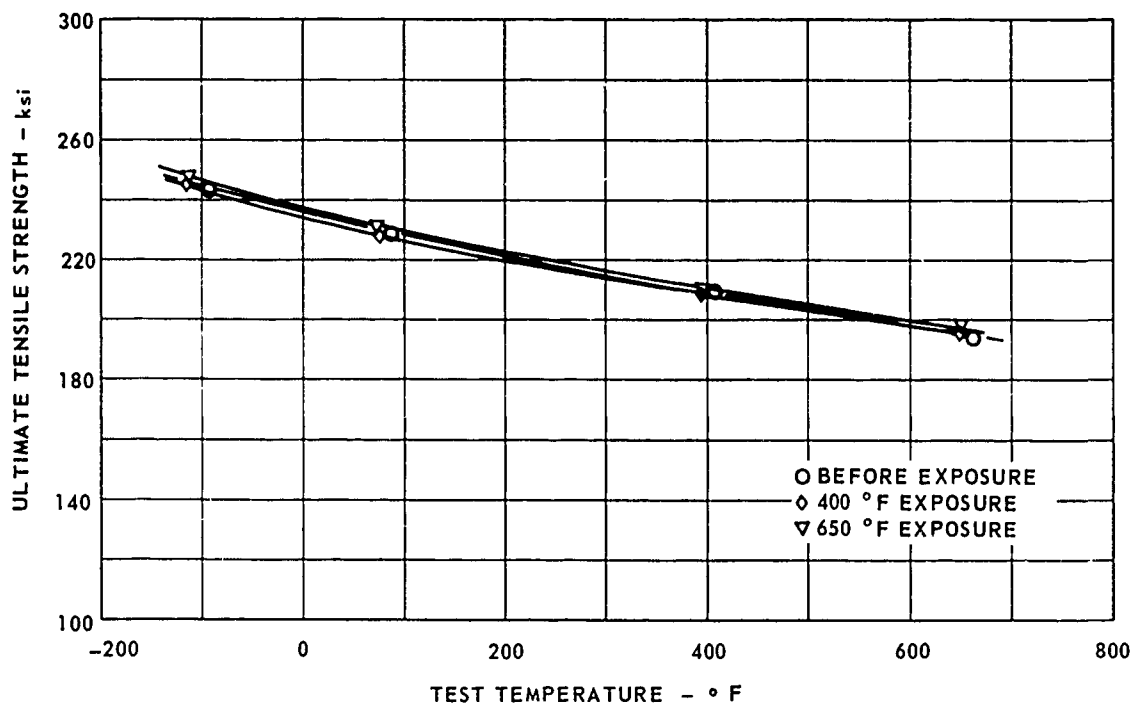


B. STRENGTH PROPERTIES

FIG. 145 EXPOSURE EFFECTS OF 1000 HOURS ON MODIFIED 9Ni-4Co FOR HEAT 588

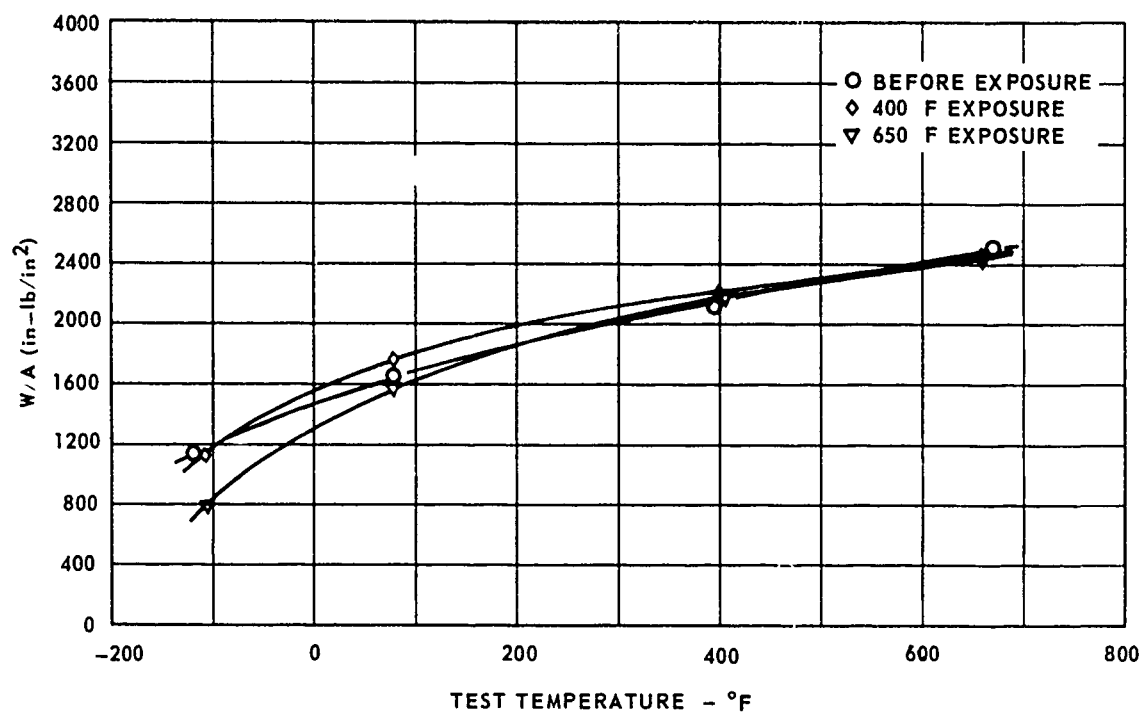


A. CHARPY TOUGHNESS PROPERTIES

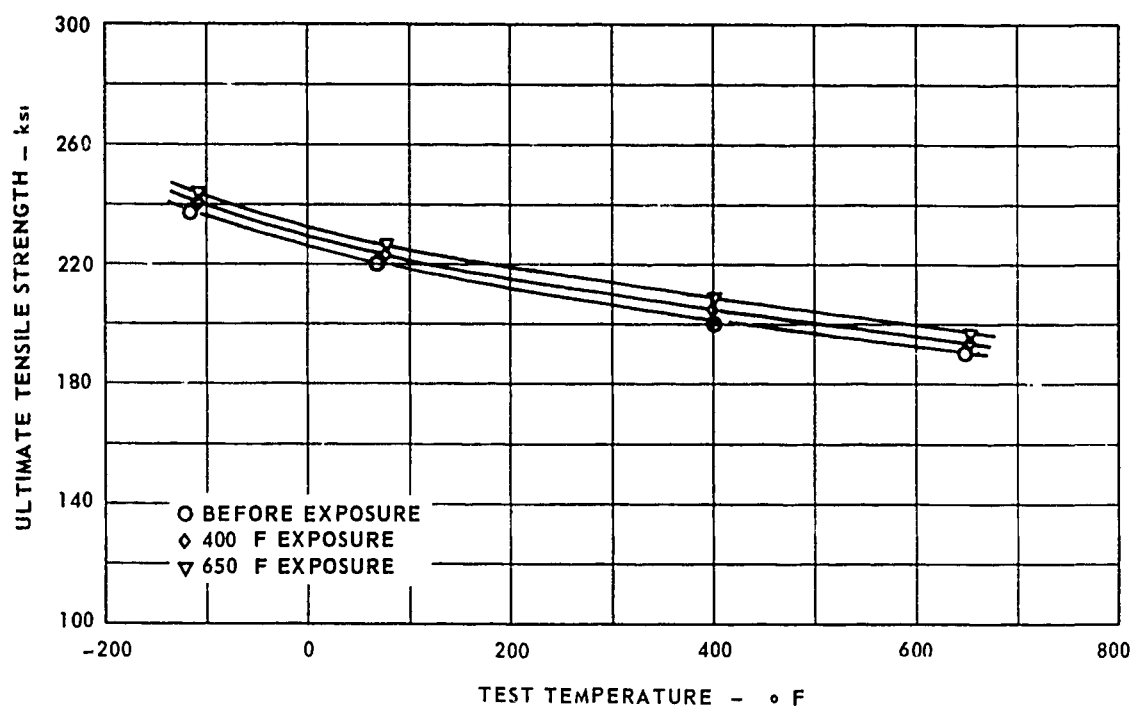


B. STRENGTH PROPERTIES

FIG. 146 EXPOSURE EFFECTS OF 1000 HOURS ON MODIFIED 9Ni-4Co FOR HEAT 655



A. CHARPY TOUGHNESS PROPERTIES



B. STRENGTH PROPERTIES

FIG. 147 EXPOSURE EFFECTS OF 1000 HOURS ON MODIFIED 9Ni-4Co FOR HEAT 656

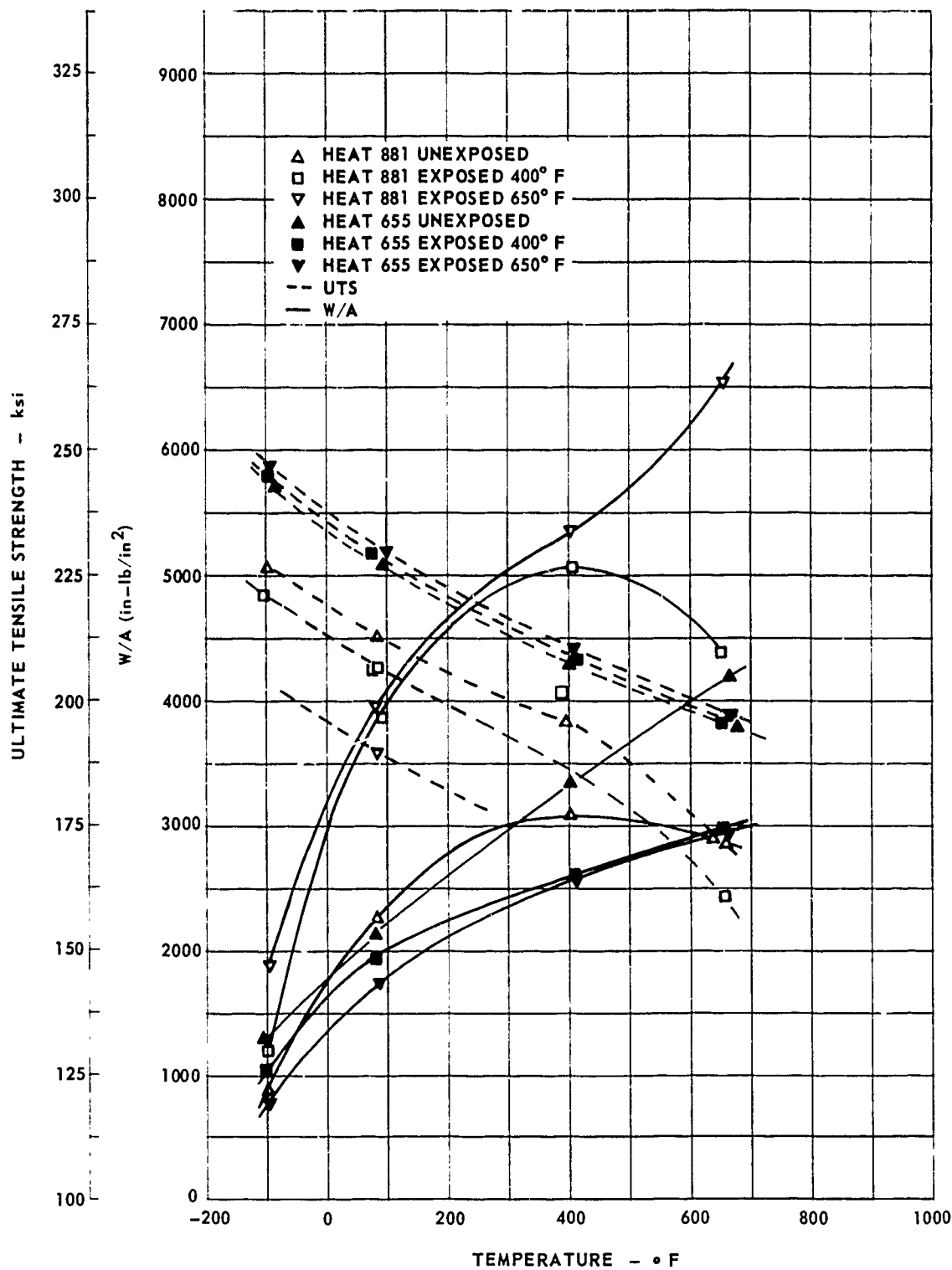


FIG. 148 9Ni-4Co EXPOSURE EFFECTS COMPARISON OF INITIAL HEAT 881 AND BEST MODIFIED HEAT 665

SECTION 11 SELECTION OF THE FOUR MOST PROMISING ALLOYS

In the first part of the program plane stress and plane-strain critical-stress intensities were determined for the eight alloys over the service temperature range of a supersonic transport. It was also desired to know how the other service conditions such as high strain rate, extended exposure to high temperature, and corrosive environment would affect these stress intensities. To keep the program to a reasonable size, further investigation was limited to the four alloys considered most promising for the supersonic transport. The same specimen design and grain direction was used for comparative purposes.

Round notched tensile specimens from the transverse grain direction were considered most practical. Transverse properties were generally minimum. Since transverse grain direction is usually considered the more sensitive to embrittling mechanisms such as stress corrosion, round notched specimens were required because they were the only specimens yielding transverse K_{1C} values.

The selection of four alloys for further study required several considerations other than toughness alone. The toughness-density ratios had to be considered because density would determine the stress level to which an alloy could be worked in designing. This means, with lower operating stresses, flaws could be larger before becoming critical. To aid in the comparison of the eight alloys, the K_C and K_{1C} data, and K_C and K_{1C} data divided by density are shown in Figs. 149 through 156. Curves for ultimate strength and ultimate strength divided by density are also included (Figs. 157 and 158). In addition a summary chart of the four toughest alloys for each specimen type at each temperature is shown in Table 36.

The titanium alloys in particular are enhanced by consideration of density as demonstrated by the comparison curves of Figs. 150, 152, 154, and 156. The summary chart (Table 37) indicates that both Ti 6Al-4V and Ti 6Al-6V-2Sn annealed were among the four toughest alloys. Ti 6Al-4V had the higher strength and more production experience so it was selected for further study.

Inco 718 had exceptionally high toughness, especially at low temperatures. Although it had a rather low yield strength, its toughness-to-density ratio was still among the top four. The design requirements for the supersonic transport will be most critical at the low temperatures; therefore Inco 718 was also selected.

Both stainless steels had excellent toughness at higher temperatures, especially in the longitudinal grain directions. However, they both displayed poor toughness at -110°F which, as mentioned before, will be a critical temperature.

The 9 Ni-4Co displayed excellent toughness throughout the temperature range. However, precracked Charpy stability testing revealed a serious problem. Because there will be applications for forgings on the supersonic transport which will not be subjected to very high temperatures, and because it appeared that a change in alloying elements could overcome the instability, this alloy was selected.

Maraging 250 proved to be among the four toughest alloys in the center notch specimens with a drop to fifth in the round notched specimens. It was selected for further study because it also had the highest strength of any of the alloys.

In summary, the 9Ni-4Co, Maraging 250, Inco 718 and Ti 6Al-4V were selected for further study. Actually five alloys rather than four alloys appeared promising, the fifth alloy being Ti 6Al-2V-Sn in the annealed condition.

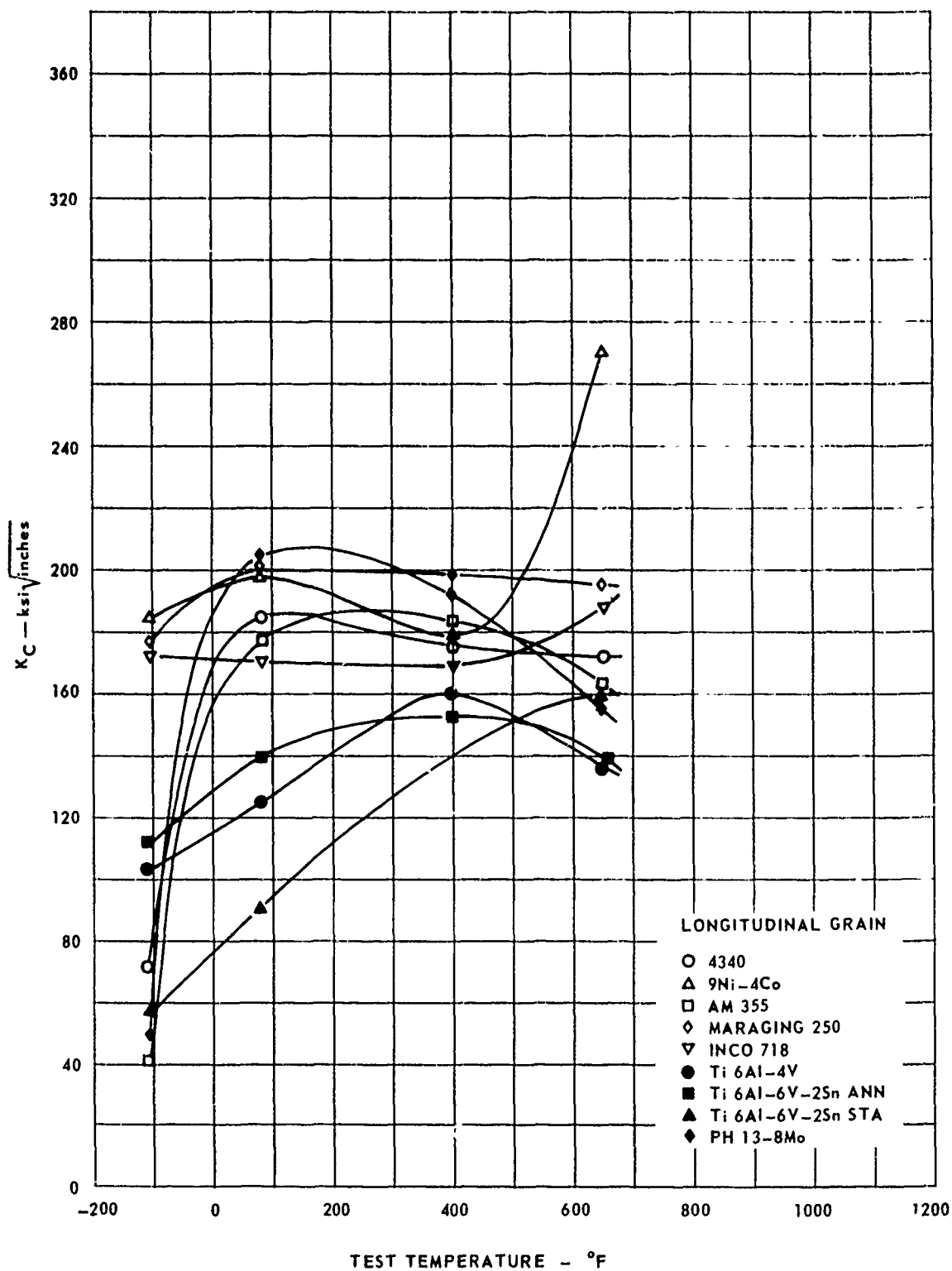


FIG. 149 3/16 INCH THICK PLATE K_{IC} COMPARISON

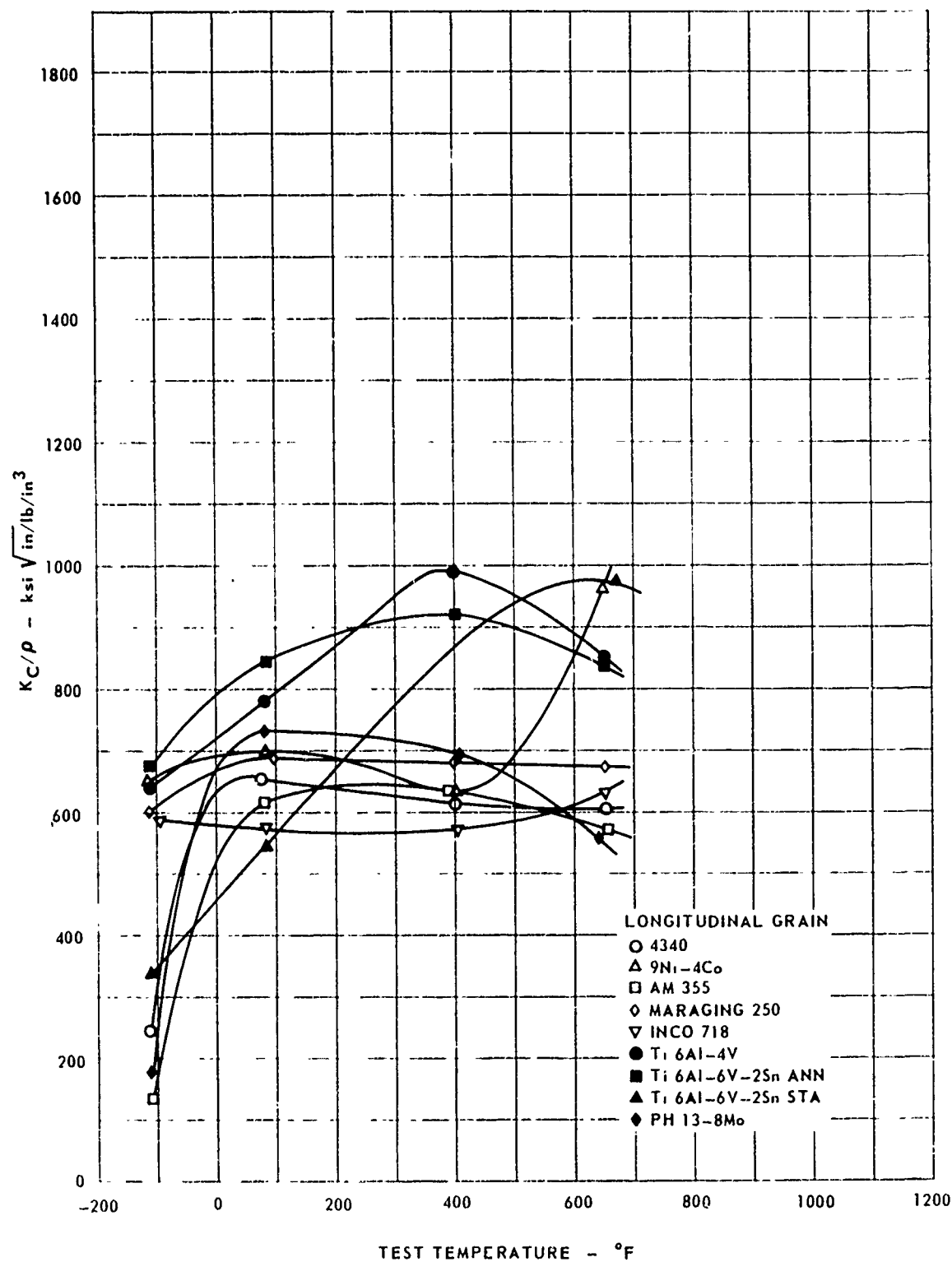


FIG. 150 3/16 INCH THICK PLATE K_C -DENSITY RATIO COMPARISON

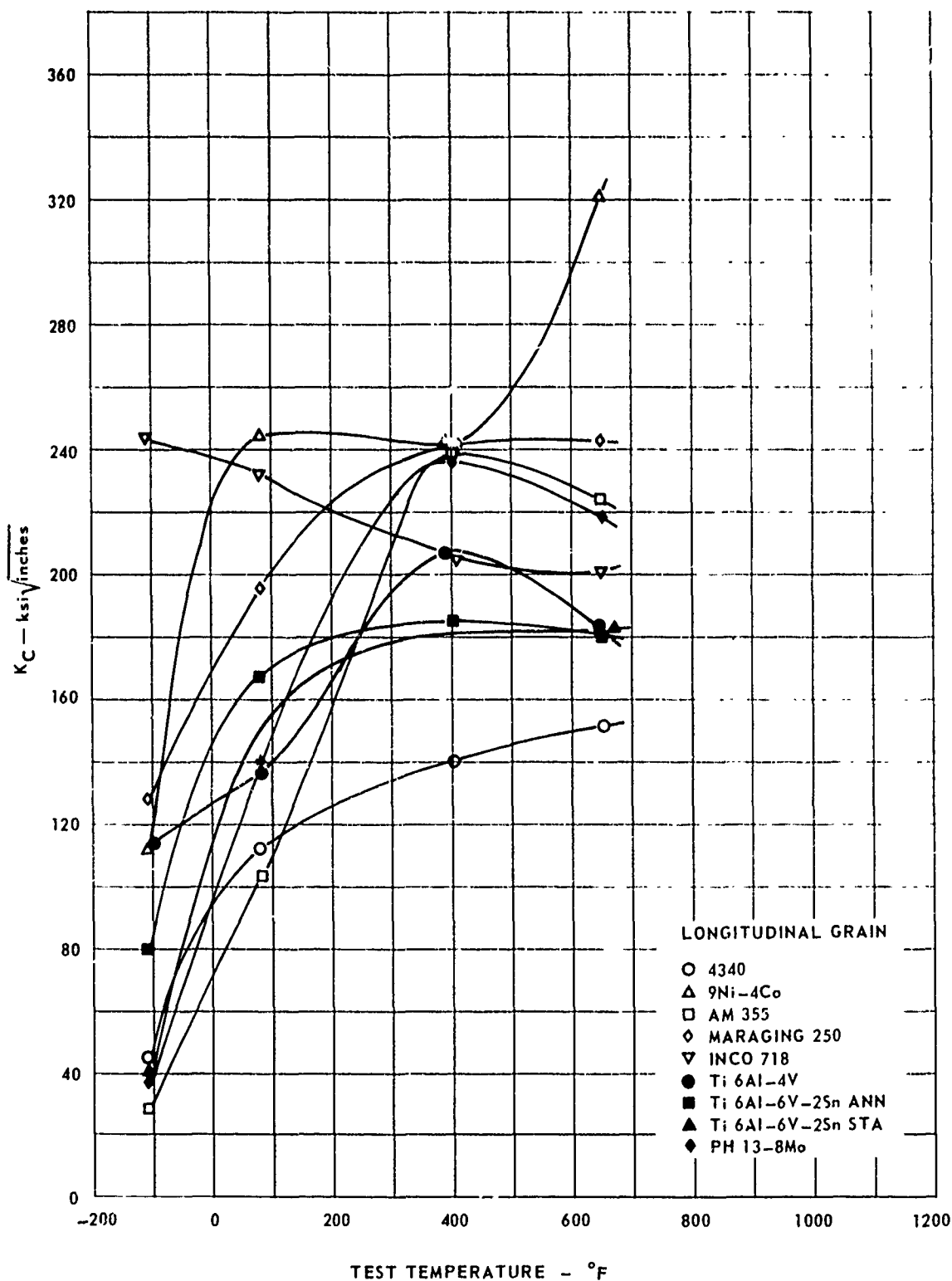


FIG. 151 3/8 INCH THICK PLATE K_{IC} COMPARISON

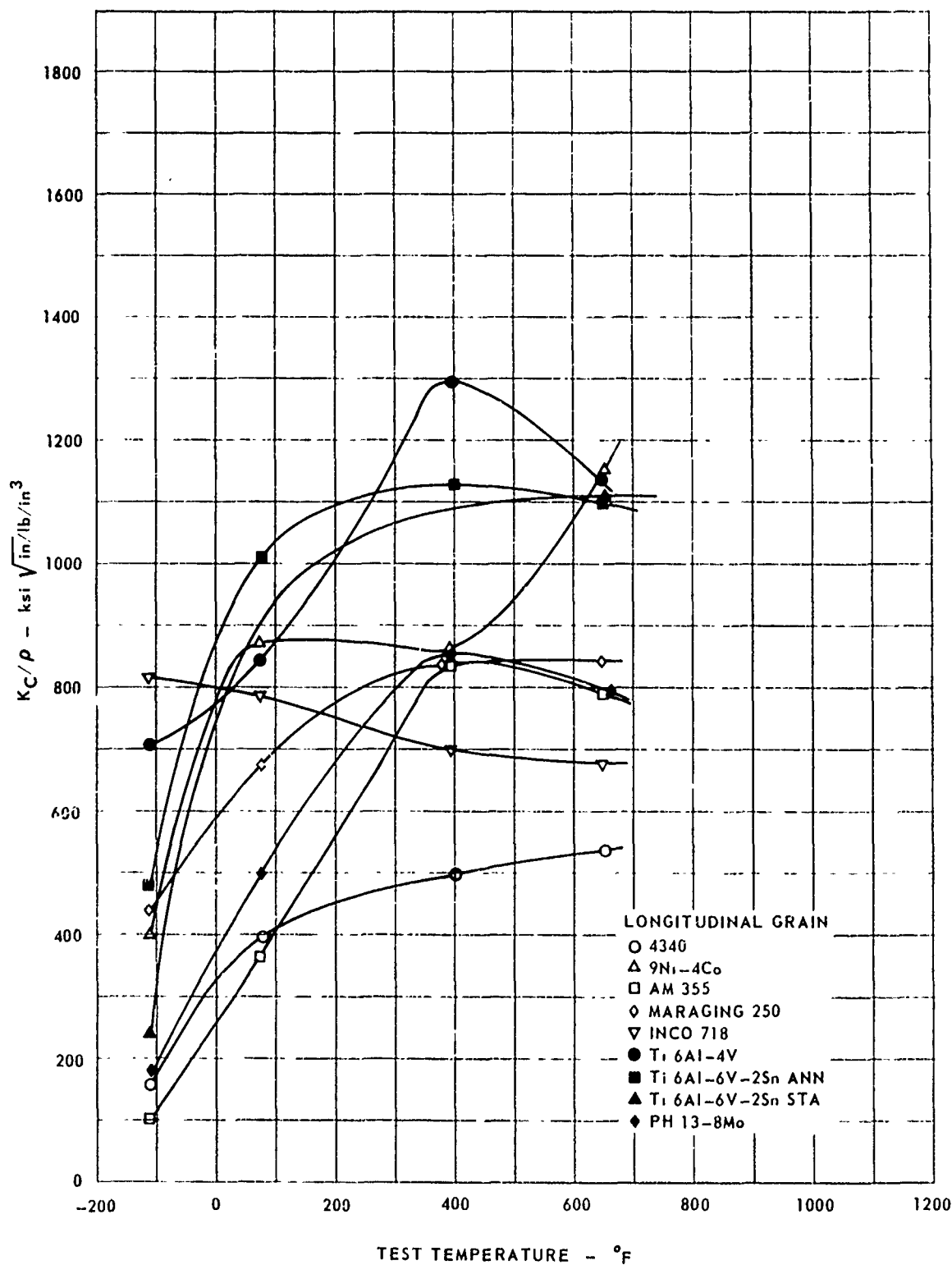


FIG. 152 3/8 INCH THICK PLATE K_{IC} -DENSITY RATIO COMPARISON

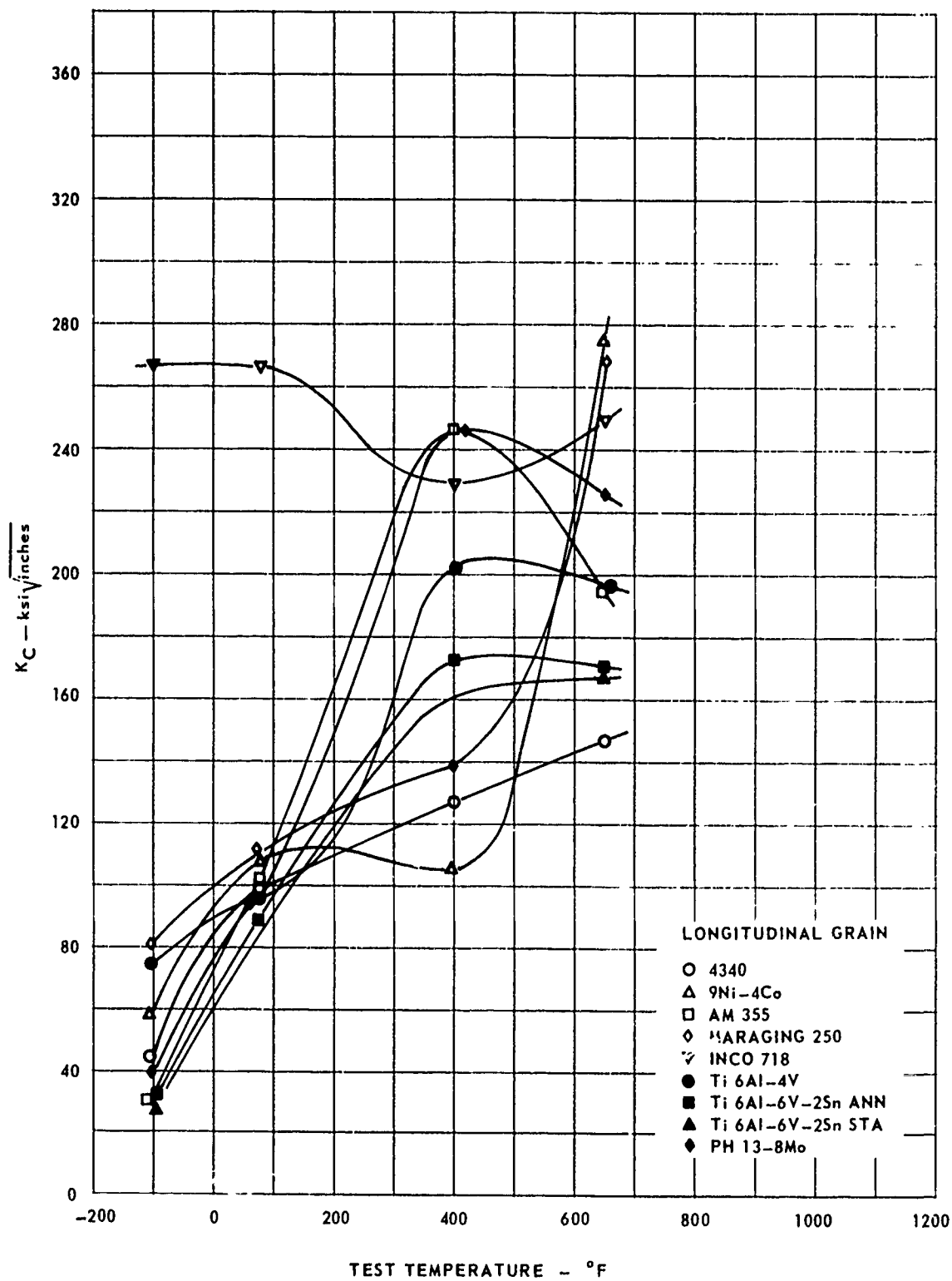


FIG. 153 1 INCH THICK PLATE K_{IC} COMPARISON

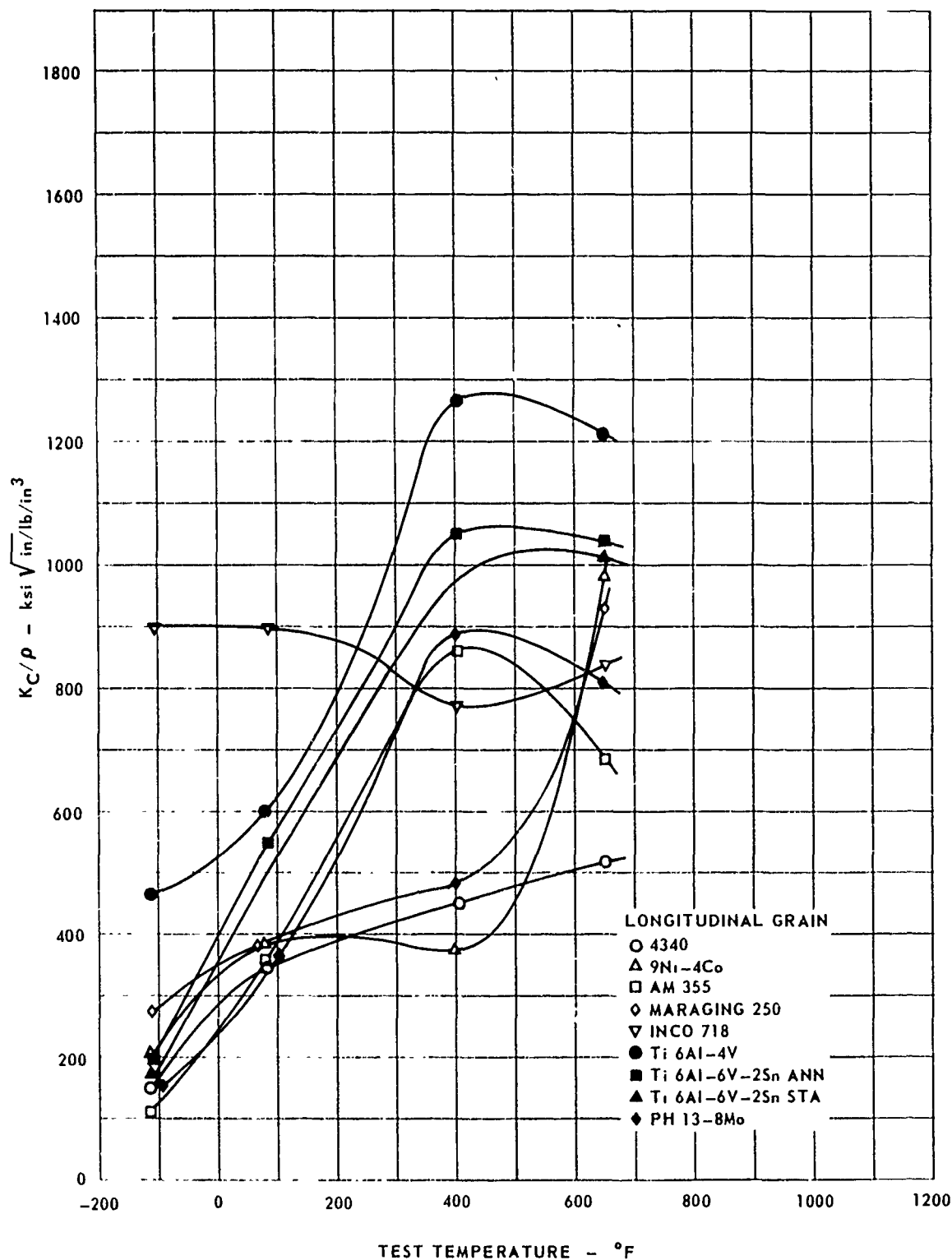


FIG. 154 1 INCH THICK PLATE K_C -DENSITY RATIO COMPARISON

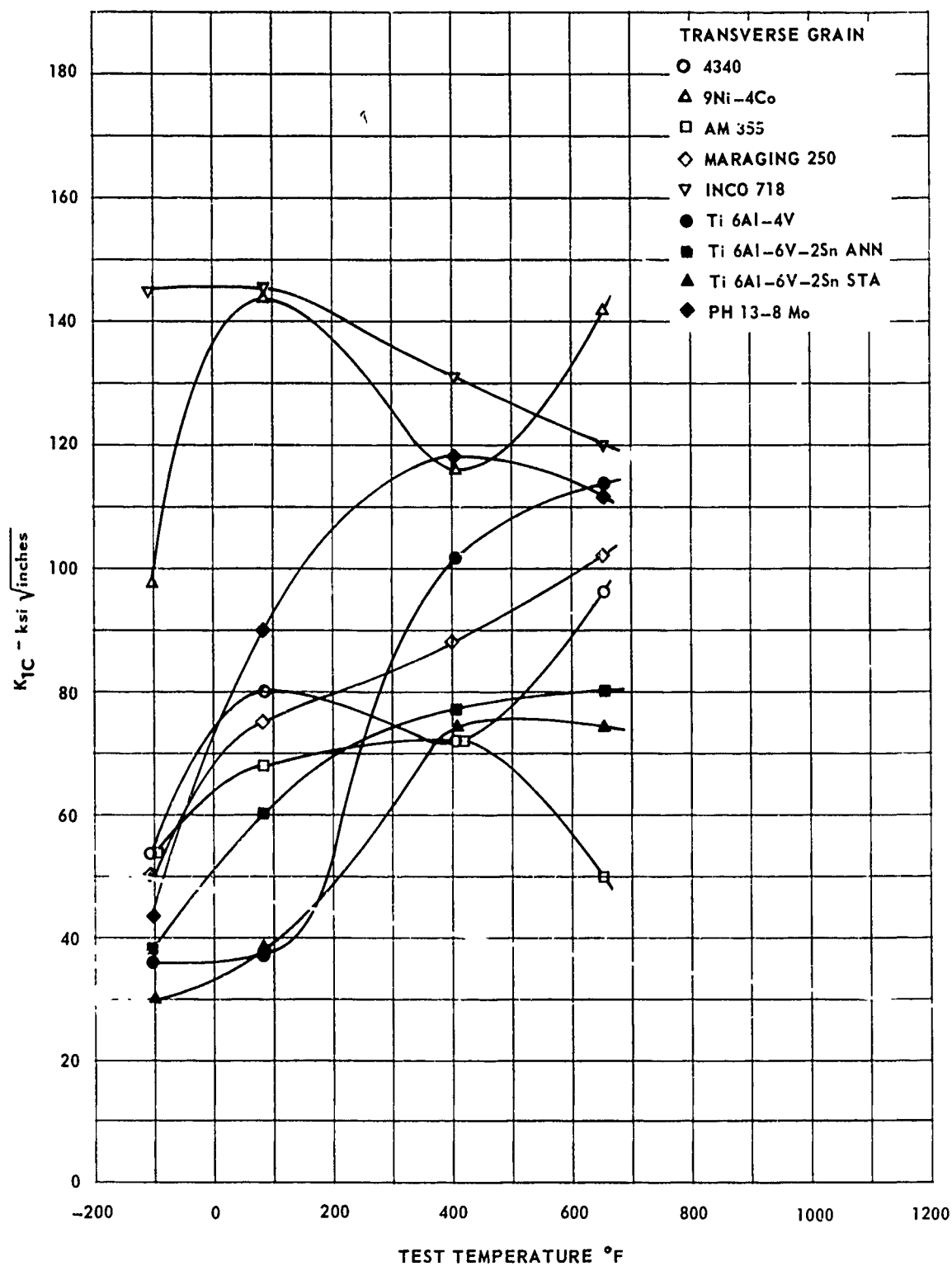


FIG. 155 ROUND NOTCH TENSILE K_{IC} COMPARISON

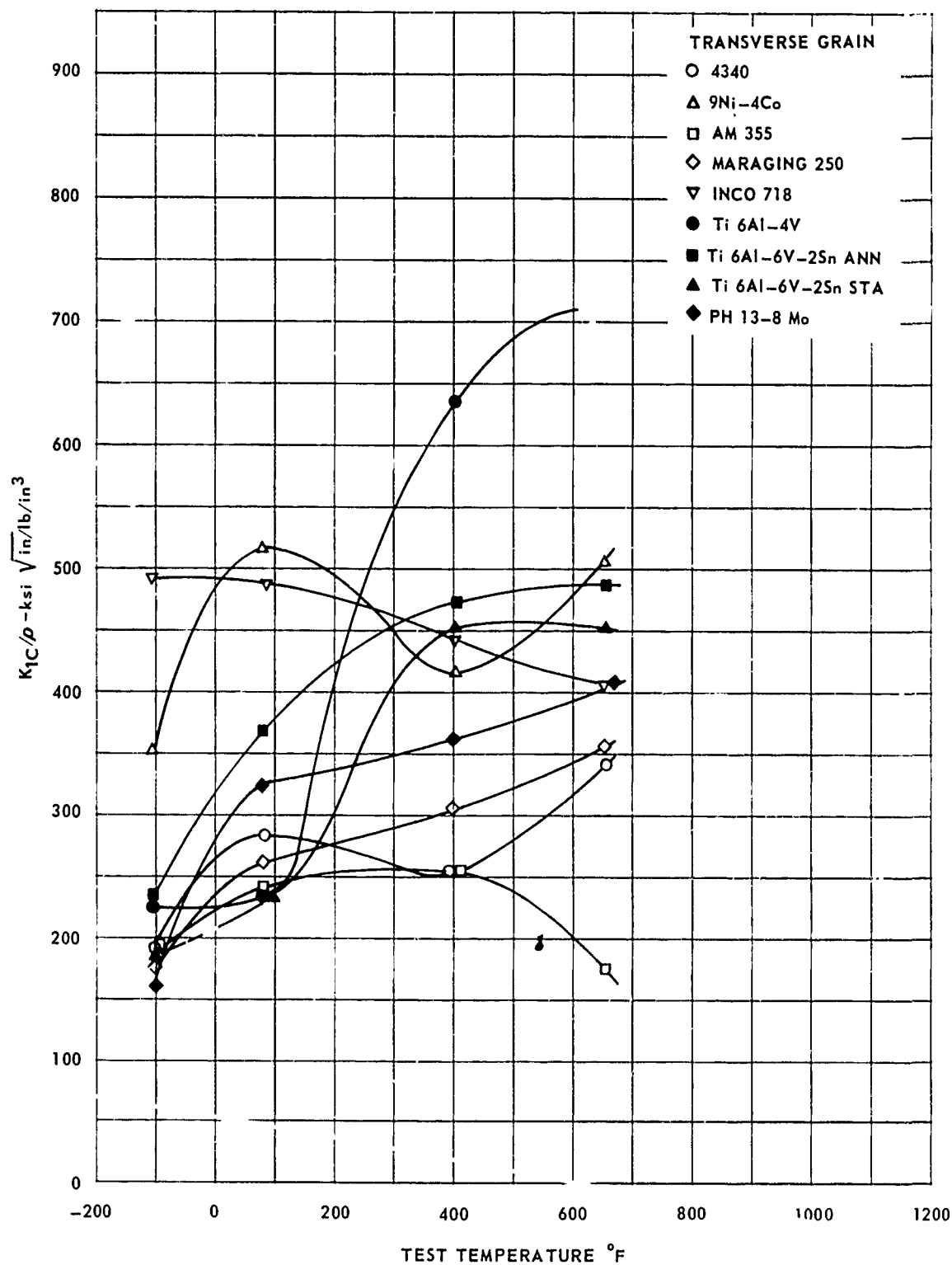


FIG. 156 ROUND NOTCH TENSILE K_{1C} - DENSITY RATIO COMPARISON

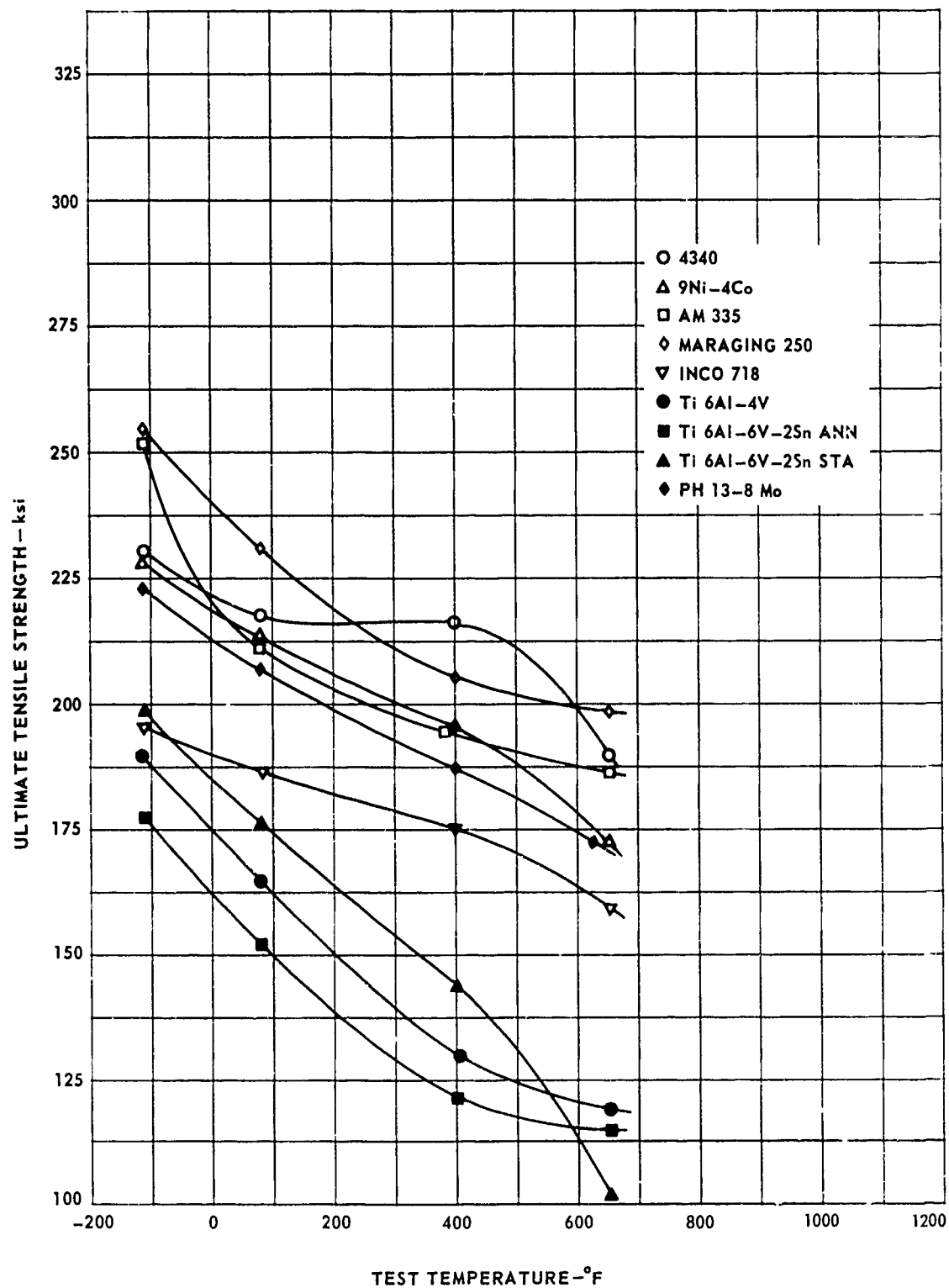


FIG. 15/ ULTIMATE STRENGTH COMPARISON

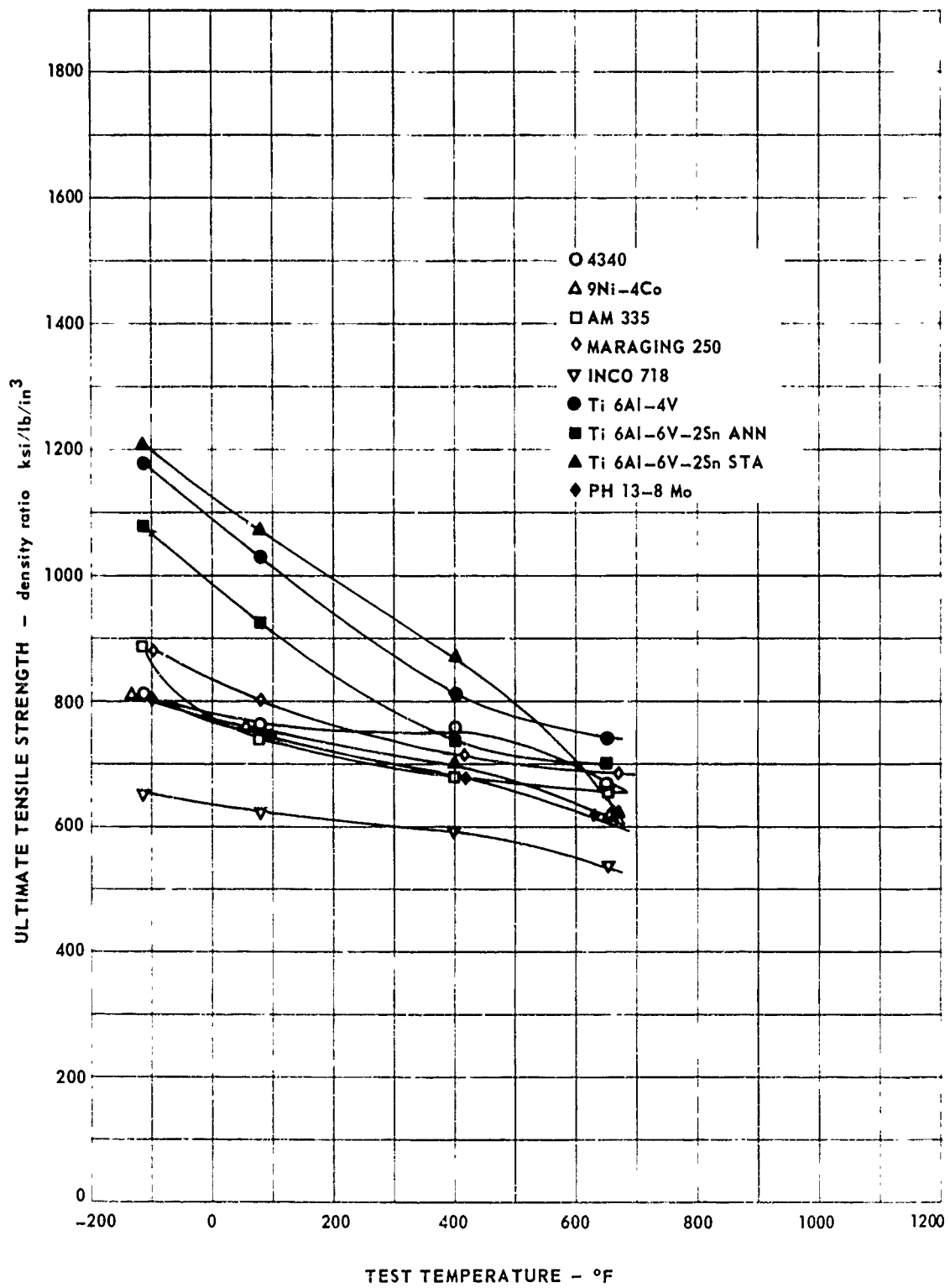


FIG. 158 STRENGTH - DENSITY RATIO COMPARISON

TABLE 37 ALLOY RATING CHART BY TOUGHNESS AND TOUGHNESS DENSITY RATIO

(A) RATED BY TOUGHNESS, K_{IC} AND K_{IC}/ρ AT VARIOUS TEST TEMPERATURES*

SPECIMEN TYPE	TOP FOUR ALLOYS RATINGS	TEST TEMP.			
		-110	RT	400	650
3/16 INCH THICK PANELS	1	9 Ni-4Co	PH 13-8 Mo	MARAGING 250	9 Ni-4Co
	2	MARAGING 250	MARAGING 250	PH 13-8 Mo	MARAGING 250
	3	INCO 718	9 Ni-4Co	AM 355	INCO 718
	4	Ti 6Al-6V-2Sn ANN	4340	9 Ni-4Co	4340
3/8 INCH THICK PANELS	1	INCO 718	9 Ni-4Co	9 Ni-4Co	9 Ni-4Co
	2	MARAGING 250	INCO 718	MARAGING 250	MARAGING 250
	3	Ti 6Al-4V	MARAGING 250	AM 355	AM 355
	4	9 Ni-4Co	Ti 6Al-6V-2Sn ANN	PH 13-8 Mo	PH 13-8 Mo
1 INCH THICK PANELS	1	INCO 718	INCO 718	AM 355	9 Ni-4Co
	2	MARAGING 250	MARAGING 250	PH 13-8 Mo	MARAGING 250
	3	Ti 6Al-4V	9 Ni-4Co	INCO 718	INCO 718
	4	9 Ni-4Co	4340	Ti 6Al-4V	PH 13-8 Mo
ROUND NOTCH SPECIMENS	1	INCO 718	INCO 718	INCO 718	9 Ni-4Co
	2	9 Ni-4Co	9 Ni-4Co	PH 13-8 Mo	INCO 718
	3	4340	PH 13-8 Mo	9 Ni-4Co	Ti 6Al-4V
	4	AM 355	4340	Ti 6Al-4V	PH 13-8 Mo

(B) RATED BY TOUGHNESS-DENSITY RATIOS, K_{IC}/ρ AND K_{IC}/ρ AT VARIOUS TEST TEMPERATURES*

SPECIMEN TYPE	TOP FOUR ALLOYS RATINGS	TEST TEMP.			
		-110	RT	400	650
3/16 INCH THICK PANELS	1	Ti 6Al-6V-2Sn ANN	Ti 6Al-6V-2Sn ANN	Ti 6Al-4V	Ti 6Al-6V-2Sn STA
	2	9 Ni-4Co	Ti 6Al-4V	Ti 6Al-6V-2Sn ANN	9 Ni-4Co
	3	Ti 6Al-4V	PH 13-8 Mo	PH 13-8 Mo	Ti 6Al-4V
	4	MARAGING 250	9 Ni-4Co	MARAGING 250	Ti 6Al-6V-2Sn ANN
3/8 INCH THICK PANELS	1	INCO 718	Ti 6Al-6V-2Sn ANN	Ti 6Al-4V	9 Ni-4Co
	2	Ti 6Al-4V	9 Ni-4Co	Ti 6Al-6V-2Sn ANN	Ti 6Al-4V
	3	Ti 6Al-6V-2Sn ANN	Ti 6Al-4V	9 Ni-4Co	Ti 6Al-6V-2Sn STA
	4	MARAGING 250	INCO 718	AM 355	Ti 6Al-6V-2Sn ANN
1 INCH THICK PANELS	1	INCO 718	INCO 718	Ti 6Al-4V	Ti 6Al-4V
	2	Ti 6Al-4V	Ti 6Al-4V	Ti 6Al-6V-2Sn ANN	Ti 6Al-6V-2Sn ANN
	3	MARAGING 250	Ti 6Al-6V-2Sn ANN	PH 13-8 Mo	Ti 6Al-6V-2Sn STA
	4	9 Ni-4Co	9 Ni-4Co	AM 355	9 Ni-4Co
ROUND NOTCH SPECIMENS	1	INCO 718	9 Ni-4Co	Ti 6Al-4V	Ti 6Al-4V
	2	9 Ni-4Co	INCO 718	Ti 6Al-6V-2Sn ANN	9 Ni-4Co
	3	Ti 6Al-6V-2Sn ANN	Ti 6Al-6V-2Sn ANN	Ti 6Al-6V-2Sn STA	Ti 6Al-6V-2Sn ANN
	4	Ti 6Al-4V	PH 13-8 Mo	INCO 718	Ti 6Al-6V-2Sn STA

* AVERAGE OF TEST VALUES

SECTION 12 ROUND NOTCHED SPECIMEN EXPOSURE TESTING

In Section 10 the preliminary evaluation was made on all eight alloys by means of precracked Charpy specimens. Although these specimens are very sensitive to variations in the metallurgical structure of an alloy, the resulting data are not valid plane-strain critical-stress intensities. Therefore, a second exposure test was run on the four most promising alloys using the 1-1/8 inch round notched tensile specimens. The transverse direction of the forged blocks was investigated to ensure that minimum properties would be obtained. Exposed specimens could then be compared with the transverse round notched specimens from Section 8. Exposure conditions for the notched rounds were only those which the precracked Charpy data indicated as most severe. This was generally 1000 hours at 650°F under stress.

The exposure test procedure was outlined in Section 10. Fabrication, fatigue cracking and fracture testing were similar to those used on specimens in Section 8 so that the only variable would be metallurgical stability.

Material for tensile specimens was exposed under the same conditions to determine if tensile properties were affected to the same extent as fracture properties. After exposure, the material was fabricated into tensile specimens identical to those in the heat treat study (Section 6).

RESULTS AND DISCUSSION

Exposure data for the notched round specimens are listed in Table 38 and were plotted against fracture test temperature in Figs. 159 through 162. Transverse round notched specimen data curves from Section 8 are included in the figures for a before and after exposure comparison. Ultimate tensile strengths from exposed smooth tensile specimens on Table 39 are also shown on Figs. 159 through 162 in order to illustrate how tensile strength changes affect fracture toughness changes. The results on each alloy are discussed separately.

9 Ni-4Co

Precracked Charpy specimen data (Figure 137) for this alloy indicated a large change after 1000 hours exposure at both 400 and 650°F; It was considered that although the stability of 9 Ni-4Co should be further investigated because of its high toughness, 650°F exposure service was probably not realistic for this alloy. It was, therefore, decided to determine the extent of instability at 400°F under a stress of 40 ksi.

The effect of these exposure conditions on both the plane strain fracture toughness and tensile strength properties is shown in Figure 159. The increase in toughness which was so evident when testing precracked Charpy specimens has disappeared in the round notched specimen data. Only in room temperature K_{IC} values was the increase found. Both the exposed and unexposed specimen tests resulted in high net stress to yield strength ratios except at -110°F. The relative toughness of the exposed and unexposed specimens varied very little over the range of test temperatures. Tensile properties plotted in Fig. 159 show a very slight decrease after exposure which is within the extent of scatter. The slight change

in ultimate tensile strength also indicates the alloy is more stable than the pre-cracked Charpy values revealed.

MARAGING 250

This alloy showed a slight increase in ultimate tensile strength with a significant decrease in K_{1C} values (Fig. 160) after exposure at 650° F under 40 ksi stress. In this case testing of the precracked Charpy specimen did predict the loss of toughness (Fig. 139).

INCO 718

The precracked Charpy exposure curves for this alloy showed considerable scatter with the stressed exposure specimens indicating an increase in toughness and the unstressed exposure indicating a decrease. As stated previously, a higher solution-annealing temperature was used on this alloy in an attempt to take all the precipitates into solution. The electron fractographs (Fig. 93) showed large indications of second phase. It was felt that this accounted for the scatter in impact. The K_{1C} values from the exposed round notched specimen (Fig. 161) show the same type of scatter. Both the toughness and strength exposure properties show a small increase at some test temperatures but not at others. Therefore, the increase in fracture toughness is not considered significant.

Ti 6Al-4V

A small increase in K_{1C} values from round notched specimens exposed at 650° F is seen mainly during higher temperature testing (Fig. 162). These results are consistent with precracked Charpy testing. There appears to be no change in tensile properties during exposure.

TABLE 38 EXPOSURE ROUND NOTCH TENSILE DATA

SPECIMEN NO.	TEST TEMP. °F	EXP. TEMP. °F	EXP. STRESS ksi	MAJOR DIAMETER inches	NOTCH DIAMETER inches	NET DIAMETER inches	MAXIMUM LOAD kips	NET AREA in ²	σ_N ksi	K_{1C} ksi $\sqrt{\text{in}}$	YIELD STRENGTH .2% OFFSET ksi	$\frac{\sigma_N}{\sigma_{ys}}$
9 NI-4Co												
CB 136	-110	400	40	1.124	.850	.802	108.3	.643	215.0	94.0	218.5	.98
CB 137	-110	400	40	1.125	.849	.803	109.8	.645	217.0	94.8	218.5	.99
CB 138	RT	400	40	1.121	.836	.800	122.3	.640	244.0	106.8	203.1	1.20*
CB 139	400	400	40	1.122	.849	.807	94.0	.651	183.6	80.2	163.5	1.12*
CB 140	650	400	40	1.119	.836	.758	123.5	.575	274.0	119.8	148.0	1.85*
CB 141	650	400	40	1.120	.844	.776	125.3	.602	266.0	116.3	148.0	
MARAGING 250												
CD 136	-110	650	40	1.125	.851	.801	66.5	.641	132.1	57.9	244.5	1.80*
CD 137	-110	650	40	1.123	.853	.743	58.0	.552	134.0	58.7	244.5	.55
CD 138	RT	650	40	1.123	.853	.761	67.1	.579	148.0	64.8	224.9	.66
CD 139	400	650	40	1.120	.847	.765	85.0	.585	185.5	81.1	206.5	.90
CD 140	650	650	40	1.119	.852	.764	91.3	.584	199.3	87.2	187.0	1.06
CD 141	650	650	40	1.121	.848	.760	77.8	.577	172.0	75.3	187.0	.92
INCO 718												
CE 136	-110	650	40	1.120	.849	.725	105.5	.525	256.0	112.0	170.2	1.50*
CE 137	-110	650	40	1.121	.847	.699	95.3	.489	248.2	108.5	170.2	1.46*
CE 138	RT	650	40	1.121	.848	.680	82.0	.463	226.0	98.9	159.1	1.42*
CE 139	400	650	40	1.120	.844	.755	102.0	.670	228.0	99.7	146.8	1.55*
CE 140	650	650	40	1.121	.849	.773	96.0	.598	204.5	89.5	145.1	1.41*
CE 141	RT	650	40	1.123	.853	.583	36.8**	.340	137.5	60.2**	159.1	.86
Ti 6Al-4V												
CF 136	-110	650	25	1.122	.851	.803	40.3	.645	79.7	34.8	178.6	.45
CF 137	-110	650	25	1.121	.850	.802	35.6	.643	70.6	30.9	178.6	.40
CF 138	RT	650	25	1.122	.855	.807	47.5	.651	93.0	40.7	152.9	.61
CF 139	400	650	25	1.119	.848	.690	65.3	.476	174.5	76.4	111.2	1.57*
CF 140	650	650	25	1.112	.840	.778	78.0	.605	164.4	71.6	94.0	1.75*
CF 141	RT	650	25	1.123	.853	.665	21.6**	.442	62.3	27.2*	152.9	.41

** FAILED DURING FATIGUE CRACKING FRACTURE TEST LOAD RATE WAS 150 ksi/min TRANSVERSE GRAIN DIRECTION

* THESE RATIOS ARE ABOVE THE 1.1 LIMIT RECOMMENDED BY

FATIGUE DATA:

THE ASTM COMMITTEE ON FRACTURE TOUGHNESS

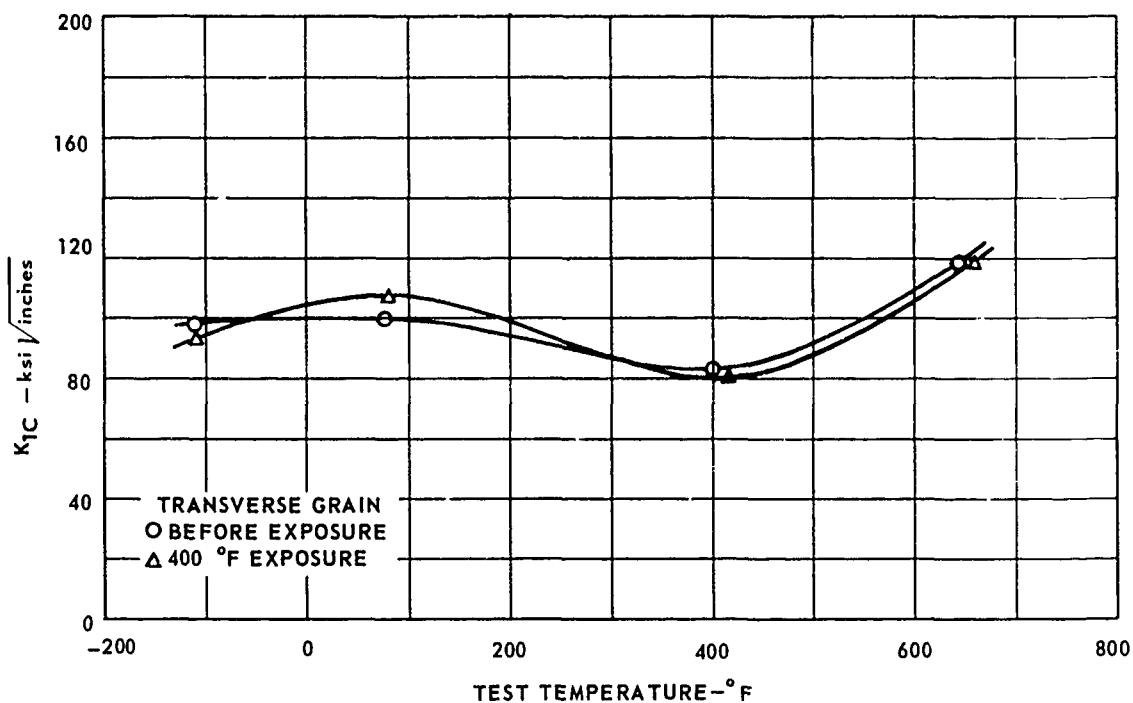
MAX CYCLING STRESS .33 YIELD STRENGTH

R = .05

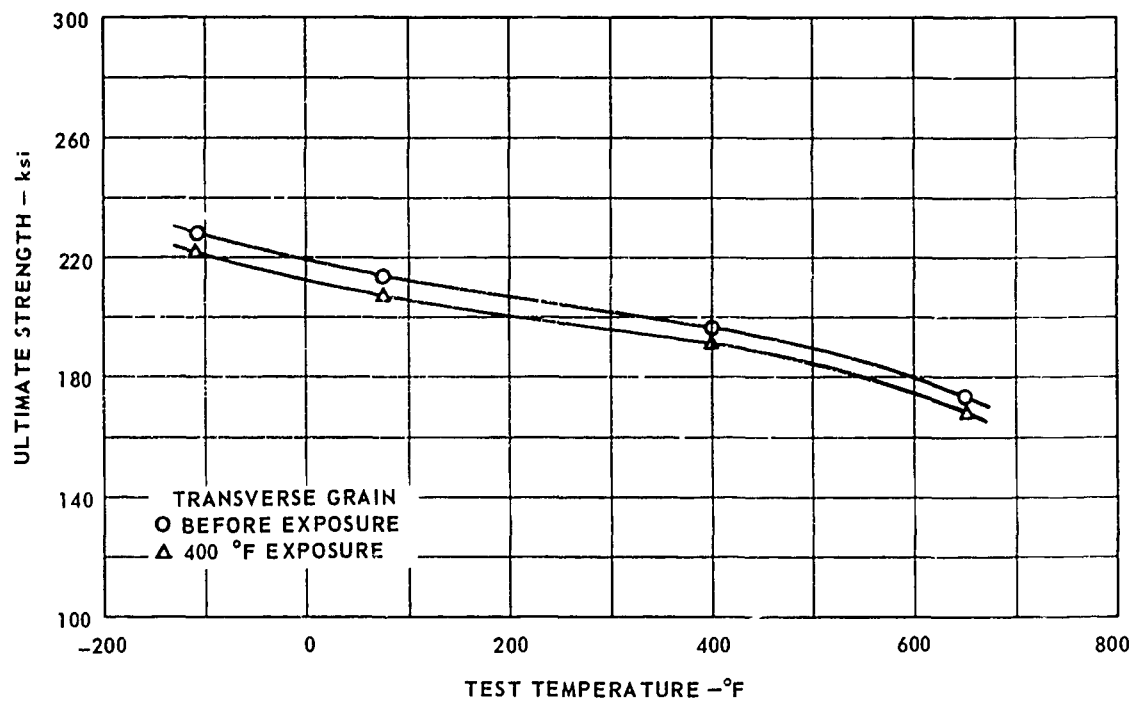
CYCLING RATE 120 TO 600 CPM

TABLE 39 EXPOSURE TENSILE DATA

ALLOY	EXPOSURE TEMP °f	EXPOSURE STRESS ksi	TEST TEMP °f	ULTIMATE STRENGTH ksi	.2% YIELD STRENGTH ksi	ELONG 1 inch percent	R.A. percent
9Ni-4Co	400	40	RT	207.4	203.2	15	59
	400	40	RT	207.0	203.0	15	60
	400	40	RT	206.1	203.0	15	60
	650	40	RT	189.3	182.9	17	61
	650	40	RT	188.3	183.9	16	60
	650	40	RT	188.6	184.3	17	61
	400	40	-110	220.4	213.3	14	58
	400	40	-110	220.4	214.7	15	59
	400	40	RT	205.3	198.7	14	59
	400	40	RT	204.1		14	60
	400	40	400	203.6	175.1	19	69
	400	40	400	203.7	173.8	18	68
	400	40	650	159.0	140.5	21	83
	400	40	650	162.0	139.7	21	82
MARAGING 250	650	40	-110	256.4	244.5	9	36
	650	40	-110	255.8		10	38
	650	40	RT	235.1	224.9	10	39
	650	40	400	217.1	206.5	11	44
	650	40	650	201.0	187.6	11	48
	650	40	650	203.2	186.3	11	48
INCO 718	650	40	-110	199.1	170.9	16	26
	650	40	-110	208.1	169.4	20	24
	650	40	RT	186.5	159.1	15	23
	650	40	400	173.0	146.8	11	15
	650	40	650	167.4	145.4	17	26
	650	40	650	167.7	144.8	16	24
Ti6Al-4V	650	25	-110	190.2	178.1	12	35
	650	25	-110	190.1	179.0	10	33
	650	25	RT	165.7	152.9	13	47
	650	25	400	131.3	111.2	17	63
	650	25	650	117.3	93.4	16	62
	650	25	650	117.1	94.5	16	66

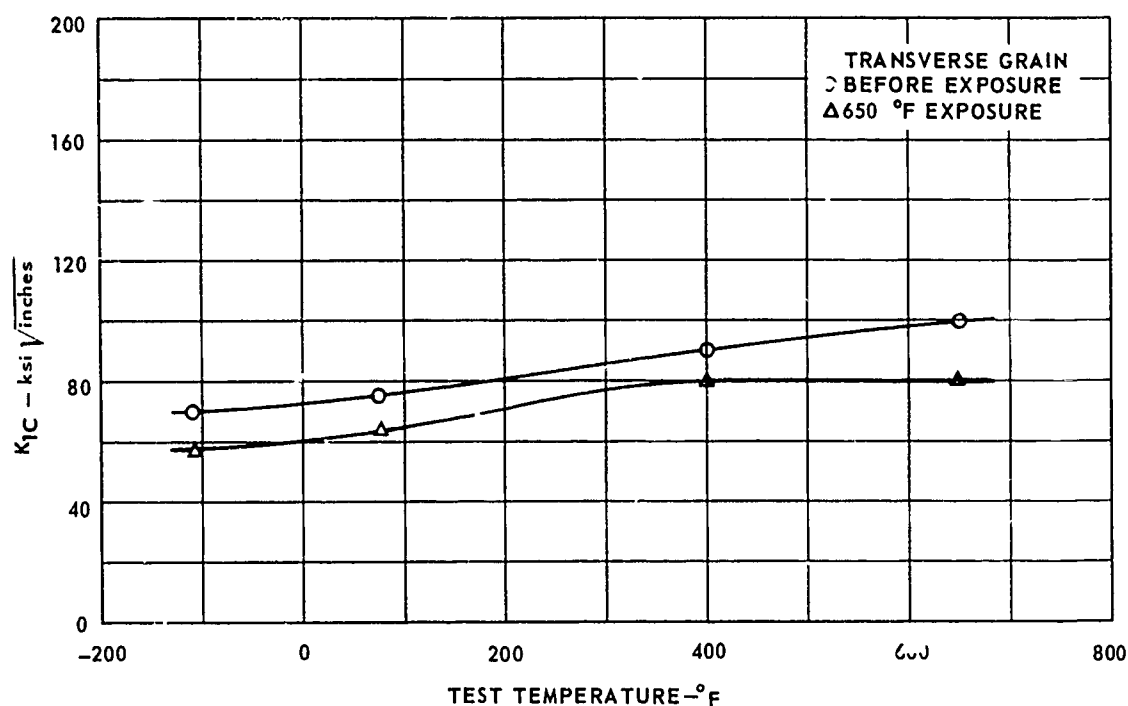


A. TOUGHNESS PROPERTIES - 1 1/8 INCH DIA ROUND NOTCH SPECIMENS

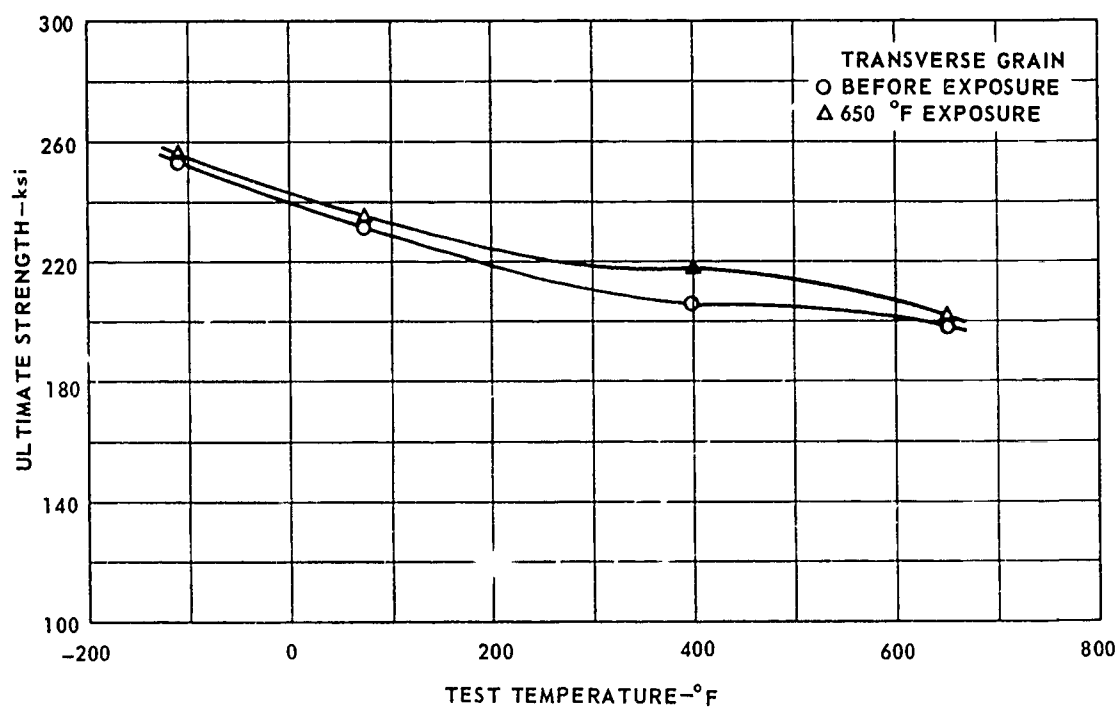


B. STRENGTH PROPERTIES - UNNOTCHED TENSILE SPECIMENS

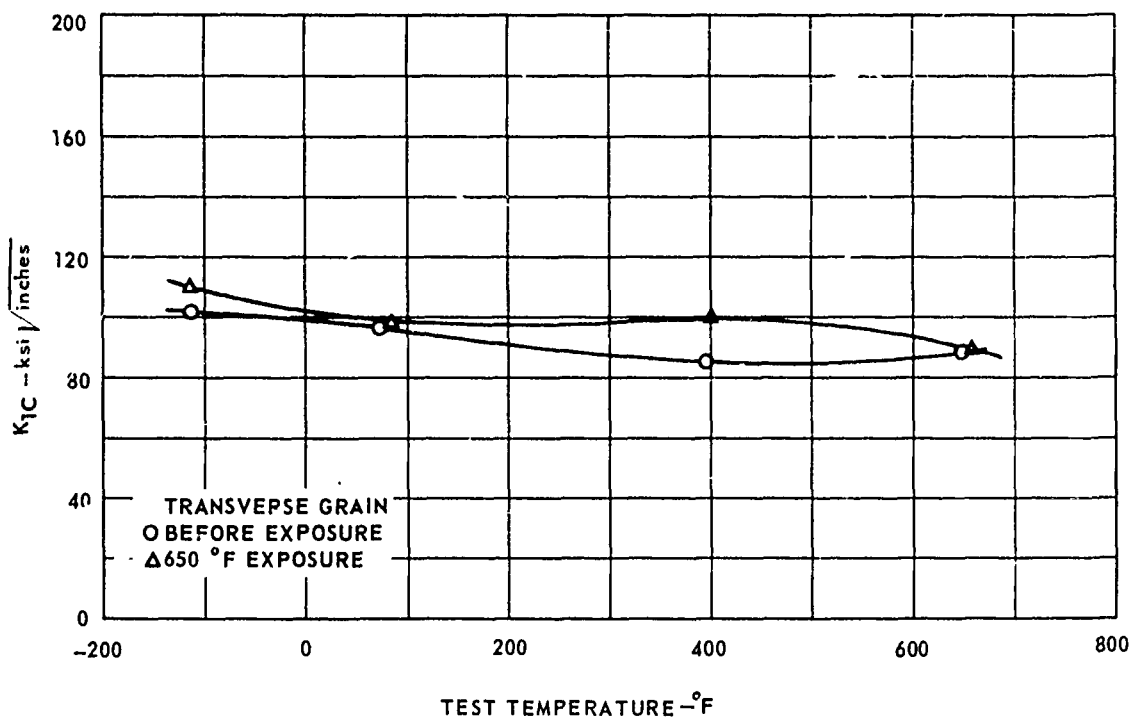
FIG. 159 EFFECTS OF 1000 HOUR STRESS AND TEMPERATURE ON PROPERTIES FOR 9Ni-4Co



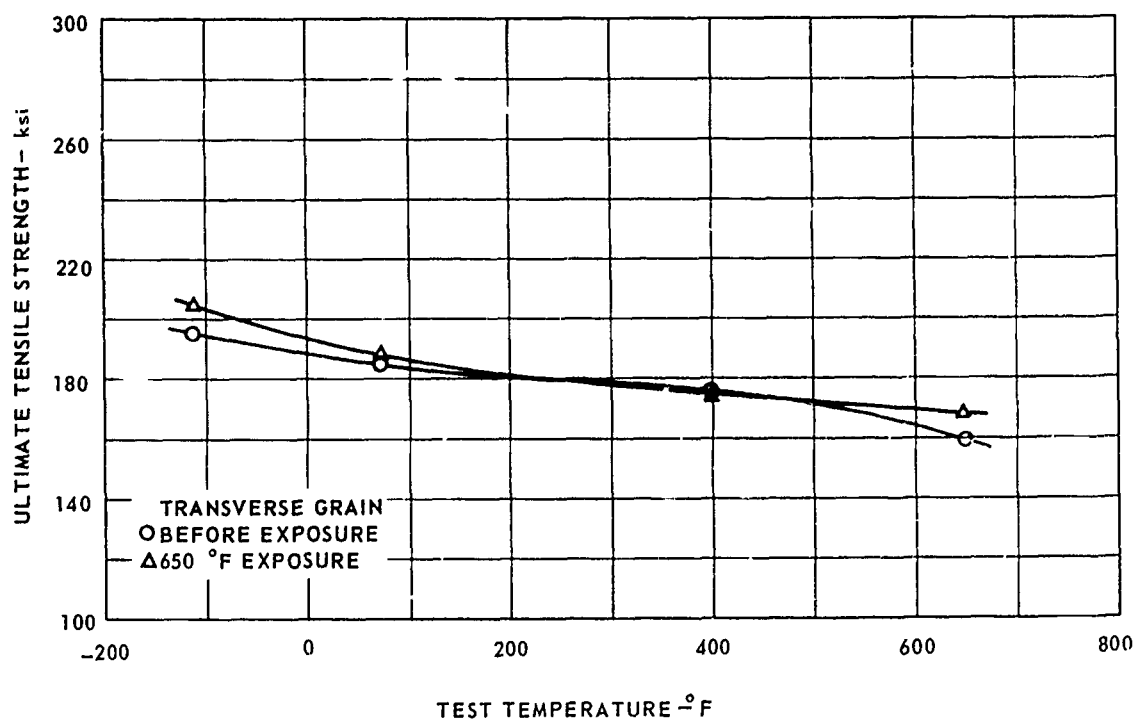
A. TOUGHNESS PROPERTIES - 1 1/8 INCH DIA ROUND NOTCH SPECIMENS



B. STRENGTH PROPERTIES - UNNOTCHES TENSILE SPECIMENS
FIG. 160 EFFECTS OF 1000 HOUR STRESS AND TEMPERATURE ON PROPERTIES
FOR MARAGING 250

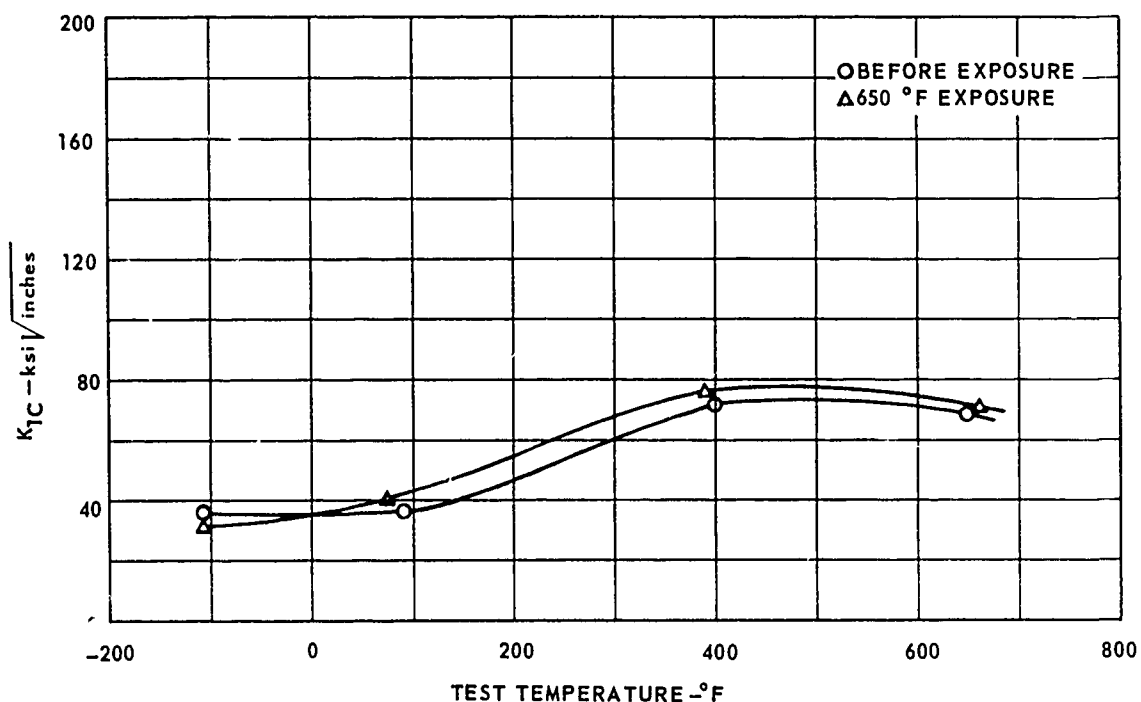


A. TOUGHNESS PROPERTIES - 1 1/8 INCH DIA ROUND NOTCH SPECIMENS

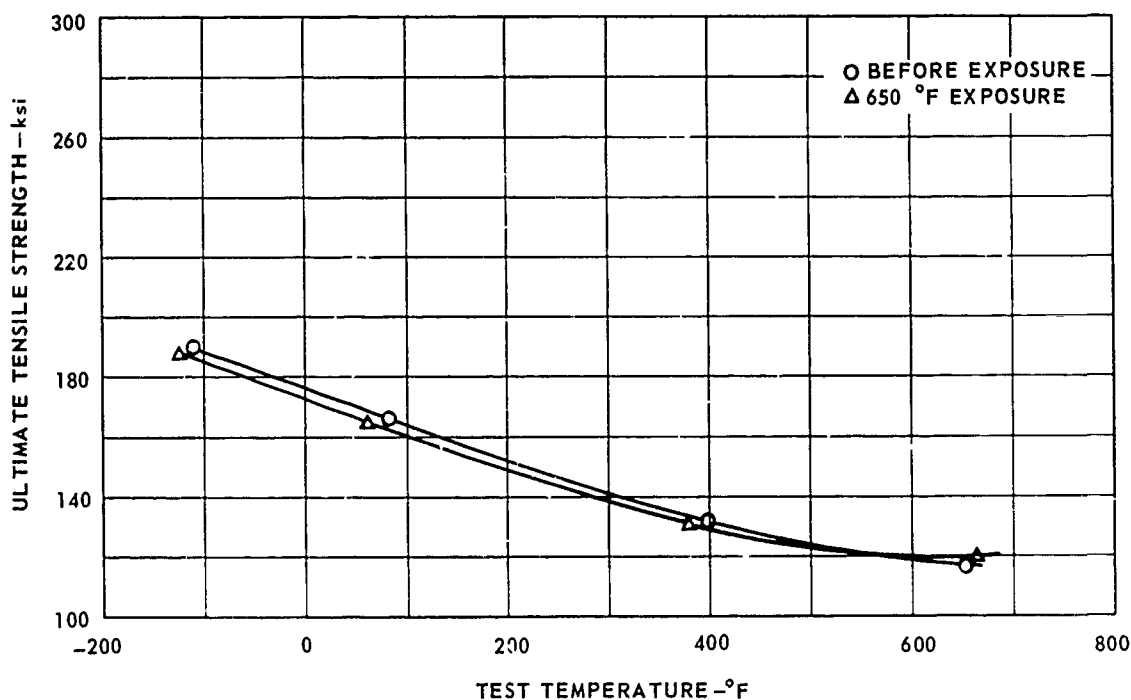


B. STRENGTH PROPERTIES - UNNOTCHED TENSILE SPECIMENS

FIG. 161 EFFECTS OF 1000 HOUR STRESS AND TEMPERATURE ON PROPERTIES FOR INCO 718



A. TOUGHNESS PROPERTIES - 1 1/8 INCH DIA ROUND NOTCH SPECIMENS



B. STRENGTH PROPERTIES - UNNOTCHED TENSILE SPECIMENS

FIG. 162 EFFECTS OF 1000 HOUR STRESS AND TEMPERATURE ON PROPERTIES FOR Ti 6Al-4V

SECTION 13 ENVIRONMENTAL TESTING

An understanding of the effect of a corrosive environment on a crack under sustained load in each of the four most promising alloys was desired. The corrosive environment used for this test was distilled water at both room temperature and 200°F. Specimens used for this test were fatigue-cracked round notch specimens identical to those used in the exposure and high load rate tests. Specimens were fabricated from the transverse direction of the forged blocks as indicated in Figs. 8 and 11. It was felt that the transverse direction would be more sensitive to corrosive action and would, therefore, reveal the minimum resistance times.

TEST PROCEDURE

The four most promising alloys involved in this test are nominally resistant to stress corrosion cracking and hydrogen embrittlement. In addition, increasing the toughness as occurred in these alloys results in increasing resistance to these embrittling mechanisms (Ref. 29). Therefore, in an attempt to cause failure to occur within 100 hours, the first specimen from each alloy was loaded to approximately 80 percent of the K_{1C} values determined from the round notch testing of Section 6. For the 200°F specimens the K_{1C} value was obtained from the transverse round notch curve at that temperature.

If the specimens, loaded to 80 percent of K_{1C} , survived 100 hours it was pulled to failure, still in the same environment, and the load was measured. The next specimen was loaded to a higher percentage until a curve of sustained load versus time to failure was obtained.

The specimens were fatigue cracked as described in the 1-1/8 inch round notch fatigue test procedure. All specimens for a given alloy were fatigue cracked the same number of cycles in order to produce, as close as possible, the same crack depth from specimen to specimen in order to accurately predict the percent K_{1C} sustained load. However, differences in crack depth and normal scatter of data caused some of the specimens to fail during loading under loads at which they would be predicted to last for many hours. Predicting the correct loads to produce a good curve was therefore difficult. The problem was amplified by the fact that the alloys were so resistant to failing within 100 hours that loading to a high percentage of K_{1C} was often necessary.

Sustained loads were applied to the specimens using three vertical test jigs with hydraulic ram-accumulator load systems. Each specimen was connected in series with the ram through universal pin joints and threaded connectors. Long-time loads, up to 100 hours, were easily maintained using a hydraulic accumulator in the ram pressure line.

Room temperature specimens were immersed in distilled water filled polyethylene beakers. Holes 1-1/8 inch in diameter were drilled in 150 ml polyethylene beakers and sealed to the specimen just above the bottom load fitting. To ensure a constant oxygen supply, water-cleaned air was bubbled through the distilled water during the test.

A large cylindrical polyethylene container was used for the distilled water in the 200°F test. To ensure a constant 200°F temperature, the load fittings and specimens were immersed in a large volume of water (Fig.163). This procedure overcame heat loss through the loading frame. The container was sealed between the bottom load fitting and clevis connector with a neoprene rubber gasket.

Each load fitting was phosphate and teflon coated so that only the specimen would react with the water. Glyptal was used to seal the specimen fitting thread area from the water. The water temperature was maintained at $202 \pm 3^\circ\text{F}$ using glass immersion heaters. The water level was maintained with a reflux condenser.

Water-cleaned air was bubbled through the water continuously to replenish the oxygen supply. All loads were measured using calibrated load cells in series with the specimen.

EXPERIMENTAL RESULTS

After testing, specimen fracture faces were examined under a low power microscope. Both the fatigue crack diameter and any evidence of slow growth were measured with a filar eyepiece and the results are listed in Tables 40 through 43. Slow crack growth was included for specimens which failed on loading as well as those that failed during sustained loading. The specimens which failed during sustained loading generally exhibited a discolored ring inside the fatigue crack. However, faint growth rings could also be seen on some of the specimens which failed on loading, particularly at the 200°F testing temperature. The final loading condition was approached very slowly in order not to overshoot, therefore, all the specimens had a small amount of time to react with the water. K_{1C} values were calculated from both diameters and are listed in the Tables as initial and final K_{1C} . In the applied stress column of the Table the percent of K_{1C} was based on values taken from the transverse curves of Section 8.

In those cases where the specimens sustained 100 hours under load without failing, the maximum loads are listed both for sustained load and the final load to cause failure.

The net stress to yield strength ratio was also included in the Tables to aid in analyzing the data. The net stress used in the ratio was the final net stress which was higher and therefore resulted in a slightly higher ratio.

Stresses applied to the specimens during the sustained loading are plotted against time to failure in Figs. 164 through 167. Both room temperature and 200°F data are included in the same figures for comparison.

DISCUSSION

Scatter bands for the data appear rather flat even for the 9 Ni-4Co and Maraging 250 steels. This fact caused considerable trouble in predicting stresses to cause failure within 100 hours without having the specimen fail on loading. Figs. 164 through 167 reveal a number of the specimens did fail on loading at low percentages of the dry strength K_{1C} . However, it has been reported (Ref. 29)

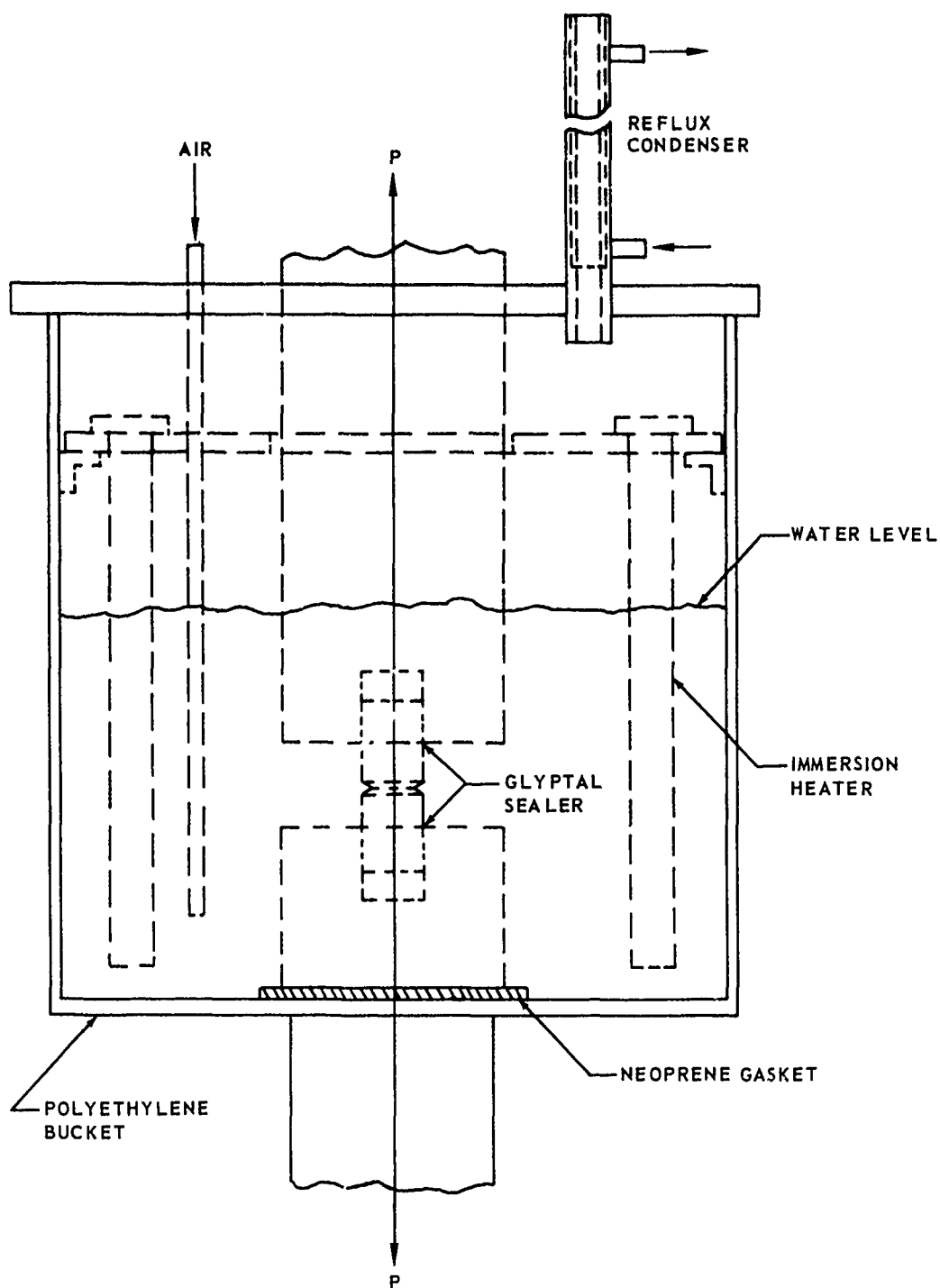


FIG. 163 200° F TEST SETUP FOR ENVIRONMENTAL SPECIMENS

TABLE 40 ENVIRONMENTAL TEST DATA FOR 9 Ni-4Co

SPECIMEN NO.	TEST TEMP °F	APPLIED STRESS % K _{1C}	MAJOR DIAMETER inches	NOTCH DIAMETER inches	NET DIAMETER INITIAL** inches	NET DIAMETER FINAL inches	MAXIMUM LOAD kips	σ_N INITIAL ksi	σ_N FINAL ksi	K _{1C} INITIAL ksi $\sqrt{\text{in}}$	K _{1C} FINAL ksi $\sqrt{\text{in}}$	FAILURE TIME HOURS	σ_{ys}	$\frac{\sigma_N}{\sigma_{ys}}$
CB 148	RT	78.4	1.122	.836	.802	.798	90.8	180.0	181.2	78.7	79.3	107.0	204.7	.89
CB 149	RT	86.5	1.123	.829	.801	.763	100.0 115.0	198.6	252.0	86.9	110.2	116.0***	204.7	1.23*
CB 150	RT	93.8	1.123	.830	.800	.782	108.0 117.2	215.3	244.0	94.2	106.8	13.0***	204.7	1.19*
CB 151	RT	91.2	1.123	.830	.798	.786	105.0	209.5	216.5	91.6	94.9	16.1	204.7	1.06*
CB 152	RT	111.8	1.123	.832	.772	.768	120.0	256.5	259.0	112.2	113.3	FL	204.7	1.27*
CB 153	RT	90.2	1.122	.829	.793	.751	102	207.0	230.0	90.5	100.5	.05	204.7	1.12*
100.0% K _{1C} = AVERAGE OF 100.3 ksi $\sqrt{\text{inches}}$ FROM 1 1/8 DIA. ROUND NOTCH SPECIMEN TESTS														
CB 154	200	82.4	1.124	.833	.789	.789	90.0	184.5	184.5	80.7	80.7	.05	198.3	.93
CB 155	200	72.2	1.123	.828	.794	.784	80.0	161.5	166.0	70.7	72.6	1.95	198.3	.84
CB 156	200	62.8	1.123	.829	.795	.789	70.0	141.0	143.5	61.6	62.8	3.37	198.3	.72
CB 157	200	48.9	1.123	.829	.801	.747	55.0	109.5	125.5	47.9	54.9	81.90	198.3	.63
CB 158	200	60.3	1.122	.828	.784	.780	65.0	135.0	136.3	59.1	59.6	.23	198.3	.68
CB 159	200	55.9	1.123	.831	.781	.781	60.0	125.5	125.5	54.9	54.9	.75	198.3	.63
100.0% K _{1C} = AVERAGE OF 98.0 ksi $\sqrt{\text{inches}}$ FROM ROUND NOTCH SPECIMEN DATA CURVE AT 200° F														

FL=FAILED ON LOADING

*THESE RATIOS ARE ABOVE THE 1.1 LIMIT RECOMMENDED BY THE ASTM COMMITTEE FOR FRACTURE TOUGHNESS

**INITIAL CRACK BASED ON FATIGUE CRACK DIMENSIONS

***TEST STOPPED SPECIMEN PULLED TO FAILURE

ALL SPECIMENS TRANSVERSE GRAIN DIRECTION

FATIGUE DATA: MAX CYCLING STRESS .33 YIELD STRENGTH

R = .05

CYCLING RATE WAS 120 TO 600 CPM

FRACTURE TEST LOAD RATE 150 ksi/min

TABLE 41 ENVIRONMENTAL TEST DATA FOR MARAGING 250

SPECIMEN NO	TEST TEMP °F	APPLIED STRESS % K _{1C}	MAJOR DIAMETER inches	NOTCH DIAMETER inches	NET DIAMETER INITIAL** inches	NET DIAMETER FINAL inches	MAXIMUM LOAD kips	σ_N INITIAL ksi	σ_N FINAL ksi	K _{1C} INITIAL ksi \sqrt{in}	K _{1C} FINAL ksi \sqrt{in}	FAILURE TIME HOURS	σ_{ys}	$\frac{\sigma_N}{\sigma_{ys}}$
CD 148	RT	73.2	1.124	.855	.831	.815	67.9	125.0	130.0	54.7	56.8	15.25	216.5	.60
CD 149	RT	82.8	1.123	.855	.825	.823	75.5	141.4	142.0	61.9	62.1	.01	216.5	.66
CD 150	RT	64.6	1.124	.855	.797	.787	55.1/62.5	110.5	128.6	48.3	56.3	120.0***	216.5	.59
CD 151	RT	88.0	1.121	.857	.781	.781	72.0	150.5	150.5	65.8	65.8	.13	216.5	.69
CD 152	RT	80.5	1.120	.855	.785	.775	66.5	137.7	141.0	60.2	61.6	18.60	216.5	.65
CD 153	RT	71.6	1.121	.857	.783	.769	58.8	122.3	126.7	53.5	55.3	34.25	216.5	.58
100.0 % = K _{1C} AVERAGE OF 74.8 ksi \sqrt{inches} FROM 1.1/8 DIAMETER ROUND NOTCH SPECIMEN TESTS														
CD 154	200	73.9	1.118	.850	.800	.800	69.5	138.4	138.4	60.6	60.6	FL	205.0	.68
CD 155	200	62.6	1.123	.854	.796	.796	58.3	117.3	117.3	51.3	51.3	FL	205.0	.57
CD 156	200	72.6	1.118	.851	.787	.787	66.0	136.0	136.0	59.5	59.5	.42	205.0	.66
CD 157	200	68.5	1.119	.853	.797	.781	64.0	128.5	131.5	56.2	57.5	1.21	205.0	.64
CD 158	200	67.5	1.118	.851	.777	.765	60.0	126.5	130.5	55.4	57.1	.58	205.0	.64
CD 159	200	62.7	1.120	.852	.772	.722	55.0	117.4	134.5	51.4	58.8	1.69	205.0	.66
100.0 % = K _{1C} AVERAGE OF 82.0 ksi \sqrt{inches} FROM ROUND NOTCH SPECIMEN DATA CURVE AT 200°F														

FL = FAILED ON LOADING

** = INITIAL CRACK BASED ON FATIGUE CRACK DIMENSIONS

*** = TEST STOPPED, SPECIMEN PULLED TO FAILURE

ALL SPECIMENS TRANSVERSE GRAIN DIRECTION

FATIGUE DATA:

MAX CYCLING STRESS .33 YIELD STRENGTH

R = .05 CYCLING RATE 120 TO 600 CPM

FRACTURE TEST LOAD RATE 150 ksi/min

TABLE 42 ENVIRONMENTAL TEST DATA FOR INCO 718

SPECIMEN NO.	TEST TEMP °F	APPLIED STRESS % K _{1C}	MAJOR DIAMETER inches	NOTCH DIAMETER inches	NET DIAMETER INITIAL** inches	NET DIAMETER FINAL inches	MAXIMUM LOAD kips	σ_N INITIAL ksi	σ_N FINAL ksi	K _{1C} INITIAL ksi $\sqrt{\text{in}}$	K _{1C} FINAL ksi $\sqrt{\text{in}}$	FAILURE TIME HOURS	σ_{ys}	$\frac{\sigma_N}{\sigma_{ys}}$
CE 148	RT	102.0	1.121	.847	.723	.723	91.4	223.0	223.0	97.6	97.6	FL	154.5	1.44*
CE 149	RT	79.3	1.121	.848	.776	.752	82.1 102.9	173.5	232.0	75.9	101.3	97.8***	154.5	1.50*
CE 150	RT	90.1	1.122	.845	.771	.771	92.0	197.0	197.0	86.2	86.2	22.4	154.5	1.28*
CE 151	RT	87.7	1.121	.846	.806	.788	97.8	191.7	200.5	83.8	87.8	FL	154.5	1.30*
CE 152	RT	91.9	1.123	.850	.776	.776	95.0 96.3	201.0	203.5	87.9	89.0	113.7***	154.5	1.32*
CE 153	RT	102.7	1.121	.847	.729	.717	93.8	225.0	232.2	98.4	101.4	FL	154.5	1.50*
100.0% K _{1C} =AVERAGE OF 95.7 ksi $\sqrt{\text{inches}}$ FROM 1 1/8 DIA. ROUND NOTCH SPECIMEN TESTS														
CE 154	200	102.8	1.121	.849	.749	.749	92.0	209.0	209.0	91.4	91.4	FL	151.5	1.38*
CE 155	200	99.4	1.121	.847	.743	.733	87.5	202.0	207.5	88.4	90.7	.03	151.5	1.37*
CE 156	200	83.0	1.121	.845	.791	.785	83.0	169.0	172.0	73.9	75.2	23.6	151.5	1.14*
CE 157	200	82.1	1.120	.846	.776	.760	79.0 102.4	167.0	226.0	73.1	98.8	116.0***	151.5	1.49*
CE 158	200	87.0	1.121	.849	.775	.763	83.4	177.0	182.4	77.4	79.8	FL	151.5	1.20*
CE 159	200	95.8	1.120	.848	.736	.730	83.0	195.0	198.6	85.3	86.8	.17	151.5	1.31*
100.0% K _{1C} =AVERAGE OF 89.0 ksi $\sqrt{\text{inches}}$ FROM ROUND NOTCH SPECIMEN DATA CURVE AT 200° F														

FL FAILED ON LOADING

** INITIAL CRACK BASED ON FATIGUE CRACK DIMENSIONS

*** TEST STOPPED SPECIMEN PULLED TO FAILURE

ALL SPECIMENS TRANSVERSE GRAIN DIRECTION

FATIGUE DATA: MAX CYCLING STRESS .33 YIELD STRENGTH

R=.05

CYCLING RATE 120 TO 600 CPM

FRACTURE TEST LOAD RATE 150 ksi/min

*THESE RATIOS ARE ABOVE THE 1.1 LIMIT RECOMMENDED BY THE ASTM COMMITTEE ON FRACTURE TOUGHNESS

TABLE 43 ENVIRONMENTAL TEST DATA FOR T₁ 6Al-4V

SPECIMEN NO.	TEST TEMP °F	APPLIED STRESS % K _{1C}	MAJOR DIAMETER inches	NOTCH DIAMETER inches	NET DIAMETER INITIAL* inches	NET DIAMETER FINAL inches	MAXIMUM LOAD kips	σ_N INITIAL ksi	σ_N FINAL ksi	K _{1C} INITIAL ksi $\sqrt{\text{in}}$	K _{1C} FINAL ksi $\sqrt{\text{in}}$	FAILURE TIME hours	σ_{ys}	$\frac{\sigma_N}{\sigma_{ys}}$
CF 148	RT	89.2	1.124	.851	.819	.819	38.8/50.0	73.7	94.9	32.2	41.4	100.0**	152.2	.62
CF 149	RT	108.8	1.122	.854	.786	.786	43.6	89.9	89.9	39.3	39.3	FL	152.2	.59
CF 150	RT	102.0	1.123	.852	.816	.804	44.0	84.2	86.8	36.8	37.9	.05	152.2	.57
CF 151	RT	93.1	1.124	.852	.814	.812	40.0	76.9	77.3	33.6	34.8	.04	152.2	.51
CF 152	RT	96.4	1.122	.850	.790	.780	39.0	79.7	81.8	34.8	35.8	.05	152.2	.54
CF 153	RT	87.3	1.123	.851	.809	.809	37.0	72.2	72.2	31.5	31.5	.10	152.2	.47
100.0% = K _{1C} AVERAGE OF 36.1 ksi $\sqrt{\text{inches}}$ FROM 1 1/8 DIA. ROUND NOTCH SPECIMEN TESTS														
CF 154	200	83.3	1.122	.853	.721	.647	40.0	98.1	121.6	42.9	53.2	.22	139.0	.87
CF 155	200	75.3	1.123	.850	.748	.690	39.0	88.8	104.2	38.8	45.6	30.75	139.0	.75
CF 156	200	79.6	1.121	.854	.728	.682	39.0	93.8	106.8	41.0	46.7	FL	139.0	.77
CF 157	200	83.1	1.122	.852	.712	.676	39.0	98.0	108.7	42.8	47.5	FL	139.0	.78
CF 158	200	72.6	1.121	.852	.742	.692	37.0	85.6	98.4	37.4	43.0	FL	139.0	.71
CF 159	200	56.2	1.122	.851	.761	.735	30.0/45.5	66.0	107.2	28.9	46.9	115.4**	139.0	.77
100.0% = K _{1C} AVERAGE OF 51.5 ksi $\sqrt{\text{inches}}$ FROM ROUND NOTCH SPECIMEN DATA CURVE AT 200° F														

FL FAILED ON LOADING

* INITIAL CRACK BASED ON FATIGUE CRACK DIMENSIONS

** TEST STOPPED SPECIMEN PULLED TO FAILURE

ALL SPECIMENS TRANSVERSE GRAIN DIRECTION

FATIGUE DATA: MAX CYCLING STRESS .33 YIELD STRENGTH

R = .05

CYCLING RATE 1800 cpm

FRACTURE TEST LOAD RATE 150 ksi min

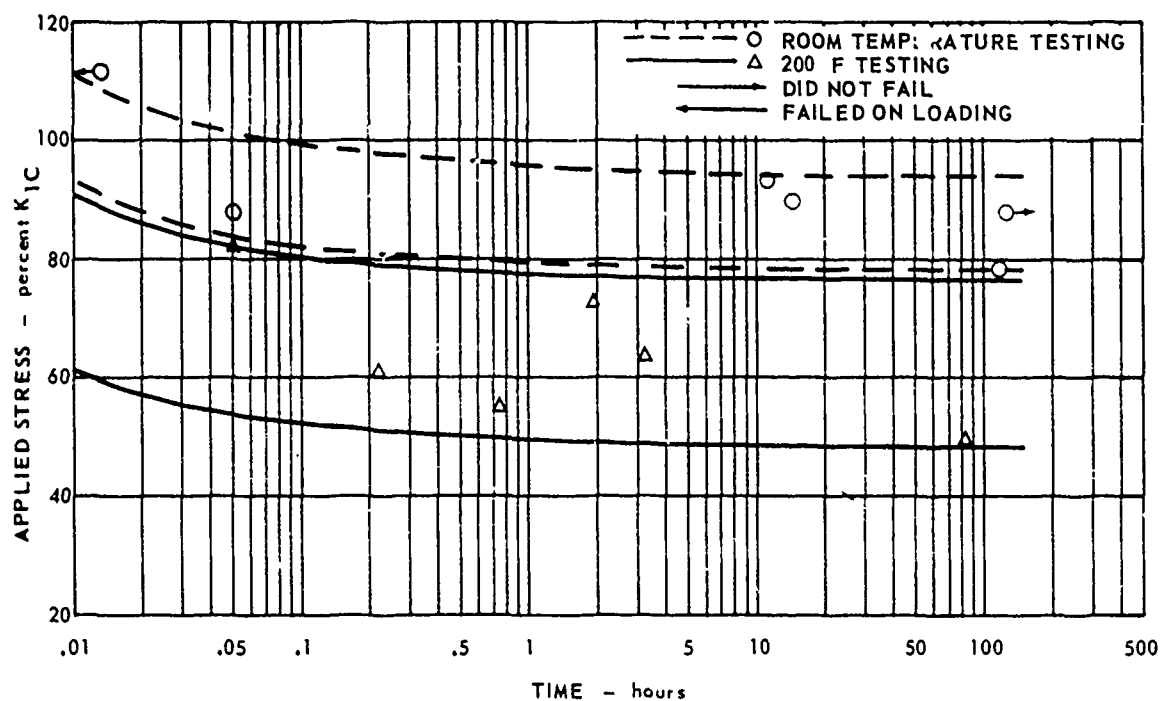


FIG. 164 ENVIRONMENTAL EFFECTS ON 9Ni - 4 Co

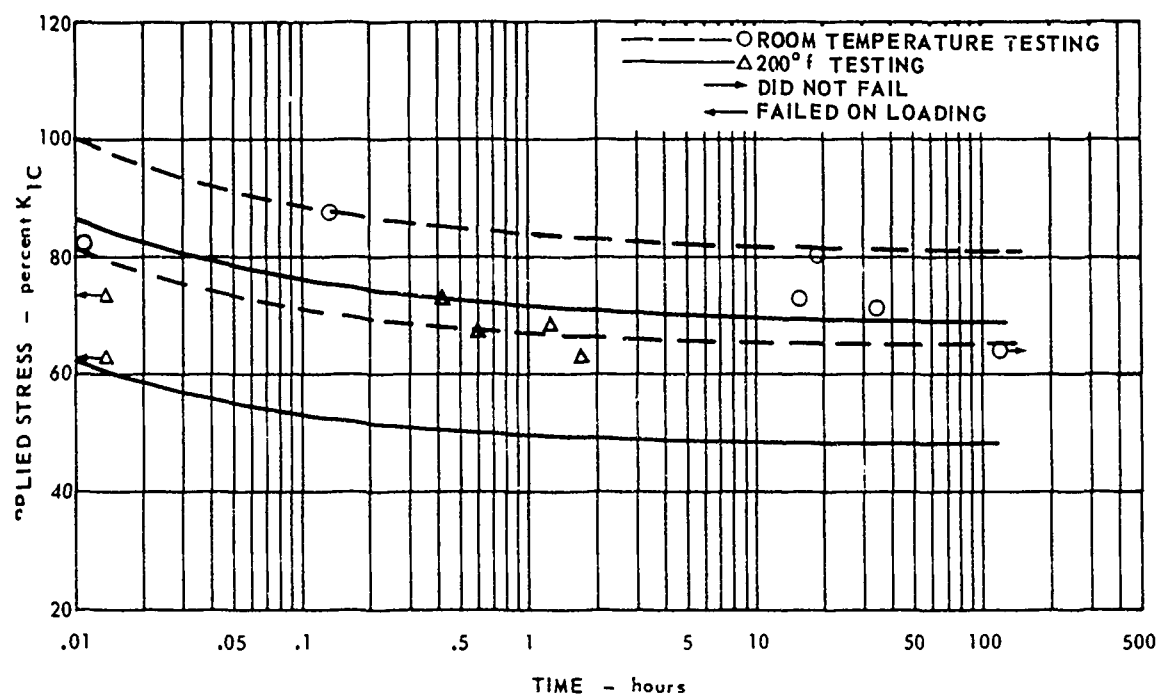


FIG. 165 ENVIRONMENTAL EFFECTS ON MARAGING 250

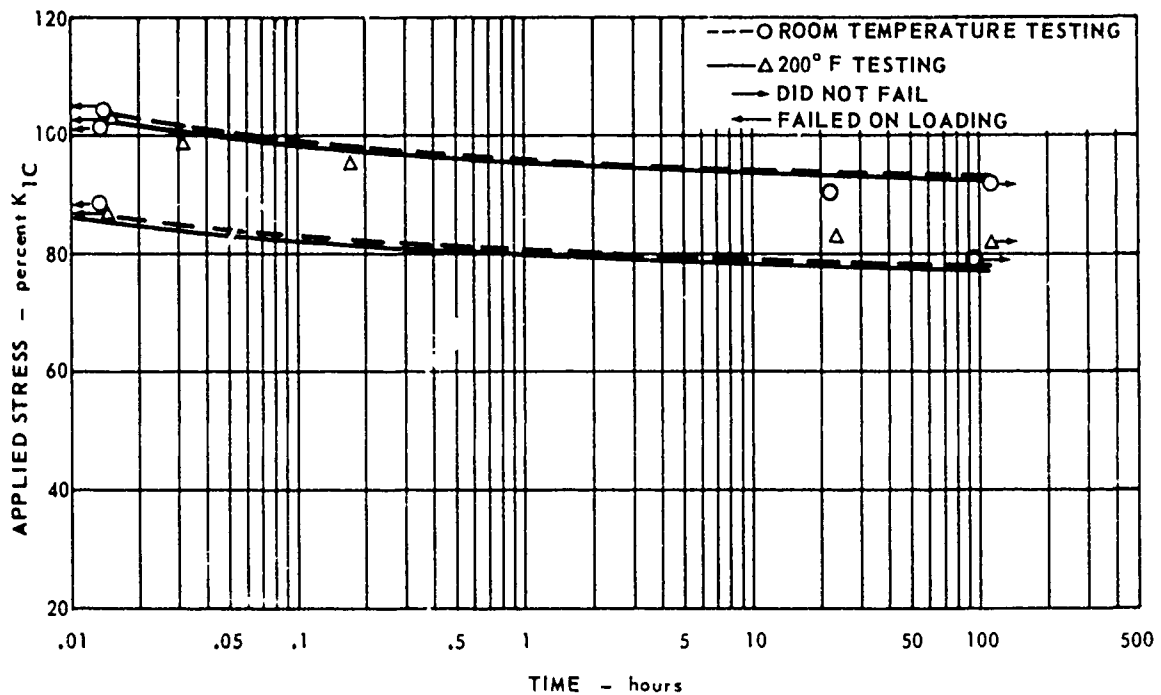


FIG. 166 ENVIRONMENTAL EFFECTS ON INCO 718

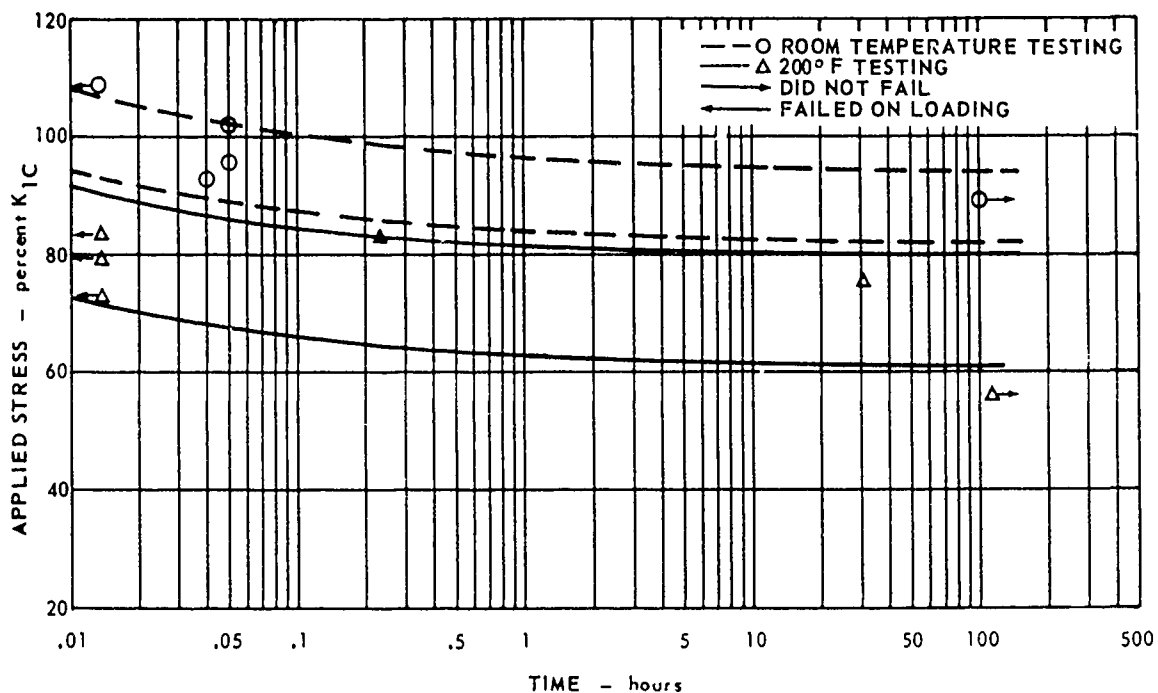


FIG. 167 ENVIRONMENTAL EFFECTS ON Ti 6Al-4V

that liquid environments can cause a lowering of notch tensile strength in high strength steels during relatively slow strain rate tensile tests. Similarly, the strain rate of these specimens was slow. Specimens were loaded slowly up to the sustaining load in order to avoid possible overloading. It is therefore probable that the liquid environment did affect even those specimens which appeared to fail from overloading alone. Although these alloys had high toughness, the specimens were cut from the transverse direction of large forged blocks, a condition highly susceptible to stress corrosion.

It is also possible that the mechanism responsible for delayed fracture involved hydrogen embrittlement. However, titanium and high nickel austenitic alloys, such as Inco 718, are not considered to be affected by hydrogen at room temperature. Both these alloys had delayed failures at room temperature with applied stresses as low as 80 percent K_{1C} .

Although there were only 6-specimens tested at each temperature per alloy, it appears that the 200°F testing temperature was more detrimental to toughness than was room temperature. Inco 718 is a possible exception. Both failure on loading and delayed fracture seem to be affected. This result is not unexpected, since a small increase in temperature causes a large change in chemical activity.

Although there are not enough data points to define reliable scatterbands, it appears that delayed failures may occur at fairly low stresses, in fatigue cracked specimens cut from the transverse grain direction of large tough alloy forgings. The data indicates that applied stresses as low as: 50 percent of K_{1C} on 9 Ni-4Co and Maraging 250; 60 percent on Ti 6Al-4V; and 80 percent on Inco 718 will cause delayed fracture in 200°F distilled water within 100 hours.

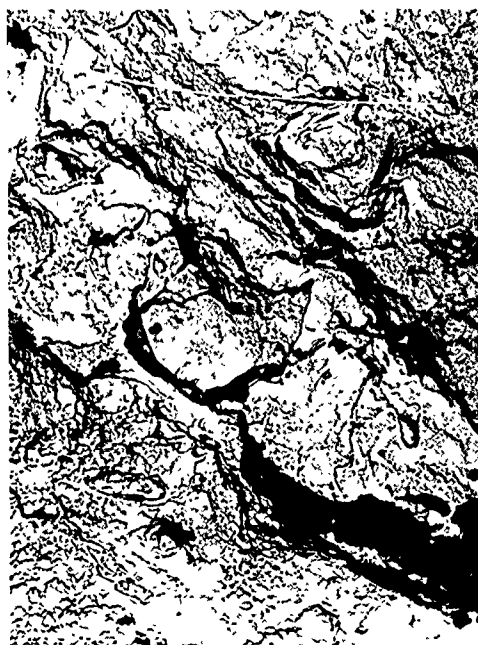
ELECTRON FRACTOGRAPHY

Round notched environmental specimen fracture faces were replicated to investigate the mode of failure during delayed fracture. Specimens of 9 Ni-4Co, Maraging 250, Inco 718, and Ti 6Al-4V subjected to room temperature distilled water until failure, are shown in Figs. 168, 169, 170, and 171. Replicas were made in the slow growth region at the fatigue interface and in the fast fracture area near the specimen center.

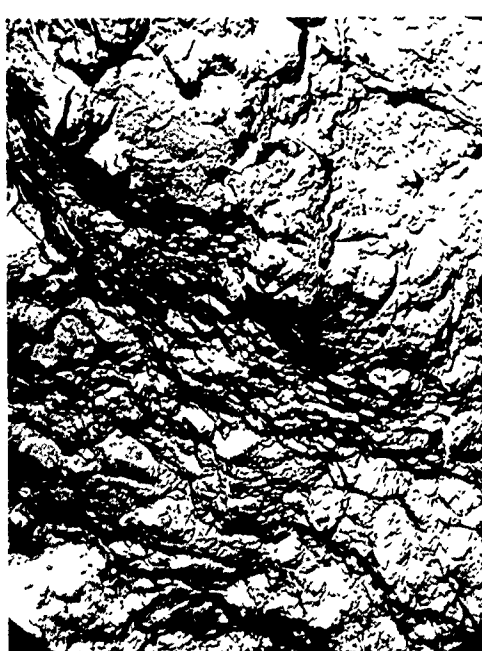
Figures 168, 169, 170, and 171 show that the sustained stresses were high in every case. In addition, each of the alloys had a high toughness and resistance to stress corrosion. Therefore, it was understandable that very few areas of intergranular crack propagation could be found. In general, the topography at the fatigue crack interface was similar to the rapid crack growth area. However, the 9 Ni-4Co and the Maraging 250 showed somewhat less dimples and more flat areas adjacent to the fatigue zone. The Inco 718 showed extensive dimples in both regions (Fig. 170). In this alloy the size of the dimples seems to be governed by the size of the second phase. The large inclusions (Fig. 170D) resulted in a high degree of triaxiality which formed large microvoids and therefore large dimples.



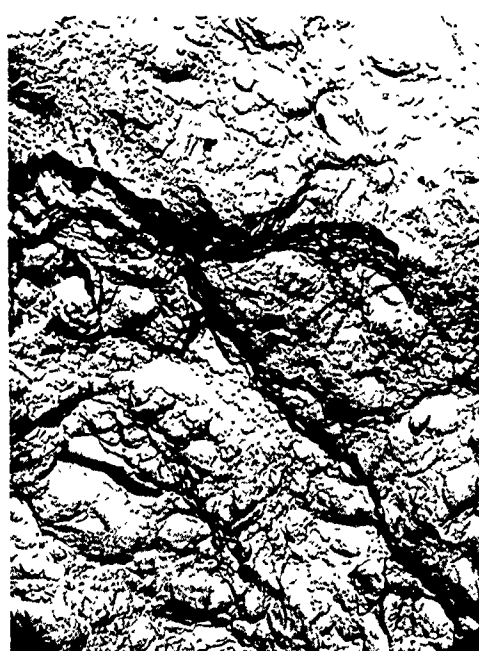
(A) AREA ADJACENT TO FATIGUE
CRACK INTERFACE



(B) AREA ADJACENT TO FATIGUE
CRACK INTERFACE



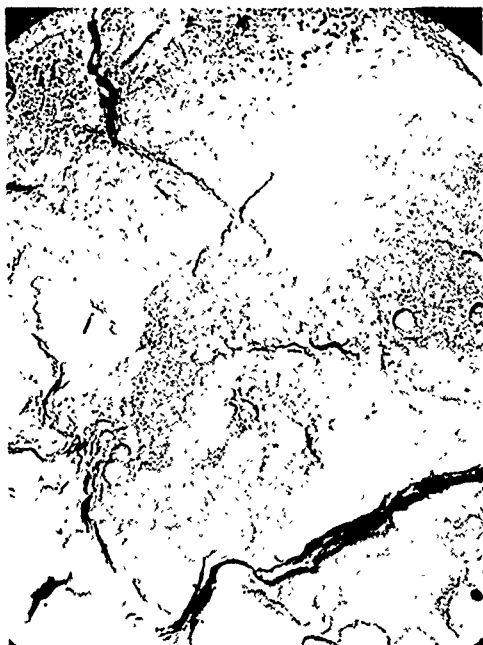
(C) FAST FRACTURE AREA



(D) FAST FRACTURE AREA

NOTE: CB148 Specimen Tested in Distilled Water at Room Temperature (1700x)

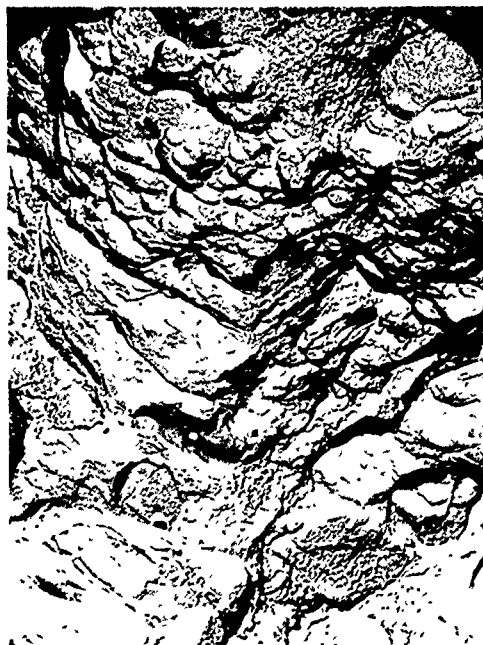
FIG. 168 ELECTRON FRACTOGRAPHS OF ENVIRONMENTAL SPECIMEN FOR 9Ni-4Co



(A) CORRODED FATIGUE AREA



(B) INTERFACE BETWEEN FATIGUE
AND SLOW GROWTH AREA



(C) DIMPLED STRUCTURE 0.01 INCHES
FROM FATIGUE INTERFACE



(D) DIMPLES IN FINAL FAST FRACTURE
AREA

NOTE: Specimen Tested in Distilled Water at Room Temperature (Specimen CD153) (1700x)

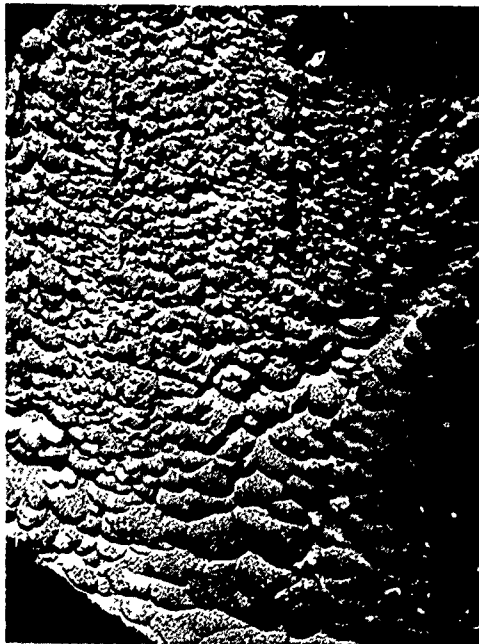
FIG.169 ELECTRON FRACTOGRAPHS OF ENVIRONMENTAL SPECIMEN FOR MARAGING 250



(A) AREA AT THE FATIGUE CRACK INTERFACE SHOWING INDICATIONS OF FATIGUE MARKINGS



(B) SMALL ELONGATED DIMPLE AREA NEAR THE FATIGUE CRACK INTERFACE



(C) SMALL ELONGATED DIMPLES IN FAST FRACTURE AREA.



(D) LARGE DIMPLES IN FAST FRACTURE AREA

NOTE: Tested in Distilled Water at Room Temperature (Specimen CE150) (1700x)

FIG.170 ELECTRON FRACTOGRAPHS OF ENVIRONMENTAL SPECIMEN FOR INCO 718



(A) AREA ADJACENT TO FATIGUE
CRACK INTERFACE



(B) AREA ADJACENT TO FATIGUE
CRACK INTERFACE



(C) LARGE DIMPLES IN FAST
FRACTURE AREA



(D) LARGE DIMPLES IN FAST
FRACTURE AREA

NOTE: Tested in Distilled Water at Room Temperature (Specimen CF153) (1700x)

FIG.171 ELECTRON FRACTOGRAPHS OF ENVIRONMENTAL SPECIMEN FOR Ti 6Al-4V

SECTION 14 HIGH LOAD RATE TESTING

The purpose of this testing was to determine the effect of high loading rates on plane-strain fracture characteristics of the four most promising alloys. Round notched transverse specimens (1.125 inch diameter) were tested at gross area stress rates of 10^5 and 10^6 psi/sec and test temperatures of -110, 75, 400 and 650°F. The results were compared with those obtained previously at normal tensile test loading rates.

TEST PROCEDURE

Specimen fabrication, fatigue cracking, and heating and cooling procedures for the high- and low-temperature tests were the same as those used previously for the round notched specimens.

The specimens were fracture tested at nominal stress rates of 10^5 and 10^6 psi/sec in a specially constructed test rig. The test rig consisted of a vertical frame structure with a 10-inch diameter hydraulic load cylinder mounted at the upper end. The cylinder ram was connected to the specimen in series and the load was applied to the specimen through pin ended adapters threaded on the specimens. Loading eccentricities were minimized by maintaining the loading pins at right angles to each other. The load was measured by a transducer in line with the specimen and was recorded graphically. The desired load rate was programmed into the electronic control unit which compared at every instant the actual load versus the programmed load and adjusted the inlet flow valve to the cylinder accordingly. Figs. 172 and 173 show the hydraulic and electrical systems in detail. The exact stress rate was measured for each specimen from the recording oscillograph trace and is shown in Table 44. The stress rate for most of the specimens was within 10 percent of the target rates of 10^5 and 10^6 psi/sec. The loading linearity is illustrated by the load versus time graph shown in Fig. 174.

For the elevated-temperature tests, the specimens were enclosed in a box-like container and heated by introducing heated air. Liquid nitrogen was used for the -110°F tests.

TEST RESULTS

The test data are presented in Table 44. The loading stress rate and K_{1C} toughness value are listed in the table for each specimen. Also listed is the ratio of net stress to yield strength based on the yield strength at normal loading rates (2500 psi/sec). These ratios are only approximate since the high loading rates would probably cause some change in yield strength. The ratios indicate that many of the toughness values reported are conservative.

The effect of loading rate change on the toughness at the various test temperatures is shown in Figs. 175 through 178. The values in the figures for a stress rate of 2500 psi/sec are from the round notch specimen testing of Section 8 of the program. At test temperatures below 650°F, the alloys show either no change or an increase in plane strain fracture toughness with increasing loading rate. At the test temperature of 650°F, each alloy reacted differently.

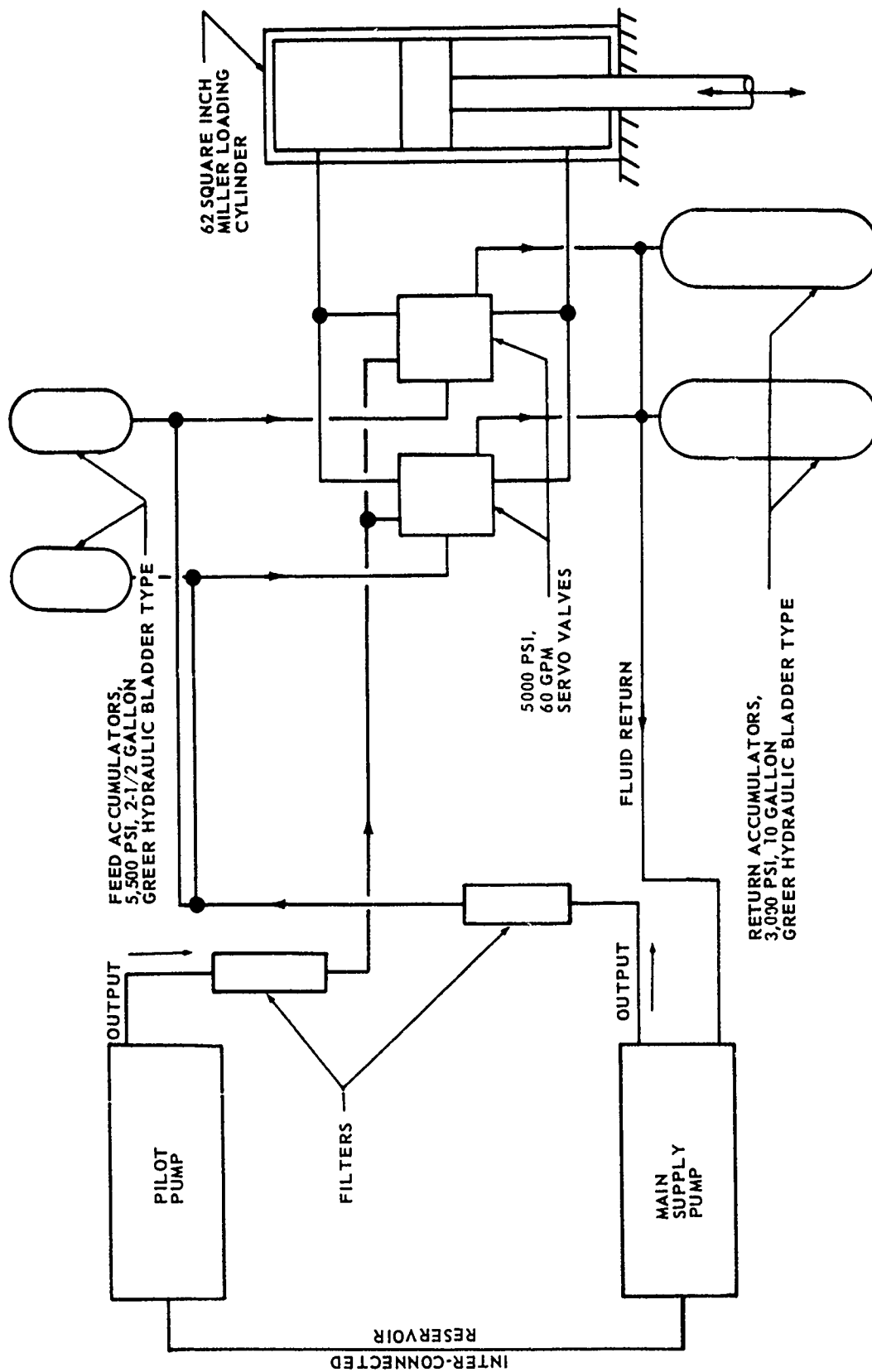
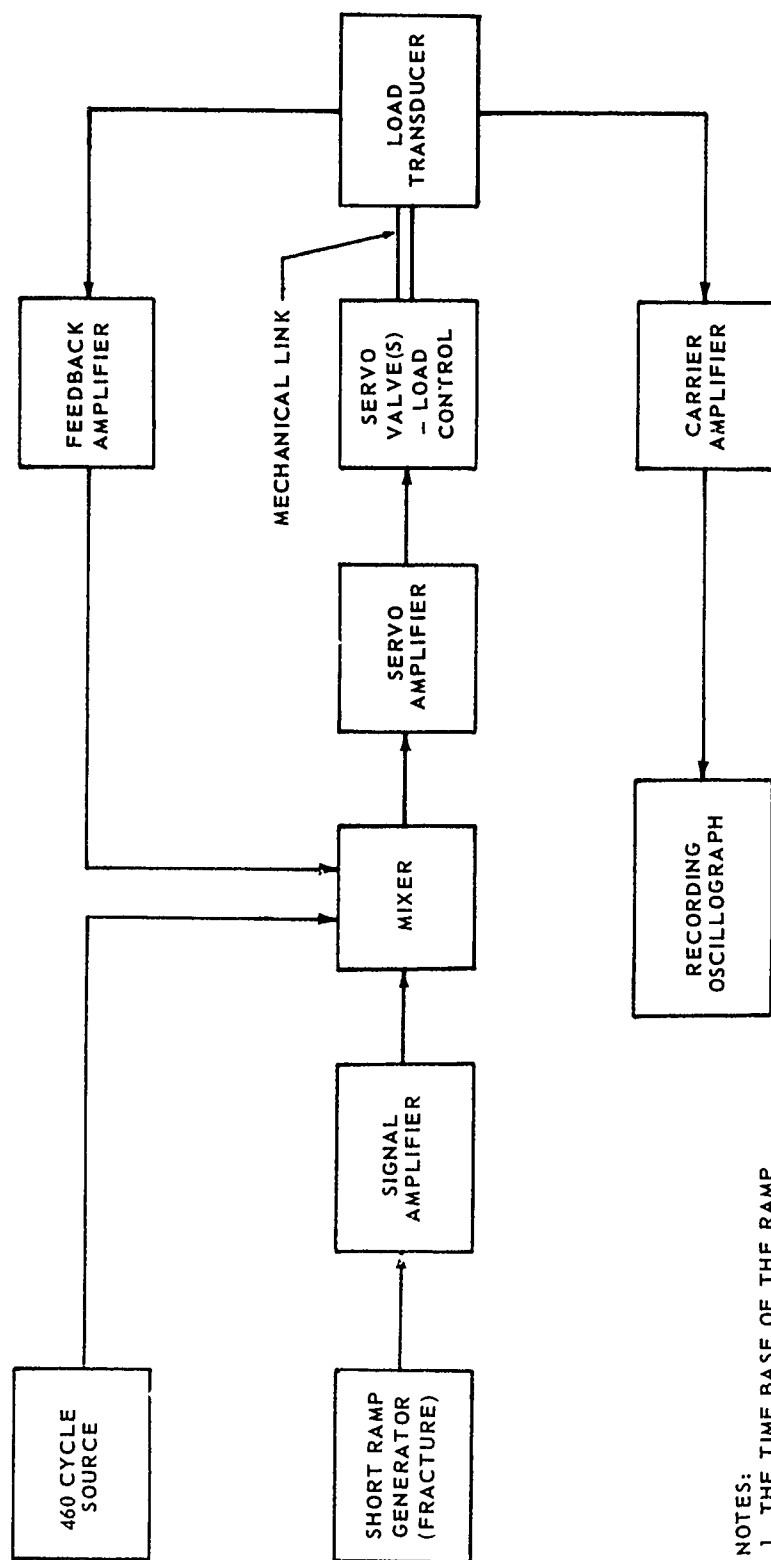





FIG. 172 HYDRAULIC SYSTEM OF HIGH LOAD RATE TEST RIG



NOTES:
 1. THE TIME BASE OF THE RAMP
 GENERATOR CIRCUIT IS ADJUSTABLE
 FROM .05 TO 11 SECONDS

FIG. 173 LOAD CONTROL SYSTEM OF HIGH LOAD RATE TEST RIG

TABLE 44 HIGH LOAD RATE DATA

SPECIMEN NO.	TEST TEMP. °F	STRESS RATE ksi/sec	MAJOR DIAMETER inches	NOTCH DIAMETER inches	NET DIAMETER inches	MAXIMUM LOAD kips	NET AREA in ²	σ_N ksi	K_{IC} ksi $\sqrt{\text{in}}$	YIELD STRENGTH .2% OFFSET ksi	$\frac{\sigma_N}{\sigma_{ys}}$
9 Ni-4Co											Approx 
B2I9	-110	93	1.122	.851	.773	122.3	.470	260.3	113.9	220.6	1.18 *
B2I10	-110	97	1.125	.852	.816	135.4	.523	258.9	113.4	220.6	1.17 *
B2I14	-110	1060	1.121	.852	.802	132.9	.505	263.1	115.1	220.6	1.19 *
B2I15	-110	946	1.121	.850	.811	137.3	.517	265.6	116.3	220.6	1.20 *
B2I11	75	95	1.123	.852	.806	137.3	.511	268.8	117.7	204.7	1.31 *
B2I16	75	986	1.121	.852	.816	143.6	.524	274.3	119.8	204.7	1.34 *
B2I12	400	94	1.122	.852	.784	107.7	.492	223.4	97.8	165.1	1.35 *
B2I17	400	935	1.121	.851	.804	129.0	.508	254.1	111.2	165.1	1.54 *
B2I13	650	97	1.123	.852	.800	118.7	.503	236.2	103.4	149.5	1.58 *
B2I18	650	995	1.121	.852	.809	109.5	.514	213.0	93.2	149.5	1.42 *
MARAGING 250											
D2I9	-110	103	1.126	.852	.724	61.10	.412	148.4	65.0	233.5	.64
D2I10	-110	106	1.127	.852	.688	59.65	.372	160.3	70.0	233.5	.69
D2I14	-110	1180	1.125	.852	.730	64.40	.418	154.1	67.5	233.5	.66
D2I15	-110	1123	1.126	.853	.742	67.90	.432	157.0	68.8	233.5	.67
D2I11	75	101	1.127	.852	.753	75.80	.445	170.2	74.6	216.7	.79
D2I16	75	1122	1.120	.853	.758	74.60	.451	165.5	72.4	216.7	.76
D2I12	400	114	1.126	.853	.728	89.10	.417	213.9	93.7	189.8	1.13 *
D2I17	400	1122	1.126	.852	.728	81.95	.417	196.8	86.2	189.8	1.04
D2I13	650	97	1.127	.852	.706	70.65	.391	180.7	79.2	187.0	.97
D2I18	650	1080	1.127	.852	.748	103.80	.439	236.2	103.5	187.0	1.26 *

NOTE: 1.125 INCH ROUND NOTCH TRANSVERSE GRAIN SPECIMENS

 THE YIELD STRENGTHS WERE OBTAINED AT NORMAL LOADING RATES (2500 psi/sec) AND THEREFORE ONLY APPROXIMATELY CORRECT FOR LISTED STRESS RATES

 STRESS RATES ARE BASED ON NOTCH DIAMETER


* THESE RATIOS ARE ABOVE THE 1.1 LIMIT RECOMMENDED BY THE ASTM COMMITTEE ON FRACTURE TOUGHNESS

FATIGUE DATA (1800 cpm, R = .05)

9 Ni-4Co: MAXIMUM CYCLING STRESS APPROXIMATELY 67 ksi, 6000 To 8000 CYCLES

MARAGING 250: MAXIMUM CYCLING STRESS APPROXIMATELY 72 ksi, 8000 to 9000 CYCLES

TABLE 44 HIGH LOAD RATE DATA (continued)


SPECIMEN NO.	TEST TEMP. °F	STRESS RATE ksi/sec	MAJOR DIAMETER inches	NOTCH DIAMETER inches	NET DIAMETER inches	MAXIMUM LOAD kips	NET AREA in ²	σ_N ksi	K_{IC} ksi $\sqrt{\text{in}}$	YIELD STRENGTH .2% OFFSET ksi	$\frac{\sigma_N}{\sigma_{ys}}$
INCONEL 718											
E219	-110	94	1.123	.848	.737	103.4	.427	242.4	106.1	164.2	1.48*
E2110	-110	100	1.126	.849	.743	105.5	.433	243.5	106.7	164.2	1.48*
E2114	-110	1082	1.123	.848	.714	99.0	.400	247.3	108.3	164.2	1.50*
E2115	-110	1118	1.123	.848	.720	108.5	.407	266.5	116.7	164.2	1.62*
E2111	75	106	1.124	.848	.745	102.8	.435	236.2	103.4	154.5	1.53*
E2116	75	993	1.124	.848	.766	116.0	.461	251.6	110.1	154.5	1.63*
E2112	400	88	1.124	.848	.739	88.0	.429	205.0	89.8	145.1	1.41*
E2117	400	1016	1.120	.849	.783	107.6	.481	223.7	97.9	145.1	1.54*
E2113	650	107	1.125	.848	.695	70.6	.379	186.1	81.2	137.3	1.35*
E2118	650	1274	1.124	.849	.740	87.5	.430	203.7	89.2	137.3	1.48*
TITANIUM 6Al-4V											
F219	-110	101	1.120	.853	.736	44.0	.426	103.4	45.2	174.0	.59
F2110	-110	98	1.122	.853	.737	35.9	.426	84.3	36.9	174.0	.48
F2114	-110	1200	1.120	.852	.750	44.4	.442	100.5	44.0	174.0	.58
F2111	75	108	1.122	.853	.784	50.6	.483	104.8	45.9	152.7	.73
F218	75	1065	1.124	.853	.780	53.0	.478	110.9	48.5	152.7	.69
F2115	75		1.121	.854							
F2112	400	93	1.123	.852	.730	72.1	.418	172.5	75.5	111.0	1.55*
F2117	400	1118	1.121	.854	.767	89.5	.462	193.7	84.8	111.0	1.74*
F217	650	200	1.120	.853	.707	70.8	.392	180.5	78.8	95.0	1.90*
F2118	650	1055	1.120	.852	.748	82.9	.439	188.9	82.7	95.0	1.99*

NOTE: 1.125 INCH ROUND NOTCH TRANSVERSE GRAIN SPECIMENS

 YIELD STRENGTHS WERE OBTAINED AT NORMAL LOADING RATES

(2500 psi/sec) AND THEREFORE ONLY APPROX CORRECT FOR

LISTED STRESS RATES

 STRESS RATES ARE BASED ON NOTCH DIAMETER

* THESE RATIOS ARE ABOVE THE ... MIT RECOMMENDED BY THE ASTM COMMITTEE ON FRACTURE TOUGHNESS

 THIS SPECIMEN FAILED IN FATIGUE MACHINE

FATIGUE DATA (1800 cpm, R = .05)

INCO 718 : MAX CYCLING STRESS APPROX 52 ksi, 40,000 TO 45,000 CYCLES

Ti 6Al-4V. MAX CYCLING STRESS APPROX 52 ksi, 6,000 TO 7,000 CYCLES

9 Ni-4Co

This alloy showed an increase in toughness with loading rate except at 650°F, (Fig. 175). At 650°F, the alloy showed a large drop in toughness with increasing loading rate resulting in the 650°F value being the lowest one at the 10^6 psi/sec stress rate. At the normal tensile testing stress rate (2.5×10^3 psi/sec), the 650°F value was the highest.

MARAGING 250

At test temperatures below 650°F, the toughness values did not vary with loading rate (Fig. 176). This was the only alloy that did not show an increase in toughness value with testing rate at the test temperatures below 650°F. At 650°F, the toughness values showed a drop at the intermediate stress rate of 10^5 psi/sec.

INCO 718

At test temperatures below 650°F, the toughness values increased slightly with loading rate (Fig. 178). At 650°F, the values did not change significantly with loading rate.

Ti 6Al-4V

The test values increased slightly at all test temperatures with loading rate (Fig. 178). This was the only alloy that showed an increase in toughness with loading rate at all test temperatures.

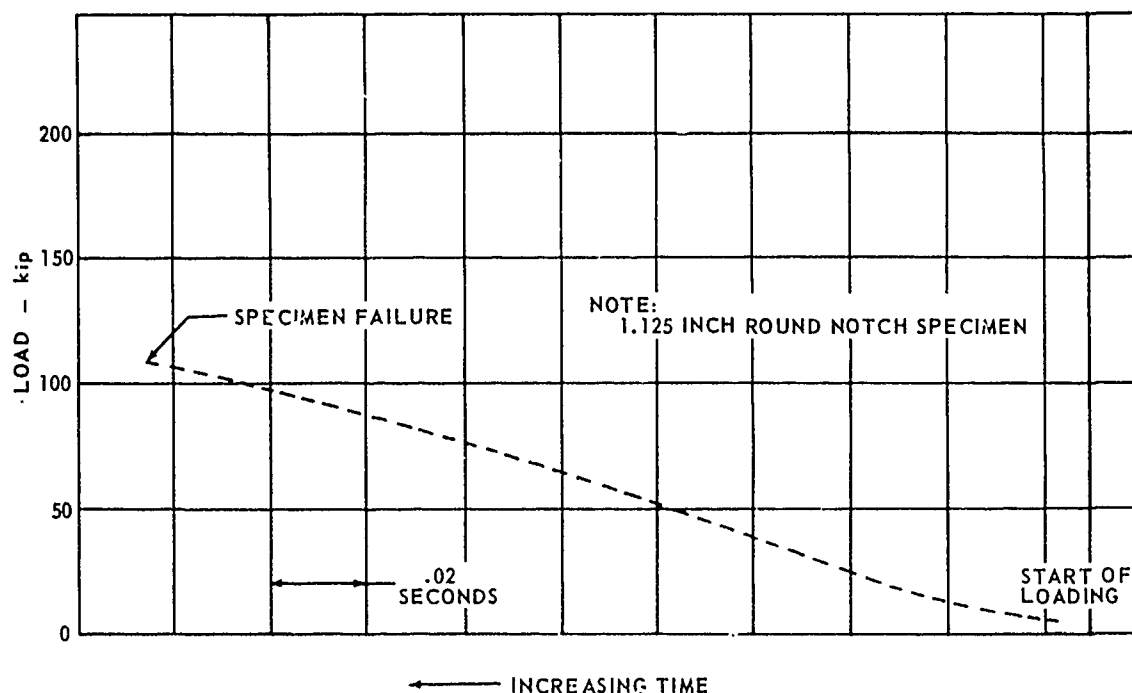


FIG. 174 TYPICAL HIGH LOAD RATE CURVE

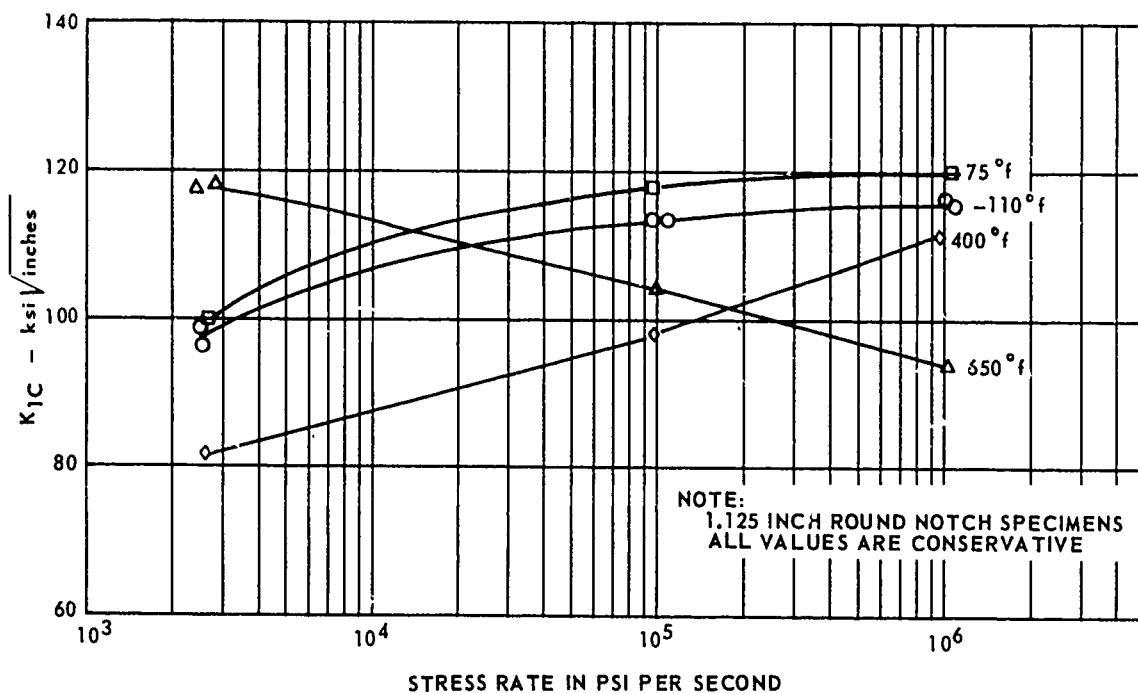


FIG. 175 EFFECT OF STRESS RATE ON K_{1C} VALUES FOR 9 Ni-4Co

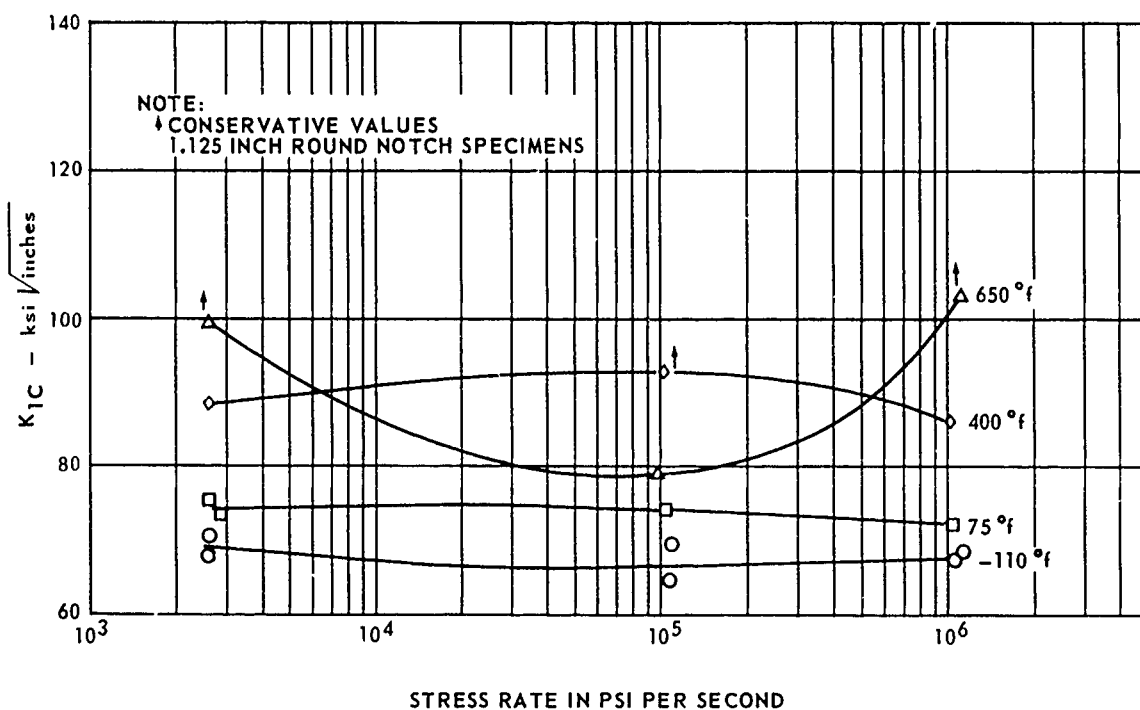


FIG. 176 EFFECT OF STRESS RATE ON K_{1C} VALUES FOR MARAGING 250

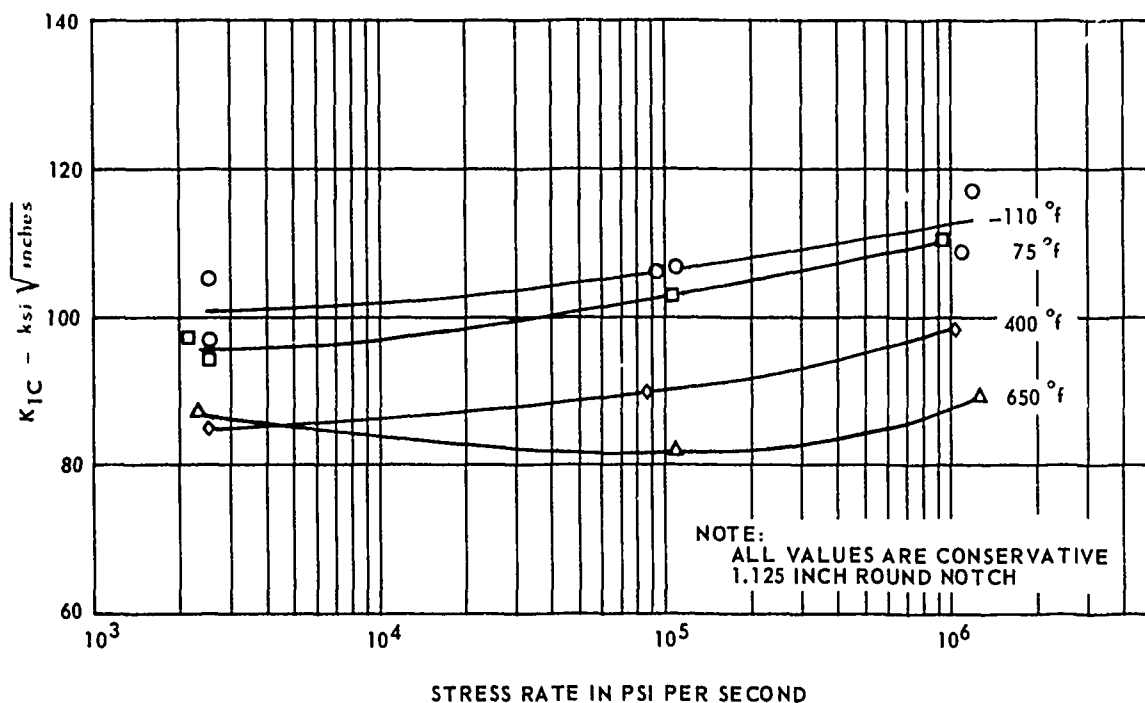


FIG. 177 EFFECT OF STRESS RATE ON K_{1C} VALUES FOR INCO 718

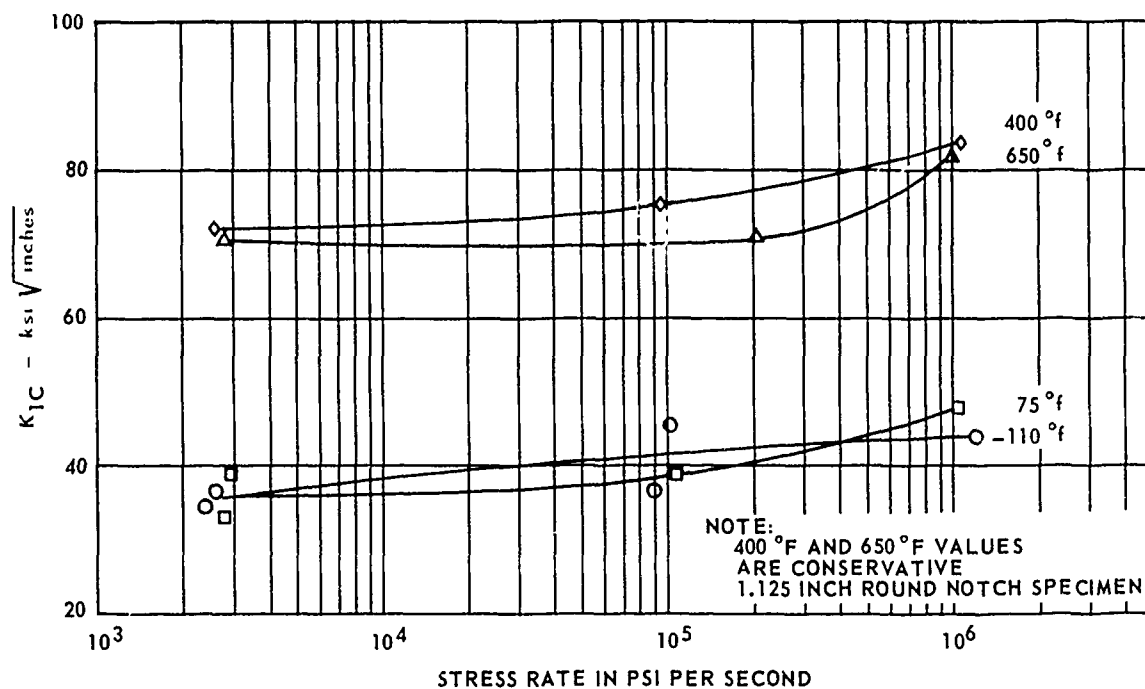


FIG. 178 EFFECT OF STRESS RATE ON K_{1C} VALUES FOR Ti 6Al-4V

SECTION 15 CONCLUSIONS

1. Material plane stress fracture toughness as derived from center notched specimens generally increased with test temperature and decreased with increasing panel thickness. Reversal of these trends was noted with Inco 718 and was considered to be the effect of very high net section stresses which tend to make the data more conservative. A summary of center notched specimen K_{IC} values is presented in Figs. 179 and 180 for the 3/8" and 1" thick panels. Data for only the more critical testing temperature of -110° F is plotted.
2. AM355 reveals a definite decrease in critical stress intensity values for both the center notched and round notched specimens tested at 650° F. With this alloy, the decrease in plane stress fracture toughness does not appear to be the result of high net section stresses. Precracked Charpy specimen data did not reveal this decrease in fracture toughness.
3. K_{IC} values derived from the notched round specimens indicate a general increase with testing temperature. However, 4340 and 9Ni-4Co revealed a decrease in K_{IC} between room temperature and 400° F testing. AM355 indicated a substantial decrease between the 400° F and 650° F testing temperature for all three grain directions.

A summary of the notched round specimen K_{IC} values, normalized by density is shown in Fig. 181 for the most critical testing conditions; transverse and -110° F.

4. Correlation of K_{IC} values from round notched, surface cracked, and center notched specimens was in general best for 4340 and Maraging 250. Fig. 182 is included as a partial illustration of this correlation. The temperature used for this comparison was determined by the temperature at which the surface cracked specimens were tested.
5. The rating order of K_{IC} and K_{IC} values for the alloys varied over the temperature range from -110° F to 650° F for various thicknesses of center notched panels and for the notched round specimens as indicated in the Rating Chart of Table 36. However, four of the alloys; 9Ni-4Co, Maraging 250, Inco 718 and Ti 6Al-4V (not in order of preference) were concluded to be the most promising for further study. Although Ti 6Al-6V-2Sn was not selected for further study, the fracture toughness of this alloy in the annealed condition was rated very closely to the first four alloys.
6. The steel alloys yielded the greatest number of pop-in indications from the center notched specimens. The titanium alloys and Inco 718 resulted in relatively few. Correlation of plane strain fracture toughness determined from the pop-in phenomenon and from round notched specimens was only fair at best. It was considered that the fracture toughness of the alloys tested was too high to yield satisfactory pop-in indications in the center-notched testing.

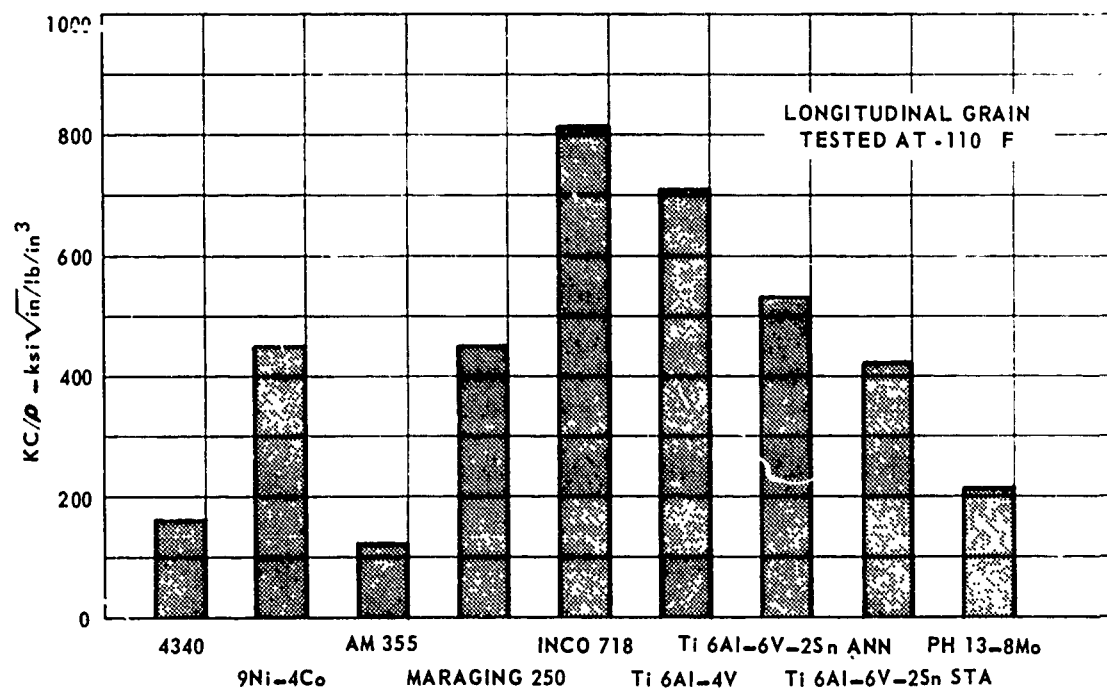


FIG. 179 3/8 INCH THICK PLATE K_C - DENSITY RATIO COMPARISON

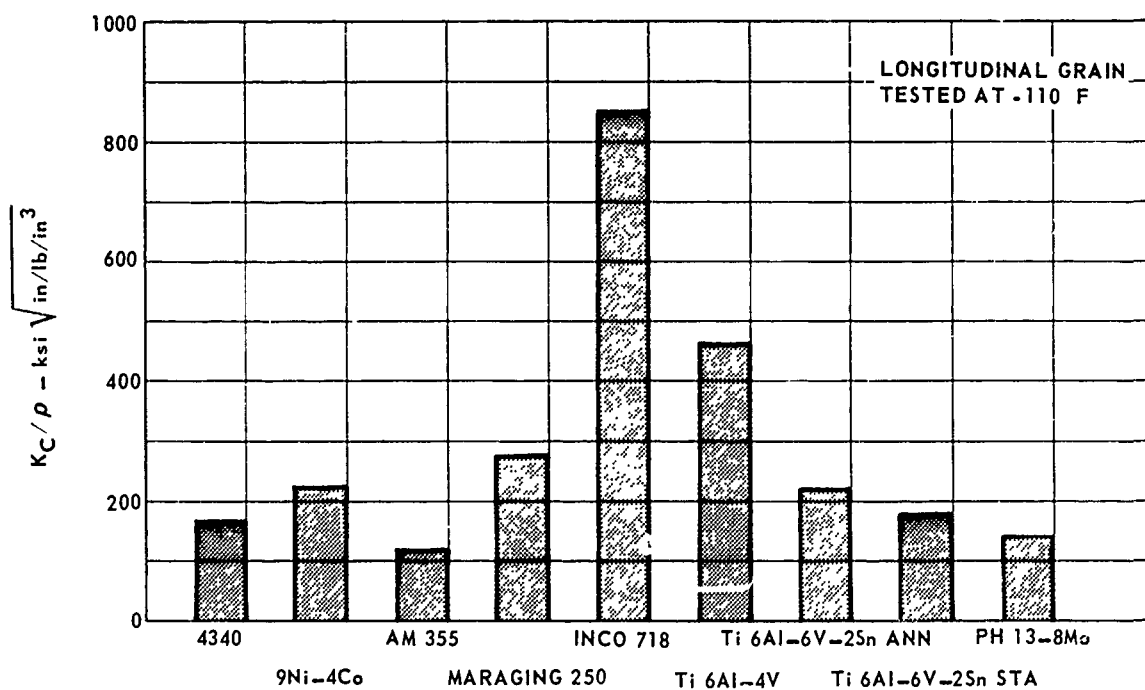


FIG. 180 1 INCH THICK PLATE K_C - DENSITY RATIO COMPARISON

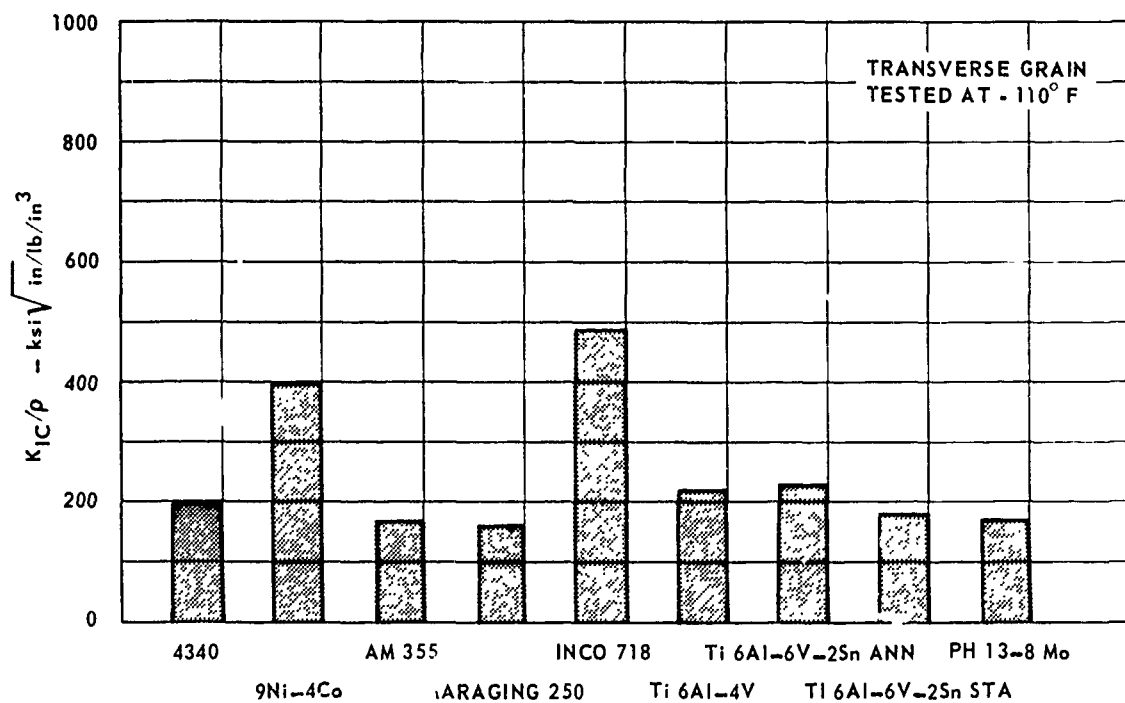


FIG. 181 ROUND NOTCH TENSILE K_{IC} - DENSITY RATIO COMPARISON

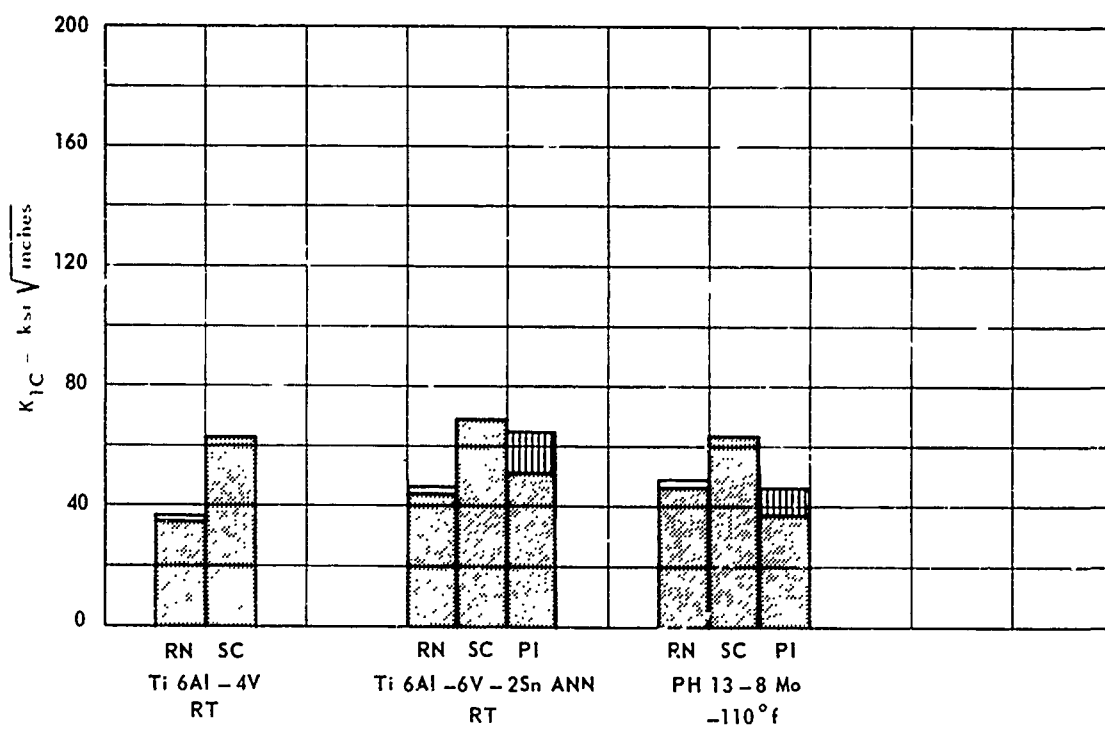
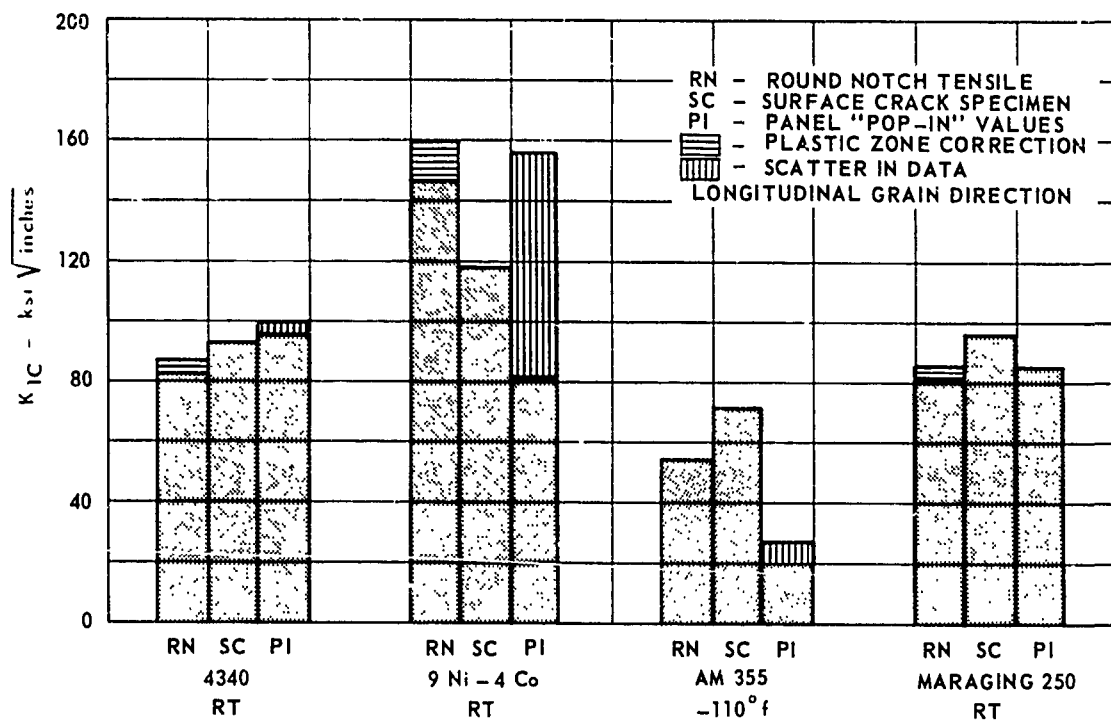


FIG.182 VARIATION IN K_{IC} TEST RESULTS WITH SPECIMEN TYPE

7. Investigation of the three grain directions of forged blocks, using round notched specimens, revealed the greatest variation in fracture toughness for stainless steels and the least for titanium alloys.
8. Round notched specimens from the short transverse grain direction of forged down blocks of 4340, AM355, and Maraging 250 had lower plane strain fracture toughness than the specimens from the transverse grain direction of the 9 x 9-inch blocks. The greatest difference in K_{1C} values at room temperature due to forging from 9-inch down to 3-inch was a decrease of 10 ksi $\sqrt{\text{in.}}$ for Maraging 250.
9. The test data indicate the critical stress intensity equation for surface cracks is only valid for gross area fracture stresses up to about 90 percent of the yield strength. At higher fracture stresses, general plastic yielding occurs and the apparent toughness values fall below the true value.
10. The predicted fracture stresses for the surface cracked specimens, based on round notched specimen K_{1C} values, ranged from 28 percent above to 39 percent below the actual stresses. The relationship between the actual and predicted fracture stresses was a function of the alloy toughness level. By converting the round bar toughness value for each alloy (by the conversion curve of Fig. 131) to an equivalent surface cracked specimen toughness value, the predicted stresses based on the corrected value would all be within 10 percent of actual stresses.
11. Exposure testing of notched round specimens for 1000 hours at 650° F under stress, revealed significant instability in only the Maraging 250 specimens. K_{1C} values were decreased an average of 16 percent for the Maraging 250 and increased an average of 6 percent for the Inco 718 when stressed to 40 ksi. The Ti 6Al-4V specimens stressed to 25 ksi were increased only an average of 5 percent of K_{1C} .

The 9Ni-4Co was exposed at the lower temperature of 400° F and at a stress level of 40 ksi which caused an average increase of less than one percent in K_{1C} values.

12. Environmental testing of transverse notched round specimens in distilled water at room temperature and 200° F caused delayed fracture to occur in each of the four most promising alloys within 100 hours. Sustained loading in room temperature distilled water caused delayed fracture stress intensity values as low as 78 percent of the dry test K_{1C} values for 9Ni-4Co, 65 percent for Maraging 250, 78 percent for Inco 718 and 82 percent for Ti 6Al-4V.

Raising the distilled water temperature to 200° F lowered the delayed fracture stress intensity values to 48 percent of K_{1C} for 9Ni-4Co, 48 percent for Maraging 250, 77 percent for Inco 718 and 65 percent for Ti 6Al-4V.

13. Increasing the rate of loading from 2.5×10^3 psi/sec to 10^6 psi/sec for notched round specimens tested at room temperature increased the room temperature K_{1C} values for 9Ni-4Co 19 percent, decreased the Maraging 250 values 2 percent, increased the Inco 718 values 11 percent, and increased the Ti 6Al-4V values 20 percent.

SECTION 16 RECOMMENDATIONS

1. The effect of chemistry variations on fracture toughness characteristics was not investigated in this program, except to a limited extent with 9 Ni-4Co. This chemistry variable has a large effect on fracture toughness; therefore, it is recommended that further work be conducted on selected alloys using several different heats. It would also be advisable to investigate some of the alloying variations such as the modified 9 Ni-4Co included in this program.
2. For design, the compromise between strength and toughness will require fracture toughness characteristics to be known over a range of strength levels. Future work should, therefore, include fracture testing at a number of strength levels to obtain a strength versus K_{IC} curve.
3. In this program, crack growth data was not obtained because of time limitations. However, in future work with center-notched specimens, crack growth should be one of the main considerations. More over, these measurements should be made on specimens from the three grain directions of forgings.
4. Environmental testing should be more fully explored with other possible service environments that the supersonic transport may encounter. Sustained loading should be continued out to at least 1000 hours to more fully develop the stress level versus time-to-failure curve.
5. Since most alloys showed some instability under stress and heat exposure, further work is necessary on this problem. A study with other stresses and temperatures with considerably longer times is required. A better understanding of the phenomenon affecting the metallurgical stability of each alloy should be attempted.
6. The data from this program has shown apparent variations in plane strain fracture toughness among the different specimen geometries. Theoretically these differences should not occur, therefore further work remains in analyzing the relationship between fracture characteristics of the various specimen geometries.
7. The alloys most useful in structural applications present the greatest problem in testing. The large specimen size imposed by the high fracture toughness of the most useful alloys may not be practical. Therefore, further analysis is required to determine more useful plane strain fracture toughness data in cases of plastic yielding.

SECTION 17 REFERENCES

1. Orner, G. M., and Hartbower, C. E., "Sheet Fracture Toughness Evaluated by Charpy Impact and Slow Bend," *Welding Research Supplement*, September, 1961.
2. Hartbower, C. E., and Orner, G. M., "Metallurgical Variables Affecting Fracture Toughness in High Strength Sheet Alloys," ASD-TDR-62-868, Project No. 7381, June, 1963.
3. Griffith, A. A., "The Phenomena of Rupture and Flow in Solids," *Philosophical Transactions of the Royal Society of London, Series A*, Vol. 221, 1920.
4. Inglis, C. E., "Stresses in a Plate Due to the Presence of Cracks and Sharp Corners," *Proc. Inst. Naval Architects*, March 14, 1913.
5. Irwin, G. R., "Fracture Dynamics," *Fracturing of Metals*, American Society of Metals, 1948, pp.147-166.
6. Irwin, G. R., and Kies, J. A., "Fracturing and Fracture Dynamics," *Welding Journal Research Supplement*, February 1952, pp. 95s-100s.
7. Orowan, E., "Fundamentals of Brittle Behavior of Metals," Fatigue and Fracture of Metals, John Wiley and Sons, New York, 1952, p. 154.
8. Irwin, G. R., "Analysis of Stresses and Strains Near the End of a Crack Traversing a Plate," *Journal of Applied Mechanics*, Transactions of ASME, Vol. 24, No. 3, September 1957.
9. Irwin, G. R., "Relation of Stresses Near a Crack to the Crack Extension Force," *IXth International Congress of Applied Mechanics*, University of Brussels, September 1957.
10. Murphy, G., "Advanced Mechanics of Materials", McGraw-Hill Book Co., 1946, p. 61.
11. Westergaard, H. M., "Bearing Pressures and Cracks," *Journal of Applied Mechanics*, June 1939.
12. Williams, M. L., "On the Stress Distribution Near the Base of a Stationary Crack," *Journal of Applied Mechanics*, March 1957.
13. Sneddon, I. N., "The Distribution of Stress in the Neighborhood of a Crack in an Elastic Solid," *Proceedings of the Royal Society of London*, Vol. A-187, 1946.
14. Irwin, G. R., "Dimensional and Geometric Aspects of Fracture," *ASM Conference on Fracture of Engineering Materials*, Troy, New York, August 24-25, 1959.

15. Irwin, G. R., "Plastic Zone Near a Crack and Fracture Toughness," Seventh Sagamore Ordnance Materials Research Conference, Racquette Lake, New York, August 16-19, 1960.
16. Irwin, G. R., "Crack Extension Force for a Part-Through Crack in a Plate," Journal of Applied Mechanics, Vol. 84E No. 4, December 1962, pp. 651-654.
17. Irwin, G. R., "Analytical Aspects of Crack Stress Field Problems," University of Illinois, Theoretical and Applied Mechanics Report No. 213, March 1962.
18. Fifth Report of a Special ASTM Committee, "Progress in Measuring Fracture Toughness and Using Fracture Mechanics," Materials Research and Standards, Vol. 4, No. 3, March 1964.
19. Irwin, G. R., "Supplement to Notes for May 1961 Meeting of ASTM Committee for Fracture Testing of High Strength Metallic Materials" (Unpublished)
20. Gallagher, W. C., "Izod Impact Testing of 4340," Boeing Technical Document D6-9820TN, November 1963.
21. Dreyer, G. A., and Gallagher, W. C., "Investigation of the Effects of Stress Corrosion on High Strength Steel Alloys," Materials Laboratory Technical Document 64-3, A. F. 33(657)8705, February 1964.
22. Banerjee, B. R., and Hauser, J. J., "Research and Application to Determine the Effect of Processing Variables on Crack Propagation of High Strength Steels and Titanium," Technical Documentary Report ASD-TDR-62-1034, Part I, December 1962.
23. Steigerwald and Hanna, "Initiation of Slow Crack Propagation in High-Strength Materials," ASTM, June 1962 Meeting, Preprint No. 74.
24. Boyle, R. W., Sullivan, A. M., and Krafft, J. M., "Determination of Plane Strain Fracture Toughness with Sharply Notched Sheets," Welding Research Supplement, September, 1962.
25. Banerjee, B. R., and Hauser, J. J. "Research and Application Engineering to Determine the Effect of Processing Variables on Crack Propagation of High Strength Steels and Titanium," Technical Documentary Report No. ASD-TDR-62-1034, Part I, December 1962.
26. Pelloux, Regie, M. N., "The Analysis of Fracture Surfaces by Electron Microscopy," D1-82-0169-R1 Boeing Scientific Research Laboratories, December 1963.
27. Beachem, C. D., "An Electron Fractographic Study of the Influence of Plastic Strain Conditions Upon Ductile Rupture Processes in Metals," Transactions ASM, 56, 318, 1963.

28. Raring, R. H., Freeman, J. W., Schultz, J. W., Voorhees, H. R.,
"Progress Report of the NASA Special Committee on Materials Research
for Supersonic Transports," NASA Technical Note D-1798, May 1963.
29. Steigerwald, E. A., "Delayed Failure of High Strength Steel in Liquid
Environments," Technical Memorandum TM1574CM, July 1, 1960.